Norwegian University of
Science and Technology

# Possibilities and Implications by Designing an Aluminium Integrated Template Structure.

**Kjell Petter Løkling Lunde**
**Henrik Westersjø Nesheim**

Subsea Technology
Submission date: June 2017
Supervisor: Tor Berge Gjersvik, IGP
Co-supervisor: Roy Johnsen, MTP

Norwegian University of Science and Technology
Department of Geoscience and Petroleum

# Preface

This master thesis is submitted to the Norwegian University of Science and Technology (NTNU) as a part of the master's degree program within Subsea Technology with specialization in operation and maintenance. The thesis was written at the Department of Geoscience and Petroleum, in the spring semester of 2017.


### Acknowledgement

We would like to thank our supervisor Tor Berge Gjersvik for his engagement. And a special thanks to our co-supervisor Roy Johnson and Ole Terje Midling in Marine Aluminium AS for their interest in the project.


Trondheim, June 9, 2017

Henrik W. Nesheim        Kjell P. Lunde

*Henrik W. Nesheim*        *Kjell P. Lunde*

# Summary

Steel has historically been the governing material for use in subsea applications. This master thesis looks into the possibility of using aluminium rather than steel in subsea structures. A four-slots integrated template structure installed on the Gjøa field in the Norwegian Sea is used as design basis. The use of aluminium represents a lighter structure with a potential in reducing life cycle cost. The aluminium alloys 5083 and 6082 are the only ones approved for structural seawater applications by the NORSOK M-121 standard, where H116 and T6 are the strongest approved tempers, respectively. However, material properties has to be fully understood in order to utilize aluminium in a subsea environment. Especially with respect to corrosion behaviour, mechanical properties and joining methods. Bolting, metal inert gas and friction stir welding are identified as preferred joining methods.

The structure is redesigned utilizing appropriate alloys and joining methods. Load simulations are subsequently performed using finite element method, where the structure withstands design loads defined by industry standards with acceptable results. The main load types are drilling, trawling, tie-in and weight of equipment installed on the integrated template structure.

The utilization of aluminium in subsea structures looks very promising for the integrated template structure, although there is a need for more research, especially with respect to corrosion of aluminium buried in soil. A total weight reduction of 36% is achieved by utilizing aluminium. Total cost for the aluminium made structure is competitive to steel, where aluminium fabrication cost is the decisive factor.

# Sammendrag

Stål har historisk vært det mest brukte materialet for bruk i undervannskonstruksjoner. Denne masteroppgaven ser på mulighetene for å bruke aluminium i stedet for stål i undervannsstrukturer. En fire-slots bunnramme installert på Gjøa feltet i Norskehavet er brukt som et design grunnlag. Bruk av aluminium resulterer i en lettere struktur med potensial i å redusere livssykluskostnadene. Aluminiumslegeringene 5083 og 6082 er de eneste som er godkjent for strukturelt bruk i undervannsmiljøet ifølge NORSOK M-121 standarden, hvor H116 og T6 er de sterkeste temperamentene. En grundig forståelse for materialegenskapene må ligge til grunn for å kunne anvende aluminium i undervannsmiljøet. Spesielt med hensyn til korrosjonsadferd, mekaniske egenskaper og sammenføyningsmetoder. Bolting, metall inert gass og friksjons sveising er identifisert som foretrukne sammenføyningsmetoder.

Foretrukne sammenføyningsmetoder og de godkjente aluminiumslegeringene er benyttet for å redesigne strukturen. Last simulasjoner er gjennomført ved å anvende elementmetoden. Strukturen tåler påsatte belastninger definert av industri-standarder med akseptable resultater. Evaluerte last typer er boring, tråling, opp-kobling og vekt av installerte komponenter.

Å anvende aluminium i undervansstrukturer ser lovende ut for den evaluerte bunnrammen, selv om det er behov for mer forskning, spesielt med hensyn til korrosjon av aluminium som er begravet i sedimenter. En total vektreduksjon på 36% er oppnåd ved å bruke aluminium i stedet for stål. Samlet sett er kostnaden for aluminiumskonstruksjonen konkurransedyktig med stål, hvor fabrikasjonskostnadene er avgjørende for hvorvidt stål eller aluminium fremstår som mest kostnadseffektivt.

# Contents

Preface . . . . . . . . . . i
Summary . . . . . . . . . . iii
Abbreviations . . . . . . . . . . xix

**1 Introduction** **1**
1.1 Background . . . . . . . . . . 1
1.2 Objective . . . . . . . . . . 1
1.3 Historical overview . . . . . . . . . . 2
1.3.1 Use of aluminium in the subsea environment . . . . . . . . . . 2
1.3.2 Selection of structure . . . . . . . . . . 3

**2 Subsea Equipment** **5**
2.1 Integrated template structure . . . . . . . . . . 5
2.1.1 X-mas tree . . . . . . . . . . 8
2.1.2 Manifold . . . . . . . . . . 9

**3 Aluminium** **11**
3.1 Aluminium designation . . . . . . . . . . 11
3.2 Material properties . . . . . . . . . . 13
3.2.1 Operating temperature . . . . . . . . . . 13
3.2.2 Cryogenic toughness . . . . . . . . . . 14
3.2.3 Hydrogen embrittlement . . . . . . . . . . 14
3.3 Extrusion . . . . . . . . . . 14
3.4 Recycling . . . . . . . . . . 16
3.5 Corrosion . . . . . . . . . . 16
3.5.1 Crevice corrosion . . . . . . . . . . 16
3.5.2 Pitting corrosion . . . . . . . . . . 18

3.5.3 Intercrystalline corrosion . . . 19
3.5.4 Corrosion in soil . . . 20
3.5.5 Seawater flow rates influence on corrosion rates . . . 22
3.5.6 Galvanic corrosion . . . 26
3.5.7 Coating . . . 28
3.5.8 Corrosion and protection of aluminium in seawater . . . 28
3.6 Welding . . . 32
3.6.1 Arc welding . . . 32
3.6.2 Friction stir welding . . . 37
3.6.3 Hybrid metal extrusion and bonding . . . 41
3.6.4 Laser welding . . . 42
3.6.5 Hybrid laser . . . 44
3.6.6 Summary of welding methods . . . 45
3.7 Brazing . . . 45
3.8 Bolting . . . 46
3.9 Adhesives . . . 53
3.10 Formability . . . 55
3.10.1 Machining . . . 56
3.11 Buckling . . . 56
3.12 Fatigue . . . 58

**4 Integrated Template Structure Analysis** **61**
4.1 Design of beams . . . 61
4.2 Design of joints . . . 70
4.2.1 Bolted joints . . . 70
4.2.2 Welded joints . . . 75
4.3 Loads . . . 77
4.3.1 Lift off and splash zone loads . . . 77
4.3.2 Pull in of umbilicals and pipelines . . . 78
4.3.3 Drilling and trawling loads . . . 79
4.3.4 Dropped objects . . . 79
4.3.5 Static loads . . . 79
4.4 Model . . . 80

4.4.1 Load cases . . . . . . . . . . . . . . . . . . . . . . . . . . . . . . . . . . 82
4.4.2 Results . . . . . . . . . . . . . . . . . . . . . . . . . . . . . . . . . . . . 83
4.5 Anode mass estimation . . . . . . . . . . . . . . . . . . . . . . . . . . . . 91
4.6 Weight saving . . . . . . . . . . . . . . . . . . . . . . . . . . . . . . . . . 94

**5 Cost Estimations and Comparison** **97**
5.1 Installation cost . . . . . . . . . . . . . . . . . . . . . . . . . . . . . . . 97
5.2 Fabrication cost . . . . . . . . . . . . . . . . . . . . . . . . . . . . . . . 98
5.2.1 Steel structure cost . . . . . . . . . . . . . . . . . . . . . . . . . . . . 99
5.2.2 Aluminium structure cost . . . . . . . . . . . . . . . . . . . . . . . . 99
5.2.3 Anode material cost . . . . . . . . . . . . . . . . . . . . . . . . . . . 102
5.2.4 Total cost estimates comparison . . . . . . . . . . . . . . . . . . . . 102

**6 Discussion** **103**
6.1 Connection methods . . . . . . . . . . . . . . . . . . . . . . . . . . . . . 103
6.2 Corrosion protection strategy . . . . . . . . . . . . . . . . . . . . . . . . 104
6.2.1 Corrosion challenges . . . . . . . . . . . . . . . . . . . . . . . . . . . 104
6.3 Fatigue concerns . . . . . . . . . . . . . . . . . . . . . . . . . . . . . . . 105
6.4 Design implications . . . . . . . . . . . . . . . . . . . . . . . . . . . . . 105
6.4.1 Deflection . . . . . . . . . . . . . . . . . . . . . . . . . . . . . . . . . 106
6.4.2 Insert . . . . . . . . . . . . . . . . . . . . . . . . . . . . . . . . . . . 106
6.4.3 Bolt calculations . . . . . . . . . . . . . . . . . . . . . . . . . . . . . 107
6.4.4 Manifold support . . . . . . . . . . . . . . . . . . . . . . . . . . . . . 107
6.4.5 Formability . . . . . . . . . . . . . . . . . . . . . . . . . . . . . . . . 108
6.5 FEM Analysis . . . . . . . . . . . . . . . . . . . . . . . . . . . . . . . . . 108
6.5.1 Validation of modelled cases . . . . . . . . . . . . . . . . . . . . . . . 108
6.5.2 Dropped objects . . . . . . . . . . . . . . . . . . . . . . . . . . . . . 109
6.6 Weight saving . . . . . . . . . . . . . . . . . . . . . . . . . . . . . . . . . 110
6.7 Coating . . . . . . . . . . . . . . . . . . . . . . . . . . . . . . . . . . . . 110
6.8 Cost uncertainties . . . . . . . . . . . . . . . . . . . . . . . . . . . . . . 110

**7 Conclusion** **113**

**8 Future Work** **115**

**Bibliography** **117**

**Appendix** **124**

**A Loads** **125**

A.1 Splash zone loads . . . . . 125

A.2 Static loads . . . . . 126

A.3 Trawling loads . . . . . 127

A.4 Dropped objects impact energy . . . . . 127

A.5 Sealine loads . . . . . 127

A.6 Drilling loads . . . . . 128

**B E-mail Correspondences** **129**

B.1 E-mail correspondence with Keld Reimer Hansen regarding production capabilities at STEP-G. . . . . . 130

B.2 E-mail correspondence with Andreas Fellhauer regarding production capabilities at Constellium. . . . . . 132

B.3 E-mail correspondence with Ole Øystein Knudsen regarding aluminium subsea properties. . . . . . 134

B.4 E-mail correspondence with Tor Berge Gjersvik. . . . . . 138

B.5 E-mail correspondence with Asbjørn Wathne in Subsea 7 regarding ITS installation details. . . . . . 142

B.6 E-mail correspondence with Ole Terje Midling in Marine Aluminium. . . . . . 147

B.7 E-mail correspondence with Skarpenord regarding aluminium anodes . . . . . 148

B.8 E-mail correspondence with Halvard Torget Eriksen regarding cost of phosphated bolts . . . . . 149

**C Bolt Calculations** **151**

C.1 Design sheets exported from excel . . . . . 151

**D Beam Design** **165**

D.1 Design sheets exported from excel . . . . . 165

**E Anode Calculation** **193**

**F Additional Figures** **195**

F.1 Extrusion limits . . . 195

F.2 seawater properties as a function of depth . . . 196

F.3 Illustration of suction anchor with welds. . . . 197

**G Que$tor Cost Estimates** **199**

G.1 Full subsea layout. . . . 200

G.2 One ITS and riser base. . . . 213

G.3 Two integrated template structures and riser base. . . . 218

**H Cost Estimates** **225**

H.1 Part list sent to STEP-G . . . 226

H.2 Price offer recieved from STEP-G . . . 230

H.3 Constellium price offer . . . 236

**I FEM Analysis** **237**

I.1 Case-A . . . 238

I.1.1 Without convergence . . . 238

I.1.2 With convergence . . . 248

I.2 Case-B . . . 258

I.2.1 Without convergence . . . 258

I.2.2 With convergence . . . 270

I.3 Case-C . . . 282

I.3.1 Without convergence . . . 282

I.3.2 With convergence on top corner . . . 296

I.3.3 With convergence on support beam . . . 305

I.3.4 Overtrawlable/snagfree design load, 400kN instead of 1000kN. . . . 318

I.4 Case-D . . . 329

I.5 Case-E . . . 346

I.5.1 Without convergence . . . 346

I.5.2 With convergence . . . 359

I.6 Case-F . . . 372

I.6.1 Without convergence . . . 372

I.6.2 With convergence . . . 388

I.7 Case-G . . . . . . . . . . 404

# List of Tables

3.1 Wrought and cast series [1]. . . . . 12
3.2 Temper designations [2]. . . . . 12
3.3 Properties of aluminium alloys 5083-H116 and 6083-T6 [2]. . . . . 13
3.4 Chemical composition of aluminium alloy 5083-H116 and 6082-T6 [wt%] [3]. . 13
3.5 Extrusion limits at STEP-G [4], SAPA [5], Constellium [6] and KUMZ [7]. . . . . 15
3.6 Corrosion potentials for 5xxx and 6xxx alloys [8]. . . . . 28
3.7 Preheating limits for arc welding of thick members [9]. . . . . 33
3.8 Strength of weld metal for alloy 5083 and 6082 [2]. . . . . 35
3.9 Strength reductions in HAZ [2]. . . . . 35
3.10 Extent of HAZ for different base metal thicknesses [2]. . . . . 36
3.11 Filler materials [2]. . . . . 36
3.12 Mechanical properties of FSW. . . . . 39
3.13 Laser weld strength characteristics1) [10]. . . . . 43
3.14 Summary of welding methods. . . . . 45
3.15 Properties of 316 stainless and 8.8 carbon steel bolts. . . . . 48
3.16 Minimum, regular and maximum values for spacing between bolts ans edges [2]. 52
3.17 Strength values of recommended adhesives [2]. . . . . 54
3.18 Minimum bend factors for cold bending of alloy 6082-T6 tubes and profiles [9]. 55
3.19 Slenderness parameters [2]. . . . . 58

4.1 MOI of beams, MOI ratios and buckling classification. . . . . 63
4.2 Forces acting on the bolted connections. . . . . 72
4.3 Dimensions of bolt plating and number of bolts required. . . . . 74
4.4 Input numbers for mesh and resulting number of elements and nodes. . . . . 81
4.5 ITS load cases. . . . . 83

4.6 Summary from analyses for all the selected cases. . . . . . . . . . . . . . . . . . . . 91
4.7 Anode specifications according to section 6.9.1 in NORSOK-M-CR-503 [11]. . . 92
4.8 Input numbers used in estimation of anode mass. . . . . . . . . . . . . . . . . . . . 93
4.9 Current demand and anode mass calculations. . . . . . . . . . . . . . . . . . . . . 93
4.10 Weight changes for each component, and total weight comparison. . . . . . . . 94

5.1 Installation vessel size influence on installation cost. . . . . . . . . . . . . . . . . . 98
5.2 Cost estimation for aluminium based on numbers in e-mail correspondence seen in appendix B.6. . . . . . . . . . . . . . . . . . . . . . . . . . . . . . . . . 100
5.3 Cost comparison between stainless, carbon and phosphated carbon M36 steel bolts [12, 13]. . . . . . . . . . . . . . . . . . . . . . . . . . . . . . . . . . . . 101
5.4 Anode cost estimation. . . . . . . . . . . . . . . . . . . . . . . . . . . . . . . . . . 102
5.5 Cost comparison for the two alternatives (aluminium and steel). . . . . . . . . . . 102

A.1 Manifold and christmas tree weights with resulting forces. . . . . . . . . . . . . . 126
A.2 Trawling loads [14]. . . . . . . . . . . . . . . . . . . . . . . . . . . . . . . . . . . . 127
A.3 Dropped objects impact energy [14]. . . . . . . . . . . . . . . . . . . . . . . . . . . 127
A.4 Sealine loads scenarios [15]. . . . . . . . . . . . . . . . . . . . . . . . . . . . . . . 127
A.5 Drilling loads for depths up to 750 m [14]. . . . . . . . . . . . . . . . . . . . . . . . 128

# List of Figures


2.1 Several suction anchors lined up, each with a height of ca. 6.5 meters [16]. . . . 6

2.2 Figure of X-mas and manifold placement on the ITS seen from above, orange is space for X-mas while the red is space for manifold. . . . . . . . . . . . . . . . 6

2.3 Position of X-mas tree on permanent guide-base on the ITS, only two out of four wells are shown on the left figure. . . . . . . . . . . . . . . . . . . . . . . . . . 8

2.4 Picture of a manifold manufactured by Agility Group [17]. . . . . . . . . . . . . . 9

3.1 Circumference limits for the extrusion press at STEP-G [4]. . . . . . . . . . . . . 15

3.2 Crevice corrosion in an overlapping joint [18]. . . . . . . . . . . . . . . . . . . . . . 17

3.3 Poor design in A and good design in B with respect to crevices [19]. . . . . . . . 18

3.4 Illustration of localized corrosion around intermetallic particles in the acidic pit and adjacent alkaline cathodic site [20]. . . . . . . . . . . . . . . . . . . . . . . . 19

3.5 Cathodic phase at the grain boundaries, [mV] vs Saturated calomel electrode (SCE) [19]. . . . . . . . . . . . . . . . . . . . . . . . . . . . . . . . . . . . . . . . 20

3.6 Resistivity versus aggressiveness for soils [19]. . . . . . . . . . . . . . . . . . . . . . 21

3.7 Cathodic current density in soil at -1100 mV vs Ag/AgCl for different temperatures [21]. . . . . . . . . . . . . . . . . . . . . . . . . . . . . . . . . . . . . . . . 21

3.8 Corrosion rate in soil polarized to -1100 mV vs Ag/AgCl for several temperatures [21]. . . . . . . . . . . . . . . . . . . . . . . . . . . . . . . . . . . . . . . . 22

3.9 Example of long circular tubes on the structure with small ventilation holes to the outside seawater. . . . . . . . . . . . . . . . . . . . . . . . . . . . . . . . . . . . 23

3.10 Velocities influence on corrosion rate for alloy 5456 connected to CP, 1 mdd = 13.5 $\mu m$[22]. . . . . . . . . . . . . . . . . . . . . . . . . . . . . . . . . . . . . . 24

3.11 Maximum pit depth for Al 99,5, AlMg3 and AlMgSi1 (alloy 6082) after two months of exposure under open-circuit potential [23]. . . . . . . . . . . . . . . . . . . . . 25

3.12 A split rubber grommet to restrict seawater flow in/out of compartments [24]. 25
3.13 Galvanic series in seawater [25]. . . . . . . . . . . . . . . . . . . . . . . . . . . . 27
3.14 Galvanic interconnection between aluminium alloy 5083-H116, 6082-T6 and filler metal 5556A. . . . . . . . . . . . . . . . . . . . . . . . . . . . . . . . . 28
3.15 Pourbaix diagram for alloy 5086 [20]. . . . . . . . . . . . . . . . . . . . . . . . . 29
3.16 Cathodic polarization curve for steel and aluminium at 8 cm/s flow rate [26]. AlMgSi1 is equivalent to 6082 and AlMg3 is equivalent to 5754. . . . . . . . . . . 30
3.17 Mechanism of CP on aluminium in seawater [20]. . . . . . . . . . . . . . . . . . 31
3.18 Typical current density vs time for a cathodically protected aluminium alloy in seawater [20]. . . . . . . . . . . . . . . . . . . . . . . . . . . . . . . . . . . . 31
3.19 MIG (left) and TIG (right) welding [27]. . . . . . . . . . . . . . . . . . . . . . . 34
3.20 Extent of HAZ for different welding geometries [2]. . . . . . . . . . . . . . . . . 36
3.21 Friction stir welding process [28]. . . . . . . . . . . . . . . . . . . . . . . . . . . 37
3.22 Microstructure after friction stir welding [29]. . . . . . . . . . . . . . . . . . . . 38
3.23 Comparison of Vickers hardness after friction stir welding for alloy 6082-T6 and alloy 6061-T6 [29]. . . . . . . . . . . . . . . . . . . . . . . . . . . . . . . . . . 40
3.24 Hybrid metal and extrusion [30]. . . . . . . . . . . . . . . . . . . . . . . . . . . 41
3.25 Laser keyhole welding principle [31]. . . . . . . . . . . . . . . . . . . . . . . . . 42
3.26 Hybrid laser principle [31]. . . . . . . . . . . . . . . . . . . . . . . . . . . . . . 44
3.27 Bolt assembly with CP between aluminium and steel with zinc phosphated carbon steel bolts and sealing compound. . . . . . . . . . . . . . . . . . . . . . . 47
3.28 In-plane moment. . . . . . . . . . . . . . . . . . . . . . . . . . . . . . . . . . . 50
3.29 Out-of-plane moment ($T_i = F_{t,i}$) [32]. . . . . . . . . . . . . . . . . . . . . . . . 50
3.30 Beam splices [32]. . . . . . . . . . . . . . . . . . . . . . . . . . . . . . . . . . . 51
3.31 Fastener spacing [2]. . . . . . . . . . . . . . . . . . . . . . . . . . . . . . . . . 52
3.32 Right figure: Structure of an adhesive metal to metal joint. Left figure: Delamination mechanism of an adhesive bonded joint: a) The oxide /primer interface is weakened due to stress and water. b) Crevice corrosion products accelerates the delamination [27]. . . . . . . . . . . . . . . . . . . . . . . . . . . . . . . . 54

4.1 The ITS with identification letters, where beam 'a' refers to the beam marked with an 'a' etc. . . . . . . . . . . . . . . . . . . . . . . . . . . . . . . . . . . 62

4.2 I-beam with a built-in guideway for the 5083-H116 plate in the 6082-T6 flange profile. Along with illustration of linear distribution of bending stress and orientation of fillet welds. . . . . 65
4.3 Stress distribution in beam 'n' when loaded with 1000 kN (yellow vector). . . . . 66
4.4 Merged 'b' and 'c' beam. . . . . 68
4.5 Heightened Beam 'h'. . . . . 68
4.6 Beam 'f' with respective x and y MOI directions. . . . . 69
4.7 Two alternatives for beam 'm' and 'n', where the left one is in accordance with NORSOK U-002 for D ≥ 250mm. . . . . 69
4.8 Joints designated with roman numerals. . . . . 71
4.9 Assumed bending moment distribution in beam 'a'. . . . . 72
4.10 Angled bolt plating on joint '$\mathrm{XIII}_{s-t}$' (left) and '$\mathrm{XIV}_{d-s}$' (right). . . . . 73
4.11 Weldments on suction anchor and beam 'i', dark lines are weldments. . . . . 76
4.12 Weldments on insert, dark lines are weldments and the insert is colored blue for better vision. . . . . 76
4.13 Assembly model of the redesigned integrated template structure. . . . . 81
4.14 Stress singularity for case-A, with convergence plot. . . . . 84
4.15 Stress singularity for case-B, with convergence plot. . . . . 85
4.16 Stress singularity for case-C, with convergence plot. . . . . 86
4.17 Stress in top corner for case-C, with convergence plot. . . . . 87
4.18 Local stress for case-E, with convergence plot. . . . . 89
4.19 Local stress for case-F, with convergence plot. . . . . 90

5.1 Gjøa south field layout, and subsea layout with three integrated template structures. . . . . 99

6.1 Integrated template structure with protection structures on top and connection of the whole side top beam [33]. . . . . 109

F.1 Circumference limits for the extrusion press at SAPA [5]). . . . . 195
F.2 Seawater's change in properties by depth [19]). . . . . 196

H.1 First table with bold letters received from Constellium, cost estimates in the second table are based on numbers in the first table (received from Constellium).236

# Abbreviations

**AS** Advancing Side

**BM** Base Material

**CAD** Computer Aided Design

**CAPEX** Capital Expenditure

**CASA** Center for Advanced Structural Analyses

**CP** Cathodic Protection

**DAF** Dynamic Amplification Factor

**DT** Drawn Tube

**DNV** Det Norske Veritas

**DVS** Deutscher Verband für Schweißtechnik

**Eq** Equation

**ET** Extruded Tube

**FCC** Face Centered Cubic

**FEM** Finite Element Method

**FSW** Friction Stir Welding

**HAZ** Heat Affected Zone

**HB** Brinell Hardness number

**HE** Hydrogen Embrittlement

**HYB** Hybrid metal extrusion and Bonding

**HT** Heat Treatable

**HV** Vickers Hardness

**ISO** International Organization for Standardization

**ITS** Integrated Template Structure

**LW** Laser Welding

**MIG** Metal Inert Gas

**MOI** Moment Of Inertia

**NCS** Norwegian Continental Shelf

**Nd:YAG** Neodymium: Doped Yttrium Aluminium Garnet

**NHT** Non Heat Treatable

**NORSOK** Norsk Sokkels Konkurranseposisjon

**NTNU** Norges Teknisk-Naturvitenskapelige Universitet

**OPEX** Operating Expenditure

**RFW** Rotary Friction Welding

**PL** Plate

**PTFE** Poly Tetra Fluoro Ethylene

**RS** Retreating Side

**SCE** Saturated Calomel Electrode

**Shell** Royal Dutch Shell plc

**SINTEF** Stiftelsen for Industriell og Teknisk Forskning ved Norges Tekniske Høgskole

**SKL** Skew Load factor

**Subsea 7** Subsea 7 SA

**SZ** Stir Zone

**Te** Metric Ton

**TEC** Thermal Expansion Coefficient

**TIG** Tungsten Inert Gas

**TMAZ** Thermal-Mechanically Affected Zone

**TS** Tensile Strength

**TSA** Thermal Sprayed Aluminium

**VAT** Value Added Tax

**YS** Yield Strength

**X-mas** Subsea christmas tree

# Chapter 1

# Introduction

## 1.1 Background

Oil companies are constantly looking for ways to reduce CAPEX (capital expenditure including installation cost) on field developments. Especially in the current market as the oil price has dropped significantly over the last couple of years (since 2014), putting an extra pressure on the field developments to reduce costs. This master thesis is based on the idea that the extensive use of aluminium in subsea structures may be beneficial to steel in terms of capital expenditures. Steel has been the governing material for use in subsea structures since the early days of subsea engineering, as it possess good and well-known mechanical properties and joining methods making it an easy choice. This study will focus on aluminium as a competitive alternative to steel.

## 1.2 Objective

The main objective of this study is to map aluminium properties related to subsea applications and to study design implications. Design possibilities will be based on one of the most extensively used integrated template structure (ITS) designs on the Norwegian Continental Shelf (NCS). A similar model of an aluminium integrated template structure will be build using appropriate software design tools. The main objectives are described in bullet points below.

- Map essential aluminium properties for subsea applications.

- Identify and describe possible joining methods for aluminium in a subsea environment.
- Identify the geometry and scale of an extensively used integrated template structure design.
- Redesign integrated template structure to suit aluminium's properties.
- Perform a cost comparison between steel and aluminium as construction materials for an integrated template structure.
- Identify research areas and areas with a need for further documentation.

## 1.3 Historical overview

Aluminium was introduced into the marine environment in the 1890's, and was mainly used in shipbuilding as an alternative to more conventional steel ships. Alfred Nobel's yacht "Mignon" was among the first ships to utilize an aluminium made hull structure [19]. Many of the earliest ships utilizing aluminium corroded heavily as the corrosion mechanisms for aluminium were not fully understood at the time [19]. Today, these technical difficulties have been solved or mitigated, and aluminium is now widely used in ship building [19].

### 1.3.1 Use of aluminium in the subsea environment

To date, most of the aluminium used in subsea equipment is only meant for short term exposure to the subsea environment, with a few exceptions. Aluminium made protection structures (hatches) were permanently installed on a satellite template structure on the Lille-Frigg field from 1991-2001. These hatches were protected by the use of sacrificial anodes and the aluminium structures were not in galvanic contact with the surrounding steel structures. According to Ole Terje Midling, a contact in Marine Aluminium, there was not observed any more degradation than expected after 10 years in service, meaning the design worked as expected [34]. Another example is the protection structures on the Gullfaks field installed in 2000 [35].

### 1.3.2 Selection of structure

An integrated template structure has been selected for all case studies in this thesis for several reasons. It is normally the heaviest structure to be installed, thus reducing the weight of the ITS provides the possibility to use smaller installation vessels with lower crane capacity. Another reason is the load scenario of an ITS, where the ITS is mainly statically loaded. Aluminium structures have lower fatigue properties compared to steel, which is the reason for choosing a statically loaded structure. More on aluminium's fatigue properties are presented in section 3.12. In addition, the operating temperature for aluminium alloys should generally not be higher than 80-100 $^oC$ [2], as described in section 3.2.1. Exceedance of the operating temperature may lead to unwanted material strength loss. The production fluids in the manifold and christmas tree (X-mas) may have a higher temperature than those mentioned above which is one of the reasons for not studying the use of aluminium on these structures in this thesis. The manifold and X-mas trees are important interfaces to the ITS, and will therefore be described in detail in chapter 2.

# Chapter 2

# Subsea Equipment

## 2.1 Integrated template structure

The ITS is a subsea structure with several important functions. The structure protects petroleum processing equipment from trawling (fishing gear) and dropped objects/impacts. It is also the base/foundation for the wells it is hosting. The ITS is kept in place using suction anchors to "suck" itself into the soil, or mud mats on hard subsea surfaces. The ITS model used in this study has 7.0 meter tall suction anchors with a diameter of ca. 5 meters. A figure of a suction anchor can be seen in figure 2.1. The length and diameter of the suction anchors depends on soil properties and the amount of weight to support.

This study will focus on a four-well slots ITS, as this is the most common size on the NCS. Larger template structures exist and are in operation, e.g. the eight-well slots ITS on the Ormen Lange field operated by Shell. A X-mas tree will be installed on each well slot prior to petroleum production, as well as a manifold located in the center of the structure, as seen in figure 2.2. The manifold is installed prior to the X-mas trees.

The selected ITS is installed on the Gjøa field, located approximately 65 km southwest from Florø. The ITS commenced start-up of production in 2010 [36]. The original weight of the structure is 270 metric ton (Te) [37]. It should be noted that the weight is dependent upon the dimensions of the suction anchors.


Figure 2.1: Several suction anchors lined up, each with a height of ca. 6.5 meters [16].

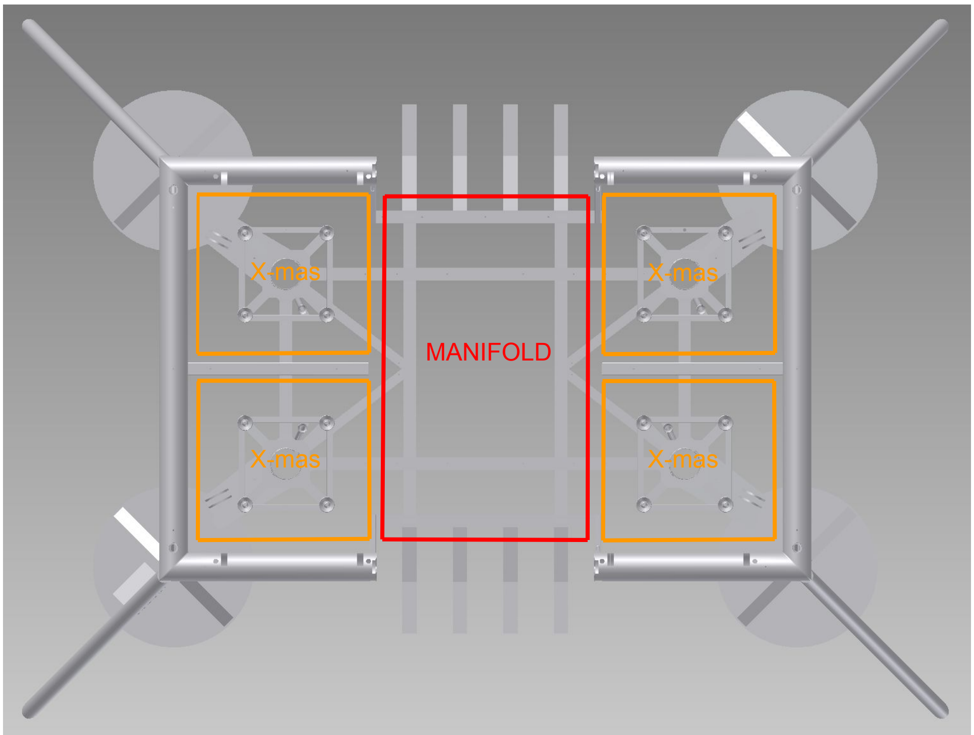


Figure 2.2: Figure of X-mas and manifold placement on the ITS seen from above, orange is space for X-mas while the red is space for manifold.

One of the purposes of this study is to reduce the weight of the ITS, and thereby reduce installation cost as lighter construction vessels with smaller crane capacity can be used to install the structure. There are several ways to install an ITS, where the most common ones are:

- Installation from subsea construction vessel, utilizing the vessels crane capacity to lift the structure overboard and install it.
- Perform a submerged tow from land to offshore, and then install it. This method has been developed more recently, and Subsea 7 had it patent pending in 2011 according to reference [38].
- Use a barge to transport the structure from shore and install it using an offshore crane vessel.

This thesis will focus on the first mentioned installation method, installation from subsea construction vessel, as this installation method is widely used by the industry [39].

The weight reduction will be achieved by implementing new construction materials for the ITS, where aluminium is believed to be the most promising material because of it's light weight compared to mechanical properties and corrosion resistance in seawater. Many of the same joining methods can be used for both steel and aluminium which makes the introduction of aluminium realistic in an industrial perspective. The fabrication cost of aluminium made structures are competitive with steel, exemplified by the extensive use of aluminium in topside structures [9].

A model of the selected ITS including markups has been received from Subsea 7, making it possible to rebuild a realistically sized ITS in a computer aided design program (CAD-program). In order to perform structural analysis on the structure, using finite element method (FEM) and conventional stress formulas. Most parts of the structure will have to be redesigned to utilize aluminium's properties in a positive way, especially with respect to difference in yield strength, joining and fabrication methods.

### 2.1.1 X-mas tree

The X-mas tree is the connection between the well and subsea production system, and it is connected to the wellhead. The X-mas tree acts as an essential integrity barrier, and it is therefore designed to be in a functional state under demanding operating conditions (all X-mas trees are pressure rated). The weight of a subsea X-mas tree ranges from 30-70Te [17]. The interface between the ITS and the X-mas tree can be seen in figure 2.3.

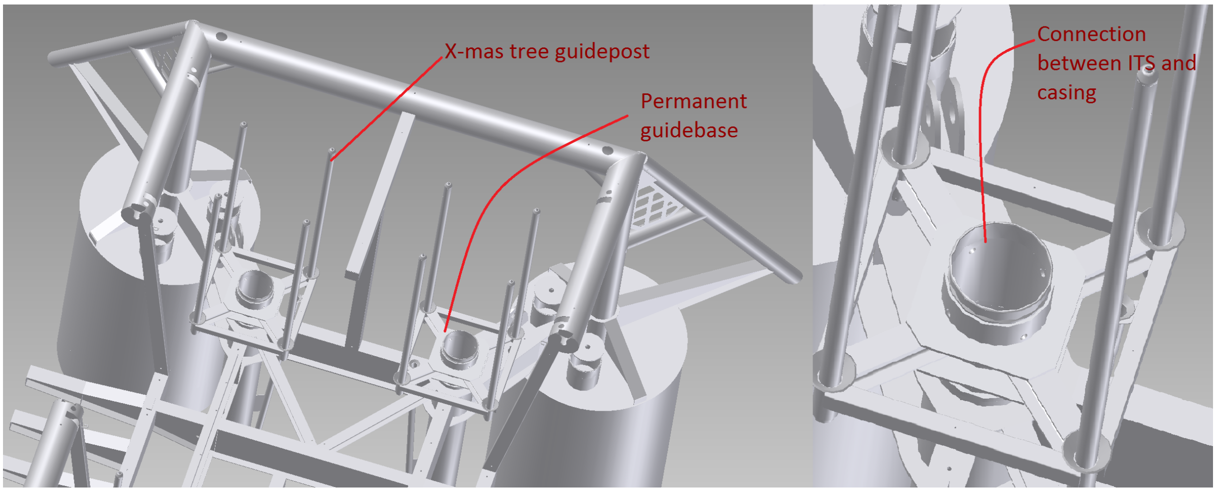


Figure 2.3: Position of X-mas tree on permanent guide-base on the ITS, only two out of four wells are shown on the left figure.

### 2.1.2 Manifold

The purpose of the manifold is to co-mingle the production fluids from several wells and transport it to a hosting facility in one pipeline (in some cases several pipelines). This method of commingling the production minimizes the use of expensive pipelines and risers. A manifold uses several independently operated valves to control the production from each well. The weight of a manifold normally ranges from 50 to 400Te [17]. The manifold installed on the selected ITS weights approximately 80Te [40]. There is no need for a weight reduction of the manifold at this stage as the weight of the concerned manifold is substantially lower than the weight of the concerned ITS. Figure 2.4 shows the type and size of a manifold installed on the ITS.

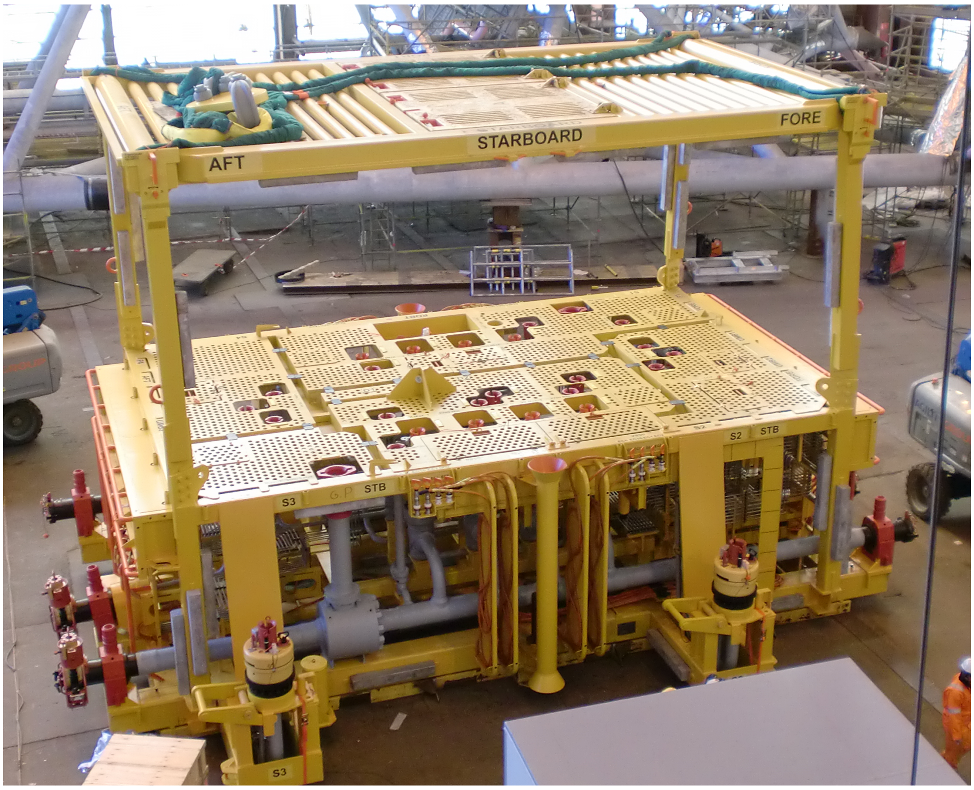


Figure 2.4: Picture of a manifold manufactured by Agility Group [17].

# Chapter 3

# Aluminium

Aluminium alloys offers many positive properties that have been proven to be successful in the aerospace [41], automobile [42] and naval [43] industry. An article [43] published in 2008 on the use of aluminium in naval applications estimated the life cycle cost of aluminium to be more cost efficient than steel. These findings resulted in a recommendation to the U.S Navy to increase the use of aluminium in ship structures [43].

This chapter describes properties of aluminium that are considered to be of importance in order to utilize aluminium in subsea structures.

## 3.1 Aluminium designation

Aluminium alloys are normally either wrought or casted, where they are further designated in series ranging from 1xxx-9xxx for wrought and 1xx.x-9xx.x for casted alloys. Table 3.1 presents the principal alloy in each series, and which series that is susceptible to heat treatment [1]. Extruded and rolled products are examples of wrought products, which generally possess higher strength than casted products [1].

The wrought aluminium alloys 5083 and 6082 are the only ones approved for immersed seawater applications in NORSOK M-121 [44], where the latter is more suited for extrusion while the first is often made in plated product forms due to strengthening by cold work. The strongest acceptable tempers for the mentioned alloys are H116 and T6 respectively [44].

Table 3.1: Wrought and cast series [1].

| Wrought alloys[1)] | | Casted alloys[1)] | |
|---|---|---|---|
| Series | Principal alloy | Series | Alloy family |
| 1xxx (Al) | Unalloyed. NHT | 1xx.0 | Unalloyed. NHT |
| 2xxx (AlCu) | Copper. HT | 2xx.0 | Copper. HT |
| 3xxx (AlMn) | Manganese. NHT | 3xx.0 | Silicon and/or copper. HT |
| 4xxx (AlSi) | Silicon. Primarily NHT | 4xx.0 | Silicon. HT |
| 5xxx (AlMg) | Magnesium. NHT | 5xx.0 | Magnesium. NHT |
| 6xxx (AlMgSi) | Magnesium and Silicon. HT | 6xx.0 | Not used |
| 7xxx (AlMgZn) | Zinc. HT | 7xx.0 | Zinc. HT |
| 8xxx (Other) | (e.g. Iron or Tin) | 8xx.0 | Tin. HT |
| 9xxx | Unassigned | 9xx.0 | Other |

1) HT= Heat treatable. NHT= Non heat treatable.

The alloy designation is always followed by a capital letter indicating the hardening method applied as illustrated in table 3.2. The strongest approved temper designations for immersed seawater applications are also presented.

Table 3.2: Temper designations [2].

| Temper designation | | Detailed temper designation | |
|---|---|---|---|
| F | As fabricated | | |
| O | Annealed | | |
| H | Strain hardened | H116[1)] | Treated against exfoliation and intergranular corrosion and optimum resistance against stress corrosion [44]. |
| W | Solution heat treated | | |
| T | Thermally treated | T6 | Solution heat treated followed by artificially aging. |

1) Equivalent mechanical properties as H32 stated in EN-1999-1-1 [2, 44].

## 3.2 Material properties

General properties of aluminium alloy 5083-H116 and 6083-T6 are presented in table 3.3, and the chemical composition is tabulated in table 3.4. Note that the modulus of elasticity for aluminium is ca. 33% of steel's modulus of elasticity, which may lead to higher displacement under loading. The density of aluminium is 35% compared to steel, and aluminium has a higher absorption of energy per unit weight during impact loading compared to steel [45]. Yield strength (YS) for aluminium is defined at 0.2% elongation offset the modulus of elasticity line.

Table 3.3: Properties of aluminium alloys 5083-H116 and 6083-T6 [2].

| | Density [kg/m$^3$] | Young's modulus [GPa] | YS [MPa] | TS$^{1)}$ [MPa] | Brinell Hardness [HB] | TEC$^{2)}$ [$1/^oC$] | Thermal conductivity [W/(m·$K$)] | Durability$^{3)}$ rating |
|---|---|---|---|---|---|---|---|---|
| 5083-H116 | 2660 | 70 | 215 | 305 | 85 | $23{,}8 \cdot 10^{-6}$ | 117 | A |
| 6082-T6 | 2700 | 70 | 255 | 300 | 91 | $23{,}4 \cdot 10^{-6}$ | 170 | B |

1) Tensile Strength.
2) Thermal Expansion Coefficient.
3) A= The need for protection for freely exposed members in seawater depends on inspection availability and planned maintenance [2].
B= Protection of freely exposed members generally required for seawater immersion [2].

Table 3.4: Chemical composition of aluminium alloy 5083-H116 and 6082-T6 [wt%] [3].

| Alloy | Si | Fe | Cu | Mn | Mg | Cr | Zn | Ti |
|---|---|---|---|---|---|---|---|---|
| 5083-H116 | 0.4 | 0.4 | 0.1 | 0.4-1.0 | 4.0-4.9 | 0.05-0.25 | 0.25 | 0.15 |
| 6082-T6 | 0.7-1.3 | 0.5 | 0.1 | 0.4-1.0 | 0.6-1.2 | 0.25 | 0.2 | 0.1 |

### 3.2.1 Operating temperature

Operating temperature for aluminium alloys should in general not be higher than 80 - 100 $^oC$ [2]. However, the 5083 alloy is more sensitive to high temperatures, hence the operating temperature for this alloy shall not be higher than 65 $^oC$ [44]. Exceedance of operating temperature may lead to unwanted strength losses.

### 3.2.2 Cryogenic toughness

Aluminium alloys have the ability to maintain ductility and improve toughness while the strength is increasing when subjected to very low temperatures due to the face centered cubic crystal structure (FCC) [46]. The 5xxx and 6xxx series are particularly noteworthy for their abilities in extremely low temperatures where their properties improves when exposed to temperatures close to absolute zero compared to room temperature [1]. For arctic temperatures which subsea structures may be subjected to during transport the ductility is maintained or increased [1]. The comparative steel material may develop brittle properties in these environments.

### 3.2.3 Hydrogen embrittlement

Hydrogen may be produced from cathodic protection (CP) at the cathode (see section 3.5.8), which can diffuse into susceptible materials and cause embrittlement. Three factors need to be present in order to be in danger of hydrogen embrittlement (HE): susceptible material, hydrogen and stress. A typical example of a susceptible material is duplex stainless steels [47]. Aluminium alloys are however considered immune to HE according to DNV-RP-B401 [47]. A study [48] on the effect of CP and susceptibility to HE in aluminium alloys concluded that the alloys 5083-H321 and 6082-T6 are not particularly prone to HE. Composition and thermal treatment did not effect the results. However, an alloy within the 7xxx series showed a decrease in strength due to HE [48].

## 3.3 Extrusion

The ability to extrude aluminium alloys enables advantages in structures; complex shapes and profiles readily forms through a die in order to obtain the optimal and desired design. The cross-section can be designed in such a way that a low weight is obtained while at the same time possess an excellent structural strength efficiency. For instance, where installation of stiffeners allows for an enhanced steel design, the extrusion process have the potential to achieve improved properties simply by adjusting the cross-sectional die shape of the extruded components. Extruded profiles can in theory be manufactured in any two dimensional profile where the only limitation is the press capabilities. Table 3.5 illustrates the extrusion limits for the three largest identified extrusion companies in Europe, and one from Russia (KUMZ). An illustration of the circumference limits at STEP-G and SAPA can be seen in figure 3.1 and appendix F.1, respectively.

Table 3.5: Extrusion limits at STEP-G [4], SAPA [5], Constellium [6] and KUMZ [7].

| | STEP-G | SAPA | Constellium | KUMZ |
|---|---|---|---|---|
| Max. Press force | 90 MN | 65 MN | 100 MN | - |
| Weight pr. meter | 190 kg/m | 65 kg/m | 80[3)] kg/m | - |
| Total weight | 535 kg | - | - | - |
| Max. Length | 30 m | 26 m | 30 m | 6 m |
| Max. diameter | 500[1)] mm | 320 mm | 520[2)] mm | 553 mm |
| Max. width | 750 mm | 620 mm | 750 mm | 480 mm |

1) Max. thickness is 30 mm for tubes.
2) Alloy 6082, Max. Ø 500x20 mm with length 6 m.
3) For alloy 6082.

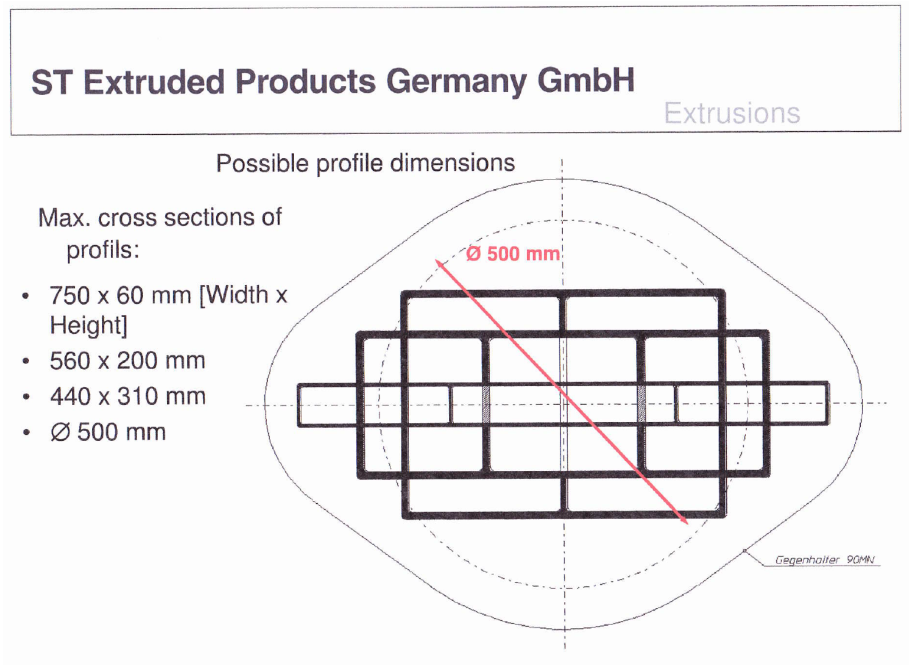


Figure 3.1: Circumference limits for the extrusion press at STEP-G [4].

A disadvantage by extrusion is the fact that each profile requires a unique die, if the die is not readily obtainable through standards the die must be custom made causing increased costs. Therefore, the designer should limit both the amount and complexity of the profiles needed and establish contact with competent fabricators.

## 3.4 Recycling

Aluminium can be recycled very efficient, requiring only a fraction (ca. 5 percent) of the energy consumed producing primary aluminium for the remelting process. About 75 percent of all extracted aluminium remains in use, whereas some are recycled through multiple cycles. However, Only 20-25 percent of the total aluminum demand is covered from recycled products due to the extended lifetime of many aluminium products. Basically all products made of aluminium are possible sources of recycled aluminium [49]. Recycling has a potential in being environmentally friendly by lowering emissions and saving energy.

There is a special concern with aluminium recycling. As aluminium is recycled over and over again impurities will build up. The accumulation of impurities/contamination may result in a chemical composition, which will influence the aluminium's properties. This is a growing problem due to the increased amount of recycled aluminium but it can be handled in the remelting process by using several technologies. Further description on applicable technologies can be seen in reference [50].

## 3.5 Corrosion

The corrosion properties of aluminium alloys in seawater have to be assessed in detail to ensure there are no problems by utilizing aluminium alloys subsea. A protection strategy for aluminium in the concerned environments will be described based on existing literature. Several types of corrosion are relevant to the two types of environments, aluminium in seawater and aluminium buried in soil. Relevant corrosion types are crevice corrosion, intercrystalline corrosion, pitting corrosion, galvanic corrosion and uniform corrosion [19].

### 3.5.1 Crevice corrosion

Crevice corrosion is localized corrosion happening in crevices, i.e. around overlapping zones such as bolting, riveting and welding. These crevices are difficult to enter for seawater, and when an electrochemical reaction occurs in the crevice the local environment will change as a result of the difficult access. The potential becomes more electronegative, and aluminium in the crevice will be oxidized as described by reaction 3.1 [19].

$$Al \rightarrow Al^{3+} + 3e^- \tag{3.1}$$

While the outside of the crevice will have an oxygen reduction by the reaction occurring in the crevice. The aluminium chloride will hydrolyze by the chemical reaction 3.2.

$$AlCl_3 + 3H_2O \rightarrow Al(OH)_3 + 3H^+ + 3Cl^- \tag{3.2}$$

The aluminium hydrolyze is caused by the local geometry limiting diffusion rates causing depletion of oxygen, and an excess of $Al^{3+}$ ions which leads to an inflow of $Cl^-$ ions. Figure 3.2 illustrates the reactions and where they take place in relation to a crevice [19].

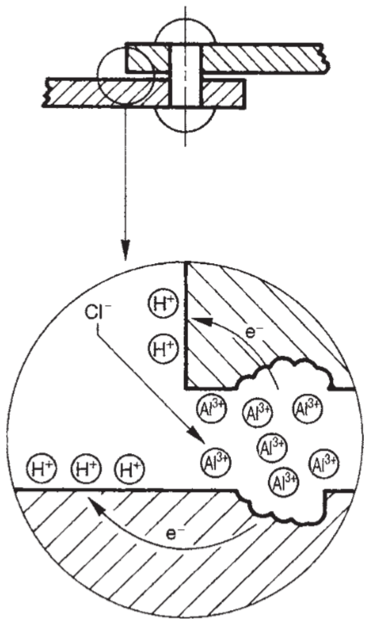


Figure 3.2: Crevice corrosion in an overlapping joint [18].

Aluminium's susceptibility towards crevice corrosion is rather low compared to some other alloys , e.g. stainless steel. Aluminium crevices are often sealed by the corrosion products of aluminium, which is one of the reasons for the low susceptibility compared to stainless steel. However, crevice corrosion can and should be avoided by design. Either by using gaskets or sealing compounds to avoid liquid from penetrating into crevices. Or by designing in such a way that crevices are avoided, a figure of poor and good design can be seen in figure 3.3.

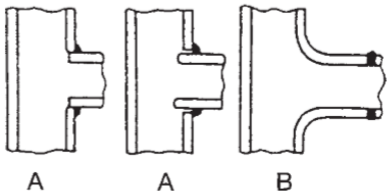


Figure 3.3: Poor design in A and good design in B with respect to crevices [19].

### 3.5.2 Pitting corrosion

Localized corrosion of aluminium in the passive pH range is usually subjected to a formation of pits. See figure 3.15 for illustration of the pitting potential, ($E_P$) and ($E_{CC}$), at various pH values for alloy 5086. Aluminium alloys polarized to a potential greater than the $E_P$ potential and lower than $E_{CC}$ in the passive region are in danger of encountering pitting corrosion. When polarized and kept in the passive area the protective oxide layer can readily maintain its integrity (anodic polarization) and thereby avoid initiation of pits [51]. At lower or higher potentials than the passivity area the oxide layer is no longer able to maintain an adequate integrity, and the oxide layer breaks at weak spots where it cannot repair itself. Pitting is often produced by chloride ions ($Cl^-$), in for instance seawater [51].

The localized corrosion of aluminium alloys is primarily determined by the properties of the intermetallic particles [20], as seen in figure 3.4. It is secondarily determined by the alloy composition, as long as copper is absent. Pitting initiates around the intermetallic particles, which is the "weak spot" for commercial alloys. Figure 3.4 illustrates this scenario, and also illustrates how the local environment changes, and the pH value increases locally [20]. For further reading about this phenomenon, see reference [20].

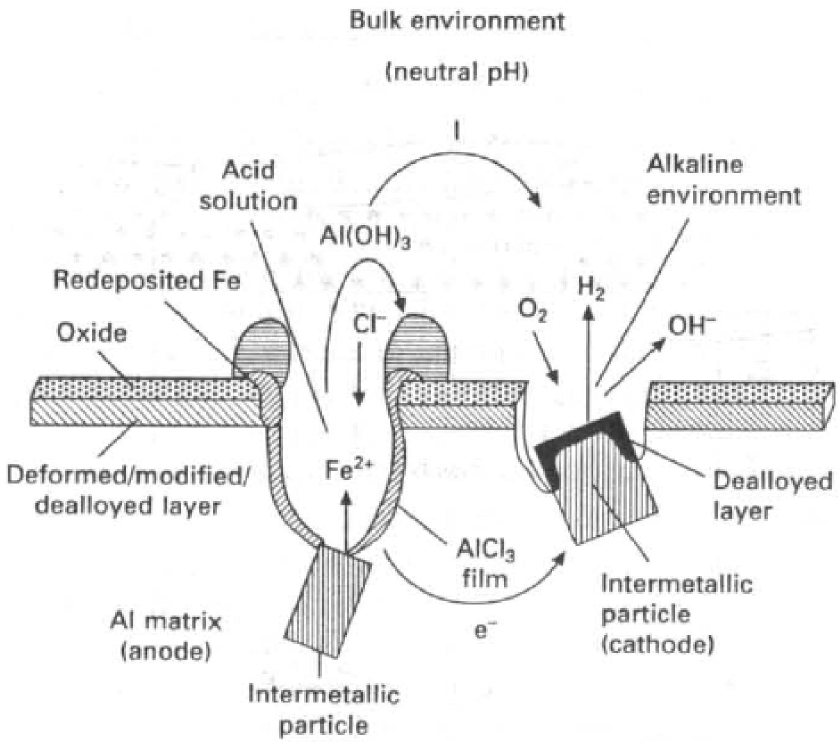


Figure 3.4: Illustration of localized corrosion around intermetallic particles in the acidic pit and adjacent alkaline cathodic site [20].

### 3.5.3 Intercrystalline corrosion

Intercrystalline corrosion may propagate within the grains or through grain boundaries, referred to as transgranular or intergranular corrosion respectively [19]. This type of corrosion initiates at pits described in section 3.5.2. It propagates due to an electrochemical potential between the grain boundaries (intermetallic phases) and the grains (bulk), see figure 3.5. The intermetallic compound can have a more negative and a more positive potential, therefore the grain boundaries can act as an anode or as a cathode with respect to the solid solution (bulk of the grains). Aluminium alloys are in danger of encountering intercrystalline corrosion if a corrosive environment, a potential difference of more than 100 mV, and a continuous precipitation of intermetallics are present. The intensity of intecrystalline corrosion depends on the amount of grain layers attacked. If there is no more than three to four influenced layers, it is considered as superficial. Superficial intercrystalline corrosion occurs in alloys of the 6xxx series without copper content. 5xxx and 6xxx series with magnesium content more than 3.5%, may be susceptible to intercrystalline corrosion [19]. However, alloy 5083 with temper H116 should not be susceptible to this type of corrosion [19, 44].

#### Exfoliation corrosion

Intercrystalline corrosion may also occur in the form of exfoliation corrosion, which propagates near the surface parallel to the direction of extrusion or rolling [44]. This type of corrosion may occur in the 5xxx series that possesses long-grained structures. The temper H116 for alloy 5083 are specially developed to mitigate the susceptibility towards exfoliation corrosion [44]. Exfoliation does not have to be in the form of intercrystalline corrosion [19].

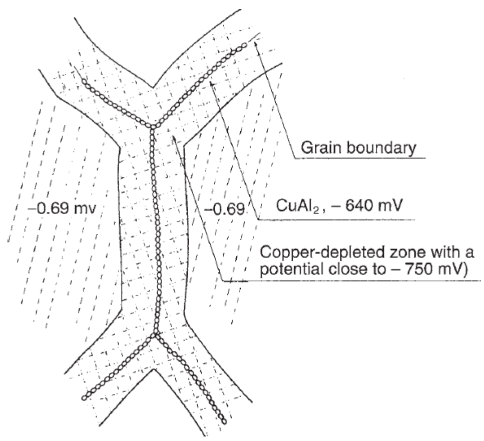


Figure 3.5: Cathodic phase at the grain boundaries, [mV] vs Saturated calomel electrode (SCE) [19].

#### Stress corrosion cracking

If a susceptible aluminium alloy is subjected to tensile stress (static or dynamic) and a corrosive environment it may encounter stress corrosion cracking. These cracks always propagates through grain boundaries. 5xxx series with sufficient amount of magnesium may be susceptible to this type of corrosion [19]. Alloy 5083-H116 is however developed to possess an optimum resistance against stress corrosion cracking [44]. The 6xxx series are not susceptible [19]. Stress corrosion cracking lowers the crack's fracture toughness [52].

### 3.5.4 Corrosion in soil

The suction anchors will be buried in soil, which represents a different environment from natural seawater. It is therefore necessary to study the corrosion conditions for aluminium in soil more in detail. A soil's aggressiveness is related to its resistivity, where the corrosion rate is high for low resistivities, as seen in figure 3.6 [19].

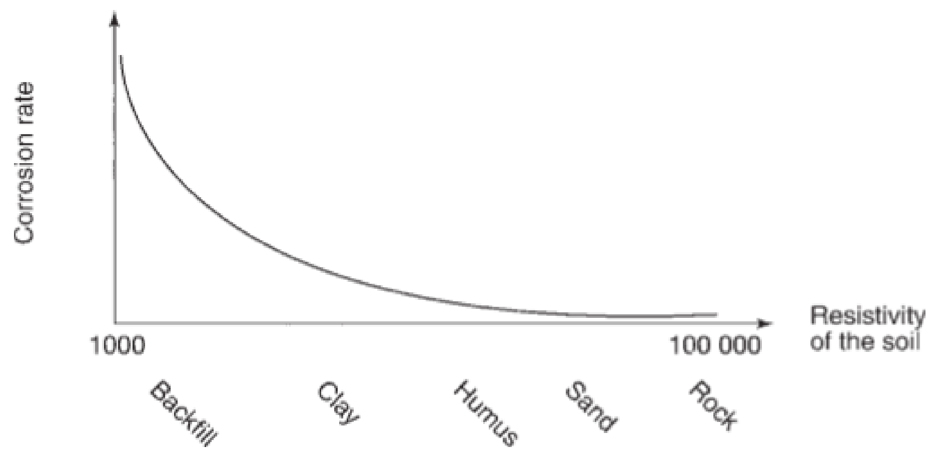


Figure 3.6: Resistivity versus aggressiveness for soils [19].

Experiments on cathodically polarized thermally sprayed aluminium (TSA) in soil has been carried out [21], the set-up can be seen in figure 1, page 562 in the reference [21]. The experiment was aimed at higher temperatures, ranging from ambient temperature up to 95 $^{o}$C. As seen in the figure 3.7, the cathodic current density decreased from $-50$ mA/m$^2$ to ca. $-10$ mA/m$^2$. The cathodic current is negative because the TSA is acting as an anode, not a cathode [21].

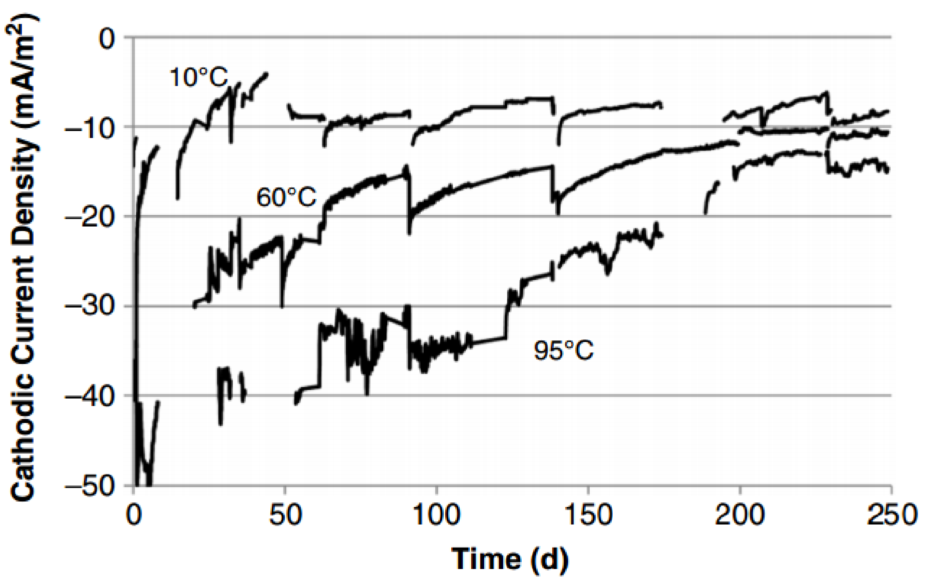


Figure 3.7: Cathodic current density in soil at -1100 mV vs Ag/AgCl for different temperatures [21].

The corrosion rate of the cathodically polarized TSA buried in soil decreases with time due to passivation of the TSA surface, as seen in figure 3.8. After 250 days the corrosion rate is below 10 $\mu$m/year. The pH value at the TSA/soil interface is kept between 8.2 (pH of soil before the tests started) and 6.5 (pH at 95 degrees Celsius) [21]. TSA is typically applied in a 200 to 400 micrometer thick layer, resulting in a lifetime of ca. 20 years for a 200 micrometer thick layer of TSA.

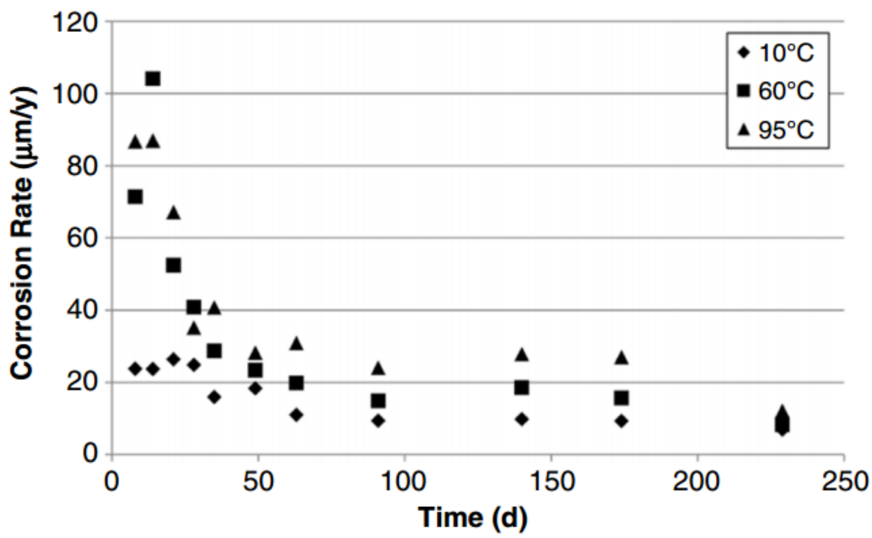


Figure 3.8: Corrosion rate in soil polarized to -1100 mV vs Ag/AgCl for several temperatures [21].

The corrosion properties of TSA and alloy 5083 or alloy 6082 are not the same. Alloy 5083 and alloy 6082 shows better corrosion resistance against uniform corrosion according to email correspondence with Ole Øystein Knudsen, seen in appendix B.3. Corrosion of aluminium in soil is considered to be a relatively undiscovered area with ongoing research. The literature within this topic is therefore very limited, and there is a need for more research in order to state a valid conclusion regarding the use of aluminium components buried permanently in soil.

### 3.5.5 Seawater flow rates influence on corrosion rates

As a result of the integrated template structure's geometry it is expected to be areas with limited seawater flow rate, so called stagnant conditions. This condition is especially expected inside circular tubes with small holes to the outside as seen in figure 3.9.

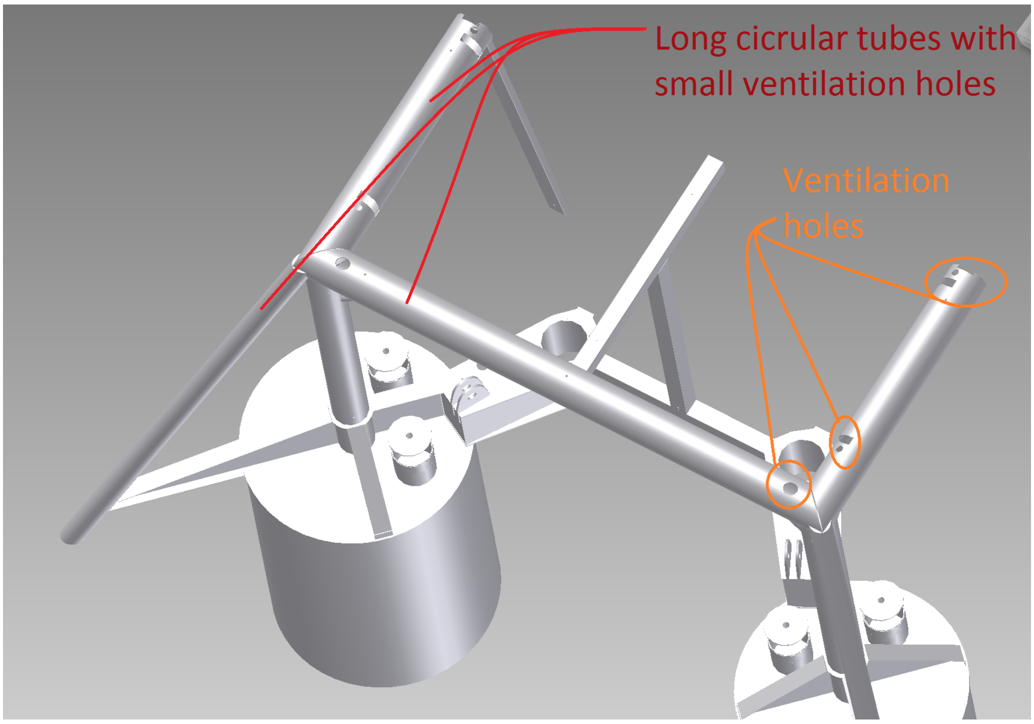


Figure 3.9: Example of long circular tubes on the structure with small ventilation holes to the outside seawater.

Kemal Nisancigolu and Torgeir Wenn conducted an experiment [23] on corrosion protection of aluminium in flowing seawater, where aluminium alloys were exposed to seawater at various seawater flow rates (0 - 100 cm/s). The result did not show any critical pitting depth after two months of exposure under open-circuit conditions for low velocities, as seen in figure 3.11. 2.5 cm/s flow rate seems to be more critical with respect to pitting corrosion depth than 0 cm/s (stagnant conditions) for AlMgSi1 (alloy 6082) [23].

Stagnant seawater conditions are not a corrosive problem according to the reviewed literature, and there has not been found any evidence to support the case of stagnant conditions being a corrosive problem, which is different from the same condition for steel (unless it is a closed compartment).

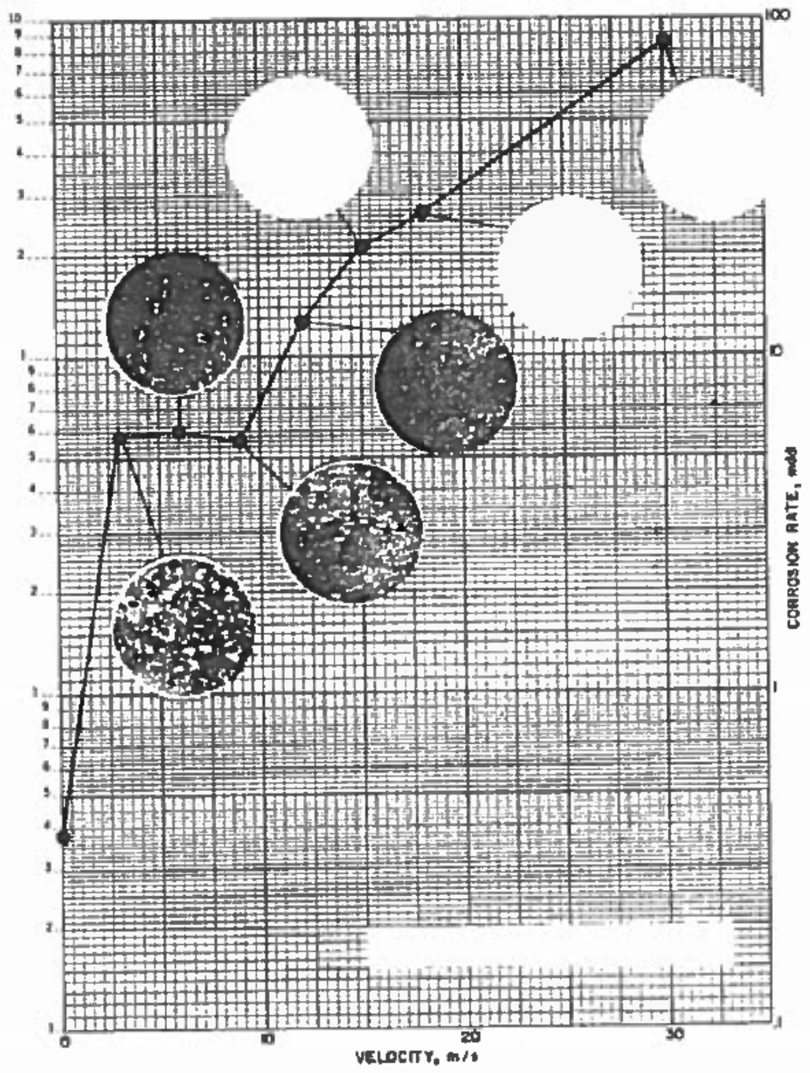


Figure 3.10: Velocities influence on corrosion rate for alloy 5456 connected to CP, 1 mdd = 13.5 $\mu m$[22].

For steel structures the internal tubing is treated as closed compartments by using "split rubber grommets" to close the compartment [53]. All internal tubing has to be filled with seawater in order to avoid a high differential pressure which can lead to structural collapse at high pressure differences [53]. NORSOK M-001 [54], section 4.3.7 can be used for corrosion protection of closed compartments, where no internal corrosion protection is needed for completely closed seawater filled compartments in carbon steel. This is assuming there is no seawater exchange between internal and outer part of the structure, achieved by using split rubber grommets as seen in figure 3.12.

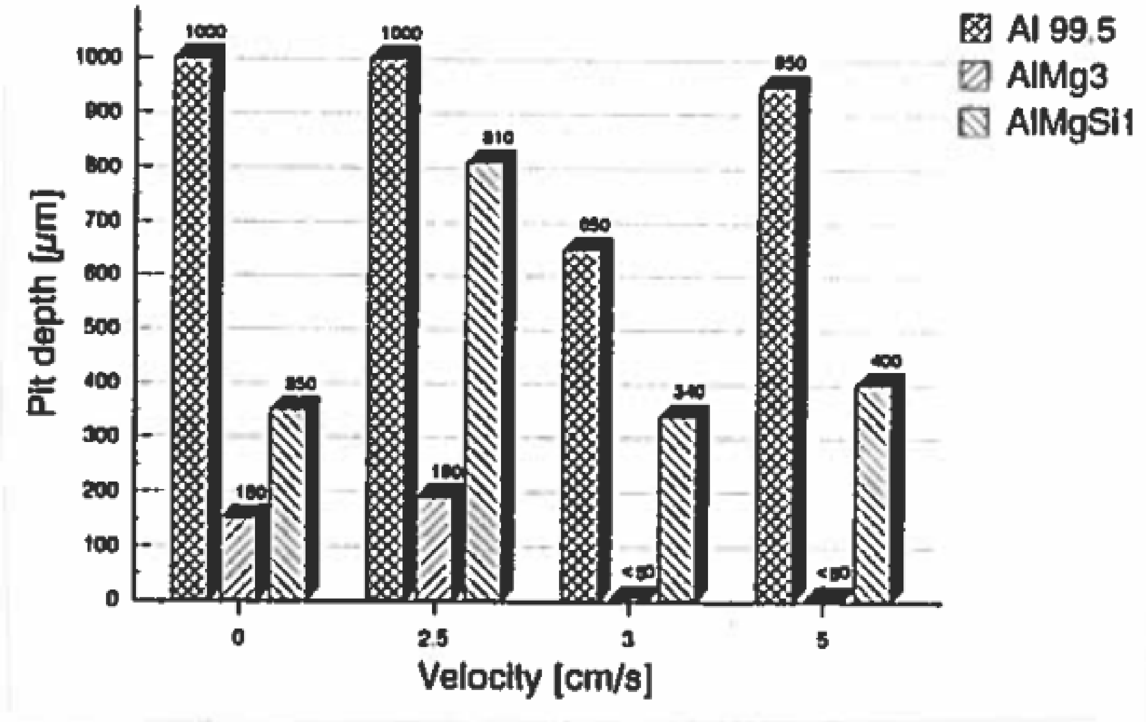


Figure 3.11: Maximum pit depth for Al 99,5, AlMg3 and AlMgSi1 (alloy 6082) after two months of exposure under open-circuit potential [23].

Figure 3.12: A split rubber grommet to restrict seawater flow in/out of compartments [24].

A SINTEF report from 1986 [22], concerning corrosion of aluminium in special environments relevant to applications in the petroleum industry studied flowing seawater velocities influence on corrosion rate. Figure 3.10 shows the corrosion rate as a function of flowing seawater velocity, low seawater velocity results in low corrosion rate. The corrosion rate at the plateau, from 3 to 9 m/s is about 0.08 mm/year [22], the corrosion rate is almost independent of the seawater velocity in this range [22]. The nearly constant corrosion rate in this region is related to oxygen transport and the corrosion reactions at the anodic sites [22]. Above 9 m/s, the corrosion rate increases rapidly due to erosion-corrosion [22]. Flow induced corrosion cannot be mitigated by CP, it may actually increase the corrosion rate [20]. The transition velocity between pitting at low velocities (stagnant conditions) and uniform corrosion due to flowing seawater were estimated to occur around 10 cm/s for alloy 6082 [20]. A transition velocity for alloy 5754, also tested in the experiment, was not identified [20].

### 3.5.6 Galvanic corrosion

Structural members surrounded by an electrolyte (seawater) are in danger of encountering galvanic corrosion if there is a metallic contact between dissimilar metals possessing different corrosion potentials. Coupling between steel and aluminium is an example of a galvanic coupling, where the aluminium is acting as anode and steel as a cathode, resulting in corrosion of aluminium and CP of steel. The galvanic series are illustrated in figure 3.6, where the more noble materials possesses more positive potentials. Cathodic protection that utilizes sacrificial anodes with lower corrosion potentials are therefore an effective method to mitigate galvanic corrosion, which is confirmed by a recent study seen in reference [55]. See section 3.5.8 and 3.5.1 for more information about CP and crevice corrosion of aluminium alloys in seawater.

A galvanic coupling may also occur between aluminium alloys and filler material used in welding or brazing for instance, as these possess varying corrosion potentials due to their respective chemical composition [56]. Hence, it is important to ensure proper CP of these interconnections. Corrosion potentials for 5xxx and 6xxx alloys are tabulated in table 3.6. Figure 3.14 illustrates an example of a galvanic interconnection between alloy 5083, 6082 and filler material. Considering such a welded coupling without CP, one may assume that the alloys in the 5xxx series would suffer more from corrosion due to possession of a more negative corrosion potential.

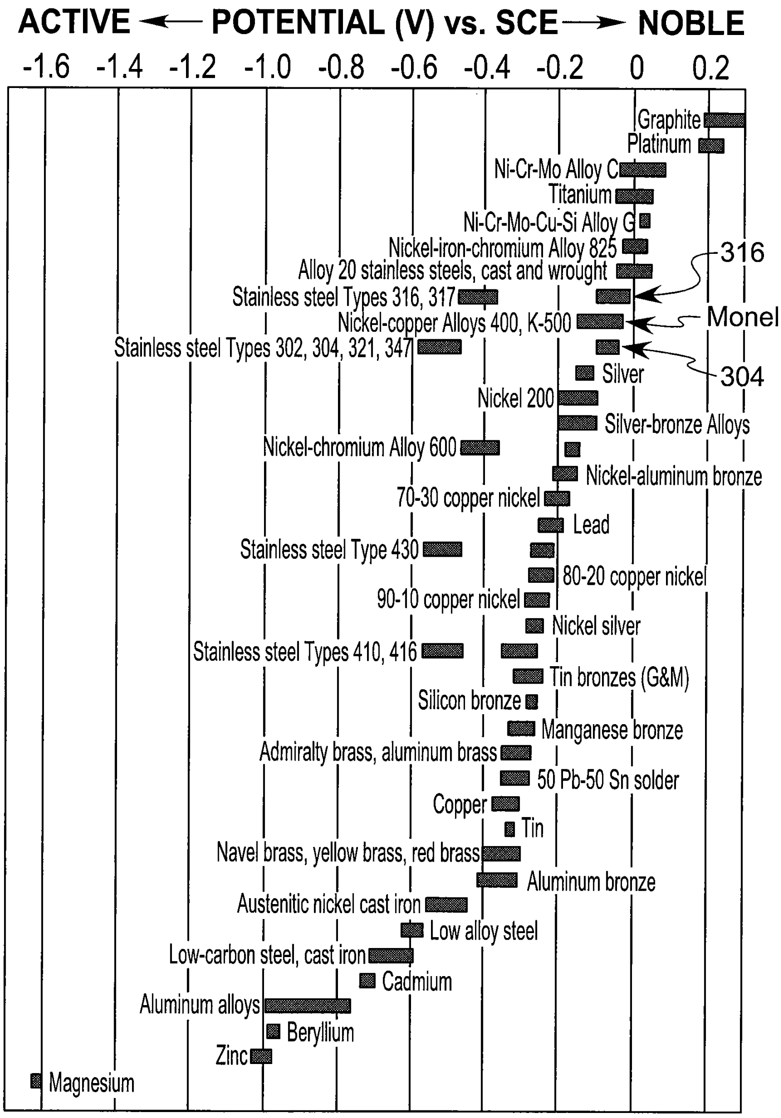


Figure 3.13: Galvanic series in seawater [25].

For bolted joints one may introduce extra material that are different from the main structure, such as carbon or stainless steel bolt, nut and washer that can contribute to galvanic corrosion. Bolted joints are in addition externally sealed to avoid mitigation of crevice corrosion. All components in a bolted connection must be cathodically protected and ensured to posses the correct protection potential. Wiring can be used to ensure an electrical contact of isolated parts. Corrosion issues with the use of bolts are further discussed in section 3.8.

Table 3.6: Corrosion potentials for 5xxx and 6xxx alloys [8].

| Material | Corrosion potential [Volt vs SCE] |
|---|---|
| 5xxx alloys | -0.78 to -0.76 |
| 6xxx alloys | -0.73 to -0.70 |

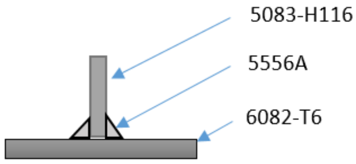


Figure 3.14: Galvanic interconnection between aluminium alloy 5083-H116, 6082-T6 and filler metal 5556A.

### 3.5.7 Coating

The selected corrosion strategy does not make coating of the aluminium surface necessary, as the structure will be protected by a passive oxide layer and cathodic protection. This is in line with the NORSOK M-501 [57] standard stating:

*"The following shall not be coated unless otherwise specified:*

- *Aluminium, titanium, uninsulated stainless steel, insulated stainless steel heating ventilation/air conditioning ducts, chrome plated, nickel plated, copper, brass, lead, plastic or similar;*
- *Jacketing materials on insulated surfaces."*

### 3.5.8 Corrosion and protection of aluminium in seawater

The passivation of aluminium in seawater is dependent upon the aluminium alloy composition and pH. The presence of manganese and magnesium as alloying components will increase the aluminium alloys resistance to high pH, as a result of this alloy 5086 in figure 3.15 can achieve passivation at pH values similar to seawater (seawater pH dependency of depth can be seen in appendix F.2) [20]. According to a recent study [58] it was found that the Pourbaix diagram in figure 3.15 is a good estimate for alloy 5083 and 6082 at pH 8.2 (seawater condition). At pH 3 it was found to be a rough estimate, and at pH 10 it was not valid [58].

Cathodic protection of aluminium differs from CP of other metals e.g. steel in two ways. The aluminium oxide layer is not stable in alkaline or acid environments where the aluminium will start corroding actively [26]. The local environment is influenced by the seawater flow speed, further discussed in section 3.5.5. The second difference is the low current demand compared to the current demand for steel. The difference in current demand is because the current is confined by the cathodic intermetallic areas for aluminium. These areas are small compared to the exposed area of aluminium in contrast to steel where the whole exposed area demands current [26]. How aluminium compares to steel can be seen in figure 3.16, showing cathodic polarization curves, where plates sized 10 · 19 cm are inserted into a flow channel at a flow rate of 8 cm/s. The data were measured before the onset of calcareous deposition [26].

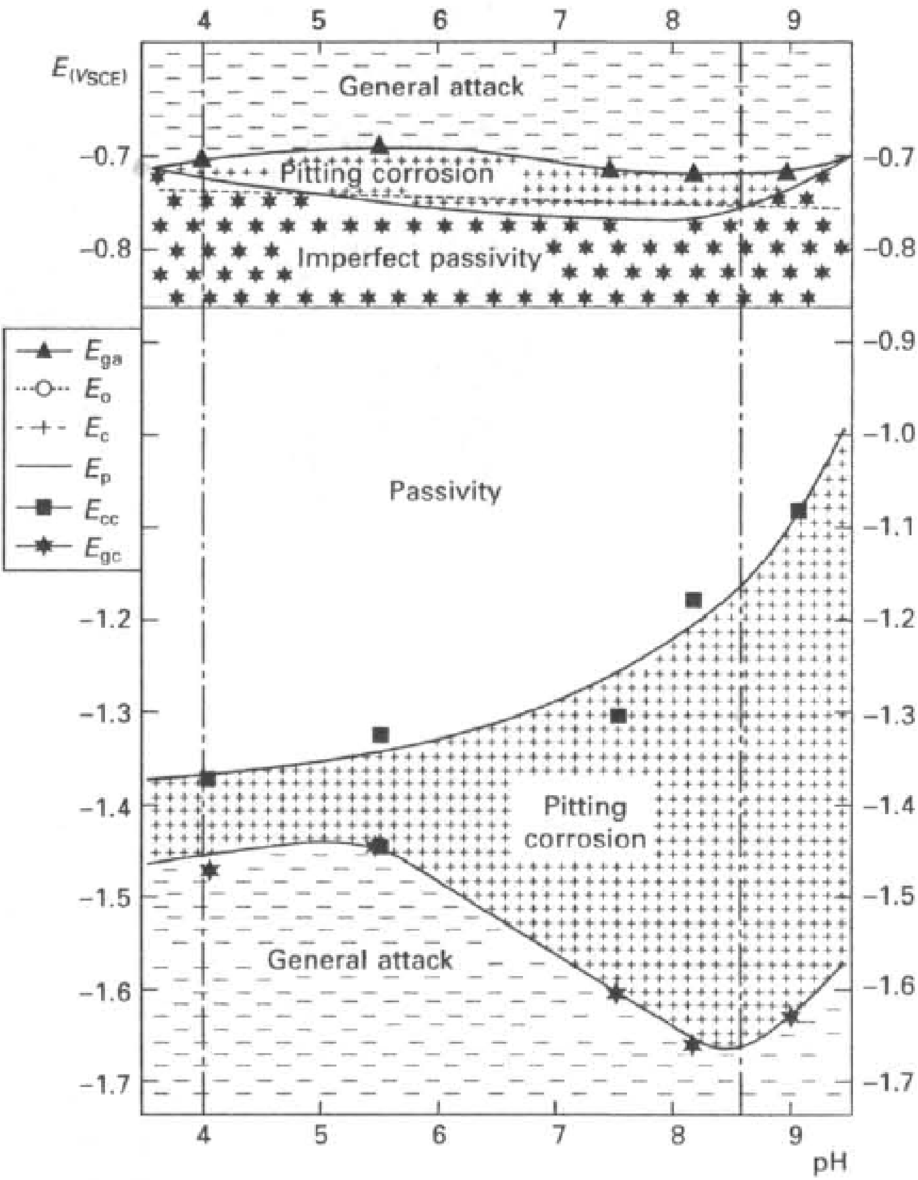


Figure 3.15: Pourbaix diagram for alloy 5086 [20].

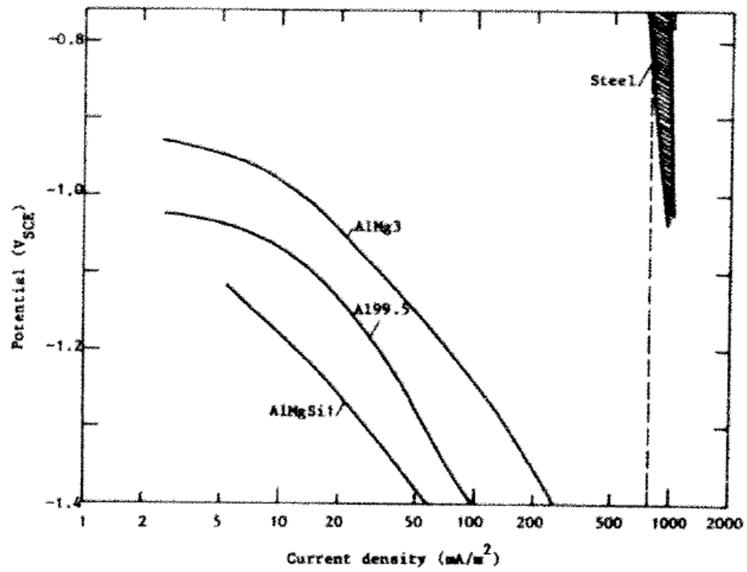


Figure 3.16: Cathodic polarization curve for steel and aluminium at 8 cm/s flow rate [26]. AlMgSi1 is equivalent to 6082 and AlMg3 is equivalent to 5754.

**Cathodic protection strategy**

Cathodic protection is selected to act as the main barrier against pitting corrosion, uniform corrosion on coated steel components and to mitigate the consequences of a galvanic coupling. Cathodic protection is achieved by placing the material to be protected in the situation of an cathode. This is performed by electrically linking it to a metal with lower corrosion potential where the two materials are placed in the same electrolyte.

Protection of aluminium is achieved by keeping the aluminium surface in a passive zone according to a Pourbaix diagram, seen for alloy 5086 in figure 3.15. And not by bringing the potential into an immunity range, which is the case for steel [19]. The cathodic protection potential should therefore be kept more negative than the critical pitting potential to achieve satisfying protection. Figure 3.17 shows schematically how the pits surrounding the intermetallic particles will develop when it is connected to a CP system [20].

The current demand for CP of aluminium will typically decline by one order of magnitude with time compared to freshly exposed areas. It is because of the passive layer (oxide layer) combined with the detachment of intermetallic particles, which are removed as shown in 3.17. Figure 3.18 shows how the current demand decreases with time [20].

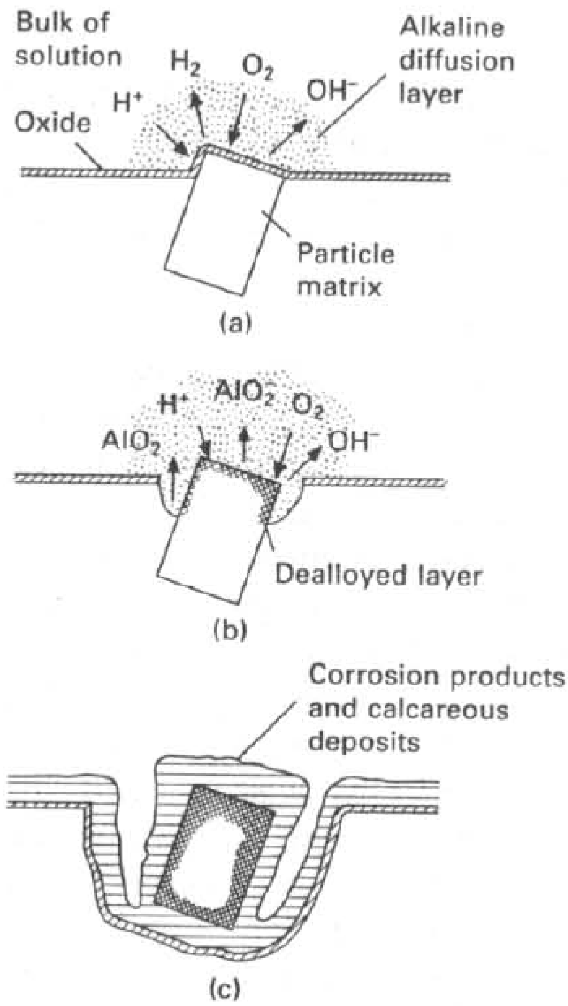


Figure 3.17: Mechanism of CP on aluminium in seawater [20].

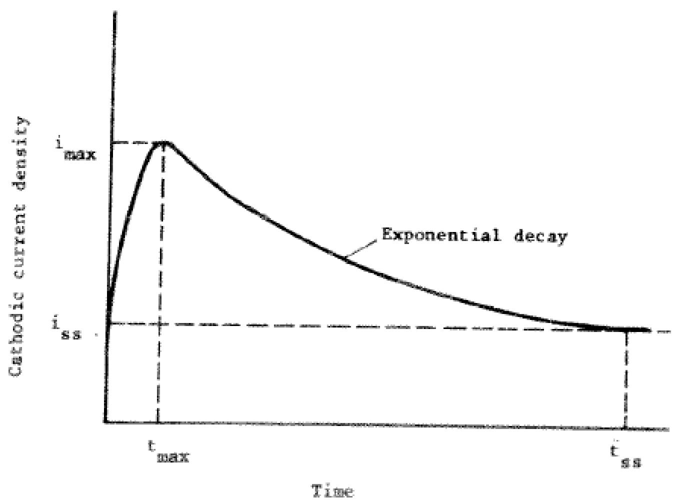


Figure 3.18: Typical current density vs time for a cathodically protected aluminium alloy in seawater [20].

Cathodic protection is less or ineffective if the seawater current reach a certain level, ca. 10 cm/s, as described in section 3.5.5. Uniform corrosion becomes critical when the seawater flow is above ca. 9 m/s because the oxide layer is mechanically removed continuously, as seen from figure 3.10.

## 3.6 Welding

Aluminium may be welded by several different methods. The relevant welding techniques for aluminium applications are: metal inert gas (MIG) welding, tungsten inert gas (TIG) welding, friction stir welding (FSW), and laser welding (LW). Each method has their individual advantages and drawbacks. MIG and TIG are well documented in Eurocode 9 [2], FSW and LW are however mentioned as alternative methods that has to be approved appropriately through testing before structural use [2].

Generally, structural members shall only be welded by workers with proper certification, and at an appropriate location, preferable in a welding workshop. An approval should be at hand if the welding has to be done elsewhere [9]. Additionally, proper closing of welds are important to avoid cracks and crevices that may lead to crevice corrosion in the welded zones [9].

### 3.6.1 Arc welding

MIG and TIG welding are the most common welding methods for structural aluminium [9]. MIG welds aluminium members by subjecting the filler metal to a current, hence, the supplied filler material is acting as the electrode. TIG welding is equipped with a non-consumable tungsten electrode, the filler must therefore be added separately during welding. An argon and/or helium inert gas is applied during welding to protect against oxide development in the molten metal. TIG and MIG provides high quality aluminium welds [59], and the welds may be produced with minimal distortions. An advantage with this type of welding is it does not require any protective flux that may affect the corrosion resistance, and the actual welding operation can be performed in challenging positions [60].

MIG welding are extensively used in the industry due to its user friendliness and low cost compared to TIG welding. MIG welding is also known to be a faster process than TIG [59]. However, TIG produces more precise welds of higher quality, which should be regarded as an advantage for members that undergoes very strict design requirements. TIG welding is a more environmental friendly process than MIG, since there are hardly any air contaminants produced in the process. On the other hand, TIG welding requires highly skilled welders [59]. For welding of aluminium, alternating current is normally preferred for TIG and direct current for MIG, where the consuming electrode is positively charged [27]. See figure 3.19 for illustrations of the two arc welding methods.

Thick members must be preheated in order to ensure a proper TIG and MIG joining, due to a requirement of possessing sufficient local heat [2]. It is important to perform any necessary preheating in a controlled manner, where particular concern should be directed to maximum allowable temperature and exposure time that may alter the material properties if exceeded. Table 3.7, presents maximum temperature and exposure time for alloy 5083 and 6082 at certain thicknesses. Additionally, temperature restrictions of the base metal when adding additional layers for multi-layer welds are tabulated [9].

Table 3.7: Preheating limits for arc welding of thick members [9].

| Alloy | Thickness [mm] | Max. Temperature [$^oC$] | Max. Exposure time [min] | Temperature limit multi-layer welds [$^o$C] |
|---|---|---|---|---|
| 5083 | 6-12 | 200 | 10 | 120 |
| 6082 | above 10 | 200 | 30 | 100 |

The pistol used for MIG welding has a significant size, which may cause problems in less accessible areas. The diameter of the mouthpiece is ca. 30 mm and the filler wire extend 10-15 mm beyond the mouthpiece. This geometry on the end of the MIG pistol imposes difficulties in areas with too sharp angles between two profiles for example. The angle between structural members should therefore not be less than 35-40$^o$ [9], and there must be enough space for the pistol itself in order to weld in the correct positioning of the pistol. Welding accessibility should be an important factor in design of structures as poor access often results in poor welds [9].

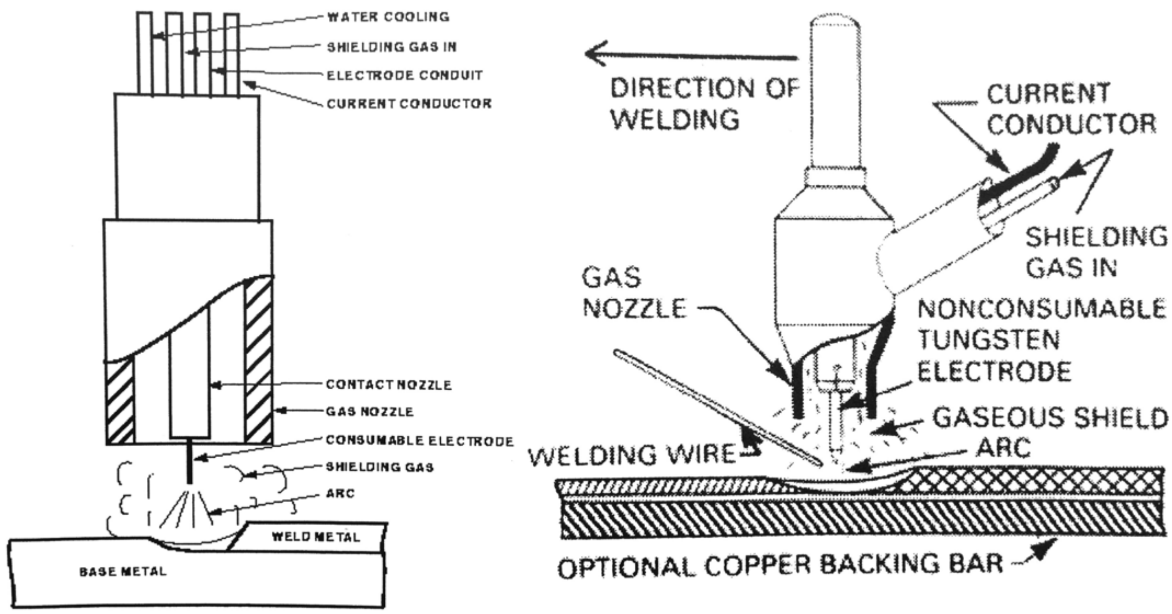


Figure 3.19: MIG (left) and TIG (right) welding [27].

In Eurocode 9 [2], the strength of the heat affected zone (HAZ) for several common aluminium alloys and product forms are listed. The HAZ values are only valid for MIG and TIG welds for thicknesses up to 15 mm, however according to a recent study [61] of HAZ values for larger thicknesses it is found that the HAZ strength will not be negatively influenced for thicknesses up to 30 mm [61].

The characteristic strength reductions and product forms for the NORSOK approved alloys are tabulated in table 3.9. The strength reductions varies with product form and welding method, different products are therefore tabulated along the with the respective strength reduction. Strength of the HAZ in TIG welds may also be influenced by thickness. The strength values for the 6xxx series are valid after 3 days due to the occurrence of natural ageing. The welded materials must be held above 10 $^{o}$C to fulfill the ageing phenomenon [2].

It is noteworthy that the strength reduction for the tensile strength (TS) is greater than the loss of YS in the aluminum HAZ, and the strength characteristics after MIG and TIG (up to 6mm) for the 5xxx series are equivalent. The difference in strength between plate (PL) and the two other products (extruded tube and drawn tube) may be regarded as negligible, an exception is however observed when comparing the TS of the products for the alloy 5083-H116.

There are also listed strength characteristics of weld metal in the Eurocode [2]. The strength of the weld metal is normally lower than the base metal, but higher when compared to the HAZ. The strength of weld metal, which is tabulated in table 3.8, are applicable given that the recommendations presented in table 3.11 are followed [2].

Table 3.8: Strength of weld metal for alloy 5083 and 6082 [2].

| Filler material | 5083 | 6082 |
|---|---|---|
| Type 4 | - | 190 MPa |
| Type 5 | 250 MPa | 210 MPa |

As mentioned, the strength in the HAZ is for most cases lower than the weld metal, one should therefore be more concerned about designing structures to accommodate the lower HAZ strength, however both strength characteristics must be accounted for in structural design [54].

Table 3.9: Strength reductions in HAZ [2].

| | | MIG[1)] | | TIG[2)] | | TIG[3)] | |
|---|---|---|---|---|---|---|---|
| | | YS [%] | TS [%] | YS [%] | TS [%] | YS [%] | TS [%] |
| 5083-H116 | PL[4] | 28 | 10 | 28 | 10 | 35.1 | 18.9 |
| | DT[4] | 32.5 | 3.6 | 32.5 | 3.6 | 39.3 | 13.2 |
| 6082-T6 | PL[4] | 51 | 38.3 | 60.7 | 50.6 | 68.6 | 60.7 |
| | ET[4] | 52 | 40.3 | 61.5 | 52.3 | 69.2 | 61.9 |

1) Up to 15 mm thickness.
2) Up to 6 mm thickness.
3) Thickness between 6-15 mm.
4) PL = Plate, ET = Extruded tube, DT = Drawn tube.

The extent of the HAZ for different shapes and welds are measured as shown in figure 3.20. The HAZ is larger and more severe in TIG welds due to greater heat input. Furthermore, values of the HAZ wideness varies with thickness; increasing thickness leads to a more severe HAZ [2]. The extension of HAZ is tabulated in table 3.10 for both MIG and TIG welding. The values given in table 3.10, are coinciding with figure 3.20.

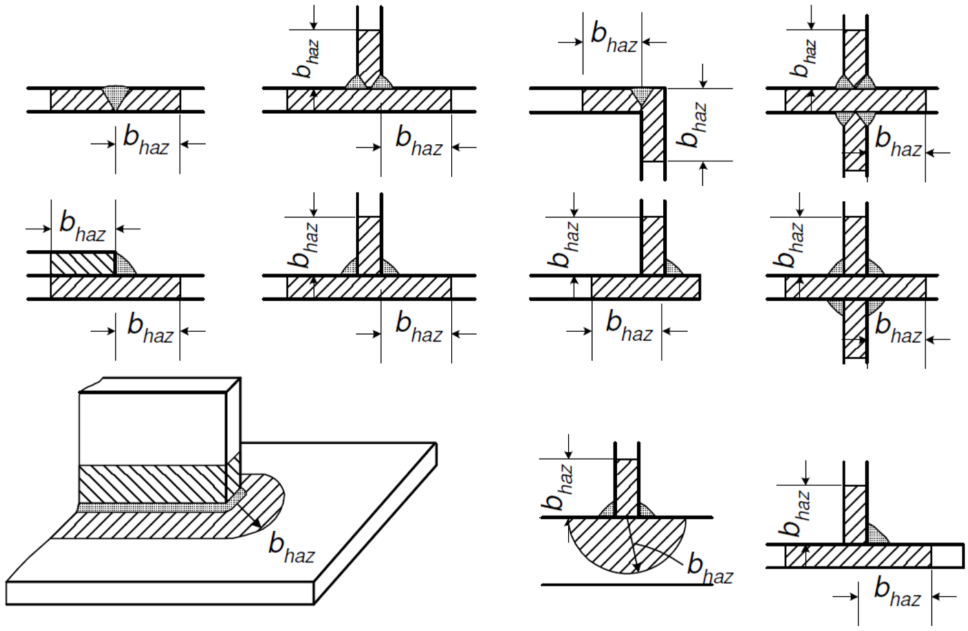


Figure 3.20: Extent of HAZ for different welding geometries [2].

Table 3.10: Extent of HAZ for different base metal thicknesses [2].

| Thickness | 0-6mm | 6-12mm | 12-25mm | above 25mm |
|---|---|---|---|---|
| MIG | $b_{HAZ} = 20$mm | $b_{HAZ} = 30$mm | $b_{HAZ} = 35$mm | $b_{HAZ} = 40$mm |
| TIG | $b_{HAZ} = 30$mm | - | - | - |

According to Eurocode 9 [2], the filler metal may be chosen based on weld strength, corrosion resistance or weld cracking [2]. Table 3.11, summarizes the recommended filler materials for different base metal combinations and demands. Primary filler material selection should be alloy 5183 for both 5xxx and 6xxx series according to NORSOK M-121 [44]. The consumption of filler material should be frugal, meaning that one should not overfill welding grooves as filler material is quite expensive (the same apply for cover gas) [9].

Table 3.11: Filler materials [2].

| | | 5083 | 6082 |
|---|---|---|---|
| 5083 | Weld strength | 5556A | Type 5 |
| | Corrosion resistance | Type 5 | Type 5 |
| | Weld porosity | Type 5 | type 5 |
| 6082 | Weld strength | | Type 5 |
| | Corrosion resistance | | Type 4 |
| | Weld porosity | | Type 4 |
| Type 5: | 5056A, 5356/5356A, 5556A/5556B, 5183/5183A | | |
| Type 4: | 4043A, 4047A | | |

There will always exist weld deformations to some extent, one should therefore be aware of precautionary actions. Firstly, it is important to make sure that the bonding components are sufficiently fastened (e.g. clamped) to reduce welding stress that may cause cracking, however in some rare cases where it is of interest to perform corrective measures it is preferable to avoid any constraints in order to reduce residual stresses [9]. Tack welding should also be commenced sufficiently to make sure the welding process takes place at the desired position. Welding speed should be as high as possible and prior bending may neutralize weld deformations in some cases [9]. For load bearing structural members, butt welds should be fully penetrated [2].

### 3.6.2 Friction stir welding

Friction stir welding is a new version of the conventional rotary friction welding. It was developed at The Welding Institute, Cambridge in 1991. The method was originally aimed for solid-state joining of aluminium but has now been successfully applied on other harder metals and plastic as well [29].

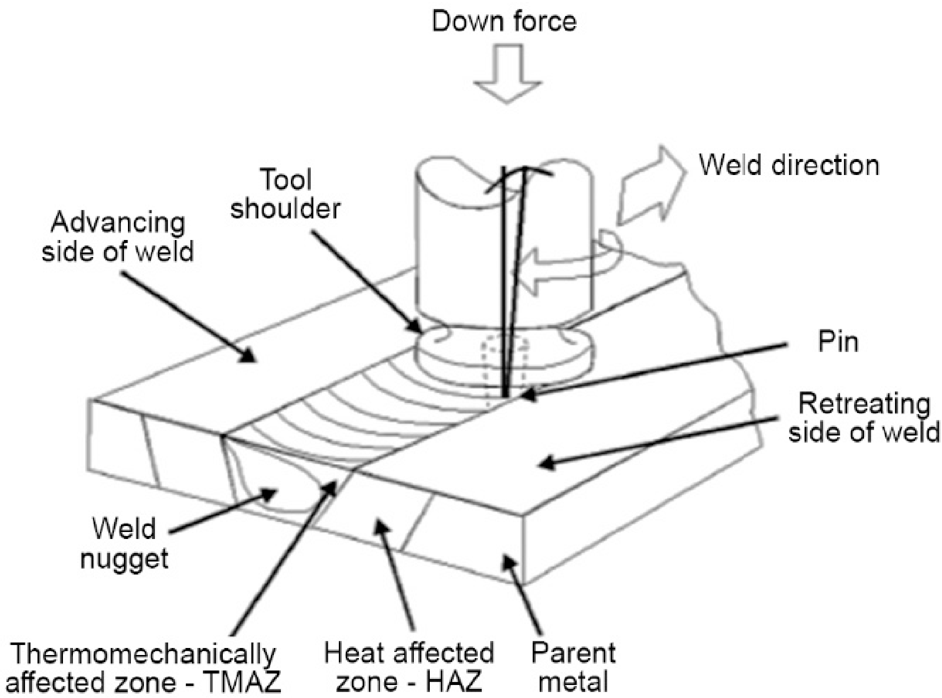


Figure 3.21: Friction stir welding process [28].

The principle of FSW is to use a rotating pin tool with a shoulder to generate heat from friction and plastic deformation of the substrate [29]. The substrates have to be rigidly clamped to avoid misalignment. The rotating pin generates a material flow from the front to the tailing end where the metal is forged into a joint, this material flow causes a plastic deformed area around the weld, as shown in figure 3.22. Notice the plastic zone surrounding the pin is uneven, caused by the rotating direction of the pin, where one side is called advancing side (AS) and the other is called retreating side (RS) [29], figure 3.21 shows the principle of FSW.

#### Microstructure

The friction stir welded material can be divided into four different microstructural zones according to how they are affected by the welding [29].

1. Base material, BM in figure 3.22.
2. Heat affected zone, HAZ in figure 3.22.
3. Thermo-mechanically affected zone, TMAZ in figure 3.22.
4. Stir zone, also called weld nugget, SZ in figure 3.22.

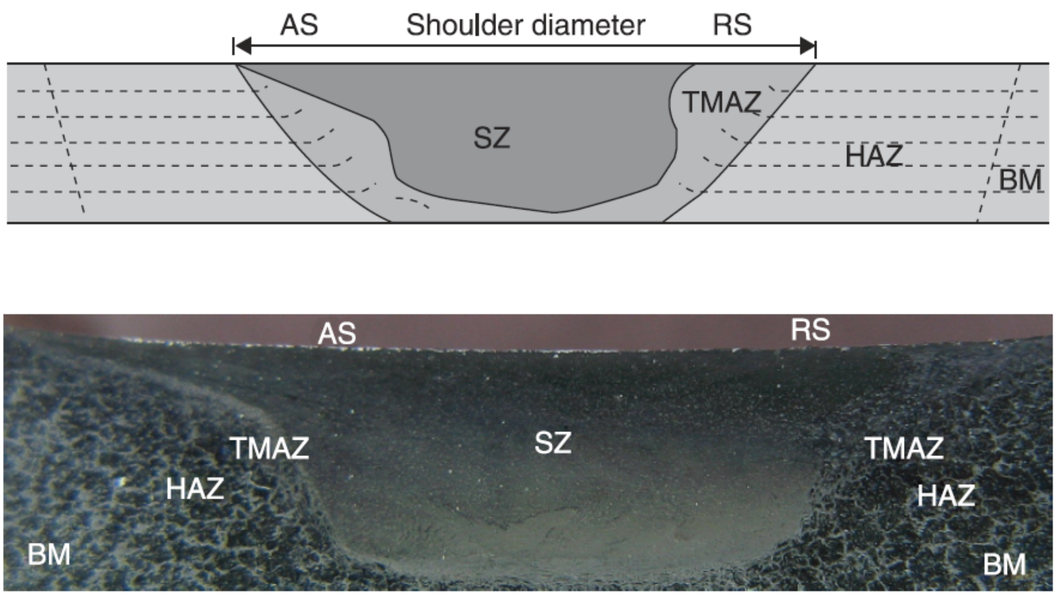


Figure 3.22: Microstructure after friction stir welding [29].

The base material is not affected by the weld, hence there is no significant change in the materials microstructure in this zone [29]. The HAZ is only heat affected by the welding process, and there is no mechanical deformation. The thermo-mechanically affected zone (TMAZ) is affected by mechanical plastic deformation, without undergoing recrystallization. There is no recrystallization due to insufficient temperature and insufficient mechanical strain. The stir zone (SZ) has undergone recrystallization due to high temperature caused by frictional heat and high plastic deformation. The transition from stir zone to base material is relatively smooth and continuous on the RS side, while the transition is sharper on the AS side of the weld [29].

Mechanical properties are changed and some of the most important properties will be significantly reduced. Especially with respect to yield strength, ca. 50% decreased for alloy 6082-T6. Tensile strength is reduced by ca. 30% for alloy 6082-T6. The FSW effect on mechanical properties for alloy 5083-O and 6082-T6 can be seen in table 3.12. The material hardness is reduced as seen in figure 3.23, showing the Vickers hardness (HV) against the distance from weld centre for alloy 6082-T6 and alloy 6061-T6 [29].

Table 3.12: Mechanical properties of FSW.

| **Material** | | **TS [MPa]** | **Efficiency [%]** | **YS [MPa]** | **Reference** |
|---|---|---|---|---|---|
| 5083-O | BM | 285-298 | 95-119 | - | [62] |
| | FSW | 271-344 | | - | |
| 6082-T6 | BM | 323 | 68 | 276 | [63] |
| | FSW | 224 | | 134 | |

Friction stir welding has been introduced into several industries working with aluminium. For example, Marine Aluminium has a FSW machine capable of welding 15 meters long large sized panels [64] and SpaceX has a special made FSW machine to weld their Falcon 9 rockets [65].

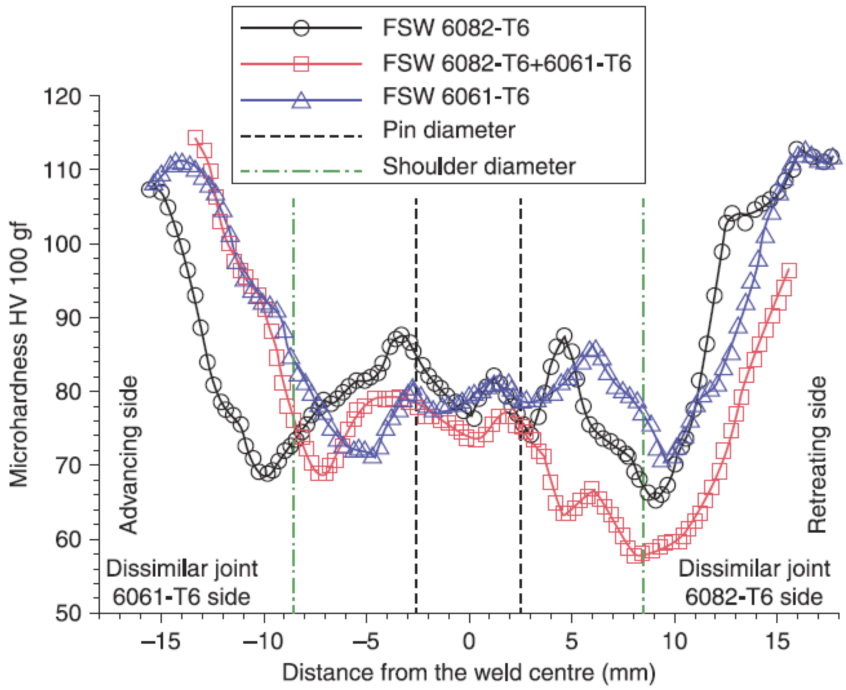


Figure 3.23: Comparison of Vickers hardness after friction stir welding for alloy 6082-T6 and alloy 6061-T6 [29].

**Rotary friction welding**

In principle, rotary friction welding (RFW) bonds two members by rotating one member against the other with a specified rpm and pressure [66]. The heat generated from the friction softens both surfaces, which leads to material plasticity. After sufficient friction heat and plasticity are reached, the rotating components are forced together by applying hydraulic pressure. The pressure may be held for a period after the rotation stops, sometimes referred to as forging force. The interface material is consequently extruded outwards, which leaves behind clean and pure metal in the whole cross-section of the joint. The base metal is not melted during this process, which means the weld is formed in a solid state. A typical application for this bonding method is joining of steel axles in vehicles [66].

It is noteworthy that the microstructure for a RFW is very similar to the one caused by FSW. The resulting strength properties of RFW are dependent on variables such as heat characteristics and welding time etc. Based on such process variables, strength values can be obtained for the HAZ by using appropriate process models [66].

### 3.6.3 Hybrid metal extrusion and bonding

A new patented process called hybrid metal extrusion and bonding (HYB) is an innovative low temperature solid state method that allows joining without any strength reductions in the HAZ [30]. The technology developed at NTNU is still in an early phase. However, in 2014 Statoil and Cardo Partners became part of the owner group in order to implement the new technology in fabrication of the new Johan Sverdrup oil field [30].

The principle of the HYB method is illustrated in figure 3.24. The filler metal is plasticized where it interacts with the base metal [30]. The oxide layer on the base metals to be bonded are subsequently removed during the process. Removal of the oxide layer is beneficial in terms of interatomic bonding between the atoms. The process temperature is below 300 $^{o}$C and the filler metal possess the same properties as the base metal. HYB do not require heavy clamping, as required for FSW due to large reaction forces during welding. Low reaction forces is advantageous in terms of robotic automation [30].

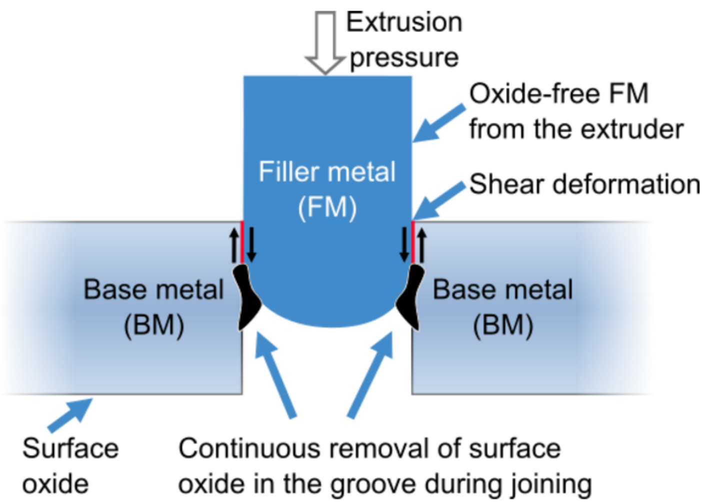


Figure 3.24: Hybrid metal and extrusion [30].

### 3.6.4 Laser welding

Laser welding (LW) is a process that requires no contact between the bonding members, it is a so called non-contact process [27]. The heat created by the concentrated laser beam causes coalescence of the joining materials. The type of lasers that are mostly seen in industries are the Nd:YAG (solid state laser) and $CO_2$ (gas laser) lasers where the YAG possesses a wavelength 10% of the latter [27]. The Nd:YAG laser light may be transmitted through fiber optics instead of copper used for the $CO_2$ laser light [31]. Gas shielding (i.e. helium and argon) is usually applied to protect the melted material from oxidation. The fact that this type of welding only require access from one side of the joint impose low-heat input that subsequently cools rapidly [10], and bonds without filler material, should be regarded as advantages. The laser joining process may be conducted with a pulsating or continuous beam [67].

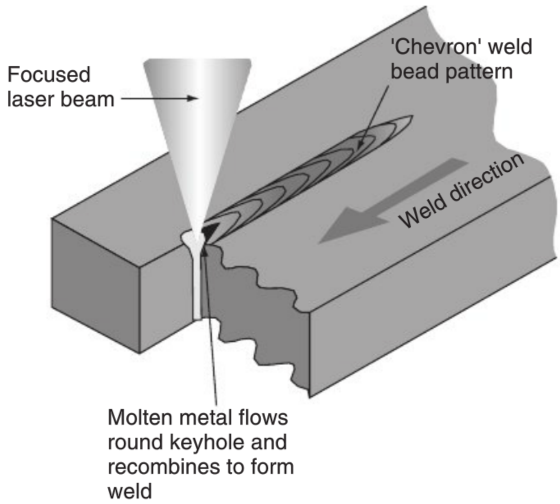


Figure 3.25: Laser keyhole welding principle [31].

There are some important limitations concerning the use of LW that should be mentioned. Magnesium and zinc, that are often seen in aluminium alloys with significant amounts, are quite easily vaporized from the heat of the laser, which may lead to formation of a beam blocking plasma layer [68]. Entrapped vapour pores and hydrogen may also occur during LW. Gas shielding are usually implemented to withstand the hydrogen diffusion, where helium is preferred for high quality welds at maximum depth applications [68]. Pores that causes porosity often seen in LW [31] may also arise from vaporization of alloying elements, for instance magnesium [67].

Pre-surface cleaning is very important for LW as a preventive measure for porosity [10]. Removal of deteriorating contaminants that may alter characteristics of the weld, and the fact that the LW process does not have the ability to remove oxide during welding. Aluminium is in addition one of the best light reflectors, which complicates the LW process due to a low power absorption. The reflection effect together with the relatively high temperature expansion coefficient of aluminium leads to a requirement for using much more powerful lasers for welding aluminium than for steel, although the absorption slightly increases when aluminium liquefies [67]. The Nd:YAG laser are preferable to use in order to overcome the reflection issues [68]. A disadvantage is the high fit-up tolerances required. The strict fit-up requirements are tabulated in the ISO 13919-2 standard [69] for multiple cases. Moreover, LW generally requires a significant investment [67].

With the use of high energy density lasers (above 40 $kW/mm^2$) one is able to produce welds in the so called keyhole regime, which improves the absorption due to a positive reflection effect within the cavity [31] seen in figure 3.25. The deep keyhole penetration reduces the width and strength losses of HAZ, minimizes distortion and the loss of alloying elements containing a lower boiling point are reduced (e.g. magnesium) [31]. It is important to have control over the power in order to create a stable keyhole. Another difficulty is the relatively low viscosity of the liquefied weld metal that may lead to drop-through of the molten metal. One can overcome this problem by welding in the horizontal-vertical position [31].

Strength in the as welded condition and in the base metal together with the respective strength reduction of laser welding are tabulated in table 3.13.

Table 3.13: Laser weld strength characteristics[1)] [10].

| Alloy | Strength reduction YS [%] | Strength reduction TS [%] |
|---|---|---|
| 5083-H21 | 7 | 11 |
| 6061-T6 | 25 | 34 |

1) $CO_2$ laser welding on 2-3 mm thick plates (butt weld).

### 3.6.5 Hybrid laser

Laser and the conventional arc welding can be combined to form a hybrid laser. The most popular combination is Nd:YAG laser implemented with MIG. This type of hybrid laser enables improved fit-up tolerances i.e. positioning of the components to be welded and the conventional welding speed possessed in arc welding is improved [27]. The Nd:YAG laser creates a keyhole ahead of the MIG that is depositing the weld metal, as illustrated in figure 3.26. It is claimed that the characteristic shape of the weld pool from a hybrid laser enables hydrogen to escape the joint, which reduces incidents of hydrogen entrapment and thereby reduces porosity defects [31].

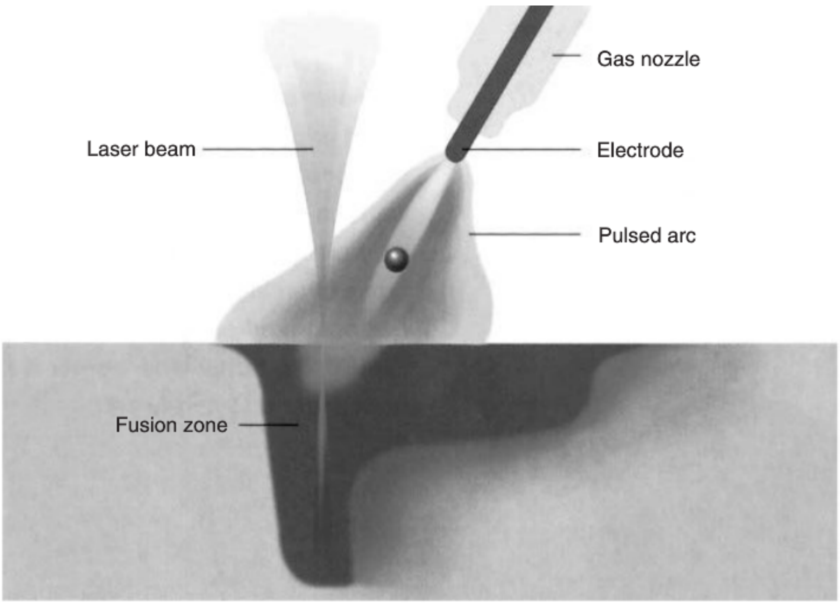


Figure 3.26: Hybrid laser principle [31].

### 3.6.6 Summary of welding methods

A brief summary of the advantages and disadvantages for the welding methods described in section 3.6 are presented in table 3.14. Brazing is excluded from table 3.14, as it is not a welding technique.

Table 3.14: Summary of welding methods.

| **Method** | **Advantages** | **Disadvantages** |
|---|---|---|
| MIG | Commercial and cost efficient.<br>Hand held apparatus. | 30-50% strength reduction. |
| TIG | High quality welds. | Requires highly skilled welders.<br>Larger HAZ than MIG. |
| FSW | High speed welding<br>Brilliant strength and ductility characteristics. | Only applicable to butt welds.<br>Bonding members must be rigidly clamped.<br>Not a hand held apparatus |
| LW | Good strength characteristics. | Costly method to implement.<br>Light reflection complicates the use of laser. |
| RFW | Brilliant strength and ductility characteristics. | Only applicable to joining of circular members.<br>Not a hand held apparatus. |
| Hybrid laser | Improved fit up tolerances, and the welding speed of the conventional MIG method is improved. | Costly method to implement. |
| HYB | Joining without any strength reductions. | Method is recently developed.<br>Limited literature on the technology. |

## 3.7 Brazing

Joining aluminium alloys by brazing is a method that does not involve melting of the structural components, the parts are instead joined by a filler material.

Brazing differs from soldering by the fact that brazing filler material for aluminium alloys are always aluminium-based, and the heat required for the brazing process is considerably higher. The brazing filler material typically exhibit a composition that is just below the melting temperature of the base metal. By definition from DVS (Deutscher Verband für Schweißtechnik), the brazing and soldering process is distinguished according to an applied temperature of 450 $^{o}$C [56].

The filler metal distributes throughout the joint surfaces at brazing temperature. During this process the filler and base metal will be combined by inter-atomic attraction, which result in a permanent metallic bonding [56]. The bonding may also partly be a result of an atomic interchange between the base and filler material due to diffusion at the working temperature. Diffusion may also lead to a reduced mechanical strength as the intermetallic phases are precipitating [56].

The heat required for the brazing process of aluminium alloys leads to a strength reduction of the base metal surrounding the brazed joint, in the magnitude of 50-60% reduction of its initial YS [56].

As for welding, the oxide layer on aluminium alloys complicates the brazing process. Removal of the oxide layer must therefore be commenced before initiation, and the bare surface needs to be protected against post oxide formation. Thick oxide layers has to be removed either chemically or mechanically. However, thinner layers may be displaced by brazing flux [56].

Aluminium alloys are generally restricted to filler material based on aluminium together with silicon. Hence, the 2xxx and 7xxx aluminium series are not suitable for brazing, as the melting temperature for these alloys are too low. The filler metal used in brazing may lead to a more corrosive behavior in seawater as it may possess a more noble potential in the galvanic series than the base metal. Furthermore, alloys with a raised amount of magnesium, more or less above 1-2% (e.g. 5083-H116), are more challenging to braze due to a more aggressive oxide development that is more complicated to handle by common removal methods.

## 3.8 Bolting

Bolted sections enables joining without any significant strength reduction in the base metal of bonding sections, as is the case for joining methods (e.g. welding) that imposes enough heat to degrade strength properties of aluminium alloys. No reduction in strength is an advantage, however bolting imposes some drawbacks.

Bolted joints in subsea applications are in danger of encountering crevice corrosion and/or galvanic corrosion, as described in section 3.5.1 and 3.5.6, respectively. Protective measures must therefore be applied to all connections that possess a crevice (bolt heads, nuts, washers) and/or galvanic coupling between various materials used in the joint. Sealing compound, coating and CP are considered effective protection methods [2, 20]. The sealing compound shall function as an external seal to prevent water ingress in openings and cracks of the assembly. All contact surfaces of the bolt assembly shall be free of coating to ensure adequate friction and electrical continuity throughout the bolt assembly [11]. See figure 3.27 for illustration of two bolted plates made of steel and aluminium with sealing compound. The components in the bolt assembly should have an electric resistance of less than 0.1 ohm with respect to an anode to ensure proper CP of the joint members. The continuity shall be verified by actual measurements [11].

Submerged carbon steel bolts should have a protective layer of phosphating or coated with poly tetra fluoro ethylene (PTFE) as long as electrical continuity is verified [54]. Phosphating is therefore advantageous in terms of electrical continuity. Hot dip galvanizing should not be implemented on structural bolts, as it may cause loss of pretension in the bolt due to dissolution of zinc layer [54]. Stainless steel bolts do not require any coating [54]. See appendix B.3 for e-mail correspondence with Ole Øystein Knudsen regarding CP of phosphated bolts.

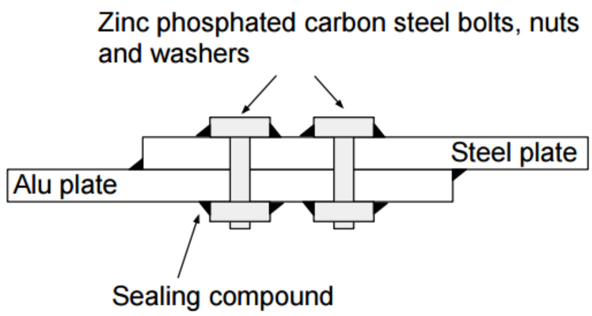


Figure 3.27: Bolt assembly with CP between aluminium and steel with zinc phosphated carbon steel bolts and sealing compound.

If elements in the bolt assembly (or structure) do not possess an adequate continuity (<0.1 ohm) one can use copper wires that can be fastened either by welding or bracing at each end, or with braced cable shoes fitted to desired bolt size. Minimum cross section of the copper wire is 16 mm$^2$ [11].

It must be decided if bolted joints shall be slip resistant or not if they are subjected to shear loading, and if the bolt(s) shall be preloaded or not for tension loading. A slip resistant and preloaded coupling requires more bolt tightening, which further implies the bolt type to be used. For the case of slip resistant connection the yield strength of the bonded material (except bolts) shall not be lower than 200 MPa [2]. According to NORSOK M-001 [54], bolts for subsea applications shall not have a higher hardness than 300 Brinell hardness number (HB) and strength class 8.8. Mechanical properties of grade 8.8 carbon steel bolts are tabulated in table 3.15. The hardness of the carbon steel bolt is ranging from 270-331 HB, it must therefore be ensured that the bolts are manufactured with a hardness below 300 HB. The hardness of stainless steel 316 is below 300 HB [70]. Properties for stainless steel bolts grade A4 (stainless steel 316) are also presented in table 3.15. Note, for subsea structural applications the bolts should generally be made of carbon steel [54].

Table 3.15: Properties of 316 stainless and 8.8 carbon steel bolts.

| Material | Grade | Property class | Yield strength | Tensile strength | Elongation after fracture |
|---|---|---|---|---|---|
| Carbon steel$^{1)}$ [71] | 8.8 | - | 640 MPa | 800 MPa | 12 % |
| Stainless steel 316 [72] | A4$^{3)}$ | 70 | 450 MPa | 700 MPa | 0.4d$^{2)}$ mm |

1) Valid for bolt diameter larger than 16 mm.
2) d = Bolt size.
3) Marine grade [72].

Bolting requires a higher number of tolerances and alignments than welding. Holes must be machined in an exact position, both for structural members and the bonding components between them. Clearance between bolt and machined holes should not be more than 3 mm for high strength slip resistant connections [73].

The recommended preloading per bolt in slip resistant joints can be calculated according to equation 3.3 [2], and the resulting slip resistance per bolt ($F_{sr}$) are found from equation 3.4. If the bolted connection are subjected to additional tensile force, equation 3.5 should be used as the tensile force lowers the slip resistance. The 1.25 fraction represents the safety factor at ultimate limit state [2]. For total joint thicknesses larger than 30 mm, the slip factor can be set to 0.4 [2].

$$F_p = 0.7\sigma_{ub} A_s \tag{3.3}$$

Where:
$F_p$ = Preloading force.
$\sigma_{ub}$ = Ultimate strength of bolt material.
$A_s$ = Bolt tensile stress area.

$$F_{sr} = \frac{n\mu F_p}{1.25} \tag{3.4}$$

$$F_{sr} = \frac{n \cdot \mu(F_p - 0.8F_t)}{1.25} \tag{3.5}$$

Where:
$n$ = Number of friction interfaces.
$\mu$ = Slip factor.
$F_t$ = Required tensile force per bolt for ultimate limit state.

The required shear ($F_{s,i}$) and tensile force ($F_{t,i}$) (per bolt) for a bolt group subjected to combined shear and moment are calculated from equation 3.6 and 3.7 respectively, where the first are valid for in-plane loading and the latter for out-of-plane loading [32]. See illustration of the two load cases in figure 3.28 and 3.29.

$$F_{s,i} = \sqrt{\left(\frac{P_x}{n} + \frac{M \cdot y_i}{\sum\left(x_i^2 + y_i^2\right)}\right)^2 + \left(\frac{P_y}{n} + \frac{M \cdot x_i}{\sum\left(x_i^2 + y_i^2\right)}\right)^2} \tag{3.6}$$

$P_x$ and $P_y$ are the vertical and horizontal shear loads acting on the bolt group. Number of bolts are denoted $n$, and $M$ is the moment around the centre of the bolt group. $x_i$ and $y_i$

represents the orientation of each bolt relative to the centre of rotation in figure 3.28. The bolts must be orientated with positive or negative values as appropriate. Use of equation 3.6 implies three assumptions: Plate deformations are negligible, total shear is distributed equally, and shear from applied moment is proportional to the distance between bolt and center of rotation [32].

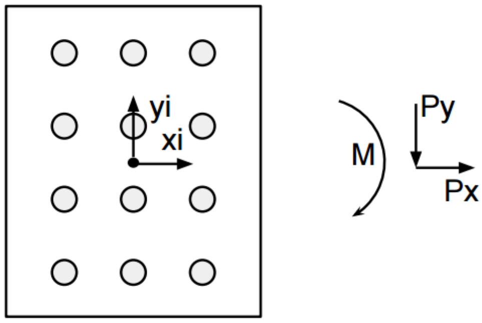


Figure 3.28: In-plane moment.

$$F_{t,i} = \frac{M \cdot l_i}{\sum(l_i \cdot L_i)} \tag{3.7}$$

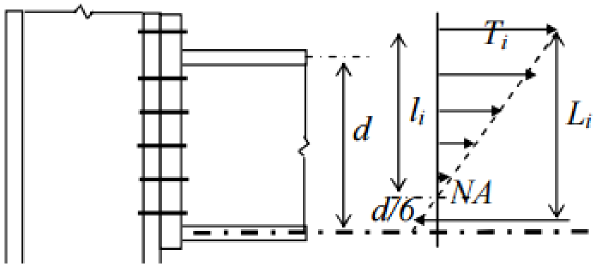


Figure 3.29: Out-of-plane moment ($T_i = F_{t,i}$) [32].

In the case of an out-of-plane loading, the point of rotation is assumed to be one-sixth of the beam height above the bottom of the beam, where $F_{t,i}$ is assumed to be proportional to the distance from point of rotation. However, if there is a hard spot in the lower area of the beam such as a flange, the point of rotation may be assumed to act in the middle of that spot. In equation 3.7, the distance between bolt "i" and center of rotation is denoted $l_i$ and the distance between the lowest bolt and bolt "i" is denoted $L_i$. The equation assumes proportional relation between $F_{t,i}$ and $l_i$, as illustrated in figure 3.29 [32].

For structural members limited by available lengths due to for example fabrication or transport restrictions, one may combine them with the use of beam splices illustrated in figure 3.30. Beam splices are known to resist large shear forces and bending moment. If a beam splice joint is oriented at a point with somewhat lower moment, one can make an assumption where the flange splice takes up the moment and the shear force is carried by the web splice [32]. However, if that assumption is not accurate, the moment should be split between the flange and web in accordance with the stress distribution between them. In the case of shared moment, the web splice is subjected to both moment and shear loading.

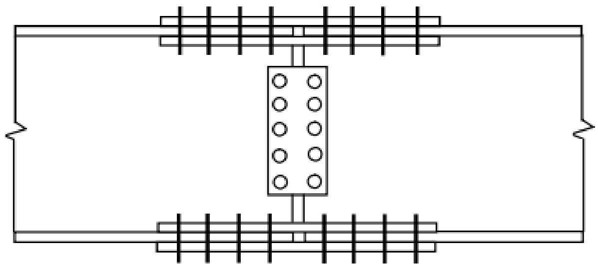

Figure 3.30: Beam splices [32].

The respective design resistance for bolts subjected to shearing ($\sigma_{sr}$) and/or tension ($\sigma_{tr}$) are found from equation 3.8 and 3.9. $\alpha_s = 0.6$ for class 8.8 steel bolts and 0.5 for stainless steel bolts. For the case of combined shearing and tension, the criteria in equation 3.10 shall be fulfilled [2].

$$\sigma_{sr} = \frac{\alpha_s \sigma_{ub}}{1.25} \tag{3.8}$$

$$\sigma_{tr} = \frac{0.9\sigma_{ub}}{1.25} \tag{3.9}$$

$$\frac{F_s, i}{\sigma_{sr} A_s} + \frac{F_t, i}{1.4\sigma_{tr} A_s} \leq 1 \tag{3.10}$$

For bolted connections there are specified minimum, regular and maximum spacing between bolts and edges. The maximum values are strongly dependent on exposed environment, where corrosive environments lowers the maximum value due to a need for proper closing of the connection, which hinders the occurrence of crevice corrosion. See figure 3.31 and table 3.16 for approved spacing values [2]. The maximum values are also influenced by the susceptibility of encountering buckling during compression, as described in section 3.11. Local buckling between fasteners are considered to be satisfactory if the ratio $p_1/t$ is lower than $9\epsilon$, see eq. 3.15 in section 3.11 for calculation of $\epsilon$. The edge distance $e_2$ is tolerable as long as it is not exceeding the maximum value. However, the distance $e_1$ do not affect the occurrence of local buckling [2], and placement of fasteners should enable enough space for tightening tools.

Table 3.16: Minimum, regular and maximum values for spacing between bolts ans edges [2].

| Spacing | Minimum[1] | Regular[1] | Maximum[2] (corrosive environment) |
|---|---|---|---|
| $e_1$ | $1.2d_0$ | $2.0d_0$ | 4t + 40 mm |
| $e_2$ | $1.2d_0$ | $1.5d_0$ | 4t + 40 mm |
| $p_1$ | $2.2d_0$ | $2.5d_0$ | Smallest of 14t or 200 mm |
| $p_2$ | $2.4d_0$ | $3.0d_0$ | Smallest of 14t or 200 mm |

1) $d_0$ = Diameter of hole.
2) t = Thinnest thickness of the outer connected member.

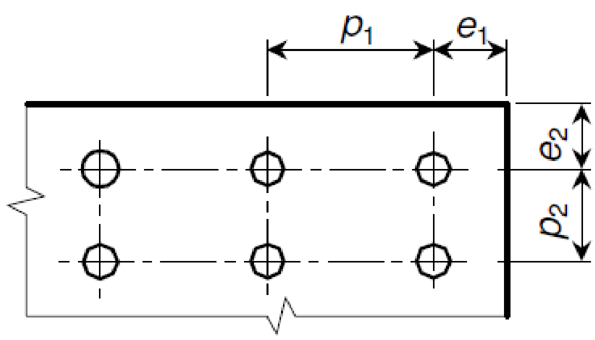


Figure 3.31: Fastener spacing [2].

Tightened bolts shall be re-tightened after 72 hours due to effects like creep, relaxation and settlement [73]. The applied tightening torque shall be continuously and smooth [74].

## 3.9 Adhesives

As for bolting, adhesive bonding does not negatively alter the mechanical properties of jointed structural members. The use of adhesives also enables joining of different materials with a wide range of properties. Furthermore, adhesive joints possesses an excellent uniform stress distribution. A drawback is adhesive's sensitivity to different environments, and the comprehensive validation required before any use of adhesives in structures [27]. Figure 3.32, illustrates the structure of an adhesive bonded joint.

According to Eurocode 9 [2], structural joints may be connected with the use of adhesives. The bonding requires an expert technique and it should only be used with care. For main structural joints comprehensive environmental and fatigue testing must be approved in order to establish its validity. A combination of plate and stiffeners may be more suitable for adhesive joining. In general, adhesives should only be subjected to shear stress [2].

The strength of the adhesive itself may be measured according to tests described in the standard ISO 11003-2 [75]. However, it is not enough to only have insight in the specific strength of the adhesive to ensure the strength of the joint, it has to be tested thoroughly in terms of strength through laboratory tests, where pretreatment, adhesive, environment and ageing are accounted for. If an adhesive joint passes the laboratory tests, it has to be validated even further in real tests conditions. The results obtained at the laboratory should only be treated as advisory [2].

High strength adhesives recommended by Eurocode 9 [2] for structural applications are illustrated in table 3.17. These values are based on extended research. Higher values for strength of adhesives may be utilized if the respective adhesive is tested and approved according to ISO 11003-2 [2, 75]. A safety factor of 3.0 is imposed [2]. Adhesives combined with riveting or bolting may increase the joints robustness [27].

Table 3.17: Strength values of recommended adhesives [2].

| Adhesive types | Strength [Mpa] |
|---|---|
| Modified epoxide, heat cured, 1 component | 35 |
| Modified epoxide, cold cured, 2 components | 25 |
| Modified acrylic, cold cured, 2 components | 20 |

Pre-treatment is very important for an adhesive joint, especially if it has to perform over extended periods, and the durability in environments that may degrade the adhesive is highly dependent on the chosen pretreatment. Examples of environments that may degrade the quality and/or contribute to ageing of the adhesives are waterish environments (saltwater), humid atmosphere and other aggressive environments [2]. Delamination process in the interface of an adhesive bonded joint are schematically illustrated in figure 3.32. Adhesive failure occurs in the metal-adhesive interface due to environmental degradation and stress, which can ultimately lead to crevice corrosion in the interface [27].

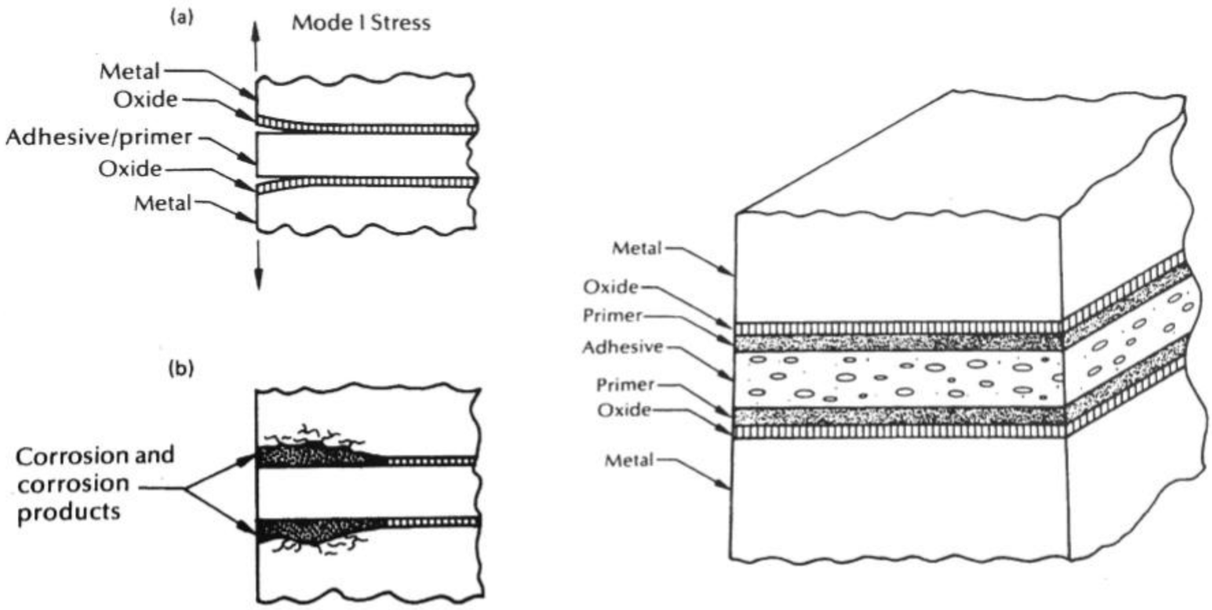


Figure 3.32: Right figure: Structure of an adhesive metal to metal joint. Left figure: Delamination mechanism of an adhesive bonded joint: a) The oxide /primer interface is weakened due to stress and water. b) Crevice corrosion products accelerates the delamination [27].

## 3.10 Formability

Aluminium is generally easy to form and machine, especially compared to steel. Bending of aluminium are roughly performed the same way as for steel, however one must be careful when it comes to the relatively soft aluminium surface that may be accumulated with metal particles during the bending process, which may lead to local corrosion [9]. Preventive actions are proper cleaning and use of lubricants.

Plates are normally formed when cold. Generally when bending aluminium it is of importance to make sure the bending radius is not too small. The radius requirement is dependent upon thickness and alloy [9]. Too small bending radius may cause fracture, especially for high strength alloys with low ductility and plastic necking (decreased thickness) will always occur in the bend zone. Aluminium must be bent more than the desired angle due to an elastic return effect. Minimum bending radius for a 12.5 mm 5083-H116 alloy plate with a $90^o$ angle is 4 four times thickness [76].

Tubes and profiles may be bent when cold, which is preferable considering loss of mechanical properties when heated. As for plates, the radius should not be too small for profiles and tubes, however the radius is also dependent on the profile shape. The minimum bending profile and tubing radius, $R$, for alloy 6082-T6 can be calculated according to formula 3.11 and table 3.18 [9]. $z$ is the external diameter or cross sectional profile height. If the relation $z$/wall-thickness is greater than 20, the table values are not valid. All components to be bent should be bent uniformly. Profiles can be made with stiffeners in order to avoid buckling of the profile that is exposed to compression. Tubes with thin walls may be filled with sand or alloys with low melting point. Generally, tube benders and jigs are the recommended bending processes for both profiles and tubes [9].

$$R = \sqrt{Bend\ factor \cdot z^2} \tag{3.11}$$

Table 3.18: Minimum bend factors for cold bending of alloy 6082-T6 tubes and profiles [9].

| Tube | Profile |
|---|---|
| 2.0-2.5 | 2.5-3.0 |

### 3.10.1 Machining

Aluminium is readily machined by commercial methods such as sawing, plasma cutting and water jet cutting. However, torch cutting should not be applied to aluminium, due to the HAZ created by the torch [9]. Water jet cutting has the advantage that it does not create any HAZ, as the process does not involve any heating of the material. Water jet cutting of aluminium alloys can be used on all components on the concerned ITS.

## 3.11 Buckling

The cross section buckling resistance for structural members can be assessed by identifying the appropriate buckling class described in Eurocode 9 [2]. The cross sectional classification assess if the resistance and rotational capacity is confined by its resistance to local buckling. The buckling class are found by calculating the width and thickness ratio of all the parts that may be subjected to compression under considered load combinations.

There are four buckling classes described in Eurocode 9, where the first one has the best buckling resistance. The classes are defined as follows:

- Class 1 posses the required rotation capacity for plastic analysis, due to formation of plastic hinge without reduction of resistance ($\beta \leq \beta_1$).
- Class 2 can reach their plastic moment resistance, but local buckling limits the rotational capacity ($\beta_1 < \beta \leq \beta_2$).
- Class 3 may reach its yield strength in the most compressed parts, but local buckling restricts full development of plastic moment resistance ($\beta_2 < \beta \leq \beta_3$).
- Class 4 develop local buckling before yield stress is reached in one or more compressed parts ($\beta > \beta_3$).

For class 4 cross sections, an effective thickness may be used to accommodate the low buckling resistance. The different compression parts of a cross section (e.g. web and flange) can in theory possess different classes, however the least favourable class apply for the whole cross section [2].

The buckling calculation process is related to the member's slenderness, which is dependent upon the cross sectional profile, shape of the compressed parts, and whether it is internal or outstanding. The parts may also be reinforced (e.g. ribs, edge lips or bulbs), which further affect the calculation procedure. The web and flange of a symmetrical unreinforced I-beam can be calculated by finding the individual slenderness parameter, $\beta$, according to eq. 3.12 and 3.13, respectively [2]. The web is regarded as an internal part while the flange is an outstanding part. $h$ is the height of the web, and $b$ is half the flange width excluding the web width. Slenderness parameter of a tube can be found from eq. 3.14 (internal part), Where $D$ is the mid-thickness diameter and $t$ is the respective thicknesses. By comparing obtained slenderness parameter with the tabulated values in table 3.19, one will be able to find the right class for each compressed part of a cross section. See the class description for the respective slenderness criteria, and use equation 3.15 to find the required value for $\epsilon$ by inserting the yield strength of considered material.

$$\beta_w = 0.4h/t \tag{3.12}$$

$$\beta_f = b/t \tag{3.13}$$

$$\beta_t = 3\sqrt{\frac{D}{t}} \tag{3.14}$$

$$\epsilon = \sqrt{250/YS} \tag{3.15}$$

Reinforcement has potential in improving buckling resistance. Slenderness parameter for a reinforced flange ($\beta_r$) fitted with single sided rib or lip possessing the same thickness as the flange throughout an I-beam, can be calculated according to equation 3.16 [2]. $c$ is the length of the rib or lip, measured from the internal edge of the flange. The other parameters are the same as described in equation 3.13. Table 3.19 also apply for equation 3.16.

$$\beta_r = b/(t\sqrt{1+0,1(c/t-1)^2}\,) \tag{3.16}$$

Table 3.19: Slenderness parameters [2].

| Material classification | Internal parts | | | Outstand parts | | |
|---|---|---|---|---|---|---|
| | $\beta_1/\epsilon$ | $\beta_2/\epsilon$ | $\beta_3/\epsilon$ | $\beta_1/\epsilon$ | $\beta_2/\epsilon$ | $\beta_3/\epsilon$ |
| Class A[1] | 11 | 16 | 22 | 3 | 4.5 | 6 |
| Class A welded | 9 | 13 | 18 | 2.5 | 4 | 5 |
| Class B[2] | 13 | 16.5 | 18 | 3.5 | 4.5 | 5 |
| Class B welded | 10 | 13.5 | 15 | 3 | 3.5 | 4 |

1) 6082-T6
1) 5083-H116

If a part happens to be classified as class four and it is not practical to enhance the local buckling by design it is possible to introduce a reduction factor (eq. 3.17), which gives an effective thickness. $C_1$ and $C_2$ varies with material class, if the part is welded or not and whether it is internal or not. For internal parts, $C_1$=25 and $C_2$=150 apply for alloy 5083-H116 with welds, and $C_1$=29 and $C_2$=198 for alloy 6082-T6 with welds [2].

$$\rho_r = \frac{C_1}{(\beta/\epsilon)} - \frac{C_2}{(\beta/\epsilon)^2} \tag{3.17}$$

## 3.12 Fatigue

The fatigue resistance compared to static resistance is significant for aluminium alloys, meaning that the fatigue resistance is significantly lower than static resistance. Fracture due to fatigue may occur without necessarily exceeding its strength capabilities if subjected to intolerable load cycles [52]. Typical initiation spots are welds, cracks, holes (pitting), notches, recesses, etc. Varying compressive stress cycles are usually not a problem with regards to encountering fatigue failure, however tensile and compressive-tensile load cycles are [52].

Design against fatigue failure may be performed according to one of the three following methods [77]:

- Safe life design
- Damage tolerant design
- Design assisted by testing

Safe life design means that the structure shall perform throughout its estimated lifetime without any required inspections. This method is a conservative fatigue life approach, which may be used on structures where it is difficult or not economically beneficial to perform inspections. The second method accepts small cracks, which is justified by fatigue crack monitoring in order to set up an appropriate inspection program. It is intended that the first and second method shall have the same reliability [77]. Damage tolerant design may be used where fatigue significantly affects design cost and in structures where it is permissible with somewhat more fatigue cracking than for safe life design, however inspections of the structure must be possible. If there is not obtained enough fatigue data for any relevant structure, one can design the structure against fatigue by performing tests in accordance with standards [77].

S-N design curves, stress range and load cycle must be established in order to assess the fatigue capacity of a structure. The S-N design curves are determined based on many factors such as: material quality, direction of extrusion, type of weld and its orientation relative to direction of stress, transitions in cross section, and other geometric factors [77]. The S-N curves which are constructed based on test, are plotted logarithmically as a function of stress range and load cycles, and can be found for many structural details. If the appropriate detail is nowhere to be found in approved standards, one can conduct full-scale fatigue testing on the missing details [77]. It is noteworthy that the S-N curves are not sensitive to different alloy compositions within the 5xxx and 6xxx series according to Eurocode 9 [77], however there may be different curves between the series itself due to lower durability rating in seawater for the 6xxx series. The curves do not distinguish between different temper designations of the alloys (e.g. T4 and T6) [9].

Structures may encounter resonant effects, which can cause magnification of dynamic stress. Slender structures with low natural frequency are particularly susceptible to this effect. In addition, structures supporting vibrating equipment (e.g. X-mas tree) should be carefully assessed for resonance [77]. If the structure is subjected to transport loads prior to its final destination, the integrity of the structure should be validated appropriately.

Fatigue damage during sea transport from wind and wave loads should be assessed if the structure is exposed to significant cyclic loading according to DNV-OS-H102 [78], which shall be based on specified environmental load history for weather restricted operations.

Fabrication quality of aluminium is very important for the fatigue capacity, and the relatively soft aluminium surface should be protected against any damage during fabrication, transport and assembly, as uniform surfaces possess better fatigue characteristics. Welds are often the most critical locations of encountering fractures due to fatigue (even when exposed to low loading), it is therefore very important that welding is performed appropriately in excess of inspections before installation [77].

Corrosion of aluminium alloys in seawater can affect fatigue crack growth, due to anodic dissolution at the apex of a crack (e.g. pit). Anodic dissolution is a relatively slow process, it is therefore most effective for small crack growth rates, meaning it effectively reduces the threshold region [52]. More on fatigue challenges are discussed in section 6.3.

# Chapter 4

# Integrated Template Structure Analysis

This chapter will focus on the practical design of the structure, where design possibilities by the use of aluminium alloys will be provided. The aluminium design will be based on the literature in chapter 3. The new size and geometry of the reviewed components are based on mechanical integrity, where the moment of inertia and yield strength are used as the most important design parameters, seen in detail in section 4.1. This approach is checked by modelling the structure in Autodesk Inventor and applying realistic design loads in a finite element method (FEM) analysis to check if the mechanical integrity is maintained and acceptable.

## 4.1 Design of beams

The mechanical integrity of the ITS has to be maintained in order to make a comparable analysis between steel and aluminium. All the beams are originally made from steel type S355, the aluminium redesign is therefore mainly based on increasing the moment of inertia (MOI) to accommodate the difference in yield strength. However, the final design is a result of an iterative optimization procedure between moment of inertia criteria, buckling, extrusion limits and weight savings. Applicable joining methods further affects the final outcome of the beam design. See section 3.2 for more information about mechanical properties of considered aluminium alloys.

Emphasize has been directed to the number of different extrusion dies needed for the whole structure to lower fabrication costs. The plate thicknesses are always divisible by five in order to ease plate procurement, as standard plate thicknesses can be used.

Each beam is given its own designation to organize the structure, an overview of all the beams designations can be seen in figure 4.1.

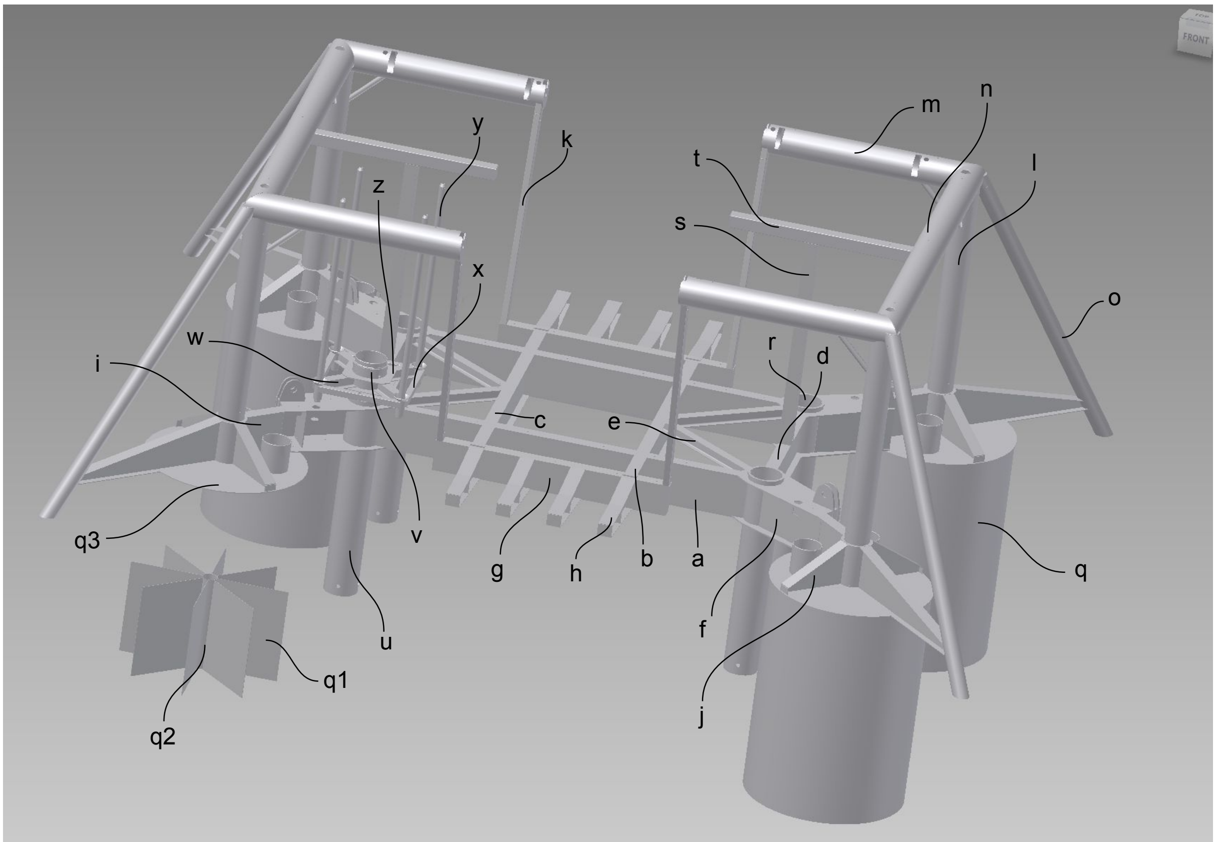


Figure 4.1: The ITS with identification letters, where beam 'a' refers to the beam marked with an 'a' etc.

Both original and new MOI for all beams along with the respective ratios in addition to buckling factor of the redesigned beams can be seen in table 4.1 . The calculations for all beams are attached in appendix D. The results in table 4.1 are based on a formula for mechanical bending stress (eq. 4.1), and the buckling assessment is based on Eurocode 9 [2]. More detailed information regarding local buckling resistance can be seen in section 3.11. The same method is used on beam number 'b' to 'y' as seen in table 4.1.

Table 4.1: MOI of beams, MOI ratios and buckling classification.

| Beam[1)] | $I_{xx,old}$ $10^6$ [mm$^4$] | $I_{xx,new}$ $10^6$[mm$^4$] | $I_{yy,old}$ $10^6$[mm$^4$] | $I_{yy,new}$ $10^6$[mm$^4$] | $I_{xx,ratio}$ [-] | $I_{yy,ratio}$ [-] | $J^{3)}_{co,ratio}$ [-] | $A_{ratio}$ [-] | Buckling[4)] [-] |
|---|---|---|---|---|---|---|---|---|---|
| a | 30134 | 40011 | 3862 | 5687 | 0.753 | 0.679 | 0.744 | 1.027 | Class 2 |
| b, c, d | 10762 | 19407 | 999 | 1411 | 0.555 | 0.708 | 0.565 | 0.519 | Class 3 |
| b* | 4948 | 7081 | 768 | 983 | 0.699 | 0.781 | 0.709 | 0.577 | Class 3 |
| e | 357 | 526 | 183 | 264 | 0.679 | 0.693 | 0.684 | 0.679 | Class 2 |
| f | 43559 | 60618 | 19258 | 28359 | 0.719 | 0.679 | 0.706 | 0.679 | Class 2 |
| g | 6468 | 9648 | 1125 | 1605 | 0.670 | 0.701 | 0.675 | 0.514 | Class 3 |
| h | 4948 | 9050 | 768 | 1288 | 0.547 | 0.596 | 0.553 | 0.469 | Class 2 |
| h* | 636 | 1020 | 421 | 635 | 0.624 | 0.664 | 0.639 | 0.525 | Class 2 |
| i | 11810 | 24215 | 1248 | 2006 | 0.488 | 0.622 | 0.498 | 0.579 | Class 3 |
| i* | 486 | 822 | 449 | 727 | 0.591 | 0.618 | 0.603 | 0.554 | Class 2 |
| j | 11811 | 24215 | 1248 | 2006 | 0.488 | 0.622 | 0.498 | 0.579 | Class 3 |
| j* | 137 | 213 | 335 | 560 | 0.642 | 0.598 | 0.610 | 0.539 | Class 3 |
| k | 298 | 486 | 99 | 226 | 0.613 | 0.420 | 0.550 | 0.781 | Class 4 |
| l | 5357 | 12652 | 5357 | 12652 | 0.423 | 0.423 | 0.423 | 0.595 | Class 3 |
| m, n | 4088 | 7040 | 4088 | 7040 | 0.581 | 0.581 | 0.581 | 0.575 | Class 1 |
| $m_2$, $n_2^{5)}$ | 4090 | 5806 | 4090 | 1231 | 0.704 | 3.323 | 1.163 | 0.500 | Class 4 |
| o | 1183 | 2070 | 1183 | 2070 | 0.572 | 0.572 | 0.572 | 0.591 | Class 1 |
| q | $1155\cdot10^3$ | $1907\cdot10^3$ | $1155\cdot10^3$ | $19057\cdot10^3$ | 0.606 | 0.606 | 0.606 | 0.602 | Class 1 |
| $q_1$ | $108\cdot10^3$ | $180\cdot10^3$ | 1.7 | 8.0 | 0.600 | 0.216 | 0.600 | 0.600 | Class 4 |
| $q_2$ | 575 | 1109 | 575 | 1109 | 0.519 | 0.519 | 0.519 | 0.480 | Class 1 |
| $q_3$ | 6.6 | 39 | $276\cdot10^3$ | $497\cdot10^3$ | 0.171 | 0.556 | 0.556 | 0.556 | Class 4 |
| r, u, v, z[2)] | - | - | - | - | - | - | - | - | - |
| s, t | 485 | 1042 | 485 | 710 | 0.466 | 0.684 | 0.554 | 0.538 | Class 3 |
| w | 418 | 597 | 186 | 280 | 0.699 | 0.666 | 0.689 | 0.651 | Class 2 |
| x | 46 | 64 | 46 | 64 | 0.719 | 0.719 | 0.719 | 0.685 | Class 1 |
| y | 73 | 103 | 74 | 103 | 0.711 | 0.711 | 0.711 | 0.504 | Class 1 |

1) Slim end of beam is marked with *.
2) The beams are made of steel, and hence no change in MOI.
3) Torsional MOI ($J_{co} = I_{xx}+I_{yy}$).
4) See section 3.11.
5)Not in accordance with NORSOK U-002, MOI in y-direction is not within criteria.

Equation 4.2 calculating the necessary moment of inertia to maintain the same bending stress in relation to yield strength with the same applied load is based on bending stress being the only significant form of stress, as the resulting cross sectional area withstanding the moment is large enough to carry the resulting shear and axial stresses. A maximum moment of inertia ratio of 0.718 between original steel and new aluminium design is necessary when considering alloy 6082-T6, and 0.606 for alloy 5083-H116. This conservative beam design approach has been selected since the exact magnitude and location of the loads acting on the beams are uncertain.

$$\sigma = \left(\frac{M \cdot y}{I}\right) \qquad [Pa] \tag{4.1}$$

Where $\sigma$ is the bending stress [MPa], $M$ is the moment about the neutral axis [Nmm], $y$ is the perpendicular distance to the neutral axis and $I$ is the second moment of inertia about the neutral axis [$mm^4$].

By dividing equation 4.1 for aluminium alloy 6082 with 255 MPa in yield strength by the same equation for steel S355 with 355 MPa in yield strength the following is obtained:

$$\frac{\sigma_{Al}}{\sigma_{St}} = \frac{\left(\frac{M*y}{I_{Al}}\right)}{\left(\frac{M*y}{I_{St}}\right)} \Rightarrow \frac{255}{355} = \left(\frac{I_{St}}{I_{Al}}\right) = 0.718 \tag{4.2}$$

The height has been changed for some of the beams ('a', 'b', 'c', 'd', 'f', 'i' and 'j') erecting the base frame in order to increase the second moment of inertia, meaning the "y" in eq. 4.2 is different for aluminium and original design. To exemplify, the height change from 1.4 meters to 1.5 meters results in a "y-factor" of $0.75/0.7 = 1.07$. This will have an amplification on the identified ratio of 0.718 by $0.718 \cdot 1.07 = 0.769$ for the mentioned beams.

Beam 'a', 'f', 'k', 's' and 't' originally designed as squared pipes have been changed to an I-beam design. I-beams have greater potential in reducing weight since the I-beams possess a more effective design in terms of moment resistance. Closed compartments followed by squared pipes are in addition avoided.

For large I-beams that are impossible to extrude as one profile ('a', 'b', 'c', 'd', 'f', 'g', 'h', 'i' and 'j'), the top and bottom flange shall be extruded in alloy 6082-T6 with a built-in guide way for the web, and a 5083-H116 alloy web plate. The web and flanges shall be joined with two fillet welds each oriented at the guide way by MIG welding, as illustrated in figure 4.2. The guide way is designed to avoid a HAZ in the extruded part of the web, and to orient the weld at an area with lower bending stress. The length of the web extrusion is based on a linear distribution of stress from the neutral axis towards the top or bottom of the beam where bending stress is peaking. The length is estimated such that the bending stress in the HAZ will not exceed the HAZ strength of alloy 5083-H116 (150 MPa). See section 3.6.1 for relevant theory of the HAZ effect. For beams erected with an extruded flange, it is appropriate to use 0.718 as the design criteria between original steel beam and new aluminium beam since the moment is known to be highest at the location farthest away from the neutral axis.

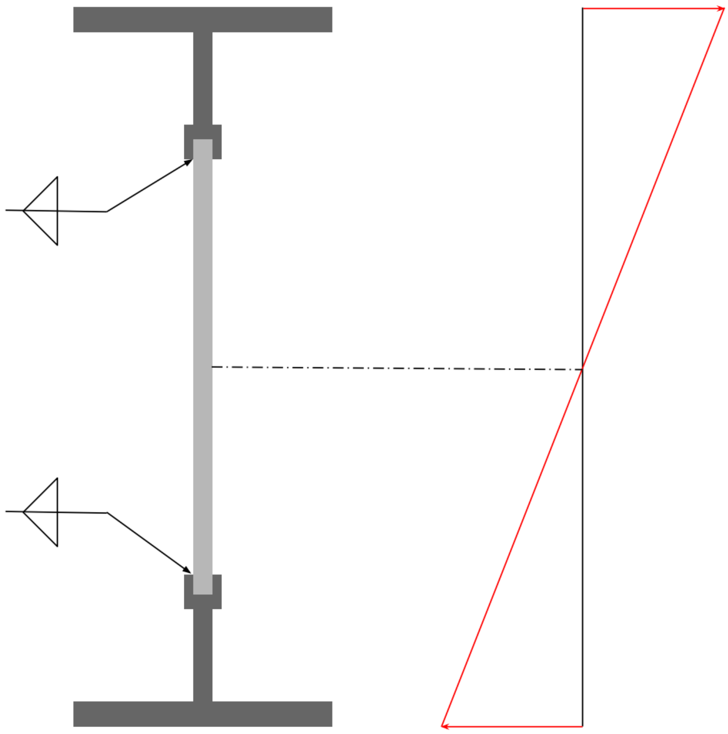

Figure 4.2: I-beam with a built-in guideway for the 5083-H116 plate in the 6082-T6 flange profile. Along with illustration of linear distribution of bending stress and orientation of fillet welds.

The beams ('l', 'm', 'n' and 'o') erecting the overtrawlable grid, is intended to be manufactured by bending a 5083-H116 plate into a circular tube closed by the use of FSW or MIG welding. The longitudinal welds shall be oriented as close to $90^o$ to the direction of overtrawlable loads as possible in order to locate the HAZ away from maximum bending stress. The weld in for instance beam 'n' should therefore be located down and inwards as shown in figure 4.3. The HAZ magnitude is only 2.8% of total cross sectional area, loss of shear and axial resistance is thereby negligible. The 0.606 MOI criteria is used for tubes made of alloy 5083-H116.

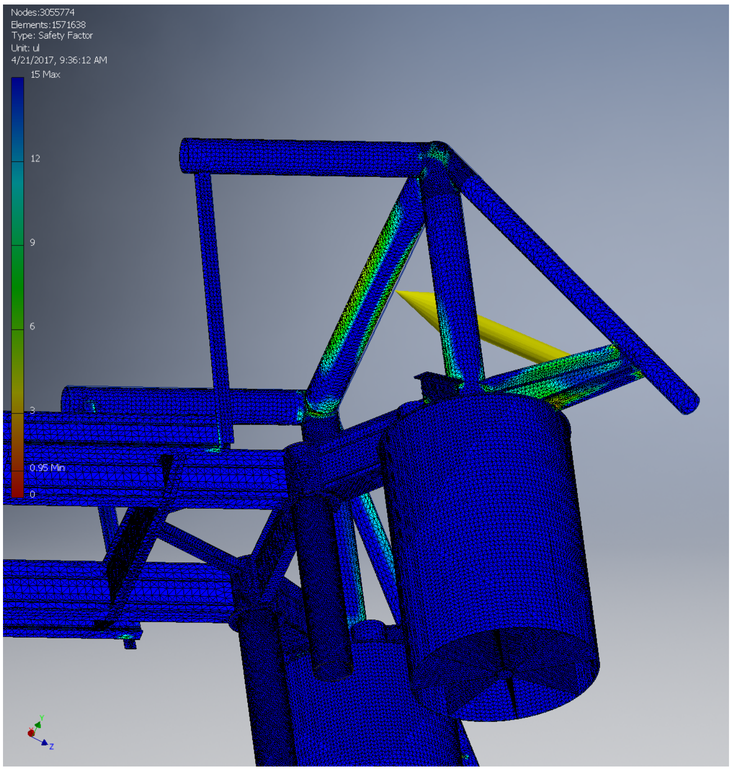


Figure 4.3: Stress distribution in beam 'n' when loaded with 1000 kN (yellow vector).

Two manufacturing methods for the cylindrical suction anchor (beam 'q') is evaluated. These two methods are based on plate size restrictions, 3.05 m width and 36 m length [79], that must be fulfilled in shaping a 15.675 m cylindrical perimeter. One possibility is to bend two plates into a tube, and bond them with one vertical and one horizontal friction stir weld. Another possibility is to friction stir weld six plates and subsequently bend them into a cylinder. The latter is regarded as the optimal alternative in consideration of preserving full strength from top to bottom of the anchor when a horizontal weld is avoided. However, the first method mentioned offers less welding but not more than the equivalence of three vertical welds as one horizontal weld approximately equals the length of two verticals (14 m). The top plate is too big to be made from one plate due to the large diameter (4.992 m) exceeding the plate size restriction, it should therefore be shaped by bonding two plates with the use of FSW. One plate is intended to be larger than the other, where the largest has a length and width of $4.992 \cdot 3.05$ m due to larger stresses towards the center. See section 4.2.2 for welding methods applicable to each joint on the structure. An illustration of the suction anchor with welds can be seen in appendix F.3.

Beam ’$q_1$’ and ’$q_3$’ are denoted with buckling class 4 as seen in table 4.1, the buckling class for the beams is however not considered to be problematic. Beam ’$q_3$’ is supported by the crossing beams ’i’ and ’j’, which are assumed to be enough reinforcement against local buckling. In addition, the only design change for these beams from the original steel design is an increase in thickness, meaning that the buckling resistance in new design should not be any lower than the original.

The insufficient buckling class of beam ’k’ seen in table 4.1 is assessed by calculating the MOI’s with a lowered effective thickness, 15 mm instead of 20 mm. The effective thickness is found from eq. 3.17 in section 3.11. The obtained effective MOI is thereby lower than the actual, which results in a reduction of maximum design moment. The relation between design moment and MOI can be seen from eq. 4.1.

The moment of inertia ratio for beam ’b’ (small end of beam) in y-direction (along the web) is 0.781, meaning it is violating the 0.718 criteria. That is because beam ’c’ is designed continuously through beam ’b’, which hinders an individual iterative procedure on the slanting beam ’b’ as the dimensions are set for beam ’c’. However, the extruded flange oriented at the bottom of beam ’b’ as illustrated in figure 4.4 is designed individually meaning it is subject to change to accommodate the moment criteria. Optimization of the bottom ’b’ flange is neglected as it is believed to not significantly influence the outcome of the complete design.

The slanting beams ’h’, ’i’ and ’j’ are heightened in the small end to create enough space for the built-in guide way extrusions and web plate, see figure 4.5 for illustration of beam ’h’. Otherwise it would cause unnecessary difficulties erecting the beams. For beam ’h’, only the bottom slant is changed due to sealine interaction on top of beam.

Dimensions of I-beam ’k’ and ’e’ are within the extrusion limits listed in table 3.5, and are therefore intended to be fully erected by extrusion. I-beam ’s’ and ’t’ are designed to be made of two extruded flanges with large enough web length to accommodate for the beam height, where they can be subsequently bonded by FSW or MIG welding at the neutral axes of bending moment.

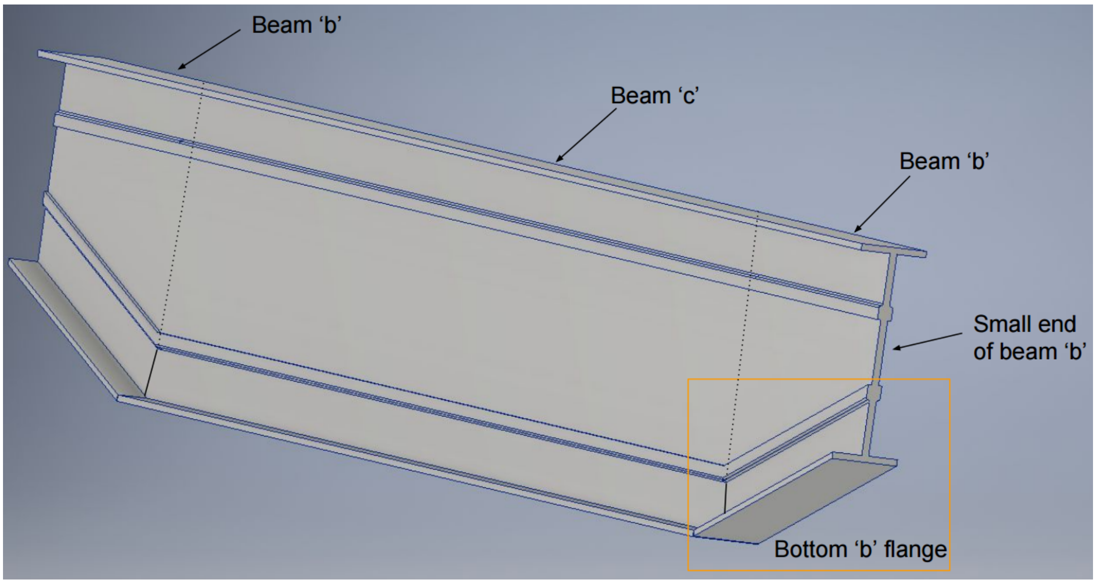


Figure 4.4: Merged ’b’ and ’c’ beam.

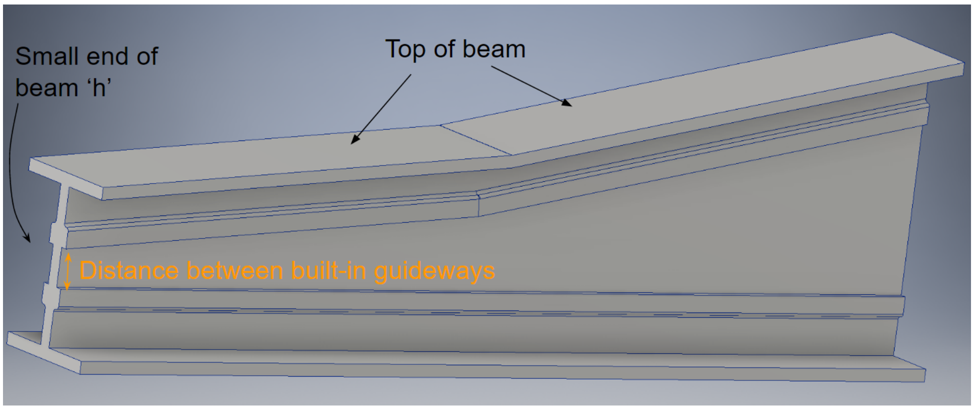


Figure 4.5: Heightened Beam ’h’.

Beam ’f’ is intended to be erected by two I-beams in order to match the MOI from the original square steel beam, see figure 4.6. The I-beams are intended to be connected by the use of FSW on the top and bottom flange facing each other. The moment resistance in the y-direction seen in figure 4.6 should not be decreased significantly as the weld is oriented at the center of rotation (low stress area). Generally, the HAZ caused by welding the I-beams in figure 4.6 does not affect the beam’s strength significantly, as the HAZ area is small compared to the affected area.

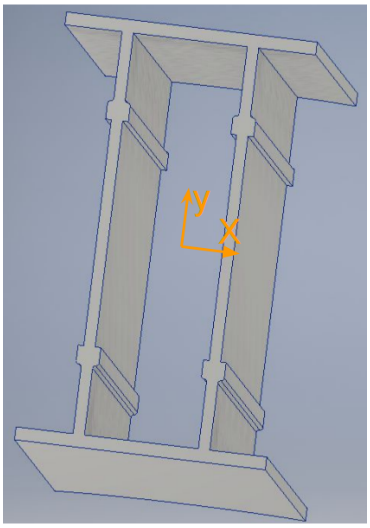


Figure 4.6: Beam ’f’ with respective x and y MOI directions.

Beam ’m’ and ’n’ cannot be made by extrusion, as their dimensions are way too large for any of the identified extrusion presses given in table 3.5. Two types of beam design have been reviewed, and both can be seen in figure 4.7 and table 4.1. In table 4.1 the beams ’$m_2$’ and ’$n_2$’ has an unfavourable $I_{yy}$ ratio, due to the change in geometry as seen in figure 4.7. This design is not in accordance with NORSOK U-002 [14], as the requirement for external edges/members shall have a minimum radius of 250 mm, which is not fulfilled. However, placing the beam in such a way that the circular edge is facing the external loads (trawl loads) could be sufficient, dependent upon the interpretation of the NORSOK U-002 standard [14]. Emphasize has been on producing a realistic design which can be introduced into the industry, thus the NORSOK approved design is therefore selected as a basis for all further design analyses.

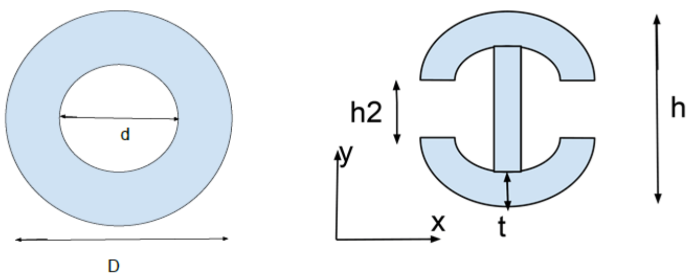


Figure 4.7: Two alternatives for beam ’m’ and ’n’, where the left one is in accordance with NORSOK U-002 for D ≥ 250mm.

## 4.2 Design of joints

Some of the structure's joints will have to be redesigned to accommodate the use of aluminium as construction material. This is especially so with respect to welds as aluminium MIG welds result in a reduced mechanical strength of approximately 30-50% in the HAZ zone, dependent upon the aluminium alloy as described in section 3.6.1. Bolting has also been introduced as an alternative joining method to welding, as bolted sections enables joining without any significant strength reduction in the base metal of bonding section. A more detailed review of bolting with its advantages and drawbacks has been conducted in section 3.8.

The X-mas tree supports (beam 'x', 'y' and 'z') are regarded as negligible in terms of structural integrity of the base frame connected to suction anchors, since the X-mas support is resting on the steel tube (beam 'r'), which is designed to be jointed with the intersecting base frame beams ('a', 'c', 'd' and 'e'). The X-mas tree support is however important in itself supporting the X-mas, but an aluminium joint design of the support is left out of this study, as it is known to be achievable.

All joints on the concerned ITS is designated with roman numerals in figure 4.8. The joints are further designated with a subscript specifying the beams to be bonded (e.g. $V_{a-a}$), which should ease the understanding of orientating for each joint when described below.

### 4.2.1 Bolted joints

An analysis of all the bolted connections have been conducted in accordance with Eurocode 9 [2]. Forces acting on each joint are presented in table 4.2, and dimension of bolt plating, arrangement and number of stainless steel bolts are tabulated in table 4.3. The results given in table 4.3 are only valid for stainless steel bolts as this is the most conservative approach comparing the use of stainless and carbon steel bolts. Only difference in calculation input between the two bolt materials in this analysis is the TS entered in eq. 3.3. The difference in plate dimensions and total number of bolts, 1468 vs 1336, used in weight and cost assessments are therefore regarded as negligible. The numerical calculation sheets created in the analysis can be found in appendix C. The bolts are designed as slip resistant, eq. 3.3 and 3.4 are thereby used to find the number of bolts required for different bolt types ranging from M20 - M39. M36 are found to be suitable for all joints, considering the number of bolts and joint size. All bolt joints designed as spliced beam connections are assumed to support all shear forces in the web while the flange supports all tension and compressive forces, which is mainly obtained from moment. An ultimate limit safety factor of 1.25 is used in the bolt calculations and the slip factor is set to 0.4 in accordance with standards [2].

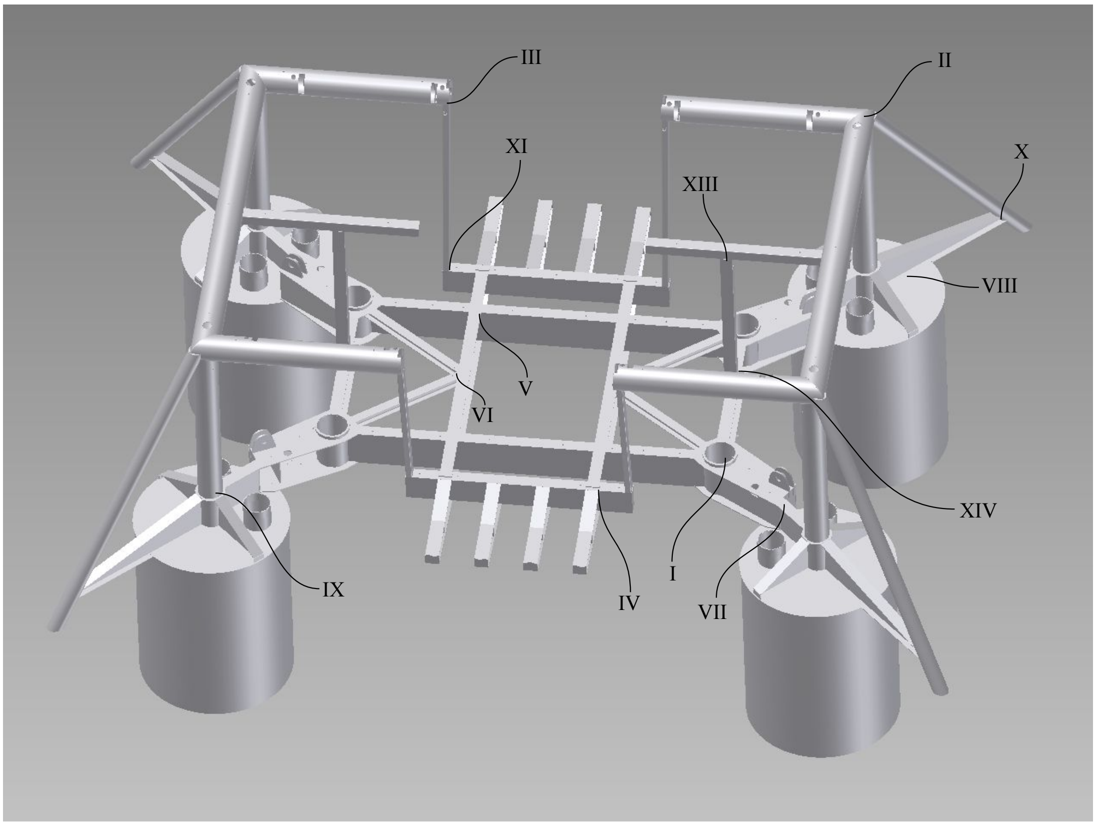


Figure 4.8: Joints designated with roman numerals.

There are uncertainties related to which structural joints the loads are applied on for the base frame connected to suction anchors, the maximum moment in beam 'a' is therefore calculated by using the moment of inertia and design strength of the original steel beam, where the design strength is obtained by dividing the yield strength with a safety factor for steel, 1.15, stated in NORSOK N-001 [80]. By re-arranging eq. 4.1, 1300 kNm is obtained as the maximum moment. The resulting moment distribution along the beam is further assumed linear between the mid point (maximum load) and the suction anchor support, where the moment is assumed to be zero as outlined in figure 4.9. Table 4.2 presents the calculated values of the respective moments and forces in joint $V_{a-a}$, $I_a$ and $I_f$. Since the beam is designed to accommodate maximum moment it will be overly conservative to find shear forces from geometry of the beam. Maximum shear force in beam 'a' is found by dividing the maximum moment by half the beam length, resulting in 1625 kN. Considering the amount of weight supported by the base frame, the magnitude of the calculated shear force is coherent. Beam 'f' is however calculated with 2000 kN shear force as this beam is assumed to be subjected to the highest shear forces.

Table 4.2: Forces acting on the bolted connections.

| Connection | Moment [kNm] | Flange force [kN] | Web force [kN] | Comment |
|---|---|---|---|---|
| $I_a$ | 4998 | 3452[4)] | 1625 | Moment is 3/8 of maximum moment (1300 kNm). |
| $I_d$ | 1662 | 1131[4)] | 100 | Moment is 1/8 of maximum moment[1)]. |
| $I_f$ | 3326 | 2301[4)] | 1625 | Moment is 2/8 of maximum moment. |
| $I_e$ | 0 | 200 | 0 | Assume 200 kN tensile force[2)]. |
| $V_{a-a}$ | 9977 | 6904[4)] | 1625 | Moment is 6/8 of maximum moment. |
| $V_{b-c}$ | 518 | 652[4)] | 100 | 5180 mm moment arm[3)]. Only one internal bottom flange. |
| $IV_{h-g}$ | 340 | 650[4)] | 100 | 3400 mm moment arm[3)]. |
| $IV_{b-g}$ | 380 | 692[4)] | 100 | 3800 mm moment arm[3)]. |
| $VI_{c-e}$ | 0 | 200 | 0 | Assume 200 kN tensile force[2)]. |
| $XI_{g-k}$ | 460 | 66 | - | Calculated from geometry of beam 'k'. |
| $XIV_{d-s}$ | 750 | 111 | - | Calculated from geometry of beam 's'. |
| $XIII_{s-t}$ | 0 | 111 | - | Calculated from geometry of beam 's'. No moment acting on beam 't'. |

1) Loads on beam 'd' are uncertain. Conservative to use 1/8 of maximum moment.
2) Joint force is not known. An assumption is made.
3) Arises from pull in forces (section 4.3.2).
4) Flange force = Moment/Height of beam.

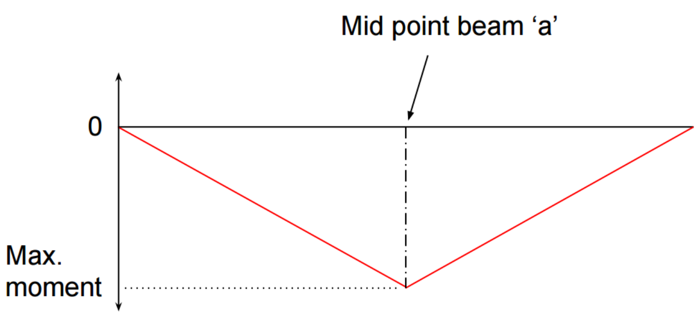


Figure 4.9: Assumed bending moment distribution in beam 'a'.

Connection ’$V_{b-c}$’ and ’IV’ are dimensioned for maximum axial and vertical sealine loads. Maximum tensile sealine load (between $0^o$-$15^o$ horizontally) on one beam is 300 kN, and maximum loading on all four sealine supports are 600 kN, giving rise to various scenarios of sealine loads described in section 4.3.2. However, $2 \cdot 300$ kN is considered in calculations. Some extra loading is added vertically in bolt calculations due to an unknown weight of sealine. Vertical load used in bolt calculations on one sealine support is then 100 kN. These loads creates moment, tensile and shear forces in joint ’IV’ and ’V’, the resulting shearing loads are negligible and the connections are therefore designed with only spliced flanges that have capacity to support all forces.

The ’$XIV_{d-s}$’ connection is designed to accommodate maximum moment and resulting shear force calculated from geometry of beam ’s’ as seen in table 4.2. The connection between beam ’d’ and ’s’ is retrofitted with a $90^o$ angled plate on the top and bottom flange of beam ’d’. Connection ’$XI_{g-k}$’ is jointed in the same way with an angled plate that is fitted to the angle between beam ’g’ and ’k’. Plates on each flange is used in connection ’$XIII_{s-t}$’ to carry the calculated shear force in table 4.2. See figure 4.10 for illustration of joint ’$XIII_{s-t}$’ and ’$XIV_{d-s}$’.

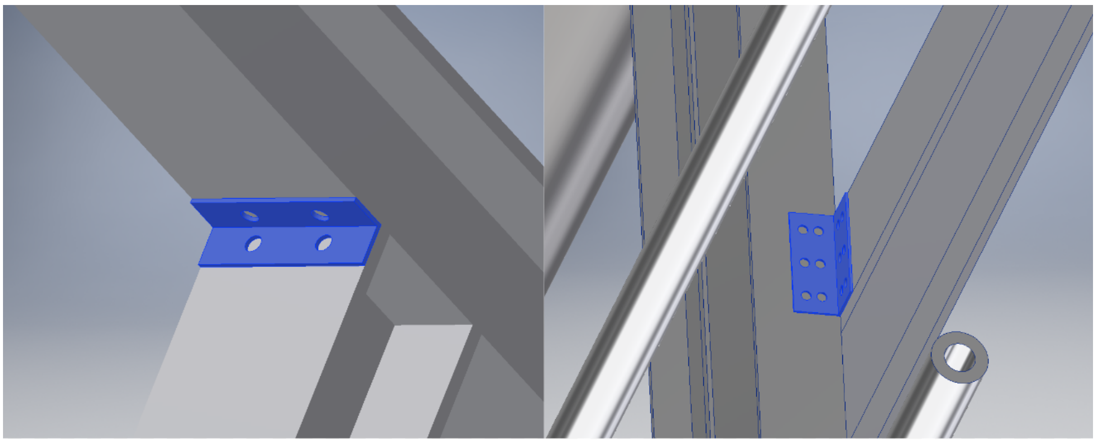

Figure 4.10: Angled bolt plating on joint ’$XIII_{s-t}$’ (left) and ’$XIV_{d-s}$’ (right).

Table 4.3: Dimensions of bolt plating and number of bolts required.

| Connection | Flange plate dimension external/internal (l-$w_e$/$w_i$-$t_e$/$t_i$) [mm] | Web plate dimension (h-w-t) [mm] | Length of cross section flange/web [mm] | Number of flange/web bolts for all connections[1)] | Sum M36 stainless steel bolts |
|---|---|---|---|---|---|
| $I_a$ | 610-500-25 | 600-200-10 | 80/70 | 208 (4x7)/ 48 (2x6) | 256 |
| $I_d$ | 438-500-10 | 200-150-10 | 40/55 | 72 (2x5)/ 8 (1x2) | 80 |
| $I_e$ | 188-300/ 0-10/0 | 0 | 42/0 | 16 (2x1)/0 | 16 |
| $I_f$ | 400-880-25 | 600-200-20 | 70/60 | 208 (8x4)/ 60 (2x4) | 268 |
| $V_{a-a}$ | 1220-500/ 420-40/40 | 600-150-10 | 135/80 | 416 (4x9)/ 48 (1x6) | 464 |
| $V_{b-c}$ | 532-0/ 550-0/15 | 0 | 45/0 | 48 (2x3)/0 | 48 |
| $IV_{h-g}$ | 360-330/ 265-10/10 | 0 | 50/0 | 128 (2x2)/0 | 128 |
| $IV_{b-g}$ | 360-330/ 265-10/10 | 0 | 50/0 | 64 (2x2)/0 | 64 |
| $VI_{c-e}$ | 188-300/ 0-10/0 | 0 | 42/0 | 16 (2x1)/0 | 16 |
| $XI_{g-k}$ | 180-300-10 | - | 50/- | 64 (2x2)/- | 64 |
| $XIV_{d-s}$ | 180-420-10 | - | 40/- | 48 (3x2)/- | 48 |
| $XIII_{s-t}$ | 100-420-10 | - | 45/- | 16 (2x1)/- | 16 |
| Sum | | | | | 1468 |

1) Bolt arrangements are given in parentheses.

Flange and web plating used in the bolted joints must be designed to withstand the transmitting forces, meaning that stress should not exceed YS reduced by the appropriate safety factor for aluminium, 1.2, [80], and dimensioned according to bolt arrangement and required spacing as seen in figure 3.16. Plate dimensions and number of bolts together with the cross-sectional bolt length for each joint are tabulated in table 4.3.

Joint 'I' is designed as a steel tube with welded steel plates that will function as flange and web for each connected beam ('a', 'd', 'e' and 'f'). The extensive use of steel in joint 'I' is due to difficulties bonding four interconnecting beams, the joint is critical, and it is assumed to be beneficial to have a steel surface interacting with drilling equipment.

Beam ’f’ is made up of two I-beams as seen in figure 4.6, the inside of the webs and flanges will thereby possess a limited access for bolt assemblies. The web and flange bolts must therefore be fastened to the steel plates bonding joint ’I’ and beam ’f’ before welding the plates onto the steel tube. Inspection should be possible either through the opposite side of the beam or through retrofitted holes.

### 4.2.2 Welded joints

Some of the joints shall be welded as it is believed to be more beneficial than bolting in terms of fabrication cost, availability and uniform beam surface, which is required for the overtrawlable tubes on top of the structure. All welds are to be placed away from stress concentrations. Welded areas are checked for stresses with the use of FEM analysis in Autodesk Inventor. Stress in welded areas can be assessed in Autodesk Inventor using contour plot for the stress results.

MIG welding is a well established and commercial cost efficient method that is very well documented in standards as seen in section 3.6.1, and it is the recommended welding method by Marine Aluminim [34]. It should therefore be used on all fillet welds required (e.g. joint ’I’, ’III’, ’VII’, ’VIII’, ’IX’ and ’X’). For butt welds (e.g. beam ’q’), FSW is believed to be the preferable method as long it is possible to weld without a hand-held apparatus as seen in section 3.6.2. Quality of welds is critical and shall therefore be assured appropriately as outlined in standards [2].

Beam ’i’ is designed continuously through joint ’VII’ where the intersecting ’j’ beams are welded onto beam ’i’. Beam ’i’ and ’j’ are additionally intended to be welded to the suction anchor. Bottom end of beam ’l’ is further designed with four tracks welded on the intersecting beams, with additional welds on the suction anchor at the bottom. The larger beam ’f’ is functioning as an extension for beam ’i’ towards joint ’I’. Beam ’f’ should be welded onto beam ’i’ and top of suction anchor, see figure 4.11 for illustration.

Joint ’II’ is designed with an insert embedded in all four tubes intersecting the joint. An insert is used in order to accommodate strength losses from welding, which enables stress resistance obtained from moment. All tubes shall be circumferential FSW or MIG welded individually as outlined in figure 4.12.

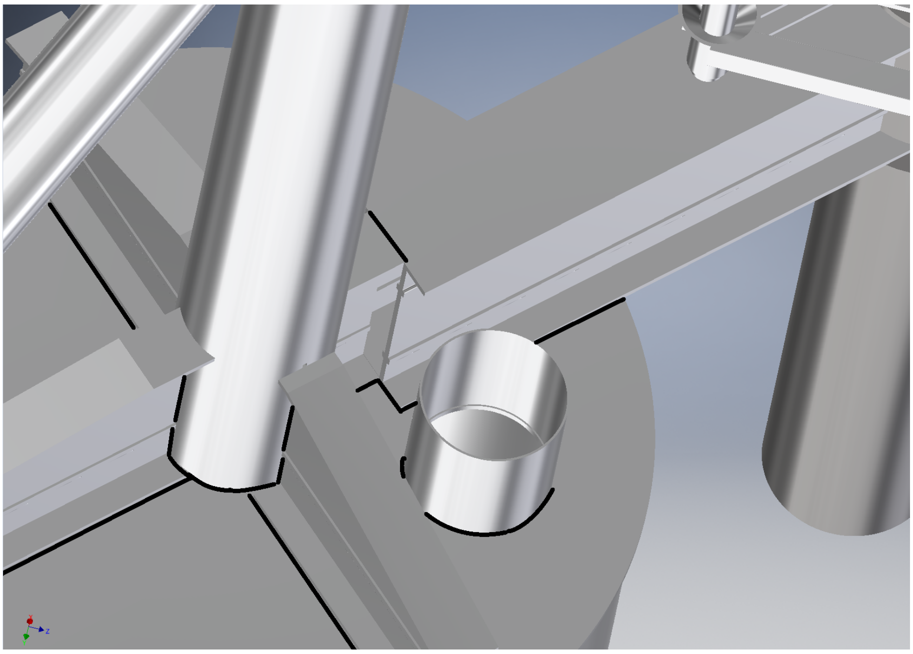

Figure 4.11: Weldments on suction anchor and beam ’i’, dark lines are weldments.

Manufacturing of the insert seen in figure 4.12 has proven to be challenging, due to the relative large size that must be machined as one unit from one of the NORSOK approved alloys. See section 6.4.2 for further discussion about this challenge.

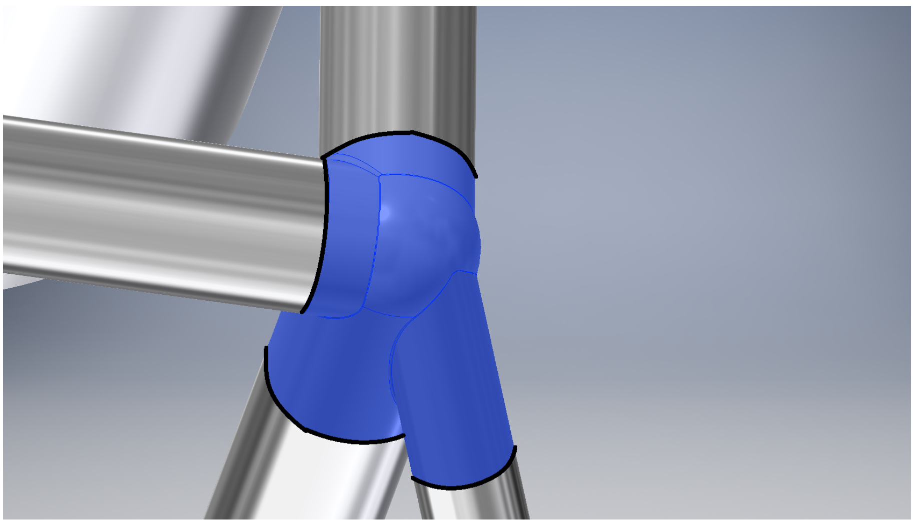

Figure 4.12: Weldments on insert, dark lines are weldments and the insert is colored blue for better vision.

All connections on the suction anchor are designed to be welded, because it is not an optimal choice to bolt through the top plate of the suction anchor. As the availability to assemble the bolts is restricted and it would be very difficult to inspect bolts inside the anchor after installation. The relatively large bonding area on the suction anchor is advantageous in terms of joining since the joint forces are spread over a large area, and stresses generally lowers with larger area. The internal stiffeners ('q1', 'q2') located at the bottom of the suction anchor is also designed intently to be fastened by welding.

Joint 'I' shall be made up of a steel tube with welded steel plates as mentioned in section 4.2.1. The effects that may mitigate from steel welding has not been analyzed, as it is out of scope for this study. However, the steel welds should not introduce any problems of concern.

## 4.3 Loads

The ITS is subjected to loads during installation and operation. Lift off, splash zone and tie-in loads are considered installation loads. Dropped objects, drilling and trawling loads are treated as operational loads. Loading from weight of X-mas trees and manifold supported by the ITS are defined as static loads. A broad explanation of relevant load scenarios are given in this chapter, while numerical summation of load values are found in appendix A. Loads that may occur during barge transport is not included in this study.

### 4.3.1 Lift off and splash zone loads

The lifting operation interval from the ITS is lifted from deck until it is completely immersed in seawater is the most critical process during installation. The ITS is subjected to added mass from seawater, slamming forces from seawater/waves and fluctuating loads when airborne. There are four dynamic forces and one static force to be considered in the splash zone [81], all of them are further described in appendix A.1. Note that the loads occurring before and during splash zone penetration mainly concern the crane capacity, and not the integrity of the ITS. However, care must be taken into account during hydration of air filled compartments (e.g. suction anchor) due to the airflow leaving the compartments and the

ITS could be buoyant enough to cause slack of lifting wire. Dynamic loads during the critical process can be accounted for by a dynamic amplification factor (DAF). A DAF value of 1.25 should be used offshore when lifting 100-300Te heavy structures [82]. The weight of the lifting rig (connecting crane wire and lifting points) on the ITS itself should in addition be added to the structural weight, the lifting rig weight is tabulated in table 4.10. For deeper waters (more than 500 m) the weight of the wire may be significant, especially for an ITS made of steel. However, an ITS made of aluminium as in this case are more readily immersed to deeper waters since the buoyancy factor is significantly lower for aluminium (0.63) than for steel (0.87). The weight of the wire is neglected in this study, in order to ease calculations.

The crane capacity must be greater than structural weight (incl. lifting rig) multiplied by the DAF. The lifting force on each of the four lifting point can not be found by simply dividing the main lifting force by four. The angle on the wire sling connecting the lifting rig and lifting points on the structure must be accounted for. A global skew load factor (SKL) of 1.25 as defined in DNV-OS-H205 [82] may be added to the force (included DAF) on each lifting point in order to calculate the resulting wire force. The SKL is only valid for angles less than $60^o$ horizontally [82]. Maximum design force on the main lifting wire is then 2453 kN, and the resulting force on each lifting point is 766 kN. See e-mail correspondence with Asbjørn Wathne (Subsea 7) in appendix B.5 for some details on ITS lifting and installation operation.

### 4.3.2 Pull in of umbilicals and pipelines

Pull in loads are related to hydraulic forces used to pull the pipeline or umbilical into desired position. In the case of an ITS used in this study, the maximum pull in load for all the sealine supports (four support arms) combined is 600 kN. Giving rise to multiple load cases, for example $4 \cdot 150$ kN or $2 \cdot 300$ kN [15]. Note that the maximum pull in load on one sealine support is 300 kN. The load direction may be in an inclination range of 0 to 15 degrees horizontally. Maximum vertical design load is therefore 77 kN. Scenarios of sealine loads are defined in appendix A.4. The weight of the sealines and umbilicals are uncertain, however it should not lead to a load of any significant size, as it is known to be much lower than pull in load. Pull in shall only be performed after the template structure is lowered into final vertical position (final setting of suction anchor).

### 4.3.3 Drilling and trawling loads

The drilling loads are found from NORSOK U-002 [14] that describes loads for different activities. There are two cases outlined in the standard, one for water depths up to 750 m and one for depths up to 1500 m. Only the first case is considered in this study to limit the scope of work. The "750 m case" is defined in appendix A.5. The largest loading occurring during drilling is when the 30" conductor is lowered. The temporary design load from the conductor weight is 600 kN in the vertical direction.

All subsea installations in Norway have to withstand overtrawling from fishing gear. Load types to be considered are trawl net friction, trawl board overpull, trawl board impact and trawling snag. See appendix A.2 for tabulation of the different trawl load scenarios. The most severe load case is snagging of trawl ground rope, which is in the magnitude of 1000 kN. However, a subsea structure may not be designed against snag loads if the structure is documented to be snagfree/overtrawlable. The most severe load case for a snagfree/overtrawlable design is $2 \cdot 200$ kN in trawl net friction. The original steel ITS design is known to possess a snagfree design, see appendix B.4 for e-mail correspondence concerning overtrawlability. Nevertheless, 1000 kN are used in section 4.4 as a conservative approach.

### 4.3.4 Dropped objects

Impact energy from dropped objects can be seen in appendix A.3. These objects are normally accidentally dropped from topside vessel, but can also come from fishing vessels. The protective hatches fitted on top of the ITS to protect the X-mas trees and manifold from dropped objects are neither modelled or designed, as it is left out of scope in this study. It should be noted that aluminium made protection structures have been successfully used on the NCS on the Lille-Frigg field [34].

### 4.3.5 Static loads

Static loads from support of X-mas trees and manifold used in calculations can be seen in appendix A.2. Note that the buoyancy factor for steel in seawater will lower the loading from components to be supported by the ITS by an estimated factor of 0.87, as the components are installed after final installation of the ITS. Buoyancy factor is not included in analysis, as the factor of 0.87 is only an estimate for the manifold and X-mas trees and excluding the buoyancy factor is the most conservative approach.

## 4.4 Model

An assembly model containing all the redesigned components in section 4.1 has been built to run global stress analyses to validate the new design. The computer aided design (CAD) software Autodesk Inventor has been used to design, assemble and analyse the structure. A figure of the assembled and meshed structure can be seen in figure 4.13. Bolt assemblies are not included in the model, however stress concentrations of concern, especially for joints and welds will be identified on the stress contour plots. All analyses are based on the finite element method, hence the results are only valid within the materials elastic area, where the materials have a linear stress-strain relation.

All the components in the model have to be designated a material before the simulation can be performed. Aluminium alloy 6082-T6, aluminium alloy 5083-H116 and steel S355 are the three materials used in the model. The different components designated material can be found in section 4.1.

The mesh is generated with an average element size of 0.100, as it is the recommended value by the software developer [83]. A smaller value would result in a more accurate and time-consuming analysis. The number of nodes and elements may vary from each load case and evaluation as there may be a need to edit the mesh set-up for each simulation, due to changes in load or fixed objects/surfaces. Approximate numbers for both element size and nodes can be seen in table 4.4. The general approach for the simulations are the following:

Create contact points →Mesh set-up→1. Simulation→Result interpretation→Fix mesh set-up→2. Simulation→Result interpretation→...

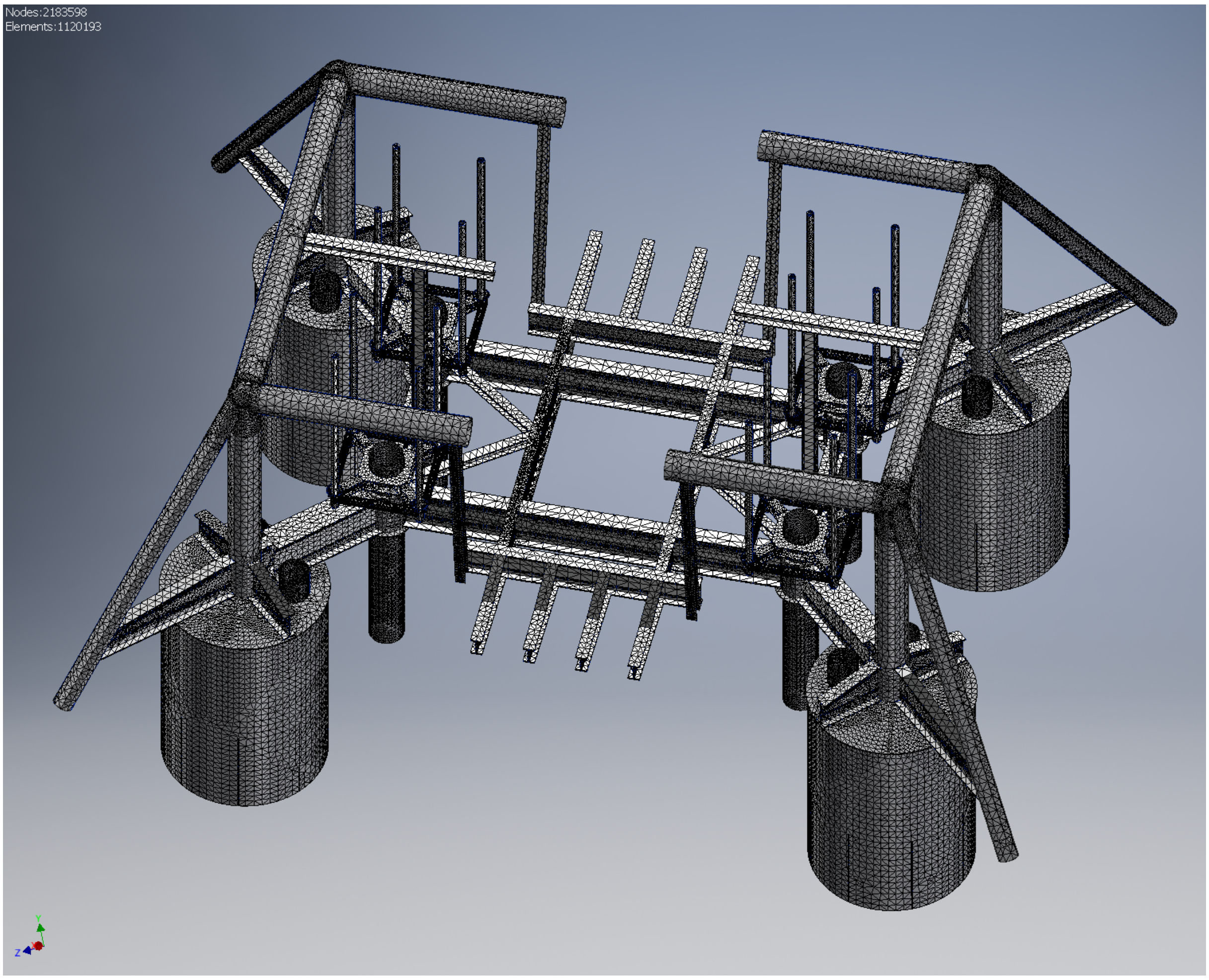


Figure 4.13: Assembly model of the redesigned integrated template structure.

Table 4.4: Input numbers for mesh and resulting number of elements and nodes.

| Number of elements | Number of nodes | Average element size[1)] | Minimum element size[1)] |
|---|---|---|---|
| ca. 1 150 000 | ca. 2 225 000 | 0.100 | 0.200 |

1) Input value for mesh-generation.

This is an iterative process where step five (Fix mesh set-up) and forward are repetitive processes. The reason for selecting this approach is to identify stress singularities that may be inaccurate near stress concentrations. The theoretical stress around such stress singularities are infinite, and should therefore be left out of the evaluation. Stress singularities are normally found surrounding sharp edges or sharp corners. A convergence plot can be made in the simulation to interpret the results and decide if there is a stress singularity present, or if the stress is caused by a stress concentration. A convergence plot is created in Autodesk Inventor by increasing mesh density on the structure locally around the peak stress several times to see how the stress changes with smaller element sizes. If the plot converges towards a limit the stress is caused by a stress concentration, if the stress is divergent (stress does not converge towards a single value) there is a stress singularity present [84].

The applied boundary conditions for the structure is not entirely realistic as a solid clay model has been applied for the suction anchors. Meaning the skirt of the suction anchor is set to fixed position (no vertical or horizontal displacement). A more realistic approach would take into account the undrained shear strength of the soil and the displacement of the suction anchor skirts. The boundary condition for each stress analysis can be seen in appendix I.

### 4.4.1 Load cases

Multiple load set-ups are necessary to accommodate all the possible load scenarios. Table 4.5 lists all modelled set-ups, the loads are taken from section 4.3 containing load definitions and combined as described in NORSOK U-002 [14] for up to 750 meters seawater depth. All events described in the NORSOK standard are covered in the cases seen in table 4.5, except for the impact loads.

The impact/dropped object loads are excluded from simulations due to uncertainties regarding modelling of impact loads and to limit the workload. Some qualitative comments regarding dropped object loads can be provided based on material properties and the geometrical design of the structure. Dropped object loads are according to NORSOK U-002 [14] designed as PLS loads, hence plastic deformation of the structure is accepted, which is positive for aluminium as it possess better ductile properties compared to steel. The aluminium structure's increased moment of inertia described in section 4.1 have to compensate for aluminium's reduction in energy absorption compared to steel. Steel has better energy absorption properties due to higher yield strength and higher E-modulus, however if energy absorption is measured per weight unit, aluminium is favourable to steel as described in reference from the automobile industry [45]. Any further assessment regarding impact/dropped object loads are left out of scope in this study.

The applicable loads for trawling and tie-in are defined with a horizontal angle, as seen in appendix A. These angles ranging from 0 to 20 degrees with the horizontal plane are not considered in FEM analyses, as it would increase the number of cases to simulate substantially, and each case is very time consuming to simulate.

Table 4.5: ITS load cases.

| Case # | Load [kN] | Load type | Reference |
|---|---|---|---|
| A | 1000-$H^{6)}$ | Trawl ground rope snag | Section 4.3 |
| B[1)] | 1000-$H^{6)}$ + 800 | Trawl ground rope snag + Manifold weight | Section 4.3 |
| C[2)] | 1000-$H^{6)}$ + 800 + $2 \cdot 300$ | Trawl ground rope snag + Manifold weight +Tie-in | Section 4.3 |
| D[4)] | $4 \cdot 600$+ (450 + 200-$H^{6)}$) + 800 + $2 \cdot 300$ | X-mas trees + Drilling loads + Manifold weight + Tie-in | Section 4.3 |
| E[4)] | 1000-$H^{6)}$ + 600 + 800 + $2 \cdot 300$ | Trawl ground rope snag + Drilling loads + Manifold weight + Tie-in | Section 4.3 |
| F[5)] | 1000-$H^{6)}$ + 4*600 +800+$2 \cdot 300$ | Trawl ground rope snag + 4* X-mas trees + Manifold weight + Tie-in | Section 4.3 |
| G[7)] | $4 \cdot 766.5$ | Offshore installation load | Section 4.3 |

1) Weight of manifold is approximately 800 kN.
2) Tie-in loads are $2 \cdot 300$ kN divided on to tie-in ports.
3) 600 kN during installation of 30" conductor (temporary drilling load).
4) Unrealistic to happen as trawling cannot happen while drilling is ongoing, but provides information regarding integrity and conservatism in design.
5) 4 installed X-mas trees, each weighting approximately 600 kN.
6) -H means the load is to be applied in horizontal direction.
7) Lifting the ITS-structure offshore, with an angle of $60^o$ the load is measured in dry weight as described in section 4.3.

### 4.4.2 Results

Results from all the simulations will be presented in this section with necessary comments concerning the results. All results can be seen in appendix I.

### Case-A

Case-A represents a trawl ground snag resulting in a maximum von-Mises stress of 189.7 MPa. This is a relatively high stress for the aluminium alloy, resulting in a safety factor of 1.13. This is a lower value than the 1.2 limit stated in NORSOK N-001 for ultimate level state [80]. However stress figures in appendix I.1 show the peak stress to be very localized and a convergence plot has been made to decide whether the peak stress is a result of a stress singularity or not. As seen in figure 4.14, the stress convergence plot suggest a divergent stress, and the von-Mises peak stress at 189.7 MPa is therefore believed to be a stress singularity which should be disregarded as a valid result. The displacement results in appendix I.1 suggest the same, as the location of the highest stress is not exposed to high displacements, while the upper cross beam has the highest displacement without any critically high stress, approximately 50 MPa von-Mises stress at the location of highest displacement. The aluminium structure is therefore believed to be well dimensioned for case-A.

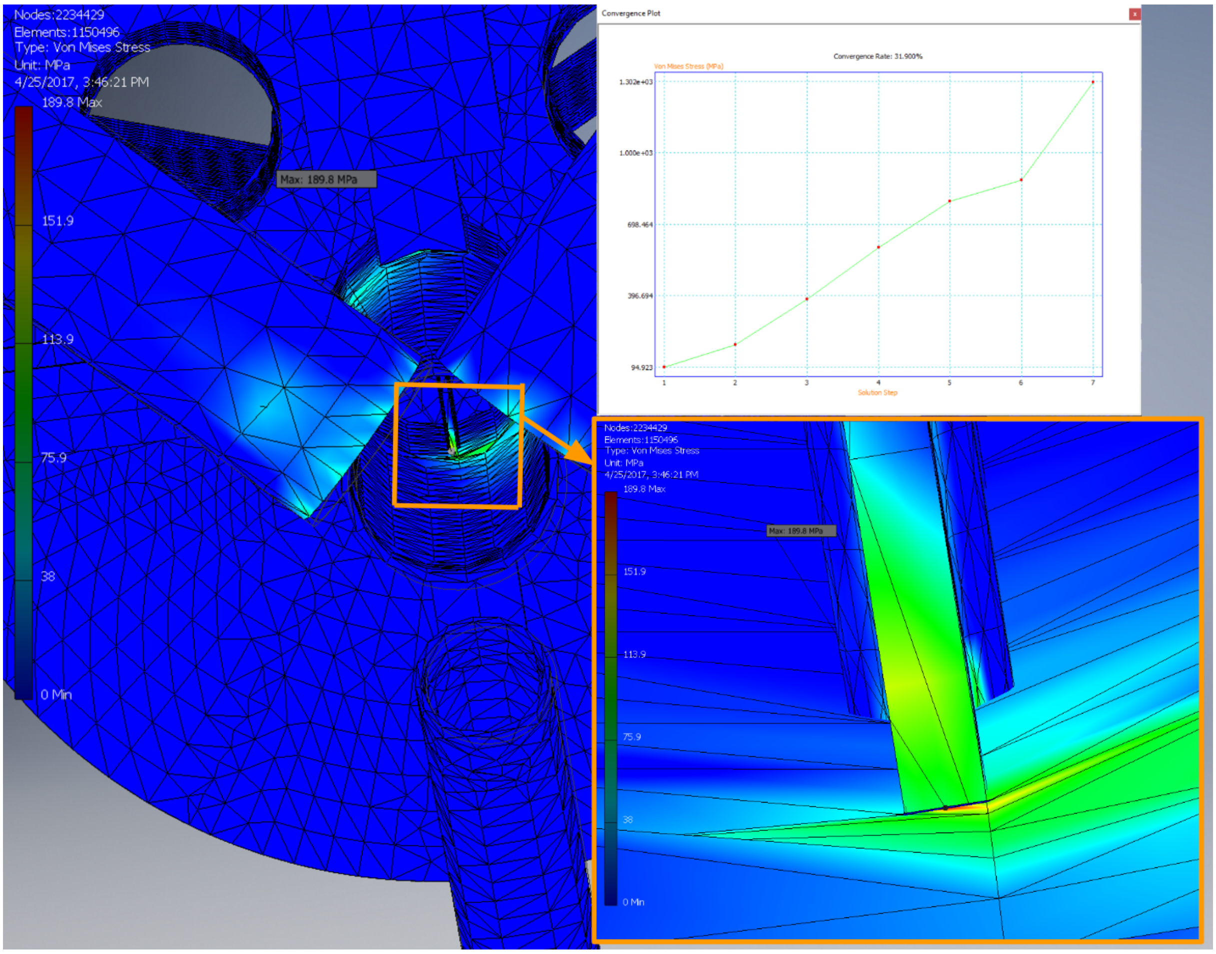


Figure 4.14: Stress singularity for case-A, with convergence plot.

**Case-B**

Case-B represent a combination of trawl ground snag (1000 kN) and the weight of the manifold in the center of the structure, 800 kN vertical load. The maximum resulting von-Mises stress on the structure is 194.7 MPa as seen in appendix I.2.1. As for case-A this stress is believed to be a stress singularity as the convergence plot in figure 4.15 suggests. The stress is limited to approximately 80 MPa, expect for the mentioned stress singularity of 194.7 MPa. The aluminium structure is therefore well dimensioned for case-B.

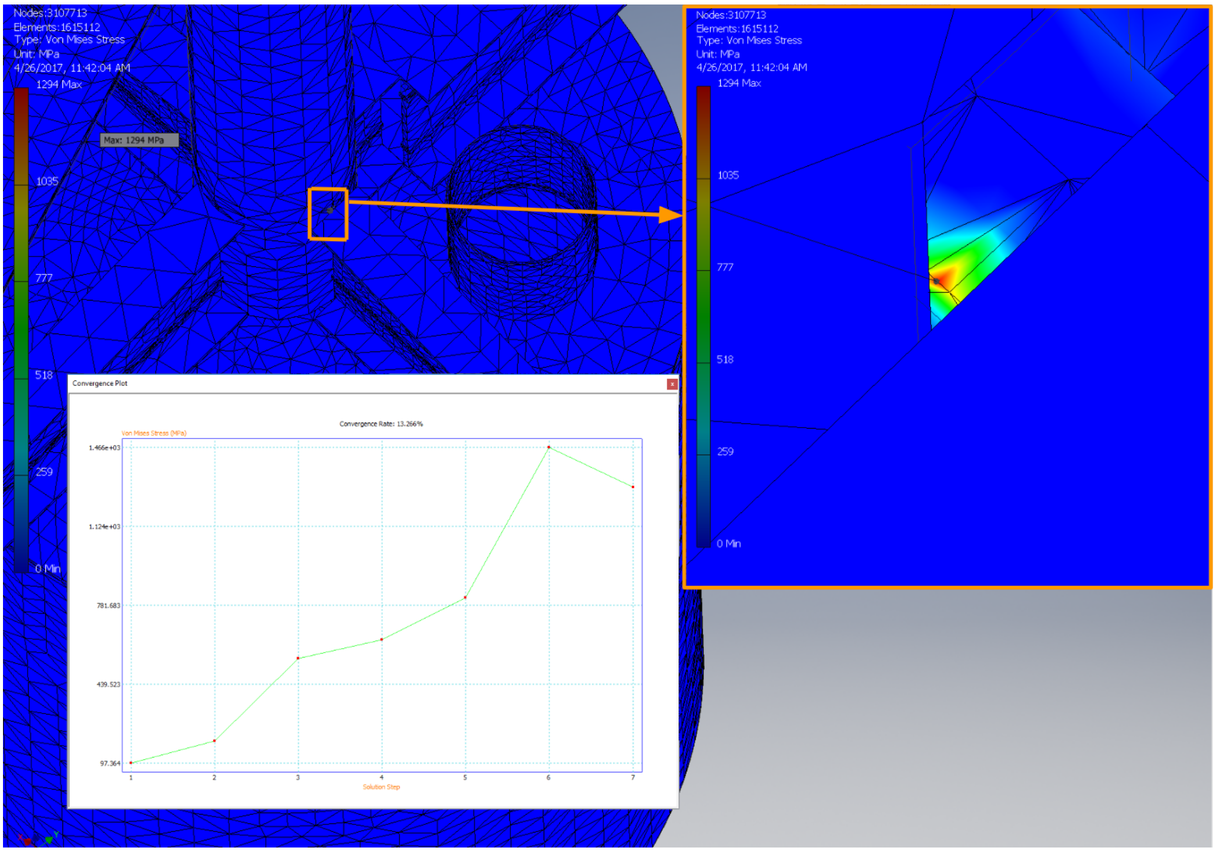


Figure 4.15: Stress singularity for case-B, with convergence plot.

**Case-C**

Case-C represent a combination of trawl ground rope snag, manifold weight and tie-in loads. The simulation set-up can be seen in appendix I.3, the resulting von-Mises peak stress is 368 MPa at a sharp corner on the beam subjected to trawl ground rope snag. A convergence plot has been created for the local stress of 368 MPa and the result as well as stress distribution and name of critical locations can be seen in figure 4.16. The convergence plot is not converging towards a final value and the stress is very localized around a sharp edge. The resulting stress of 368 MPa is therefore disregarded as a valid result.

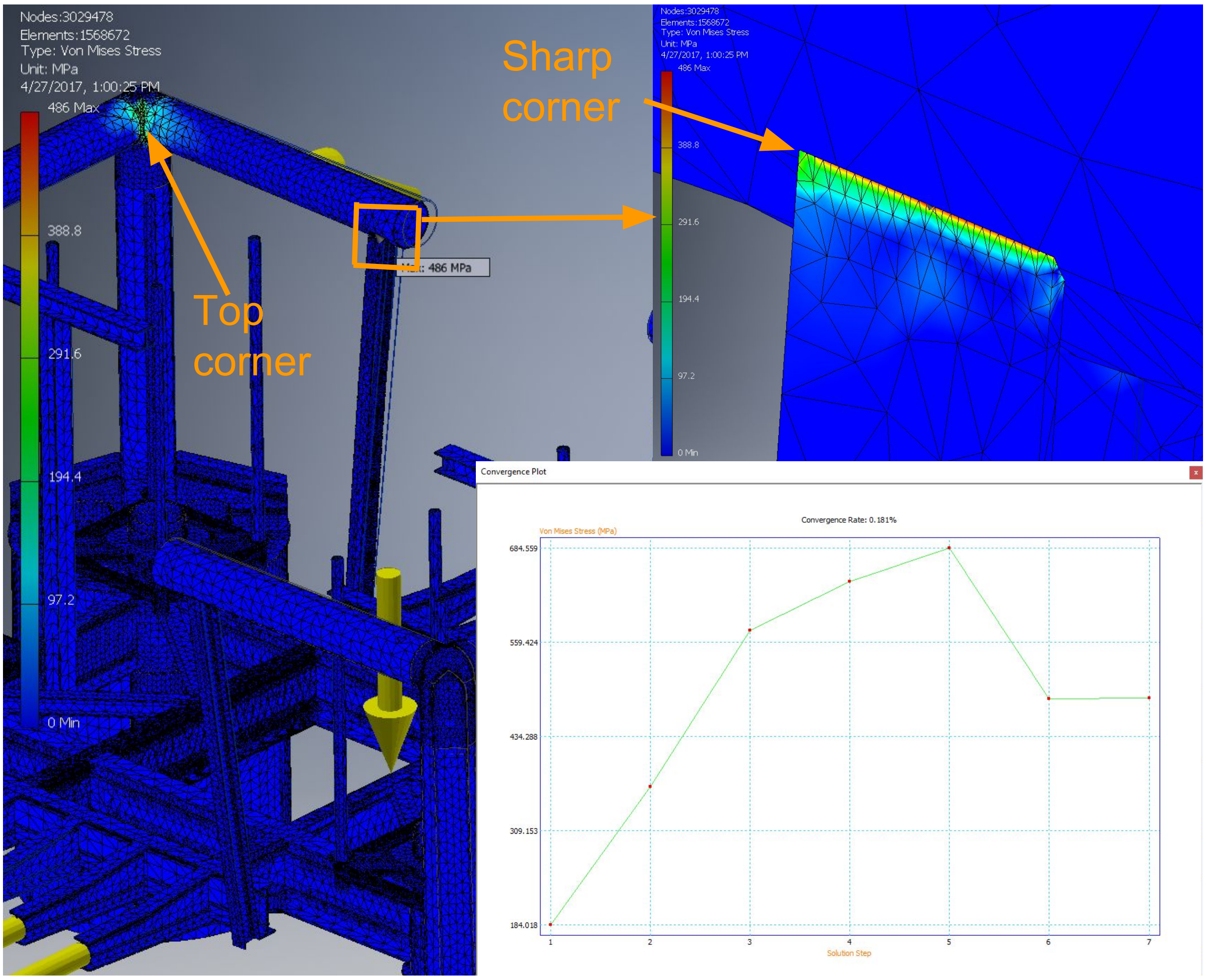


Figure 4.16: Stress singularity for case-C, with convergence plot.

The same case shows high stress in the top corner exposed to trawl ground rope snag. The local stress in the corner is approximately 300 MPa as seen in appendix I.3.1. A convergence plot has been created for this location as well, seen in figure 4.17. The convergence plot is converging and a von-Mises peak stress of 483.6 MPa can be observed in appendix I.3.2.

The modelled structure is not designed to withstand these loads without any improvements, however the displacement is very low at the location of the peak stress.

As described in section 4.3.3, the 1000 kN load is very conservative, a new simulation with 400 kN ($2 \cdot 200$ kN) instead of 1000 kN is therefore performed to see if the top corner can withstand trawlnet friction. The resulting stress is 230.4 MPa at the location of stress singularity (sharp corner) and approximately 140 MPa at the critical location in the top corner, as seen from von-Mises stress contour plot in appendix I.3.4. The difference between the load scenario of 1000 kN (not overtrawlable structure) and 400 kN (overtrawlable/snagfree structure) is therefore significant, as the structure is designed to withstand the loads applicable to an overtrawlable/snagfree structure. While it is not designed to withstand the trawling snag load of 1000 kN at the given location.

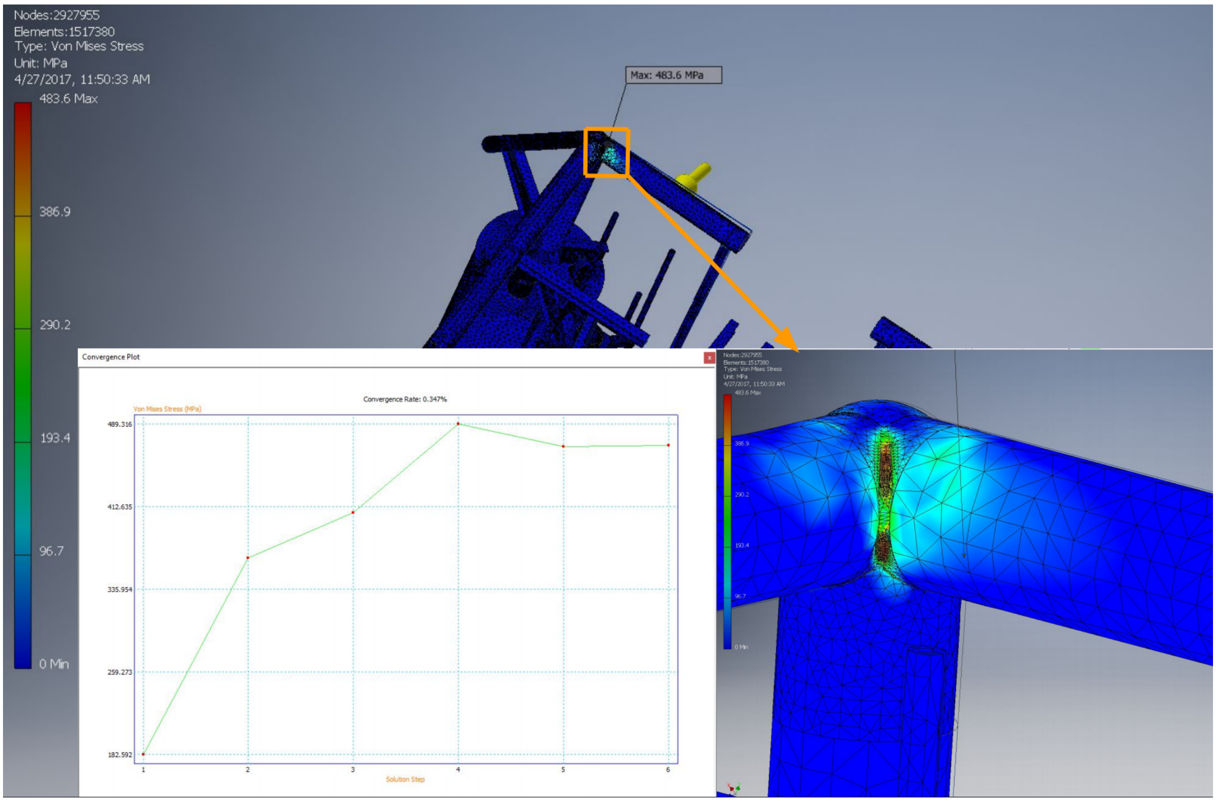


Figure 4.17: Stress in top corner for case-C, with convergence plot.

**Case-D**

Case-D represents a combination of X-mas tree weights, drilling loads, manifold weight and tie-in loads as shown in table 4.5. The set-up showing each of the forces and constraints can be seen in appendix I.4. The resulting von-Mises peak stress is 127 MPa at a location close to a well exposed to both drilling loads (450 kN vertical and 200 kN horizontal) and X-mas tree load (600 kN vertical). The resulting minimum safety factor is 2.71 which is acceptable. This design case shows how conservatively the structure is designed with respect to drilling and subsea equipment loads. The highest displacement is located where the structure is subjected to tie-in loads and the highest displacement value is 17.7 mm. All results for this load case are acceptable.

**Case-E**

Case-E represents a combination of trawl ground rope snag, drilling load, manifold weight and tie-in loads as shown in table 4.5. The case set-up and results can be viewed in appendix I.5. The resulting von-Mises peak stress of 283.3 MPa is located at the edge of a sharp corner, as seen in figure 4.18. The same location show high displacement and a convergence plot has been made to decide whether this is caused by a stress singularity or not. As seen from figure 4.18 the high stress is clearly caused by a stress singularity and is therefore disregarded as a valid result. The convergence plot shows an exponentially increase in stress with increased mesh density. The rest of the structure is limited to approximately 60 MPa in von-Mises stress, seen on stress contour plots in appendix I.5. The results for this load case are acceptable when the stress singularity is disregarded as a valid result.

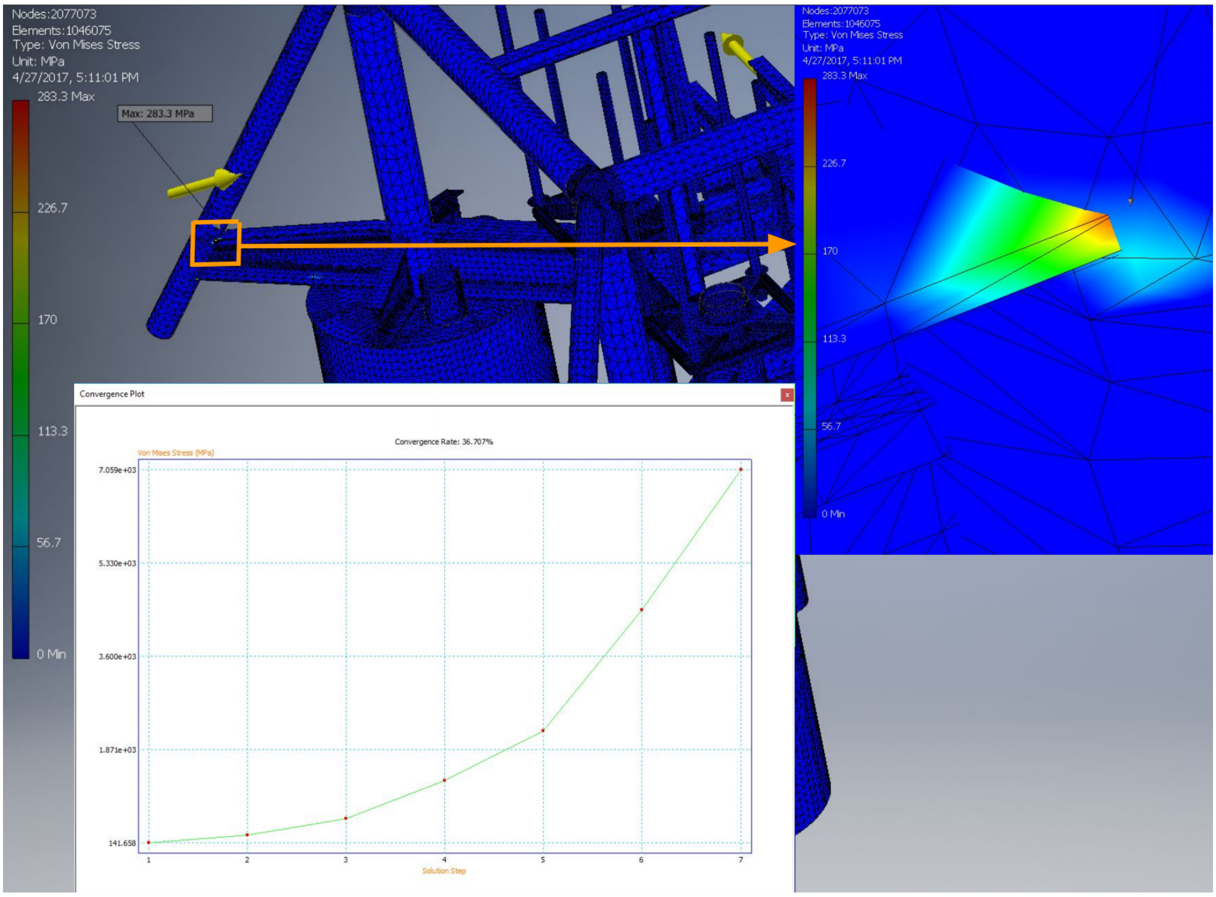


Figure 4.18: Local stress for case-E, with convergence plot.

**Case-F**

Case-F represents a combination of trawl ground rope snag, X-mas tree weights, manifold weight and tie-in loads. The trawling load is applied in the same way as in case-E. The set-up and results can be seen in appendix I.6. The resulting von-Mises maximum stress is 344 MPa at a sharp edge. A convergence plot has been made to decide if the high stress is caused by a stress singularity or not, as seen in figure 4.19 the peak stress is clearly caused by a stress singularity and is therefore disregarded as a valid result. The rest of the structure is limited to approximately 100 MPa in von-Mises stress. The maximum displacement is caused by the trawling load and results in a displacement of 65.1 mm, as seen in appendix I.6.2. The results for this load case are acceptable when the stress singularity is disregarded as a valid result.

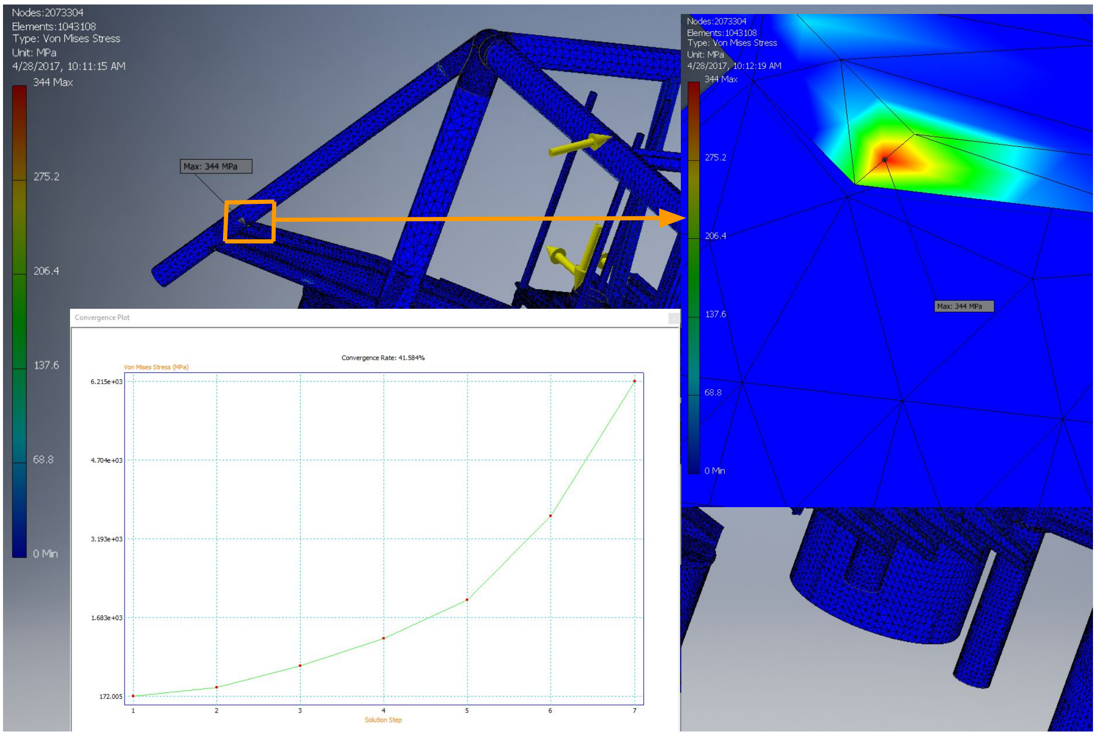


Figure 4.19: Local stress for case-F, with convergence plot.

### Case-G

Case-G represents an offshore installation case where the load in each corner is calculated to 766.5 kN in section 4.3.1. There are two lifting arrangements in each corner resulting in a bearing force of 383.3 kN modelled as a bearing load. The case set-up and results can be seen in appendix I.7. The resulting von-Mises peak stress is 65.5 MPa resulting in a safety factor of 4.2, seen on stress contour plots in appendix I.7. This safety factor is based on the yield strength of aluminium, while the location of peak stress is also subjected to MIG welding reducing the minimum safety factor to 2.3 (150 MPa/ 65.5 MPa) when welding effects are considered, as described in section 3.6. The highest displacement is located on the lifting arrangement and limited to 2.5 mm. All results for this load case are acceptable, and the structure seems to be conservatively designed with respect to offshore lifting operations.

### Summary

Table 4.6 contains a summary from all the cases with the most important findings. Case-C is the only problematic case as the stress is very high, 483.6 MPa. Possible methods to mitigate the high stress level is discussed in section 6.5.1. All the other cases are acceptable, as shown in table 4.6.

Table 4.6: Summary from analyses for all the selected cases.

| Case # | Stress[1] [MPa] | Displacement [mm] | Safety factor[2] [-] | Singularity stress [3] [MPa] |
|---|---|---|---|---|
| A | 50 | 93.3 | 4.30 | 189.7 |
| B | 80 | 94.75 | 2.69 | 194.7 |
| C[4] | 483.6 (140) | 244.4 (101.8) | 0.44 (1.54) | 368 (230.4) |
| D | 127 | 17.7 | 1.69 | N/A |
| E | 60 | 19.6 | 3.58 | 283.3 |
| F | 100 | 65.1 | 2.15 | 344 |
| G | 65.6 | 2.5 | 2.3 | N/A |

1) The approximate maximum stress when stress singularities are disregarded.
2) Safety factor as a ratio between yield strength and maximum valid stress.
3) The measured stress at a stress singularity.
4) 1000 kN trawl load case with a high stress location, 483.6 MPa and a stress singularity of 368 MPa. Numbers in parenthesis are for the 400 kN load case.

## 4.5 Anode mass estimation

An estimation of the total anode mass is necessary to conclude whether the weight of anodes will have a significant impact on the total mass and to perform cost estimations for anodes in chapter 5. The estimation is based on NORSOK-M-CR-503 [11], and DNV RP-B401[47]. Cathodic protection of the relevant aluminium alloys in seawater can be obtained for potentials ranging from −830 mV to −1130 mV vs SCE with low risk of corrosion [19], which is acceptable for protection of steel in seawater.

Aluminium anodes are selected due to their high capacity compared to zinc anodes, the technical data for the different anodes can be seen in table 4.7. According to DNV-B401 [47], the following should be applied for cathodic protection of aluminium in seawater:

*"A design current density of 0.01 $A/m^2$ is recommended for initial, final and mean value ... the design current density shall be increased by 0.0002 $A/m^2$ for each $^\circ C$ that the metal/seawater is assumed to exceed 25 $^\circ C$."*

Table 4.7: Anode specifications according to section 6.9.1 in NORSOK-M-CR-503 [11].

| | Aluminium based anode | Zinc based anode |
|---|---|---|
| Capacity, $\epsilon$ [Ah/kg] | 2000 | 780 |
| Potential [mV] vs Ag/AgCl/ Seawater | $-1050$ | $-1030$ |

The temperature is not expected to exceed 25 $^{o}$C and 0.01 A/m$^2$ will therefore be used in calculations. A design lifetime of 25 years will be used, as subsea structures are normally designed to last between 20 and 30 years. An anode utilization factor of 0.9 is imposed, as shown in appendix E and described in the DNV standard [47]. The current demand will be calculated in accordance with section 7.4, "Current Demand Calculations", in the DNV standard [47]. The surface area to be protected is calculated using the CAD-model in Autodesk Inventor, where a surface area of 1521 m$^2$ is estimated. The anode mass calculation is based on section 7.7, "Anode Mass Calculations", in the DNV standard [47]. All the input numbers can be seen in table 4.8 with reference to where the input numbers are found. The current demand calculation and the anode mass calculation can be seen in table 4.9. The number 8760 refers to the number of hours in one year.

The total anode mass must also provide current to suction anchors and well-slots, as described in NORSOK M-CR-503 [11]. Mud mats, suction piles and skirts made of steel exposed to sediments shall be designed with a current drainage of 20 mA/m$^2$, the same number is used for aluminium in calculations, as no recommendations have been found for aluminium in the literature. The limited amount of literature on the topic suggests 20 mA/m$^2$ as a conservative number, the earlier mentioned TSA in soil, outlined in section 3.5.4, had a current drainage of 10 mA/m$^2$ after ca. 250 days [21]. A subsea well shall be designed with a current drainage of 8 amps per well [11]. The additional drainage from anchors and wells will have a large impact on the total anode mass as the current raises from 15.21 amps for seawater exposed aluminium surfaces to 56.21 amps for the structure accounting for submerged anchors and all well-slots made from steel, as seen in table 4.9 and appendix E.

Table 4.8: Input numbers used in estimation of anode mass.

| | | |
|---|---|---|
| ic[1] [A/m$^2$] | 0.01 | Section 6.3.11 in DNV-RP-B401 [47]. |
| u[2] [-] | 0.9 | Appendix A- Table 10-8 in DNV-RP-B401 [47]. |
| Ac[3] [m$^2$] | 1521 | Surface area from CAD-model. |
| $I_{well}$[4] [A] | 8 | 8 amps per well, from 6.5 in NORSOK M-CR-503 [11]. |
| $i_{sa}$[5] [mA/m$^2$] | 20 | 20 mA/m$^2$ for steel suction anchors, from 6.4 in NORSOK M-CR-503 [11]. |
| $A_{sa}$[6] [m$^2$] | 112.5 | Outer surface area of one suction anchor. |
| tf[7] [years] | 25 | |

1) ic : Design current density for aluminium components, recommended for initial/final as well as mean value.
2) u : Recommended anode utilization factor for CP design calculations.
3) Ac : Total surface of all aluminium components on the structure.
4) $I_{well}$ : Current addition of 8 amps per well.
5) $i_{sa}$ : Current drainage for mud mats, skirts and piles.
6) $A_{sa}$ : Surface area pr. suction anchor.
7) tf: Design life.

Table 4.9: Current demand and anode mass calculations.

| | Formula | Result |
|---|---|---|
| Current demand aluminium, $I_{Al}$ | $I_{Al}$=Ac · ic [A] | 15.21 A |
| Current demand wells, $I_{wells}$ | $I_{wells} = 4 \cdot I_{well}$ [A] | 32.0 A |
| Current demand suction anchors, $I_{sa}$ | $I_{sa} = i_{sa} \cdot A_{sa} \cdot 4$ [A] | 9.0 A |
| Total current demand, $I_c$ | $I_c=(A_c \cdot ic) + I_{wells} + I_{sa}$ [A] | 56.21 A |
| Anode mass calculation, $M_a$ | $M_a=(I_c \cdot tf \cdot 8760)/(u \cdot \epsilon)$ [kg] | 6840 kg |

The weight of anodes are significant compared to the total weight of the structure, it is therefore included in calculation of the structures mass in section 4.6. From table 4.9 it is clear that wells and suction anchors are the main source for current drainage, responsible for approximately 73% of the current. The aluminium surfaces exposed to seawater are responsible for ca. 27% of the current drainage. The use of coating on these surfaces as a strategy to reduce the anode mass requirement would therefore have a very limited effect, as the suction anchors and wells would have the same current drainage. Current demand for coated aluminium is not included in the reviewed standards, NORSOK and DNV standard on cathodic protection. Further calculations on the impact of coating aluminium is therefore left out of scope.

## 4.6 Weight saving

The overall weight has been decreased significantly due to the introduction of aluminium. Table 4.10 shows all changes for all components, except for lifting eyes, suction anchor ventilation holes and coating weight. These weights are assumed to be insignificant (estimated to be maximum 1,5Te).

Table 4.10: Weight changes for each component, and total weight comparison.

| Component | Weight of original component [kg] | Weight of new component [kg] | Number in assembly | Weight of original components [kg] | Weight of original components [kg] | Weight ratio[2] [%] |
|---|---|---|---|---|---|---|
| a | 12439 | 4 193 | 2 | 24879 | 8387 | 0.663 |
| b | 397 | 265 | 4 | 1590 | 1061 | 0.332 |
| c | 1590 | 1213 | 2 | 3180 | 2426 | 0.237 |
| d | 1390 | 928 | 2 | 2780 | 1856 | 0.332 |
| e | 575 | 293 | 4 | 2302 | 1174 | 0.490 |
| f | 3861 | 1555 | 4 | 15444 | 6221 | 0.597 |
| g | 2452 | 1273 | 2 | 4905 | 2547 | 0.481 |
| h | 948 | 483 | 8 | 7582 | 3866 | 0.490 |
| i | 2656 | 1136 | 4 | 10623 | 4544 | 0.572 |
| j | 605 | 288 | 8 | 4837 | 2301 | 0.524 |
| k | 790 | 417 | 4 | 3160 | 1668 | 0.472 |
| l | 4486 | 2610 | 4 | 17946 | 10442 | 0.418 |
| m | 2147 | 1292 | 4 | 8418 | 4872 | 0.421 |
| n | 4209 | 2436 | 2 | 8418 | 4872 | 0.421 |
| o | 2447 | 1434 | 4 | 9789 | 5738 | 0.414 |
| q | 20442 | 11755 | 4 | 81766 | 47021 | 0.425 |
| q1 | 626 | 361 | 32 | 20038 | 11560 | 0.423 |
| q2 | 438 | 307 | 4 | 1750 | 1229 | 0.298 |
| q3 | 3984 | 2482 | 4 | 15934 | 9928 | 0.377 |
| r[3] | 2021 | 2021 | 4 | 8082 | 8082 | 0.000 |
| s | 1023 | 804 | 2 | 2046 | 1607 | 0.214 |
| t | 883 | 568 | 2 | 1767 | 1136 | 0.357 |
| u[3] | 1918 | 1918 | 4 | 7672 | 7672 | 0.000 |
| v[3] | 1085 | 1085 | 4 | 4341 | 4341 | 0.000 |
| w | 179 | 95 | 16 | 2856 | 1520 | 0.468 |
| x | 153 | 78 | 16 | 2453 | 1240 | 0.494 |
| y | 802 | 481 | 16 | 12836 | 7688 | 0.401 |
| z[3] | 321 | 321 | 8 | 2569 | 2569 | 0.000 |
| Anode weight | - | - | - | 7513[1] | 6840 | 0.090 |
| Bolt weight | - | - | - | 0 | 14000 | - |
| Bolting plates | - | - | - | 0 | 2600 | - |
| Lifting slings | - | - | - | 12500 | 12500 | - |
| Sum: | 72326 | 40035 | 174 | 310142 | 202718 | 0.346 |

1) Anode mass calculations is based on [47, 11]. Calculations can be seen in appendix E.
2) Weight ratio is defined as the weight reduction between original and new weight.
3) Made of steel.

The calculated weight is reduced from 298Te to 191Te by utilizing aluminium, which is a weight reduction of 36%. 18.1% of the new weight is steel. Anode weight is included in the mentioned weights but weight of lifting slings are excluded. As a result of this weight saving lighter subsea construction vessels can be used (250Te crane vessel class instead of 400Te crane vessel class), reducing the cost of installation. The cost implications are described in detail in chapter 5.

# Chapter 5

# Cost Estimations and Comparison

An introduction of aluminium in subsea structures are not likely to happen if it is not cost efficient. It is therefore necessary to perform a cost estimation comparison study. The study will only focus on capital expenditure (CAPEX), operating expenditures (OPEX) will not be a part of the study to limit the scope of work.

## 5.1 Installation cost

The calculated steel structure weight is 298Te, while the calculated aluminium structure weight is 191Te. The weight difference of 107Te results in a larger number of vessels capable of installing the structure. To estimate an installation cost for the two alternatives, it is necessary to estimate an installation time. The installation time in days is set to 3, 6 and 8 days, as a reference in Subsea 7 estimated 3 days for such installations [85], a source in Seabrokers estimated 5-7 days [86], while the software program Que$tor used for cost estimations estimated 8 days for the installation of an ITS as seen in appendix G. The number Que$tor estimated were identified by setting up two cases, a case with one ITS and a case with two integrated template structures, and 8 days were the installation time difference as seen in appendix G.2 and G.3. All sources have been used in the cost estimation to point out the uncertainties related to installation time. The difference in installation cost can be seen in table 5.1. The daily rate is the total cost of renting operational vessel (including onboard personnel) [39], the e-mail correspondence with Asbjørn Wathne in Subsea 7 can be seen in appendix B.5. It should be noted that the daily vessel rate changes a lot with the market situation as pointed out in e-mails from both Seabrokers [39] and Subsea 7 [85]. Vessel rates can therefore differ from the numbers used in the table 5.1, dependent upon the market situation. The daily vessel rates numbers should therefore not be used for any cost estimations in the future, as they reflect the current market.

Table 5.1: Installation vessel size influence on installation cost.

| Vessel crane size | Daily rate [NOK/day] | Installation time [days] | Installation cost [NOK] |
|---|---|---|---|
| 250Te | 1 500 000 | 3 | 4 500 000 |
| | | 6 | 9 000 000 |
| | | 8 | 12 000 000 |
| | 1 750 000 | 3 | 5 250 000 |
| | | 6 | 10 500 000 |
| | | 8 | 14 000 000 |
| | 2 000 000 | 3 | 6 000 000 |
| | | 6 | 12 000 000 |
| | | 8 | 16 000 000 |
| 400Te | 2 000 000 | 3 | 6 000 000 |
| | | 6 | 12 000 000 |
| | | 8 | 16 000 000 |
| | 2 250 000 | 3 | 6 750 000 |
| | | 6 | 13 500 000 |
| | | 8 | 18 000 000 |
| | 2 500 000 | 3 | 7 500 000 |
| | | 6 | 15 000 000 |
| | | 8 | 20 000 000 |

## 5.2 Fabrication cost

Fabrication cost for both steel and aluminium have been estimated to conclude whether aluminium is a cost efficient solution or not. Estimated costs for both alternatives are presented in this section.

### 5.2.1 Steel structure cost

The cost estimation program Que$tor from IHS Markit [87] has been used to find the cost for an steel made ITS. The program is based on historical development costs in the oil & gas industry. A Gjøa field was generated in the software by selecting structures and field specifications according to references [88, 89]. The field layout can be seen in figure 5.1, where the left figure shows the overall layout while the right figure shows the subsea layout with three integrated template structures.

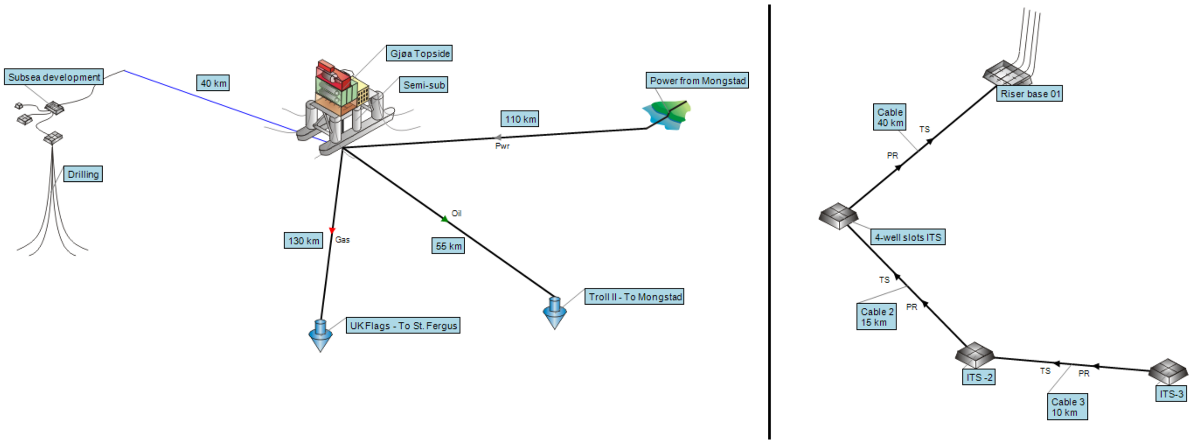


Figure 5.1: Gjøa south field layout, and subsea layout with three integrated template structures.

The cost estimation found in Que$tor for a 4-well slots ITS can be seen in table 5.5. The total cost of the main structure is 6 361 000 USD, equal to ca. 53 854 000 NOK (dependent upon the exchange current between USD and NOK). All the information extracted from the Que$tor software can be seen in appendix G.

### 5.2.2 Aluminium structure cost

The aluminium fabrication cost is not possible to identify using the Que$tor software, as an aluminium made ITS does not exist. Fabrication cost for the aluminium alternative is developed by contacting industrial companies and asking for price offers on all items. The aluminium cost has therefore been divided into the following sub-groups: fabrication cost, extrusion cost, plate cost, bolt cost and anode cost.

#### Aluminium fabrication cost

The fabrication cost is the cost of constructing the structure when the extrusion profiles, plates, bolts and anodes have been purchased. Based on numbers from Marine Aluminium, the cost of fabricating such an aluminium structure is estimated to be in the range of 200 to 300 NOK/kg, as seen from e-mail correspondence in appendix B.6. A cost estimation can be carried out based on these numbers combined with the total weight of the aluminium structure. The cost estimations can be seen in table 5.2, where the calculated structural weight is combined with several options for NOK/kg to accommodate the uncertainties regarding these values. The cost per kg (NOK/kg) numbers presented in table 5.2 are rough estimates, more details regarding cost uncertainties are presented in section 6.8.

Table 5.2: Cost estimation for aluminium based on numbers in e-mail correspondence seen in appendix B.6.

| Total weight [Te] | Cost per kg [NOK/kg] | Fabrication cost [NOK] | Fabrication cost [MNOK] |
|---|---|---|---|
| 191 | 200 | 38 200 000 | 38.20 |
| 191 | 250 | 47 750 000 | 47.75 |
| 191 | 300 | 57 300 000 | 57.30 |

#### Extrusion cost

The extrusion cost is estimated from numbers received from STEP-G. STEP-G's price offer is based on the part-list for extrusion profiles in appendix H.1 which covers all extrusion profiles used on the aluminium made ITS. The received price offer from STEP-G can be seen in appendix H.2. The cost of extruded profiles is estimated to 3 532 000 NOK, using 9.45 as exchange current between NOK and EUR. 1/3 of the extrusion cost is directed to manufacturing of the dies needed. The estimated cost is excluding VAT (Value Added Tax) and including European Standard certificate.

#### Plate cost

Plate cost is based on price offer received from Constellium, the price offer can be seen in appendix H.1 covering all plates included in the ITS design. The total cost for plates including DNV certificate and transport to Norway is approximately 550 300 EUR. Using 9.45 as exchange current between NOK and EUR results in 5 200 340 NOK.

### Bolt cost

Costs for stainless steel type 316 and carbon steel obtained from AccuGroup [12], and additional phosphating costs received from Odda Coating Technology AS [13], are presented in table 5.3. Phosphating is chosen as the optimal coating method mainly due to the possession of electrical continuity, see section 3.8 for bolt coating alternatives and bolt properties. Required bolt length and respective quantities are estimated from results provided in table 4.3.

Table 5.3: Cost comparison between stainless, carbon and phosphated carbon M36 steel bolts [12, 13].

| Bolt length [mm] | Quantity 2) | NOK/ stainless bolt | NOK/ stainless nut | NOK/ stainless washer | NOK/ carbon steel bolt 1) | NOK/ carbon steel nut 1) | NOK/ carbon steel washer 1) |
|---|---|---|---|---|---|---|---|
| 110 | 120 | 188 | 67 | 21 | 69 (219) | 9 (69) | 7 (62) |
| 120 | 352 | 200 | 67 | 21 | 73 (223) | 9 (69) | 7 (62) |
| 130 | 68 | 207 | 67 | 21 | 76 (226) | 9 (69) | 7 (62) |
| 140 | 256 | 211 | 67 | 21 | 80 (230) | 9 (69) | 7 (62) |
| 150 | 256 | 222 | 67 | 21 | 84 (234) | 9 (69) | 7 (62) |
| 210 | 416 | 352 | 67 | 21 | 111 (261) | 9 (69) | 7 (62) |
| Sum | 1468 | 364 442 | 98 826 | 30 883 | 126 345 (347 180) | 13 451 (101 531) | 20 314 (181 794) |
| Sum stainless steel bolts, nuts and washers | | | 494 151 NOK | | | | |
| Sum carbon steel bolts, nuts and washers 1) | | | | | | 160 764 NOK (630 506 NOK) | |

1) Cost for phosphated carbon steel bolts are given in parentheses.
2) Double amount of washers (2936).

### 5.2.3 Anode material cost

The anode cost estimations are based on prices received from Skarpenord, e-mail correspondence can be seen in appendix B.7. The estimated anode cost is 44 NOK/kg. Table 5.4 shows the estimated cost for 6840 kg of anodes as calculated in section 4.5.

Table 5.4: Anode cost estimation.

| Anode cost [NOK/kg] | Anode mass [kg] | Anode cost [NOK] |
|---|---|---|
| 44 | 6840 | 300 960 |

### 5.2.4 Total cost estimates comparison

The installation of an aluminium made ITS involves a 250Te crane vessel instead of a 400Te crane vessel which is the case for steel. Table 5.5 identifies the lowest cost case for aluminium as a cost competitive alternative to steel, while the upper cost case identify steel to be the most cost efficient choice. Aluminium fabrication cost is the decisive factor. It should be noted that these numbers are estimates and will differ from one field to another (as the distances changes, depth changes, installation time changes, etc.).

Table 5.5: Cost comparison for the two alternatives (aluminium and steel).

| | Aluminium | Steel |
|---|---|---|
| Fabrication cost [NOK] | 38 200 000 to 57 300 000 | 53 854 000 |
| + Extrusion cost [NOK] | 3 532 000 | N/A |
| + Plate cost [NOK] | 5 200 340 | N/A |
| + Bolt cost [NOK] | 630 506 | N/A |
| + Anode cost [NOK] | 300 960 | N/A |
| + Installation cost [NOK] | 4 500 000 to 16 000 000 | 6 000 000 to 20 000 000 |
| = Total cost [NOK] | 52 363 806 to 82 963 806 | 59 854 000 to 73 854 000 |

# Chapter 6

# Discussion

## 6.1 Connection methods

A number of different joining methods have been presented in chapter 3, it is therefore necessary to summarize and discuss relevant findings.

Joining by adhesives, bracing and laser are not used in the aluminium design. As adhesives require a comprehensive documentation and testing, which is not beneficial in terms of costs and ultimately NORSOK approval. Bracing of alloy 5083-H116 is difficult due to the relatively large magnesium content and the resulting strength reduction is high. Laser welding is believed to be a possible welding method, but the experience and knowledge within aluminium fabrication companies are limited, and costs by implementing laser could be severe.

MIG and FSW are on the other hand identified as promising and applicable joining methods for joints that needs to be welded, and are therefore implemented in design and cost analyses. MIG is an extensively used method and likely to be the most cost efficient method [9]. FSW possess a high ductility with favorable strength characteristics, but it is limited to butt welds. TIG is also a possibility, but the strength reductions are significantly higher for larger thicknesses and it is found to be a more costly process compared to MIG.

Bolting is regarded as the optimal joining method in terms of retaining strength throughout the joints, although some extra corrosion concerns must be expected.

The new HYB method shows very interesting and promising joint characteristics. The innovative joining method is however in an early stage, relevant literature is therefore very limited. HYB is thereby not implemented in the ITS redesign.

## 6.2 Corrosion protection strategy

Based on the provided evidence in section 3.5.8, cathodic protection of aluminium is regarded as an efficient and simple solution to protect the aluminium structure from corrosion attacks. At higher flow rates some degradation on the aluminium surface must be accepted. Flow induced corrosion is not found to be problematic as the resulting corrosion rate is approximately 0.08 mm/year for velocities between 3 - 9 m/s, which would result in 2 mm uniform thickness loss after 25 years in service. Flow rates higher than 9 m/s in a subsea environment is regarded as highly unlikely.

Corrosion protection strategy for the redesigned ITS is mainly to use sacrificial anodes. Total anode weight is calculated in section 4.5, but anode distribution is not analyzed in this study, to limit the scope of work. However, anode distribution requirements should be clarified. The anodes must be distributed to assure that the structural steel is polarized to the immune area of the Pourbaix diagram and the aluminium alloys shall be polarized to the passive area in order to produce a protective oxide layer, which is obtained for both materials if a potential range of $-830$ mV to $-1130$ mV vs SCE is valid throughout the structure. Extra concerns should be directed to the relatively large current drainage towards wells and suction anchors.

### 6.2.1 Corrosion challenges

A complete understanding of corrosion of aluminium in closed compartments and soil is necessary before an aluminium ITS can be considered. There are indications outlined in section 3.5.4 and 3.5.5 that the approved NORSOK alloys are resistant under these conditions, but the literature found in this study is not enough to state a valid conclusion at this point.

Sealing compounds required for bolting applications must have a durability rating that satisfies desired lifetime and subsea requirements. The use of sealing compounds as an external seal is defined as the appropriate measure against water ingress in Eurocode 9 [2] for submerged applications. Suppliers of sealing compounds have not been identified, and subsequently the durability of the mentioned compound could not be confirmed during this study.

## 6.3 Fatigue concerns

Fatigue damage that may occur from cyclic loading during the integrated template structures lifetime has not been assessed, to limit the scope of work. It should be emphasized in an aluminium redesign that steel possess a greater fatigue resistance. Possible fatigue scenario are cyclic loading during sea transport. Trawling, drilling and unstable production through X-mas may also be a source of fatigue on the ITS, but that has not been confirmed. The ITS is however known to be subjected dominantly by static loading.

A safe life fatigue design described in section 3.12 is believed to be appropriate, since it is probably not cost efficient to perform the inspections required subsea for the damage tolerant design.

## 6.4 Design implications

The design of the ITS has been a time consuming iterative process with a number of considerations, especially with respect to aluminium extrusion limits outlined in section 3.3. Note that each extrusion is not only restricted by circumferential limits but also by a maximum weight per extrusion of 535 kg [4], which ultimately restricts the extrusion length. The redesign must in addition be within acceptable values for MOI, buckling and weight reduction.

### 6.4.1 Deflection

Larger beam deflection due to lower E-modulus for aluminium compared to steel has not been regarded as a design issue for the redesigned beams, although thickness among other dimensions is increased in order to meet MOI criteria. Considering the overtrawlable grid's allowance to experience plastic deformation (larger displacement) according to NORSOK U-002 [14] and DNV-RP-C204 [90] from accidental loads defined as a PLS condition (e.g. trawl snagging). Deformation of the overtrawlable grid should not lead to difficulties opening and closing the protective hatches covering the manifold and X-mas trees. In addition, the resulting elastic deformations in the FEM model load cases seen in section 4.4 is not of any concern. Only load case-C has a stress concentration beyond the elastic region, which is further discussed in section 6.5.1.

### 6.4.2 Insert

The joint in the top corners of the overtrawlable tubes is solved by using an insert to connect all four tubes. Manufacturing of the insert has proven to be challenging. The aluminium block required to machine the insert in one piece is too big for any billets identified in this study, which means that it is not found a proper manufacturing method for the insert in the approved NORSOK M-121 [44] alloys for submerged applications. It is further difficult to cast the insert in the 5xxx or 6xxx series, since the 6xxx series is not used for casting and the 5xxx series would be very difficult to temper to an adequate strength, as it is NHT and strengthening by cold work is not feasible on a casted block. To limit the work, manufacturing of the insert has not been analyzed in detail in this study. However, two possible solutions have been evaluated; the insert could be casted in an unapproved NORSOK alloy, for example in the 7xxx series and heat treated to desired strength, another possibility is to conduct further attempts to optimize the joint design by welding the tubes together. Note that the overtrawling requirement (smoothness) makes the joint design more difficult. A price estimate for the insert has not been identified, as details concerning the insert fabrication method is unknown.

### 6.4.3 Bolt calculations

Some of the loads and moments used as inputs in section 4.2.1 are established based on some simplified judgments, and should therefore be discussed. The joint loads along beam 'a' is based on design moment calculated from original geometry of beam 'a', where it is assumed a maximum moment at mid point of the beam, which is reasonable for a beam supported in both ends with a symmetric distributed load. However, the maximum original design moment found in the bolt analysis could in theory be spread evenly over a larger area than just the "mid point", but that is highly unlikely due to the resulting shear force in each beam support, which would be unreasonably large compared to known vertical loads acting on the base frame. The assumptions made in section 4.2.1 is supported by results in the FEM analysis performed in section 4.4 in the sense that it is conservative. It is not found any stress concentrations of concern in any of the bolted joint locations, meaning the geometry in these joints are well within desired safety factor.

Hydrogen embrittlement effects on the alternative stainless steel bolts connected to a potential source of hydrogen from CP, has not been analysed in this study. It is observed that stainless steel bolts shall only be used with a diameter of 10 mm or less according to NORSOK M-001 [54]. Nevertheless it is of interest to compare both carbon and stainless steel bolts in terms of required corrosion protection, amount of bolts and costs, as the utilization of large aluminium structures permanently installed subsea is still in an early stage.

### 6.4.4 Manifold support

The extensive use of bolting assemblies may interfere with the manifolds supporting points on the ITS, due to a non uniform beam surface on the assembly area. The manifolds interaction with the integrated template structures beams have not been studied in detail.

### 6.4.5 Formability

Bending of 5083-H116 plates are required in order to erect some of the parts, especially tubes and the plates intended to shape the suction anchor. As mentioned in section 3.10, one must reassure that the minimum bending radius is not too sharp. It has not been identified any challenges with respect to the radius limit. A company with sufficient equipment for the required manufacturing of the overtrawlable tubes have in addition been identified [79].

## 6.5 FEM Analysis

The structural analyses performed in section 4.4 is based on some simplifications to limit the amount of work. These simplifications will be a source of error in the analysis, and should therefore be discussed. Welding spots are not included in the model, welded locations on the structure will have reduced mechanical properties as described in section 3.6. It is therefore necessary to study the stress results with respect to stress in welded areas in order to obtain appropriate safety factors. Dropped object loads are excluded from the analysis as impact simulations required to perform such analysis has been left out of scope to limit the work load.

### 6.5.1 Validation of modelled cases

All design load cases in section 4.4.1 are acceptable except for the original case-C, where the trawling load of 1000 kN is too large for the modelled structure while the 400 kN load case is acceptable. The model does not take into account the protection covers and connection of the whole long side. These components are believed to contribute to distribute the stress over a larger part of the structure. Figure 6.1 shows the mentioned components and their locations. The stress distribution caused by these components are not further discussed in this study, to limit the scope of work.


Figure 6.1: Integrated template structure with protection structures on top and connection of the whole side top beam [33].

In the set-up of case-G, the suction anchors has been set as "fixed" items meaning they do not have any displacement. This is not correct, as case-G is ment to describe a lifting scenario. Only the lowest tip of the suction anchors should have been set as "fixed" rather than the whole suction anchor. It is not known to which extend this influences the results, but there is no reason to believe it would change the outcome of the design as the identified safety factor is relatively high, 2.3 as shown in table 4.6 in section 4.4.2.

### 6.5.2 Dropped objects

Analyses of dropped objects has been left out of scope, but should be discussed. Protective hatches are excluded in this study, a realistic model of the different impact scenarios on the ITS can therefore not be conducted. Impact properties are however presented for aluminium in section 4.4.1. Center for advanced structural analyses (CASA) at NTNU has a lot of experience with impact testing on aluminium, which makes it a suitable organization for further impact research on subsea aluminium structures and hatches.

## 6.6 Weight saving

Total weight saving of 36% between original steel design and new aluminium design is achieved, which is regarded as an adequate reduction considering the beams that have not been changed to an aluminium design and amount of steel bolts. The new obtained weight (including lifting slings) is 202.7Te, which is just within reach for 250Te installation vessels, which saves 500 000 NOK/day compared to 400Te vessels.

## 6.7 Coating

Operating companies responsible for field developments may specify a coating or colour for aluminium as it is currently for steel, based on the yellow coating's high visibility and extensive use in today's subsea structures. This possible requirement from the field developer has not been studied any further, but it should be mentioned that an extra layer of coating would increase the fabrication cost and time.

## 6.8 Cost uncertainties

The cost estimations are not accurate for future use, as the material cost of both aluminium and steel are changing continuously. As mentioned in section 5.1, the daily vessel rates are based on the current marked, the presented numbers are therefore not applicable for future marked changes. There are some uncertainties related to the installation time, as several references reported different installation times. An upper and lower installation cost were calculated based on the difference in estimated installation times to accommodate the uncertainties. This approach will impact the accuracy of the total cost estimation, as the total cost estimation is given as a range.

Freight cost for extrusions from STEP-G is excluded in the cost estimates, they are however expected to be insignificant since the parts submitted to STEP-G, located in Germany, fits in large commercial trailers. The VAT (Value Added Tax) is excluded from the cost estimates from STEP-G and Constellium, the VAT for import goods to Norway is ca. 25 %, dependent upon the goods [91]. The plate cost estimate from Constellium includes freight cost, where the destination for delivery is set to Trondheim/Norway.

Management costs related to design and manufacturing are not included in the cost analyses, which can have a significant influence on the total cost estimation. The cost of fabricating the inserts mentioned in section 6.4.2 has also been excluded as an estimate could not be identified because of the uncertainties regarding fabrication method. It is not clear whether inserts will have a significant impact on the total cost.

The fabrication cost numbers presented in section 5.2.2 is based on total weight, overall dimensions, experience and comparable structures. Length of welds, number of alignments and number of bolted connections are thereby not used as input in the fabrication cost estimates.

# Chapter 7

# Conclusion

### Aluminium properties

Aluminium's properties with respect to subsea applications have been reviewed and the following remarks can be concluded:

- The aluminium alloys 5083-H116 and 6082-T6 have excellent corrosion properties in seawater. Coating of the aluminium surfaces is not necessary, as cathodic protection and passivation of the aluminium surfaces are sufficient.
- Cathodic protection mitigates galvanic corrosion between aluminium and welds and between steel and aluminium.
- Cathodic protection of aluminium surfaces is not effective at high flow rates.
- It is not fully understood how aluminium will degrade when buried in soil.
- Several joining methods can be applied to an aluminium subsea structure, where bolting and welding are the preferred methods.
- MIG welding of alloy 5083-H116 and 6082-T6 reduces the yield strength by 30% and 50% respectively. FSW welding reduces the tensile strength by ca. 30% for alloy 6082 and 5% for alloy 5083, FSW can also increase the tensile strength for alloy 5083 by up to 19%.
- Adhesives, laser welding, friction welding, bracing and HYB are joining methods that have not been used in the redesign.

**Cost estimates**

The following remarks can be concluded regarding cost implications by using aluminium rather than steel as construction material for an integrated template structure:

- The reduced structure weight enables installation to be performed by the use of smaller installation vessels, with lower rates (NOK/day) reducing the installation cost.
- The assembly process is the main cost for the aluminium made integrated template structure.
- Total cost for the aluminium made structure is cost competitive to steel, where the aluminium fabrication cost is the decisive factor.

**Redesigned aluminium made structure**

The integrated template structure has been rebuild using aluminium as the main construction material, and simulated for several load cases in accordance with industry standards. The following can be concluded concerning the redesign and performed simulations:

- The redesign results in a structure with thicker members and optimized beam profiles in order to maintain the mechanical integrity of the structure. All important offsets and main dimensions remain the same, e.g. the well centre distance, height, width and length of the structure.
- The weight of the integrated template structure is reduced from 298Te to 191Te, a weight reduction of 107Te or 36%.
- Simulations performed on the aluminium designed structure showed acceptable stress, displacement and safety factor results for the applied load cases, simulating trawling, tie-in and structural weights of manifold and X-mas trees.

# Chapter 8

# Future Work

- Research on aluminium in soil with respect to corrosiveness and degradation mechanisms.
- Research on aluminium in closed compartments with respect to corrosiveness and degradation mechanisms.
- Conduct more experiments on various seawater flow rates influence on corrosion rate and cathodic protection.
- Identify other relevant subsea structures where it is possible to introduce aluminium as construction material. Structures with repetitive installation and retrieval will have a larger impact on installation cost.
- Develop Pourbaix diagrams for 5083-H116, 6082-T6 and 7020-T6.
- Perform impact (dropped object) loads analysis.
- Find suitable sealing compounds to be used on steel-aluminium interfaces.
- Develop more detailed standards concerning aluminium in a subsea environment. E.g. there has not been identified any standards concerning aluminium buried in mud, as there is for steel.

# Bibliography


[1] J. Gilbert Kaufman. *Introduction to Aluminum Alloys and Tempers*, pages 1–76. ASM International, 2000.

[2] NS-EN 1999-1-1:2007. *Eurocode 9: Design of Aluminium Structures, Part 1-1: General Structural rules.* 2009 edition.

[3] NS-EN 573-3:2013. *Aluminium and aluminium alloys Chemical composition and form of wrought product, Part 3: Chemical composition and form of products*, pages 12–18. 2014.

[4] Keld Reimer Hansen. Extrusion limits at STEP-G. E-mail from Keld Reimer Hansen, seen in appendix B.1, 2017.

[5] Sapa Group. Profiles in stock - Catalogue. Available: https://www.sapagroup.com/contentassets/444999c64c4641f7b3aff58aa655f2aa/stocklist.pdf,
Date accessed: 02.05.2017.

[6] Andreas Fellhauer. Extrusion limits at Constellium. E-mail from Andreas Fellhauer, seen in appendix B.2, 2017.

[7] KUMZ. Aluminium products. Available: http://www.kumz.ru/eng/win/download/176/, Date accessed: 01.2017.

[8] Eurpean Aluminium Association. *The aluminium automotive manual, Materials - Microstructure and properties.* EAA, 2002.

[9] Marine Aluminium AS. Aluminium in the marine environment. Available: http://m-a.no/wp-content/uploads/2015/01/Literature-file.pdf, Date accessed: 02.2017.

[10] A. El-Batahgy and M. Kutsuna. *Laser Beam Welding of AA5052, AA5083, and AA6061 Aluminum Alloys.* Springer-Verlag Berlin Heidelberg, 2009.

[11] Norsk Standard. *NORSOK-M-CR-503 - Common Requirements, Cathodic Protection*. Rev.1, december 1994 edition, 1994.

[12] AccuGroup. Available: https://www.accu.co.uk/en/, Date accessed: 04.2017.

[13] Halvard Torget Eriksen. Cost phosphated bolts. E-mail from Eriksen, seen in appendix B.8, 2017.

[14] Norsk Standard. *NORSOK U-002 - Subsea Structures and Piping System*. Rev.2, june 1998 edition, 1998.

[15] Tor Berge Gjersvik. Lecture notes, TPG4200 - Subsea Production Systems, Date accessed: 12.2016.

[16] Agility group. Baobab phase 3 project ; Operator: Canadian National Resources, Customer: FMC Technologies. Available: http://www.agilitygroup.no/projects-references/, Date accessed: 31.03.2016.

[17] Yong Bai and Qiang Bai. *Subsea Engineering Handbook*, chapter 4,17,19,20,22. Elsevier, 2010.

[18] Fontana M.G and Greene N.D. *Corrosion engineering*. McGraw-Hill, 1998.

[19] Christian Vargel. *Corrosion of aluminium*. Elsevier, 2004.

[20] Kemal Nisancioglu and D Féron. *Corrosion Behaviour and Protection of Copper and Aluminium Alloys in Seawater*, volume 50. Woodhead Publishing.

[21] Ole Øystein Knudsen, Jan Van Bokhorst, George Clapp, and Graeme Duncan. Corrosion of Cathodically Polarized Thermally Sprayed Aluminum in Subsea Mud at High Temperature. *Corrosion Engineering Section*, NACE International:560–568, 2016.

[22] Kemal Nisancioglu. Corrosion of aluminium in special environments relevant to applications in the petroleum industry. *SINTEF*, 1986.

[23] Kemal Nisancioglu and Torgeir Wenn. Corrosion and cathodic protection of aluminium in flowing sea water. *12th Scandinavian Corrosion Congress & Eurocorr 92*, -:485–492, 1992.

[24] CableTiesAndMore. Figure; A split rubber grommet to restrict seawater flow in/out of structures. Available: http://www.cabletiesandmore.com/american/catalog/flexible-grommet-black-6pack-p-1192.php, Date accessed: 15.03.2017.

[25] Figure; Galvanic series. Available: https://www.google.com/patents/US20080128393, Date accessed: 16.12.2016.

[26] Kemal Nisancioglu. Cathodic protection of aluminium in seawater. *National Association of Corrosion Engineers*, Vol.46:279–285, 1990.

[27] S.Haarberg, R. Aune, H. Fostervoll, E. Halmøy, and O.M. Akselsen. *Joining technology for aluminium in automotive applications.* 2009 edition, 2001.

[28] A.Pietras and B. Rams. FSW Welding of Aluminium Casting Alloys. *Archives of Foundry Engineering*, 16:119–124, 2016. Date accessed: 22.04.2016.

[29] M.K. Beasharati Givi, P. Asadi, D.F.O. Braga, A-C.F da Silva, and P.M.G.P. Moreira. *Advances in Friction Stir Welding and Processing.* Elsevier limited, 2014.

[30] Hybond. The HYB Technology. Available: http://www.hybond.no/technology.html, Date accessed: 05.2017.

[31] Gene Mathers. *Welding of Aluminium and Its Alloys*, chapter 6-8. Woodhead publishing limited, 2002.

[32] Rangachari Narayanan, V. Kalyanaraman, A.R. Santhakumar, S. Seetharaman, S.R. Satish Kumar, S. Arul Jayachandran, and R. Senthil. Bolted connections. Available: http://www.steel-insdag.org/TeachingMaterial/chapter34.pdf, 2000
Date accessed: 02.2017.

[33] Offshore Mag. Available: http://www.offshore-mag.com/articles/print/volume-71/issue-2/flowlines-__pipelines/online-monitoring-enhances-flow-assurance.html, Date accessed: 01.05.2017.

[34] Ole Terje Midling. Marine Aluminium AS, ole.terje.midling@m-a.no, -.

[35] Christian Knutsen, Ivar Kvale, and Jan Halvor Nordlien. *Aluminium applied for Subsea Structures: Possibilities and Challenges*, pages 46–51. The International Society of Offshore and Polar Engineers, 2001.

[36] FMC Technologies. Statoil Gjøa. Available: http://www.fmctechnologies.com/en/Subsea Systems/GlobalProjects/Europe/Norway/StatoilGjoa.aspx?tab=BC56CA53-A52B-40DF-83D1-B1BE9EE11805, 2011. Date accessed: 06.03.2017.

[37] T. Næss, J. Havn, and F. Solaas. *On the importance of slamming during installation of structures with large suction anchors*, pages 99–112. Elsevier, 2014.

[38] Kenneth Aarset, Arunjyoti Sarkar, and Daniel Karunakaran. Lessons Learned from Lifting Operations and Towing of Heavy Structures in North Sea. pages 1–14, 2011.

[39] Aleksander Kjønnerød. Daily rates subsea vessels. E-mail correspondence with Aleksander Kjønnerød in Seabrokers, 2017.

[40] Agility group. Fram project ; Fram H Nord, FMC Technologies. Available: http://www.agilitygroup.no/projects-references/, Date accessed: 30.03.2016.

[41] Aluminium Insider. Aerospace industry trends and aluminium use. Available: http://aluminiuminsider.com/aersopace-industry-trends-aluminium-use/, Date accessed: 12.2016.

[42] The Aluminum Association. Automotive. Available: http://www.aluminum.org/product-markets/automotive, Date accessed: 06.2017.

[43] Thomas Lamb. *The benefits and cost impact of aluminium naval ship structure.* 2011.

[44] Norsk Standard. *Norsok Standard M-121 - Aluminum Structural Material*, pages 1–14. Edition 2, september 2015 edition, 2015.

[45] Gravita aluminium. Aluminium Facts. Available: http://www.gravitaaluminium.com/auminium-facts/, Date accessed: 08.05.2017.

[46] Gene Mathers. *The welding of aluminium and its alloys*, pages 1–90. Woodhead publishing limited, 2002.

[47] Det Norske Veritas. *Recommended Practice DNV-RP-B401.* April 2011 edition, 2010.

[48] Kjetil Fossland Veium. *Effect of Cathodic Polarization on the Susceptibility to Hydrogen Embrittlement in 5xxx, 6xxx and 7xxx Series Aluminium Alloys.* NTNU, 2015.

[49] Hydro. Recycling of Aluminium. Available: http://www.hydro.com/globalassets/1-english/about-aluminium/files/aluminium_environment-and-society.pdf, Date accessed: 12.2016.

[50] Gabrielle Gaustad, Elsa Olivetti, and Randolph Kirchain. *Improving aluminum recycling: A survey of sorting and impurity removal technologies*, pages 79–87. Elsevier, 2012.

[51] Stephen D. Cramer, Bernard S. Covino, and J.G Kaufman. *Volume 13B Corrosion: Materials.* ASM International, 2005.

[52] Stig Berge. *Fatigue and Fracture Design of Marine structures*, chapter 12. NTNU, second edition, 2016.

[53] Tor Berge Gjersvik and Harald T. Neerland. E-mail correspondence with harald t. neerland. E-mail from Harald T. Neerland, seen in Appendix B.4, 2017.

[54] Norsk Standard. *NORSOK M-001 - Material Selection.* Rev.4, august 2004 edition, 2004.

[55] Sondre Røstbø. *Cathodic Protection of Steel-Aluminium Galvanic Couples for a New Generation of Lightweight Subsea Structures .* NTNU, 2016.

[56] R. Mundt, Hoogovens, and Koblenz. *Introduction to Brazing of Aluminium Alloys.* EAA-European Aluminium Association, 1994.

[57] Norsk Standard. *NORSOK M-501 - Surface preparation and protective coating.* Rev. 5, june 2004 edition, 2004.

[58] Ove Nese. *Corrosion properties of AA5083 and AA6082 in seawater - effect of temperature, pH and potential.* NTNU, 2016.

[59] Alumac. Should You Use TIG or MIG Welding For Aluminum Welding? Available: http://www.alumac.com.au/_blog/Our_Blog/post/Should_You_Use_Tig_Or_Mig_Welding_For_Aluminum_Weldin/, 2011. Date accessed: 02.02.2017.

[60] J.M. Gomes de Salazar, A. Urena, E. Villauriz, S. Manzanedo, and I. Barrena. *TIG and MIG welding of 6061 and 7020 aluminium alloys. Microstructural studies and mechanical properties.* Taylor & Francis Group, 1999.

[61] Bård Nyhus, Stephane Dumoulin, Håkon Nordhagen, Ole Terje Midling, Ole Runar Myhr, Trond Furu, and Steinar Lundberg. *Cross-weld tensile strength of aluminium alloys EN AW 5083 and 6082*. 2016.

[62] Mishra, R.S., and Z.Y. Ma. *Friction stir welding and processing, Materials Science and Engineering*. Elsevier, 2005.

[63] Moreira and P.M.G.P. *Mechanical and metallurgical characterization of friction stir welding joints of AA6061-T6 with AA6082-T6*. Elsevier, 2009.

[64] Marine Aluminium AS. Friction Stir Welded Panels. Available: http://m-a.no/product/friction-stir-welded-panels/, Date accessed: 02.05.2017.

[65] SpaceX. FALCON 9 Progress Update. Available: http://www.spacex.com/news/2013/02/11/falcon-9-progress-update-12, Date accessed: 02.05.2017.

[66] Øyvind Frigaard. *Process modelling applied to friction welding and aluminium alloys - A state of the art review*, pages 20–32. SINTEF, 1997.

[67] L. Quintino, R. Miranda, U. Dilthey, D. Lordachescu, M. Banasik, and S. Stano. *Laser Welding of Structural Aluminium*. Springer-Verlag Berlin Heidelberg, 2011.

[68] B. Katalinic. *Laser Beam Welding of Aluminium*, volume 22. DAAAM International, 2011.

[69] NS-EN ISO 13919-2:2001. *Electron and laser beam welded joints Guidance on quality levels for imperfections, Part 2: Aluminium and its weldable alloys*. First edition, 2001.

[70] Azom. Stainless Steel - Grade 316 (UNS S31600). Available: http://www.azom.com/article.aspx?ArticleID=863, Date accessed: 12.05.2017.

[71] NS-EN ISO 898-1. *Mechanical properties of fasteners made of carbon steel and alloy steel - Part 1: Bolts, screws and studs with specified property classes - Coarse thread and fine pitch thread*. 2013.

[72] Norsk Standard. *NS-EN ISO 3506-1:2009 - Mechanical properties of corrosion-resistant stainless steel fasteners - Part 1: Bolts, screws and studs*. 2010.

[73] Norsk Standard. *NS-EN 1090-3:2008 - Execution of steel structures and aluminium structures - Part 3: Technical requirements for aluminium structures.* 2008.

[74] Norsk Standard. *NS-EN 1090-2:2008 - Execution of steel structures and aluminium structures - Part 2: Technical requirements for steel structures.* 2012.

[75] ISO 11003-2:2001. *Determination of shear behaviour of structural adhesives, Part 2: Tensile test method using thick adherends.* Second edition, 2001.

[76] NS-EN 485-2:2016. *Aluminium and aluminium alloys - Sheet, strip and plate - Part 2: Mechanical properties.* First edition, 2016.

[77] NS-EN 1999-1-3:2007. *Eurocode 9: Design of Aluminium Structures, Part 1-3: Structures susceptible to fatigue.* 2010 edition.

[78] Det Norske Veritas. *DNV-OS-H102 - Marine Operations, Design and Fabrication.* 2012.

[79] Constellium. Aluminium plates. Available: http://www.constellium.com/aluminium-products/aerospace-and-transportation/products/plates, Date accessed: 02.2017.

[80] Norsk Standard. *NORSOK N-001 - Structural design.* Rev. 4, february 2004 edition, 2004.

[81] Det Norske Veritas. *DNV-RP-H103 - Modelling and Analysis of Marine Operations*, pages 58–70. 2011.

[82] Det Norske Veritas. *DNV-OS-H205 - Lifting Operations (VMO Standard - Part 2-5)*, pages 16–19. 2014.

[83] Autodesk Inventor. Mesh settings. Available: https://knowledge.autodesk.com/support/inventor-products/learn-explore/caas/CloudHelp/cloudhelp/2014/ENU/Inventor/files/GUID-10291E2B-03E4-4A5E-AB23-BC6083B6538A-htm.html,
Date accessed: 26.04.2017.

[84] Autodesk Inventor. How to ensure accuracy of stress analysis results and convergence in inventor stress analysis. Available: https://knowledge.autodesk.com/support/inventor-products/troubleshooting/caas/sfdcarticles/sfdcarticles/Accuracy-of-Stress-Analysis-Results-and-Convergence-in-Inventor-Stress-Analysis.html,
Date accessed: 26.04.2017.

[85] Asbjørn Wathne. Gjøa ITS installation. E-mail from Asbjørn Wathne, seen in appendix B.5, 2017.

[86] Aleksander Kjønnerød. Estimated installation time for ITS. E-mail correspondence with Aleksander Kjønnerød in Seabrokers, 2017.

[87] IHS. QUE$TOR®. Available: https://www.ihs.com/products/questor-oil-gas-project-cost-estimation-software.html, Date accessed: 02.05.2017.

[88] Offshore-Technology. Gjøa Field, North Sea Northern, Norway. Available: http://www.offshore-technology.com/projects/gjoa/, Date accessed: 02.05.2017.

[89] Factpages-npd. Gjøa field specifications. Available: http://factpages.npd.no/ReportServer?/FactPages/PageView/field&rs:Command=Render&rc:Toolbar=false&rc:Parameters=f&NpdId=4467574&IpAddress=129.241.64.170&CultureCode=en, Date accessed: 02.05.2017.

[90] Det Norske Veritas. *DNV-RP-C204 - Design Against Accidential Loads*, pages 1–12. 2010.

[91] Tax Norway. VAT in Norway. Available: http://taxnorway.com/vat-in-norway, Date accessed: 11.05.2017.

# Appendix A

# Loads

## A.1 Splash zone loads

There are four types of hydrodynamic (dynamic) forces and one static load to consider during splash zone penetration according to DNV-RP-H103 [81], The following hydrodynamic forces have to be included:

$F_m$ : Characteristic hydrodynamic mass force [N], dependent upon object mass in air, heave added mass caused by water flooding of the structure, vertical acceleration of crane tip, the wave displaced volume of water and vertical water acceleration due to wave motion.

$F_d$ : Characteristic hydrodynamic drag force [N], dependent upon drag coefficient, the objects area of horizontal directed surfaces and vertical velocity for object relative to water.

$F_{slam}$ : Characteristic slamming impact force [N]. The magnitude of this load is dependent upon impact velocity (known as slamming velocity [m/s]) and the slamming area (size of structure projected to the slamming loads).

$F_{ro}$ : Characteristic varying buoyancy force [N], change in buoyancy as the wave height changes. Dependent upon the volume difference between water volume for stilled water and wave.

The static load is determined according to DNV-RP-H103 [21], section 4.2.2:

$$F_{static,min} = M_{min} \cdot g – ro \cdot V \cdot g \ [N]$$

$$F_{static,max} = M_{max} \cdot g – ro \cdot V \cdot g \ [N]$$

Where:

$V$: represents the displaced water in both cases.

$M_{min}$ : The minimum mass is equal the mass of object in air (i.e. the structure is submerged but the flooding has not yet started) [kg].

$M_{max}$ : The maximum mass is equal the mass of object in air including the full weight of the water that floods the structure (i.e. the structure is fully flooded after submergence) [kg].

## A.2 Static loads

Table A.1: Manifold and christmas tree weights with resulting forces.

| Component | Dry weight | Wet weight |
|---|---|---|
| Manifold | 80Te (800 kN) | 70Te (700 kN) |
| Christmas tree | 60Te (600 kN) | 53Te (530 kN) |

## A.3 Trawling loads

Table A.2: Trawling loads [14].

| Design load type | Design load figure | | |
|---|---|---|---|
| Trawl net friction | 2x200 kN | 0-20 deg.[4)] | ULS[1)] |
| Trawl board overpull | 300 kN | 0-20 deg.[4)] | ULS |
| Trawl board impact | 13 kJ | - | ULS |
| Trawl board snag[3)] | 600 kN | 0-20 deg.[4)] | PLS[2)] |
| Trawl ground rope snag[3)] | 1000 kN | 0-20 deg.[4)] | PLS |
| Trawl board snag on sealine[3)] | 600 kN | - | PLS |

1) ULS means it is regarded as normal operation,
something that can occur during normal operation.
2) PLS means it is regarded as an abnormal operation.
3) Negligible if the subsea structure is documented to be snagfree.
4) With respect to horizontal direction.

## A.4 Dropped objects impact energy

Table A.3: Dropped objects impact energy [14].

| Group | Impact energy | Impact area | Object diameter |
|---|---|---|---|
| Multi well structures | 50 kJ | Point load | 700 mm |
| | 5 kJ | Point load | 100 mm |
| Other structures | 20 kJ | Point load | 500 mm |
| | 5 kJ | Point load | 100 mm |

## A.5 Sealine loads

Table A.4: Sealine loads scenarios [15].

| Sealine supports in use | Maximum load on one support | Total maximum combined load |
|---|---|---|
| 1 | 300 kN | 300 kN |
| 2 | 300 kN | 600 kN |
| 3 | 200 kN | 600 kN |
| 4 | 150 kN | 600 kN |

## A.6 Drilling loads

Table A.5: Drilling loads for depths up to 750 m [14].

| Activity | Load case | Design load |
|---|---|---|
| Lowering of 30" conductor. | Weight carried by template. | Temporary 600 kN vertical. |
| Drilling 24", lowering and cementing of 18 5/8" casing. | Partly 30" and 18 5/8" casing will be transferred to soil via the cement, assuming settling of the structure. | Permanent 450 kN vertical. |
| | Normal pull off stucked drillstring (2000 kN) and rig offset 4.5 degrees, including 1.5 degrees misalignment. Vertical load will be carried by conductor. Horizontal load will be carried by templateand conductor | Vertical 0 kN, Horizontal 160 kN. |
| Drilling of subsequent sections. | A BOP stack with riser attached landing on template at 0.5 m/s. Impact load mainly taken by the conductor casing. | Vertical 31 kJ impact, assuming 40 % on template. |
| | Normal pull of stucked drill string (2000 kN) and rig offset 4.5 deg. Including 1.5 deg. Misalignment. Vertical load carried by conductor. Horizontal load to be carried by template. | Vertical 0 kN, Horizontal160 kN. |
| | Tension from riser (300 kN) will be taken up by conductor casing. Horizontal component to be carried by template and conductor. | Vertical 0 kN, Horizontal25 kN. |
| | Guideline tension, max 200 kN. Vertical load will be taken by template.Horizontal comp. from 4 off lines at 4.5 deg. to be carried by template and conductor. | Vertical 0 kN, Horizontal 15 kN. |

# Appendix B

# E-mail Correspondences

## B.1 E-mail correspondence with Keld Reimer Hansen regarding production capabilities at STEP-G.

Bonn pressen - tekniske data

Keld Reimer Hansen <keld.reimer.hansen@step-g.com>
ma 06.03, 12:41

Hej Kjell

Nej, I kan ikke udregne max gods ud fra max-vægt pr meter.

Vi kan godt presse ø500x30 mm mm rør som max størrelse, men vores sav kan ikke save det.
Ny sav kræver en investering på 100.000 €.

ø400x30 mm er største rør vi kan tilbyde og kun I 6060 T6, Lmax = 5000 mm

Alternativt kan vi producer halv skaller 500x60 og svejse sammen til et rør.

Flangen til den store I-bjælke vil komme til at veje ca 100 kg/m og da presbolten max kan veje 535 kg, kan der "kun" producer L=5000 mm.

Send gerne en tegning af flangen så skal vi kigge på optimeringer.

Mit freundlichen Grüßen / best regards

**Keld Reimer Hansen**

**ST Extruded Products Germany GmbH**
Devillestrasse 2 **|** 06749 Bitterfeld, Deutschland **|** www.step-g.com
T: **|** F: **|** M: +45 20643306 **|** keld.reimer.hansen@step-g.com

Sitz: Bergstraße 17, 88267 Vogt, Germany | Geschäftsführer: Michael Zint | Handelsregister Ulm | HRB 550822
------------------------------------------------------------------------------------------

Kjell Petter Løkling Lunde

ma 06.03, 11:05

Hei,

Takk for svar. Finner man maksimal tykkelse på de oppgitte profilene ved å bruke vekt per. m (190kg/m for pressen i Bonn)?

For et Ø500 mm rør, blir maksimal tykkelse da 50 mm? Og hva blir maksimal lengde på et slikt rør?

Vi ønsker å lage en I-profil slik som vist i vedlagt bilde. Der tanken er å ekstrudere flensen. Kan flensen ekstruderes med, bredde: 700 mm, tykkelse: 50 mm, og lengde: 12 000 mm (dimensjonen på "built-in guideway" er ikke helt bestemt enda)?

Med vennlig hilsen,
Kjell og Henrik

## B.2 E-mail correspondence with Andreas Fellhauer regarding production capabilities at Constellium.

### WG: Large Extrusion

Fellhauer, Andreas <andreas.fellhauer@constellium.com>

ma 27.02, 14:01
Kjell Petter Løkling Lunde;
martin@jnssweden.com;
Renner Juergen <juergen.renner@constellium.com>

Hi Kjell

I'm Andreas from the technical department.

Our leaflet is giving very general information. The thickness you mentioned below is the minimum thickness which is very often of interest for lightweight structures.

The diameter 600mm is valid for alloys 6060 and 6063 only, but more for profiles in rectangular shapes.
In the case of tubes we are generally limited to sizes of diameter 520 mm and looking at your requirement concerning the wall-thickness we have to speak as well about other restrictions:

- Choice of the alloy: in case of 6082 we should not exceed very much the weight per meter of 80 kg/m which is the case e.g. for 500x20 or 350x30
- Max delivery length of the tube/profile is limited according to the weight per meter and choice of alloy – e.g. tube 500x20 in 6082 is only up to 6m
- More lightweight profiles/tubes can be delivered in longer lengths

I hope this answers your question sufficiently. If you like you can send me further information so that I can support you on the design of profiles.

Mit freundlichen Grüßen / Kind regards

**Andreas FELLHAUER, Dipl.-Ing.**
**Head of Technical Customer Service Industry**
**Large Profiles**
**Automotive Structures and Industry**
Constellium Singen GmbH
Alusingen-Platz 1
78224 Singen, Germany
Office phone : +49 7731 80 3523
Mobile phone : +49 172 6397355
Fax : +49 7731 80 2436
Mail : andreas.fellhauer@constellium.com

Geschäftsführung: Rolf Schencking (Vorsitzender), Hans-Joachim Chwalisz
Bank: Deutsche Bank, Singen

**Von:** Kjell Petter Løkling Lunde [mailto:kplunde@stud.ntnu.no]
**Gesendet:** Donnerstag, 23. Februar 2017 15:29
**An:** Renner Juergen
**Cc:** Henrik Westersjø Nesheim
**Betreff:** Large Extrusion

Hi,

We are working on a project, where we are modelling a large subsea structure in aluminium. We are trying to find out how large profiles (and what shape) it is possible to extrude. Do Constellium have a product catalog of large extruded profiles, or are you able to help us?

Regards,
Kjell

## B.3 E-mail correspondence with Ole Øystein Knudsen regarding aluminium subsea properties.

### Thermal Sprayed Aluminium i mud

Ole Øystein Knudsen <Ole.Knudsen@sintef.no>

ti 28.02, 13:56

Henrik Westersjø Nesheim

Innboks

Hei

I mud blir jo betingelsene ganske stagnant, siden muden ikke er flytende. Det rant friskt sjøvann over muden hele tiden så denne ikke skulle tørke inn. I sjøvann ble vannet skifta ut hele tida. Må det, ellers vil bakterier gjøre at vannet råtner, og da er ikke betingelsene sammenlignbare med naturlig sjøvann lenger.

TSA korroderer mer enn valsa og ekstrudert Al, trolig fordi det har en annen mikrostruktur og en geometri med mye sprekker og spalter. Kan se ut som det vil angripes av generell korrosjon til en viss grad. Vi finner korrosjonsprodukter over hele overflata på TSA etter eksponering. Anodiske polarisasjonskurver til TSA viser alltid høyere anodisk reaksjonshastighet enn valsa og ekstrudert materiale. Men TSA viser også et "pittingpotensiale" på omkring -700 mV, så helt ulikt er det jo ikke. Disse resultatene er ikke publisert enda.

-øøk

Henrik Westersjø Nesheim

ti 28.02, 10:33

Hei,

Takk for paper på korrosjon i sjøvann. Har to spørsmål angående paperet:

- Er sjøvannet stillestående i begge beholderene (både for sjøvannsprøvene og for prøvene som er nedsenket i mud) ?
- Og om du vet noe om korrosjonsegenskapene til TSA i forhold til AA-5083 og AA-6082 ?

Resultatene og konklusjonen i paperet er veldig nyttig i vår masteroppgave ettersom at det viser at TSA har akseptable korrosjonsegenskaper nedsenket i mud.

Hilsen,
Henrik og Kjell

Ole Øystein Knudsen <Ole.Knudsen@sintef.no>

on 22.02, 11:30

Hei
Vedlagt finner dere et paper på dette.
Hvis dere ikke har CP på TSA er det fare for MIC, som kan akselerere korrosjon vesentlig. Den undersøkelsen blir ikke publisert før i september.

Hilsen Ole Øystein

Henrik Westersjø Nesheim
on 22.02, 10:48

Hei,

Vi er to studenter som skriver oppgave ved PTS (petroleum) om bruken av aluminium i subsea strukturer. I den forbindelse har vi identifisert et mulig problem når en begraver aluminium i mud, vi er usikre på hva som vil skje med aluminiumet.
I dag hadde vi ett møte med Professor Roy Johnsen, hvor han nevnte at du hadde sett på hva som skjer med TSA (thermal sprayed aluminium) i mud under sjøvann.

Vi lurer derfor på om du har noe informasjon om emnet som du kan dele med oss ?

Hilsen,
Henrik og Kjell

# RE: PTFE Coating subsea bolter

Ole Øystein Knudsen <Ole.Knudsen@sintef.no>

fr 28.04, 11:35
Kjell Petter Løkling Lunde
Innboks

Siden det er CP vil bolten være beskyttet. Det er kun i kontaktflata det er viktig med ekstra beskyttelse, for å hindre at sinken går i oppløsning og bolten mister forspenninga. Ser ut til at NORSOK godkjenner bare sinkfosfatering, uten ekstra lag med belegg. Med sinkfosfatering antar jeg at sinken er katodisk. Sinken kan jo strengt tatt korrodere selv med CP. Fosfatering vil passivere den, slik at den ikke korroderer.

-oøk

**From:** Kjell Petter Løkling Lunde [mailto:kplunde@stud.ntnu.no]
**Sent:** 28. april 2017 09:12
**To:** Ole Øystein Knudsen <Ole.Knudsen@sintef.no>
**Subject:** SV: PTFE Coating subsea bolter

Hei igjen,

Er sinkfosfatering alene tilstrekkelig (med CP) for å beskytte boltene? Eller må det påføres et ekstra lag med coating?

Med vennlig hilsen,
Kjell

---

**Fra:** Ole Øystein Knudsen <Ole.Knudsen@sintef.no>
**Sendt:** 26. april 2017 10:46:30
**Til:** Kjell Petter Løkling Lunde; Henrik Westersjø Nesheim
**Emne:** RE: PTFE Coating subsea bolter

Hei
Jeg tror man kjøper ferdig PTFE belagte bolter. Belegget er svært tynt, ~20 µm bare, så det er sannsynlig at det skades i monteringa og elektrisk kontakt oppnås på den måten. Eller at de skraper det av på et område. Det står at fosfatering av sinkbelegget også er et alternativ, hvilket ikke introduserer dette problemet. Tror jeg ville gått for fosfatering

-oøk

**From:** Ole Øystein Knudsen [mailto:ole.oystein.knudsen@ntnu.no]
**Sent:** 26. april 2017 10:28
**To:** Ole Øystein Knudsen <Ole.Knudsen@sintef.no>
**Subject:** Vs: PTFE Coating subsea bolter

---

**Fra:** Kjell Petter Løkling Lunde
**Sendt:** 26. april 2017 10:28:04 (UTC+01.00) Amsterdam, Berlin, Bern, Roma, Stockholm, Wien
**Til:** Ole Øystein Knudsen
**Kopi:** Henrik Westersjø Nesheim
**Subjekt:** PTFE Coating subsea bolter

Hei,

Jobber med en master angående bruk av aluminium subsea (ITS-Integrated template structure), med Roy Johnsen som veileder. Noen av de strukturelle bjelkene skal sammenføyes ved bolting, både alu-alu plater mot hverandre og alu-stål. Karbonstål bolter skal brukes (NORSOK).

Boltene skal coates i henhold til følgene (NORSOK):

"Carbon steel and/or low alloy bolting material shall be hot dip galvanised to ASTM A153 or have similar corrosion protection. For submerged applications, where dissolution of a thick zinc layer may cause loss of bolt pretension, phosphating shall be used. For sub-sea installations the use of poly-tetra-fluoro-ethylene (PTFE) based coatings can be used provided electrical continuity is verified by measurements. ."

PTFE er som kjent et ikke ledende materialet. Hvordan kan man da  sørge for elektrisk kontinuitet til bolten (fra CP på strukturen)? Er det meningen at PTFE skal påføres etter at bolten er montert, slik at det er en ubehandlet kontaktflate mellom bolt og plate for å skape elektrisk kontinuitet?

Mvh,
Kjell og Henrik

## B.4 E-mail correspondence with Tor Berge Gjersvik.

Tor Berge Gjersvik <tor.b.gjersvik@ntnu.no>

**From:** Harald Thomander Neerland [mailto:haraldt.neerland@technipfmc.com]
**Sent:** fredag 17. februar 2017 10.08
**To:** Tor Berge Gjersvik <tor.b.gjersvik@ntnu.no>
**Subject:** RE: Gjøa ITS

Hei Tor,

Gjøa er designet for å være Snag Free» når manifold og sealine protection er installert.

Designet er model testet (Tror faktisk det var i Trondheim).

Slik bildet viser er ikke Gjøa «Snag free», men temporary roof og sealine protection ble

(så vidt jeg vet) instalert i samme kampanje.

Harald

PS. Uttrykket «Snag free» er i hovedsak relatert til snag av trålbord. For oss er faktisk friksjon

fra trål et viktigere design kriteria; dvs. friksjon når trål blir dratt over strukturen.

---

**From:** Tor Berge Gjersvik [mailto:tor.b.gjersvik@ntnu.no]
**Sent:** 16. februar 2017 13:29
**To:** HaraldT.Neerland@technipfmc.com
**Subject:** Gjøa ITS

Harald,

Jeg har noen studenter som sitter å ser på noen fine bilder og figurere de har fått fra Subsea 7 og fra installasjon av template på Gjøa. Se her:


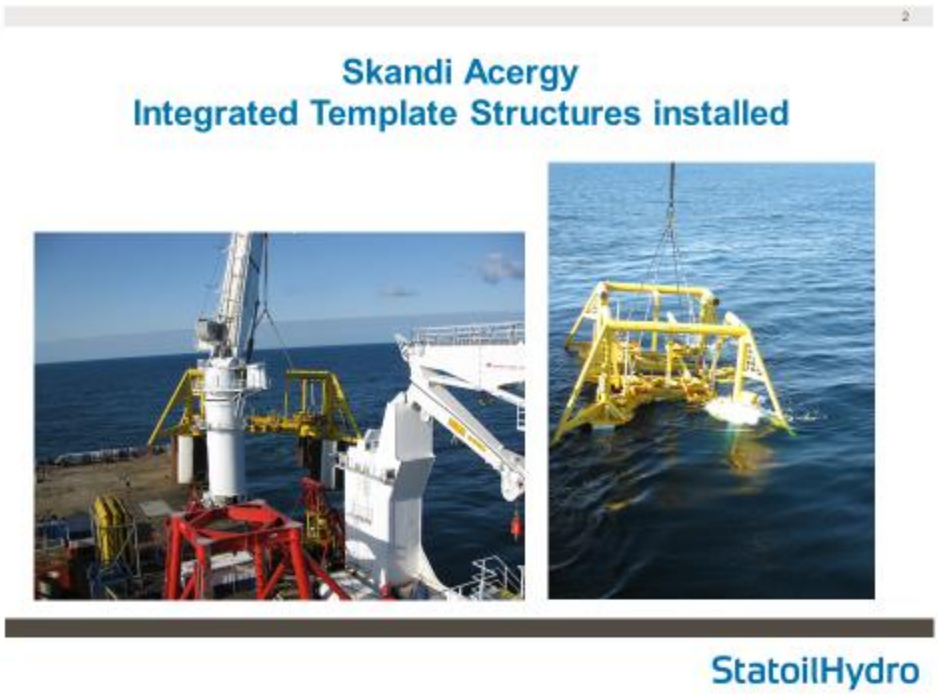


Dette er jo slik det gikk i sjøen uten luker og sea-line protection.

Så til spørsmålet: Kan du si eller finne svar på om denne typen er designet for å være «snag free»?

Hilsen,

Tor Berge

Tor Berge S. Gjersvik, siv.ing, dr.ing

Professor

Norwegian University of Science and Technology - NTNU

Faculty of Engineering Science and Technology,

Department of Geoscience and Petroleum

# Spørsmål og svar

## Tor Berge Gjersvik <tor.b.gjersvik@ntnu.no>

fr 17.03, 13:26
Henrik Westersjø Nesheim;
Kjell Petter Løkling Lunde;
Roy Johnsen;
Patrick Reurink
Innboks

Hei,

Har hatt kontakt med Harald T. Neerland i TechnipFMC nå på spørsmål som kom opp i dagens møte:

- Hva er de typiske stålkvalitetene nyttet i struktur (ramme + sugeankre) og beskyttelsesstruktur for en ITS?
  Topp ramme: S355 G15+N Norsok Y 2t
  Skørt: S355 J2+N Norsok Y05
- I trålbeskyttelsen benyttes et rammeverk av «rør». Er disse påført noen form for coating innvendig?
  Nei.  Man antar at O2 nivået blir utarmet inne i lukkete rom. For å ungå kolaps fra ytre krefter blir alle
  hullrom punktert, og diskusjonen har gått på hvorvidt vår filosofi /antagelse om utarming av O2 er riktig,
  eller om vi får utskifting av innestengt volum. For å forhinfdre dette krever Statoil (og enkelte andre) at vi
  innstallerer «Splitt Rubber Grommets) i de hull som punkterer strukturen (personlig ikke sikker på om de
  er nøvendig. Jeg vet vi har mistet noen under installasjon uten at man har ropt ulv).

Tor Berge

Tor Berge S. Gjersvik, siv.ing, dr.ing

Professor

Norwegian University of Science and Technology - NTNU

Faculty of Engineering Science and Technology,
Department of Geoscience and Petroleum

## B.5 E-mail correspondence with Asbjørn Wathne in Subsea 7 regarding ITS installation details.

Gjøa ITS installasjon

Asbjoern Wathne <asbjorn.wathne@subsea7.com>

ti 28.03, 15:18

Heisann

Bare hyggelig å være til hjelp. Dere finner svarene mine rødt nedenfor. Det er en herlig blanding av engelsk og norsk, men dere er jo smarte studenter, så det finner dere nok ut av. ☺ Lykke til!

Regards,

**Asbjørn Wathne**
Project Engineering Manager

***eMail*** Asbjorn.Wathne@subsea7.com
***Tel*** +47 51725184
***Mobile*** +47 91685582
***Switchboard*** +47 51725000
***Website*** www.subsea7.com

---

**From:** Henrik Westersjø Nesheim [mailto:henrikwn@stud.ntnu.no]
**Sent:** 27. mars 2017 15:00
**To:** Asbjoern Wathne
**Cc:** Kjell Petter Løkling Lunde
**Subject:** Gjøa ITS installasjon

Hei,

Takk for hyggelig telefon tidligere i dag, setter stor pris på at du tar deg tid til å svare på henvendelse.

Nedenfor ser du en oversikt over hva vil lurer på:

- Er vekt på wire med i beregning av vekt/løftekapasitet, slik at en må ta hensyn til vekt av wire på dypere vann ? Normalt ikke nødvendig på grunt vann, men for dypt vann, si 500m og dypere, er det viktig å ta med vekten av kranwirer. Dette kan ofte bli en showstopper på veldig dypt vann. Noen fartøy har egen fibertau winch for bruk på dypt vann. Strukturen løftes da ut med vanlig krane og overføres til fibertau winchen for videre nedsenking til sjøbunn. Husk og også legge til vekt av løfterigging på selve ITSen. Denne kan utgjøre 10-15 Te dersom det er stålslings, en del mindre om dere bruker fiberslings.

- Tidsbruk under installasjon, hvor lenge leies ett vessel for å installere en ITS, med utgangspunkt i Gjøa ITS'er og gjerne noe om variasjon i installasjonstider? Her er det store forskjeller fra ITS til ITS. Dette avhenger av flere forskjellige årsaker, som f.eks størrelse på sugeankerene, sjøbunnsforhold og tiden det tar å suge dem ned (6-18 timer). Her ville jeg sagt at selve ITS installasjonsjobben tar ca 24 timer (inkludert 4 stk XT luker) fra ankomst til feltet, til fartøyet kan returner til land. Legg til 6-12 timer i transit hver vei, avhengig av hvor feltet ligger og hvor du mobiliserer fartøyet. Dere kan også regne 24 timer i mobilisering av fartøyet (løfte om bord utstyr, ITS, luker, sjøsikring, risikomøter, crew familiarisation etc.). Så grovt sett kan en regne ca 3 dager på en ITS installasjon. Jeg har ikke inkludert for sealine protection cover. Dere kan regne 2-3 timer per cover. Normalt er det kun en SPS på en ITS som står alene. Venting på vær er ikke inkludert.

- Logg over installasjonsforløpet dersom det eksisterer. Har lagt til en røff breakdown av hvordan vi installerer en typisk FMC ITS nedenfor:

**The bullets below explains the main steps for the deployment of the ITS:**

- Set up on DP
- Preparation for launching of the ITS
- Survey of the installation area
- Connect crane to ITS rigging at deck level.
- Lift ITS clear of deck
- Slew the load to outboard until the ITS is clear of the vessel.
- Lower through splash zone to a water depth of 50m to allow for flooding of tubular members and disconnection of tugger wires.
- Continue lower the ITS to approx 10m above seabed

**The bullets below explains the main steps for the positioning of the ITS:**

- Adjust the position of the vessel and rotate the ITS with the ROV as required until the ITS is within the allowable tolerances
- Land the ITS in target position
- Gradually reduce tension and complete self-weight penetration
- Pay out slack on the main crane
- ROV to inspect the actual penetration and verify correct positioning and heading from transponder/gyro
- Disconnect rigging and recover crane and rigging to deck

**The bullets below explains the main steps for the levelling of the ITS:**

- Clean and lock the vent hatches on the suction cans
- Level and suck down ITS by use of suction pump and by operating the valves on the levelling panel
- Confirm correct inclination and depth by inclinometers, bullseye and digiquartz
- Close valves on the levelling panel and undock the ROV

**The bullets below explains the main steps for the XT hatches installation:**

- Offset vessel to a safe distance from existing subsea structures/lines.
- Connect crane to the XT hatch rigging
- Upend the XT hatch on deck and overboard
- Lower to approx 20m above seabed
- Relocate vessel to the ITS and position hatch over the dedicated position.
- Lower down XT hatch and land onto the ITS until the hinges engage

| |
|---|
| Continue to pay out on crane wire and assist with ROV to further lower the hatch to closed position<br>Lock XT hatch in closed position.<br>Repeat for remaining 3 off XT hatches<br>Perform as-left survey of complete ITS |

- Lurer også på hva som er utfordringer/begrensningene under installasjon ? (Eksempelvis waiting on weather). Den største utfordringen er selve avløftet fra dekk. Altså løft i luft. Større fartøy greier normalt disse løftene i 2-3m Hs. Farene er svingende last under avløft, samt økte dynamiske laster i rigging/kranwire. Selve deployment har også noen begrensninger, men normal mindre kritisk enn løft i luft. Her er det krefter i plaskesonen som er utfordringen. Har ITS f.eks. store sugeanker, så kan dette gi oppdrift (om ITS senkes raskere enn luften i sugeankerne kan evakueres) som igjen kan gi slakke slings og rykklaster. Lokalt, så kan f.eks. luker på ITS ødelegges/rives av pga. slamming/drag krefter. Waiting on weather er en direkte konsekvens av å ikke ha rette værforhold når ITSen skal løftes. Mye tid blir brukt på deployment analyser under forberedelsene til jobben. Vi ser da på statistiske værdata, som vind, bølgehøyde, bølgeperiode og strøm, og ser på hvilken innvirkning de har på fartøybevegelse (heave, roll, pitch etc.) og konkluderer så hvilke kombinasjoner/scenarioer vi kan operere i.

- Hvor tidkrevende (eventuelt ekstra kostnader) ved å løfte på plass beskyttelsesstruktur (hatches og sealine protection). Vil det være muligheter for å redusere antall løft ved å inkludere hatches og sealine protection i samme løft som ITS'en når ITS'en veier ca. 200 ton. Sealine protection covers må normalt installeres etter ITS er landet. På FMC sine ITSer må de 4 XMT lukene også installeres separat, da disse har for mye drag til å installeres med ITSen (de risikerer å rives av i plaskesonen). Men vi har sett ITSer med luker som har større perforering og således ikke er noe problem å inkludere i ITS løftet, gitt at totalvekten er håndterbar.

- Dagrater på relevant vessel (Ett vessel i 400Te klassen og ett i 250Te klassen). Målet med oppgaven vår er å redusere installasjonsvekten til en ITS og således bruke mindre installasjonsfartøy. Dette er konfidensiell informasjon, og variere veldig med markedsituasjonen. Her vil jeg anbefale å ta kontakt med f.eks. Seabrokers, da disser nok sitter på gjennomsnittspriser i markedet. Men husk at i tillegg til en kraftig kran, så må også kranen ha løfteradius nok til å plukke opp ITSen fra dekk. Fartøyet må også ha nok dekksplass til ITSen.

- Vet du noe om hva hvert enkelt løft veide (tenker da spesielt på løftene for hatches og sealine protection) ? Fra Gjøa prosjektet så var vektene omtrent som følger:

| | |
|---|---|
| Gjøa ITS | 275 Te (+ 10 Te for vekt av løfterigging) |
| XT luker | 3.5 Te per luke (installert separat) |
| Sealine Protection Cover | 15 Te (installert separat) |

Om dere ikke allerede er klar over det, så var det en gruppe studenter som gjorde modelltester av Gjøa ITS for oss på Marintek i 2008. Dere kan sikkert finne noe god info der også.

Vi lurer også på om noe av informasjonen du sender oss er konfidensielt ?, i så fall må vi referere til dette som konfidensielt, og unnlate det fra oppgaven ettersom at vår oppgave ikke er konfidensiell.

Informasjonen jeg har gitt dere her er ikke konfidensiell. Men vi setter alltids pris på at dere refererer til oss når dere bruke informasjonen. ☺

---



Henrik Westersjø Nesheim

ma 27.03, 14:59

Asbjorn.Wathne@subsea7.com <asbjorn.wathne@subsea7.com>;

Kjell Petter Løkling Lunde

Hei,

Takk for hyggelig telefon tidligere i dag, setter stor pris på at du tar deg tid til å svare på henvendelse.
Nedenfor ser du en oversikt over hva vil lurer på:

- Er vekt på wire med i beregning av vekt/løftekapasitet, slik at en må ta hensyn til vekt av wire på dypere vann ?
- Tidsbruk under installasjon, hvor lenge leies ett vessel for å installere en ITS, med utgangspunkt i Gjøa ITS'er og gjerne noe om variasjon i installasjonstider?
- Logg over installasjonsforløpet dersom det eksisterer.
- Lurer også på hva som er utfordringer/begrensningene under installsjon ? (Eksempelvis waiting on weather).
- Hvor tidkrevende (eventuelt ekstra kostnader) ved å løfte på plass beskyttelsesstruktur (hatches og sealine protection). Vil det være muligheter for å redusere antall løft ved å inkludere hatches og sealine protection i samme løft som ITS'en når ITS'en veier ca. 200 ton.
- Dagrater på relevant vessel (Ett vessel i 400Te klassen og ett i 250Te klassen). Målet med oppgaven vår er å redusere installasjonsvekten til en ITS og således bruke mindre installasjonsfartøy.

- Vet du noe om hva hvert enkelt løft veide (tenker da spesielt på løftene for hatches og sealine protection) ?

Vi lurer også på om noe av informasjonen du sender oss er konfidensielt ?, i så fall må vi referere til dette som konfidensielt, og unnlate det fra oppgaven ettersom at vår oppgave ikke er konfidensiell.

Vi kommer begge fra Stavanger-området og besøker dere gjerne på Forus dersom det passer. Vi er hjemme i påsken fra og med Lørdag den 06. April til og med Tirsdag den 18. April.

Hilsen,
Henrik og Kjell

## B.6 E-mail correspondence with Ole Terje Midling in Marine Aluminium.

RE: Prisoverslag - Fabrikasjon ITS

Ole Terje Midling <ole.terje.midling@m-a.no>

Svar alle ti
16.05, 16:12

Hei,

Som sagt er det en utfordring å prise denne jobben da vi ikke vet omfanget av sveisingen (annet en antall meter sveis, og MIG eller FSW prosessen som er valgt) Spekteret for fabrikasjon vil være i størrelsesorden 300-400NOK/kg avhengig av kompleksitet*).

Mvh
Ole Terje

**Ole Terje Midling**
Chief Fabrication Officer PhD , Marine Aluminium AS
**Mobile**+4793208952
**Websit Email**

**From:** Kjell Petter Løkling Lunde [mailto:kplunde@stud.ntnu.no]
**Sent:** 16. mai 2017 13:04
**To:** Ole Terje Midling <ole.terje.midling@m-a.no>; Henrik Westersjø Nesheim <henrikwn@stud.ntnu.no>
**Subject:** SV: Prisoverslag - Fabrikasjon ITS

Hei Ole,

Har dere en ca. fabrikasjonstid (timer/tonn) og fabrikasjonskostnad (kr/time) eller andre veiledende tall vi kan bruke? Det kan gjerne være i form av et spekter.

Vi har fått prisoverslag fra både STEP-G og Constellium. Ekstrusjon hos STEP-G og plater hos Constellium.

Med vennlig hilsen,
Kjell og Henrik

*) Etter diskusjon per telefon den 05.31.2017, er det avtalt å bruke spekteret 200 – 300 NOK/kg som et realistisk estimat i kostnadsanalysen.

## B.7 E-mail correspondence with Skarpenord regarding aluminium anodes

### Anode kostnader

Jørn Voje <joern.voje@skarpenord-corrosion.no>

to 27.04, 13:27

Hei,

Som et slags budsjettall foreslår jeg at dere benytter NOK 44.00 pr. kg netto legering.

Vennlig hilsen,
for Skarpenord Corrosion a.s.
Jørn Voje

*Jørn Voje*
*Skarpenord Corrosion a.s.*
*P.O. Box 46*
*N-3993 Langesund*
*Norway*
*Telephone: +47 35967941*
*Handphone: +47 91614902*
*Email: jv@scas.no*
*Web: http://www.skarpenord-corrosion.no*

Henrik Westersjø Nesheim

to 27.04, 12:50
post@skarpenord-corrosion.no;
Kjell Petter Løkling Lunde

Hei,

Vi er to studenter ved NTNU som skriver en masteroppgave innen subsea. Vi tar for oss en stor struktur som trenger anode-beskyttelse mot korrosjon.
Har du/dere en enhetskostnad (NOK/Ton eller NOK/kg) på anoder av typen "Coral 'A' High Grade" og typen "Coral 'A' Special Grade" ?

Strukturen vi ser på vil grovt regnet trenge ca. 7,5 ton med anoder.

Hilsen,
Henrik og Kjell

## B.8 E-mail correspondence with Halvard Torget Eriksen regarding cost of phosphated bolts

RE: Sinkfosfatering bolter - prisoverslag

Halvard Torget Eriksen <halvard@oddacoating.no>

fr 28.04.2017 08:59
Til:
Kjell Petter Løkling Lunde
Kopi:
Bjarne Sørum <bjarne@oddacoating.no>
Innboks

Hei og god morgen!

Et kjapt prisoverslag på dette:

Vask, blåserensing, zink-fosfatering:

- Bolter Kr. 145.-
- Mutre Kr. 60.-
- Skiver Kr. 50.-

Prisene forutsetter antallet dere antydet i forespørselen under.

Vi vil anbefale at delene får påført et tynt lag olje som er egnet for formålet rett etter fosfatering. Om dere ønsker dette vil det medføre en kostnad på Kr. 5.- per del.

Bare ta kontakt om dere ønsker utfyllende opplysninger eller om det er andre prosjekter dere ønsker hjelp til. ☺

Beste hilsen / Best Regards
**Halvard Torget Eriksen**
Project Coordinator

☎ +47 906 44 100 +47 992 06 228
www.oddacoating.no

**From:** Kjell Petter Løkling Lunde [mailto:kplunde@stud.ntnu.no]
**Sent:** 27. april 2017 14:08
**To:** Odda Coating Technology AS <post@oddacoating.no>
**Cc:** Henrik Westersjø Nesheim <henrikwn@stud.ntnu.no>
**Subject:** Sinkfosfatering bolter - prisoverslag

Hei,

Vi jobber med en master angående bruk av aluminium subsea ved NTNU. Noen av de strukturelle bjelkene vi jobber med må sammenføyes med bolter.
Har dere mulighet til å gi oss et prisoverslag på å sinkfosfatere 1468 stk karbonstålbolter i tillegg til tilhørende muttere (1468 stk) og skiver (1468*2=2936 stk)? Dimensjonen på boltene er M36 med varierende lengder mellom 110-210 mm.

Har dere en budsjetterende enhetspris pr. komponent?

Med vennlig hilsen,
Kjell og Henrik

# Appendix C

# Bolt Calculations

## C.1 Design sheets exported from excel

| | | | | | |
|---|---|---|---|---|---|
| Joint V, a-a | Accounts for both web and flange | | | Momemt 6/8 of maximum | |
| Safety factor for ultimate state | Number of friction interfaces | Slip factor (0,3-0,4?pakning?) | UTS [Mpa] | Moment [N*mm] | Height of beam [mm] |
| 1.25 | 2 | 0.4 | 700 | 9,976,568,229 | 1500 |
| | | | | | |
| Bolt Type | As [mm^2] | Preloading (F_p) [N] | Slip resistance per bolt [N] | Shear resistance per bolt [N] | Number of flange bolts required (one flange, one side) |
| M20 | 333 | 163,170 | 104,429 | 93,240 | 67 |
| M24 | 384 | 188,160 | 120,422 | 107,520 | 58 |
| M30 | 621 | 304,290 | 194,746 | 173,880 | 36 |
| M36 | 865 | 423,850 | 271,264 | 242,200 | 26 |
| M39 | 1030 | 504,700 | 323,008 | 288,400 | 22 |
| | | | | | |
| Bolt size [mm] | do [mm] +3 | Min. e1 and e2 [mm] | Min. p1 [mm] | Min. p2 [mm] | Number of bolts across the flange (ca. 420 mm space to bolt one side) |
| 20 | 23 | 28 | 51 | 56 | 7.00 |
| 24 | 27 | 33 | 60 | 65 | 6.00 |
| 30 | 33 | 40 | 73 | 80 | 5.00 |
| 36 | 39 | 47 | 86 | 94 | 4.00 |
| 39 | 42 | 51 | 93 | 101 | 4.00 |
| Flange fixturing characteristics | | Flange thickness [mm] | Flange force [N] | Web thickness [mm] | Web force [N] |
| Width of top flange plate [mm] | 500 | 55 | 6,904,199 | 60 | 1,625,000 |
| Thickness of top flange plate [mm] | 40 | | | | |
| Width of bottom flange plate (one side of web) [mm] | 210 | Total number of flange bolts | Number of web bolts (one web) | Total number of web bolts | Total number of bolts in the joint |
| Thickness of bottom flange plate [mm] | 40 | 268 | 16 | 64 | 332 |
| Axial stress in top plate (one friction interface) [Mpa] | 345 | 232 | 14 | 56 | 288 |
| Axial stress in both plate (two friction interfaces) [Mpa] | 188 | 144 | 9 | 36 | 180 |
| Length through cross-section (one friction interface) [mm] | 95 | 104 | 6 | 12 | 116 |
| Length through cross-section (two friction interfaces) [mm] | 135 | 88 | 6 | 24 | 112 |
| | | | | | |
| Web fixturing characteristics | | Number of bolts along the flange | Min. Length of coupling (one side) [mm] | Min. length of flange plate (both sides) [mm] | |
| Width of web plate [mm] | 150 | 10.00 | 515 | 1030 | |
| Height of middle plate [mm] | 600 | 10.00 | 606 | 1212 | |
| Height of top or bottom plate [mm] | 0 | 8.00 | 591 | 1182 | |
| Thickness of web plate [mm] | 10 | 7.00 | 610 | 1220 | |
| Shear stress in web plate [Mpa] | 67.70833333 | 6.00 | 567 | 1134 | |
| Length through cross-section [mm] | 80 | | | | |
| | | | | | |
| | | | | | |
| Cubic meter of flange plating [mm^3] | 89792000 | | | | |
| Cubic meter of web plating [mm^3] | 3600000 | | | | |
| Total Plate weight [kg] 4 connections | 1008.6336 | | | | |
| | | cross section length [mm] | | | |
| Total number of flange bolts | 416 | 135 | | | |
| Total number of web bolts | 48 | 80 | | | |

| | | | | | | |
|---|---|---|---|---|---|---|
| Joint I,a | Accounts for both web and flange | | | moment 3/8 of maximum | | |
| Safety factor for ultimate state | Number of friction interfaces | Slip factor (0,3-0,4?pakning?) | UTS [Mpa] | Moment [N*mm] | Height of beam [mm] | |
| 1.25 | 1 | 0.4 | 700 | 4,988,284,115 | 1500 | |
| | | | | | | |
| Bolt Type | As [mm^2] | Preloading (F_p) [N] | Slip resistance per bolt [N] | Shear resistance per bolt [N] | Number of flange bolts required (one flange, one side) | |
| M20 | 333 | 163,170 | 52,214 | 93,240 | 67 | |
| M24 | 384 | 188,160 | 60,211 | 107,520 | 58 | |
| M30 | 621 | 304,290 | 97,373 | 173,880 | 36 | |
| M36 | 865 | 423,850 | 135,632 | 242,200 | 26 | |
| M39 | 1030 | 504,700 | 161,504 | 288,400 | 22 | |
| | | | | | | |
| Bolt size [mm] | do [mm] +3 | Min. e1 and e2 [mm] | Min. p1 [mm] | Min. p2 [mm] | Number of bolts across the flange (ca. 420 mm space to bolt one side) | |
| 20 | 23 | 28 | 51 | 56 | 7.00 | |
| 24 | 27 | 33 | 60 | 65 | 6.00 | |
| 30 | 33 | 40 | 73 | 80 | 5.00 | |
| 36 | 39 | 47 | 86 | 94 | 4.00 | |
| 39 | 42 | 51 | 93 | 101 | 4.00 | |
| Flange fixturing characteristics | | Flange thickness [mm] | Flange force [N] | Web thickness [mm] | Web force [N] | |
| Width of top flange plate [mm] Steel plate | 500 | 55 | 3,452,100 | 60 | 1,625,000 | |
| Thickness of top flange plate [mm] | 25 | | | | | |
| Axial stress in top plate (one friction interface) [Mpa] | 276 | Total number of flange bolts | Number of web bolts (one web) | Total number of web bolts | Total number of bolts in the joint | |
| Length through cross-section (one friction interface) [mm] | 80 | 134 | 32 | 32 | 166 | |
| | | 116 | 27 | 27 | 143 | |
| | | 72 | 17 | 17 | 89 | |
| Web fixturing characteristics | | 52 | 12 | 12 | 64 | |
| Width of web plate [mm] | 200 | 44 | 11 | 11 | 55 | |
| Height of middle plate [mm] | 600 | | | | | |
| Height of top or bottom plate [mm] | 0 | Number of bolts along the flange | Min. Length of coupling (one side) [mm] | | | |
| Thickness of web plate [mm] | 10 | 10.00 | 515 | | | |
| Shear stress in web plate [Mpa] | 270.8333333 | 10.00 | 606 | | | |
| Length through cross-section [mm] | 70 | 8.00 | 591 | | | |
| | | 7.00 | 610 | | | |
| | | 6.00 | 567 | | | |
| | | | | | | |
| Cubic meter of flange plating [mm^3] Steel | 15250000 | | | | | |
| Cubic meter of web plating [mm^3] Steel | 1200000 | | | | | |
| Total steel plate weight [kg] 4*connections | 513.24 | | | | | |
| | | cross section length [mm] | | | | |
| Total number of flange bolts | 208 | 80 | | | | |
| Total number of web bolts | 48 | 70 | | | | |

| | | | | | |
|---|---|---|---|---|---|
| Joint I, d | Accounts for both web and flange (flange only one interface due to steel plating) | | | Moment (1/8 of maximum | |
| Safety factor for ultimate state | Number of friction interfaces | Slip factor (0,3-0,4?pakning?) | UTS [Mpa] | Moment [N*mm] | Height of beam [mm] |
| 1.25 | 1 | 0.4 | 700 | 1,662,761,372 | 1500 |
| | | | | | |
| Bolt Type | As [mm^2] | Preloading (F_p) [N] | Slip resistance per bolt [N] | Shear resistance per bolt [N] | Number of flange bolts required (one flange, one side) |
| M20 | 333 | 163,170 | 52,214 | 93,240 | 22.00 |
| M24 | 384 | 188,160 | 60,211 | 107,520 | 19.00 |
| M30 | 621 | 304,290 | 97,373 | 173,880 | 12.00 |
| M36 | 865 | 423,850 | 135,632 | 242,200 | 9.00 |
| M39 | 1030 | 504,700 | 161,504 | 288,400 | 8.00 |
| | | | | | |
| Bolt size [mm] | do [mm] +3 | Min. e1 and e2 [mm] | Min. p1 [mm] | Min. p2 [mm] | Number of bolts across the flange (ca. 250 mm space to bolt one side) |
| 20 | 23 | 28 | 51 | 56 | 4.00 |
| 24 | 27 | 33 | 60 | 65 | 3.00 |
| 30 | 33 | 40 | 73 | 80 | 3.00 |
| 36 | 39 | 47 | 86 | 94 | 2.00 |
| 39 | 42 | 51 | 93 | 101 | 2.00 |
| Flange fixturing characteristics | | Flange thickness [mm] | Flange force [N] | Web thickness [mm] | Web force [N] |
| Width of top flange plate [mm] Steel plate | 500 | 30 | 1,131,130 | 45 | 100,000 |
| Thickness of top flange plate [mm] | 10 | | | | |
| Axial stress in top plate (one friction interface) [Mpa] | 226 | Total number of flange bolts | Number of web bolts (one web) | Total number of web bolts | Total number of bolts in the joint |
| Length through cross-section (one friction interface) [mm] | 40 | 44.00 | 2.00 | 2.00 | 46.00 |
| | | 38.00 | 2.00 | 2.00 | 40.00 |
| | | 24.00 | 2.00 | 2.00 | 26.00 |
| Web fixturing characteristics | | 18.00 | 2.00 | 2.00 | 20.00 |
| Width of web plate [mm] | 150 | 16.00 | 1.00 | 1.00 | 17.00 |
| Height of middle plate [mm] | 200 | | | | |
| Height of top or bottom plate [mm] | 0 | Number of bolts along the flange | Min. Length of coupling (one side) [mm] | | |
| Thickness of web plate [mm] | 10 | 6.00 | 311 | | |
| Shear stress in web plate [Mpa] | 50 | 7.00 | 426 | | |
| Length through cross-section [mm] | 55 | 4.00 | 299 | | |
| | | 5.00 | 438 | | |
| | | 4.00 | 381 | | |
| | | | | | |
| | | | | | |
| | | | | | |
| Cubic meter of flange plating [mm^3] Steel | 4380000 | | | | |
| Cubic meter of web plating [mm^3] Steel | 300000 | | | | |
| Total steel plate weight [kg] | 146.016 | | | | |
| | | cross section length [mm] | | | |
| Total number of flange bolts | 72 | 40 | | | |
| Total number of web bolts | 8 | 55 | | | |

| | | | | | |
|---|---|---|---|---|---|
| Joint I, f | Accounts for both web and flange | | | Moment 3/8 of max | |
| Safety factor for ultimate state | Number of friction interfaces | Slip factor (0,3-0,4?pakning?) | UTS [Mpa] | Moment [N*mm] | Height of beam [mm] |
| 1.25 | 1 | 0.4 | 700 | 4,988,284,115 | 1500 |
| | | | | | |
| Bolt Type | As [mm^2] | Preloading (F_p) [N] | Slip resistance per bolt [N] | Shear resistance per bolt [N] | Number of flange bolts required (one flange, one side) |
| M20 | 333 | 163,170 | 52,214 | 93,240 | 66 |
| M24 | 384 | 188,160 | 60,211 | 107,520 | 57 |
| M30 | 621 | 304,290 | 97,373 | 173,880 | 36 |
| M36 | 865 | 423,850 | 135,632 | 242,200 | 26 |
| M39 | 1030 | 504,700 | 161,504 | 288,400 | 22 |
| | | | | | |
| Bolt size [mm] | do [mm] +3 | Min. e1 and e2 [mm] | Min. p1 [mm] | Min. p2 [mm] | Number of bolts across the flange (ca. 760 mm space to bolt one side) |
| 20 | 23 | 28 | 51 | 56 | 13.00 |
| 24 | 27 | 33 | 60 | 65 | 11.00 |
| 30 | 33 | 40 | 73 | 80 | 9.00 |
| 36 | 39 | 47 | 86 | 94 | 8.00 |
| 39 | 42 | 51 | 93 | 101 | 7.00 |
| Flange fixturing characteristics | | Flange thickness [mm] | Flange force [N] | Web thickness [mm] | Web force [N] |
| Width of top flange plate [mm] Steel plate!!!! | 880 | 45 | 3,428,374 | 40 | 2,000,000 |
| Thickness of top flange plate [mm] | 25 | | | | |
| Axial stress in top plate (one friction interface) [Mpa] | 156 | Total number of flange bolts | Number of web bolts (one web) | Total number of web bolts | Total number of bolts in the joint |
| Length through cross-section (one friction interface) [mm] | 70 | 132 | 39 | 78 | 210 |
| | | 114 | 34 | 68 | 182 |
| | | 72 | 21 | 42 | 114 |
| Web fixturing characteristics | | 52 | 15 | 15 | 67 |
| Width of web plate [mm] | 200 | 44 | 13 | 26 | 70 |
| Height of middle plate [mm] | 600 | | 2*5 arangement on each web | | |
| Height of top or bottom plate [mm] | 0 | Number of bolts along the flange | Min. Length of coupling (one side) [mm] | | |
| Thickness of web plate [mm] | 20 | 6.00 | 311 | | |
| Shear stress in web plate [Mpa] | 167 | 6.00 | 366 | | |
| Length through cross-section [mm] | 60 | 4.00 | 299 | | |
| | | 4.00 | 352 | | |
| | | 4.00 | 381 | | |
| | | | | | |
| Cubic meter of flange plating [mm^3] Steel | 15488000 | | | | |
| Cubic meter of web plating [mm^3] Steel | 2400000 | | | | |
| Total steel plate weight [kg] | 558.1056 | | | | |
| | | cross section length [mm] | | | |
| Total number of flange bolts | 208 | 70 | | | |
| Total number of web bolts | 60 | 60 | | | |

| | | | | | |
|---|---|---|---|---|---|
| Joint IV, h-g | Accounts for both web and flange | | | | |
| Safety factor for ultimate state | Number of friction interfaces | Slip factor (0,3-0,4?pakning?) | UTS [Mpa] | Moment [N*mm] | Height of beam [mm] |
| 1.25 | 2 | 0.3 | 700 | 340,000,000 | 1000 |
| | | | | | |
| Bolt Type | As [mm^2] | Preloading (F_p) [N] | Slip resistance per bolt [N] | Shear resistance per bolt [N] | Number of flange bolts required (one flange, one side) |
| M20 | 333 | 163,170 | 78,322 | 93,240 | 9 |
| M24 | 384 | 188,160 | 90,317 | 107,520 | 8 |
| M30 | 621 | 304,290 | 146,059 | 173,880 | 5 |
| M36 | 865 | 423,850 | 203,448 | 242,200 | 4 |
| M39 | 1030 | 504,700 | 242,256 | 288,400 | 3 |
| | | | | | |
| Bolt size [mm] | do [mm] +3 | Min. e1 and e2 [mm] | Min. p1 [mm] | Min. p2 [mm] | Number of bolts across the flange (ca. 265 mm space to bolt one side, beam h) |
| 20 | 23 | 28 | 51 | 56 | 4.00 |
| 24 | 27 | 33 | 60 | 65 | 4.00 |
| 30 | 33 | 40 | 73 | 80 | 3.00 |
| 36 | 39 | 47 | 86 | 94 | 2.00 |
| 39 | 42 | 51 | 93 | 101 | 2.00 |
| Flange fixturing characteristics | | Flange thickness [mm] | Flange force [N] | Web thickness [mm] | Web force [N] |
| Width of top flange plate [mm] | 330 | 30 | 650,515 | 45 | 100,000 |
| Thickness of top flange plate [mm] | 10 | | | | |
| Width of bottom flange plate (one side of web) [mm] | 132.5 | Total number of flange bolts | Number of web bolts (one web) | Total number of web bolts | Total number of bolts in the joint |
| Thickness of bottom flange plate [mm] | 10 | 36 | 2 | 4 | 40 |
| Axial stress in top plate (one friction interface) [Mpa] | 197 | 32 | 2 | 4 | 36 |
| Axial stress in both plate (two friction interfaces) [Mpa] | 109 | 20 | 1 | 2 | 22 |
| Length through cross-section (one friction interface) [mm] | 40 | 16 | 0 | 0 | 16 |
| Length through cross-section (two friction interfaces) [mm] | 50 | 12 | 1 | 2 | 14 |
| | | | | | |
| | | Number of bolts along the flange | Min. Length of coupling (one side) [mm] | Min. length of flange plate (both sides) [mm] | |
| Cubic meter of flange plating [mm^3] | 4284000 | 3.00 | 158 | 316 | |
| Cubic meter of web plating [mm^3] | 0 | 2.00 | 126 | 252 | |
| Total weight of plating [kg] 8 connections | 92.5344 | 2.00 | 153 | 306 | |
| | | 2.00 | 180 | 360 | |
| | | 2.00 | 195 | 390 | |
| | | | | | |
| | | cross section length [mm] | | | |
| Total number of flange bolts | 128 | 50 | | | |
| Total number of web bolts | 0 | 0 | | | |

| | | | | | |
|---|---|---|---|---|---|
| Joint IV, b-g | Accounts for both web and flange | | | | |
| Safety factor for ultimate state | Number of friction interfaces | Slip factor (0,3-0,4?pakning?) | UTS [Mpa] | Moment [N*mm] | Height of beam [mm] |
| 1.25 | 2 | 0.3 | 700 | 380,000,000 | 1000 |
| | | | | | |
| Bolt Type | As [mm^2] | Preloading (F_p) [N] | Slip resistance per bolt [N] | Shear resistance per bolt [N] | Number of flange bolts required (one flange, one side) |
| M20 | 333 | 163,170 | 78,322 | 93,240 | 9 |
| M24 | 384 | 188,160 | 90,317 | 107,520 | 8 |
| M30 | 621 | 304,290 | 146,059 | 173,880 | 5 |
| M36 | 865 | 423,850 | 203,448 | 242,200 | 4 |
| M39 | 1030 | 504,700 | 242,256 | 288,400 | 3 |
| | | | | | |
| Bolt size [mm] | do [mm] +3 | Min. e1 and e2 [mm] | Min. p1 [mm] | Min. p2 [mm] | Number of bolts across the flange (ca. 275 mm space to bolt one side, beam h) |
| 20 | 23 | 28 | 51 | 56 | 5.00 |
| 24 | 27 | 33 | 60 | 65 | 4.00 |
| 30 | 33 | 40 | 73 | 80 | 3.00 |
| 36 | 39 | 47 | 86 | 94 | 2.00 |
| 39 | 42 | 51 | 93 | 101 | 2.00 |
| Flange fixturing characteristics | | Flange thickness [mm] | Flange force [N] | Web thickness [mm] | Web force [N] |
| Width of top flange plate [mm] | 330 | 30 | 691,753 | 35 | 100,000 |
| Thickness of top flange plate [mm] | 10 | | | | |
| Width of bottom flange plate (one side of web) [mm] | 132.5 | Total number of flange bolts | Number of web bolts (one web) | Total number of web bolts | Total number of bolts in the joint |
| Thickness of bottom flange plate [mm] | 10 | 36 | 2 | 4 | 40 |
| Axial stress in top plate (one friction interface) [Mpa] | 210 | 32 | 2 | 4 | 36 |
| Axial stress in both plate (two friction interfaces) [Mpa] | 116 | 20 | 1 | 2 | 22 |
| Length through cross-section (one friction interface) [mm] | 40 | 16 | 0 | 0 | 16 |
| Length through cross-section (two friction interfaces) [mm] | 50 | 12 | 1 | 2 | 14 |
| | | | | | |
| | | Number of bolts along the flange | Min. Length of coupling (one side) [mm] | Min. length of flange plate (both sides) [mm] | |
| Cubic meter of flange plating [mm^3] | 4284000 | 2.00 | 107 | 214 | |
| Cubic meter of web plating [mm^3] | 0 | 2.00 | 126 | 252 | |
| Total weight of plating [kg] 4 connections | 46.2672 | 2.00 | 153 | 306 | |
| | | 2.00 | 180 | 360 | |
| | | 2.00 | 195 | 390 | |
| | | | | | |
| | | | | | |
| | | cross section length [mm] | | | |
| Total number of flange bolts | 64 | 50 | | | |
| Total number of web bolts | 0 | 0 | | | |

| | | | | | |
|---|---|---|---|---|---|
| Joint V, b-c | Accounts for both web and flange | | | tie in loads | |
| Safety factor for ultimate state | Number of friction interfaces | Slip factor (0,3-0,4?pakning?) | UTS [Mpa] | Moment [N*mm] | Height of beam [mm] |
| 1.25 | 1 | 0.4 | 700 | 518,000,000 | 1500 |
| | | | | | |
| Bolt Type | As [mm^2] | Preloading (F_p) [N] | Slip resistance per bolt [N] | Shear resistance per bolt [N] | Number of flange bolts required (one flange, one side) |
| M20 | 333 | 163,170 | 52,214 | 93,240 | 13 |
| M24 | 384 | 188,160 | 60,211 | 107,520 | 11 |
| M30 | 621 | 304,290 | 97,373 | 173,880 | 7 |
| M36 | 865 | 423,850 | 135,632 | 242,200 | 5 |
| M39 | 1030 | 504,700 | 161,504 | 288,400 | 5 |
| | | | | | |
| Bolt size [mm] | do [mm] +3 | Min. e1 and e2 [mm] | Min. p1 [mm] | Min. p2 [mm] | Number of bolts across the flange (ca. 275 mm space to bolt one side, beam h) |
| 20 | 23 | 28 | 51 | 56 | 5.00 |
| 24 | 27 | 33 | 60 | 65 | 4.00 |
| 30 | 33 | 40 | 73 | 80 | 3.00 |
| 36 | 39 | 47 | 86 | 94 | 2.00 |
| 39 | 42 | 51 | 93 | 101 | 2.00 |
| Flange fixturing characteristics | | Flange thickness [mm] | Flange force [N] | Web thickness [mm] | Web force [N] |
| Width of top flange plate [mm] | 0 | 30 | 652,381 | 35 | 100,000 |
| Thickness of top flange plate [mm] | 0 | | | | |
| Width of bottom flange plate (one side of web) [mm] | 275 | Total number of flange bolts | Number of web bolts (one web) | Total number of web bolts | Total number of bolts in the joint |
| Thickness of bottom flange plate [mm] | 15 | 26 | 2 | 4 | 30 |
| Axial stress in top plate (one friction interface) [Mpa] | 0 | 22 | 2 | 4 | 26 |
| Axial stress in both plate (two friction interfaces) [Mpa] | 79 | 14 | 2 | 4 | 18 |
| Length through cross-section (one friction interface) [mm] | 30 | 10 | 0 | 0 | 10 |
| Length through cross-section (two friction interfaces) [mm] | 45 | 10 | 1 | 2 | 12 |
| | | | | | |
| | | Number of bolts along the flange | Min. Length of coupling (one side) [mm] | Min. length of flange plate (both sides) [mm] | |
| Cubic meter of flange plating [mm^3] | 4389000 | 3.00 | 158 | 316 | |
| Cubic meter of web plating [mm^3] | 0 | 3.00 | 186 | 372 | |
| Total weight of plating [kg] 4 connections | 47.4012 | 3.00 | 226 | 452 | |
| | | 3.00 | 266 | 532 | |
| | | 3.00 | 288 | 576 | |
| | | | | | |
| | | cross section length [mm] | | | |
| Total number of flange bolts | 48 | 45 | | | |
| Total number of web bolts | 0 | 0 | | | |

| | | | | | |
|---|---|---|---|---|---|
| Joint VI, c-e | Accounts for both web and flange | | | | |
| Safety factor for ultimate state | Number of friction interfaces | Slip factor (0,3-0,4?pakning?) | UTS [Mpa] | Moment [N*mm] | Height of beam [mm] |
| 1.25 | 1 | 0.3 | 700 | 0 | |
| | | | | | |
| Bolt Type | As [mm^2] | Preloading (F_p) [N] | Slip resistance per bolt [N] | Shear resistance per bolt [N] | Number of flange bolts required (one flange, one side) |
| M20 | 333 | 163,170 | 39,161 | 93,240 | 6 |
| M24 | 384 | 188,160 | 45,158 | 107,520 | 5 |
| M30 | 621 | 304,290 | 73,030 | 173,880 | 3 |
| M36 | 865 | 423,850 | 101,724 | 242,200 | 2 |
| M39 | 1030 | 504,700 | 121,128 | 288,400 | 2 |
| | | | | | |
| Bolt size [mm] | do [mm] +3 | Min. e1 and e2 [mm] | Min. p1 [mm] | Min. p2 [mm] | Number of bolts across the flange (ca. 260 mm space to bolt one side, beam h) |
| 20 | 23 | 28 | 51 | 56 | 5.00 |
| 24 | 27 | 33 | 60 | 65 | 4.00 |
| 30 | 33 | 40 | 73 | 80 | 3.00 |
| 36 | 39 | 47 | 86 | 94 | 2.00 |
| 39 | 42 | 51 | 93 | 101 | 2.00 |
| Flange fixturing characteristics | | Flange thickness [mm] | Flange force [N] | Web thickness [mm] | Web force [N] |
| Width of top flange plate [mm] | 300 | 32 | 200,000 | 20 | 0 |
| Thickness of top flange plate [mm] | 10 | | | | |
| Width of bottom flange plate (one side of web) [mm] | 0 | Total number of flange bolts | Number of web bolts (one web) | Total number of web bolts | Total number of bolts in the joint |
| Thickness of bottom flange plate [mm] | 0 | 12 | 0 | 0 | 12 |
| Axial stress in top plate (one friction interface) [Mpa] | 67 | 10 | 0 | 0 | 10 |
| Axial stress in both plate (two friction interfaces) [Mpa] | 67 | 6 | 0 | 0 | 6 |
| Length through cross-section (one friction interface) [mm] | 42 | 4 | 0 | 0 | 4 |
| Length through cross-section (two friction interfaces) [mm] | 42 | 4 | 0 | 0 | 4 |
| | | | | | |
| | | Number of bolts along the flange | Min. Length of coupling (one side) [mm] | Min. length of flange plate (both sides) [mm] | |
| | | 2.00 | 107 | 214 | |
| | | 2.00 | 126 | 252 | |
| | | 1.00 | 80 | 160 | |
| | | 1.00 | 94 | 188 | |
| | | 1.00 | 102 | 204 | |
| | | | | | |
| | | cross section length [mm] | | | |
| Total number of flange bolts | 16 | 42 | | | |
| Total number of web bolts | 0 | 0 | | | |

| | | | | | |
|---|---|---|---|---|---|
| Joint I, e | Accounts for both web and flange | | | | |
| Safety factor for ultimate state | Number of friction interfaces | Slip factor (0,3-0,4?pakning?) | UTS [Mpa] | Moment [N*mm] | Height of beam [mm] |
| 1.25 | 1 | 0.3 | 700 | 0 | |
| | | | | | |
| Bolt Type | As [mm^2] | Preloading (F_p) [N] | Slip resistance per bolt [N] | Shear resistance per bolt [N] | Number of flange bolts required (one flange, one side) |
| M20 | 333 | 163,170 | 39,161 | 93,240 | 6 |
| M24 | 384 | 188,160 | 45,158 | 107,520 | 5 |
| M30 | 621 | 304,290 | 73,030 | 173,880 | 3 |
| M36 | 865 | 423,850 | 101,724 | 242,200 | 2 |
| M39 | 1030 | 504,700 | 121,128 | 288,400 | 2 |
| | | | | | |
| Bolt size [mm] | do [mm] +3 | Min. e1 and e2 [mm] | Min. p1 [mm] | Min. p2 [mm] | Number of bolts across the flange (ca. 260 mm space to bolt one side, beam h) |
| 20 | 23 | 28 | 51 | 56 | 5.00 |
| 24 | 27 | 33 | 60 | 65 | 4.00 |
| 30 | 33 | 40 | 73 | 80 | 3.00 |
| 36 | 39 | 47 | 86 | 94 | 2.00 |
| 39 | 42 | 51 | 93 | 101 | 2.00 |
| Flange fixturing characteristics | | Flange thickness [mm] | Flange force [N] | Web thickness [mm] | Web force [N] |
| Width of top flange plate [mm] Steel plate | 300 | 32 | 200,000 | 20 | 0 |
| Thickness of top flange plate [mm] | 5 | | | | |
| Axial stress in top plate (one friction interface) [Mpa] | 133 | Total number of flange bolts | Number of web bolts (one web) | Total number of web bolts | Total number of bolts in the joint |
| Length through cross-section (one friction interface) [mm] | 37 | 12 | 0 | 0 | 12 |
| | | 10 | 0 | 0 | 10 |
| | | 6 | 0 | 0 | 6 |
| Cubic meter of flange plating [mm^3] | 282000 | 4 | 0 | 0 | 4 |
| Cubic meter of web plating [mm^3] | 0 | 4 | 0 | 0 | 4 |
| Total weight of plating [kg] 4 connections, steel | 8.7984 | | | | |
| | | Number of bolts along the flange | Min. Length of coupling (one side) [mm] | | |
| | | 2.00 | 107 | | |
| | | 2.00 | 126 | | |
| | | 1.00 | 80 | | |
| | | 1.00 | 94 | | |
| | | 1.00 | 102 | | |
| | | | | | |
| | | cross section length [mm] | | | |
| Total number of flange bolts | 16 | 37 | | | |
| Total number of web bolts | 0 | 0 | | | |

| | | | | | |
|---|---|---|---|---|---|
| Joint XI, g-k | | | | Maximum moment from geomery of beam k | |
| Safety factor for ultimate state | Number of friction interfaces | Slip factor (0,3-0,4?pakning?) | UTS [Mpa] | Moment [N*mm] | Height of beam [mm] |
| 1.25 | 1 | 0.4 | 700 | 460,000,000 | 1000 |
| | | | | | |
| Bolt Type | As [mm^2] | Preloading (F_p) [N] | Slip resistance per bolt [N] | Shear resistance per bolt [N] | Number of flange bolts required (one flange, one side) |
| M20 | 333 | 163,170 | 52,214 | 93,240 | 9 |
| M24 | 384 | 188,160 | 60,211 | 107,520 | 8 |
| M30 | 621 | 304,290 | 97,373 | 173,880 | 5 |
| M36 | 865 | 423,850 | 135,632 | 242,200 | 4 |
| M39 | 1030 | 504,700 | 161,504 | 288,400 | 3 |
| | | | | | |
| Bolt size [mm] | do [mm] +3 | Min. e1 and e2 [mm] | Min. p1 [mm] | Min. p2 [mm] | Number of bolts across the flange (ca. 180 mm space to bolt one side) |
| 20 | 23 | 28 | 51 | 56 | 8.00 |
| 24 | 27 | 33 | 60 | 65 | 6.00 |
| 30 | 33 | 40 | 73 | 80 | 5.00 |
| 36 | 39 | 47 | 86 | 94 | 2.00 |
| 39 | 42 | 51 | 93 | 101 | 4.00 |
| Flange fixturing characteristics | | Flange thickness [mm] | Flange force [N] | Web thickness [mm] | Web force [N] |
| Width of top flange plate [mm] | 500 | 40 | 460,000 | 20 | 0 |
| Thickness of top flange plate [mm] | 10 | | | | |
| Axial stress in top plate (one friction interface) [Mpa] | 92 | Total number of flange bolts | Number of web bolts (one web) | Total number of web bolts | Total number of bolts in the joint |
| Length through cross-section (one friction interface) [mm] | 50 | 18 | 0 | 0 | 18 |
| | | 16 | 0 | 0 | 16 |
| cubic of one angle plate [mm^3] | 1750000 | 10 | 0 | 0 | 10 |
| Weight of all 8 plates [kg] | 37.8 | 16 | 0 | 0 | 16 |
| | | 6 | 0 | 0 | 6 |
| | | | | | |
| | | Number of bolts along the flange | Min. Length of coupling (one side) [mm] | Min. length of flange plate (both sides) [mm] | |
| | | 2.00 | 107 | 214 | |
| | | 2.00 | 126 | 252 | |
| | | 1.00 | 80 | 160 | |
| | | 2.00 | 180 | 360 | |
| | | 1.00 | 102 | 204 | |
| | | | | | |
| | | cross section length [mm] | | | |
| Total number of flange bolts | 64 | 50 | | | |
| Total number of web bolts | 0 | 0 | | | |

| | | | | | |
|---|---|---|---|---|---|
| Joint XIV, d-s | Accounts for both web and flange | | | | |
| Safety factor for ultimate state | Number of friction interfaces | Slip factor (0,3-0,4?pakning?) | UTS [Mpa] | Moment [N*mm] | Height of beam [mm] |
| 1.25 | 1 | 0.4 | 700 | 750,000,000 | 1500 |
| | | | | | |
| Bolt Type | As [mm^2] | Preloading (F_p) [N] | Slip resistance per bolt [N] | Shear resistance per bolt [N] | Number of flange bolts required (one flange, one side) |
| M20 | 333 | 163,170 | 52,214 | 93,240 | 10 |
| M24 | 384 | 188,160 | 60,211 | 107,520 | 9 |
| M30 | 621 | 304,290 | 97,373 | 173,880 | 6 |
| M36 | 865 | 423,850 | 135,632 | 242,200 | 6 |
| M39 | 1030 | 504,700 | 161,504 | 288,400 | 4 |
| | | | | | |
| Bolt size [mm] | do [mm] +3 | Min. e1 and e2 [mm] | Min. p1 [mm] | Min. p2 [mm] | Number of bolts across the flange (ca. 375 mm space to bolt one side, beam h) |
| 20 | 23 | 28 | 51 | 56 | 6.00 |
| 24 | 27 | 33 | 60 | 65 | 5.00 |
| 30 | 33 | 40 | 73 | 80 | 4.00 |
| 36 | 39 | 47 | 86 | 94 | 3.00 |
| 39 | 42 | 51 | 93 | 101 | 3.00 |
| Flange fixturing characteristics | | Flange thickness [mm] beam d | Flange force [N] | Web thickness [mm] | Web force [N] |
| Width of flange plate [mm] | 420 | 30 | 500,000 | 20 | 0 |
| Thickness of flange plate [mm] | 10 | | | | |
| Axial stress in top plate (one friction interface) [Mpa] | 119 | Total number of flange bolts | Number of web bolts (one web) | Total number of web bolts | Total number of bolts in the joint |
| Length through cross-section (one friction interface) [mm] | 40 | 20 | 0 | 0 | 20 |
| | | 18 | 0 | 0 | 18 |
| cubic of one angle plate [mm^3] | 2192400 | 12 | 0 | 0 | 12 |
| Weight of all 4 plates [kg] | 23.67792 | 24 | 0 | 0 | 24 |
| | | 8 | 0 | 0 | 8 |
| | | | | | |
| | | Number of bolts along the flange | Min. Length of coupling (one side) [mm] | | |
| | | 2.00 | 107 | | |
| | | 2.00 | 126 | | |
| | | 2.00 | 153 | | |
| | | 2.00 | 266 | | |
| | | 2.00 | 195 | | |
| | | | | | |
| | | cross section length [mm] | | | |
| Total number of flange bolts | 48 | 40 | | | |
| Total number of web bolts | 0 | 0 | | | |

| | | | | | |
|---|---|---|---|---|---|
| Joint XIII, s-t | Accounts for both web and flange | | | | |
| Safety factor for ultimate state | Number of friction interfaces | Slip factor (0,3-0,4?pakning?) | UTS [Mpa] | Moment [N*mm] | Height of beam [mm] |
| 1.25 | 1 | 0.3 | 700 | 0 | 400 |
| | | | | | |
| Bolt Type | As [mm^2] | Preloading (F_p) [N] | Slip resistance per bolt [N] | Shear resistance per bolt [N] | Number of flange bolts required (one flange, one side) |
| M20 | 333 | 163,170 | 39,161 | 93,240 | 3 |
| M24 | 384 | 188,160 | 45,158 | 107,520 | 3 |
| M30 | 621 | 304,290 | 73,030 | 173,880 | 2 |
| M36 | 865 | 423,850 | 101,724 | 242,200 | 2 |
| M39 | 1030 | 504,700 | 121,128 | 288,400 | 1 |
| | | | | | |
| Bolt size [mm] | do [mm] +3 | Min. e1 and e2 [mm] | Min. p1 [mm] | Min. p2 [mm] | Number of bolts across the flange (ca. 365 mm space to bolt one side, beam h) |
| 20 | 23 | 28 | 51 | 56 | 6.00 |
| 24 | 27 | 33 | 60 | 65 | 5.00 |
| 30 | 33 | 40 | 73 | 80 | 4.00 |
| 36 | 39 | 47 | 86 | 94 | 2.00 |
| 39 | 42 | 51 | 93 | 101 | 3.00 |
| Flange fixturing characteristics | | Flange thickness [mm] beam d | Flange force [N] | Web thickness [mm] | Web force [N] |
| Width of flange plate [mm] | 420 | 35 | 111,000 | 20 | 0 |
| Thickness of flange plate [mm] | 10 | | | | |
| Axial stress in top plate (one friction interface) [Mpa] | 26 | Total number of flange bolts | Number of web bolts (one web) | Total number of web bolts | Total number of bolts in the joint |
| Length through cross-section (one friction interface) [mm] | 45 | 6 | 0 | 0 | 6 |
| | | 6 | 0 | 0 | 6 |
| cubic of one angle plate [mm^3] | 747600 | 4 | 0 | 0 | 4 |
| Weight of all 4 plates [kg] | 8.07408 | 8 | 0 | 0 | 8 |
| | | 2 | 0 | 0 | 2 |
| | | | | | |
| | | Number of bolts along the flange | Min. Length of coupling (one side) [mm] | | |
| | | 1.00 | 56 | | |
| | | 1.00 | 66 | | |
| | | 1.00 | 80 | | |
| | | 1.00 | 94 | | |
| | | 1.00 | 102 | | |
| | | | | | |
| | | | | | |
| | | cross section length [mm] | | | |
| Total number of flange bolts | 16 | 45 | | | |
| Total number of web bolts | 0 | 0 | | | |

Summary

| | | | | | | | | | | | | | | | | | | | | | | | | |
|---|---|---|---|---|---|---|---|---|---|---|---|---|---|---|---|---|---|---|---|---|---|---|---|---|
| Total aluminium plate weight [kg] | 1264.39 | | | | | | | | | | | | | | | | | | | | | | | |
| Total steel plate weight [kg] | 1226.16 | | | | | | | | | | | | | | | | | | | | | | | |
| joint: | a-a | | a-x_tree | | d-x_tree | | f-x_tree | | h-g | | g-b | | c-c (a-c) | | c-e | | e-x_tree | | g-k | | d-s | | s-t | |
| | Flange | Web | Flange | Web | Flange | Web | Flange | Web | Flange | Web | Flange | Web | Flange | Web | Flange | Web | Flange | Web | Flange | Web | Flange | Web | Flange | Web |
| Cross section length [mm]: | 135 | 80 | 80 | 70 | 40 | 55 | 70 | 60 | 50 | 0 | 50 | 0 | 45 | 0 | 42 | 0 | 37 | 0 | 50 | 0 | 40 | 0 | 45 | 0 |
| Number of bolts | 416 | 48 | 208 | 48 | 72 | 8 | 208 | 60 | 128 | 0 | 64 | 0 | 48 | 0 | 16 | 0 | 16 | 0 | 64 | 0 | 48 | 0 | 16 | 0 |
| Number of joints | 4 | | 4 | | 4 | | 4 | | 8 | | 4 | | 4 | | 4 | | 4 | | 4 | | 2 | | 2 | |
| Status | ok | | ok | | ok | | ok | | ok | | ok | | ok | | ok | | ok | | ok | | ok | | ok | |
| comment | | | | | | | | | | | | | | | | | | | | | | | | |
| Required bolt length | 195 | 140 | 140 | 130 | 100 | 115 | 130 | 120 | 110 | #DIV/0! | 110 | #DIV/0! | 105 | #DIV/0! | 102 | #DIV/0! | 97 | #DIV/0! | 110 | #DIV/0! | 100 | #DIV/0! | 105 | #DIV/0! |
| purchased bolt length | 200 | 140 | 140 | 130 | 100 | 120 | 130 | 120 | 110 | 0 | 110 | 0 | 110 | 0 | 110 | 0 | 110 | 0 | 110 | 0 | 100 | 0 | 110 | 0 |
| Sum stainless bolts (M36x3) | 1468 | | | | | | | | | | | | | | | | | | | | | | | |
| Sum carbon bolts | 1336 | | | | | | | | | | | | | | | | | | | | | | | |
| Difference bolts | 132 | | | | | | | | | | | | | | | | | | | | | | | |

| | Bolt length | quantity | euro/stainless bolt | euro/ stainless nut | euro/stainless washer | euro/carbon bolt | euro/carbon nut | euro/carbon washer | | NOK/stainless bolt | NOK/ stainless nut | NOK/stainless washer | NOK/carbon bolt | NOK/carbon nut | NOK/carbon washer | NOK/posphated bol | NOK/phosphated nut | NOK/phosphated washer | | |
|---|---|---|---|---|---|---|---|---|---|---|---|---|---|---|---|---|---|---|---|---|
| | 110 | 120 | 20.13 | 7.2 | 2.25 | 7.33 | 0.98 | 0.74 | | 188 | 67 | 21 | 69 | 9 | 7 | 219 | 69 | 62 | Ph. Bolt | 145 |
| | 120 | 352 | 21.43 | 7.2 | 2.25 | 7.8 | 0.98 | 0.74 | | 200 | 67 | 21 | 73 | 9 | 7 | 223 | 69 | 62 | Ph. Nut | 60 |
| | 130 | 68 | 22.15 | 7.2 | 2.25 | 8.1 | 0.98 | 0.74 | | 207 | 67 | 21 | 76 | 9 | 7 | 226 | 69 | 62 | Ph. Washe | 50 |
| | 140 | 256 | 22.53 | 7.2 | 2.25 | 8.53 | 0.98 | 0.74 | | 211 | 67 | 21 | 80 | 9 | 7 | 230 | 69 | 62 | | |
| | 150 | 256 | 23.76 | 7.2 | 2.25 | 9 | 0.98 | 0.74 | | 222 | 67 | 21 | 84 | 9 | 7 | 234 | 69 | 62 | Oil layer | 5 |
| | 210 | 416 | 37.65 | 7.2 | 2.25 | 11.82 | 0.98 | 0.74 | | 352 | 67 | 21 | 111 | 9 | 7 | 261 | 69 | 62 | | |
| Sum euro | | | 38977.8 | 10569.6 | 6606 | | | | | 364442 | 98826 | 30883 | 126980 | 13451 | 20314 | 347180 | 101531 | 181794 | | |
| Total sum stainless bolts [NOK] | 494151 | | | | | | | | | | | | | | | | | | | |
| Total sum carbon steel bolts [NOK] | 160746 | | | | | | | | | Approx. 1/3 kr difference in stainless and carbon bolts | | | | | | | | | | |
| Total sum phosphated bolts [NOK] | 630506 | | | | | | | | | Small difference between stainless and phosphated bolts | | | | | | | | | | |
| Kilde: www.accu.co.uk | | | | | | | | | | | | | | | | | | | | |
| Exchange rate euro- NOK | 9.35 | | | | | | | | | | | | | | | | | | | |

# Appendix D

# Beam Design

## D.1 Design sheets exported from excel

Beam-A

| | | | | | | | | | | |
|---|---|---|---|---|---|---|---|---|---|---|
| | | | | | | | Density | Yield | As-welded | |
| | **Current square beam** | **New I beam (6082 extrusion and 5083 plate)** | **I_current/I_new** | **A_current/A_new** | | Steel | 7800 | 355 | | |
| Height | 1400 | 1500 | | | | Aluminium | 2700 | 255 | 150 | 5083 |
| Width | 400 | 500 | 500 | | | | | | | |
| Flange thickness | [redacted] | 50 | 55 | | | | | | | |
| Web **thickness** | 40 | 60 | 60 | | | | | | | |
| Length | 11590 | 11590 | | | 0.769 | Limit for A_current/A_new | | | | |
| I_xx | 30,134,186,667 | 40,011,666,667 | 0.753 | 1.027 | 0.718 | Limit for I_current/I_new | | | | |
| I_yy | 3,862,186,667 | 5,686,866,667 | 0.679 | | 0.718 | Limit for I_current/I_new | | | | |
| J_co | 33,996,373,333 | 45,698,533,333 | 0.744 | | 0.718 | Limit for I_current/I_new | | | | |
| | | | **weight save** | | | | | | | |
| Vekt [kg/m] | 1073.28 | 361.8 | 0.66 | % | | | | | | |
| Vekt [kg] | 12,439 | 4,193 | | | | | | | | |
| Weight extrusion [kg/m] | | 67.5 | | | | | | | | |
| Weight extrusion [kg] | | 782.325 | | | | | | | | |
| Length extrusion (max 535kg) [m] | | 7.93 | | | | | | | | |
| Length of T-flange (vertical) | | 308.8235294 | | | | | | | | |
| Weight of extruded T-flange [kg/m] | | 117.5294118 | | | | | | | | |
| LengthT-flange extrusion (max 535kg) [m] | | 4.552052052 | | | | | | | | |
| Flange bending | | 4.4 | 3.5--4,5--5 | | | | | | | |
| Web bending | | 9.333333333 | 9--13--18 | | | | | | | |
| Flange bending with stiffener | | 3.751040559 | | | | | | | | |
| Length of stiffener | | 5 | | | | | | | | |
| | | 138400 | mm^2 Tverrsnitt | | | | | | | |

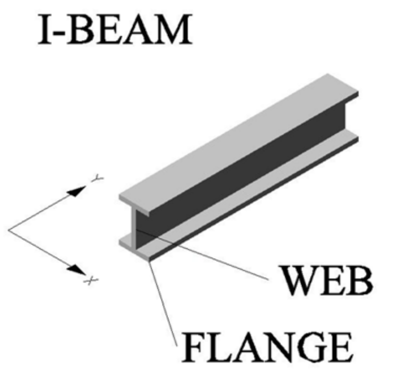

Beam-b

| | Current I beam | New I beam (6082 extrusion and 5083 plate | I_current/I_new | A_current/A-new | SMYS Ratio |
|---|---|---|---|---|---|
| Height | 1400 | 1500 | | | |
| Width | 400 | 330 | | | |
| Flange thickness | 20 | 30 | | | |
| Web thickness | 15 | 35 | | | |
| Length | 1400 | 1400 | | | |
| I_xx | 10,762,453,333 | 19,407,060,000 | 0.555 | 0.519 | 0.606 |
| I_yy | 999,115,833 | 1,411,440,000 | 0.708 | | 0.718 |
| J_co | 11,761,569,167 | 20,818,500,000 | 0.565 | | 0.606 |
| | | | | | |
| Vekt [kg/m] | 283.92 | 189.54 | 0.33 | % | |
| Vekt [kg] | 397.488 | 265.356 | | | |
| Weight extrusion [kg/m] | | 26.73 | | | |
| Weight extrusion [kg] (Flange Only) | | 37.422 | | | |
| Length extrusion (max 535kg) [m] | | 20.01 | | | |
| Length of T-flange (vertical) | | 308.8235294 | | | |
| Weight of extruded T-flange [kg/m], reell vekt | | 55.91382353 | | | |
| LengthT-flange extrusion (max 535kg) [m] | | 9.57 | 3 | | |
| | | | | | |
| Flange bending | | 4.916666667 | 3.5--4,5--5 | | |
| Web bending | | 16.45714286 | 9--13--18 | | |
| Flange bending with stiffener | | 4.270861709 | | | |
| Length of stiffener | | 5 | | | |

Small end of beam

| | Current I beam | New I beam (6082 e | I_current/ | A_current | SMYS Ratio |
|---|---|---|---|---|---|
| Height | 1000 | 1000 | | | |
| Width | 400 | 330 | | | |
| Flange thickness | 20 | 30 | | | |
| Web thickness | 15 | 35 | | | |
| Length (flange-flange) | 1400 | 1400 | | | |
| I_xx | 4,948,053,333 | 7,081,476,667 | 0.699 | 0.577 | 0.718 |
| I_yy | 768,003,333 | 983,747,292 | 0.781 | | 0.718 |
| J_co | 5,716,056,667 | 8,065,223,958 | 0.709 | | 0.718 |
| | | | | | |
| Weight [kg/m] | 237.12 | 142.29 | 0.40 | % | |
| Weight [kg] | | | | | |
| Weight extrusion [kg/m] | | 26.73 | | | |

| | Density | Yield | |
|---|---|---|---|
| Steel | 7800 | 355 | |
| Aluminiun | 2700 | 215 | 150 |
| | | 255 | |

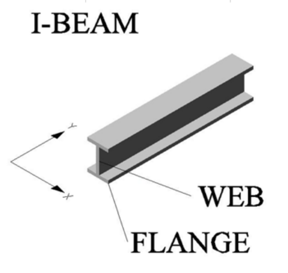

beam-c

| | Current I beam | New I beam (6082 extrusion and 5083 plate) | I_current/I_new | A_current/A-new | SMYS Ratio | | Density | Yield | |
|---|---|---|---|---|---|---|---|---|---|
| Height | 1400 | 1500 | | | | Steel | 7800 | 355 | |
| Width | 400 | 330 | | 310 | | Aluminium | 2700 | 255 | 150 |
| Flange thickness | 20 | 30 | | 30 | | | | | |
| Web thickness | 15 | 35 | | 45 | | | | | |
| Length (flange -flange) | 5600 | 6400 | | | | | | | |
| I_xx | 10,762,453,333 | 19,407,060,000 | 0.555 | 0.519 | 0.718 | | | | |
| I_yy | 999,115,833 | 1,411,440,000 | 0.708 | | 0.718 | | | | |
| J_co | 11,761,569,167 | 20,818,500,000 | 0.565 | | 0.718 | | | | |
| | | | | | | | | | |
| Vekt [kg/m] | 283.92 | 189.54 | 0.33 | % | | | | | |
| Vekt [kg] | 1,590 | 1,213 | | | | 6082 as welded | 130 Mpa | | |
| Weight extrusion [kg/m] | | 26.73 | | | | 5083 as welded | 150 Mpa | | |
| Weight extrusion [kg] (Flange Only) | | 171.072 | | | | | | | |
| Length extrusion (max 535kg) [m] | | 20.01 | | | | | | | |
| Length of T-flange (vertical) | | 308.8235294 | | | | | | | |
| Weight of extruded T-flange [kg/m], reell vekt | | 55.91382353 | | | | | | | |
| LengthT-flange extrusion (max 535kg) [m] | | 9.57 | | | | | | | |
| | | | | | | | | | |
| | | | | | | | | | |
| Flange bending | | 4.916666667 | 3.5--4,5--5 | | | | | | |
| Web bending | | 16.45714286 | 9--13--18 | | | | | | |
| Flange bending with stiffener | | 4.270861709 | | | | | | | |
| Length of stiffener | | 5 | | | | | | | |

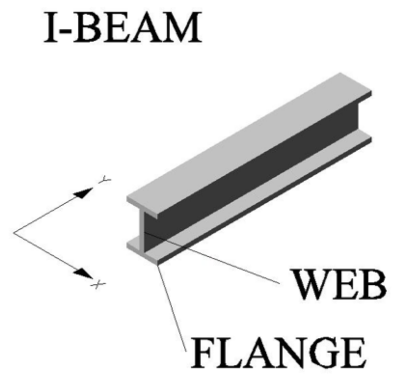

| Beam-d | | | | | | | | |
|---|---|---|---|---|---|---|---|---|
| | **Current I beam** | **New I beam (6082 extrusion and 5083 plate)** | **I_current/I_new** | **A_current/A-new** | | | Density | Yield |
| Height | 1400 | 1500 | | | | Steel | 7800 | 355 |
| Width | 400 | 330 | | | | Aluminium | 2700 | 255 |
| Flange thickness | 20 | 30 | | | | | | |
| Web thickness | 15 | 35 | | | | | | |
| Length (tube surface-tube surface) | 4895 | 4895 | | | | | | |
| I_xx | 10,762,453,333 | 19,407,060,000 | 0.555 | 0.519 | 0.718 | | | |
| I_yy | 999,115,833 | 1,411,440,000 | 0.708 | | 0.718 | | | |
| J_co | 11,761,569,167 | 20,818,500,000 | 0.565 | | 0.718 | | | |
| | | | | | | | | |
| Vekt [kg/m] | 283.92 | 189.54 | 0.33 | % | | | | |
| Vekt [kg] | 1,390 | 928 | | | | | | |

| Beam-e | | | | | | | | | |
|---|---|---|---|---|---|---|---|---|---|
| | Current I beam | New I beam (6082 extrusion) | I_current/I_new | A_current/A-new | | | Density | Yield | |
| Height | 340 | 350 | | | | Steel | 7800 | 355 | |
| Width | 300 | 300 | | | | Aluminium | 2700 | 255 | 255 |
| Flange thickness | 21.5 | 32 | | | | | | | |
| Web thickness | 13.52 | 20 | | | | | | | |
| Length (tube surface-end) | 4361.77 | 4361.77 | | | | | | | |
| I_xx | 357,164,671 | 526,023,027 | 0.679 | 0.679 | 0.718 | | | | |
| I_yy | 183,086,909 | 264,310,667 | 0.693 | | 0.718 | | | | |
| J_co | 540,251,580 | 790,333,693 | 0.684 | | 0.718 | | | | |
| | | | weight saving | | | | | | |
| Vekt [kg/m] | 131.94 | 67.28 | 0.49 | % | | | | | |
| Vekt [kg] | 575 | 293 | | | | | | | |
| Weight extrusion [kg/m] | | 25.92 | | | | | | | |
| Weight extrusion [kg] | | 113.0570784 | | | | | | | |
| Length extrusion (max 535kg) [m] | | 20.64 | | | | | | | |
| Length of T-flange (vertical) | | 0 | | | | | | | |
| Weight of extruded T-flange [kg/m] | | 25.92 | | | | | | | |
| LengthT-flange extrusion (max 535kg) [m] | | 20.64 | 3 | | | | | | |
| | | | | | | | | | |
| | | | | | | | | | |
| Flange bending | | 4.375 | 3.5--4,5--5 | | | | | | |
| Web bending | | 5.72 | 9--13--18 | | | | | | |
| Flange bending with stiffener | | 3.74402006 | | | | | | | |
| Length of stiffener | | 5 | | | | | | | |

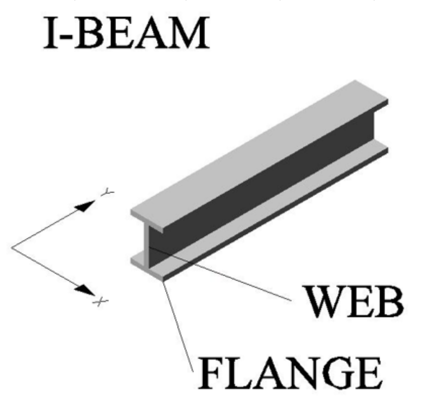

| | | | | | | | | | |
|---|---|---|---|---|---|---|---|---|---|
| Beam-f | small end | **For 2 I-beams connected together, legg inn for 1 beam** | | | | | | | |
| | **Current square beam** | **New I beam (6082 extrusion and 5083 plate)** | **I_current/I_new** | **A_current/A_new** | | | Density | Yield | |
| Height | 1400 | 1500 | | | | Steel | 7800 | 355 | |
| Width | 970 | 440 | | | | Aluminium | 2700 | 255 | 150 |
| Flange thickness (Horizontal) | 40 | 45 | | | | | | | |
| Web thickness (vertical) | 20 | 40 | | | | | | | |
| Length (ca) [mm] | 3450 | 3000 | | | | | | | |
| I_xx [mm^4] | 43,559,146,667 | 60,618,600,000 | 0.719 | 0.679 | 0.718 | | | | |
| I_yy [mm^4] | 19,258,953,333 | 28,359,040,000 | 0.679 | | 0.718 | | | | |
| J_co | 62,818,100,000 | 88,977,640,000 | 0.706 | | 0.718 | | | | |
| | Vekt fra Inventor | For en bjelke | Weight save for 2 beams | | | | | | |
| Vekt [kg/m] | 1017.12 | 259.2 | 0.60 | % | | | | | |
| Vekt [kg] | 3861 | 777.6 | | | | | | | |
| Weight extrusion [kg/m] | | 53.46 | | | | | | | |
| Weight extrusion [kg] | | 160.38 | | | | | | | |
| Length extrusion (max 535kg) [m] | | 10.01 | | | | | | | |
| Length of T-flange (vertical) | | 308.8235294 | | | | | | | |
| Weight of extruded T-flange [kg/m] | | 86.81294118 | | | | | | | |
| LengthT-flange extrusion (max 535kg) [m] | | 6.16 | | | | | | | |

| | | | | | | | | | |
|---|---|---|---|---|---|---|---|---|---|
| Beam-g | | | | | | | | | |
| | **Current square beam** | **New I beam (6082 extrusion and 5083 plate)** | **I_current/I_new** | **A_current/A_new** | | | Density | Yield | |
| Height | 1000 | 1000 | | | | Steel | 7800 | 355 | |
| Width | 400 | 400 | | | | Aluminium | 2700 | 255 | 150 |
| Flange thickness (Horizontal) | 25 | 40 | 40 | | | | | | |
| Web thickness (vertical) | 12 | 35 | | | | | | | |
| Length | 7346 | 7346 | | | | | | | |
| I_xx | 6,468,916,667 | 9,648,240,000 | 0.670 | 0.514 | 0.718 | | | | |
| I_yy | 1,125,041,067 | 1,605,253,750 | 0.701 | | 0.718 | | | | |
| J_co | 7,593,957,733 | 11,253,493,750 | 0.675 | | 0.718 | | | | |
| | | | Weight saving | | | | | | |
| Vekt [kg/m] | 333.84 | 173.34 | 0.48 | % | | | | | |
| Vekt [kg] | 2452.39 | 1273.36 | | | | | | | |
| Weight extrusion [kg/m] | | 43.2 | | | | | | | |
| Weight extrusion [kg] | | 317.3472 | | | | | | | |
| Length extrusion (max 535kg) [m] | | 12.38 | | | | | | | |
| Length of T-flange (vertical) | | 205.8823529 | | | | | | | |
| Weight of extruded T-flange [kg/m] | | 62.65588235 | | | | | | | |
| LengthT-flange extrusion (max 535kg) [m] | | 8.54 | 4.4 | | | | | | |
| | | | | | | | | | |
| | | | | | | | | | |
| Flange bending | | 4.5625 | 3.5--4,5--5 | | | | | | |
| Web bending | | 10.51428571 | 9--13--18 | | | | | | |
| Flange bending with stiffener | | 3.915378485 | | | | | | | |
| Length of stiffener | | 5 | | | | | | | |

| Beam-h | Current I beam | New I beam (6082 extrusion and 5083 plate) | I_current/I_new | A_current/A-new | SMYS Ratio |
|---|---|---|---|---|---|
| Height | 1000 | 1000 | | | |
| Width | 400 | 350 | | | |
| Flange thickness | 20 | 40 | | | |
| Web thickness | 15 | 40 | | | |
| Length | 1755 | 1755 | Control length | | |
| I_xx | 4,948,053,333 | 9,050,560,000 | 0.547 | 0.469 | 0.606 |
| I_yy | 768,003,333 | 1,288,940,000 | 0.596 | | 0.606 |
| J_co | 5,716,056,667 | 10,339,500,000 | 0.553 | | 0.606 |
| | | | | | |
| | | | weight saving | | |
| Vekt [kg/m] | 349.44 | 174.96 | 0.50 | | |
| Vekt [kg] | 613.27 | 307.05 | | | |
| Weight extrusion [kg/m] | | 37.8 | | | |
| Weight extrusion [kg] | | 66.339 | | | |
| Length extrusion (max 535kg) [m] | | 14.15 | | | |
| Length of T-flange (vertical) | | 151.1627907 | 120 | 120, max høyde | |
| Weight of extruded T-flange [kg/m] | | 54.1255814 | | | |
| LengthT-flange extrusion (max 535kg) [m] | | 9.88 | 4.4 | | |
| | | | | | |
| Flange bending | | 3.875 | 3.5--4,5--5 | | |
| Web bending | | 0.061538462 | 9--13--18 | | |
| Flange bending with stiffener | | -21.14304382 | | | |
| Length of stiffener | | 5 | | | |

| Small end of beam | Current I beam | New I beam (6082 e: | I_current/I_new | A_current/A-new | SMYS Ratio |
|---|---|---|---|---|---|
| Height | 400 | 400 | | | |
| Width | 400 | 350 | | | |
| Flange thickness | 20 | 40 | | | |
| Web thickness | 15 | 40 | | | |
| Length | 1600 | 1600 | Control length | 1625 | |
| I_xx | 636,453,333 | 1,020,160,000 | 0.624 | 0.525 | 0.606 |
| I_yy | 421,334,583 | 634,740,000 | 0.664 | | 0.606 |
| J_co | 1,057,787,917 | 1,654,900,000 | 0.639 | | 0.606 |
| | | | | | |
| | | | weight saving | | |
| Vekt [kg/m] | 209.04 | 110.16 | 0.47 | | |
| Vekt [kg] | 334.46 | 176.26 | | | |
| Weight extrusion [kg/m] | | 37.8 | | | |
| Weight extrusion [kg] | | 60.48 | | | |
| Length extrusion (max 535kg) [m] | | 14.15 | | | |
| Length of T-flange (vertical) | | 60.46511628 | | | |
| Weight of extruded T-flange [kg/m] | | 44.33023256 | | | |
| LengthT-flange extrusion (max 535kg) [m] | | 12.07 | 4.4 | | |
| | | | | | |
| Flange bending | | 3.875 | 3.5--4,5--5 | | |
| Web bending | | 3.2 | 9--13--18 | | |
| Flange bending with stiffener | | 3.252775972 | | | |
| Length of stiffener | | 5 | | | |

| | Density | Yield | |
|---|---|---|---|
| Steel | 7800 | 355 | |
| Aluminiun | 2700 | 215 | 150 |

Beam-i

| | Current I beam | New I beam (6082 extrusion and 5083 plate) | I_current/I_new | A_current/A-new | SMYS Ratio |
|---|---|---|---|---|---|
| Height | 1400 | 1500 | | | |
| Width | 400 | 400 | | | |
| Flange thickness | 20 | 40 | | | |
| Web thickness | 20 | 30 | | | |
| Length | 2420 | 2420 | | | |
| I_xx | 11,810,560,000 | 24,215,286,667 | 0.488 | 0.579 | 0.718 |
| I_yy | 1,247,840,000 | 2,006,061,667 | 0.622 | | 0.718 |
| J_co | 13,058,400,000 | 26,221,348,333 | 0.498 | | 0.718 |
| | | | | | |
| Vekt [kg/m] | 549.12 | 201.42 | 0.63 | | |
| Vekt [kg] | 1328.87 | 487.44 | | | |
| Weight extrusion [kg/m] | | 43.2 | | | |
| Weight extrusion [kg] | | 104.544 | | | |
| Length extrusion (max 535kg) [m] | | 12.38 | | | |
| Length of T-flange (vertical) | | 308.8235294 | | | |
| Weight of extruded T-flange [kg/m] | | 68.21470588 | | | |
| LengthT-flange extrusion (max 535kg) [m] | | 7.84 | 4.4 | | |
| | | | | | |
| Flange bending | | 4.625 | 3.5--4,5--5 | | |
| Web bending | | 0.056198347 | 9--13--18 | | |
| Flange bending with stiffener | | -38.84066687 | | | |
| Length of stiffener | | 5 | | | |

Small end of beam

| | Current I beam | New I beam (6082 ext | I_current/I_ne | A_current/A-r | SMYS Ratio |
|---|---|---|---|---|---|
| Height | 350 | 350 | | | |
| Width | 400 | 400 | | | |
| Flange thickness | 20 | 40 | | | |
| Web thickness | 20 | 30 | | | |
| Length (Diagonal) | 5990 | 5990 | | | |
| I_xx | 485,785,000 | 822,274,167 | 0.591 | 0.554 | 0.718 |
| I_yy | 449,140,000 | 726,974,167 | 0.618 | | 0.718 |
| J_co | 934,925,000 | 1,549,248,333 | 0.603 | | 0.718 |
| | | | Weight saving | | |
| Vekt [kg/m] | 221.52 | 108.27 | 0.51 | | |
| Vekt [kg] | 1326.90 | 648.54 | | | |
| Weight extrusion [kg/m] | | 43.2 | | | |
| Weight extrusion [kg] | | 258.768 | | | |
| Length extrusion (max 535kg) [m] | | 12.38 | | | |
| Length of T-flange (vertical) | | 72.05882353 | | | |
| Weight of extruded T-flange [kg/m] | | 49.03676471 | | | |
| LengthT-flange extrusion (max 535kg) [m] | | 10.91 | 4.4 | | |
| | | | | | |
| Flange bending | | 4.625 | 3.5--4,5--5 | | |
| Web bending | | 3.6 | 9--13--18 | | |
| Flange bending with stiffener | | 3.975615077 | | | |
| Length of stiffener | | 5 | | | |

| | Density | Yield | |
|---|---|---|---|
| Steel | 7800 | 355 | |
| Aluminiur | 2700 | 255 | 150 |

| | |
|---|---|
| Total lengde | 7406 |
| Angle | 12.66 |

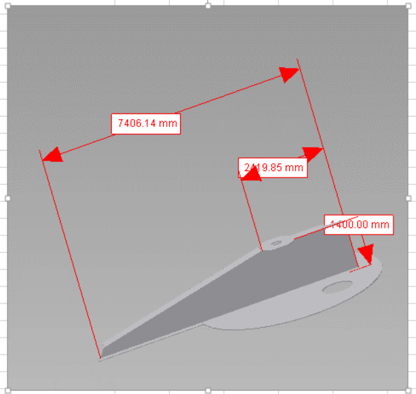

| Beam-j | | | | | |
|---|---|---|---|---|---|
| | Current I beam | New I beam (6082 extrusion and 5083 plate) | I_current/I_new | A_current/A-new | SMYS Ratio |
| Height | 1400 | 1500 | | | |
| Width | 400 | 400 | | | |
| Flange thickness | 20 | 40 | | | |
| Web thickness | 20 | 30 | | | |
| Length | 448.45 | 450 | | | |
| I_xx | 11,810,560,000 | 24,215,286,667 | 0.488 | 0.579 | 0.718 |
| I_yy | 1,247,840,000 | 2,006,061,667 | 0.622 | | 0.718 |
| J_co | 13,058,400,000 | 26,221,348,333 | 0.498 | | 0.718 |
| | | | Weight saving | | |
| Vekt [kg/m] | 549.12 | 201.42 | 0.63 | | |
| Vekt [kg] | 246.25 | 90.64 | | | |
| Weight extrusion [kg/m] | | 43.2 | | | |
| Weight extrusion [kg] | | 19.44 | | | |
| Length extrusion (max 535kg) [m] | | 12.38 | | | |
| Length of T-flange (vertical) | | 308.8235294 | | | |
| Weight of extruded T-flange [kg/m] | | 68.21470588 | | | |
| LengthT-flange extrusion (max 535kg) [m] | | 7.84 | 4.4 | | |
| Flange bending | | 4.625 | 3.5--4,5--5 | | |
| Web bending | | 18.93333333 | 9--13--18 | | |
| Flange bending with stiffener | | 3.975615077 | | | |
| Length of stiffener | | 5 | | | |

| Small end of beam | | | | | |
|---|---|---|---|---|---|
| | Current I beam | New I beam (6082 ext | I_current/ | A_current | SMYS Ratio |
| Height | 200 | 200 | | | |
| Width | 400 | 400 | | | |
| Flange thickness | 20 | 40 | | | |
| Web thickness | 20 | 30 | | | |
| Length (Diagonal) | 2050.82 | 2050 | | | |
| I_xx | 136,960,000 | 213,386,667 | 0.642 | 0.539 | 0.718 |
| I_yy | 335,040,000 | 560,136,667 | 0.598 | | 0.718 |
| J_co | 472,000,000 | 773,523,333 | 0.610 | | 0.718 |
| | | | Weight saving | | |
| Vekt [kg/m] | 174.72 | 96.12 | 0.45 | | |
| Vekt [kg] | 358.32 | 197.05 | | | |
| Weight extrusion [kg/m] | | 43.2 | | | |
| Weight extrusion [kg] | | 88.56 | | | |
| Length extrusion (max 535kg) [m] | | 12.38 | | | |
| Length of T-flange (vertical) | | 41.17647059 | | | |
| Weight of extruded T-flange [kg/m] | | 46.53529412 | | | |
| LengthT-flange extrusion (max 535kg) [m] | | 11.50 | 4.4 | | |
| Flange bending | | 4.625 | 3.5--4,5--5 | | |
| Web bending | | 1.6 | 9--13--18 | | |
| Flange bending with stiffener | | 3.975615077 | | | |
| Length of stiffener | | 5 | | | |

| | Density | Yield | |
|---|---|---|---|
| Steel | 7800 | 355 | |
| Aluminiur | 2700 | 255 | 150 |

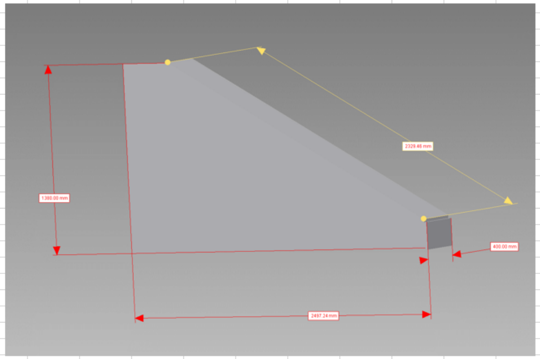

Beam-k

| | Current square beam | New I beam (6082 extrusion and 5083 plate) | I_current/I_new | A_current/A-new | SMYS Ratio |
|---|---|---|---|---|---|
| Height | 400 | 400 | | | |
| Width | 200 | 300 | | | |
| Flange thickness | | 20 | | | |
| Web **thickness** | 12.5 | 20 | | | |
| Length | 7045 | 8045 | | | |
| I_xx | 297,623,698 | 511,360,000 | 0.582 | 0.749 | 0.718 |
| I_yy | 99,186,198 | 241,440,000 | 0.411 | | 0.718 |
| J_co | 396,809,896 | 752,800,000 | 0.527 | | 0.718 |
| | | | Weight saving | | |
| Vekt [kg/m] | 112.125 | 51.84 | 0.54 | % | |
| Vekt [kg] | 789.920625 | 417.0528 | | | |
| Lengde [m] | | 10.32021605 | | | |
| | | | | | |
| epsilon | 0.990147543 | | | | |
| | | | | | |
| Flange bending | | 7.069653457 | 2.5--4,5--5 | | |
| Web bending | | 7.129062309 | 9--13--18 | | |
| Flange bending with stiffener | | 6.32455532 | | | |
| Length of stiffener | | 5 | | | |
| | | | Class 4, må bruke 18.6 mm tykkelse I utregninger | | |
| Rho_c, flange | 0.934304413 | | | | |
| Rho_c, web | 0.930486797 | | | | |

| | Density | Yield | Yield | Yield |
|---|---|---|---|---|
| Steel | 7800 | 355 | | |
| Aluminium | 2700 | 215 | 255 | 150 |
| | | | 6082 Extruded | Welded |

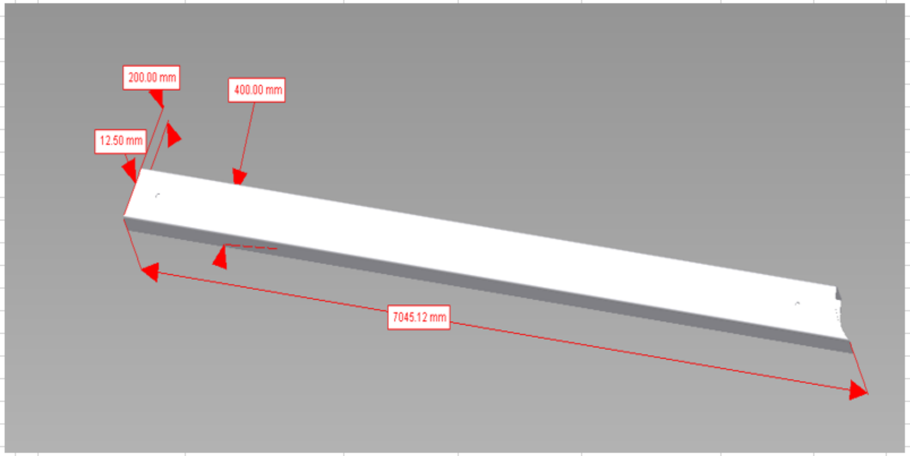

| | | | | | | | | | | |
|---|---|---|---|---|---|---|---|---|---|---|
| Beam-I | | | | | | | | | | |
| | **Current Tube** | **New Tube, 6082 extrusion** | **I_current/I_new** | **A_current/A-new** | **SMYS Ratio** | | Density | Yield | | |
| Diameter | 813 | 970 | | | | Steel | 7800 | 355 | | |
| Thickness | 28.2 | 40 | | | | Aluminium | 2700 | 215 | 150 | |
| Length | 8277 | 8277 | 7140 | | | | | | | |
| I_xx | 5,357,055,364 | 12,651,766,500 | 0.423 | 0.595 | 0.423 | 0.606 | | | | |
| I_yy | 5,357,055,364 | 12,651,766,500 | 0.423 | | 0.423 | 0.606 | | | | |
| J_co | 10,714,110,727 | 25,303,533,000 | 0.423 | | 0.423 | 0.606 | | | | |
| | | | Weight saving | | | | | | | |
| Vekt [kg/m] | 542 | 315 | 0.42 | % | | | | | | |
| Vekt [kg] | 4,486 | 2,610 | | | | | | | | |
| | | | | | | | | | | |
| | | | New T: | 41.2032492 | | | | | | |
| Tetta_c | | 1.03008123 | | | | | | | | |
| | | | | | | | | | | |
| | | | | | | | | | | |
| betta | | 14.46547614 | | | betta | 3*((D-t)/t)^0.5 | | | | |
| epsilon | | 1.078327732 | | | epsilon | (250^0,5)/(YS) | | | | |
| Betta/epsilon | | 13.41473071 | | | | | | | | |
| | | | | | Betta/epsilon < 15 --> | | | | | |
| | | | | | | | | | | |
| | | | | | Klasse 1 | < 10 | | | | |
| | | | | | Klasse 2 | 10 - 13,5 | | | | |
| | | | | | Klasse 3 | 13,5 - 15 | | | | |
| | | | | | Klasse 4 | 15 < | | | | |

| | | | | | | | | | | |
|---|---|---|---|---|---|---|---|---|---|---|
| Beam-m | | | | | | | | | | |
| | **Current Tube** | **New Tube, 6082 extrusion** | **I_current/I_new** | **A_current/A_new** | | | Density | Yield | | |
| Diameter | 914 | 920 | | | | Steel | 7800 | 355 | | |
| Thickness | 14.3 | 25 | 25 | | | Aluminium | 2700 | 215 | 150 | |
| Length | 6812 | 6812 | | | | | | | | |
| I_xx | 4,088,637,051 | 7,040,240,609 | 0.581 | 0.575 | 0.606 | 0.423 | | | | |
| I_yy | 4,088,637,051 | 7,040,240,609 | 0.581 | | 0.606 | 0.423 | | | | |
| J_co | 8,177,274,102 | 14,080,481,219 | 0.581 | | 0.606 | 0.423 | | | | |
| | | | Weight saving | | | | | | | |
| Vekt [kg/m] | 315 | 190 | 0.40 | % | | | | | | |
| Vekt [kg] | 2,147 | 1,292 | | | | | | | | |
| | | | | | | | | | | |
| Epsilon | 1.078327732 | | | | | | | | | |
| Buckling | 3.056400306 | | | | | | | | | |
| | | | | | | | | | | |
| Beam m designed according to NORSOK. | | | | | | | | | | |

Beam-m2

| | Current square beam | New I beam (6082 extrus | I_current/I_new | A_current/A_new | |
|---|---|---|---|---|---|
| Height | 914 | 1280 | | | |
| Diameter | | 500 | | | |
| Width | | | | | |
| Flange thickness (Horizontal) | 14.3 | 30 | | | |
| Web thickness (vertical) | | 30 | | | |
| Length | 6812 | 6812 | | | |
| I_xx | 4,090,710,867 | 5,806,563,575 | 0.704 | 0.500 | 0.718 |
| I_yy | 4,090,710,867 | 1,230,864,254 | 3.323 | | 0.718 |
| J_co | 8,181,421,734 | 7,037,427,829 | 1.163 | | 0.718 |
| | | | Weight saving | | |
| Vekt [kg/m] | 315.2667961 | 218.4204323 | 0.31 | % | |
| Vekt [kg] | 2147.60 | 1487.88 | | | |
| Weight extrusion [kg/m] | | 119.6004323 | | | |
| Weight extrusion [kg] | | 814.718145 | | | |
| Length extrusion (max 535kg) [m] | | 4.47 | | | |
| Length of T-flange (vertical) | | 263.5294118 | | | |
| Weight of extruded T-flange [kg/m] | | 140.9463147 | | | |
| LengthT-flange extrusion (max 535kg) [m] | | 3.80 | 6.812 | | |
| | | | | | |
| | | | | | |
| Flange bending | | 7.833333333 | 3.5--4,5--5 | | |
| Web bending | | 16.26666667 | 9--13--18 | | |
| Flange bending with stiffener | | -0.966987557 | | | |
| Length of stiffener | | 5 | | | |

| | Density | Yield | |
|---|---|---|---|
| Steel | 7800 | 355 | |
| Aluminium | 2700 | 255 | 150 |

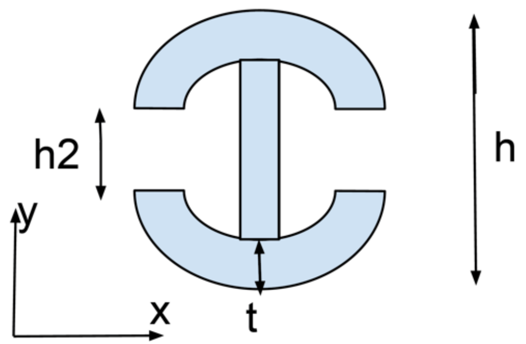

| | | | | | | | | | |
|---|---|---|---|---|---|---|---|---|---|
| Beam-n | | | | | | | | | |
| | **Current Tube** | **New Tube, 6082 extrusion** | **I_current/I_new** | **A_current/A_new** | | | Density | Yield | |
| Diameter | 914 | 920 | | | | Steel | 7800 | 355 | |
| Thickness | 14.3 | 24.01 | 25 | | | Aluminium | 2700 | 150 | 215 |
| Length | 13357 | 13357 | 12499-500 = 11999 | | | | | | |
| I_xx | 4,088,637,051 | 6,783,487,966 | 0.603 | 0.598 | 0.606 | | | | |
| I_yy | 4,088,637,051 | 6,783,487,966 | 0.603 | | 0.606 | | | | |
| J_co | 8,177,274,102 | 13,566,975,932 | 0.603 | | 0.606 | | | | |
| | | | Weight saving | | | | | | |
| Vekt [kg/m] | 315.11 | 182.38 | 0.42 | % | | | | | |
| Vekt [kg] | 4208.88 | 2436.11 | | | | | | | |
| | | | New T: | 22.84982499 | | | | | |
| Tetta_c | | 0.951679508 | | | | | | | |
| betta | | 18.32638289 | | | betta | 3*((D-t)/t)^0.5 | | | |
| epsilon | | 1.078327732 | | | epsilon | (250^0,5)/(YS) | | | |
| Betta/epsilon | | 16.99518833 | | | | | | | |
| | | | | | Betta/epsilon < 15 --> | | | | |
| | | | | | Klasse 1 | < 10 | | | |
| | | | | | Klasse 2 | 10 - 13,5 | | | |
| | | | | | Klasse 3 | 13,5 - 15 | | | |
| | | | | | Klasse 4 | 15 < | | | |

| | | | | | | | | |
|---|---|---|---|---|---|---|---|---|
| Beam-o | | | | | | | | |
| | **Current Tube** | **New Tube, 6082 extrusion** | **I_current/I_new** | **A_current/A_new** | | | Density | Yield |
| Diameter | 600.65 | 620 | | | | Steel | 7800 | 355 |
| Thickness | 15 | 25 | | | | Aluminium | 2700 | 215 |
| Length | 11374 | 11374 | 11374-1000= 10374 | | | | | |
| I_xx | 1,183,396,194 | 2,070,601,859 | 0.572 | 0.591 | 0.606 | | | |
| I_yy | 1,183,396,194 | 2,070,601,859 | 0.572 | | 0.606 | | | |
| J_co | 2,366,792,389 | 4,141,203,719 | 0.572 | | 0.606 | | | |
| | | | Weight saving | | | | | |
| Vekt [kg/m] | 215.16 | 126.11 | 0.41 | % | | | | |
| Vekt [kg] | 2447.19 | 1434.38 | | | | | | |
| | | | | | | | | |
| Epsilon | 1.078327732 | | | | | | | |
| Buckling | 2.667523237 | ok, Class 1 | | | | | | |

| | | | | | | | | |
|---|---|---|---|---|---|---|---|---|
| Beam-q | | | | | | | | |
| | **Current Tube** | **New Tube, 5083 plates *3** | **I_current/I_new** | **A_current/A_new** | | | Density | Yield |
| Diameter | 4992 | 4992 | | | | Steel | 7800 | 355 |
| Thickness | 24 | 40 | | | | Aluminium | 2700 | 215 |
| Length | 7000 | 7000 | | | | | | |
| I_xx | 1,155,063,338,496 | 1,906,645,249,946 | 0.606 | 0.602 | 0.606 | | | |
| I_yy | 1,155,063,338,496 | 1,906,645,249,946 | 0.606 | | 0.606 | | | |
| J_co | 2,310,126,676,992 | 3,813,290,499,891 | 0.606 | | 0.606 | | | |
| | | | Weight saving | | | | | |
| Vekt [kg/m] | 2920.23 | 1679.32 | 0.42 | % | | | | |
| Vekt [kg] | 20441.61 | 11755.26 | | | | | | |
| | | | | | | | | |
| Epsilon | 1.078327732 | | | | | | | |
| Buckling | 4.983948525 | Class 1 | | | | | | |

| Beam-q1 | | | | | | | | |
|---|---|---|---|---|---|---|---|---|
| | Current plate | New plate | I_current/I_new | A_current/A_new | | | Density | Yield |
| Height | 3,000 | 3,000 | | | | Steel | 7800 | 355 |
| Width | 2,230 | 2,230 | | | | Aluminiur | 2700 | 215 |
| Thickness | 12 | 20 | | | | | | |
| I_xx | 108,000,000,000 | 180,000,000,000 | 0.600 | 0.600 | 0.606 | | | |
| I_yy | 1,728,000 | 8,000,000 | 0.216 | | 0.606 | | | |
| J_co | 108,001,728,000 | 180,008,000,000 | 0.600 | | 0.606 | | | |
| | | | Weight saving | | | | | |
| Vekt [kg/m] | - | - | 0.42 | % | Epsilon | 1.078328 | | |
| Vekt [kg] | 626 | 361 | | | Buckling height | | 55.64171 | <5 |
| | | | | | Bukling width | | 41.36015 | <5 |

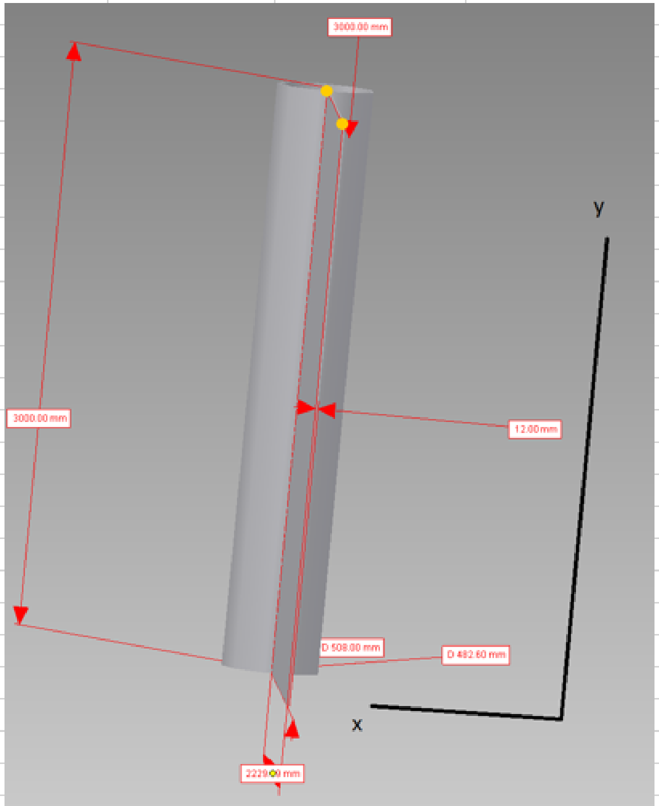


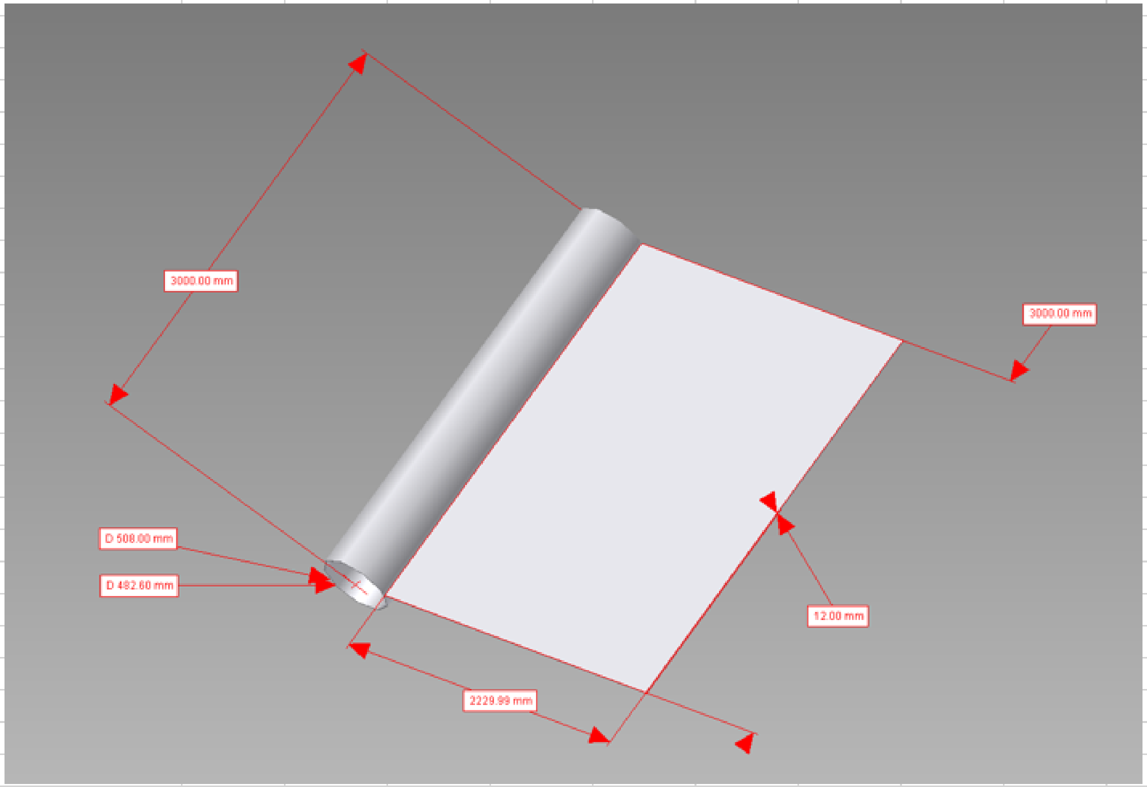

| | | | | | | | | |
|---|---|---|---|---|---|---|---|---|
| Beam-q2 | | | | | | | | |
| Diameter | | | | | | | | |
| Length | Current cylinder | New cylinder | I_current/I_new | A_current/A_new | | | Density | Yield |
| Thickness | 508 | 508 | | | | Steel | 7800 | 355 |
| I_xx | 3,000 | 3,000 | | | | Aluminiur | 2700 | 215 |
| I_yy | 12 | 25 | | | | | | |
| J_co | 575,360,829 | 1,109,183,092 | 0.519 | 0.480 | 0.606 | | | |
| | 575,360,829 | 1,109,183,092 | 0.519 | | 0.606 | | | |
| Vekt [kg/m] | 1,150,721,658 | 2,218,366,184 | 0.519 | | 0.606 | | | |
| Vekt [kg] | | | Weight saving | | | | | |
| | - | - | 0.30 | % | | | | |
| | 438 | 307 | | | | | | |
| Epsilon | 1.078327732 | | | | | | | |
| Buckling | 2.683298826 | Class 1 | | | | | | |

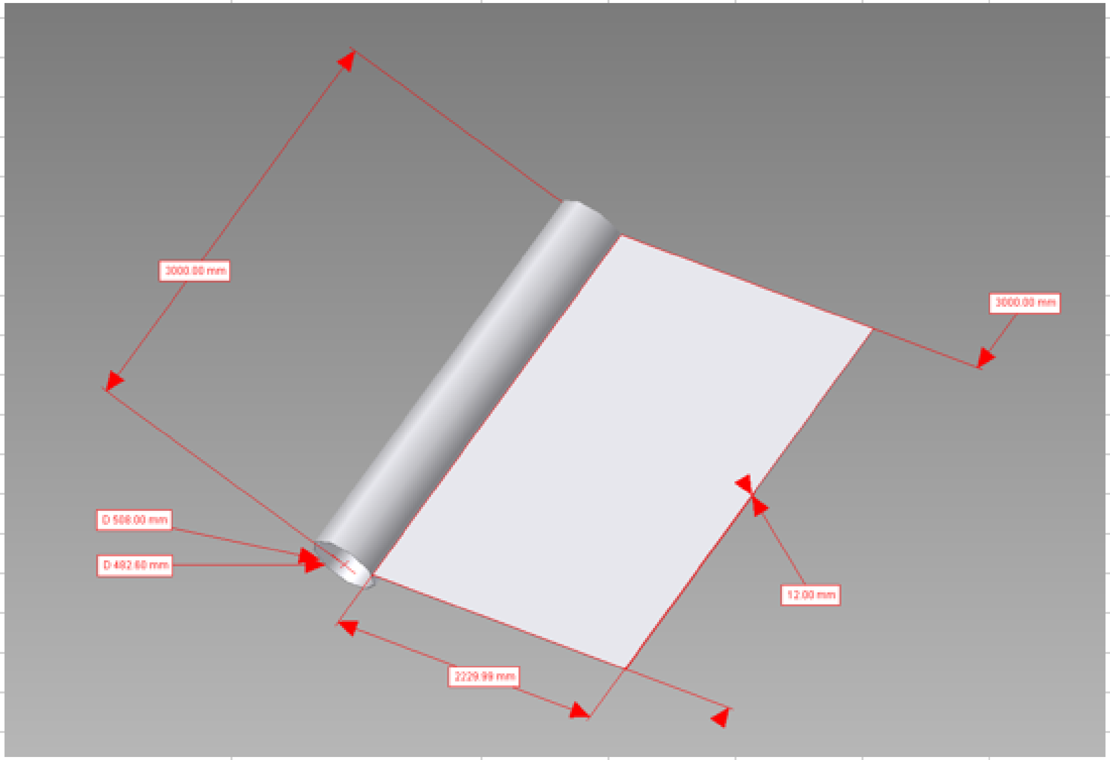

| | | | | | | | | |
|---|---|---|---|---|---|---|---|---|
| Beam-q3 | | | | | | | | |
| | Current cylinder | New cylinder | I_current/I_new | A_current/A_new | | | Density | Yield |
| Diameter | 5,100 | 5,100 | | | | Steel | 7800 | 355 |
| Length | | | | | | Aluminium | 2700 | 215 |
| Thickness | 25 | 45 | | | | | | |
| I_xx | 6,640,625 | 38,728,125 | 0.171 | 0.556 | 0.606 | | | |
| I_yy | 276,356,250,000 | 497,441,250,000 | 0.556 | | 0.606 | | | |
| J_co | 276,362,890,625 | 497,479,978,125 | 0.556 | | 0.606 | | | |
| | | | Weight saving | | | | | |
| Vekt [kg/r | - | - | 0.38 | % | | | | |
| Vekt [kg] | 3,984 | 2,482 | | | | | | |
| | | | | | | | | |
| Epsilon | 1.078327732 | | | | | | | |
| buckling | 21.02020192 | | | | | | | |

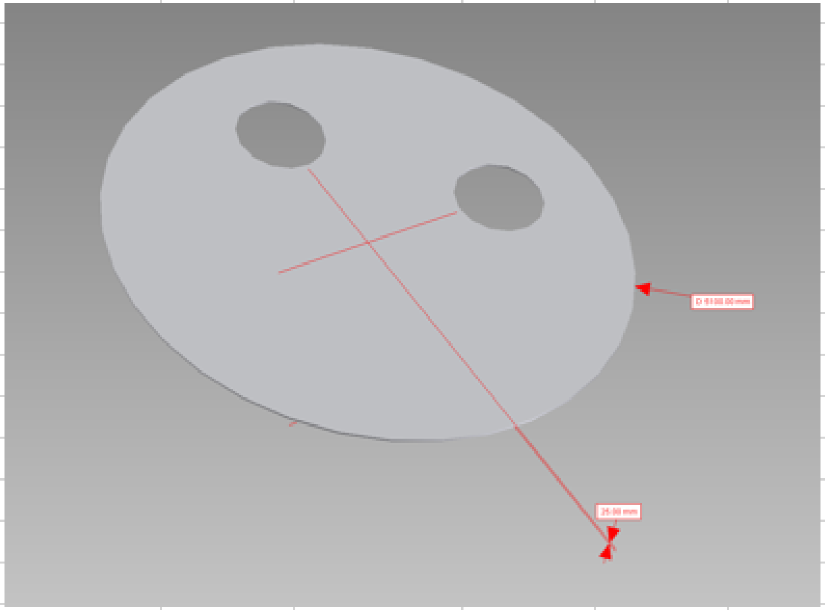

| | | | | | | | | | |
|---|---|---|---|---|---|---|---|---|---|
| Beam-s | | | | | | | Density | Yield | |
| | **Current square beam** | **New I beam (6082 extrusion and 5083 plate)** | **I_current/I_new** | **A_current/A_new** | | Steel | 7800 | 355 | |
| Height | 400 | 400 | | | | Aluminium | 2700 | 215 | 255 |
| Width | 400 | 420 | | | | | | | |
| Flange thickness | [redacted] | 35 | | | | | | | |
| Web **thickness** | 12.5 | 20 | | | | | | | |
| Length | 6768 | 8268 | 6768+1500 | | | | | | |
| I_xx | 485,384,115 | 1,042,100,000 | 0.466 | 0.538 | 0.718 | | | | |
| I_yy | 485,384,115 | 709,600,000 | 0.684 | | 0.718 | | | | |
| J_co | 970,768,229 | 1,751,700,000 | 0.554 | | 0.718 | | | | |
| | | | Weight saving | | | | | | |
| Vekt [kg/m] | 151 | 97 | 0.21 | % | | | | | |
| Vekt [kg] | 1,023 | 804 | | | | | | | |
| Lengde [m] | | 5.504115226 | 8.2 | | | | | | |
| | | | | | | | | | |
| | | Square beam | | | | | | | |
| Heigt | | 400 | | | | | | | |
| Width | | 400 | | | | | | | |
| Thickness | | 25 | | | | | | | |
| Length | | 8268 | | | | | | | |
| I_xx | | 882,812,500 | 0.550 | 0.517 | 0.606 | | | | |
| I_yy | | 882,812,500 | 0.550 | | 0.606 | | | | |
| J_co | | 1,765,625,000 | 0.550 | | 0.606 | | | | |
| | | | Weight saving | | | | | | |
| Vekt [kg/m] | 151.125 | 101.25 | 0.33 | % | | | | | |
| Vekt [kg] | 1022814 | 837135 | | | | | | | |
| | | | | | | | | | |
| | | | | | | | | | |
| Buckling in flange | | 5.714285714 | 3-6 for 6082 | | | | | | |
| Buckling in web | | 6.6 | | | | | | | |

| | | | | | | | | | |
|---|---|---|---|---|---|---|---|---|---|
| Beam-t | | | | | | | Density | Yield | |
| | **Current square beam** | **New I beam (6082 extrusion and 5083 plate)** | **I_current/I_new** | **A_current/A_new** | | Steel | 7800 | 355 | |
| Height | 400 | 400 | | | | Aluminium | 2700 | 215 | 255 |
| Width | 400 | 420 | | | | | | | |
| Flange thickness | [redacted] | 35 | | | | | | | |
| Web **thickness** | 12.5 | 20 | | | | | | | |
| Length | 5846 | 5846 | | | | | | | |
| I_xx | 485,384,115 | 1,042,100,000 | 0.466 | 0.538 | 0.718 | | | | |
| I_yy | 485,384,115 | 709,600,000 | 0.684 | | 0.718 | | | | |
| J_co | 970,768,229 | 1,751,700,000 | 0.554 | | 0.718 | | | | |
| | | | Weight saving | | | | | | |
| Vekt [kg/m] | 151 | 97 | 0.36 | % | | | | | |
| Vekt [kg] | 883 | 568 | | | | | | | |
| | | | | | | | | | |
| | | Square beam | | | | | | | |
| Heigt | | 400 | | | | | | | |
| Width | | 400 | | | | | | | |
| Thickness | | 25 | | | | | | | |
| Length | | 5846 | | | | | | | |
| I_xx | | 882,812,500 | 0.550 | 0.517 | 0.606 | | | | |
| I_yy | | 882,812,500 | 0.550 | | 0.606 | | | | |
| J_co | | 1,765,625,000 | 0.550 | | 0.606 | | | | |
| | | | Weight saving | | | | | | |
| Vekt [kg/m] | 151.125 | 101.25 | 0.33 | % | | | | | |
| Vekt [kg] | 883476.75 | 591907.5 | | | | | | | |

| Beam-w | Current I beam | New I beam (6082 extr | I_current/I_new | A_current/A-new | | | Density | Yield | |
|---|---|---|---|---|---|---|---|---|---|
| Height | 360 | 360 | | | | Steel | 7800 | 355 | |
| Width | 300 | 300 | | | | Aluminium | 2700 | 255 | 150 |
| Flange thickness | 22.5 | 35 | | | | | | | |
| Web thickness | 12.5 | 20 | | | | | | | |
| Length (tube surface-end) | 1312.5 | 1312.5 | | | | | | | |
| I_xx | 417,561,328 | 597,323,333 | 0.699 | 0.651 | 0.718 | | | | |
| I_yy | 186,203,613 | 279,493,333 | 0.666 | | 0.718 | | | | |
| J_co | 603,764,941 | 876,816,667 | 0.689 | | 0.718 | | | | |
| | | | Weight saving | | | | | | |
| Vekt [kg/m] | 136.01 | 72.36 | 0.47 | % | | | | | |
| Vekt [kg] | 179 | 95 | | | | | | | |
| Weight extrusion [kg/m] | | 28.35 | | | | | | | |
| Weight extrusion [kg] | | 37.209375 | | | | | | | |
| Length extrusion (max 535kg) [m] | | 18.87 | | | | | | | |
| Length of T-flange (vertical) | | 74.11764706 | | | | | | | |
| Weight of extruded T-flange [kg/m] | | 32.35235294 | | | | | | | |
| LengthT-flange extrusion (max 535kg) [m] | | 16.54 | 3 | | | | | | |
| | | | | | | | | | |
| Flange bending | | 4 | 3.5--4,5--5 | | | | | | |
| Web bending | | 5.8 | 9--13--18 | | | | | | |
| Flange bending with stiffener | | 3.378105528 | | | | | | | |
| Length of stiffener | | 5 | | | | | | | |
| | | | | | | | | | |
| Alt i en ekstrusjon: | Vekt [kg/m] | 72.36 | kg/m i 1 ekstrusjon | | | | | | |
| | Lengde [m] | 7.39 | m | | | | | | |

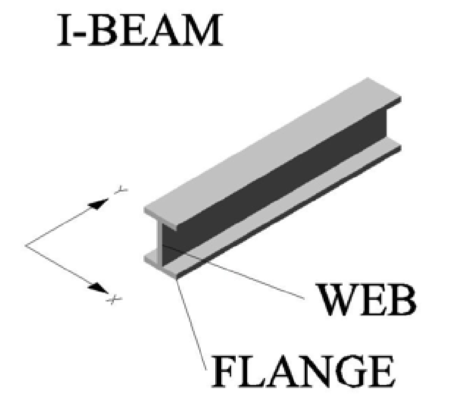


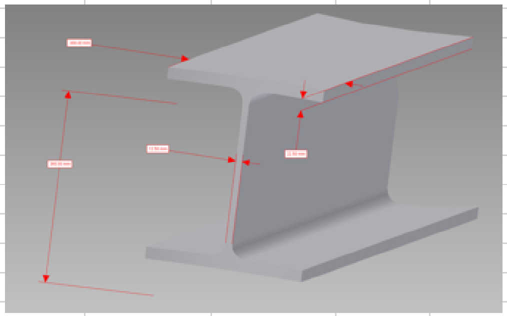

| Beam-x | | | | | | | | | | |
|---|---|---|---|---|---|---|---|---|---|---|
| | Current square beam | New I beam (6082 extrusion and | I_current/I_new | A_current/A-new | SMYS Ratio | | | Density | Yield | |
| Height | 200 | 200 | | | | | Steel | 7800 | 355 | |
| Width | 200 | 200 | | | | | Aluminiur | 2700 | 255 | 150 |
| Flange thickness | | | | | | | | | | |
| Thickness | 10 | 15 | | | | | | | | |
| Length | 2586 | 2586 | | | | | | | | |
| I_xx | 45,853,333 | 63,732,500 | 0.719 | 0.685 | 0.718 | | epsilon | 0.990148 | | |
| I_yy | 45,853,333 | 63,732,500 | 0.719 | | 0.718 | | Buckling | 11.22167 | Class 2 | |
| J_co | 91,706,667 | 127,465,000 | 0.719 | | 0.718 | | | | | |
| | | | Weight saving | | | | | | | |
| Vekt [kg/m] | 59.28 | 29.97 | 0.49 | % | | | | | | |
| Vekt [kg] | 153.29808 | 77.50242 | | | | | | | | |

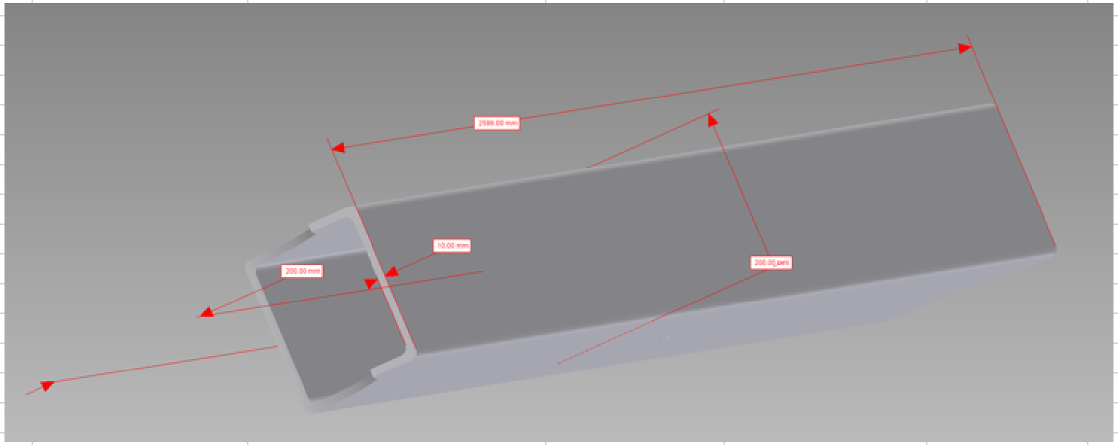

| | | | | | | | | | |
|---|---|---|---|---|---|---|---|---|---|
| Beam-y | | | | | | | | | |
| Cylinder 1 | Current cylinder | New cylinder | I_current/I_new | A_current/A_new | | | Density | Yield | |
| Diameter | 219 | 219 | | | | Steel | 7800 | 355 | |
| Length | 6,700 | 6,700 | | | | Aluminium | 2700 | 255 | Extruded |
| Thickness | 25 | 50 | | | | | | | |
| I_xx | 73,361,481 | 103,243,188 | 0.711 | 0.504 | 0.718 | | | | |
| I_yy | 73,361,481 | 103,243,188 | 0.711 | | 0.718 | | | | |
| J_co | 146,722,963 | 206,486,375 | 0.711 | | 0.718 | | | | |
| | | | Weight saving | | | | | | |
| Vekt [kg/m] | 120 | 72 | 0.40 | % | | Epsilon | 0.990147543 | | |
| Vekt [kg] | 802 | 481 | | | | Buckling | 1.515972374 | Class 1 | |

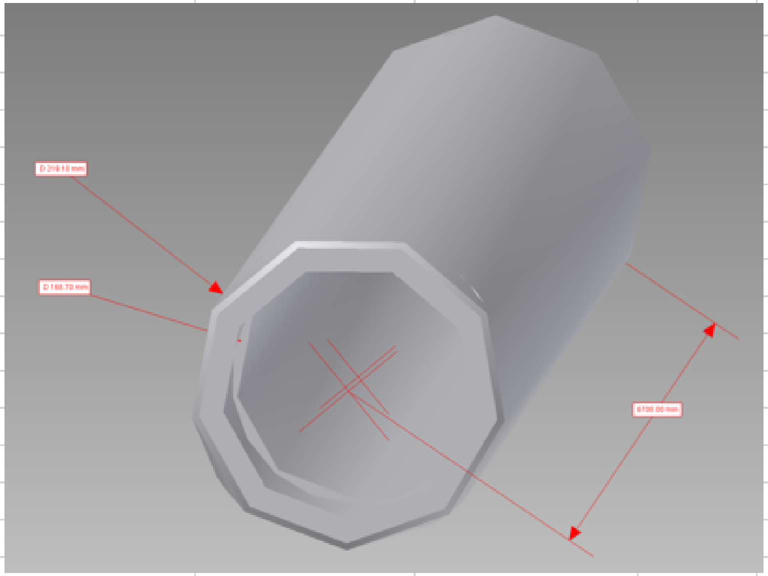

| beam-z | | | | | | | | | |
|---|---|---|---|---|---|---|---|---|---|
| Plate | Current plate | New plate | **I_current/I_new** | **A_current/A_new** | | | Density | Yield | |
| Height | 1,510 | 1,510 | | | | Steel | 7800 | 355 | |
| Width | 1,510 | 1,510 | | | | Aluminium | 2700 | 215 | 5083 Plates |
| Thickness | 30 | 50 | | | | | | | |
| Minus Hole | | | | | | | | | |
| Diameter | 1,075 | 1,075 | | | | | | | |
| I_xx | 5,501,635,313 | 9,169,392,188 | 0.600 | 0.600 | 0.606 | | | | |
| I_yy | 978,750 | 4,531,250 | 0.216 | | 0.606 | | | | |
| J_co | 5,502,614,063 | 9,173,923,438 | 0.600 | | 0.606 | | | | |
| | | | Weight saving | | | | | | |
| Vekt [kg/m] | 10,705 | 3,706 | 0.42 | % | | | | | |
| Vekt [kg] | 321 | 185 | | | | | | | |

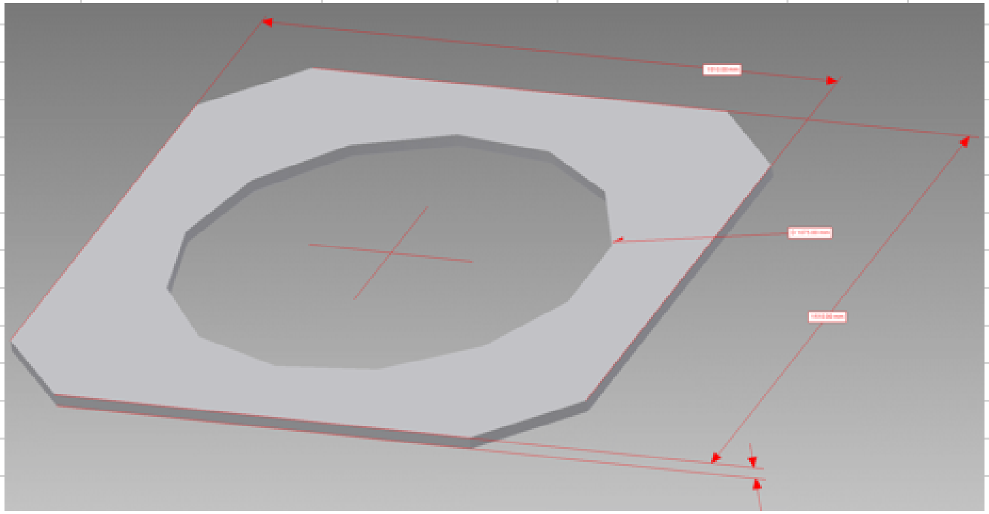

# Appendix E

# Anode Calculation

| | | | |
|---|---|---|---|
| Anode-Calculation | | | |
| | Aluminium anode | Zinc anode | Accodring to NORSOK-M-CR-503 for |
| Cap. [Ah/kg] | 2000 | 780 | Capacity for temperatures up to 30.deg Celsius |
| CCP | -1050 | -1030 | [mV vs Ag/AgCl] |

| | | | |
|---|---|---|---|
| 6.3.11 - DnV - | For aluminium components, or those coated with either aluminium or zinc, a design current density of 0.010 A/m2 is recommended for initial/final as well as mean values | | |
| ic= | 0.01 | A/m^2 | From DnV when Aluminium are to be protected |
| u= | 0.9 | Utilization factor, NORSOK-6.9.2 and from Table 10-8 in Annex A in DnV. | |
| Ac= | 1521 | m^2 | Exposed area of structure in aluminium |

**__ALUMINIUM CP__**

| | | | | |
|---|---|---|---|---|
| NORSOK-M-CR503 | | | | |
| 4 Wells | 8 Amps/well | I_well | 32 | A |

| | | | |
|---|---|---|---|
| 20mA/m^2 for suction anchor | i= 20mA/m^2 | | |
| Area pr. suction anchor | A=pi*D*H | D=5100 | H= 7025 |
| | 112555410.8 | mm^2 | 112.5554 |
| 4 suction anchors | I=4*A*i | 9004.43286 | mA |
| | I_sa | 9.00443286 | A |

| | | | |
|---|---|---|---|
| | Ac*ic | 15.21 | |
| Current Demand Calculation | (Ac*ic)+I_well+I_sa | 56.2144329 | A |

| | | |
|---|---|---|
| Anode Mass Calculation | Ma=(Icm*tf*8760)/(u*CCP) | |
| 20 yrs | 5471.538132 | kg |
| 25 yrs | 6839.422665 | kg |
| 30 yrs | 8207.307198 | kg |

**__STEEL CP__**

| | | | |
|---|---|---|---|
| 8 amps per well: | I_well | 32 | A |
| | i_sa | 20 | mA/m^2 |
| 4 SA | A | 484 | m^2 |
| Surface structure: | A_st | 1521 | m^2 |
| Current surface: | I_st= A_st*i_st*fc | | |

where, fc is coating breakdown factor, i_st is current density and A_st is steel surface area (initially coated by a 2 layer epoxy, total DFT = 350 µm.

| DnV: | ic and fc are then to be selected according to (6.3) and (6.4), respectively. |
|---|---|
| | 2 layer epoxt, 350 µm DFT --> **a=0.02** and **b = 0.008** |
| | fc = a+ b*t |

| initial | mean | final | |
|---|---|---|---|
| 0.22 | 0.11 | 0.17 | A/m^2 for seawater exposed bare metal |

Depth more than 300m (assumption) and Temperature range 7-11 degrees celsius:

Ma= (Icm*tf*8760)/(u*CCP)

| Icm = | I_st + I_well + I_sa = (A_st*i_mean*fcm) + (I_well) + (i_sa*A) |
|---|---|

Current calc:

| years | fc | I_st [A] | I_well [A] | I_sa [A] | I_tot [A] |
|---|---|---|---|---|---|
| 20 | 0.1 | 16.731 | 32 | 9.68 | 58.411 |
| 25 | 0.12 | 20.0772 | 32 | 9.68 | 61.7572 |
| 30 | 0.14 | 23.4234 | 32 | 9.68 | 65.1034 |

| Anode Mass Calculat | Ma=(Icm*tf*8760)/(u*CCP) | |
|---|---|---|
| 20 yrs | 5685.337333 | kg |
| 25 yrs | 7513.792667 | kg |
| 30 yrs | 9505.0964 | kg |

# Appendix F

# Additional Figures

## F.1 Extrusion limits

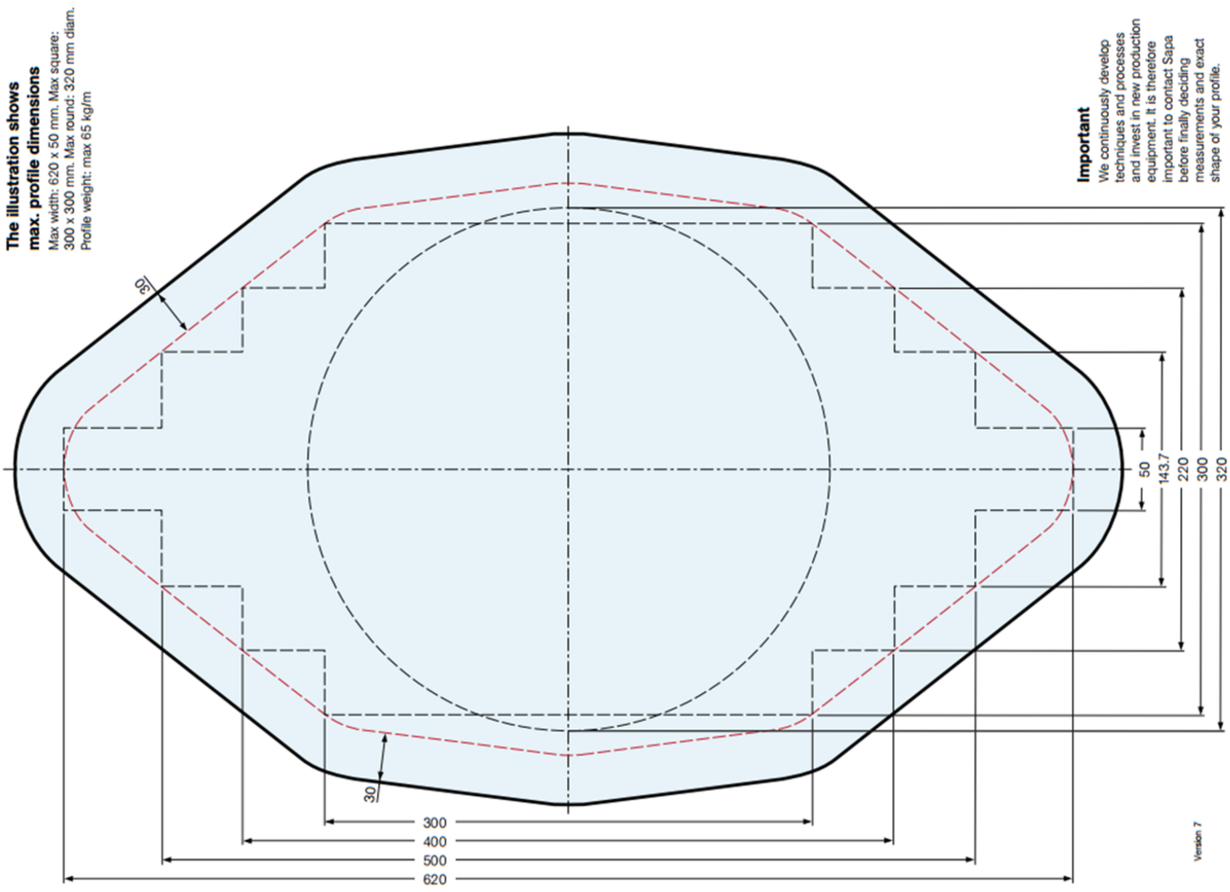


Figure F.1: Circumference limits for the extrusion press at SAPA [5]).

## F.2 seawater properties as a function of depth

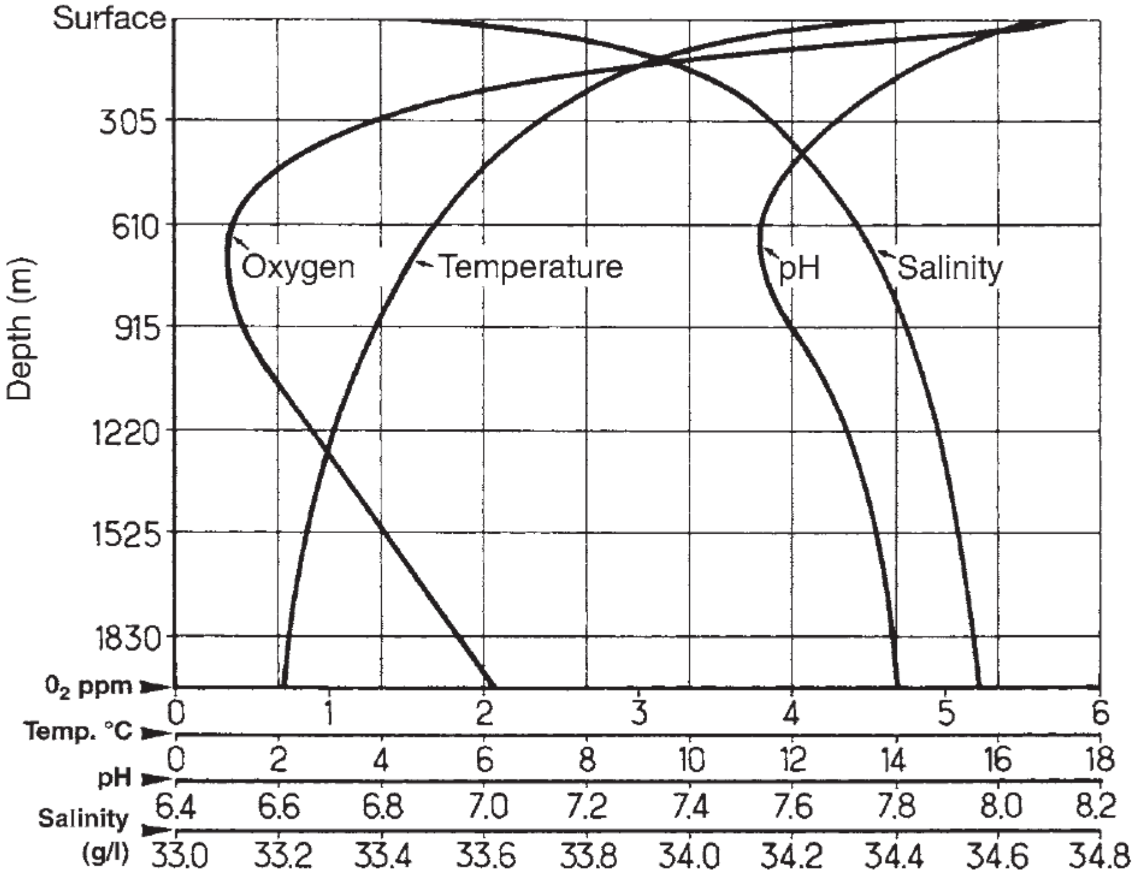


Figure F.2: Seawater's change in properties by depth [19]).

## F.3 Illustration of suction anchor with welds.

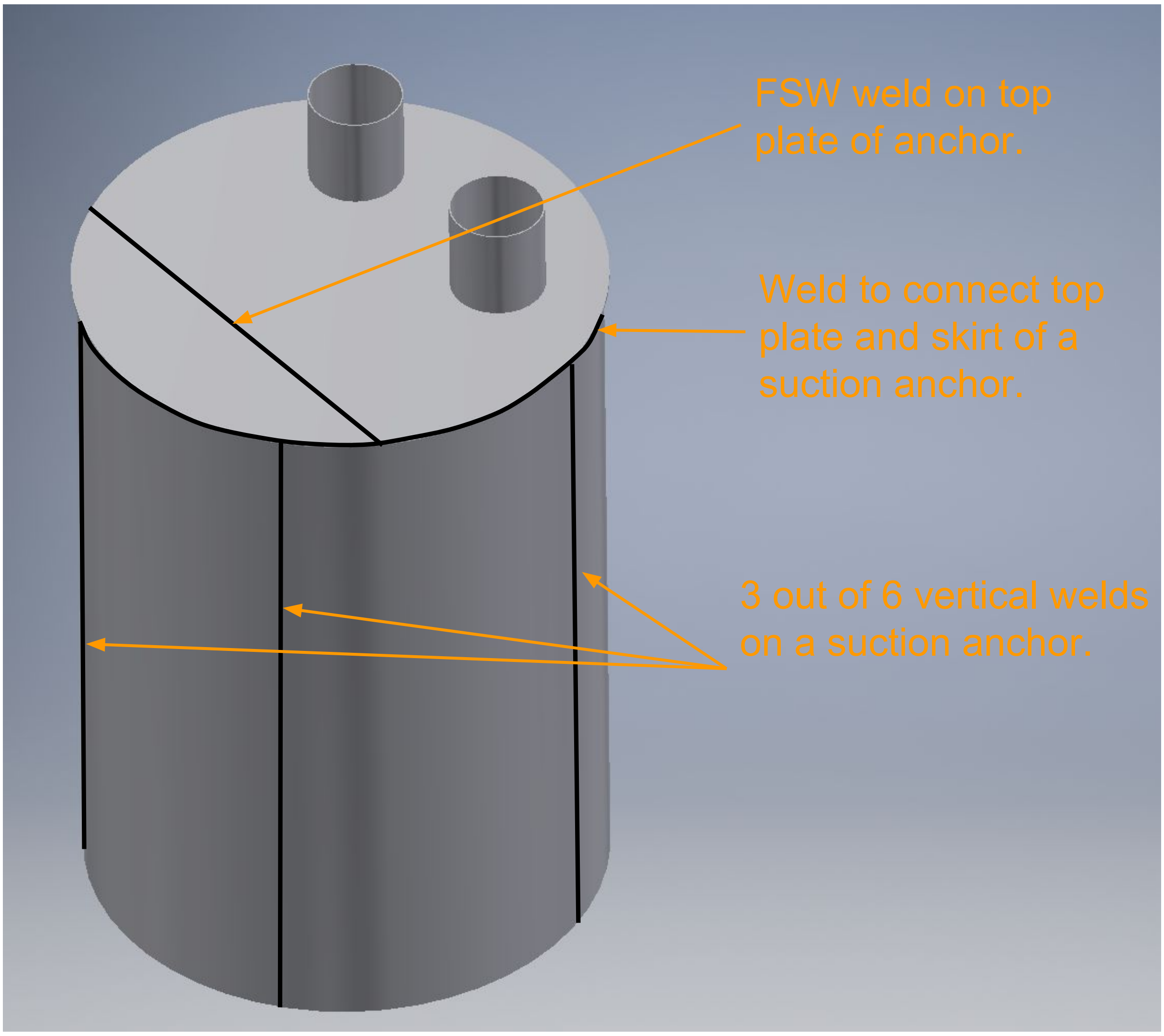

# Appendix G

# Que$tor Cost Estimates

## G.1 Full subsea layout.

OFFSHORE PROJECT SUMMARY

| | |
|---|---|
| Project name | ITS-Project |
| Region | Europe |
| Country | Norway (North) |
| Basin | Trondelag Platform |

| Procurement strategy | | Currency | Rate/$ |
|---|---|---|---|
| Offshore | ITS-test | $ | 1.00 |
| Contingency | N. North Sea (Norway) | $ | 8.17 |
| Equipment | N. North Sea (Norway) | $ | 8.17 |
| Materials | N. North Sea (Norway) | $ | 8.17 |
| Fabrication | N. North Sea (Norway) | $ | 8.17 |
| Linepipe | N. North Sea (Norway) | $ | 8.17 |
| Installation | N. North Sea (Norway) | $ | 8.17 |
| Design & PM | N. North Sea (Norway) | $ | 8.17 |
| Opex | N. North Sea (Norway) | $ | 8.17 |
| Certification | N. North Sea (Norway) | $ | 8.17 |
| Freight | N. North Sea (Norway) | $ | 8.17 |

| | |
|---|---|
| Technical database | N. North Sea (Norway) |

| | |
|---|---|
| Unit set | Oilfield |
| Development type | Oil |
| Development concept | Semi-submersible + Subsea tie-back |

Overall input

| | | | | | |
|---|---|---|---|---|---|
| Design oil production flowrate | 52.80 | Mbbl/day | Reserves | 120.00 | MMbbl |
| Design associated gas flowrate | 118.00 | MMscf/day | Water depth | 269.00 | m |
| Design gross liquids flowrate | 58.70 | Mbbl/day | Reservoir depth | 2310.00 | m |
| Water injection | Yes | | Reservoir pressure | 246.00 | bara |
| Water injection capacity factor | 1.10 | | Reservoir temperature | 71.20 | °C |
| Design water injection flowrate | 64.50 | Mbbl/day | Reservoir length | 4.89 | km |
| Gas injection | Yes | | Reservoir width | 2.45 | km |
| Design gas injection rate | 118.00 | MMscf/day | | | |
| Gas oil ratio | 2230.00 | scf/bbl | | | |
| Design factor | 1.10 | | | | |

Fluid characteristics

| | | | | | |
|---|---|---|---|---|---|
| Oil density @ STP | 40.20 | °API | H2S content | 0.00 | ppm |
| CO2 content | 0.30 | % | Gas molecular weight | 30.00 | |
| Initial water cut | 10.00 | % | | | |

Production profile characteristics

| | | | | | |
|---|---|---|---|---|---|
| Plateau rate | 48.00 | Mbbl/day | Years to plateau | 2.00 | year |
| Productivity | 16.00 | MMbbl/well | Plateau duration | 3.00 | year |
| Peak well flow | 6.00 | Mbbl/day | Field life | 11.00 | year |
| Maximum drilling stepout | 3.00 | km | Onstream days | 350.00 | day |
| Concurrent drilling operations | 1 | | Wells per year per operation | 4.90 | |

Export methods

| | | | | | |
|---|---|---|---|---|---|
| Oil export method | via existing pipeline | | Gas export method | via existing pipeline | |
| Distance to delivery / tie-back point | 55.00 | km | Distance to delivery / tie-back point | 130.00 | km |

Number of wells

| | | | |
|---|---|---|---|
| Production wells | 12 | Gas injection wells | 4 |
| Water injection wells | 5 | | |

| Field level miscellaneous data | | | BOE equivalent values | | |
|---|---|---|---|---|---|
| Distance to operations base | 120.00 | km | BOE oil | 1.00 | BOE/bbl |
| Distance to delivery point | 120.00 | km | BOE condensate | 0.94 | BOE/bbl |
| Maximum drilling stepout | 3.00 | km | BOE gas | 0.17 | BOE/Mscf |
| Maximum ambient temperature | 22.00 | °C | | | |
| Average seawater temperature | 10.00 | °C | | | |

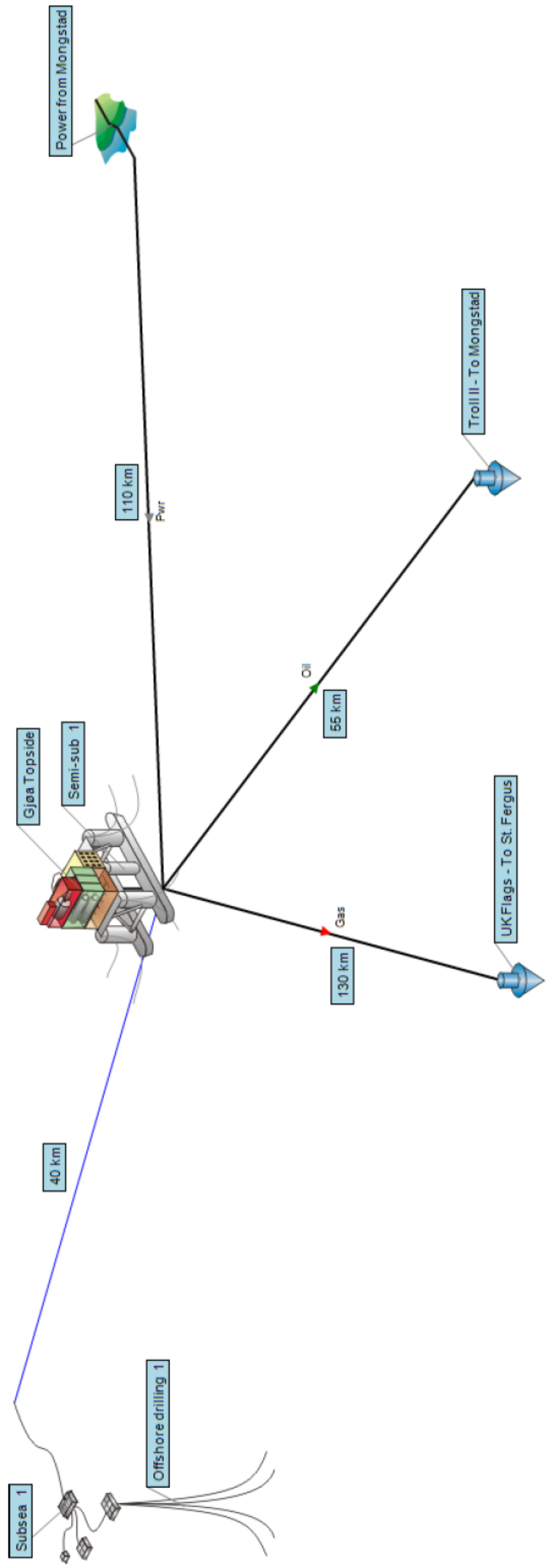
Power from Mongstad
110 km
Pwr
Troll II - To Mongstad
Oil
55 km
Gjøa Topside
Semi-sub 1
Gas
130 km
UKFlags - To St. Fergus
40 km
Offshore drilling 1
Subsea 1

Subsea input report

| | |
|---|---|
| Component name | Subsea 1 |

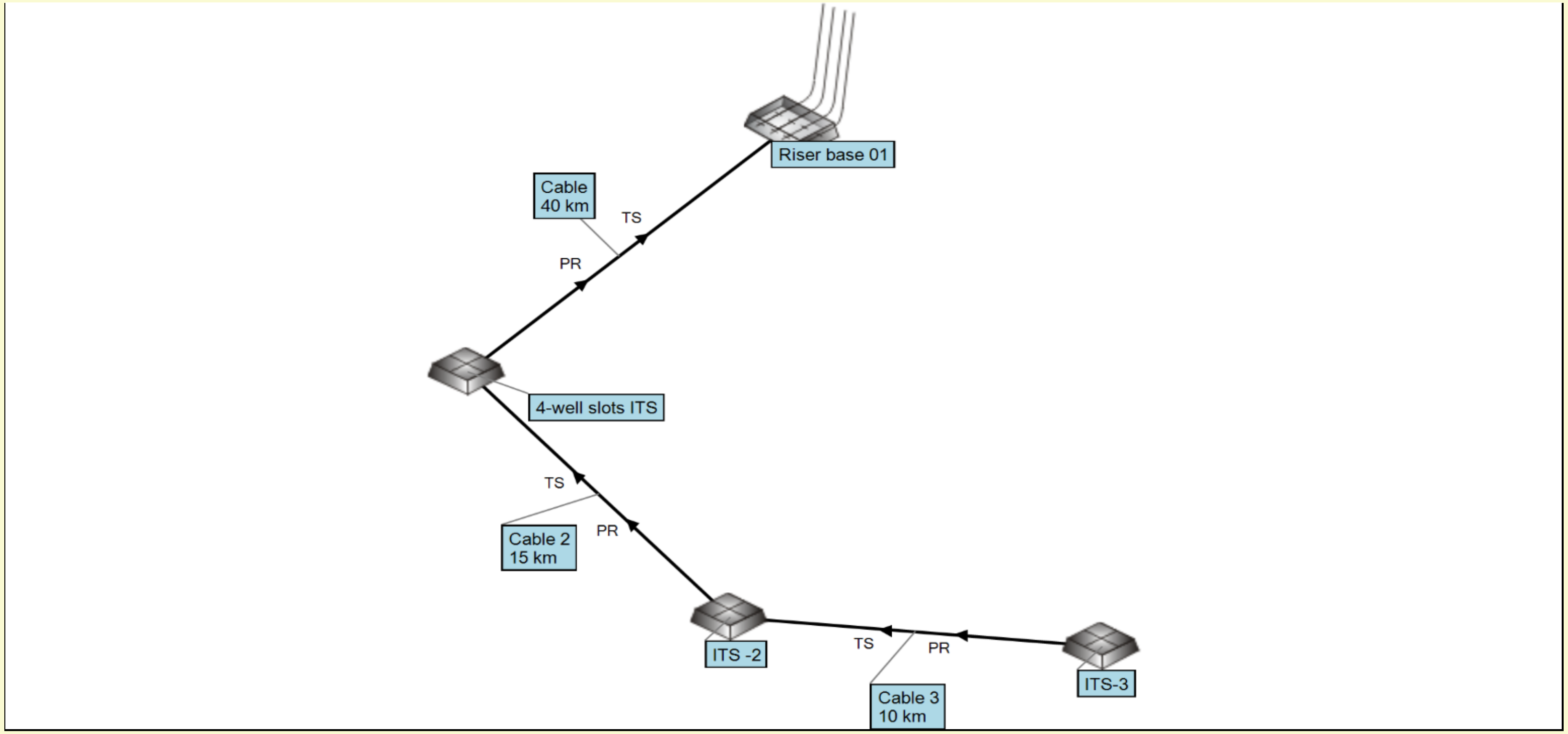


| | Well count | Flow | Type |
|---|---|---|---|
| Production | 12 | 52.8 Mbbl/day | |
| Water injection | 0 | 64.5 Mbbl/day | |
| Gas injection | 0 | 118 MMscf/day | |
| Spare slots | 0 | | - |

| | Present | Flow rate |
|---|---|---|
| Multiphase metering | No | |
| Test | Yes | |
| Gas lift | No | - |
| Chemical injection | No | |

| | |
|---|---|
| Schematic edited | Yes |

| |
|---|
| Layout |

| | | | |
|---|---|---|---|
| Development type | Cluster manifold | Maximum wells per item | 4 |
| Infield flowline length | 1.63 km | Tie-back | No |
| Tie-back length | - | | |

| Features | | | |
|---|---|---|---|
| Water depth | 350 m | Wellhead shut in pressure | 203 bara |
| Pressure rating | 345 barg | Wellhead temperature | 64.7 °C |
| Soil conditions | Average | Acid gas | No |
| HIPPS | No | HIPPS minimum flowline length | - |
| Through pigging | No | Retrievable subsea | No |
| Trawler protection | No | Intervention tools | No |
| Diverless system | Yes | | |

| Tie-in point | | | |
|---|---|---|---|
| Production delivery pressure | 35 bara | Water injection pressure | 136 bara |
| Gas injection pressure | 220 bara | Test service delivery pressure | 35 bara |
| Gas lift pressure | 205 bara | Production / test service design pressure | 202 barg |
| Production temperature | 10.4 °C | | |

| Flowlines | |
|---|---|
| Lay vessel | S-lay without DP |
| Flowline type | Steel |
| Buried lines | No |

| Umbilicals | |
|---|---|
| Control system | Electro-hydraulic |
| Tube material | Duplex |
| Inhibitor chemicals | Yes |
| Power cable | No |

| Flowline fluid | Production | Water Injection | Gas injection | Test service | Gas lift | Chemical injection |
|---|---|---|---|---|---|---|
| Flowline material | Carbon steel X60 | Carbon steel X60 | Carbon steel X60 | Carbon steel X60 | Carbon steel X60 | Carbon steel X60 |
| Insulation material | None | None | None | None | None | None |
| Insulation U value | - | - | - | - | - | - |
| PLET selected | Yes | Yes | Yes | Yes | Yes | Yes |

| | |
|---|---|
| Distance to supply base | 120 km |
| Weather downtime (small vessels) | 15 % |
| Weather downtime (large vessels) | 10 % |

| Vessel durations (days) | Pipelay spread | DSV | SSCV | SSDV | Trench vessel | Survey vessel | Dredge vessel | Rock install vessel | Supply vessel |
|---|---|---|---|---|---|---|---|---|---|
| Template | 0.0 | 18.4 | 0.0 | 0.0 | 0.0 | 0.0 | 0.0 | 0.0 | 0.0 |
| Satellite | 0.0 | 0.0 | 0.0 | 0.0 | 0.0 | 0.0 | 0.0 | 0.0 | 0.0 |
| Cluster | 0.0 | 0.0 | 0.0 | 0.0 | 0.0 | 0.0 | 0.0 | 0.0 | 0.0 |
| Manifold | 0.0 | 2.3 | 0.0 | 0.0 | 0.0 | 0.0 | 0.0 | 0.0 | 0.0 |
| Equipment | 0.0 | 0.0 | 0.0 | 0.0 | 0.0 | 0.0 | 0.0 | 0.0 | 0.0 |
| Risers | 10.7 | 0.0 | 0.0 | 0.0 | 0.0 | 0.0 | 0.0 | 0.0 | 0.0 |
| Flowline links | 67.1 | 0.0 | 0.0 | 0.0 | 0.0 | 0.0 | 0.0 | 0.0 | 0.0 |
| PLETs | 8.8 | 14.8 | 0.0 | 0.0 | 0.0 | 0.0 | 0.0 | 0.0 | 0.0 |
| Umbilical links | 9.7 | 8.5 | 0.0 | 0.0 | 0.0 | 0.0 | 0.0 | 0.0 | 0.0 |
| Trenching | 0.0 | 0.0 | 0.0 | 0.0 | 0.0 | 0.0 | 0.0 | 0.0 | 0.0 |
| Surveying | 0.0 | 0.0 | 0.0 | 0.0 | 0.0 | 13.0 | 0.0 | 0.0 | 0.0 |
| Dredging | 0.0 | 0.0 | 0.0 | 0.0 | 0.0 | 0.0 | 0.0 | 0.0 | 0.0 |
| Rock installation | 0.0 | 0.0 | 0.0 | 0.0 | 0.0 | 13.0 | 0.0 | 0.0 | 0.0 |
| Transit loadout | 1.9 | 3.8 | 0.0 | 0.0 | 0.0 | 1.3 | 0.0 | 0.0 | 26.0 |
| Weather downtime | 9.8 | 7.2 | 0.0 | 0.0 | 0.0 | 2.1 | 0.0 | 0.0 | 3.9 |
| Mob/demob | 8.0 | 8.0 | 0.0 | 0.0 | 0.0 | 8.0 | 0.0 | 0.0 | 8.0 |
| Total | 116.1 | 63.0 | 0.0 | 0.0 | 0.0 | 24.4 | 0.0 | 0.0 | 37.9 |

| Subsea components | Type | Water depth | Production wells | Production flow per well | Water injection wells | Water injection flow per | Gas injection wells | Gas injection flow per well | Test service |
|---|---|---|---|---|---|---|---|---|---|
| 4-well slots ITS | Template manifold | 350 m | 4 | 4.4 Mbbl/day | 0 | 0 Mbbl/day | 0 | 0 MMscf/day | Yes |
| ITS -2 | Template manifold | 350 m | 4 | 4.4 Mbbl/day | 0 | 0 Mbbl/day | 0 | 0 MMscf/day | Yes |
| ITS-3 | Template manifold | 350 m | 4 | 4.4 Mbbl/day | 0 | 0 Mbbl/day | 0 | 0 MMscf/day | Yes |

| Subsea components | Gas lift | Chemical injection | HIPPS | MFM on test service | MFM on production | MFM on wellheads | Spare slots | Spare slots type | Total slots count |
|---|---|---|---|---|---|---|---|---|---|
| 4-well slots ITS | No | No | No | No | No | No | 0 | - | 4 |
| ITS -2 | No | No | No | No | No | No | 0 | - | 4 |
| ITS-3 | No | No | No | No | No | No | 0 | - | 4 |

| Subsea components | SDU selected | SDU wells serviced | SDU hydraulic flying | SDU electrical flying leads | UTA wells serviced | UTA hydraulic flying leads | UTA electrical flying leads |
|---|---|---|---|---|---|---|---|
| 4-well slots ITS | Yes | 4 | 0 | 0 | 4 | 1 | 2 |
| ITS -2 | Yes | 4 | 0 | 0 | 4 | 1 | 2 |
| ITS-3 | Yes | 4 | 0 | 0 | 4 | 1 | 2 |

| Riser base manifold | Water depth | Termination type | Sub-type | Riser systems | Riser length |
|---|---|---|---|---|---|
| Riser base 01 | 350 m | Riser | Flexible lazy S | 1 | 562 m |

| Cable | Length | Well end name | Well end water depth | Tie-back end name | Tie-back end water depth |
|---|---|---|---|---|---|
| | 40 km | 4-well slots ITS | 350 m | Riser base 01 | 350 m |

| Production oil flow | Production water flow | Production gas flow | Water injection flow | Gas injection flow |
|---|---|---|---|---|
| 52.8 Mbbl/day | 5.87 Mbbl/day | 118 MMscf/day | 0 Mbbl/day | 0 MMscf/day |

| Production flowline | | | | | | | | |
|---|---|---|---|---|---|---|---|---|
| | Number of lines | 1 | Material | Carbon steel X60 | Oil flow per line | 52.8 Mbbl/day | Water flow per line | 5.87 Mbbl/day |
| | Gas flow per line | 118 MMscf/day | Fixed pressure | Outlet pressure | Pressure In | 63.9 bara | Pressure out | 45.1 bara |
| | Design pressure | 203 bara | Buckle arrestors | Yes | Inlet temperature | 32.3 °C | Outlet temperature | 10.5 °C |
| | Nominal diameter | 20 in | Wall thickness | 22 mm | Corrosion allowance | 3 mm | Cladding thickness | 0 mm |
| | Coating | Yes | Weight coating | No | Cathodic protection | Yes | Insulation material | None |
| | Insulation U value | - | | | | | | |

| PLETs | PLET required | Valve | Soil conditions | Pressure rating | Trawler protection | Jumper type |
|---|---|---|---|---|---|---|
| Well end | Yes | Yes | Average | 345 barg | No | Rigid |
| Tie-back | Yes | Yes | Average | 345 barg | No | Rigid |

| Test service flowline | | | | | | | | |
|---|---|---|---|---|---|---|---|---|
| | Number of lines | 1 | Material | Carbon steel X60 | Oil flow per line | 8.8 Mbbl/day | Water flow per line | 0.978 Mbbl/day |
| | Gas flow per line | 19.6 MMscf/day | Fixed pressure | Outlet pressure | Pressure In | 84.5 bara | Pressure out | 45.9 bara |
| | Design pressure | 203 bara | Buckle arrestors | Yes | Inlet temperature | 47 °C | Outlet temperature | 10 °C |
| | Nominal diameter | 8 in | Wall thickness | 11.2 mm | Corrosion allowance | 3 mm | Cladding thickness | 0 mm |
| | Coating | Yes | Weight coating | No | Cathodic protection | Yes | Insulation material | None |
| | Insulation U value | - | | | | | | |

| PLETs | PLET required | Valve | Soil conditions | Pressure rating | Trawler protection | Jumper type |
|---|---|---|---|---|---|---|
| Well end | Yes | Yes | Average | 345 barg | No | Rigid |
| Tie-back | Yes | Yes | Average | 345 barg | No | Rigid |

| Umbilicals | Control and chemical tube material | Primary control tubes | | Secondary control tubes | | Primary chemical tubes | | Secondary chemical tubes | |
|---|---|---|---|---|---|---|---|---|---|
| | | Number of | Size | Number of | Size | Number of | Size | Number of | Size |
| | Duplex | 6 | 25.4 mm | 0 | 9.52 mm | 6 | 25.4 mm | 0 | 9.52 mm |

| Cable 2 | Length | Well end name | Well end water depth | Tie-back end name | Tie-back end water depth |
|---|---|---|---|---|---|
| | 15 km | ITS -2 | 350 m | 4-well slots ITS | 350 m |

| Production oil flow | Production water flow | Production gas flow | Water injection flow | Gas injection flow |
|---|---|---|---|---|
| 35.2 Mbbl/day | 3.91 Mbbl/day | 78.5 MMscf/day | 0 Mbbl/day | 0 MMscf/day |

| | | | | | | | | |
|---|---|---|---|---|---|---|---|---|
| Production flowline | Number of lines | 1 | Material | Carbon steel X60 | Oil flow per line | 35.2 Mbbl/day | Water flow per line | 3.91 Mbbl/day |
| | Gas flow per line | 78.5 MMscf/day | Fixed pressure | Outlet pressure | Pressure In | 72.7 bara | Pressure out | 63.9 bara |
| | Design pressure | 203 bara | Buckle arrestors | Yes | Inlet temperature | 44.1 °C | Outlet temperature | 16.1 °C |
| | Nominal diameter | 16 in | Wall thickness | 18.2 mm | Corrosion allowance | 3 mm | Cladding thickness | 0 mm |
| | Coating | Yes | Weight coating | No | Cathodic protection | Yes | Insulation material | None |
| | Insulation U value | - | | | | | | |

| PLETs | PLET required | Valve | Soil conditions | Pressure rating | Trawler protection | Jumper type |
|---|---|---|---|---|---|---|
| Well end | Yes | Yes | Average | 345 barg | No | Rigid |
| Tie-back | Yes | Yes | Average | 345 barg | No | Rigid |

| | | | | | | | | |
|---|---|---|---|---|---|---|---|---|
| Test service flowline | Number of lines | 1 | Material | Carbon steel X60 | Oil flow per line | 8.8 Mbbl/day | Water flow per line | 0.978 Mbbl/day |
| | Gas flow per line | 19.6 MMscf/day | Fixed pressure | Outlet pressure | Pressure In | 96.4 bara | Pressure out | 84.5 bara |
| | Design pressure | 203 bara | Buckle arrestors | Yes | Inlet temperature | 48.5 °C | Outlet temperature | 11.5 °C |
| | Nominal diameter | 8 in | Wall thickness | 11.2 mm | Corrosion allowance | 3 mm | Cladding thickness | 0 mm |
| | Coating | Yes | Weight coating | No | Cathodic protection | Yes | Insulation material | None |
| | Insulation U value | - | | | | | | |

| PLETs | PLET required | Valve | Soil conditions | Pressure rating | Trawler protection | Jumper type |
|---|---|---|---|---|---|---|
| Well end | Yes | Yes | Average | 345 barg | No | Rigid |
| Tie-back | Yes | Yes | Average | 345 barg | No | Rigid |

| Umbilicals | Control and chemical tube material | Primary control tubes | | Secondary control tubes | | Primary chemical tubes | | Secondary chemical tubes | |
|---|---|---|---|---|---|---|---|---|---|
| | | Number of | Size | Number of | Size | Number of | Size | Number of | Size |
| | Duplex | 6 | 19 mm | 0 | 9.52 mm | 6 | 19 mm | 0 | 9.52 mm |

| Cable 3 | Length | Well end name | Well end water depth | Tie-back end name | Tie-back end water depth |
|---|---|---|---|---|---|
| | 10 km | ITS-3 | 350 m | ITS -2 | 350 m |

| Production oil flow | Production water flow | Production gas flow | Water injection flow | Gas injection flow |
|---|---|---|---|---|
| 17.6 Mbbl/day | 1.96 Mbbl/day | 39.2 MMscf/day | 0 Mbbl/day | 0 MMscf/day |

| | | | | | | | | |
|---|---|---|---|---|---|---|---|---|
| Production flowline | Number of lines | 1 | Material | Carbon steel X60 | Oil flow per line | 17.6 Mbbl/day | Water flow per line | 1.96 Mbbl/day |
| | Gas flow per line | 39.2 MMscf/day | Fixed pressure | Outlet pressure | Pressure In | 84.9 bara | Pressure out | 72.7 bara |
| | Design pressure | 203 bara | Buckle arrestors | Yes | Inlet temperature | 64.7 °C | Outlet temperature | 23.4 °C |
| | Nominal diameter | 10 in | Wall thickness | 13.2 mm | Corrosion allowance | 3 mm | Cladding thickness | 0 mm |
| | Coating | Yes | Weight coating | No | Cathodic protection | Yes | Insulation material | None |
| | Insulation U value | - | | | | | | |

| PLETs | PLET required | Valve | Soil conditions | Pressure rating | Trawler protection | Jumper type |
|---|---|---|---|---|---|---|
| Well end | Yes | Yes | Average | 345 barg | No | Rigid |
| Tie-back | Yes | Yes | Average | 345 barg | No | Rigid |

| | | | | | | | | |
|---|---|---|---|---|---|---|---|---|
| Test service flowline | Number of lines | 1 | Material | Carbon steel X60 | Oil flow per line | 8.8 Mbbl/day | Water flow per line | 0.978 Mbbl/day |
| | Gas flow per line | 19.6 MMscf/day | Fixed pressure | Outlet pressure | Pressure In | 104 bara | Pressure out | 96.4 bara |
| | Design pressure | 203 bara | Buckle arrestors | Yes | Inlet temperature | 64.7 °C | Outlet temperature | 16.2 °C |
| | Nominal diameter | 8 in | Wall thickness | 11.2 mm | Corrosion allowance | 3 mm | Cladding thickness | 0 mm |
| | Coating | Yes | Weight coating | No | Cathodic protection | Yes | Insulation material | None |
| | Insulation U value | - | | | | | | |

| PLETs | PLET required | Valve | Soil conditions | Pressure rating | Trawler protection | Jumper type |
|---|---|---|---|---|---|---|
| Well end | Yes | Yes | Average | 345 barg | No | Rigid |
| Tie-back | Yes | Yes | Average | 345 barg | No | Rigid |

| Umbilicals | Control and chemical tube material | Primary control tubes | | Secondary control tubes | | Primary chemical tubes | | Secondary chemical tubes | |
|---|---|---|---|---|---|---|---|---|---|
| | | Number of | Size | Number of | Size | Number of | Size | Number of | Size |
| | Duplex | 4 | 19 mm | 0 | 9.52 mm | 4 | 19 mm | 0 | 9.52 mm |

**Subsea 1**

| Name | Subsea 1 |
| --- | --- |

| TOTAL COST | US Dollars | 385,208,000 |
| --- | --- | --- |

| EQUIPMENT | | | Procured from: N. North Sea (Norway) |
| --- | --- | --- | --- |
| | QUANTITY | UNIT RATE | COST |
| 4-well slots ITS | | | 34,374,000 |
| ITS -2 | | | 33,696,000 |
| ITS-3 | | | 32,183,000 |
| Riser base 01 | | | 2,263,000 |
| Platform controls - main | 1 | 471,000 | 471,000 |
| Platform controls - additional | 12 | 68,700 | 824,000 |
| Sub Total | | | 103,811,000 |
| Freight | 3.00% | | 3,114,000 |
| Total Equipment | | $ | **106,925,000** |

| MATERIALS | | | Procured from: N. North Sea (Norway) |
| --- | --- | --- | --- |
| | QUANTITY | UNIT RATE | COST |
| Cable | | | 66,800,000 |
| Cable 2 | | | 25,359,000 |
| Cable 3 | | | 14,480,000 |
| Riser 01 | | | 8,661,000 |
| Riser systems ( arch/buoy ) | 1 | 410,087 | 410,000 |
| Sub Total | | | 115,710,000 |
| Freight | 2.00% | | 2,314,000 |
| Total Materials | | $ | **118,024,000** |

| INSTALLATION | | | Location: N. North Sea (Norway) |
| --- | --- | --- | --- |
| | QUANTITY | UNIT RATE | COST |
| Pipelay spread ( S-lay without DP ) | 117 day | 293,916 | 34,388,000 |
| Diving support vessel tie ins | 63 day | 249,725 | 15,733,000 |
| Diving support vessel test & commissioning | 14 day | 249,725 | 3,496,000 |
| Testing & commissioning equipment | 26 day | 19,097 | 497,000 |
| Semi-submersible crane vessel | 0 day | 355,001 | 0 |
| Semi-submersible drilling vessel | 0 day | 141,021 | 0 |
| Trench vessel | 0 day | 147,019 | 0 |
| Survey vessel | 25 day | 99,155 | 2,479,000 |
| Dredge vessel | 0 day | 226,466 | 0 |
| Rock install vessel | 0 day | 97,931 | 0 |
| Supply vessel | 38 day | 41,743 | 1,586,000 |
| Total Installation | | $ | **58,179,000** |

| DESIGN & PROJECT MANAGEMENT | | | N. North Sea (Norway) |
| --- | --- | --- | --- |
| | QUANTITY | UNIT RATE | COST |
| Design | 79,000 mhr | 176 | 13,904,000 |
| Project management | 26,900 mhr | 323 | 8,689,000 |
| Total Design & Project management | | $ | **22,593,000** |

| INSURANCE & CERTIFICATION | | | N. North Sea (Norway) |
| --- | --- | --- | --- |
| | QUANTITY | UNIT RATE | COST |
| Certification | 1.00% | | 3,057,000 |
| Insurance | 4.00% | | 12,229,000 |
| Total Insurance & Certification | | $ | **15,286,000** |

| CONTINGENCY | | | N. North Sea (Norway) |
| --- | --- | --- | --- |
| | QUANTITY | UNIT RATE | COST |

| | | | |
|---|---|---|---|
| Contingency | 20.00% | | 64,201,000 |
| Total Contingency | | $ | **64,201,000** |

## 4-well slots ITS

| TOTAL COST | US Dollars | 34,374,000 |
|---|---|---|

| MAIN STRUCTURE | | | |
|---|---|---|---|
| | QUANTITY | UNIT RATE | COST |
| Structure | 260 te | 17,897 | 4,653,000 |
| Guide base | 4 | 360,911 | 1,444,000 |
| Protection structure | 0 te | 15,393 | 0 |
| Piles | 55 te | 4,807 | 264,000 |
| Total Main structure | | $ | **6,361,000** |

| XMAS TREES | | | |
|---|---|---|---|
| | QUANTITY | UNIT RATE | COST |
| Production | 4 | 3,478,800 | 13,915,000 |
| Water injection | 0 | 3,261,100 | 0 |
| Gas injection | 0 | 3,261,100 | 0 |
| Total Xmas trees | | $ | **13,915,000** |

| MANIFOLDING (PIPING & VALVES) | | | |
|---|---|---|---|
| | QUANTITY | UNIT RATE | COST |
| Production | 18 te | 91,653 | 1,650,000 |
| Test | 8 te | 91,653 | 733,000 |
| Total Manifolding (piping & valves) | | $ | **2,383,000** |

| MULTIPHASE METERING | | | |
|---|---|---|---|
| | QUANTITY | UNIT RATE | COST |
| Multiphase meters (0-8 Mbbl/day) | 0 | 758,967 | 0 |
| Multiphase meters (8-30 Mbbl/day) | 0 | 1,065,002 | 0 |
| Multiphase meters (30-75 Mbbl/day) | 0 | 1,517,934 | 0 |
| Total Multiphase metering | | $ | **0** |

| CONNECTORS / HUBS | | | |
|---|---|---|---|
| | QUANTITY | UNIT RATE | COST |
| 8 in connectors | 2 | 287,673 | 575,000 |
| 16 in connectors | 1 | 465,173 | 465,000 |
| 20 in connectors | 1 | 465,173 | 465,000 |
| Umbilical connectors | 2 | 119,966 | 240,000 |
| Hydraulic connectors | 2 | 42,845 | 86,000 |
| Electrical connectors | 4 | 21,178 | 85,000 |
| Total Connectors / hubs | | $ | **1,916,000** |

| FLYING LEADS | | | |
|---|---|---|---|
| | QUANTITY | UNIT RATE | COST |
| Hydraulic (x 1) | 50 m | 2,399 | 120,000 |
| Electrical (x 2) | 100 m | 66 | 7,000 |
| Total Flying leads | | $ | **127,000** |

| CONTROL AND TESTING | | | |
|---|---|---|---|
| | QUANTITY | UNIT RATE | COST |
| Subsea distribution unit | 1 | 3,427,592 | 3,428,000 |
| Subsea controls | 4 | 1,481,209 | 5,925,000 |
| System testing | 4 | 79,820 | 319,000 |
| Total Control and testing | | $ | **9,672,000** |

ITS -2

| TOTAL COST | US Dollars | 33,696,000 |
|---|---|---|

| MAIN STRUCTURE | | | |
|---|---|---|---|
| | QUANTITY | UNIT RATE | COST |
| Structure | 260 te | 17,897 | 4,653,000 |
| Guide base | 4 | 360,911 | 1,444,000 |
| Protection structure | 0 te | 15,393 | 0 |
| Piles | 55 te | 4,807 | 264,000 |
| Total Main structure | | $ | **6,361,000** |

| XMAS TREES | | | |
|---|---|---|---|
| | QUANTITY | UNIT RATE | COST |
| Production | 4 | 3,478,800 | 13,915,000 |
| Water injection | 0 | 3,261,100 | 0 |
| Gas injection | 0 | 3,261,100 | 0 |
| Total Xmas trees | | $ | **13,915,000** |

| MANIFOLDING (PIPING & VALVES) | | | |
|---|---|---|---|
| | QUANTITY | UNIT RATE | COST |
| Production | 14 te | 91,653 | 1,283,000 |
| Test | 6 te | 91,653 | 550,000 |
| Total Manifolding (piping & valves) | | $ | **1,833,000** |

| MULTIPHASE METERING | | | |
|---|---|---|---|
| | QUANTITY | UNIT RATE | COST |
| Multiphase meters (0-8 Mbbl/day) | 0 | 758,967 | 0 |
| Multiphase meters (8-30 Mbbl/day) | 0 | 1,065,002 | 0 |
| Multiphase meters (30-75 Mbbl/day) | 0 | 1,517,934 | 0 |
| Total Multiphase metering | | $ | **0** |

| CONNECTORS / HUBS | | | |
|---|---|---|---|
| | QUANTITY | UNIT RATE | COST |
| 8 in connectors | 2 | 287,673 | 575,000 |
| 10 in connectors | 1 | 336,639 | 337,000 |
| 16 in connectors | 1 | 465,173 | 465,000 |
| Umbilical connectors | 2 | 119,966 | 240,000 |
| Hydraulic connectors | 2 | 42,845 | 86,000 |
| Electrical connectors | 4 | 21,178 | 85,000 |
| Total Connectors / hubs | | $ | **1,788,000** |

| FLYING LEADS | | | |
|---|---|---|---|
| | QUANTITY | UNIT RATE | COST |
| Hydraulic (x 1) | 50 m | 2,399 | 120,000 |
| Electrical (x 2) | 100 m | 66 | 7,000 |
| Total Flying leads | | $ | **127,000** |

| CONTROL AND TESTING | | | |
|---|---|---|---|
| | QUANTITY | UNIT RATE | COST |
| Subsea distribution unit | 1 | 3,427,592 | 3,428,000 |
| Subsea controls | 4 | 1,481,209 | 5,925,000 |
| System testing | 4 | 79,820 | 319,000 |
| Total Control and testing | | $ | **9,672,000** |

## ITS-3

| TOTAL COST | US Dollars | 32,183,000 |
|---|---|---|

| MAIN STRUCTURE | | | |
|---|---|---|---|
| | QUANTITY | UNIT RATE | COST |
| Structure | 260 te | 17,897 | 4,653,000 |
| Guide base | 4 | 360,911 | 1,444,000 |
| Protection structure | 0 te | 15,393 | 0 |
| Piles | 55 te | 4,807 | 264,000 |
| Total Main structure | | $ | **6,361,000** |

| XMAS TREES | | | |
|---|---|---|---|
| | QUANTITY | UNIT RATE | COST |
| Production | 4 | 3,478,800 | 13,915,000 |
| Water injection | 0 | 3,261,100 | 0 |
| Gas injection | 0 | 3,261,100 | 0 |
| Total Xmas trees | | $ | **13,915,000** |

| MANIFOLDING (PIPING & VALVES) | | | |
|---|---|---|---|
| | QUANTITY | UNIT RATE | COST |
| Production | 9 te | 91,653 | 825,000 |
| Test | 4 te | 91,653 | 367,000 |
| Total Manifolding (piping & valves) | | $ | **1,192,000** |

| MULTIPHASE METERING | | | |
|---|---|---|---|
| | QUANTITY | UNIT RATE | COST |
| Multiphase meters (0-8 Mbbl/day) | 0 | 758,967 | 0 |
| Multiphase meters (8-30 Mbbl/day) | 0 | 1,065,002 | 0 |
| Multiphase meters (30-75 Mbbl/day) | 0 | 1,517,934 | 0 |
| Total Multiphase metering | | $ | **0** |

| CONNECTORS / HUBS | | | |
|---|---|---|---|
| | QUANTITY | UNIT RATE | COST |
| 8 in connectors | 1 | 287,673 | 288,000 |
| 10 in connectors | 1 | 336,639 | 337,000 |
| Umbilical connectors | 1 | 119,966 | 120,000 |
| Hydraulic connectors | 2 | 42,845 | 86,000 |
| Electrical connectors | 4 | 21,178 | 85,000 |
| Total Connectors / hubs | | $ | **916,000** |

| FLYING LEADS | | | |
|---|---|---|---|
| | QUANTITY | UNIT RATE | COST |
| Hydraulic (x 1) | 50 m | 2,399 | 120,000 |
| Electrical (x 2) | 100 m | 66 | 7,000 |
| Total Flying leads | | $ | **127,000** |

| CONTROL AND TESTING | | | |
|---|---|---|---|
| | QUANTITY | UNIT RATE | COST |
| Subsea distribution unit | 1 | 3,427,592 | 3,428,000 |
| Subsea controls | 4 | 1,481,209 | 5,925,000 |
| System testing | 4 | 79,820 | 319,000 |
| Total Control and testing | | $ | **9,672,000** |

## Cable

| TOTAL COST | US Dollars | 66,800,000 |
|---|---|---|

| PRODUCTION FLOWLINE | | | |
|---|---|---|---|
| | QUANTITY | UNIT RATE | COST |
| Linepipe - 1 x (D = 20 in, t = 22 mm, Carbon steel X60) | 40.00 km | 356,800 | 14,272,000 |
| Coating | 40.00 km | 47,700 | 1,908,000 |
| Anodes | 63.80 te | 8,600 | 549,000 |
| Subsea crossings | 0 | 563,100 | 0 |
| PLETs | 2 | | 4,294,000 |
| Total Production flowline | | $ | **21,023,000** |

| TEST SERVICE FLOWLINE | | | |
|---|---|---|---|
| | QUANTITY | UNIT RATE | COST |
| Linepipe - 1 x (D = 8 in, t = 11.2 mm, Carbon steel X60) | 40.00 km | 100,700 | 4,028,000 |
| Coating | 40.00 km | 23,700 | 948,000 |
| Anodes | 27.50 te | 8,600 | 237,000 |
| Subsea crossings | 0 | 563,100 | 0 |
| PLETs | 2 | | 1,760,000 |
| Total Test service flowline | | $ | **6,973,000** |

| UMBILICALS | | | |
|---|---|---|---|
| | QUANTITY | UNIT RATE | COST |
| **Control tubes** | | | |
| 6 x D = 25.4 mm | 240.00 km | 61,210 | 14,690,000 |
| **Chemical tubes** | | | |
| 6 x D = 25.4 mm | 240.00 km | 61,210 | 14,690,000 |
| **Electrical signal cable** | | | |
| 4 x XSA = 2.5 mm² | 160.00 km | 7,720 | 1,235,000 |
| **Power cable** | | | |
| 2 x XSA = 25 mm² | 80.00 km | 88,140 | 7,051,000 |
| UTA | 1 | 1,138,450 | 1,138,000 |
| Total Umbilicals | | $ | **38,804,000** |

## G.2 One ITS and riser base.

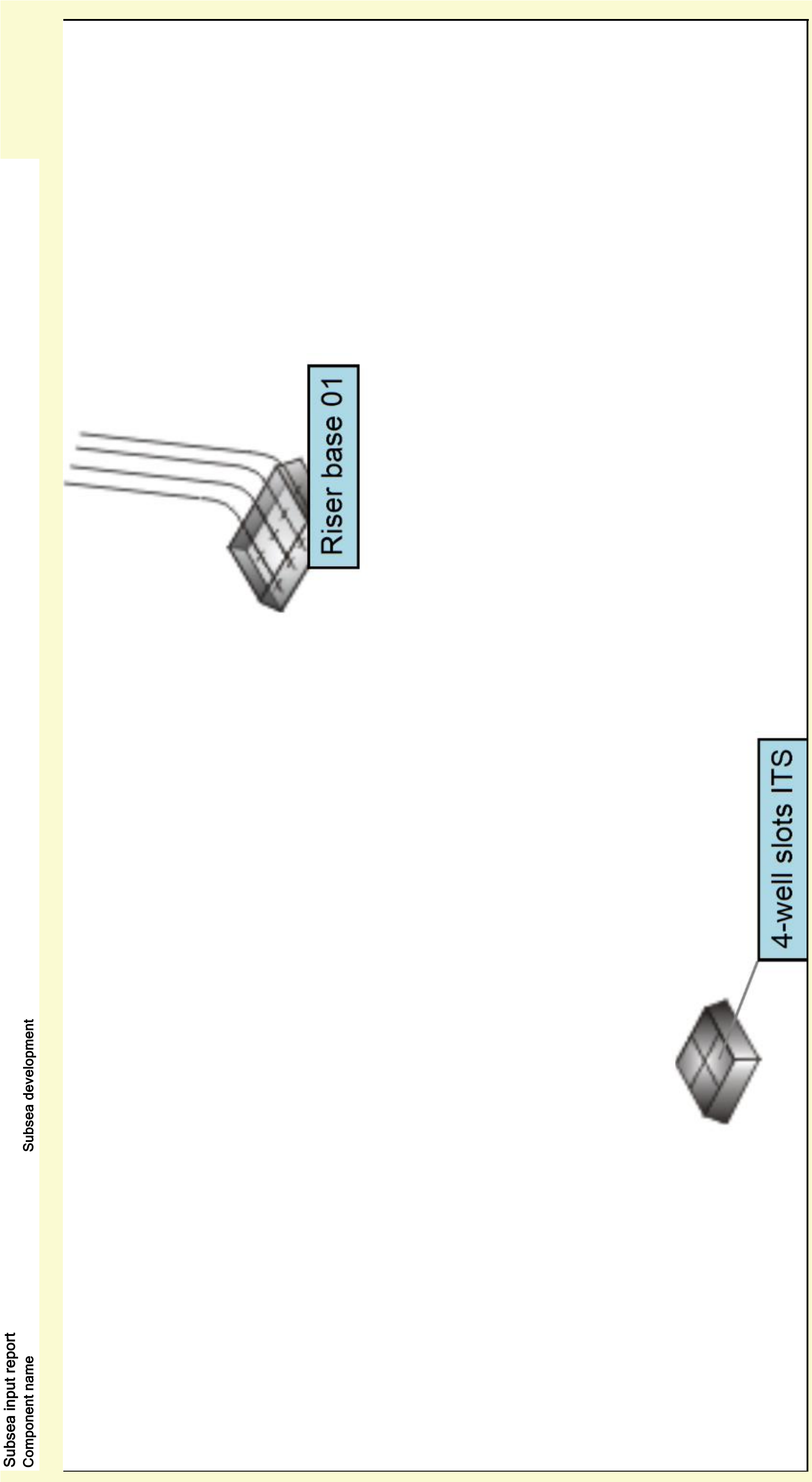


| | Well count | Flow | Type |
|---|---|---|---|
| Production | 0 | 52.8 Mbbl/day | |
| Water injection | 0 | 64.5 Mbbl/day | |
| Gas injection | 0 | 118 MMscf/day | |
| Spare slots | 0 | | - |

| | Present | Flow rate |
|---|---|---|
| Multiphase metering | No | |
| Test | Yes | |
| Gas lift | No | - |
| Chemical injection | No | |

| | |
|---|---|
| Schematic edited | Yes |

| | | | |
|---|---|---|---|
| Layout | | | |
| Development type | Cluster manifold | Maximum wells per item | 4 |
| Infield flowline length | 1.63 km | Tie-back | No |
| Tie-back length | - | | |

| | | | |
|---|---|---|---|
| Features | | | |
| Water depth | 350 m | Wellhead shut in pressure | 203 bara |
| Pressure rating | 345 barg | Wellhead temperature | 64.7 °C |
| Soil conditions | Average | Acid gas | No |
| HIPPS | No | HIPPS minimum flowline length | - |
| Through pigging | No | Retrievable subsea | No |
| Trawler protection | No | Intervention tools | No |
| Diverless system | Yes | | |

| | | | |
|---|---|---|---|
| Tie-in point | | | |
| Production delivery pressure | 35 bara | Water injection pressure | 136 bara |
| Gas injection pressure | 220 bara | Test service delivery pressure | 35 bara |
| Gas lift pressure | 205 bara | Production / test service design pressure | 37.5 barg |
| Production temperature | 10 °C | | |

| | |
|---|---|
| Flowlines | |
| Lay vessel | Reel-lay |
| Flowline type | Steel |
| Buried lines | No |

| | |
|---|---|
| Umbilicals | |
| Control system | Electro-hydraulic |
| Tube material | Duplex |
| Inhibitor chemicals | Yes |
| Power cable | No |

| Flowline fluid | Production | Water Injection | Gas injection | Test service | Gas lift | Chemical injection |
|---|---|---|---|---|---|---|
| Flowline material | Carbon steel X60 | Carbon steel X60 | Carbon steel X60 | Carbon steel X60 | Carbon steel X60 | Carbon steel X60 |
| Insulation material | None | None | None | None | None | None |
| Insulation U value | - | - | - | - | - | - |
| PLET selected | Yes | Yes | Yes | Yes | Yes | Yes |

| | |
|---|---|
| Distance to supply base | 120 km |
| Weather downtime (small vessels) | 15 % |
| Weather downtime (large vessels) | 10 % |

| Vessel durations (days) | Pipelay spread | DSV | SSCV | SSDV | Trench vessel | Survey vessel | Dredge vessel | Rock install vessel | Supply vessel |
|---|---|---|---|---|---|---|---|---|---|
| Template | 0.0 | 6.2 | 0.0 | 0.0 | 0.0 | 0.0 | 0.0 | 0.0 | 0.0 |
| Satellite | 0.0 | 0.0 | 0.0 | 0.0 | 0.0 | 0.0 | 0.0 | 0.0 | 0.0 |
| Cluster | 0.0 | 0.0 | 0.0 | 0.0 | 0.0 | 0.0 | 0.0 | 0.0 | 0.0 |
| Manifold | 0.0 | 2.3 | 0.0 | 0.0 | 0.0 | 0.0 | 0.0 | 0.0 | 0.0 |
| Equipment | 0.0 | 0.0 | 0.0 | 0.0 | 0.0 | 0.0 | 0.0 | 0.0 | 0.0 |
| Risers | 0.0 | 0.0 | 0.0 | 0.0 | 0.0 | 0.0 | 0.0 | 0.0 | 0.0 |
| Flowline links | 0.0 | 0.0 | 0.0 | 0.0 | 0.0 | 0.0 | 0.0 | 0.0 | 0.0 |
| PLETs | 0.0 | 0.0 | 0.0 | 0.0 | 0.0 | 0.0 | 0.0 | 0.0 | 0.0 |
| Umbilical links | 0.0 | 0.0 | 0.0 | 0.0 | 0.0 | 0.0 | 0.0 | 0.0 | 0.0 |
| Trenching | 0.0 | 0.0 | 0.0 | 0.0 | 0.0 | 0.0 | 0.0 | 0.0 | 0.0 |
| Surveying | 0.0 | 0.0 | 0.0 | 0.0 | 0.0 | 0.0 | 0.0 | 0.0 | 0.0 |
| Dredging | 0.0 | 0.0 | 0.0 | 0.0 | 0.0 | 0.0 | 0.0 | 0.0 | 0.0 |
| Rock installation | 0.0 | 0.0 | 0.0 | 0.0 | 0.0 | 0.0 | 0.0 | 0.0 | 0.0 |
| Transit loadout | 0.0 | 2.5 | 0.0 | 0.0 | 0.0 | 0.0 | 0.0 | 0.0 | 1.7 |

| | | | | | | | | | |
|---|---|---|---|---|---|---|---|---|---|
| Weather downtime | 0.0 | 1.7 | 0.0 | 0.0 | 0.0 | 0.0 | 0.0 | 0.0 | 0.3 |
| Mob/demob | 0.0 | 8.0 | 0.0 | 0.0 | 0.0 | 0.0 | 0.0 | 0.0 | 8.0 |
| Total | 0.0 | 20.7 | 0.0 | 0.0 | 0.0 | 0.0 | 0.0 | 0.0 | 10.0 |

| Subsea components | Type | Water depth | Production wells | Production flow per well | Water injection wells | Water injection flow per | Gas injection wells | Gas injection flow per well | Test service |
|---|---|---|---|---|---|---|---|---|---|
| 4-well slots ITS | Template manifold | 350 m | 4 | 0 Mbbl/day | 0 | 0 Mbbl/day | 0 | 0 MMscf/day | Yes |

| Subsea components | Gas lift | Chemical injection | HIPPS | MFM on test service | MFM on production | MFM on wellheads | Spare slots | Spare slots type | Total slots count |
|---|---|---|---|---|---|---|---|---|---|
| 4-well slots ITS | No | No | No | No | No | No | 0 | - | 4 |

| Subsea components | SDU selected | SDU wells serviced | SDU hydraulic flying | SDU electrical flying leads | UTA wells serviced | UTA hydraulic flying leads | UTA electrical flying leads |
|---|---|---|---|---|---|---|---|
| 4-well slots ITS | Yes | 4 | 0 | 0 | 4 | 1 | 2 |

| Riser base manifold | Water depth | Termination type | Sub-type | Riser systems | Riser length |
|---|---|---|---|---|---|
| Riser base 01 | 350 m | Riser | Flexible lazy S | 0 | 0 m |

## Subsea development

| Name | Subsea development |
|---|---|

| TOTAL COST | US Dollars | 59,875,000 |
|---|---|---|

| EQUIPMENT | | | Procured from: N. North Sea (Norway) |
|---|---|---|---|
| | QUANTITY | UNIT RATE | COST |
| 4-well slots ITS | | | 29,423,000 |
| Riser base 01 | | | 213,000 |
| Platform controls - main | 1 | 471,000 | 471,000 |
| Platform controls - additional | 0 | 68,700 | 0 |
| Sub Total | | | 30,107,000 |
| Freight | 3.00% | | 903,000 |
| Total Equipment | | $ | **31,010,000** |

| INSTALLATION | | | Location: N. North Sea (Norway) |
|---|---|---|---|
| | QUANTITY | UNIT RATE | COST |
| Pipelay spread ( reel-lay ) | 0 day | 195,862 | 0 |
| Diving support vessel tie ins | 21 day | 249,725 | 5,244,000 |
| Diving support vessel test & commissioning | 0 day | 249,725 | 0 |
| Testing & commissioning equipment | 0 day | 19,097 | 0 |
| Semi-submersible crane vessel | 0 day | 355,001 | 0 |
| Semi-submersible drilling vessel | 0 day | 141,021 | 0 |
| Trench vessel | 0 day | 147,019 | 0 |
| Survey vessel | 0 day | 99,155 | 0 |
| Dredge vessel | 0 day | 226,466 | 0 |
| Rock install vessel | 0 day | 97,931 | 0 |
| Supply vessel | 10 day | 41,743 | 417,000 |
| Total Installation | | $ | **5,661,000** |

| DESIGN & PROJECT MANAGEMENT | | | N. North Sea (Norway) |
|---|---|---|---|
| | QUANTITY | UNIT RATE | COST |
| Design | 37,600 mhr | 176 | 6,618,000 |
| Project management | 13,100 mhr | 323 | 4,231,000 |
| Total Design & Project management | | $ | **10,849,000** |

| INSURANCE & CERTIFICATION | | | N. North Sea (Norway) |
|---|---|---|---|
| | QUANTITY | UNIT RATE | COST |
| Certification | 1.00% | | 475,000 |
| Insurance | 4.00% | | 1,901,000 |
| Total Insurance & Certification | | $ | **2,376,000** |

| CONTINGENCY | | | N. North Sea (Norway) |
|---|---|---|---|
| | QUANTITY | UNIT RATE | COST |
| Contingency | 20.00% | | 9,979,000 |
| Total Contingency | | $ | **9,979,000** |

## 4-well slots ITS

| | | |
|---|---|---|
| TOTAL COST | US Dollars | 29,423,000 |

| MAIN STRUCTURE | | | |
|---|---|---|---|
| | QUANTITY | UNIT RATE | COST |
| Structure | 260 te | 17,897 | 4,653,000 |
| Guide base | 4 | 360,911 | 1,444,000 |
| Protection structure | 0 te | 15,393 | 0 |
| Piles | 55 te | 4,807 | 264,000 |
| Total Main structure | | $ | **6,361,000** |

| XMAS TREES | | | |
|---|---|---|---|
| | QUANTITY | UNIT RATE | COST |
| Production | 4 | 3,135,600 | 12,542,000 |
| Water injection | 0 | 3,261,100 | 0 |
| Gas injection | 0 | 3,261,100 | 0 |
| Total Xmas trees | | $ | **12,542,000** |

| MANIFOLDING (PIPING & VALVES) | | | |
|---|---|---|---|
| | QUANTITY | UNIT RATE | COST |
| Production | 4 te | 91,653 | 367,000 |
| Test | 2 te | 91,653 | 183,000 |
| Total Manifolding (piping & valves) | | $ | **550,000** |

| MULTIPHASE METERING | | | |
|---|---|---|---|
| | QUANTITY | UNIT RATE | COST |
| Multiphase meters (0-8 Mbbl/day) | 0 | 758,967 | 0 |
| Multiphase meters (8-30 Mbbl/day) | 0 | 1,065,002 | 0 |
| Multiphase meters (30-75 Mbbl/day) | 0 | 1,517,934 | 0 |
| Total Multiphase metering | | $ | **0** |

| CONNECTORS / HUBS | | | |
|---|---|---|---|
| | QUANTITY | UNIT RATE | COST |
| Umbilical connectors | 0 | 119,966 | 0 |
| Hydraulic connectors | 2 | 42,845 | 86,000 |
| Electrical connectors | 4 | 21,178 | 85,000 |
| Total Connectors / hubs | | $ | **171,000** |

| FLYING LEADS | | | |
|---|---|---|---|
| | QUANTITY | UNIT RATE | COST |
| Hydraulic (x 1) | 50 m | 2,399 | 120,000 |
| Electrical (x 2) | 100 m | 66 | 7,000 |
| Total Flying leads | | $ | **127,000** |

| CONTROL AND TESTING | | | |
|---|---|---|---|
| | QUANTITY | UNIT RATE | COST |
| Subsea distribution unit | 1 | 3,427,592 | 3,428,000 |
| Subsea controls | 4 | 1,481,209 | 5,925,000 |
| System testing | 4 | 79,820 | 319,000 |
| Total Control and testing | | $ | **9,672,000** |

## G.3 Two integrated template structures and riser base.

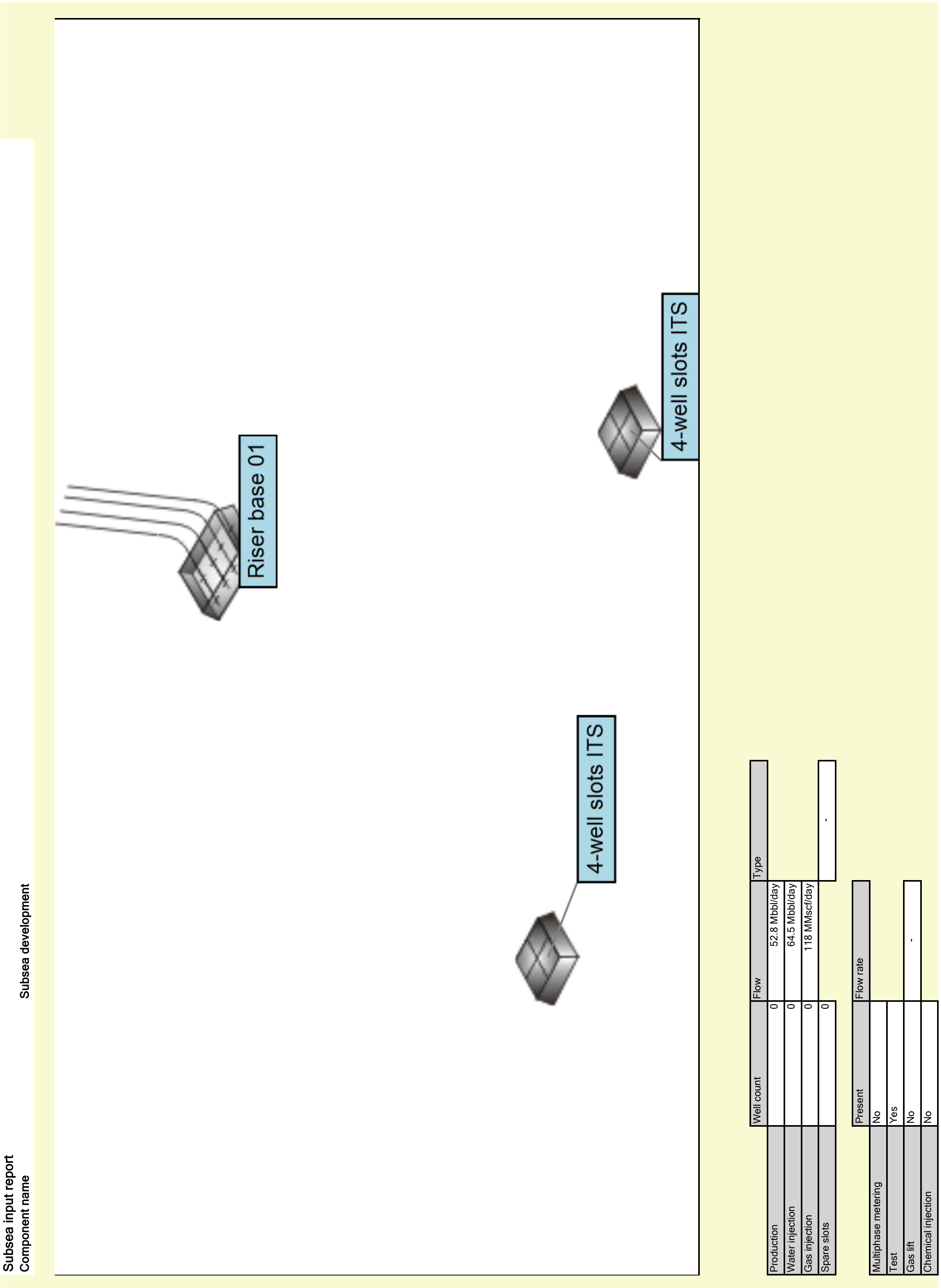

| | |
|---|---|
| Schematic edited | Yes |

| Layout | | | |
|---|---|---|---|
| Development type | Cluster manifold | Maximum wells per item | 4 |
| Infield flowline length | 1.63 km | Tie-back | No |
| Tie-back length | - | | |

| Features | | | |
|---|---|---|---|
| Water depth | 350 m | Wellhead shut in pressure | 203 bara |
| Pressure rating | 345 barg | Wellhead temperature | 64.7 °C |
| Soil conditions | Average | Acid gas | No |
| HIPPS | No | HIPPS minimum flowline length | - |
| Through pigging | No | Retrievable subsea | No |
| Trawler protection | No | Intervention tools | No |
| Diverless system | Yes | | |

| Tie-in point | | | |
|---|---|---|---|
| Production delivery pressure | 35 bara | Water injection pressure | 136 bara |
| Gas injection pressure | 220 bara | Test service delivery pressure | 35 bara |
| Gas lift pressure | 205 bara | Production / test service design pressure | 37.5 barg |
| Production temperature | 10 °C | | |

| Flowlines | |
|---|---|
| Lay vessel | Reel-lay |
| Flowline type | Steel |
| Buried lines | No |

| Umbilicals | |
|---|---|
| Control system | Electro-hydraulic |
| Tube material | Duplex |
| Inhibitor chemicals | Yes |
| Power cable | No |

| Flowline fluid | Production | Water Injection | Gas injection | Test service | Gas lift | Chemical injection |
|---|---|---|---|---|---|---|
| Flowline material | Carbon steel X60 | Carbon steel X60 | Carbon steel X60 | Carbon steel X60 | Carbon steel X60 | Carbon steel X60 |
| Insulation material | None | None | None | None | None | None |
| Insulation U value | - | - | - | - | - | - |
| PLET selected | Yes | Yes | Yes | Yes | Yes | Yes |

| | |
|---|---|
| Distance to supply base | 120 km |
| Weather downtime (small vessels) | 15 % |
| Weather downtime (large vessels) | 10 % |

| Vessel durations (days) | Pipelay spread | DSV | SSCV | SSDV | Trench vessel | Survey vessel | Dredge vessel | Rock install vessel | Supply vessel |
|---|---|---|---|---|---|---|---|---|---|
| Template | 0.0 | 12.3 | 0.0 | 0.0 | 0.0 | 0.0 | 0.0 | 0.0 | 0.0 |
| Satellite | 0.0 | 0.0 | 0.0 | 0.0 | 0.0 | 0.0 | 0.0 | 0.0 | 0.0 |
| Cluster | 0.0 | 0.0 | 0.0 | 0.0 | 0.0 | 0.0 | 0.0 | 0.0 | 0.0 |
| Manifold | 0.0 | 2.3 | 0.0 | 0.0 | 0.0 | 0.0 | 0.0 | 0.0 | 0.0 |
| Equipment | 0.0 | 0.0 | 0.0 | 0.0 | 0.0 | 0.0 | 0.0 | 0.0 | 0.0 |
| Risers | 0.0 | 0.0 | 0.0 | 0.0 | 0.0 | 0.0 | 0.0 | 0.0 | 0.0 |
| Flowline links | 0.0 | 0.0 | 0.0 | 0.0 | 0.0 | 0.0 | 0.0 | 0.0 | 0.0 |
| PLETs | 0.0 | 0.0 | 0.0 | 0.0 | 0.0 | 0.0 | 0.0 | 0.0 | 0.0 |
| Umbilical links | 0.0 | 0.0 | 0.0 | 0.0 | 0.0 | 0.0 | 0.0 | 0.0 | 0.0 |
| Trenching | 0.0 | 0.0 | 0.0 | 0.0 | 0.0 | 0.0 | 0.0 | 0.0 | 0.0 |
| Surveying | 0.0 | 0.0 | 0.0 | 0.0 | 0.0 | 0.0 | 0.0 | 0.0 | 0.0 |
| Dredging | 0.0 | 0.0 | 0.0 | 0.0 | 0.0 | 0.0 | 0.0 | 0.0 | 0.0 |
| Rock installation | 0.0 | 0.0 | 0.0 | 0.0 | 0.0 | 0.0 | 0.0 | 0.0 | 0.0 |
| Transit loadout | 0.0 | 3.1 | 0.0 | 0.0 | 0.0 | 0.0 | 0.0 | 0.0 | 3.3 |

| | | | | | | | | | |
|---|---|---|---|---|---|---|---|---|---|
| Weather downtime | 0.0 | 2.7 | 0.0 | 0.0 | 0.0 | 0.0 | 0.0 | 0.0 | 0.5 |
| Mob/demob | 0.0 | 8.0 | 0.0 | 0.0 | 0.0 | 0.0 | 0.0 | 0.0 | 8.0 |
| Total | 0.0 | 28.4 | 0.0 | 0.0 | 0.0 | 0.0 | 0.0 | 0.0 | 11.8 |

| Subsea components | Type | Water depth | Production wells | Production flow per well | Water injection wells | Water injection flow per | Gas injection wells | Gas injection flow per well | Test service |
|---|---|---|---|---|---|---|---|---|---|
| 4-well slots ITS | Template manifold | 350 m | 4 | 0 Mbbl/day | 0 | 0 Mbbl/day | 0 | 0 MMscf/day | Yes |
| 4-well slots ITS | Template manifold | 350 m | 4 | 0 Mbbl/day | 0 | 0 Mbbl/day | 0 | 0 MMscf/day | Yes |

| Subsea components | Gas lift | Chemical injection | HIPPS | MFM on test service | MFM on production | MFM on wellheads | Spare slots | Spare slots type | Total slots count |
|---|---|---|---|---|---|---|---|---|---|
| 4-well slots ITS | No | No | No | No | No | No | 0 | - | 4 |
| 4-well slots ITS | No | No | No | No | No | No | 0 | - | 4 |

| Subsea components | SDU selected | SDU wells serviced | SDU hydraulic flying | SDU electrical flying leads | UTA wells serviced | UTA hydraulic flying leads | UTA electrical flying leads |
|---|---|---|---|---|---|---|---|
| 4-well slots ITS | Yes | 4 | 0 | 0 | 4 | 1 | 2 |
| 4-well slots ITS | Yes | 4 | 0 | 0 | 4 | 1 | 2 |

| Riser base manifold | Water depth | Termination type | Sub-type | Riser systems | Riser length |
|---|---|---|---|---|---|
| Riser base 01 | 350 m | Riser | Flexible lazy S | 0 | 0 m |

**Subsea development**

| Name | Subsea development |
|---|---|

| TOTAL COST | US Dollars | 104,542,000 |
|---|---|---|

| EQUIPMENT | | | Procured from: N. North Sea (Norway) |
|---|---|---|---|
| | QUANTITY | UNIT RATE | COST |
| 4-well slots ITS | | | 29,423,000 |
| 4-well slots ITS | | | 29,423,000 |
| Riser base 01 | | | 213,000 |
| Platform controls - main | 1 | 471,000 | 471,000 |
| Platform controls - additional | 0 | 68,700 | 0 |
| Sub Total | | | 59,530,000 |
| Freight | 3.00% | | 1,786,000 |
| Total Equipment | | $ | **61,316,000** |

| INSTALLATION | | | Location: N. North Sea (Norway) |
|---|---|---|---|
| | QUANTITY | UNIT RATE | COST |
| Pipelay spread ( reel-lay ) | 0 day | 195,862 | 0 |
| Diving support vessel tie ins | 29 day | 249,725 | 7,242,000 |
| Diving support vessel test & commissioning | 0 day | 249,725 | 0 |
| Testing & commissioning equipment | 0 day | 19,097 | 0 |
| Semi-submersible crane vessel | 0 day | 355,001 | 0 |
| Semi-submersible drilling vessel | 0 day | 141,021 | 0 |
| Trench vessel | 0 day | 147,019 | 0 |
| Survey vessel | 0 day | 99,155 | 0 |
| Dredge vessel | 0 day | 226,466 | 0 |
| Rock install vessel | 0 day | 97,931 | 0 |
| Supply vessel | 12 day | 41,743 | 501,000 |
| Total Installation | | $ | **7,743,000** |

| DESIGN & PROJECT MANAGEMENT | | | N. North Sea (Norway) |
|---|---|---|---|
| | QUANTITY | UNIT RATE | COST |
| Design | 49,300 mhr | 176 | 8,677,000 |
| Project management | 16,200 mhr | 323 | 5,233,000 |
| Total Design & Project management | | $ | **13,910,000** |

| INSURANCE & CERTIFICATION | | | N. North Sea (Norway) |
|---|---|---|---|
| | QUANTITY | UNIT RATE | COST |
| Certification | 1.00% | | 830,000 |
| Insurance | 4.00% | | 3,319,000 |
| Total Insurance & Certification | | $ | **4,149,000** |

| CONTINGENCY | | | N. North Sea (Norway) |
|---|---|---|---|
| | QUANTITY | UNIT RATE | COST |
| Contingency | 20.00% | | 17,424,000 |
| Total Contingency | | $ | **17,424,000** |

## 4-well slots ITS

| TOTAL COST | US Dollars | 29,423,000 |
|---|---|---|

| MAIN STRUCTURE | | | |
|---|---|---|---|
| | QUANTITY | UNIT RATE | COST |
| Structure | 260 te | 17,897 | 4,653,000 |
| Guide base | 4 | 360,911 | 1,444,000 |
| Protection structure | 0 te | 15,393 | 0 |
| Piles | 55 te | 4,807 | 264,000 |
| Total Main structure | | $ | **6,361,000** |

| XMAS TREES | | | |
|---|---|---|---|
| | QUANTITY | UNIT RATE | COST |
| Production | 4 | 3,135,600 | 12,542,000 |
| Water injection | 0 | 3,261,100 | 0 |
| Gas injection | 0 | 3,261,100 | 0 |
| Total Xmas trees | | $ | **12,542,000** |

| MANIFOLDING (PIPING & VALVES) | | | |
|---|---|---|---|
| | QUANTITY | UNIT RATE | COST |
| Production | 4 te | 91,653 | 367,000 |
| Test | 2 te | 91,653 | 183,000 |
| Total Manifolding (piping & valves) | | $ | **550,000** |

| MULTIPHASE METERING | | | |
|---|---|---|---|
| | QUANTITY | UNIT RATE | COST |
| Multiphase meters (0-8 Mbbl/day) | 0 | 758,967 | 0 |
| Multiphase meters (8-30 Mbbl/day) | 0 | 1,065,002 | 0 |
| Multiphase meters (30-75 Mbbl/day) | 0 | 1,517,934 | 0 |
| Total Multiphase metering | | $ | **0** |

| CONNECTORS / HUBS | | | |
|---|---|---|---|
| | QUANTITY | UNIT RATE | COST |
| Umbilical connectors | 0 | 119,966 | 0 |
| Hydraulic connectors | 2 | 42,845 | 86,000 |
| Electrical connectors | 4 | 21,178 | 85,000 |
| Total Connectors / hubs | | $ | **171,000** |

| FLYING LEADS | | | |
|---|---|---|---|
| | QUANTITY | UNIT RATE | COST |
| Hydraulic (x 1) | 50 m | 2,399 | 120,000 |
| Electrical (x 2) | 100 m | 66 | 7,000 |
| Total Flying leads | | $ | **127,000** |

| CONTROL AND TESTING | | | |
|---|---|---|---|
| | QUANTITY | UNIT RATE | COST |
| Subsea distribution unit | 1 | 3,427,592 | 3,428,000 |
| Subsea controls | 4 | 1,481,209 | 5,925,000 |
| System testing | 4 | 79,820 | 319,000 |
| Total Control and testing | | $ | **9,672,000** |

## 4-well slots ITS

| | | |
|---|---|---|
| TOTAL COST | US Dollars | 29,423,000 |

| MAIN STRUCTURE | | | |
|---|---|---|---|
| | QUANTITY | UNIT RATE | COST |
| Structure | 260 te | 17,897 | 4,653,000 |
| Guide base | 4 | 360,911 | 1,444,000 |
| Protection structure | 0 te | 15,393 | 0 |
| Piles | 55 te | 4,807 | 264,000 |
| Total Main structure | | $ | **6,361,000** |

| XMAS TREES | | | |
|---|---|---|---|
| | QUANTITY | UNIT RATE | COST |
| Production | 4 | 3,135,600 | 12,542,000 |
| Water injection | 0 | 3,261,100 | 0 |
| Gas injection | 0 | 3,261,100 | 0 |
| Total Xmas trees | | $ | **12,542,000** |

| MANIFOLDING (PIPING & VALVES) | | | |
|---|---|---|---|
| | QUANTITY | UNIT RATE | COST |
| Production | 4 te | 91,653 | 367,000 |
| Test | 2 te | 91,653 | 183,000 |
| Total Manifolding (piping & valves) | | $ | **550,000** |

| MULTIPHASE METERING | | | |
|---|---|---|---|
| | QUANTITY | UNIT RATE | COST |
| Multiphase meters (0-8 Mbbl/day) | 0 | 758,967 | 0 |
| Multiphase meters (8-30 Mbbl/day) | 0 | 1,065,002 | 0 |
| Multiphase meters (30-75 Mbbl/day) | 0 | 1,517,934 | 0 |
| Total Multiphase metering | | $ | **0** |

| CONNECTORS / HUBS | | | |
|---|---|---|---|
| | QUANTITY | UNIT RATE | COST |
| Umbilical connectors | 0 | 119,966 | 0 |
| Hydraulic connectors | 2 | 42,845 | 86,000 |
| Electrical connectors | 4 | 21,178 | 85,000 |
| Total Connectors / hubs | | $ | **171,000** |

| FLYING LEADS | | | |
|---|---|---|---|
| | QUANTITY | UNIT RATE | COST |
| Hydraulic (x 1) | 50 m | 2,399 | 120,000 |
| Electrical (x 2) | 100 m | 66 | 7,000 |
| Total Flying leads | | $ | **127,000** |

| CONTROL AND TESTING | | | |
|---|---|---|---|
| | QUANTITY | UNIT RATE | COST |
| Subsea distribution unit | 1 | 3,427,592 | 3,428,000 |
| Subsea controls | 4 | 1,481,209 | 5,925,000 |
| System testing | 4 | 79,820 | 319,000 |
| Total Control and testing | | $ | **9,672,000** |

# Appendix H

# Cost Estimates

## H.1 Part list sent to STEP-G

Profiles for extrusion:

**<u>Profille type 1:</u>**
Flange thickness: Tf [mm]
Web thickness: Tw [mm]
Flange width: Wf [mm]
Web height: Hw [mm]
Length: L [mm]

| | Beam # | Tf | Tw | Wf | Hw | L |
|---|---|---|---|---|---|---|
| a | 1 | 50 | 60 | 400 | 310 | 46360 |
| (b-c)+d | 2 | 30 | 35 | 330 | 310 | 56400 |
| f | 3 | 45 | 40 | 440 | 310 | 60800 |
| g | 4 | 40 | 35 | 400 | 210 | 29600 |
| h | 5 | 40 | 40 | 350 | 120 | 54400 |
| i+j | 6 | 40 | 30 | 400 | 310 | 88000 |
| s+t | 7 | 35 | 20 | 420 | 200 | 113600 |

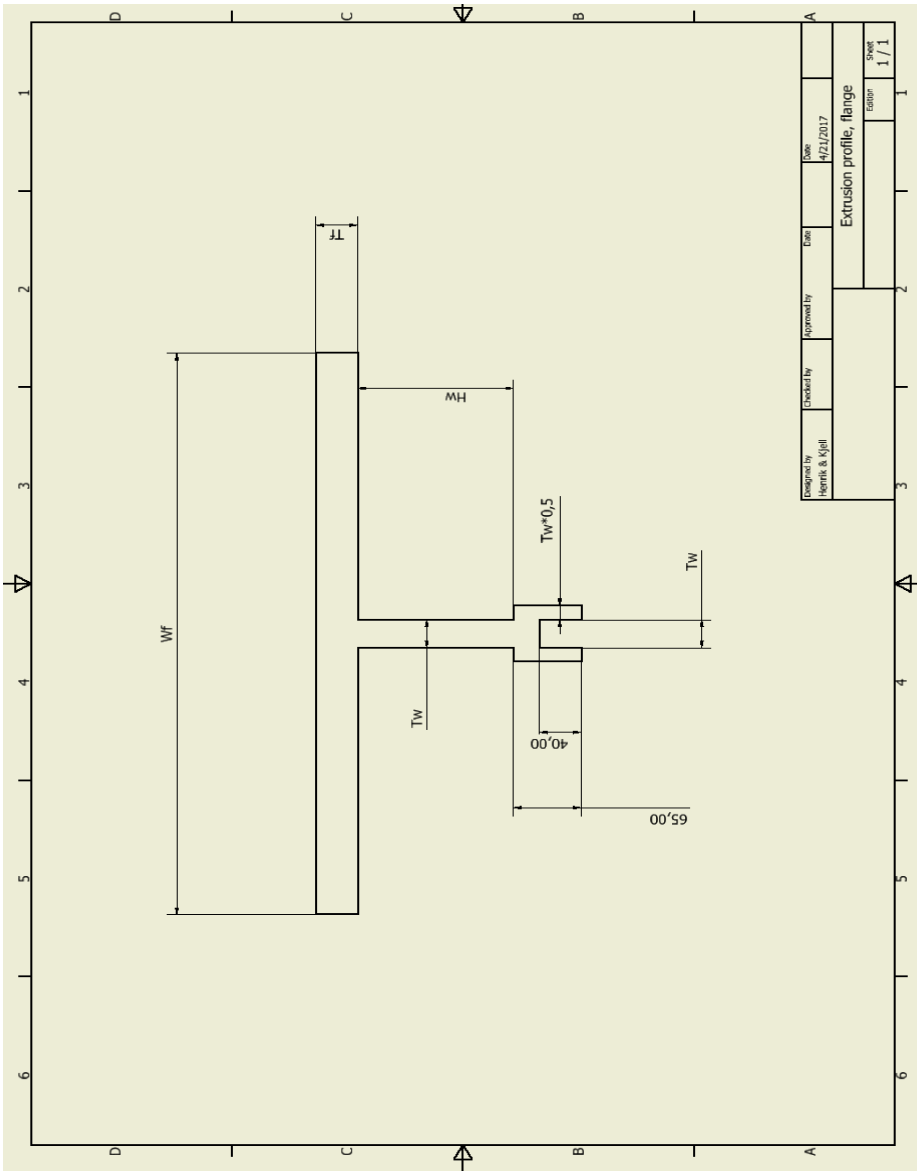

**Profile type 2**

| | Beam # | Tf | Tw | Wf | H | L |
|---|---|---|---|---|---|---|
| e | 8 | 32 | 20 | 300 | 350 | 17600 |
| k | 9 | 15 | 20 | 300 | 400 | 32200 |
| w | 10 | 35 | 20 | 300 | 360 | 21600 |

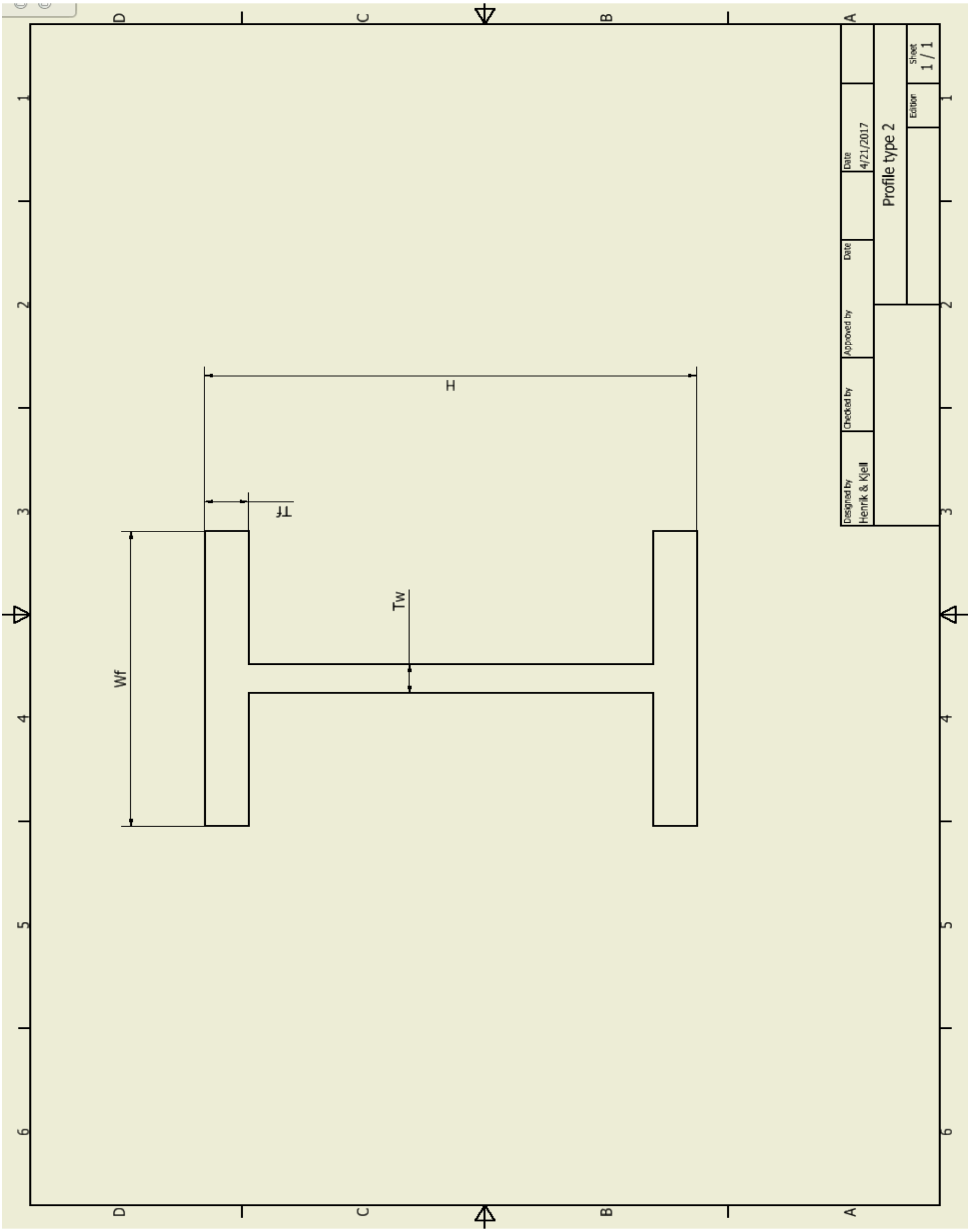

**Profile type 3**

Outer diameter: D [mm]
Thickness: T [mm]
Length: L [mm]

| | Tube # | D | T | L |
|---|---|---|---|---|
| q2 | 1 | 500 | 25 | 12000 |
| y | 2 | 219 | 50 | 107200 |

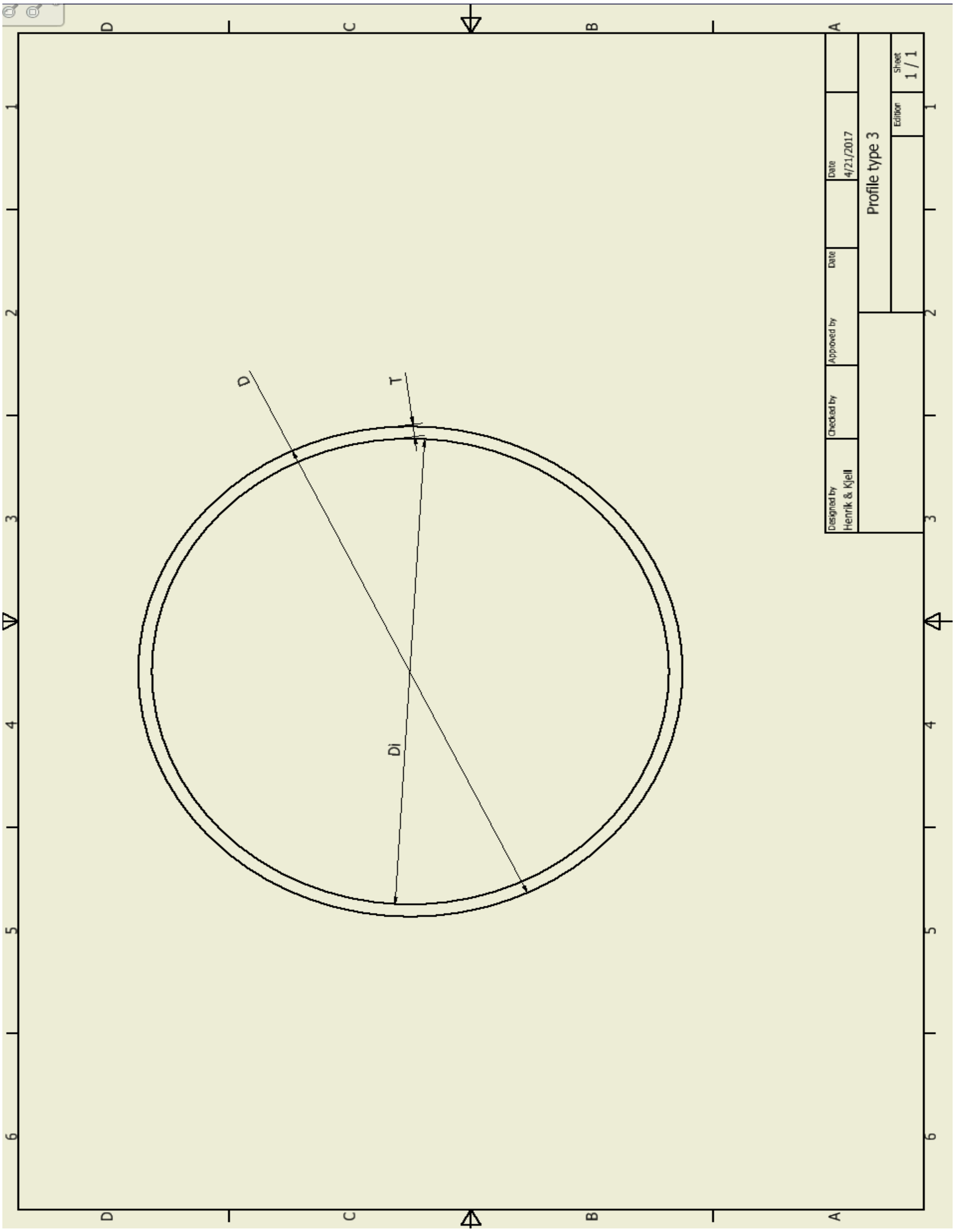

**Profile type 4**

Width: W [mm]
Height: H [mm]
Thickness: T [mm]
Length: L [mm]

| | Tube # | W | H | T | L |
|---|---|---|---|---|---|
| x | 3 | 200 | 200 | 15 | 41600 |

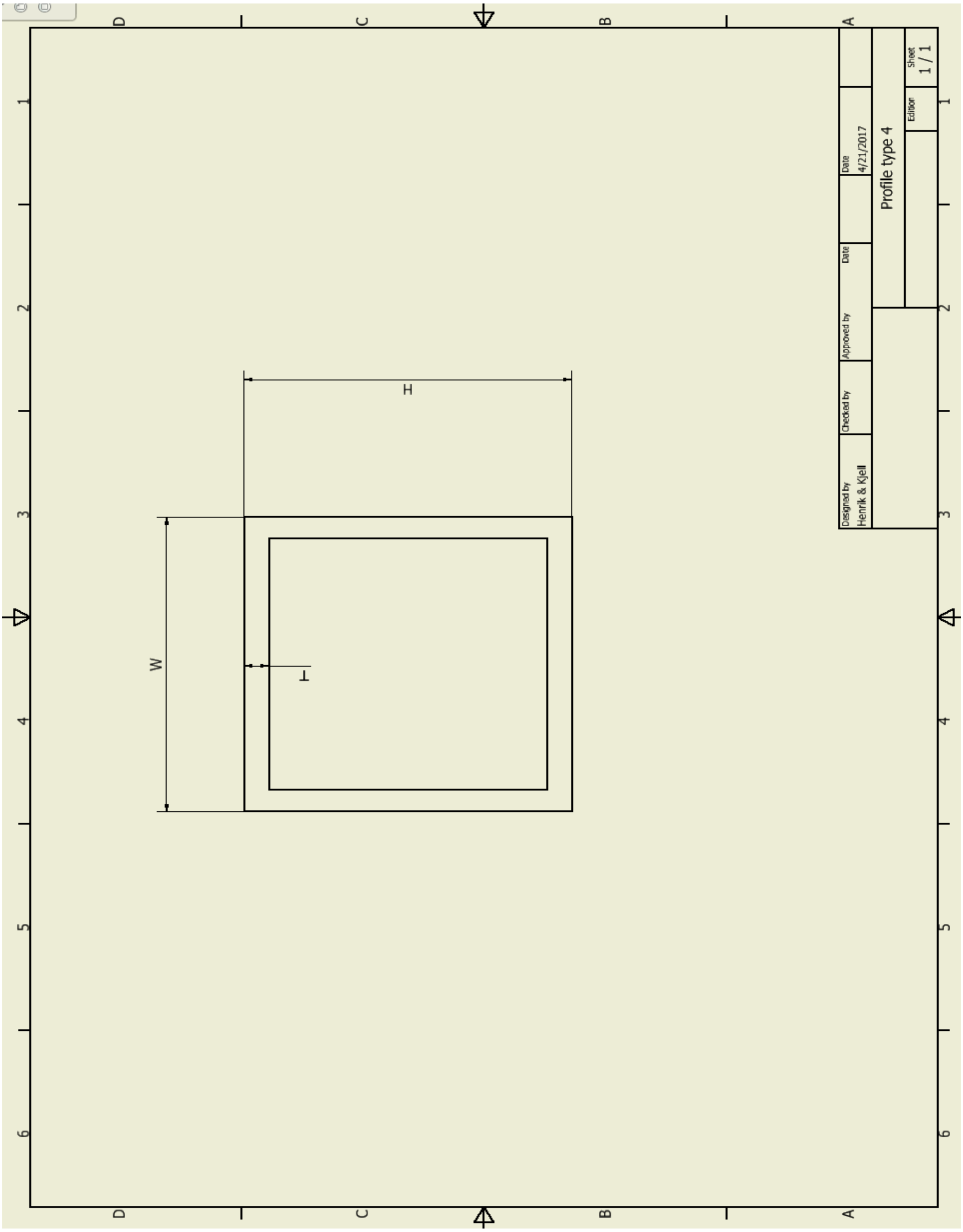

## H.2 Price offer recieved from STEP-G

| | | | | | | | | | | | | | |
|---|---|---|---|---|---|---|---|---|---|---|---|---|---|
| | **Profiles for extrusion (alloy 6082-T6):** | | | | | | | | | | | | |
| | Feasibility check STEP-G | | Total cost = | | 385742 | Euro | | | | **Remarks** | | | |
| | Klaus Funken | | | | 3,645,258 | NOK | With 9,45 NOK/EUR | | | Standard packaging | | | |
| | 5/4/2017 | | | | | Price excludes VAT tax | | | | min lotsizes to be respected | | | |
| | | | | | | | | | | Tolerances acc. EN 755-9 | | | |
| | | | | | | | | | | Alloy 6082 T6 according EN 755-2 & EN 573 | | | |
| | | | | | | | | | | max/min delivery length to be agreed | | | |
| | | | | | | | | | | just indicational offer, as details open | | | |
| | **Profille type 1:** | | | | | | | | | Delivery ex works | | | |
| | Flange thickness: Tf [mm] | | | | | | | | | | | | |
| | Web thickness: Tw [mm] | | | | | | | | | | | | |
| | Flange width: Wf [mm] | | | | | | | | | | | | |
| | Web height: Hw [mm] | | | | | | | | | | | | |
| | Length: L [mm] | | | | | | | | | | | | |
| | Beam # | Tf | Tw | Wf | Hw | L | kg/m | total weight kg | €/kg | die cost | du | comment | |
| a | 1 | 50 | 60 | 400 | 310 | 46360 | 118.8 | 5508 | 4.61 | 13,000 € | 548 | | |
| (b-c)+d | 2 | 30 | 35 | 330 | 310 | 56400 | 64.53 | 3639 | 4.61 | 12,000 € | 500 | | |
| f | 3 | 45 | 40 | 440 | 310 | 60800 | 96.66 | 5877 | 4.61 | 15,000 € | 578 | | |
| g | 4 | 40 | 35 | 400 | 210 | 29600 | 71.55 | 2118 | 4.61 | 12,000 € | 485 | | |
| h | 5 | 40 | 40 | 350 | 120 | 54400 | 60.48 | 3290 | 4.61 | 6,000 € | 396 | | |
| i+j | 6 | 40 | 30 | 400 | 310 | 88000 | 75.6 | 6653 | 4.61 | 13,000 € | 548 | | |
| s+t | 7 | 35 | 20 | 420 | 200 | 113600 | 55.35 | 6288 | 4.61 | 12,000 € | 497 | | |
| | | | | | | | | **33373** | with LME 1,76 and Billet prime 0,48 | **83,000 €** | | | |
| | | | | | | | Profile 1 cost | | 236847 | Euro | | | |

| | | | | | | | | | | | | | |
|---|---|---|---|---|---|---|---|---|---|---|---|---|---|
| Total die cost | 155000 | Euro | | Total extrusion cost | 230742 | Euro | | Die prosentage of cost | 33% | | Extrusion prosentage of cost | | 67% |
| | | | | | | | | | | | | | |
| | **Profile type 2** | | | | | | | | | | | | |
| | Beam # | Tf | Tw | Wf | H | L | kg/m | total weight kg | €/kg | die cost | du | comment | |
| e | 8 | 32 | 20 | 300 | 350 | 17600 | 67.28 | 1184 | 4.61 | 12,000 € | 461 | max 10 m length | |
| k | 9 | 15 | 20 | 300 | 400 | 32200 | 44.28 | 1426 | 4.61 | 12,000 € | 500 | | |
| w | 10 | 35 | 20 | 300 | 360 | 21600 | 72.36 | 1563 | 4.61 | 12,000 € | 469 | max 8 m length | |
| | | | | | | | | **4173** | | **36,000 €** | | | |
| | | | | | | | Profile 2 cost = | | 55237 | Euro | | | |
| | | | | | | | | | | | | | |
| | | | | | | | | | | | | | |
| | **Profile type 3** | | | Outer diameter: D [mm] | | | | | | | | | |
| | | | | Thickness: T [mm] | | | | | | | | | |
| | | | | Length: L [mm] | | | | | | | | | |
| | Tube # | D | T | L | kg/m | total weight kg | €/kg | die cost | comment | | | | |
| q2 | 1 | 500 | 25 | 12000 | 106.0 | 1272 | | | | | | | |
| y | 2 | 219 | 50 | 107200 | 92.9 | 9957 | | | | | | | |
| | | | | | | **11229** | | | | | | | |
| | | | | | | | | | | | | | |
| | | Profile 3 cost = | | 75767 | Euro | | Anta 12,000 i die cost, og 4,61 i euro/kg | | | | | | |
| | | | | | | | | | | | | | |
| | | | | | | | | | | | | | |
| | | | | | | | | | | | | | |
| **Profile type 4** | | | Width: W [mm] | | Length: L [mm] | | Height: H [mm] | | Thickness: T [mm] | | | | |
| | | | | | | | | | | | | | |
| | Tube # | W | H | T | L | kg/m | total weight kg | €/kg | die cost | du | | | |
| x | 3 | 200 | 200 | 15 | 41600 | 32.4 | 1348 | 4.37 | 12,000 € | 283 | | | |
| | | | | | | | | | | | | | |
| | | | | | Profile 4 cost = | 17890 | Euro | | | | | | |
| | | | | | | | | | | | | | |

Profile-1:

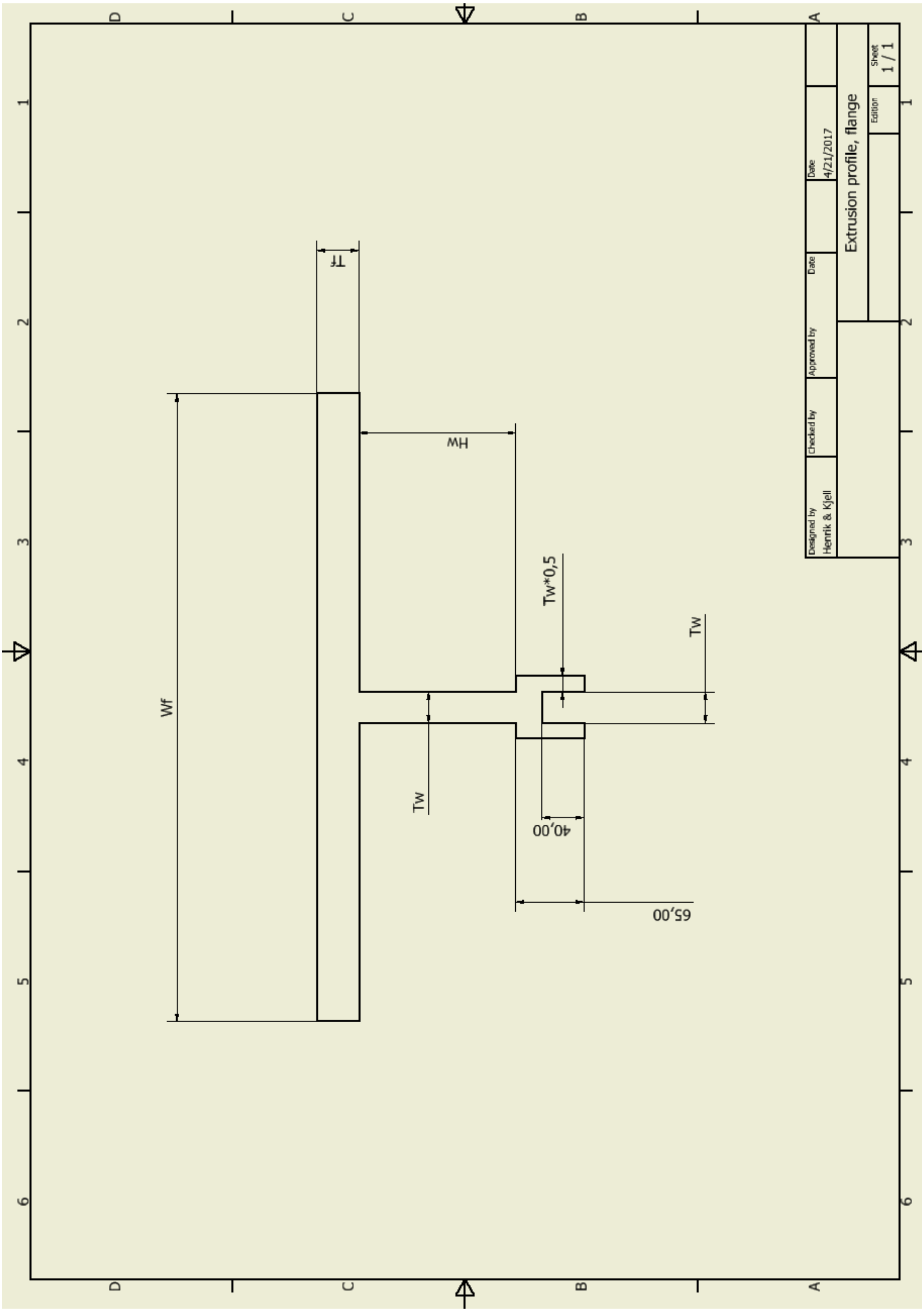
Extrusion profile, flange
Designed by
Henrik & Kjell
Checked by
Approved by
Date
Date
4/21/2017
Edition
Sheet
1 / 1
Tf
Hw
Wf
Tw*0,5
Tw
Tw
40,00
65,00

Profile-2:

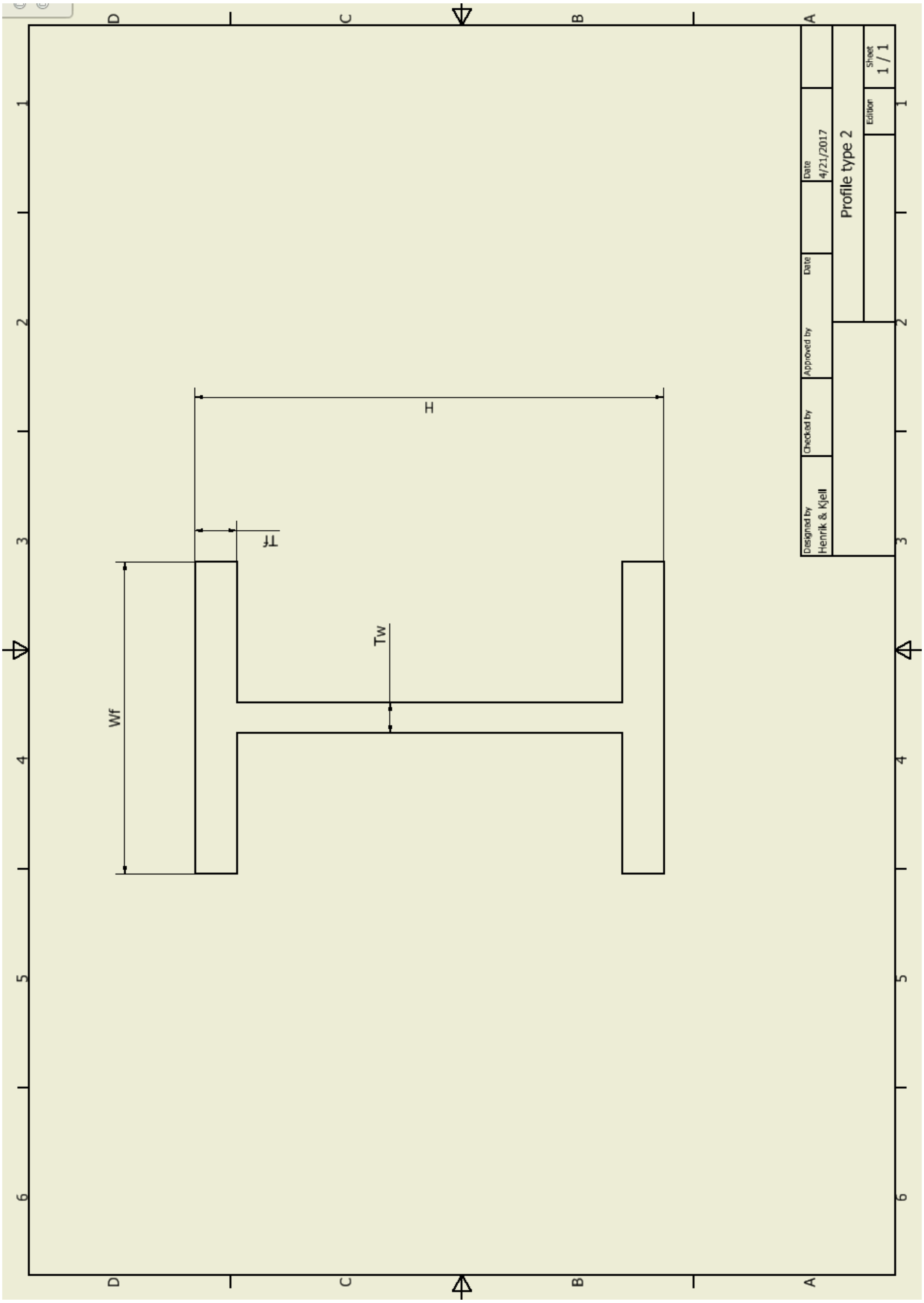

Profile type 2
Designed by
Henrik & Kjell
Checked by
Approved by
Date
Date
4/21/2017
Edition
Sheet
1 / 1
H
Tf
Tw
Wf

Profile-3:

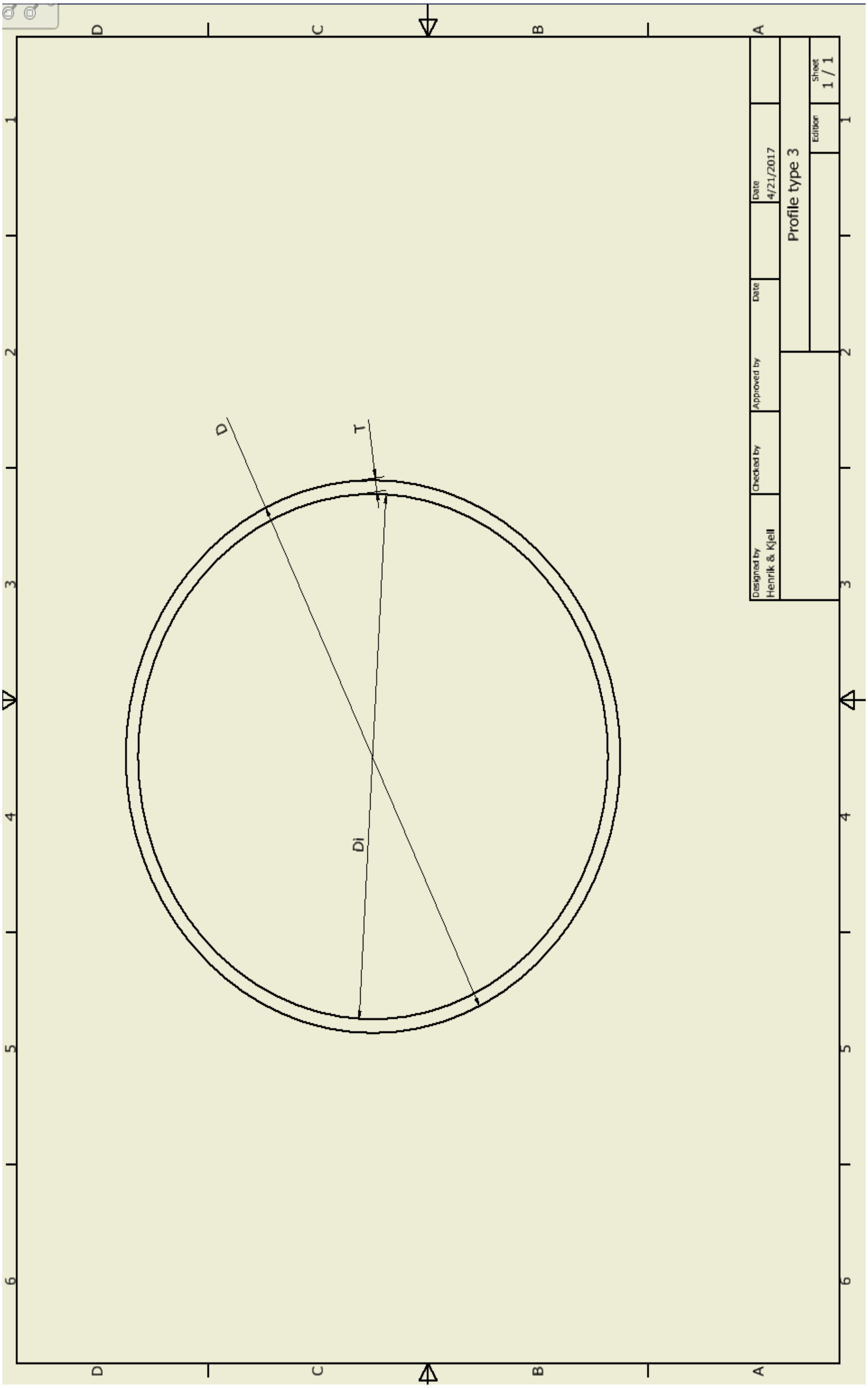
D
T
Di
Designed by
Henrik & Kjell
Checked by
Approved by
Date
Date
4/21/2017
Profile type 3
Edition
1
Sheet
1 / 1

Profile-4:

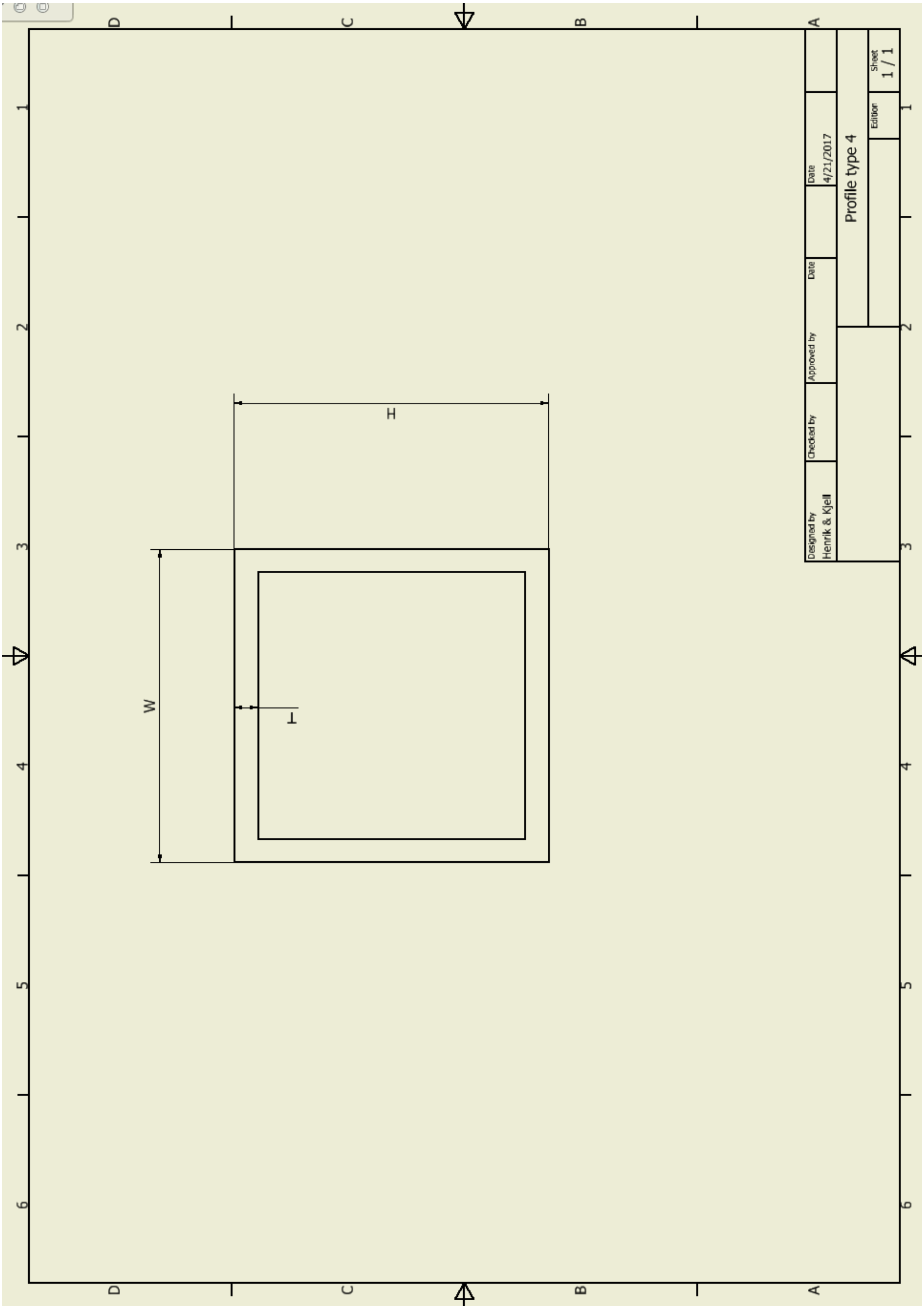
H
W
T
Designed by
Henrik & Kjell
Checked by
Approved by
Date
Date
4/21/2017
Profile type 4
Edition
Sheet
1 / 1

## H.3 Constellium price offer

| Alloy | Temper | Norm | Certificate | Thickness | Width (mm) | Length (mm) | MOQ (nbr of pces) | Full price with DNV certificate included (EUR/T) DAP Trondheim/Norway |
|---|---|---|---|---|---|---|---|---|
| 5083 | H116 | ASTM B928 | DNV | 20 | 2500 max | 7000 | 1 pc | 3850 |
| 5083 | H116 | ASTM B928 | DNV | 25 | 2000 | 11400 | 1 pc | 3650 |
| 5083 | H116 | ASTM B928 | DNV | 25 | 2500 max | 13400 | 1 pc | 3850 |
| 5083 | H116 | ASTM B928 | DNV | 25 | 2500 max | 13400 | 1 pc | 3850 |
| 5083 | H116 | ASTM B928 | DNV | 30 | 800 | 1100 | 20 pcs | 3650 |
| 5083 | H116 | ASTM B928 | DNV | 35 | 500 | 7350 | 6 pcs | 3650 |
| 5083 | H116 | ASTM B928 | DNV | 35 | 850 | 4900 | 4 pcs | 3650 |
| 5083 | H116 | ASTM B928 | DNV | 35 | 850 | 9200 | 2 pcs | 3650 |
| 5083 | H116 | ASTM B928 | DNV | 40 | 680 | 3360 | 6 pcs | 3750 |
| 5083 | H116 | ASTM B928 | DNV | 40 | 790 | 3800 | 6 pcs | 3750 |
| 5083 | H116 | ASTM B928 | DNV | 40 | 2500 max | 10000 max | 1 pc | 3950 |
| 5083 | H116 | ASTM B928 | DNV | 40 | 2500 max | 8300 | 1 pc | 3950 |
| 5083 | H116 | ASTM B928 | DNV | 45 | 2050 | 5100 | 1 pc | 3750 |
| 5083 | H116 | ASTM B928 | DNV | 45 | 2500 | 5100 | 1 pc | 3950 |
| 5083 | H116 | ASTM B928 | DNV | 50 | 1510 | 1510 | 7 pcs | 3750 |
| 5083 | H116 | ASTM B928 | DNV | 60 | 780 | 11600 | 1 pc | 3850 |

5083 Plates

Density 2700 kg/m^3

| | Plate # | Number of plates | H | W | T | MOQ | Full price [EUR/T] | Limit | MOQ | Weight [kg] | Price [EUR] |
|---|---|---|---|---|---|---|---|---|---|---|---|
| a | 1 | 2 | 780 | 11600 | 60 | 1 | 3850 | | Y | 2932 | 11286.4752 |
| bc | 2 | 2 | 850 | 9200 | 35 | 2 | 3650 | | Y | 1478 | 5394.627 |
| d | 3 | 2 | 850 | 4900 | 35 | 4 | 3650 | | N | 787 | 2873.22525 |
| f | 4 | 8 | 790 | 3800 | 40 | 6 | 3750 | | Y | 2594 | 9726.48 |
| g | 5 | 2 | 500 | 7350 | 35 | 6 | 3650 | | N | 695 | 2535.19875 |
| h | 6 | 8 | 680 | 3360 | 40 | 6 | 3750 | | Y | 1974 | 7402.752 |
| i+j | 7 | 4 | 800 | 11000 | 30 | 20 | 3650 | | N | 2851 | 10406.88 |
| l | 8 | 4 | 8300 | 3140 | 40 | 1 | 3950 | W=2500 | Y | 11259 | 44472.1968 |
| m | 9 | 4 | 6820 | 2900 | 25 | 1 | 3850 | W=2500 | Y | 5340 | 20559.231 |
| n | 10 | 2 | 13400 | 2900 | 25 | 1 | 3850 | W=2500 | Y | 5246 | 20197.485 |
| o | 11 | 4 | 2000 | 11400 | 25 | 1 | 3850 | | Y | 6156 | 23700.6 |
| q | 12 | 24 | 2700 | 7000 | 40 | 1 | 3950 | W=2500 | | 48989 | 193505.76 |
| q1 | 13 | 32 | 3000 | 7000 | 20 | 1 | 3850 | W=2500 | Y | 36288 | 139708.8 |
| q3 | 14 | 4 | 3800 | 5100 | 45 | 1 | 3950 | W=2500 | Y | 9419 | 37203.786 |
| q3-2 | 15 | 4 | 1300 | 5100 | 45 | 1 | 3750 | | Y | 3222 | 12083.175 |
| z | 16 | 8 | 1510 | 1510 | 50 | 7 | 3750 | | Y | 2463 | 9234.405 |
| | | | | | | | | | Total | 141691 | 550291 |

| | |
|---|---|
| EUR to NOK | 9.45 |
| Total price [NOK] | 5200251 |

Cost includes DNV certificate and delivery to Trondheim/Norway

Figure H.1: First table with bold letters received from Constellium, cost estimates in the second table are based on numbers in the first table (received from Constellium).

# Appendix I

# FEM Analysis

# I.1 Case-A

## I.1.1 Without convergence

# Stress Analysis Report

AUTODESK

| | |
|---|---|
| Analyzed File: | Assembly.iam |
| Autodesk Inventor Version: | 2017 (Build 210142000, 142) |
| Creation Date: | 4/26/2017, 9:26 AM |
| Study Author: | Henrikwn |
| Summary: | |

---

## ⊟ Project Info (iProperties)

### ⊟ Summary

| | |
|---|---|
| Title | |
| Author | Henrikwn |

### ⊟ Project

| | |
|---|---|
| Part Number | Assembly |
| Designer | Henrikwn |

### ⊟ Physical

| | |
|---|---|
| Mass | 182983 kg |
| Area | 3.56846E+09 mm^2 |
| Volume | 6.09185E+10 mm^3 |
| Center of Gravity | x=-41359.7 mm<br>y=-19499.7 mm<br>z=32758.2 mm |

Note: Physical values could be different from Physical values used by FEA reported below.

---

## ⊟ Case-a

**General objective and settings:**

| | |
|---|---|
| Design Objective | Single Point |
| Study Type | Static Analysis |
| Last Modification Date | 4/26/2017, 9:17 AM |
| Detect and Eliminate Rigid Body Modes | No |
| Separate Stresses Across Contact Surfaces | No |
| Motion Loads Analysis | No |

## ⊟ Operating conditions

## ⊟ Force:1

| | |
|---|---|
| Load Type | Force |
| Magnitude | 1000000.000 N |
| Vector X | 481601.661 N |
| Vector Y | 554956.253 N |
| Vector Z | 678294.477 N |

## ⊟ Selected Face(s)

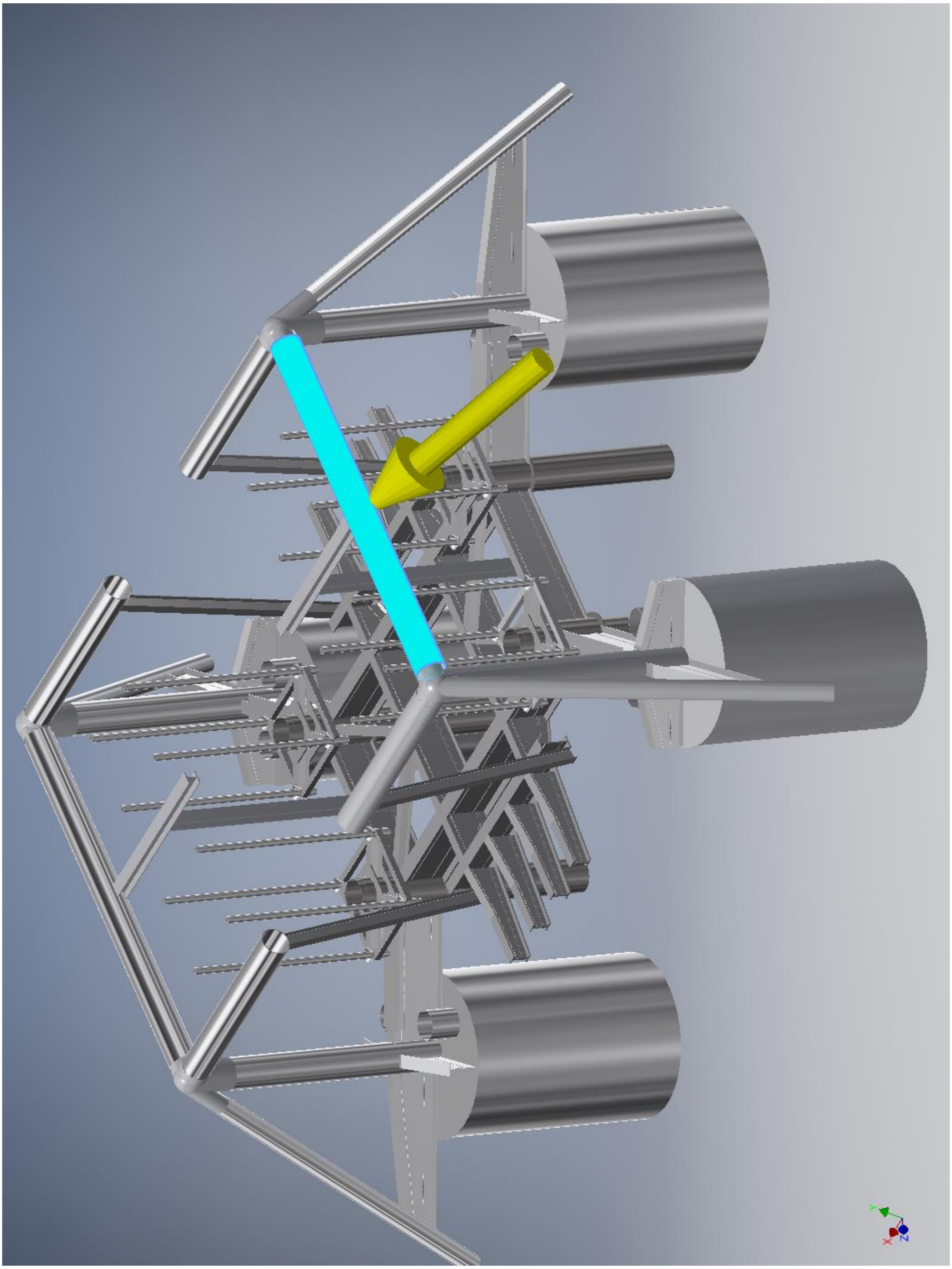

## ⊟ Fixed Constraint:1

| Constraint Type | Fixed Constraint |
|---|---|

### ⊟ Selected Face(s)

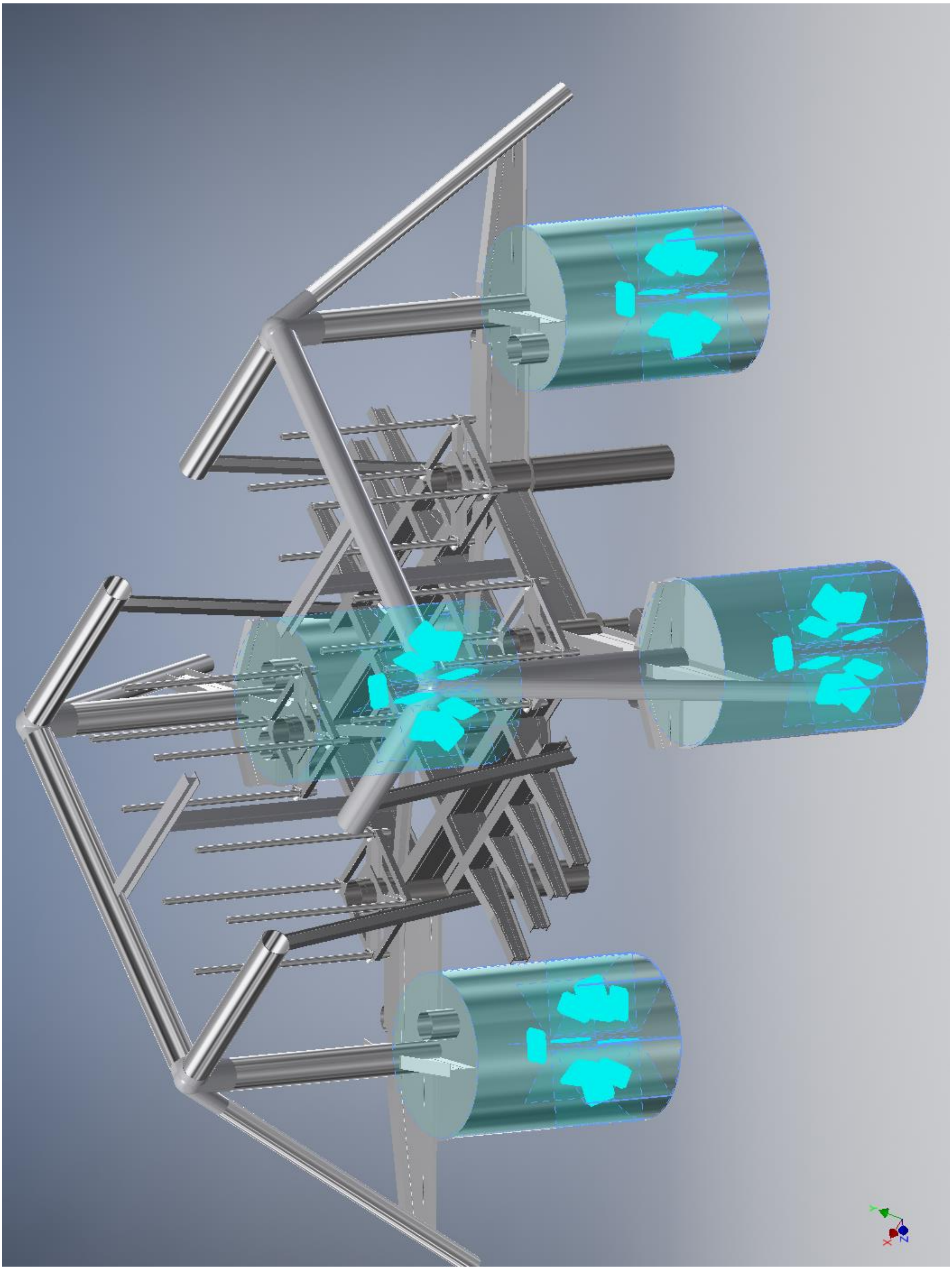

# ⊟ Results

## ⊟ Reaction Force and Moment on Constraints

<table>
<tr><th rowspan="2">Constraint Name</th><th colspan="2">Reaction Force</th><th colspan="2">Reaction Moment</th></tr>
<tr><th>Magnitude</th><th>Component (X,Y,Z)</th><th>Magnitude</th><th>Component (X,Y,Z)</th></tr>
<tr><td rowspan="3">Fixed Constraint:1</td><td rowspan="3">1000000 N</td><td>-481602 N</td><td rowspan="3">15329500 N m</td><td>-10128600 N m</td></tr>
<tr><td>-554956 N</td><td>11318400 N m</td></tr>
<tr><td>-678295 N</td><td>-2072920 N m</td></tr>
</table>

## ⊟ Result Summary

| Name | Minimum | Maximum |
|---|---|---|
| Volume | 6.09185E+10 mm^3 | |
| Mass | 182983 kg | |
| Von Mises Stress | 0 MPa | 189.657 MPa |
| 1st Principal Stress | -112.152 MPa | 299.466 MPa |
| 3rd Principal Stress | -264.441 MPa | 119.904 MPa |
| Displacement | 0 mm | 93.2757 mm |
| Safety Factor | 1.13362 ul | 15 ul |

## ⊟ Figures

## ⊟ Von Mises Stress

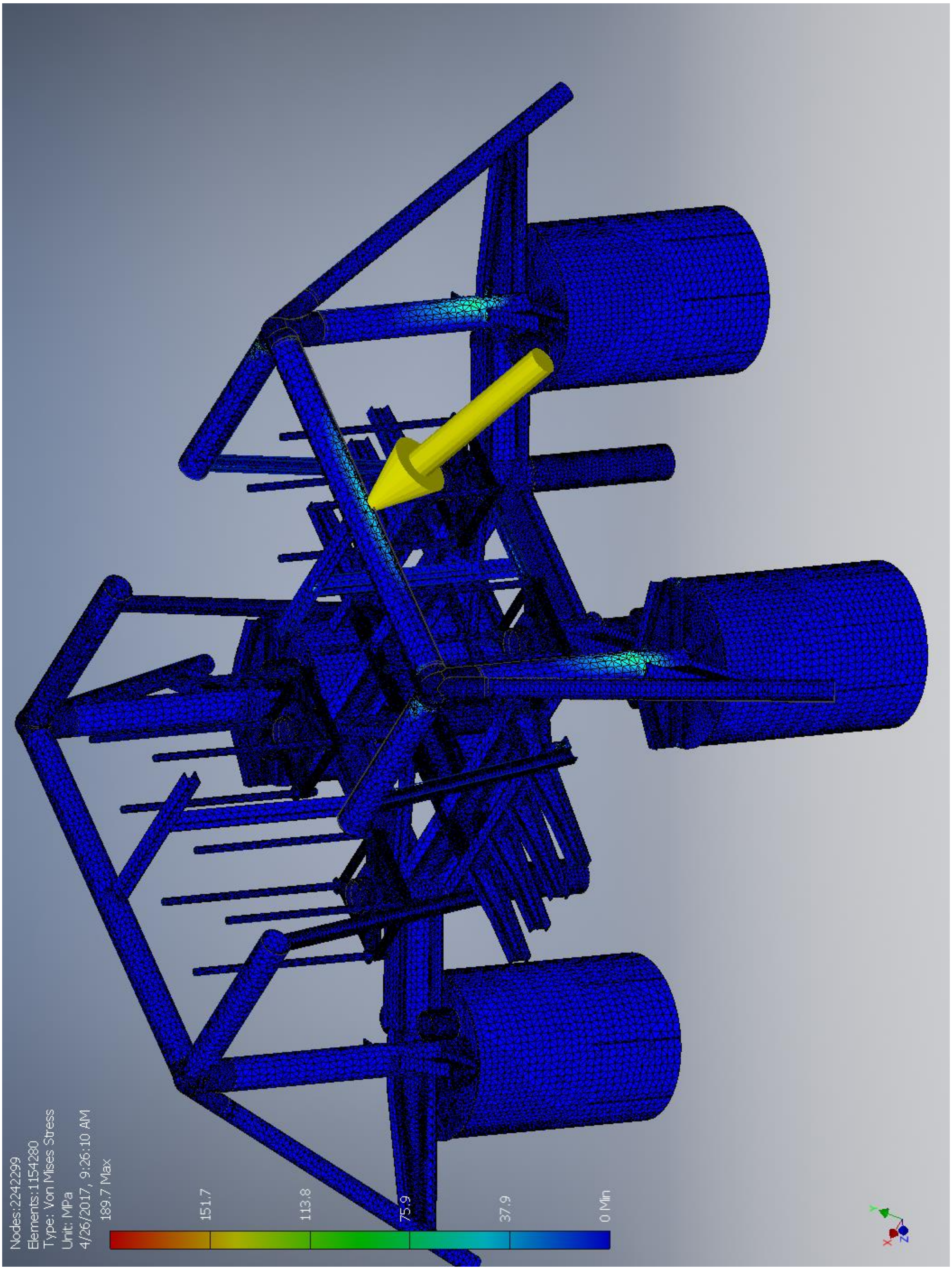

## ⊟ 1st Principal Stress

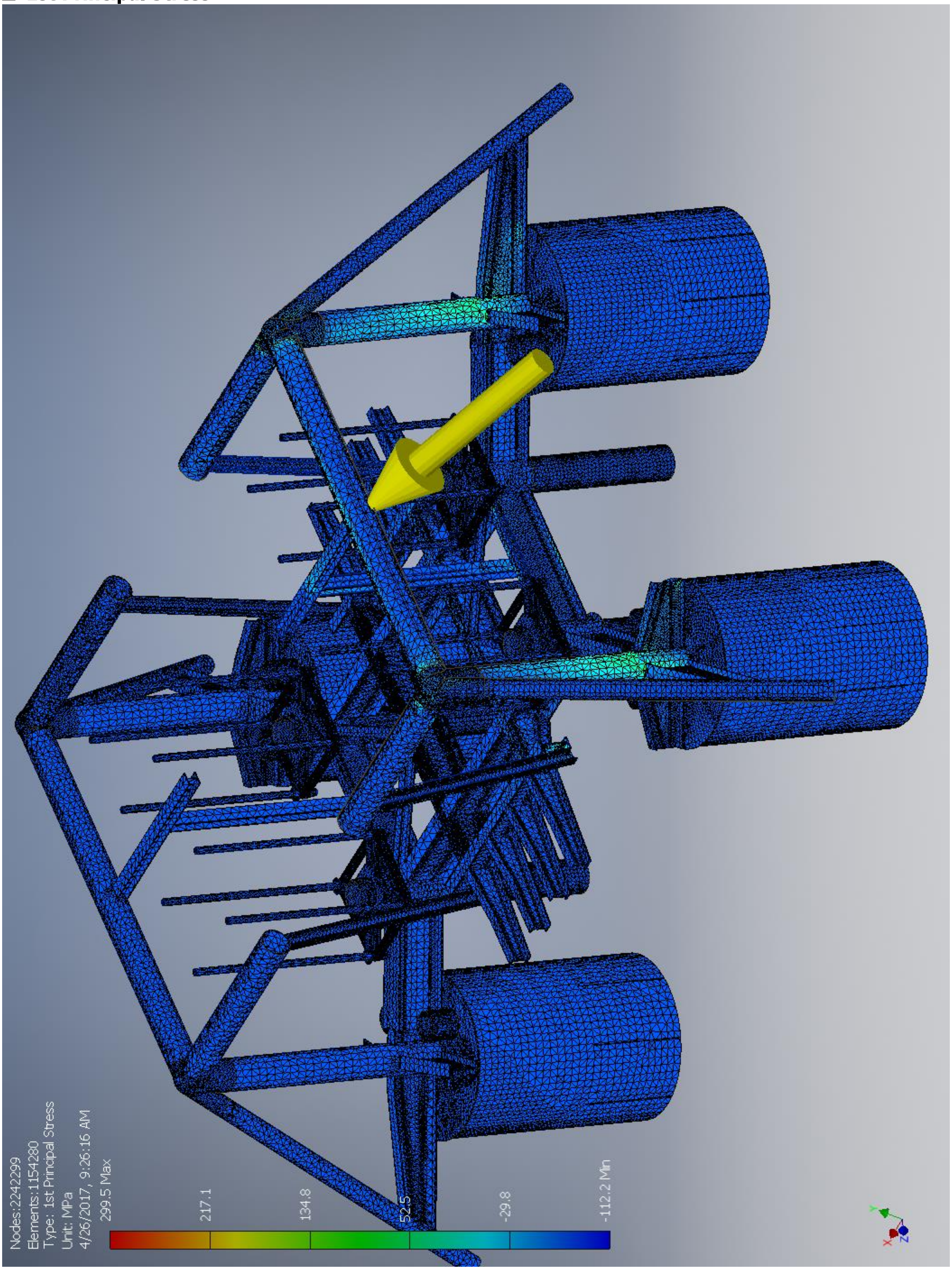

### ⊟ 3rd Principal Stress

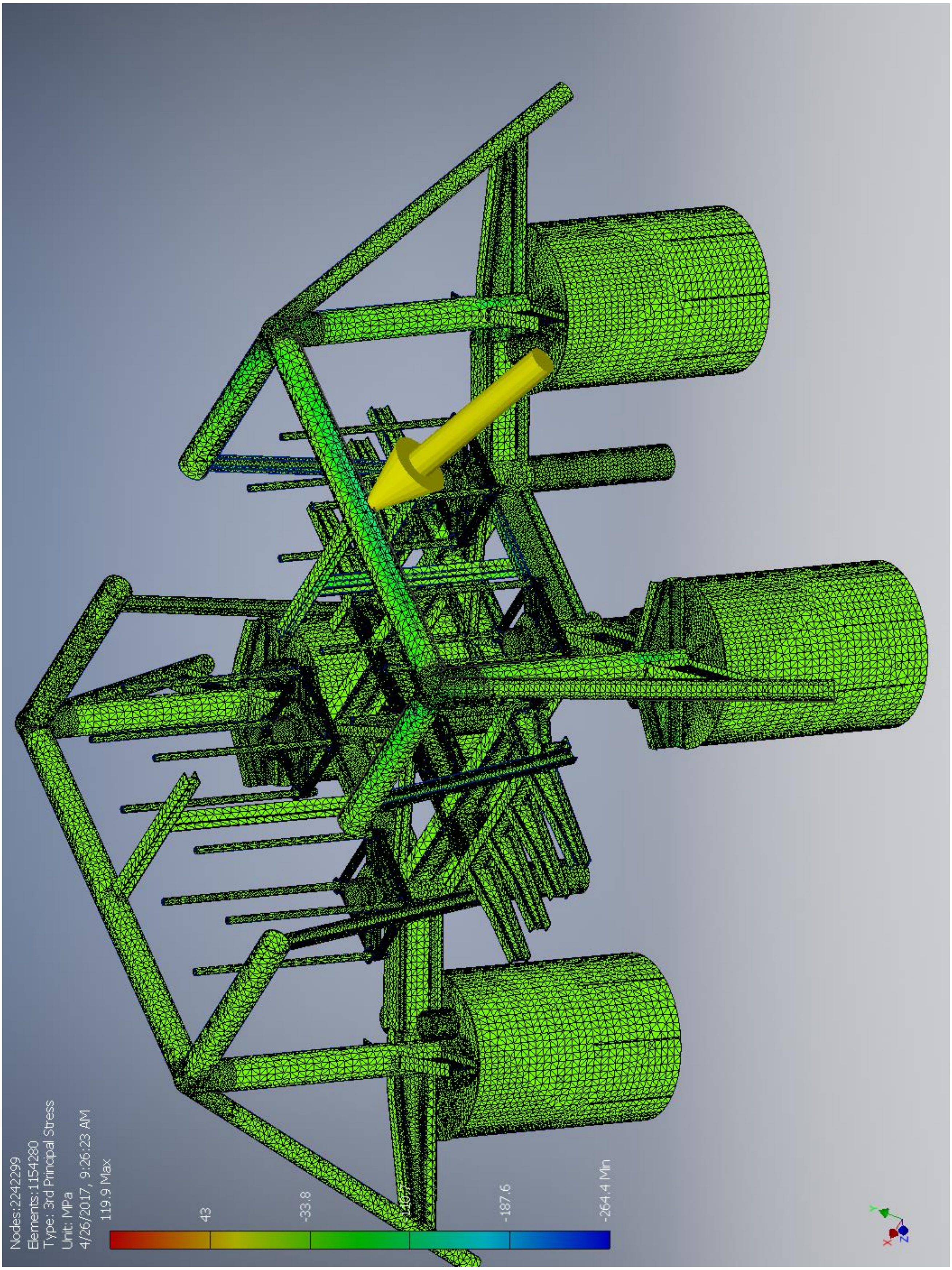

## ⊟ Displacement

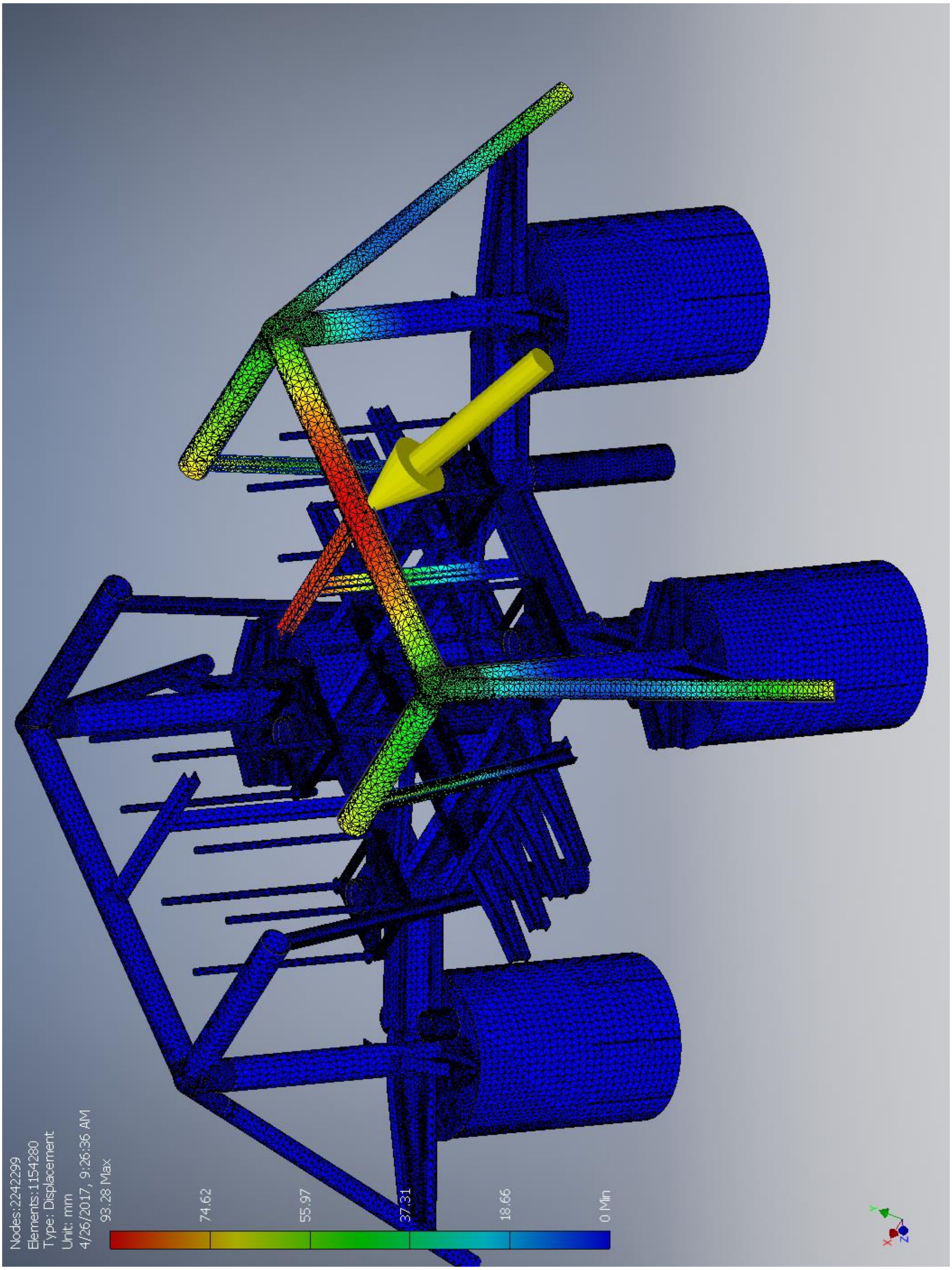

⊟ **Safety Factor**

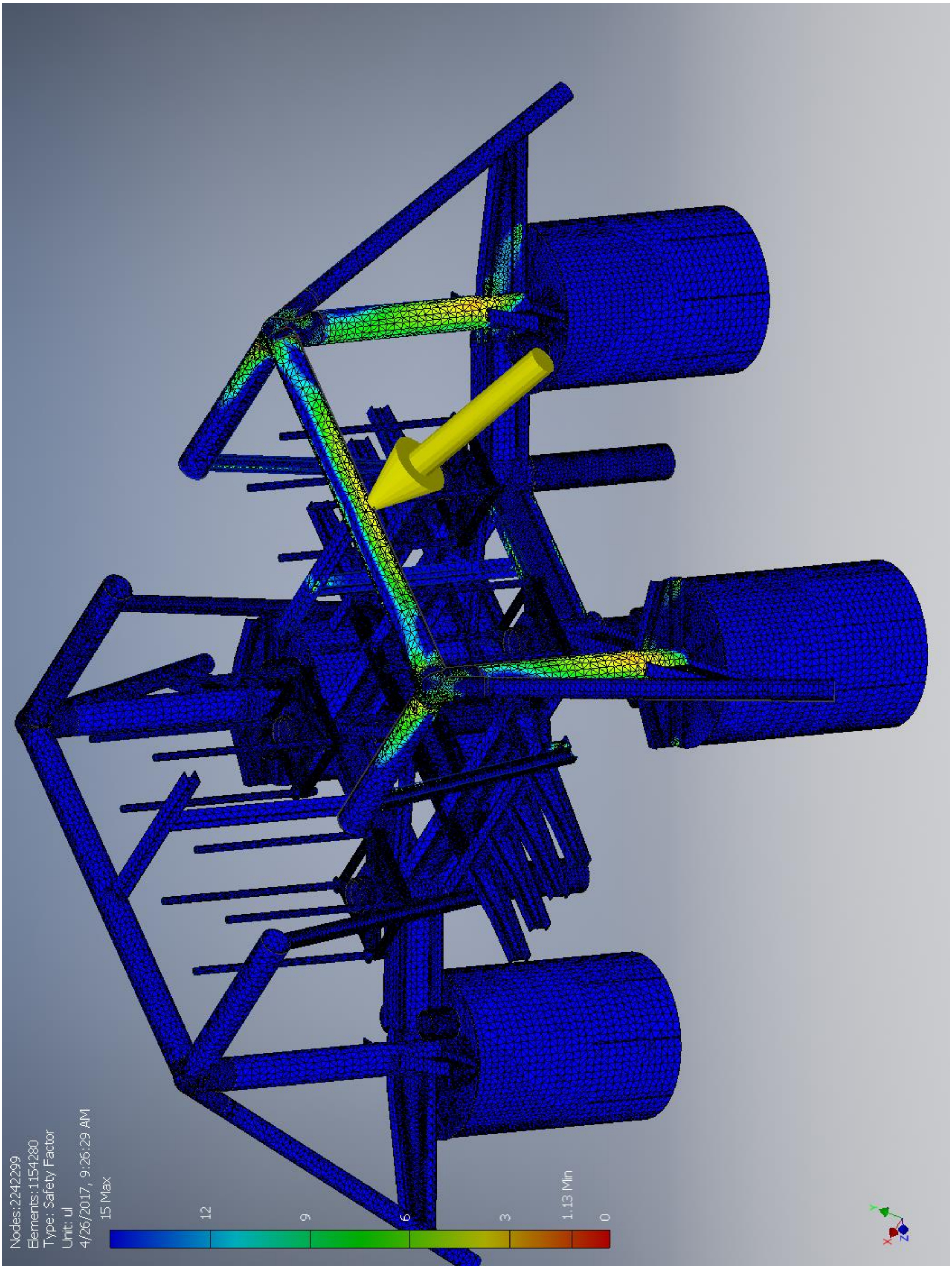

### I.1.2 With convergence

# Stress Analysis Report

AUTODESK

| | |
|---|---|
| Analyzed File: | Assembly.iam |
| Autodesk Inventor Version: | 2017 (Build 210142000, 142) |
| Creation Date: | 4/25/2017, 4:50 PM |
| Study Author: | henrikwn |
| Summary: | |

---

## ⊟ Project Info (iProperties)

### ⊟ Summary

| | |
|---|---|
| Title | |
| Author | henrikwn |

### ⊟ Project

| | |
|---|---|
| Part Number | Assembly |
| Designer | henrikwn |

### ⊟ Physical

| | |
|---|---|
| Mass | 182983 kg |
| Area | 3.56846E+09 mm^2 |
| Volume | 6.09185E+10 mm^3 |
| Center of Gravity | x=-41359.7 mm<br>y=-19499.7 mm<br>z=32758.2 mm |

Note: Physical values could be different from Physical values used by FEA reported below.

---

## ⊟ Case-a

**General objective and settings:**

| | |
|---|---|
| Design Objective | Single Point |
| Study Type | Static Analysis |
| Last Modification Date | 4/25/2017, 4:47 PM |
| Detect and Eliminate Rigid Body Modes | No |
| Separate Stresses Across Contact Surfaces | No |
| Motion Loads Analysis | No |

### ⊟ Operating conditions

### ⊟ Force:1

| | |
|---|---|
| Load Type | Force |
| Magnitude | 1000000.000 N |
| Vector X | 481601.661 N |
| Vector Y | 554956.253 N |
| Vector Z | 678294.477 N |

⊟ **Selected Face(s)**

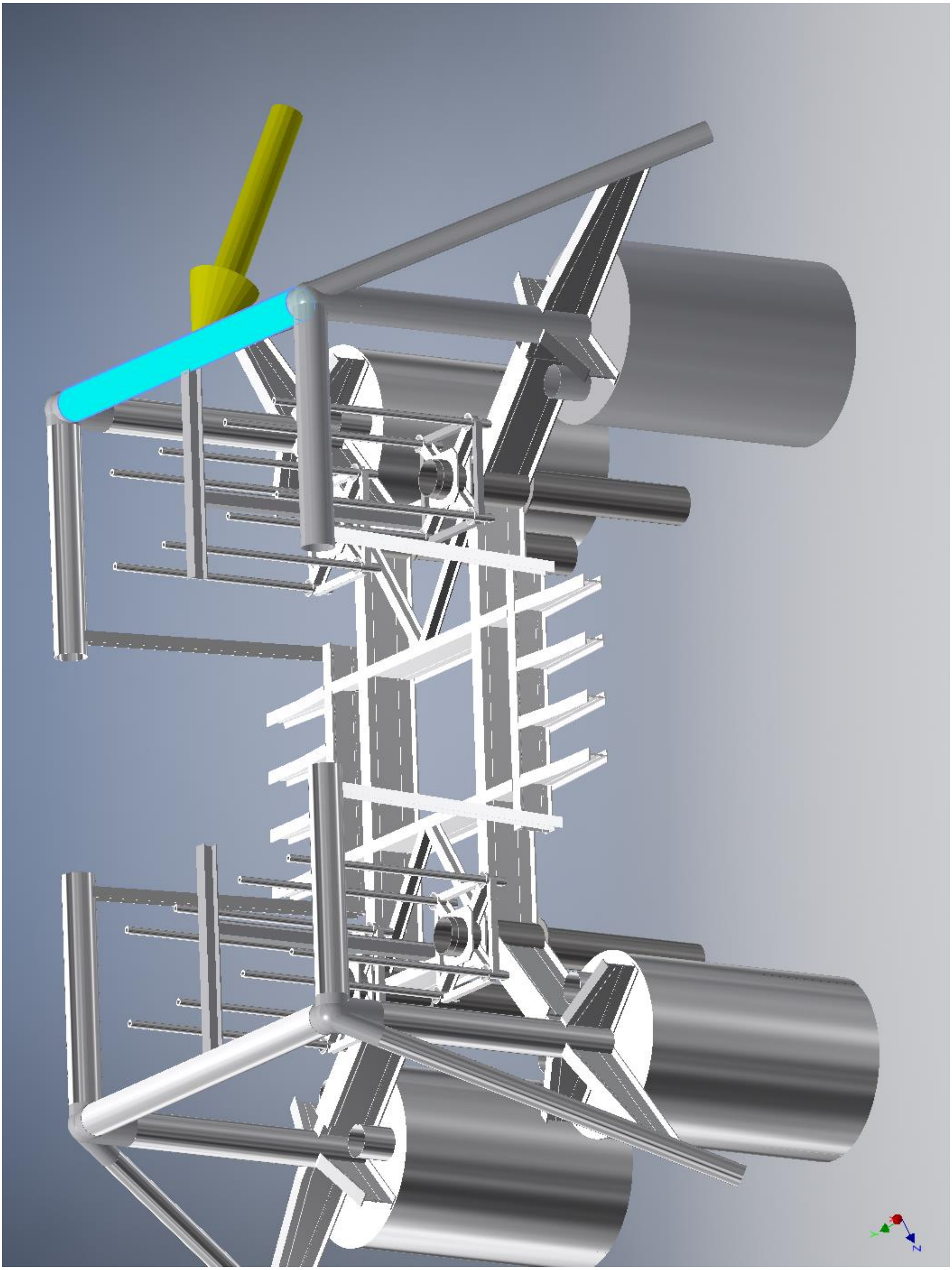

## ⊟ Fixed Constraint:1

| Constraint Type | Fixed Constraint |
|---|---|

### ⊟ Selected Face(s)

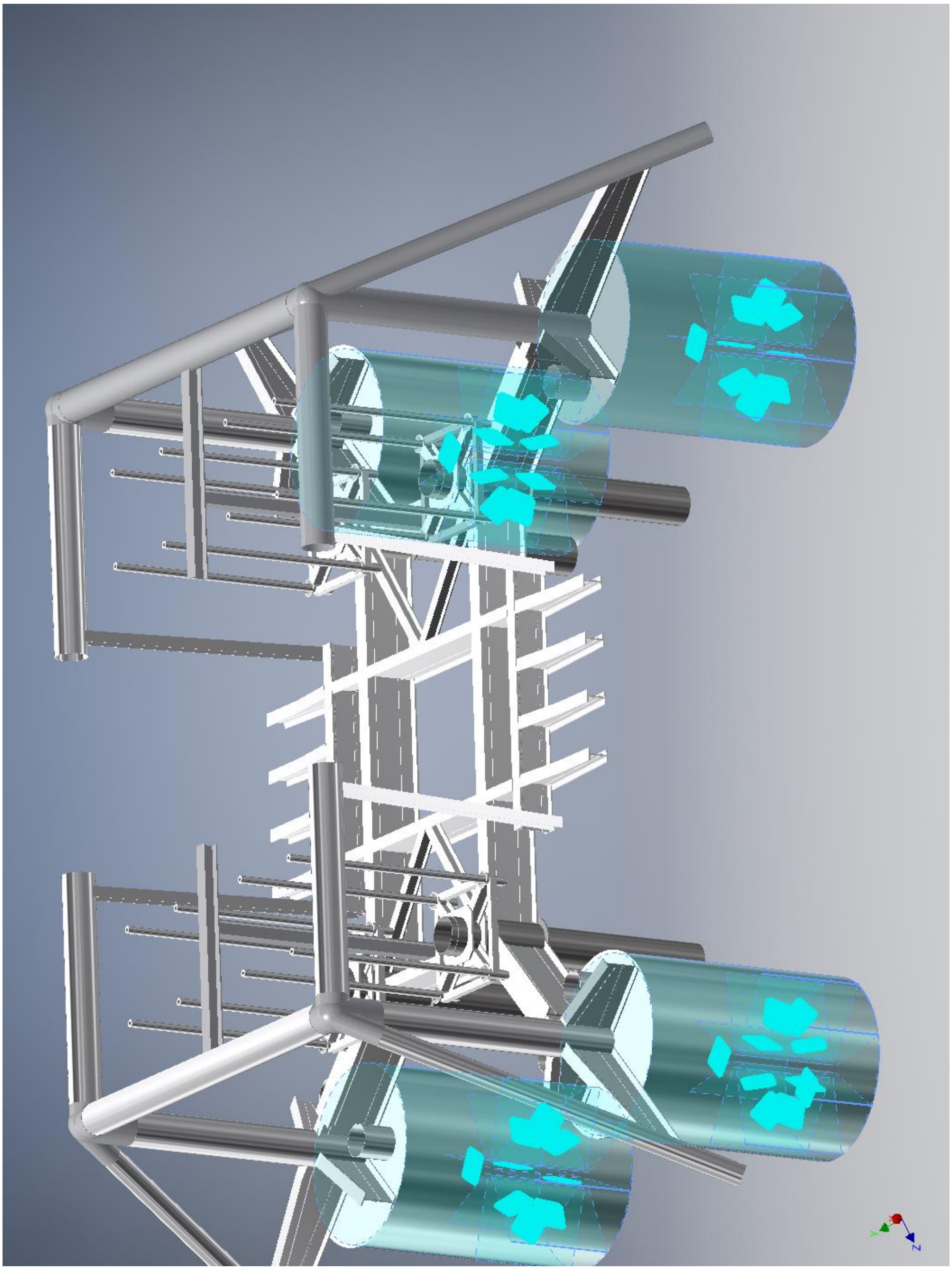

# ⊟ Results

## ⊟ Reaction Force and Moment on Constraints

| Constraint Name | Reaction Force | | Reaction Moment | |
|---|---|---|---|---|
| | Magnitude | Component (X,Y,Z) | Magnitude | Component (X,Y,Z) |
| Fixed Constraint:1 | 1000000 N | -481602 N | 15257000 N m | -10055100 N m |
| | | -554956 N | | 11286400 N m |
| | | -678295 N | | -2070320 N m |

## ⊟ Result Summary

| Name | Minimum | Maximum |
|---|---|---|
| Volume | 6.09185E+10 mm^3 | |
| Mass | 182983 kg | |
| Von Mises Stress | 0 MPa | 1302 MPa |
| 1st Principal Stress | -111.021 MPa | 1701.07 MPa |
| 3rd Principal Stress | -369.69 MPa | 330.557 MPa |
| Displacement | 0 mm | 92.7268 mm |
| Safety Factor | 0.211213 ul | 15 ul |

## ⊟ Figures

⊟ **Von Mises Stress**

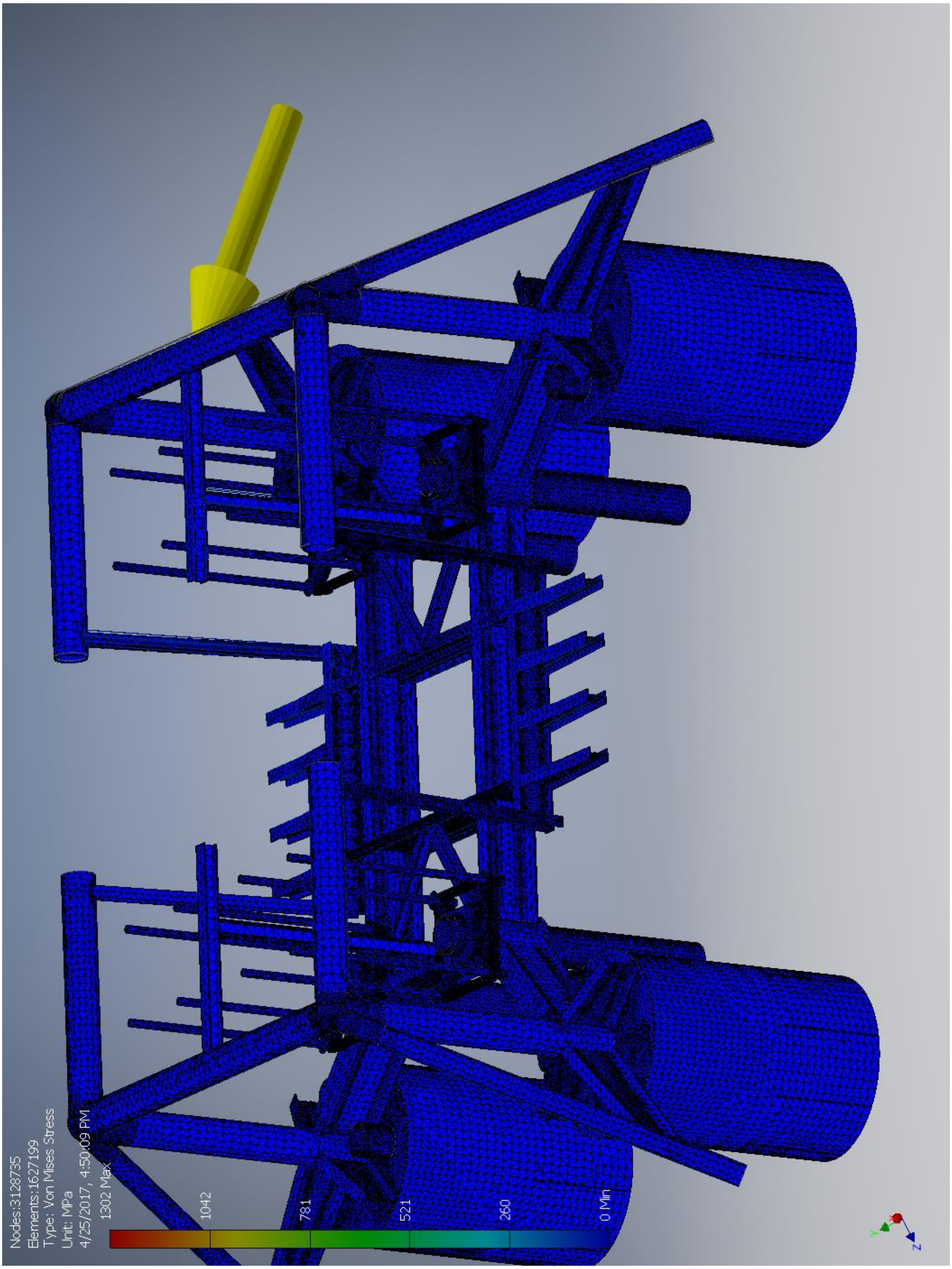

⊟ **1st Principal Stress**

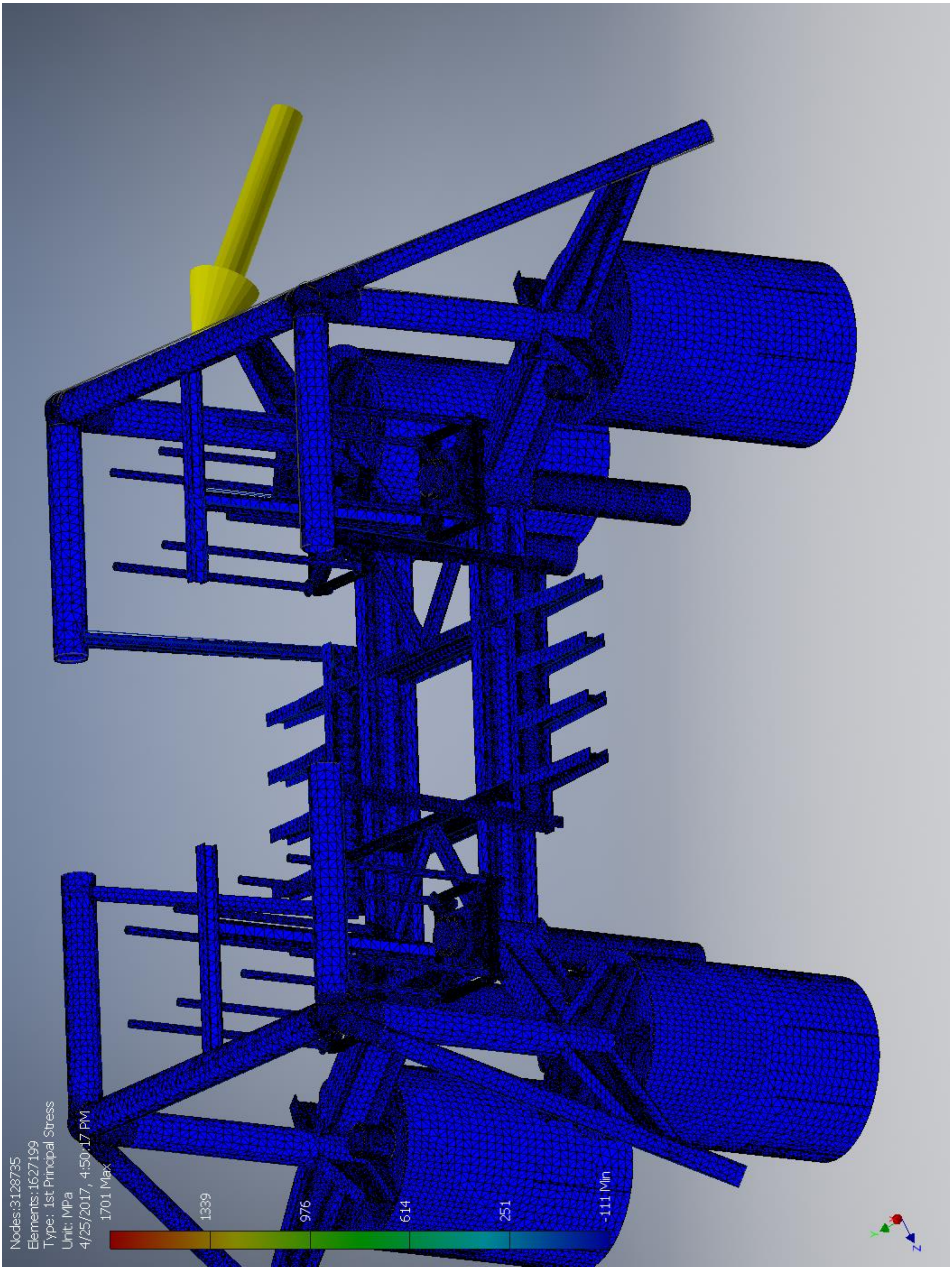

## ⊟ 3rd Principal Stress

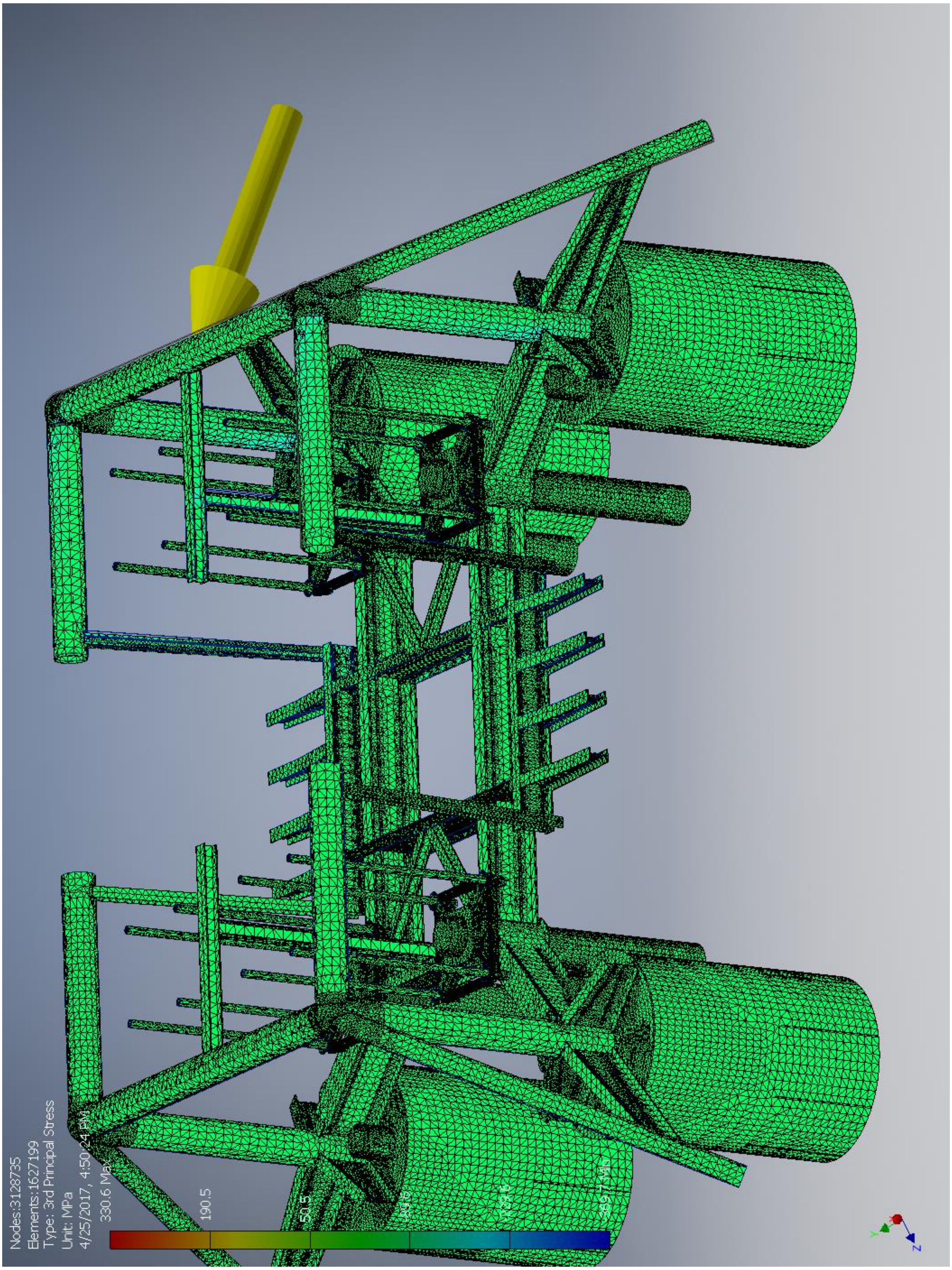

## ⊟ Displacement

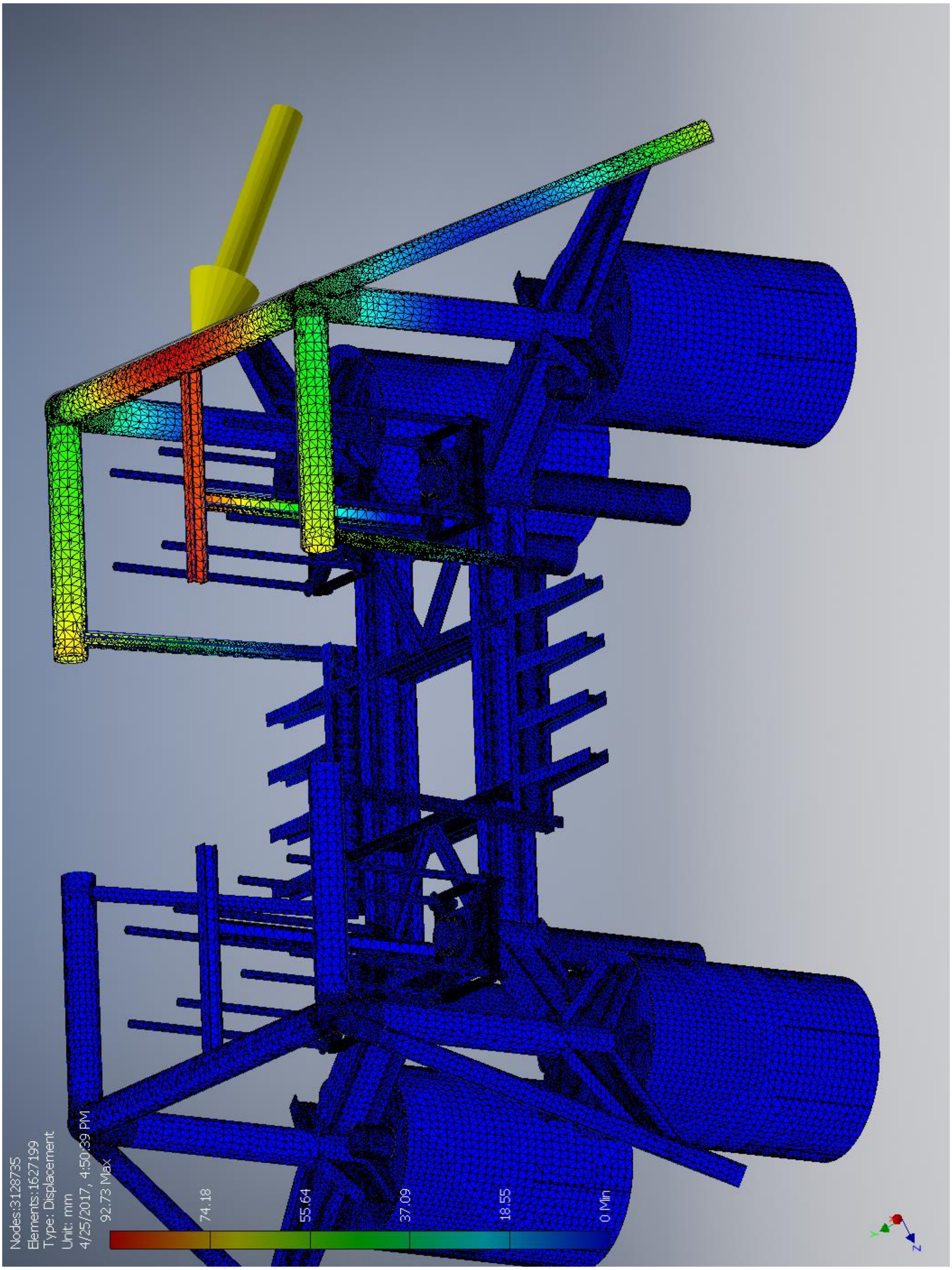

## ⊟ Safety Factor

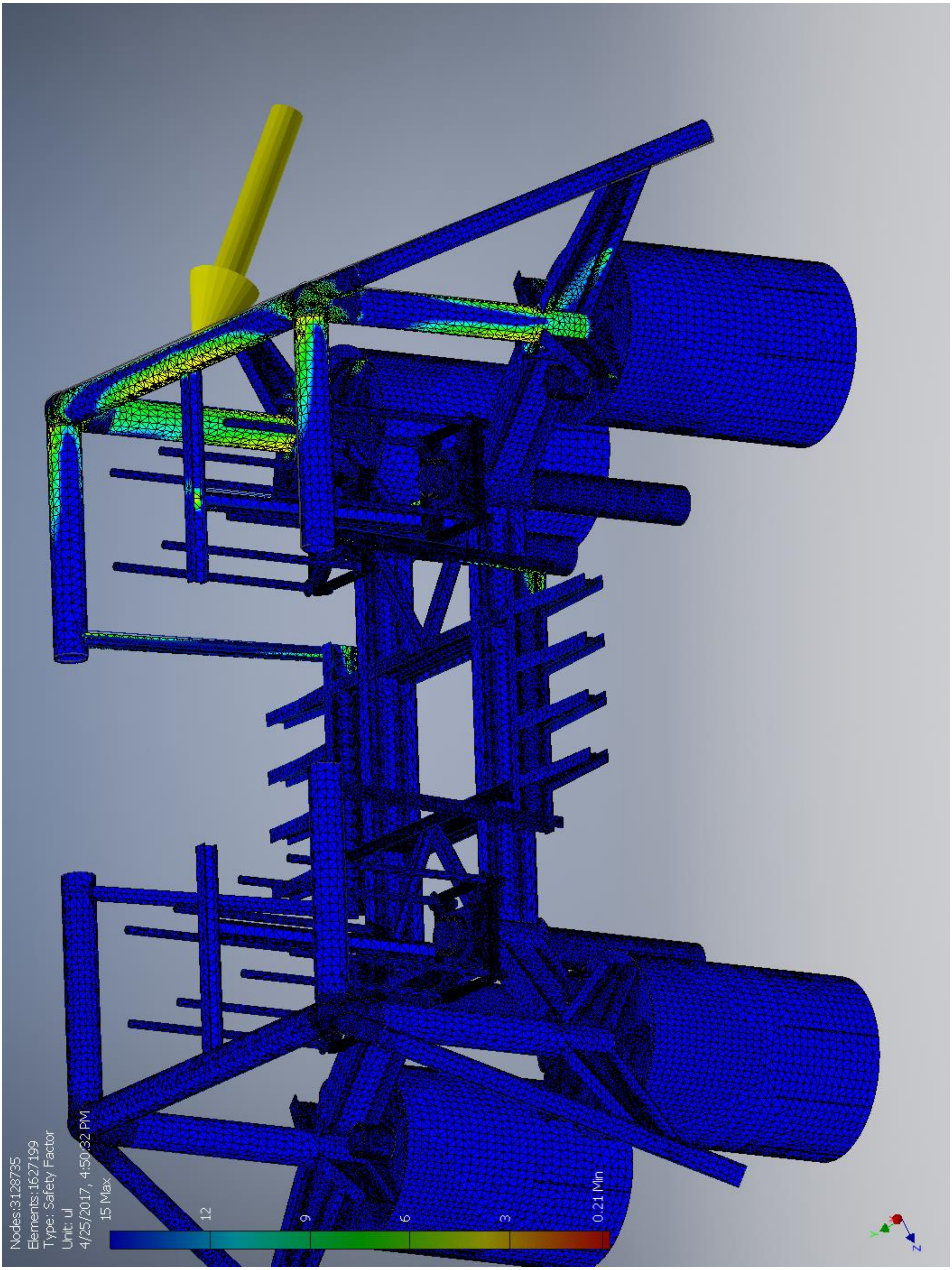

## I.2 Case-B

### I.2.1 Without convergence

# Stress Analysis Report

AUTODESK

| | |
|---|---|
| Analyzed File: | Assembly.iam |
| Autodesk Inventor Version: | 2017 (Build 210142000, 142) |
| Creation Date: | 4/26/2017, 12:13 PM |
| Study Author: | henrikwn |
| Summary: | |

---

## ⊟ Project Info (iProperties)

### ⊟ Summary

| | |
|---|---|
| Title | |
| Author | henrikwn |

### ⊟ Project

| | |
|---|---|
| Designer | henrikwn |

### ⊟ Physical

| | |
|---|---|
| Mass | 182983 kg |
| Area | 3.56846E+09 mm^2 |
| Volume | 6.09185E+10 mm^3 |
| Center of Gravity | x=-41359.7 mm<br>y=-19499.7 mm<br>z=32758.2 mm |

Note: Physical values could be different from Physical values used by FEA reported below.

---

## ⊟ Case-B

**General objective and settings:**

| | |
|---|---|
| Design Objective | Single Point |
| Study Type | Static Analysis |
| Last Modification Date | 4/26/2017, 12:09 PM |
| Detect and Eliminate Rigid Body Modes | No |
| Separate Stresses Across Contact Surfaces | No |
| Motion Loads Analysis | No |

### ⊟ Operating conditions

## ⊟ Force:1

| | |
|---|---|
| Load Type | Force |
| Magnitude | 1000000.000 N |
| Vector X | 481601.661 N |
| Vector Y | 554956.253 N |
| Vector Z | 678294.477 N |

⊟ **Selected Face(s)**

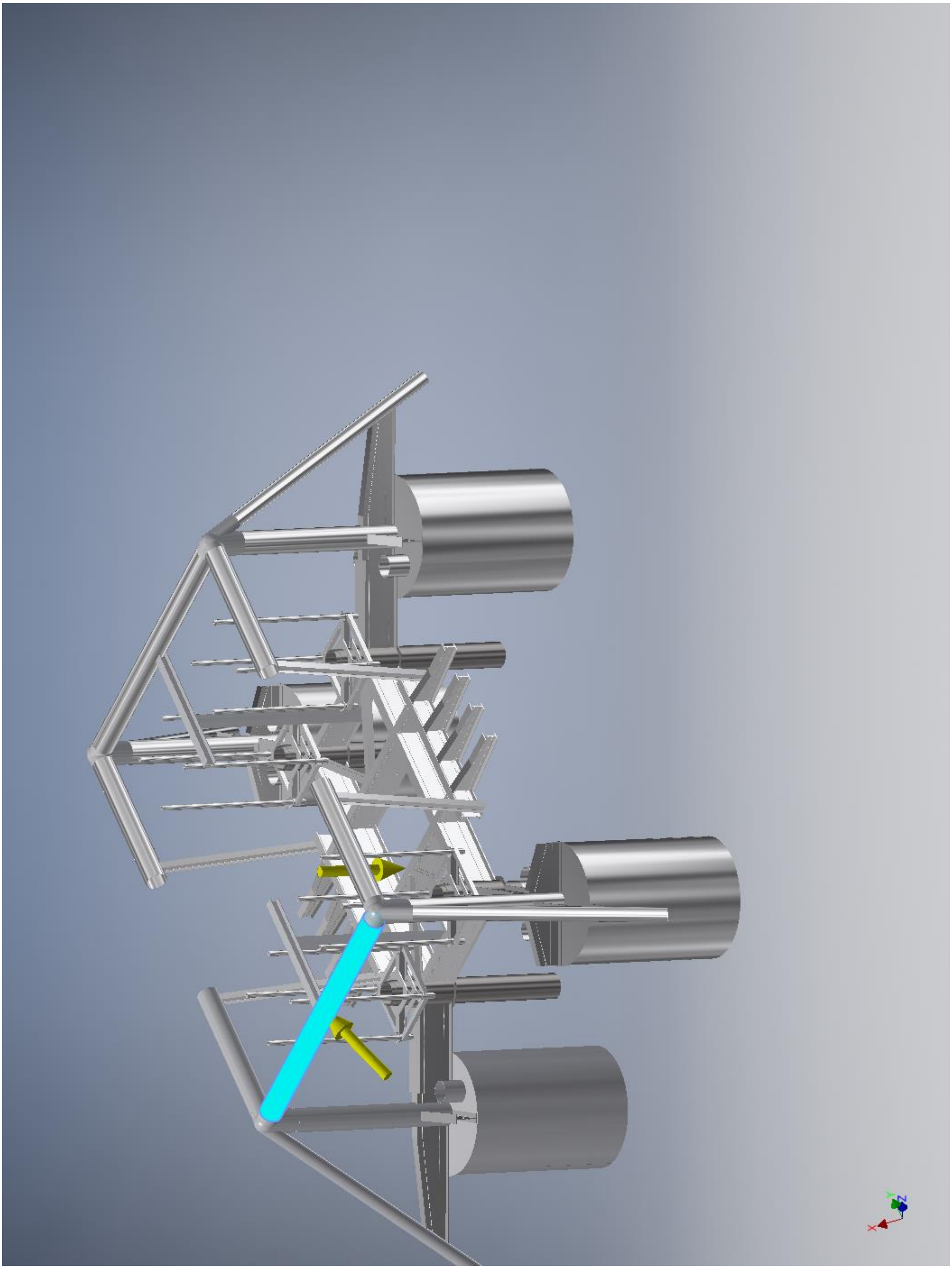

### ⊟ Force:5

| | |
|---|---|
| Load Type | Force |
| Magnitude | 800000.000 N |
| Vector X | -575687.094 N |
| Vector Y | -456689.119 N |
| Vector Z | 316258.468 N |

## ⊟ Selected Face(s)

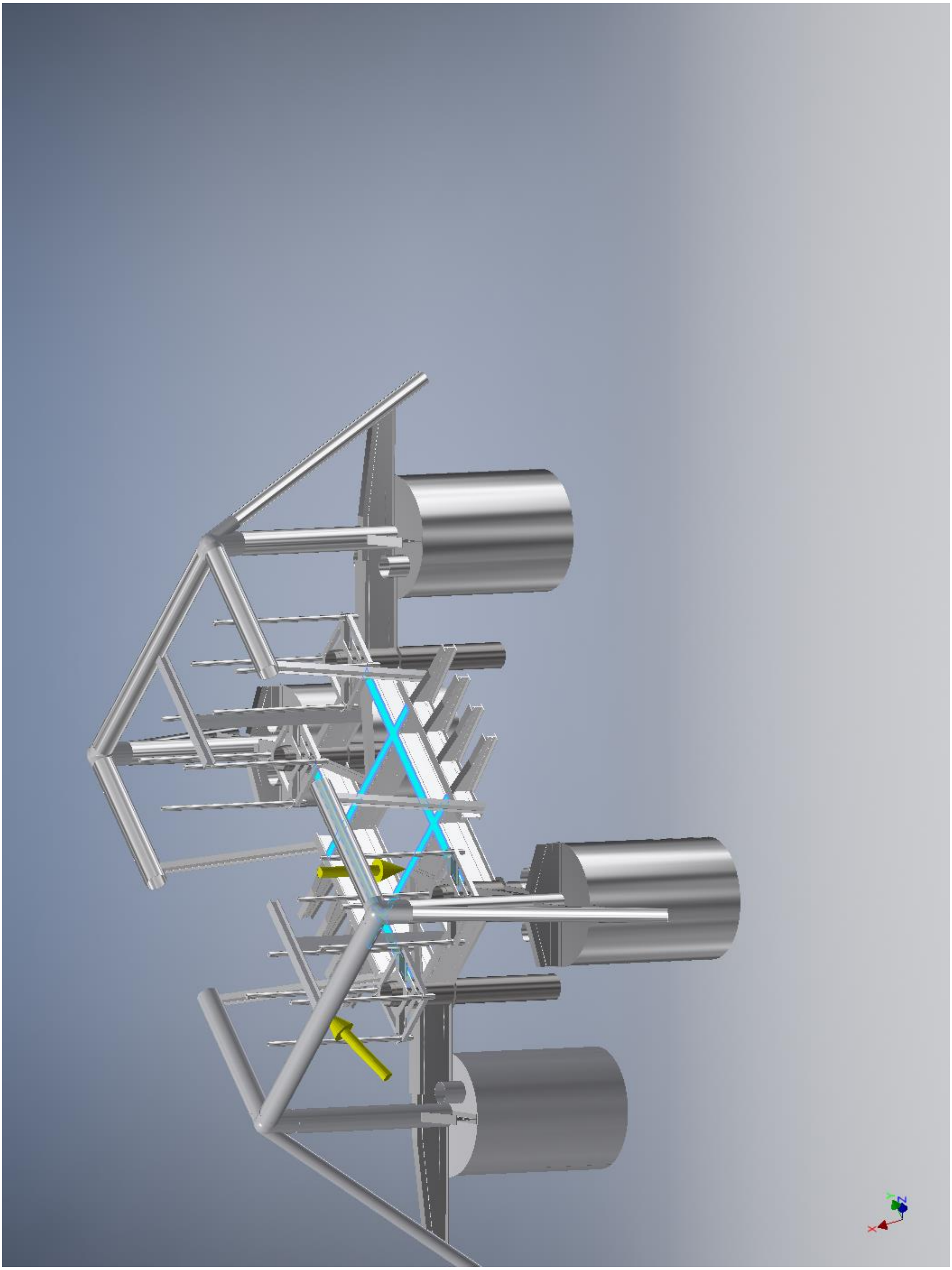

## ⊟ Fixed Constraint:1

| Constraint Type | Fixed Constraint |
|---|---|

### ⊟ Selected Face(s)

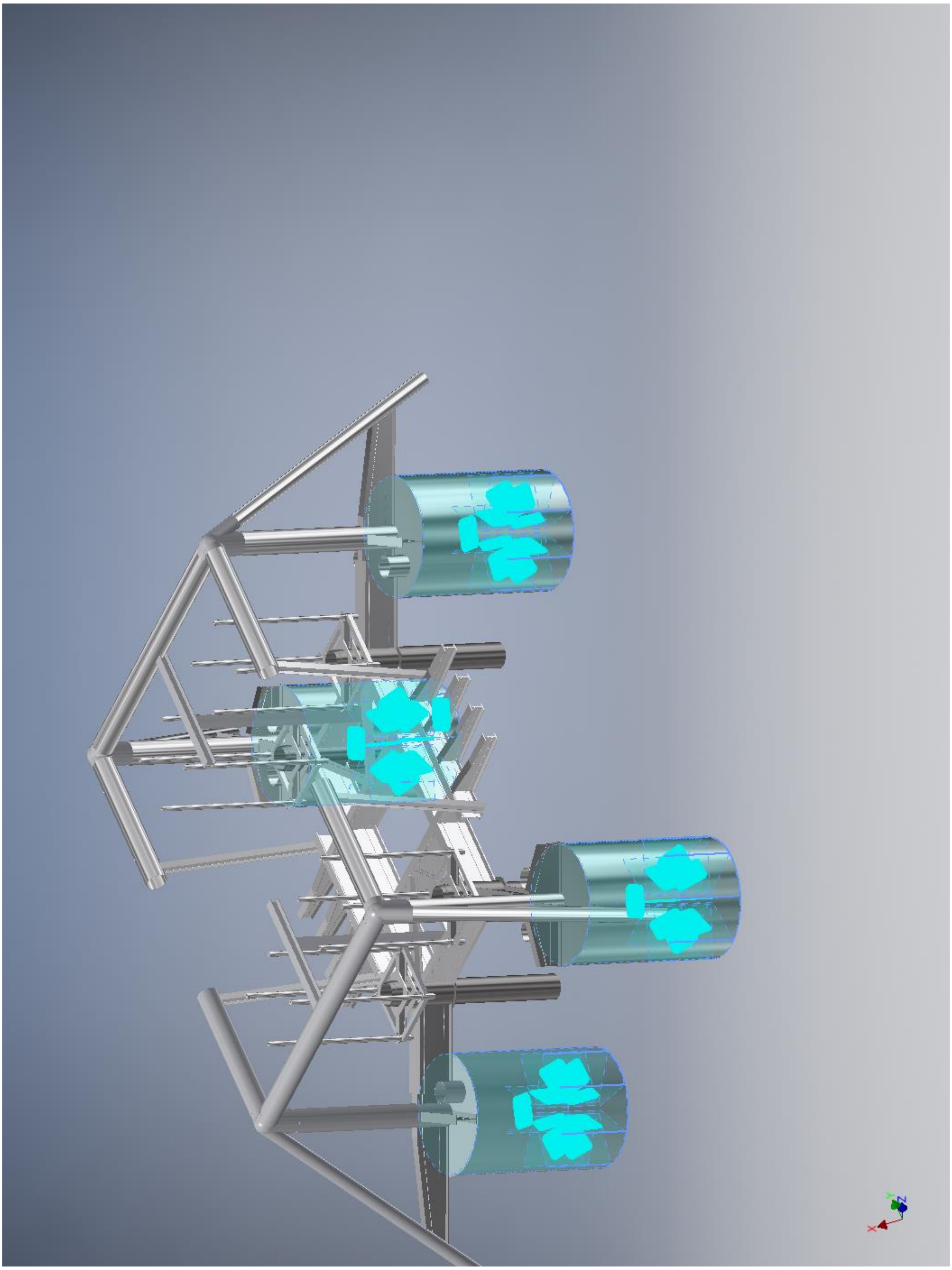

## ⊟ Results

### ⊟ Reaction Force and Moment on Constraints

| Constraint Name | Reaction Force | | Reaction Moment | |
|---|---|---|---|---|
| | Magnitude | Component (X,Y,Z) | Magnitude | Component (X,Y,Z) |
| Fixed Constraint:1 | 1003810 N | 94085.4 N | 15253600 N m | -10070300 N m |
| | | -98267.1 N | | 11269000 N m |
| | | -994553 N | | -2066750 N m |

### ⊟ Result Summary

| Name | Minimum | Maximum |
|---|---|---|
| Volume | 6.09185E+10 mm^3 | |
| Mass | 182983 kg | |
| Von Mises Stress | 0 MPa | 194.682 MPa |
| 1st Principal Stress | -110.804 MPa | 306.814 MPa |
| 3rd Principal Stress | -262.644 MPa | 125.266 MPa |
| Displacement | 0 mm | 93.9621 mm |
| Safety Factor | 1.10436 ul | 15 ul |

### ⊟ Figures

## ⊟ Von Mises Stress

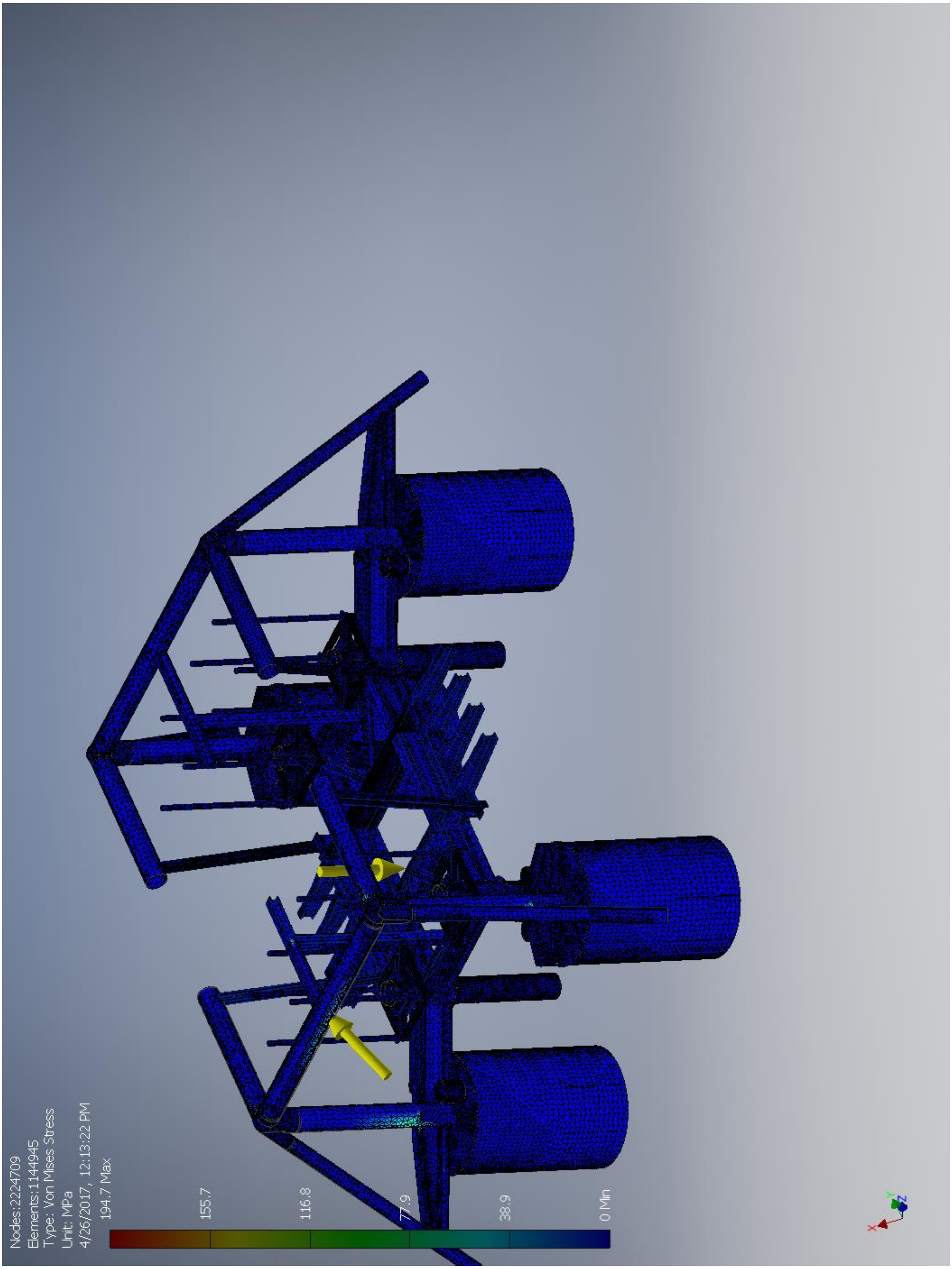

## ⊟ 1st Principal Stress

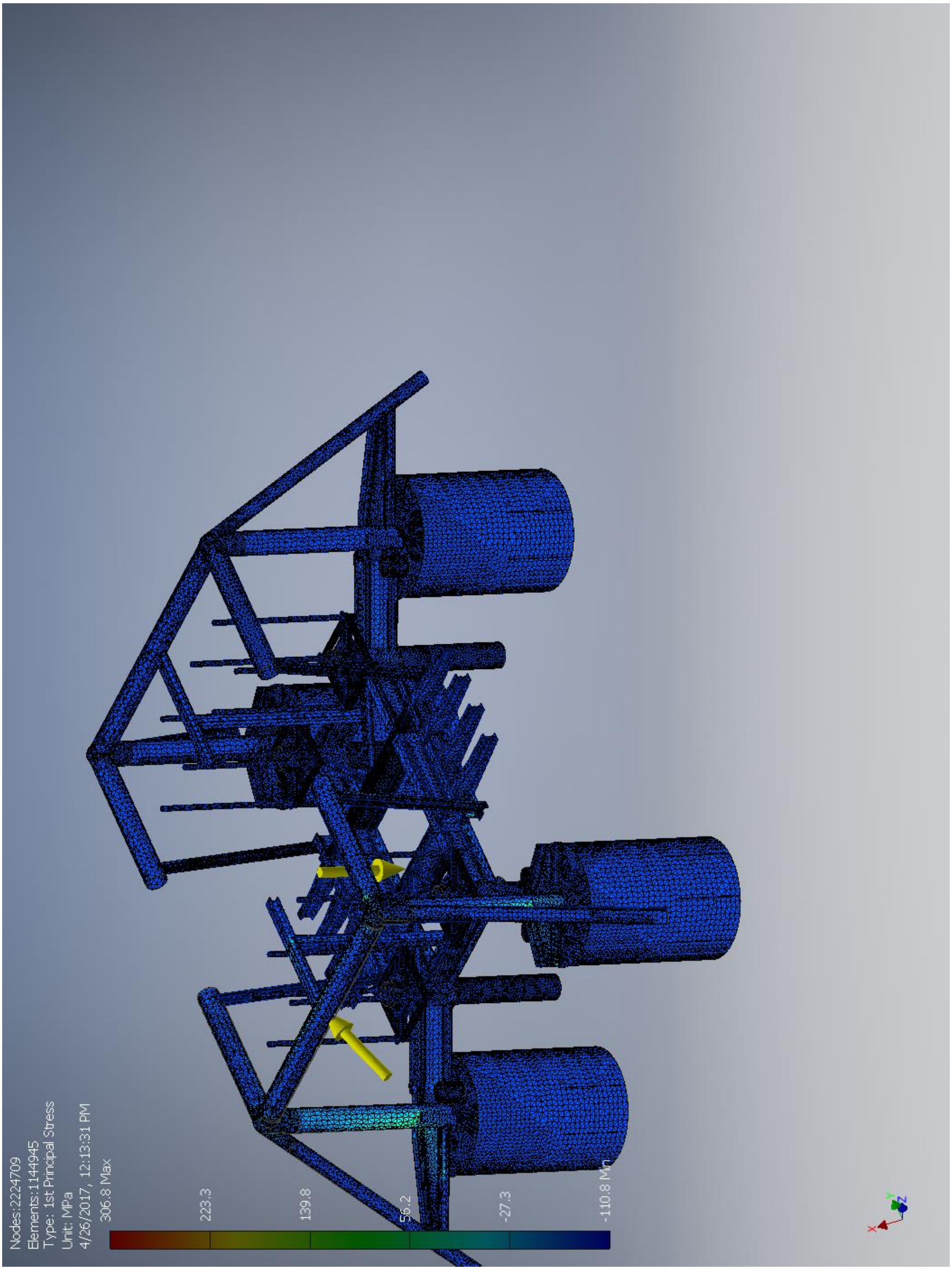

## ⊟ 3rd Principal Stress

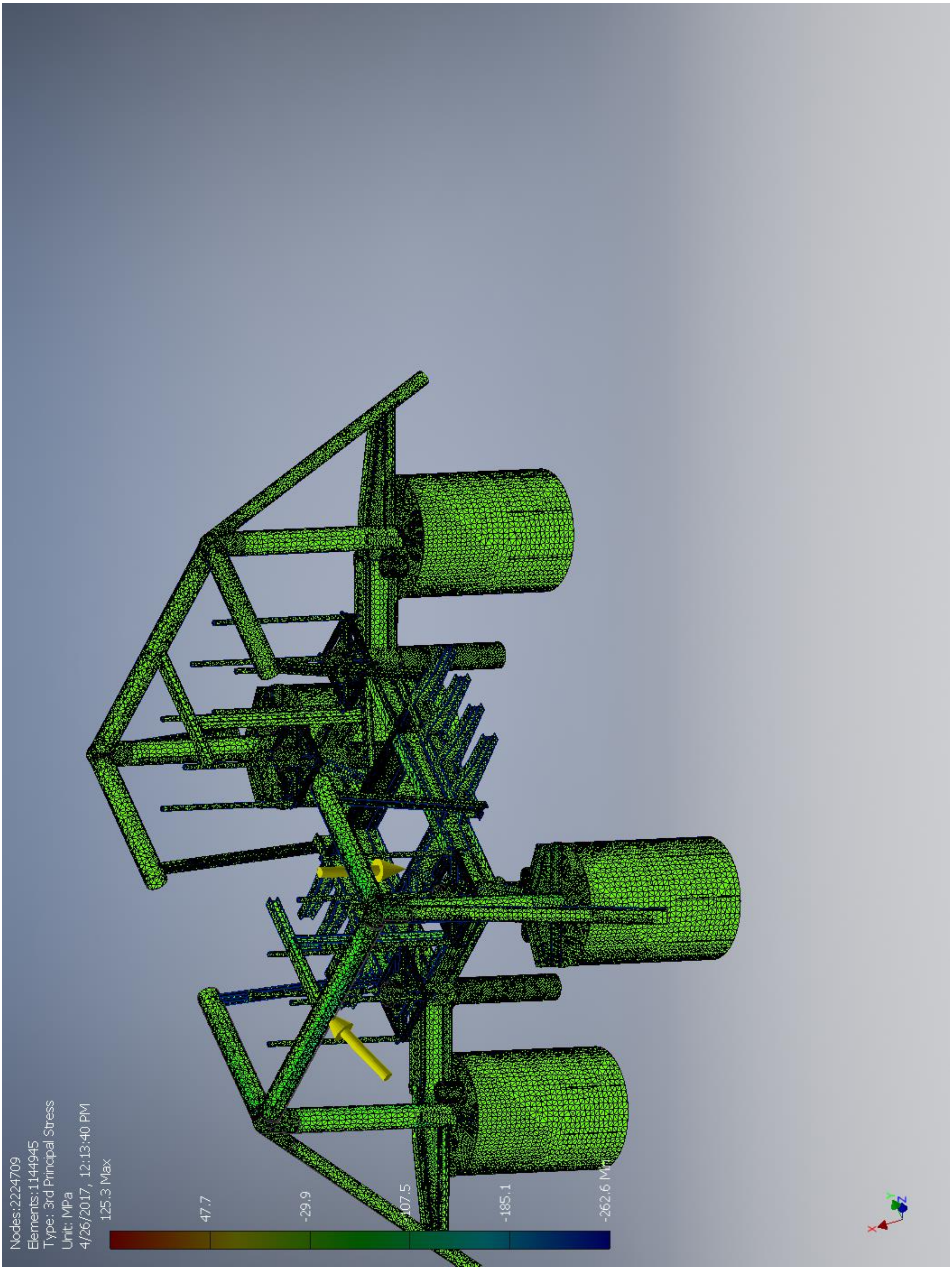

## ⊟ Displacement

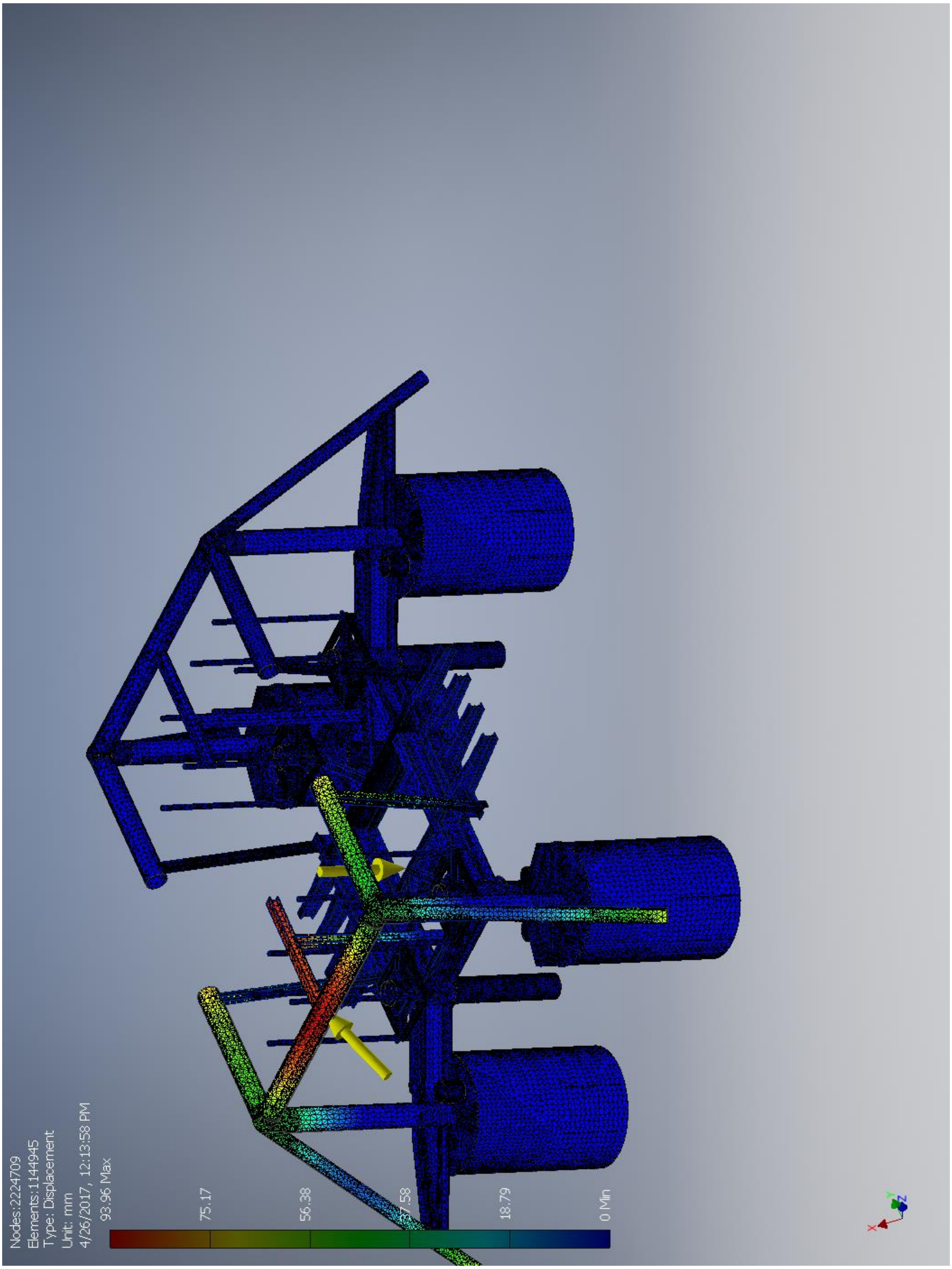

### ⊟ Safety Factor

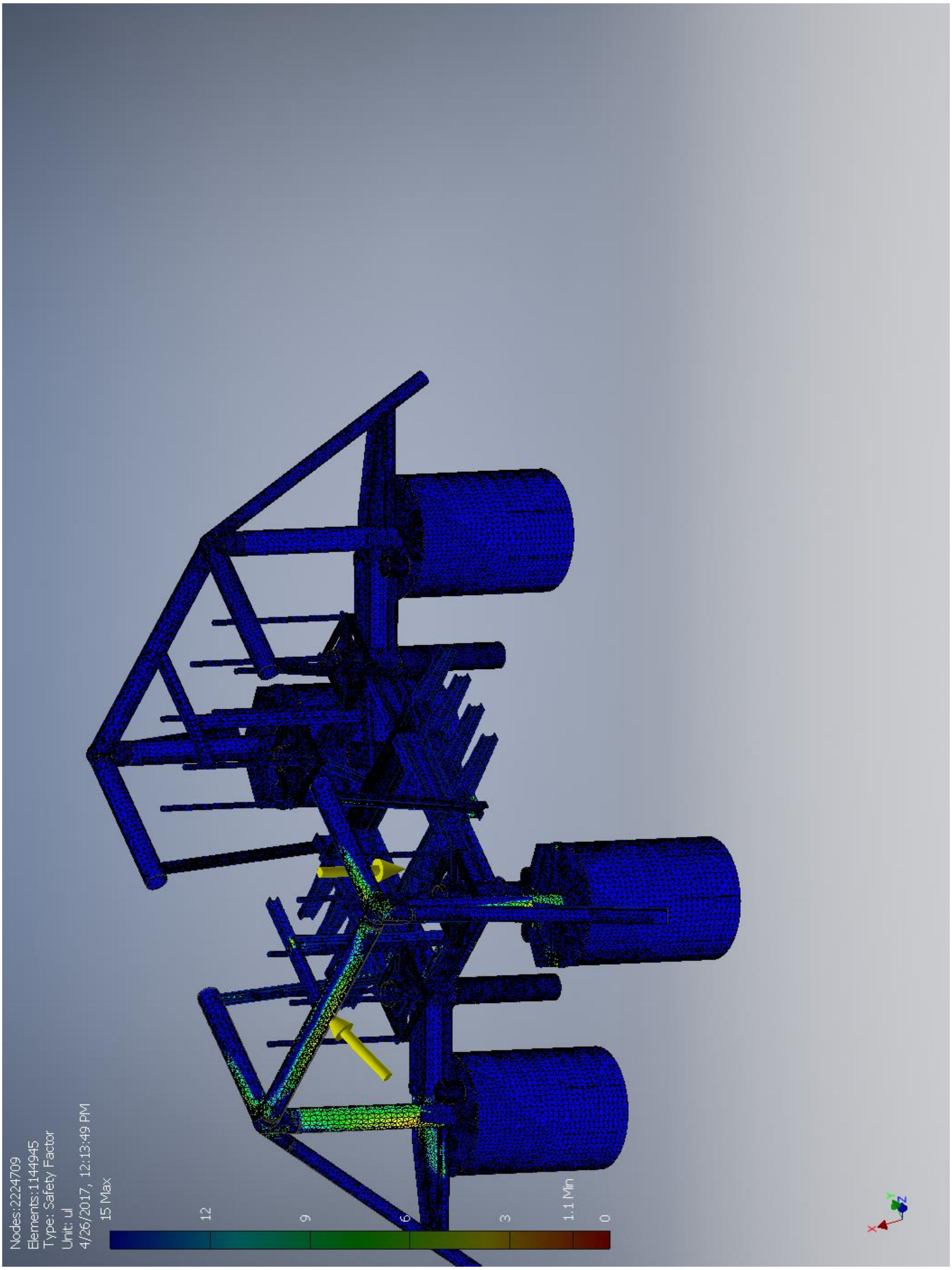

### I.2.2 With convergence

# Stress Analysis Report

AUTODESK

| | |
|---|---|
| Analyzed File: | Assembly.iam |
| Autodesk Inventor Version: | 2017 (Build 210142000, 142) |
| Creation Date: | 4/26/2017, 11:56 AM |
| Study Author: | henrikwn |
| Summary: | |

---

## Project Info (iProperties)

### Summary

| | |
|---|---|
| Title | |
| Author | henrikwn |

### Project

| | |
|---|---|
| Part Number | Assembly |
| Designer | henrikwn |

### Physical

| | |
|---|---|
| Mass | 182983 kg |
| Area | 3.56846E+09 mm^2 |
| Volume | 6.09185E+10 mm^3 |
| Center of Gravity | x=-41359.7 mm<br>y=-19499.7 mm<br>z=32758.2 mm |

Note: Physical values could be different from Physical values used by FEA reported below.

---

## Case-B

**General objective and settings:**

| | |
|---|---|
| Design Objective | Single Point |
| Study Type | Static Analysis |
| Last Modification Date | 4/26/2017, 11:41 AM |
| Detect and Eliminate Rigid Body Modes | No |
| Separate Stresses Across Contact Surfaces | No |
| Motion Loads Analysis | No |

## Operating conditions

### Force:1

| Load Type | Force |
|---|---|
| Magnitude | 1000000.000 N |
| Vector X | 481601.661 N |
| Vector Y | 554956.253 N |
| Vector Z | 678294.477 N |

**Selected Face(s)**

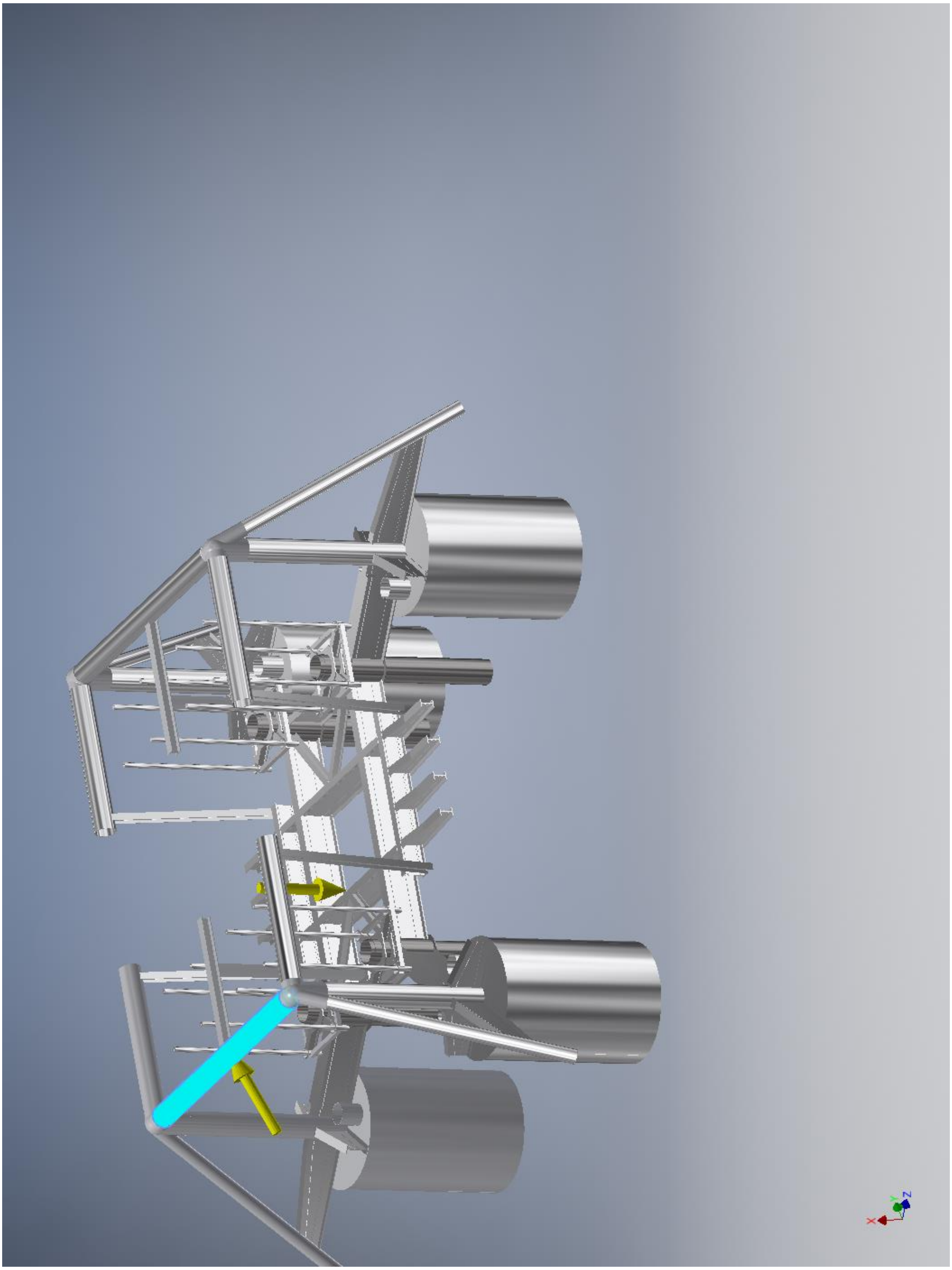

## Force:5

| | |
|---|---|
| Load Type | Force |
| Magnitude | 800000.000 N |
| Vector X | -575687.094 N |
| Vector Y | -456689.119 N |
| Vector Z | 316258.468 N |

**Selected Face(s)**

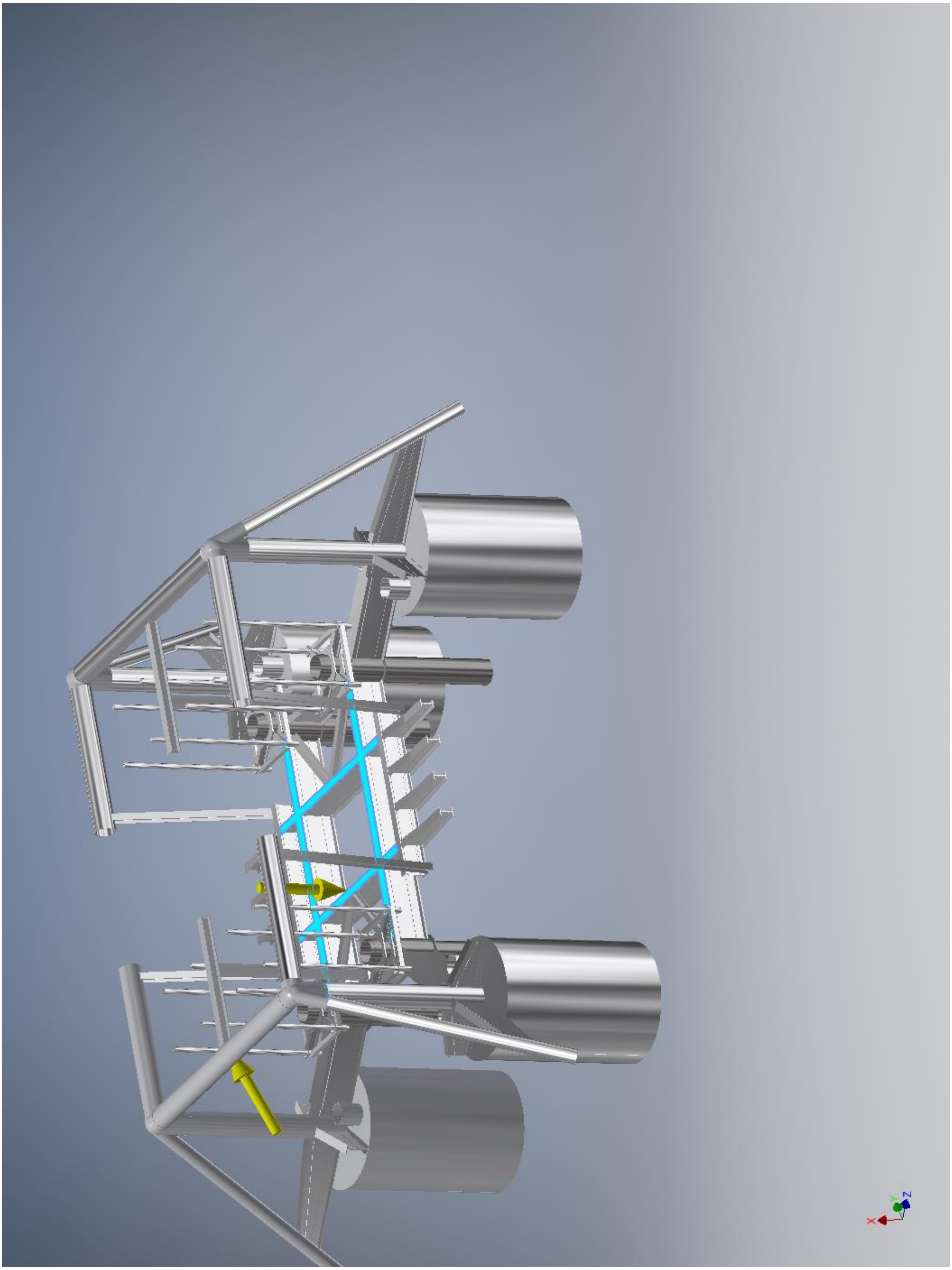

## Fixed Constraint:1

| Constraint Type | Fixed Constraint |
| --- | --- |

### Selected Face(s)

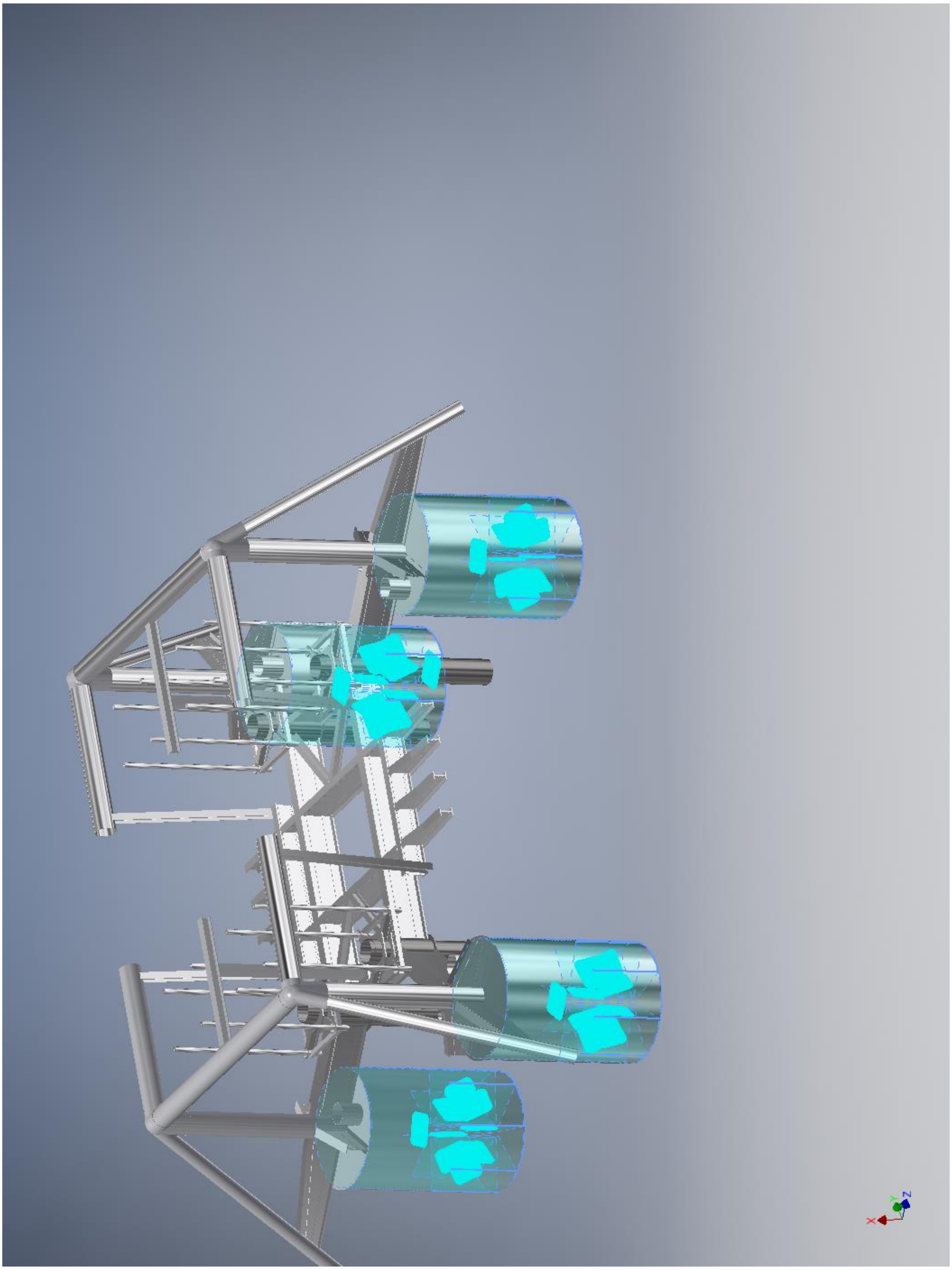

# Results

## Reaction Force and Moment on Constraints

| Constraint Name | Reaction Force | | Reaction Moment | |
|---|---|---|---|---|
| | Magnitude | Component (X,Y,Z) | Magnitude | Component (X,Y,Z) |
| Fixed Constraint:1 | 1003810 N | 94085.4 N | 15255000 N m | -10061700 N m |
| | | -98267.1 N | | 11278500 N m |
| | | -994553 N | | -2067110 N m |

## Result Summary

| Name | Minimum | Maximum |
|---|---|---|
| Volume | 6.09185E+10 mm^3 | |
| Mass | 182983 kg | |
| Von Mises Stress | 0 MPa | 1294.3 MPa |
| 1st Principal Stress | -108.756 MPa | 1526 MPa |
| 3rd Principal Stress | -320.304 MPa | 169.333 MPa |
| Displacement | 0 mm | 94.1343 mm |
| Safety Factor | 0.21247 ul | 15 ul |

## Figures

**Von Mises Stress**

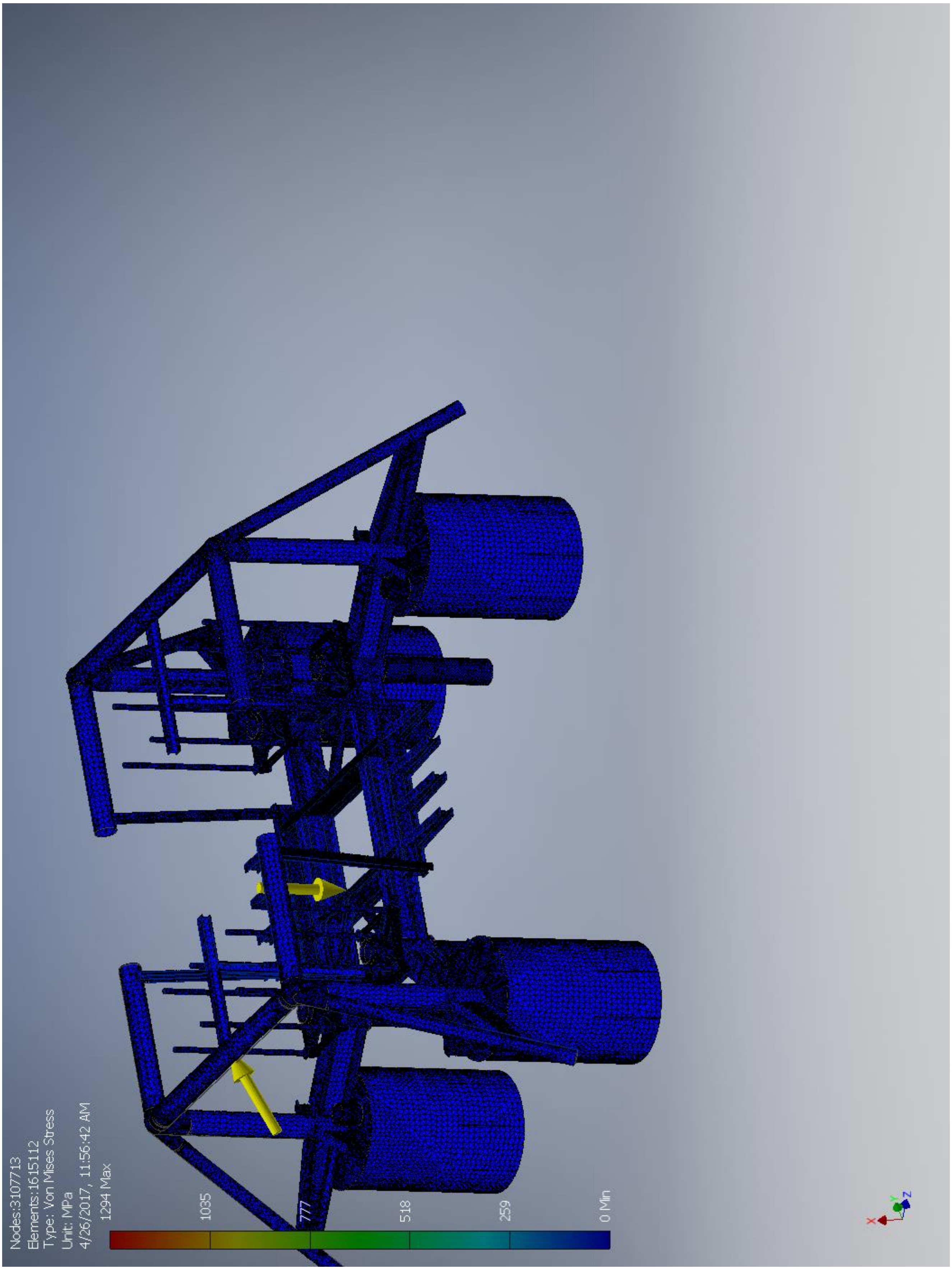

**1st Principal Stress**

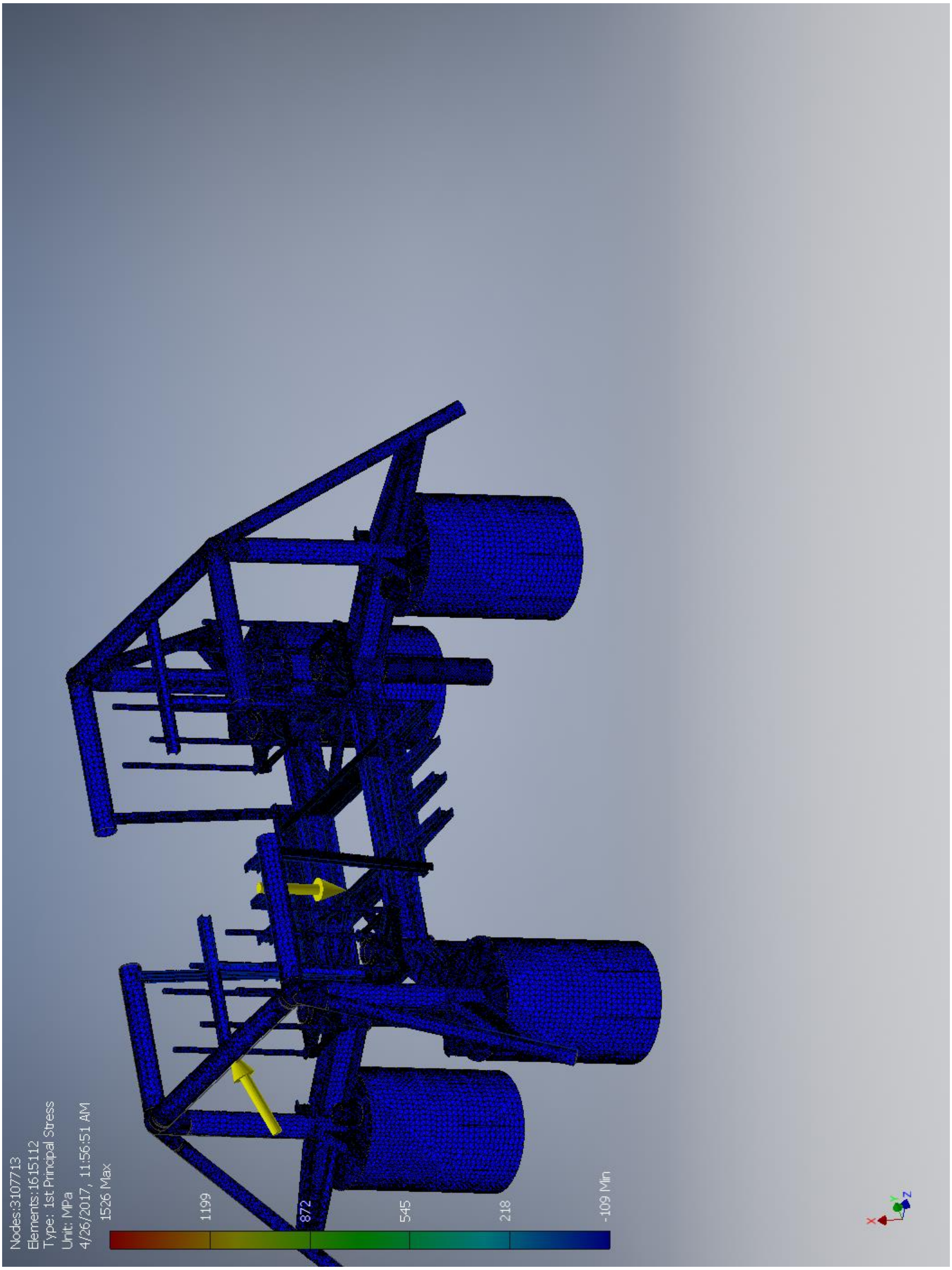

**3rd Principal Stress**

**Displacement**

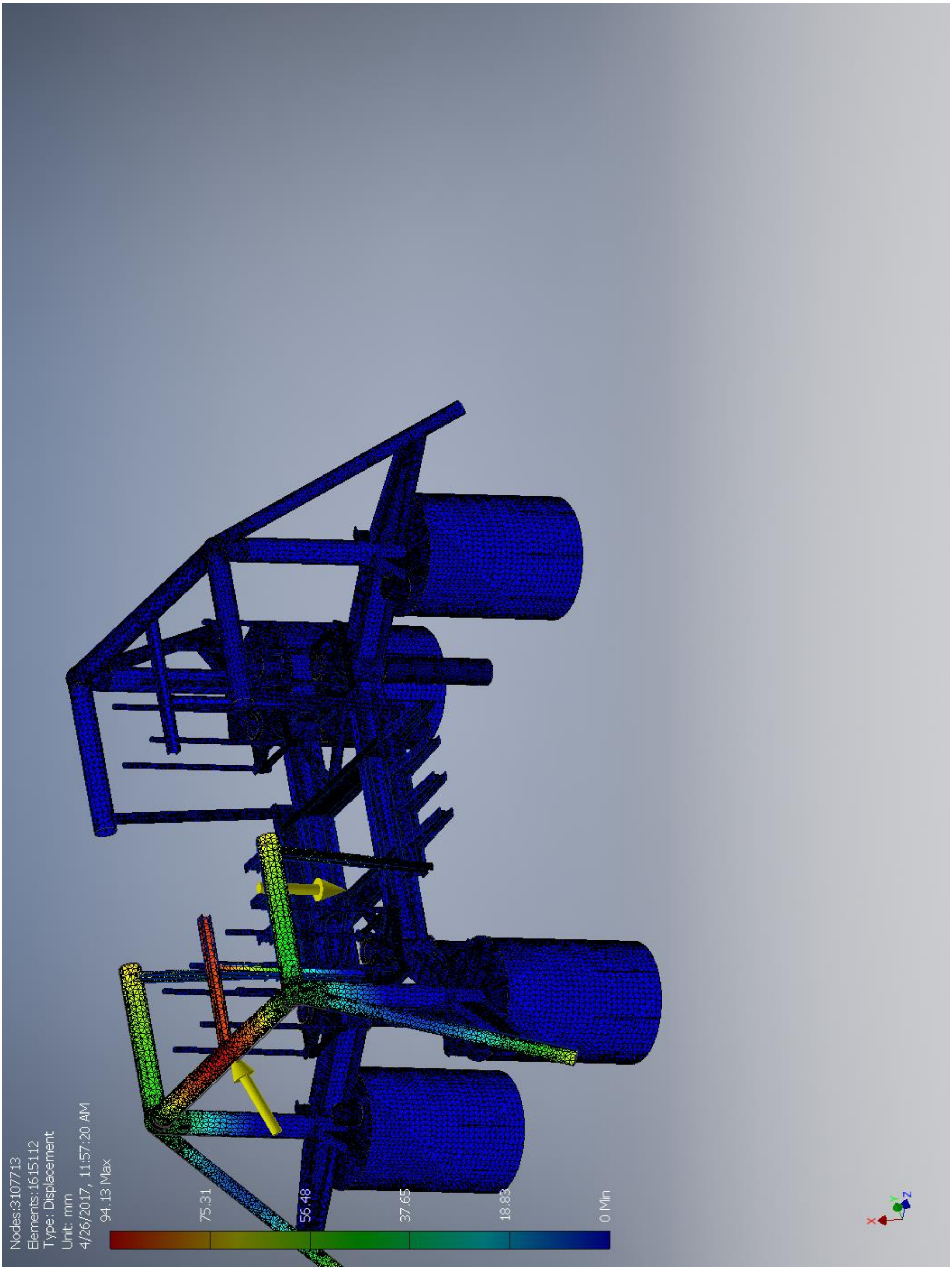

**Safety Factor**

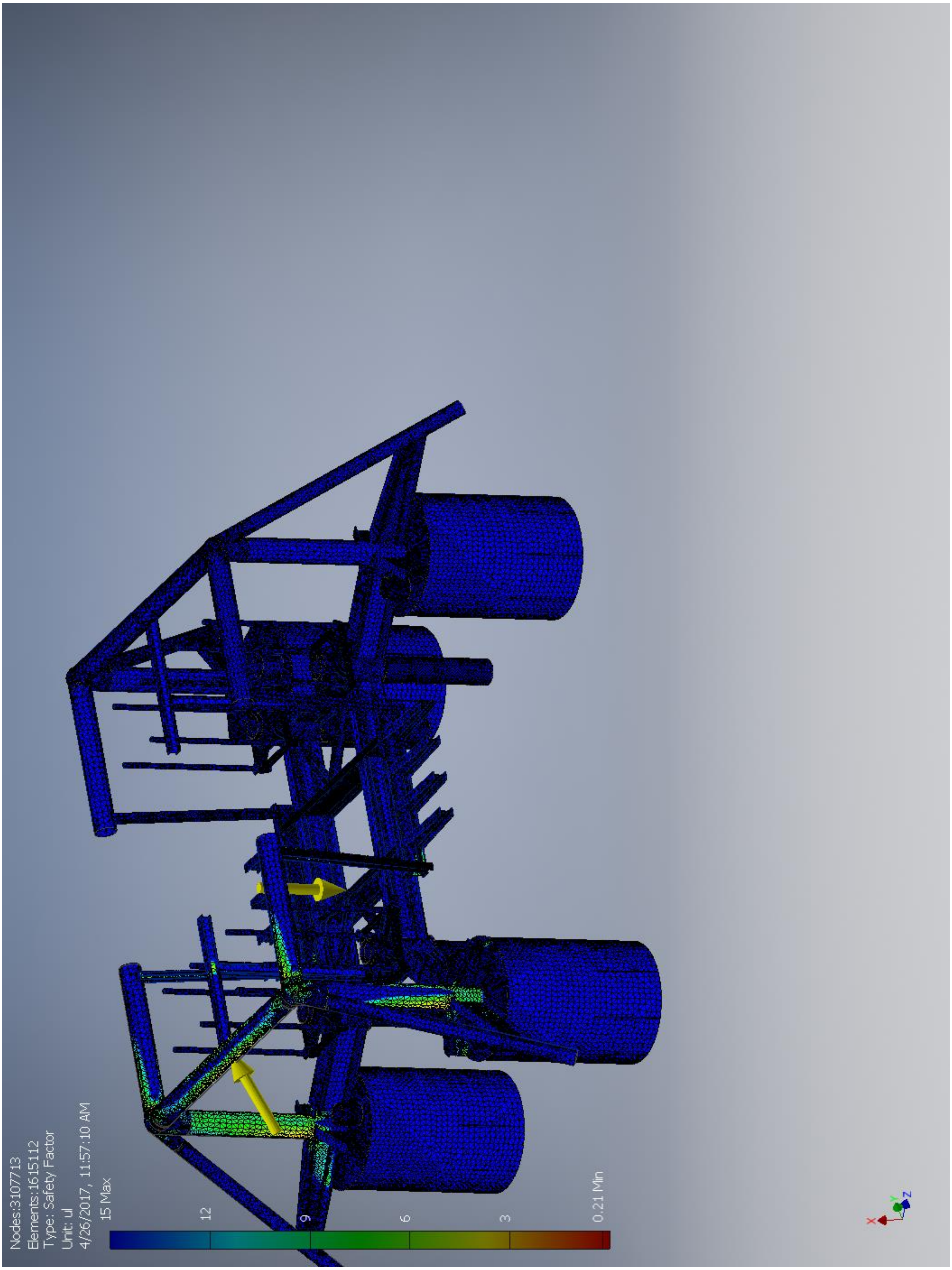

## I.3 Case-C

### I.3.1 Without convergence

# Stress Analysis Report

| | |
|---|---|
| Analyzed File: | Assembly.iam |
| Autodesk Inventor Version: | 2017 (Build 210142000, 142) |
| Creation Date: | 4/27/2017, 12:23 PM |
| Study Author: | henrikwn |
| Summary: | |

---

## ⊟ Project Info (iProperties)

### ⊟ Summary

| | |
|---|---|
| Title | |
| Author | henrikwn |

### ⊟ Project

| | |
|---|---|
| Designer | henrikwn |

### ⊟ Physical

| | |
|---|---|
| Mass | 182983 kg |
| Area | 3.56846E+09 mm^2 |
| Volume | 6.09185E+10 mm^3 |
| Center of Gravity | x=-41359.7 mm<br>y=-19499.7 mm<br>z=32758.2 mm |

Note: Physical values could be different from Physical values used by FEA reported below.

---

## ⊟ Case-C

**General objective and settings:**

| | |
|---|---|
| Design Objective | Single Point |
| Study Type | Static Analysis |
| Last Modification Date | 4/27/2017, 12:15 PM |
| Detect and Eliminate Rigid Body Modes | No |
| Separate Stresses Across Contact Surfaces | No |
| Motion Loads Analysis | No |

## ⊟ Operating conditions

## ⊟ Force:1

| | |
|---|---|
| Load Type | Force |
| Magnitude | 1000000.000 N |
| Vector X | 936001.935 N |
| Vector Y | -341194.991 N |
| Vector Z | -86523.732 N |

⊟ **Selected Face(s)**

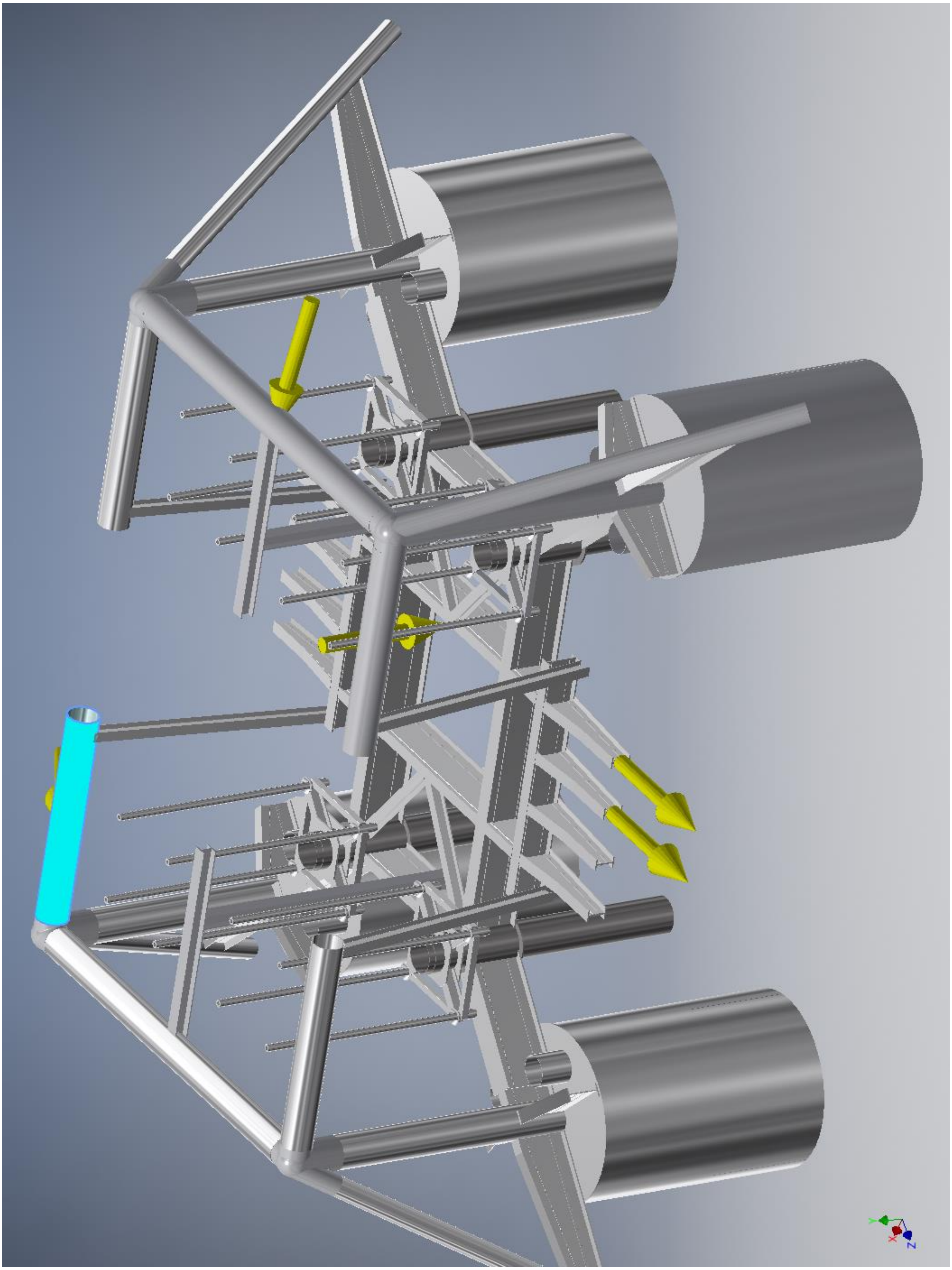

## ⊟ Force:2

| | |
|---|---|
| Load Type | Force |
| Magnitude | 1000000.000 N |
| Vector X | 319421.899 N |
| Vector Y | 439526.628 N |
| Vector Z | 839515.333 N |

### ⊟ Selected Face(s)

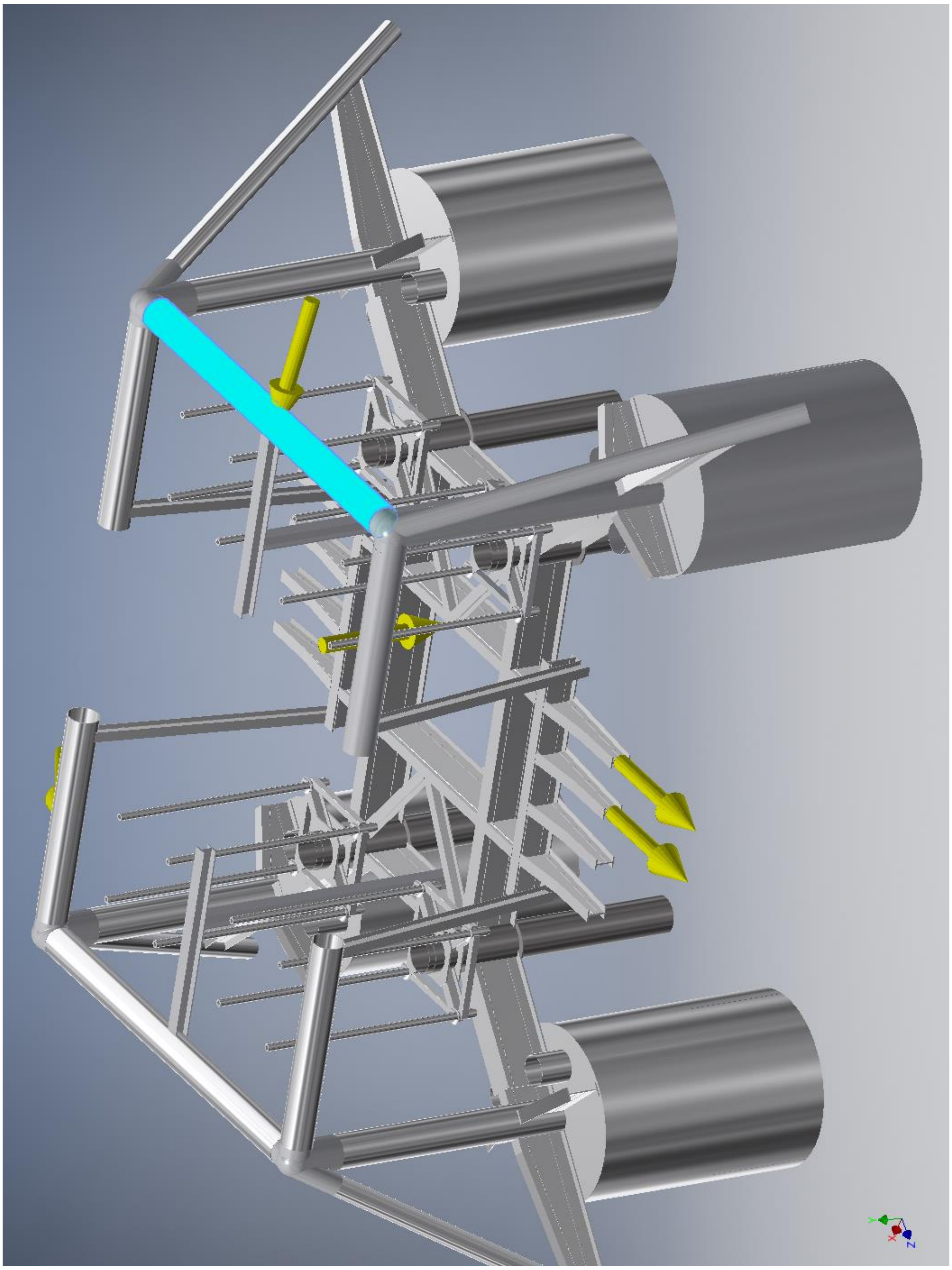

## ⊟ Force:3

| | |
|---|---|
| Load Type | Force |
| Magnitude | 80000.000 N |
| Vector X | -57568.709 N |
| Vector Y | -45668.912 N |
| Vector Z | 31625.847 N |

### ⊟ Selected Face(s)

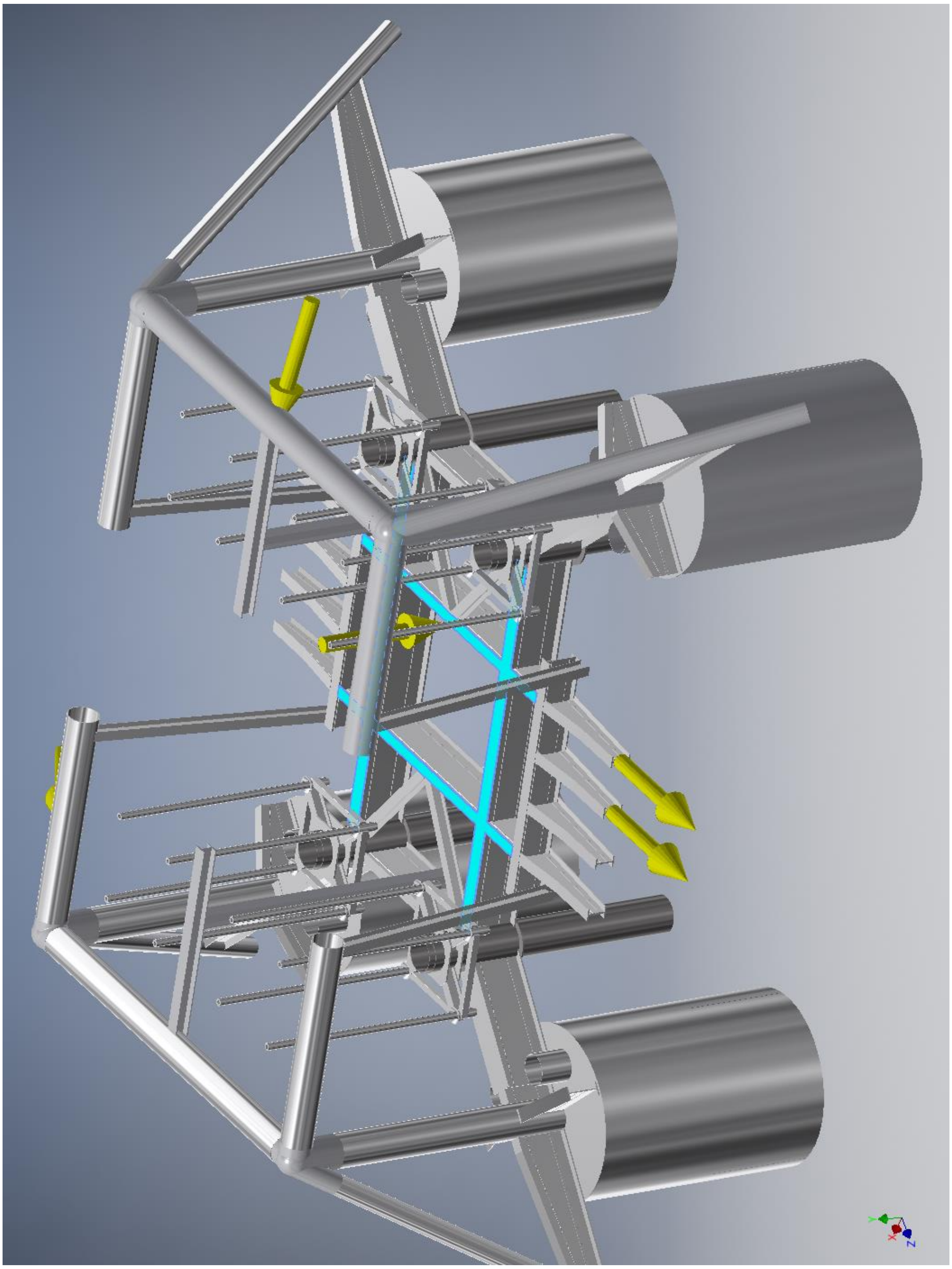

## ⊟ Force:4

| | |
|---|---|
| Load Type | Force |
| Magnitude | 300000.000 N |
| Vector X | 198108.677 N |
| Vector Y | -221589.070 N |
| Vector Z | 40635.406 N |

### ⊟ Selected Face(s)

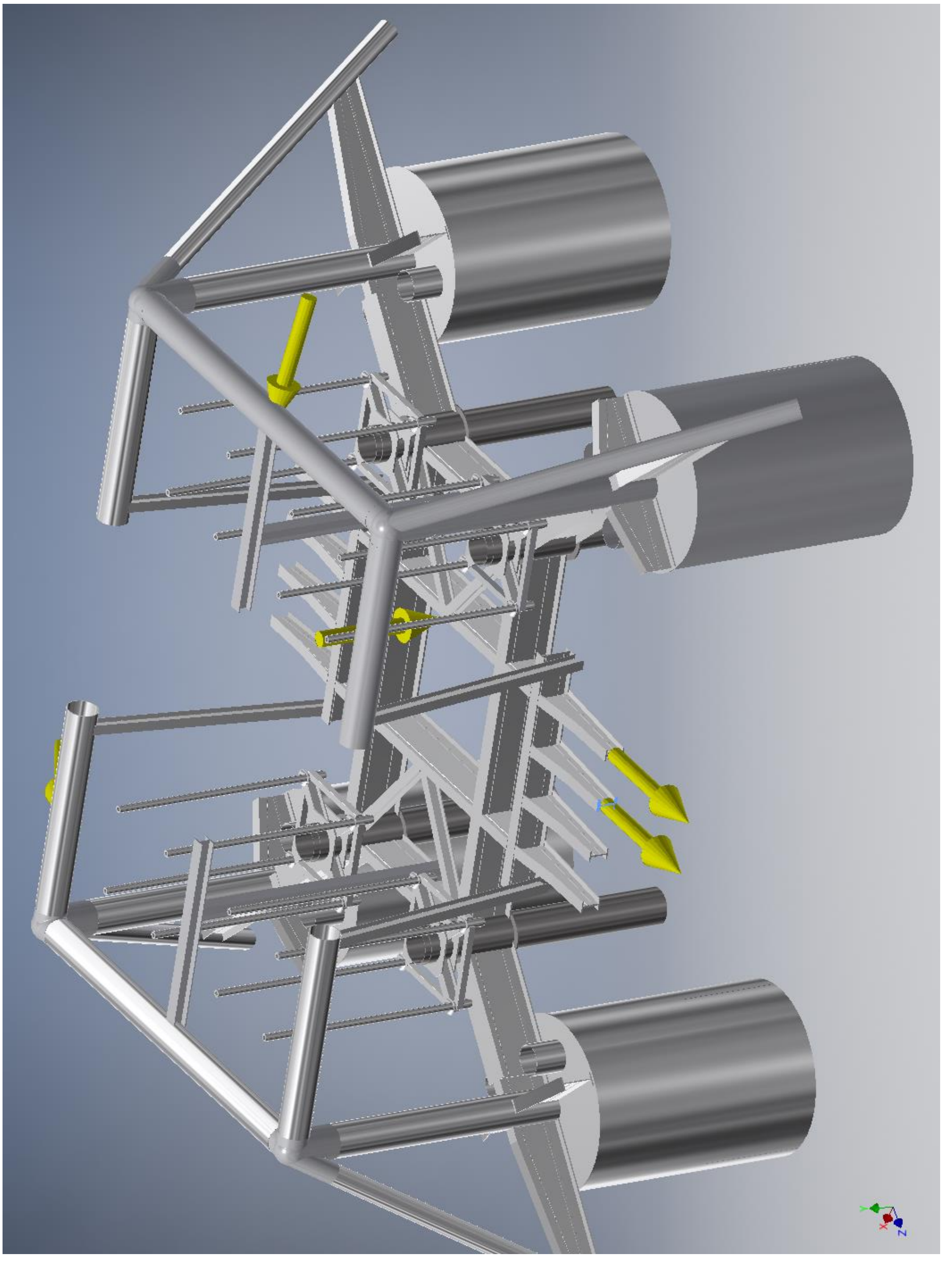

## ⊟ Force:5

| | |
|---|---|
| Load Type | Force |
| Magnitude | 300000.000 N |
| Vector X | 198108.677 N |
| Vector Y | -221589.070 N |
| Vector Z | 40635.406 N |

### ⊟ Selected Face(s)

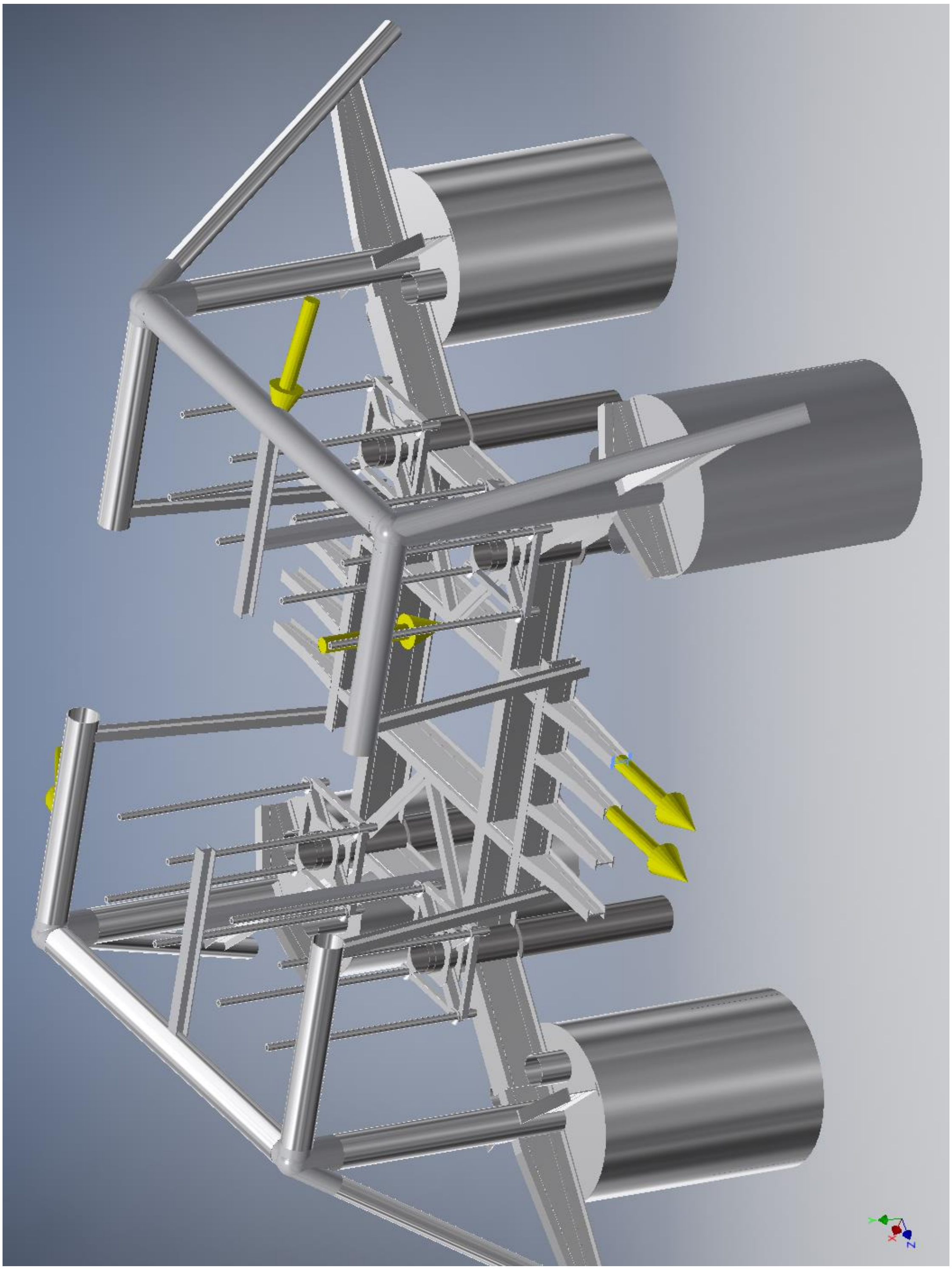

## ⊟ Fixed Constraint:1

| Constraint Type | Fixed Constraint |
| --- | --- |

### ⊟ Selected Face(s)

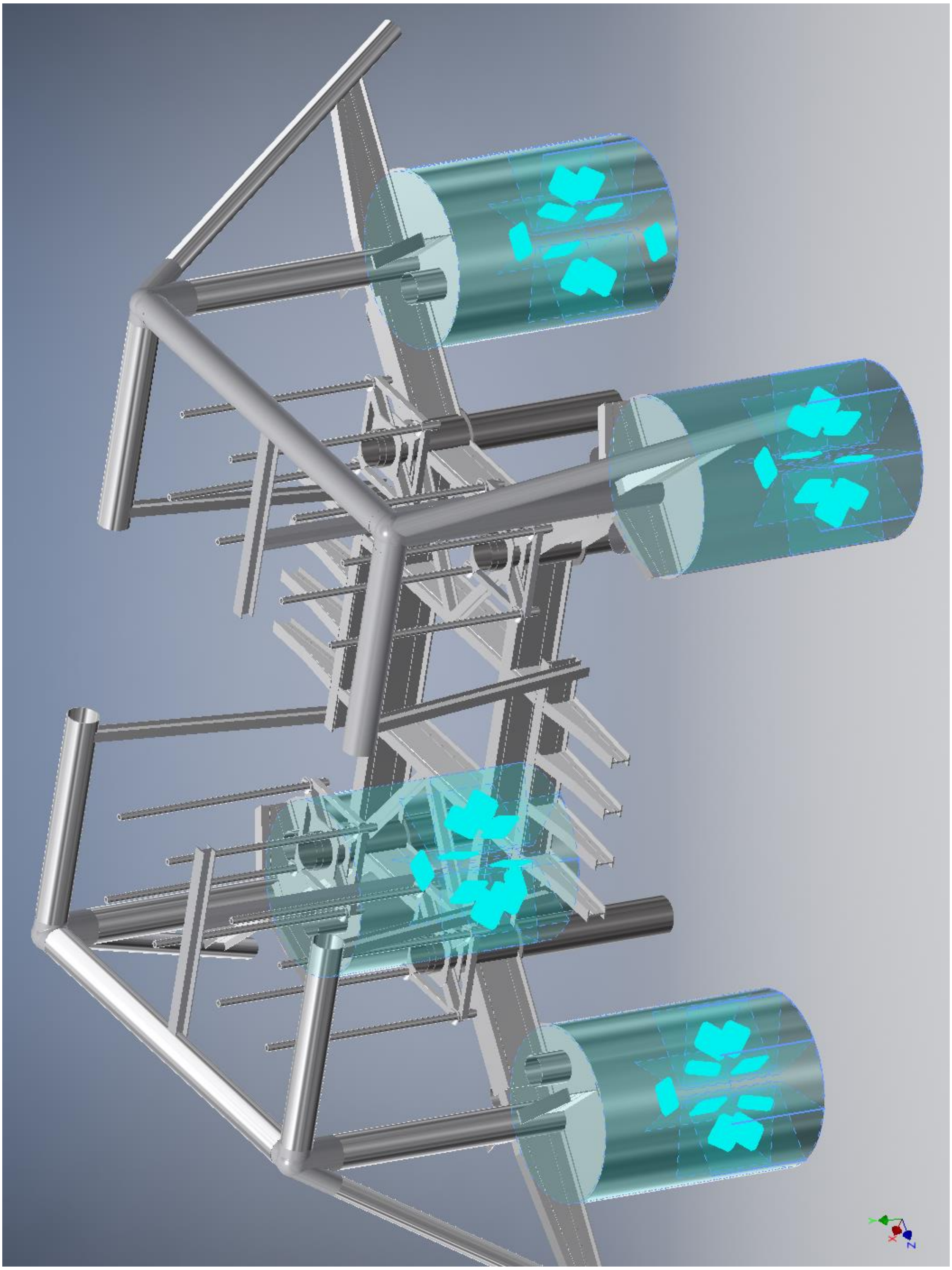

## ⊟ Results

### ⊟ Reaction Force and Moment on Constraints

| Constraint Name | Reaction Force | | Reaction Moment | |
|---|---|---|---|---|
| | Magnitude | Component (X,Y,Z) | Magnitude | Component (X,Y,Z) |
| Fixed Constraint:1 | 1855620 N | -1594070 N | 20742400 N m | -6426080 N m |
| | | 390515 N | | 11683200 N m |
| | | -865888 N | | 15888900 N m |

### ⊟ Result Summary

| Name | Minimum | Maximum |
|---|---|---|
| Volume | 6.09185E+10 mm^3 | |
| Mass | 182983 kg | |
| Von Mises Stress | 0 MPa | 368.035 MPa |
| 1st Principal Stress | -103.538 MPa | 457.664 MPa |
| 3rd Principal Stress | -464.726 MPa | 113.157 MPa |
| Displacement | 0 mm | 244.38 mm |
| Safety Factor | 0.588644 ul | 15 ul |

### ⊟ Figures

### ⊟ Von Mises Stress

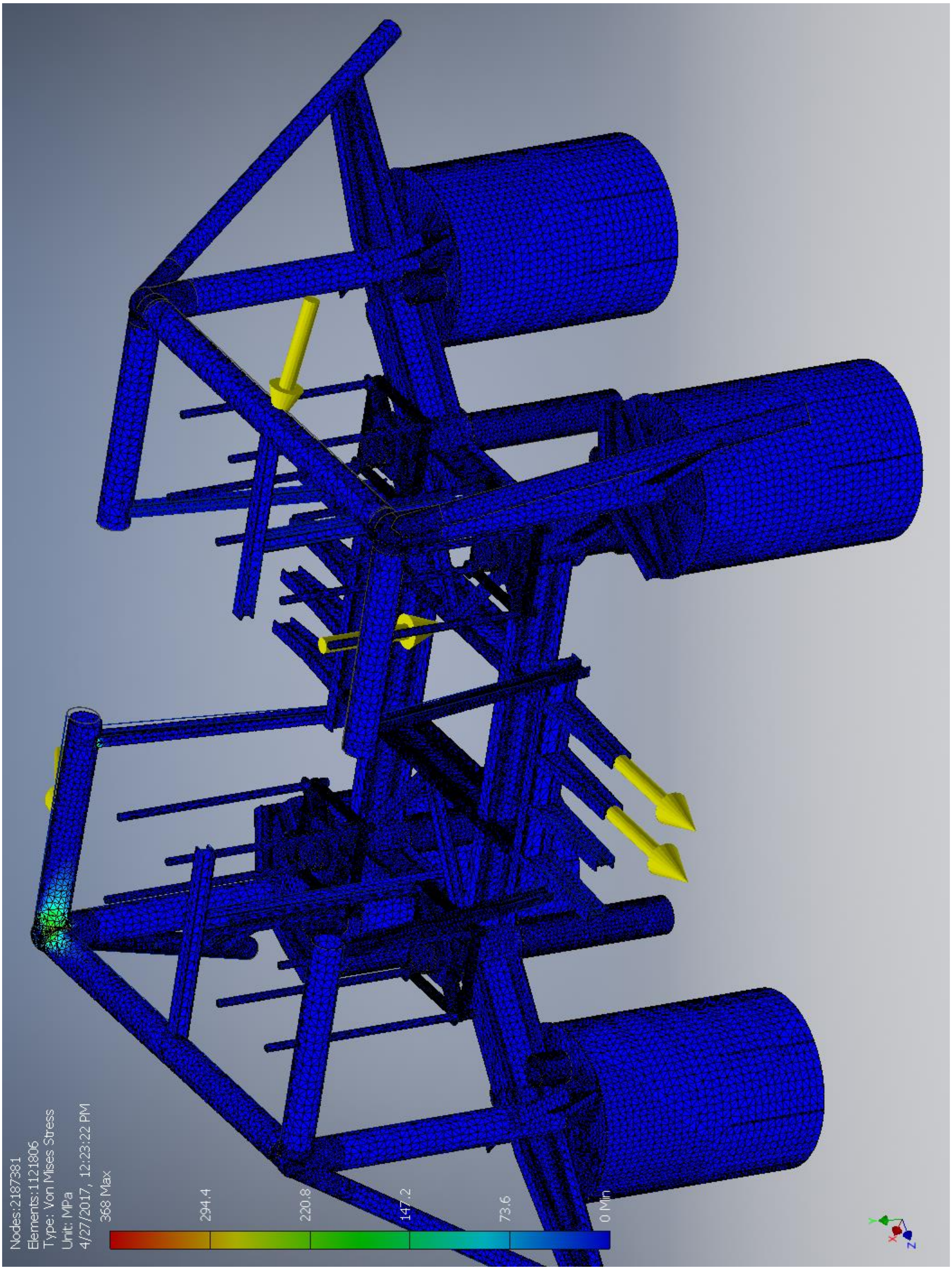

## ⊟ 1st Principal Stress

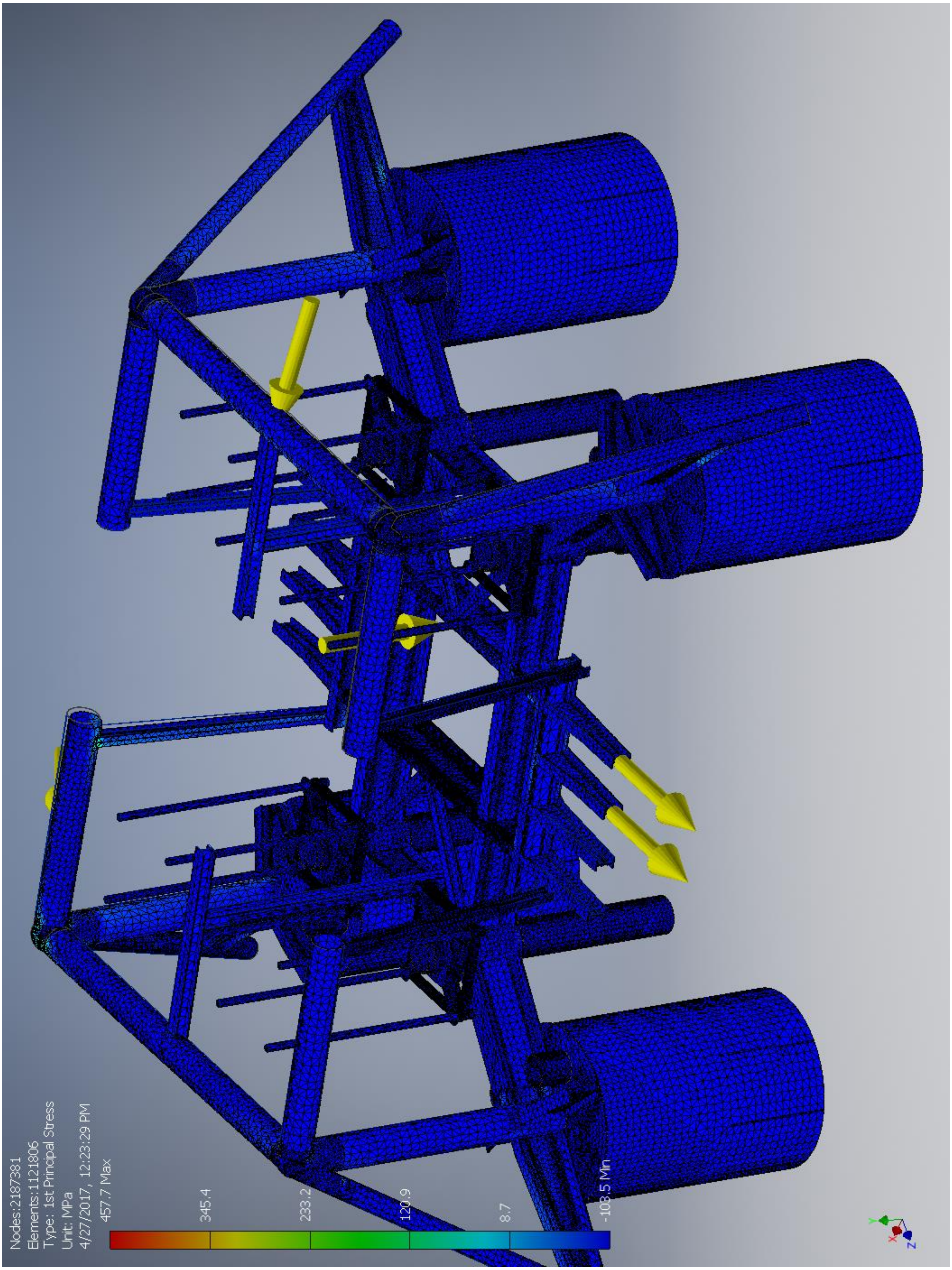

## ⊟ 3rd Principal Stress

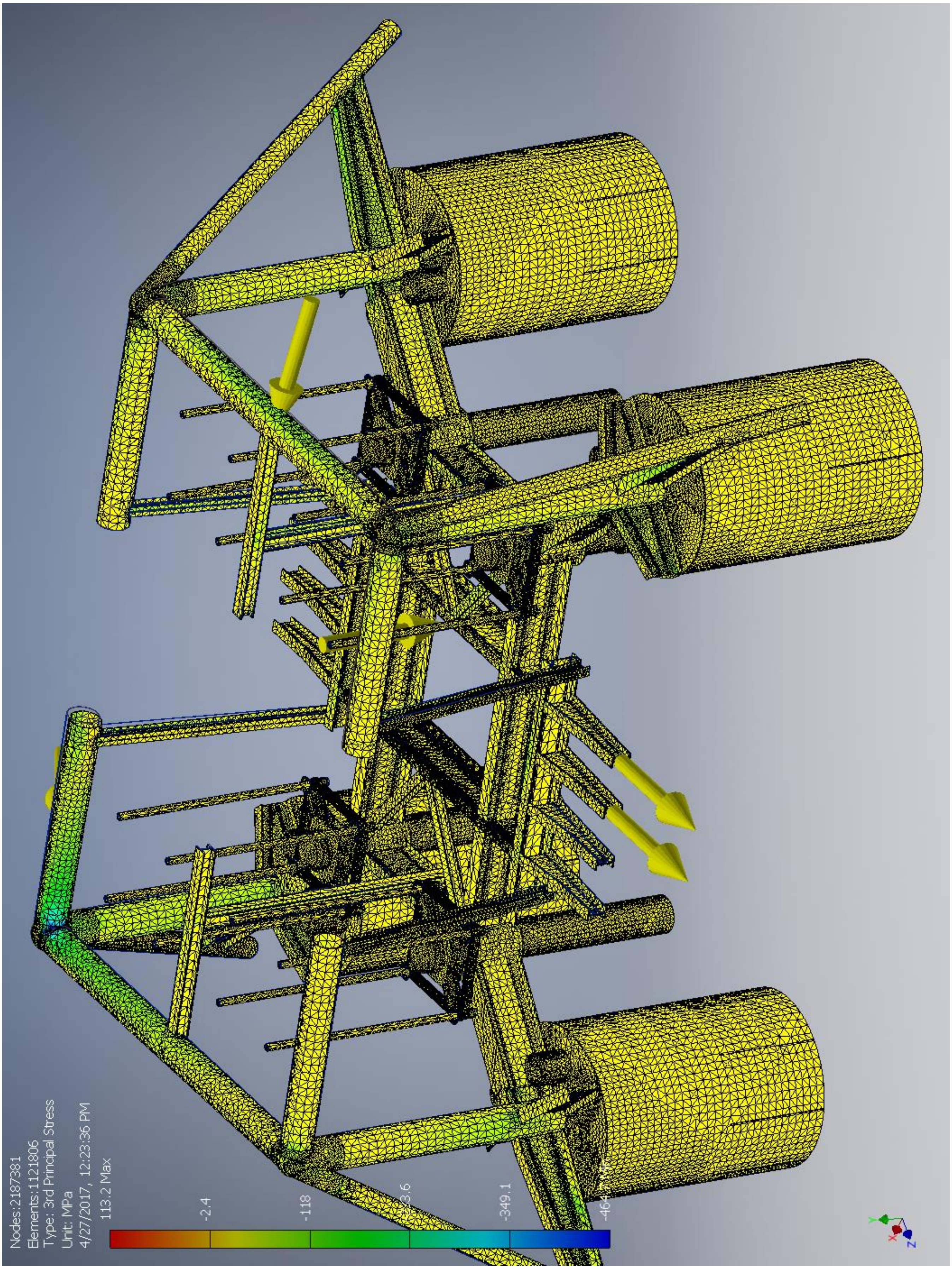

⊟ **Displacement**

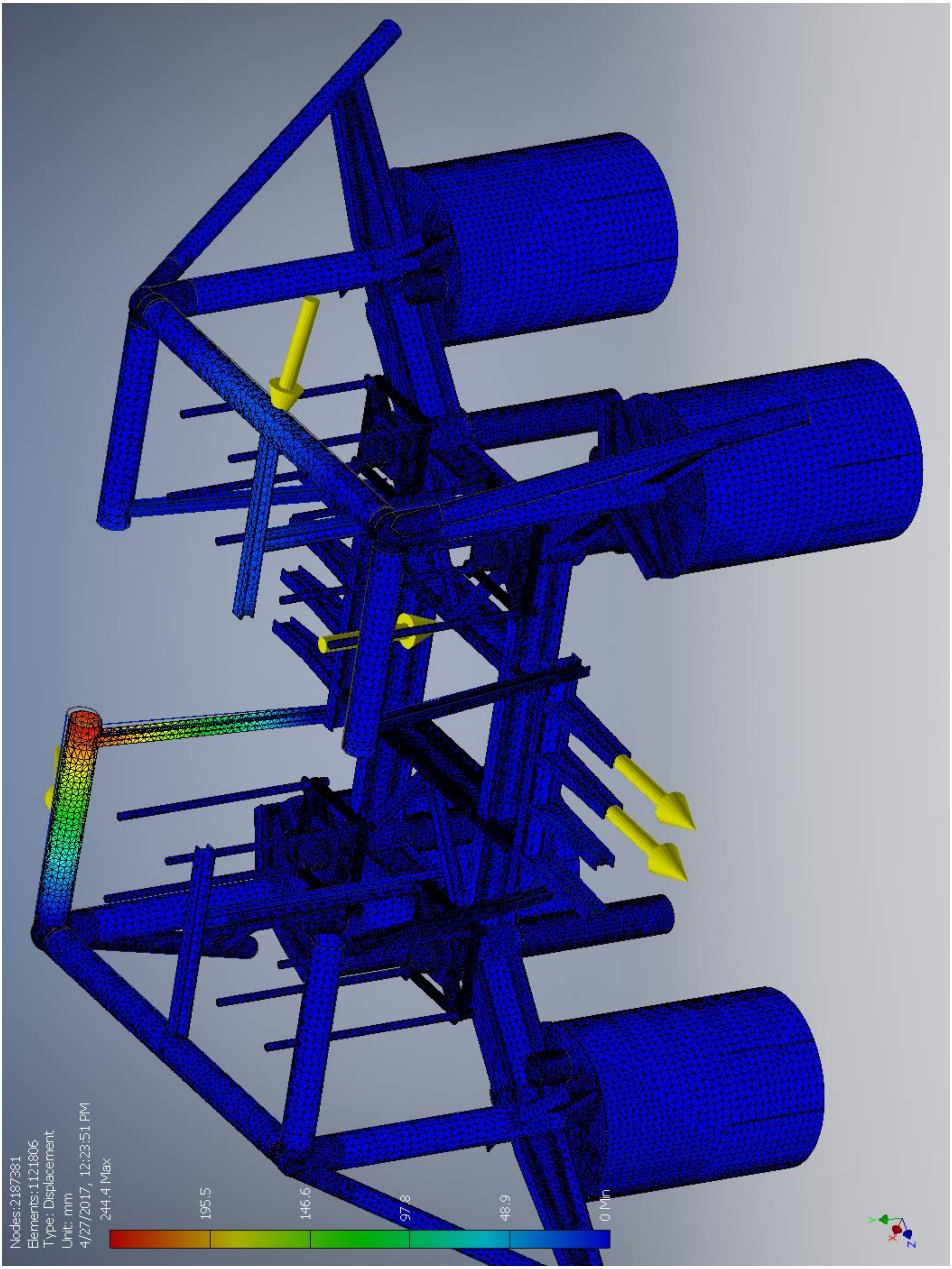

## ⊟ Safety Factor

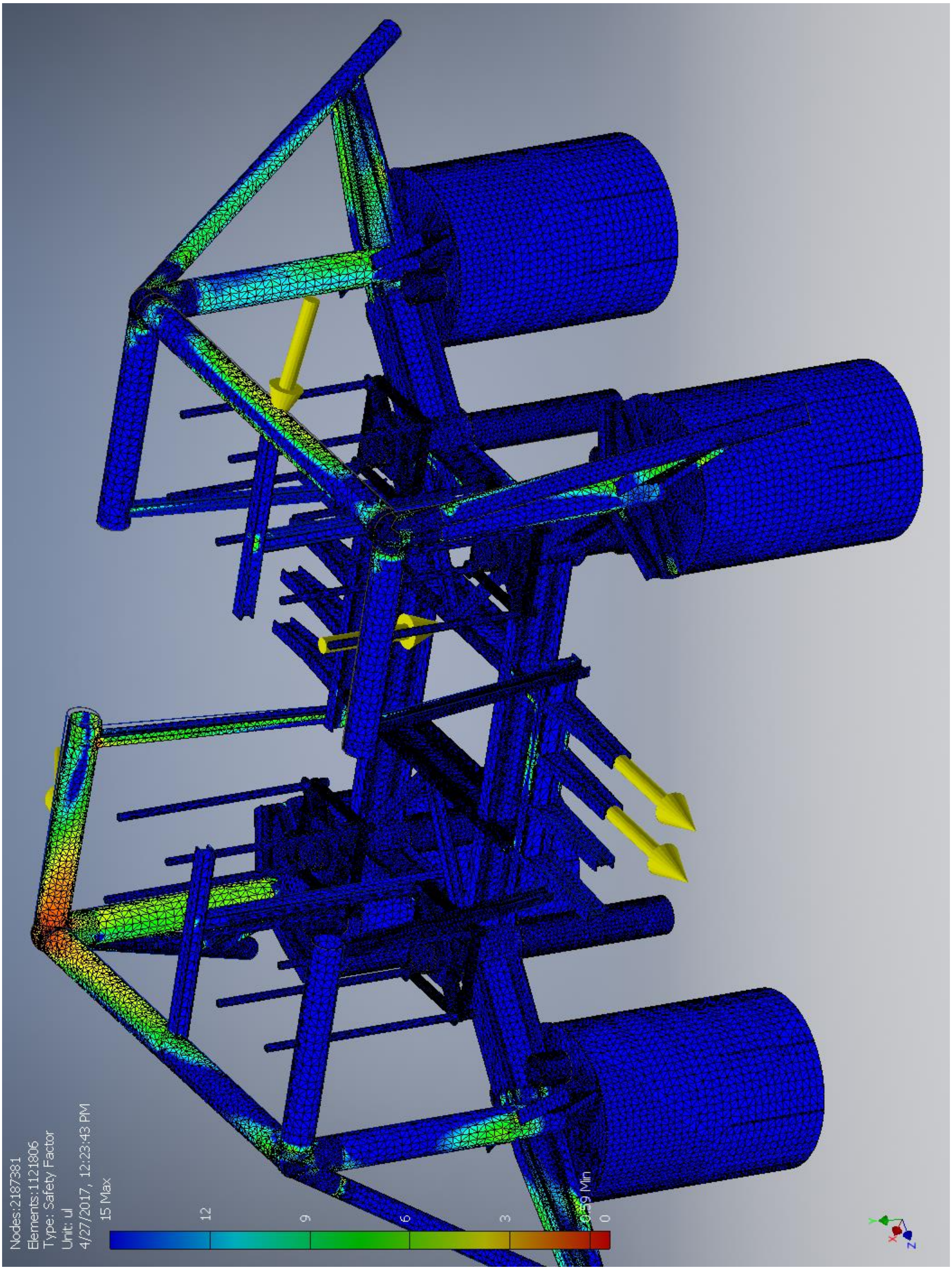

### I.3.2 With convergence on top corner

# Stress Analysis Report

| | |
|---|---|
| Analyzed File: | Assembly.iam |
| Autodesk Inventor Version: | 2017 (Build 210142000, 142) |
| Creation Date: | 4/27/2017, 12:03 PM |
| Study Author: | henrikwn |
| Summary: | |

## ⊟ Project Info (iProperties)

### ⊟ Summary

| | |
|---|---|
| Title | |
| Author | henrikwn |

### ⊟ Project

| | |
|---|---|
| Designer | henrikwn |

### ⊟ Physical

| | |
|---|---|
| Mass | 182983 kg |
| Area | 3.56846E+09 mm^2 |
| Volume | 6.09185E+10 mm^3 |
| Center of Gravity | x=-41359.7 mm<br>y=-19499.7 mm<br>z=32758.2 mm |

Note: Physical values could be different from Physical values used by FEA reported below.

## ⊟ Case-C

**General objective and settings:**

| | |
|---|---|
| Design Objective | Single Point |
| Study Type | Static Analysis |
| Last Modification Date | 4/27/2017, 11:50 AM |
| Detect and Eliminate Rigid Body Modes | No |
| Separate Stresses Across Contact Surfaces | No |
| Motion Loads Analysis | No |

## ⊟ Operating conditions

## ⊟ Force:1

| | |
|---|---|
| Load Type | Force |
| Magnitude | 1000000.000 N |
| Vector X | 936001.935 N |
| Vector Y | -341194.991 N |
| Vector Z | -86523.732 N |

### ⊟ Selected Face(s)

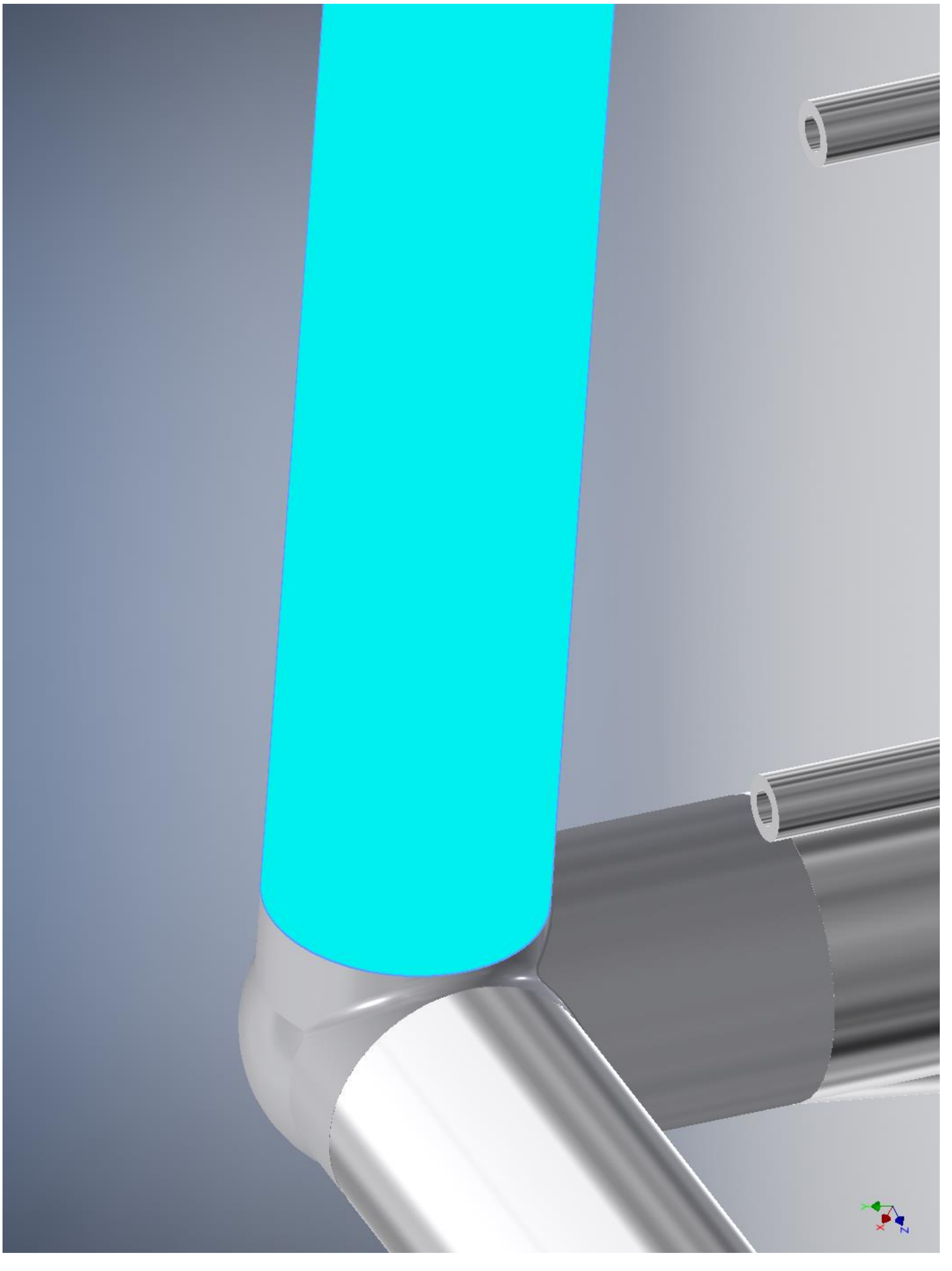

## ⊟ Force:2

| | |
|---|---|
| Load Type | Force |
| Magnitude | 1000000.000 N |
| Vector X | 319421.899 N |
| Vector Y | 439526.628 N |
| Vector Z | 839515.333 N |

### ⊟ Selected Face(s)

## ⊟ Force:3

| | |
|---|---|
| Load Type | Force |
| Magnitude | 80000.000 N |
| Vector X | -57568.709 N |
| Vector Y | -45668.912 N |
| Vector Z | 31625.847 N |

### ⊟ Selected Face(s)

## ⊟ Force:4

| | |
|---|---|
| Load Type | Force |
| Magnitude | 300000.000 N |
| Vector X | 198108.677 N |
| Vector Y | -221589.070 N |
| Vector Z | 40635.406 N |

### ⊟ Selected Face(s)

## ⊟ Force:5

| | |
|---|---|
| Load Type | Force |
| Magnitude | 300000.000 N |
| Vector X | 198108.677 N |
| Vector Y | -221589.070 N |
| Vector Z | 40635.406 N |

### ⊟ Selected Face(s)

## ⊟ Fixed Constraint:1

| | |
|---|---|
| Constraint Type | Fixed Constraint |

### ⊟ Selected Face(s)

## ⊟ Results

### ⊟ Reaction Force and Moment on Constraints

| Constraint Name | Reaction Force | | Reaction Moment | |
|---|---|---|---|---|
| | Magnitude | Component (X,Y,Z) | Magnitude | Component (X,Y,Z) |
| Fixed Constraint:1 | 1855620 N | -1594070 N | 20792300 N m | -6465650 N m |
| | | 390515 N | | 11709100 N m |
| | | -865888 N | | 15918900 N m |

### ⊟ Result Summary

| Name | Minimum | Maximum |
|---|---|---|
| Volume | 6.09185E+10 mm^3 | |
| Mass | 182983 kg | |
| Von Mises Stress | 0 MPa | 483.624 MPa |
| 1st Principal Stress | -97.5239 MPa | 589.698 MPa |
| 3rd Principal Stress | -575.036 MPa | 133.04 MPa |
| Displacement | 0 mm | 245.483 mm |
| Safety Factor | 0.444559 ul | 15 ul |

### ⊟ Figures

## ⊟ Von Mises Stress

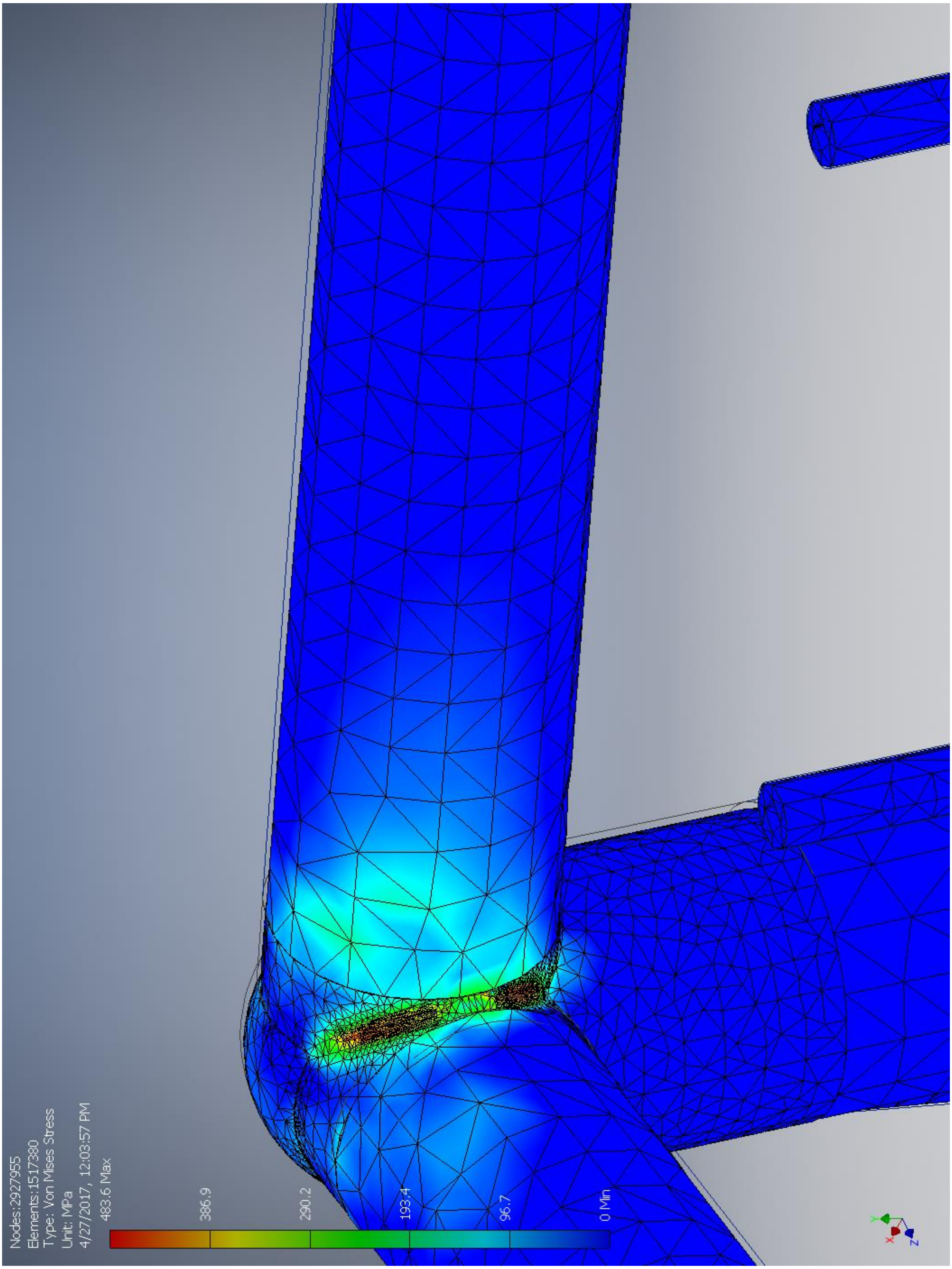

⊟ **1st Principal Stress**

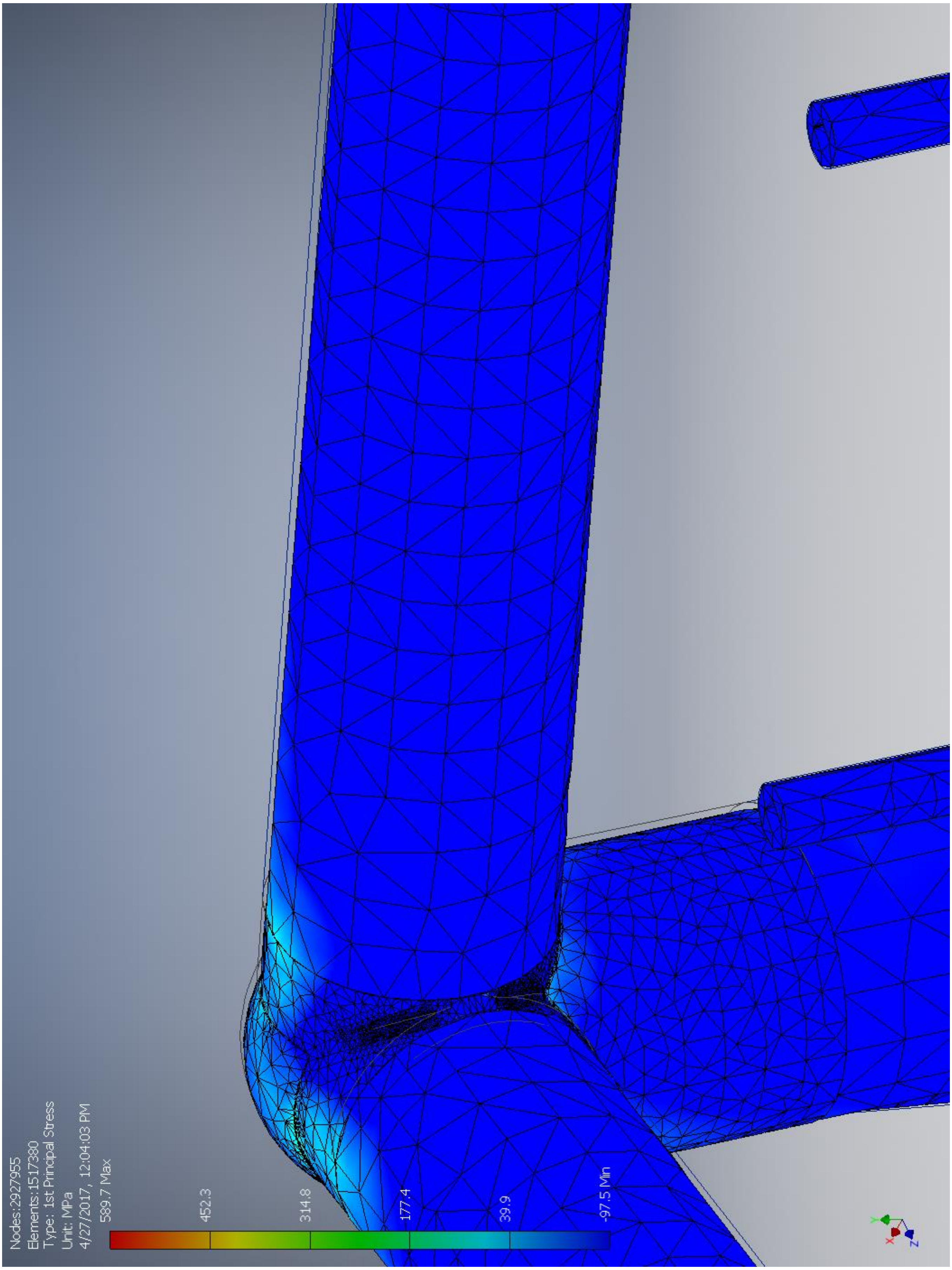

### ⊟ 3rd Principal Stress

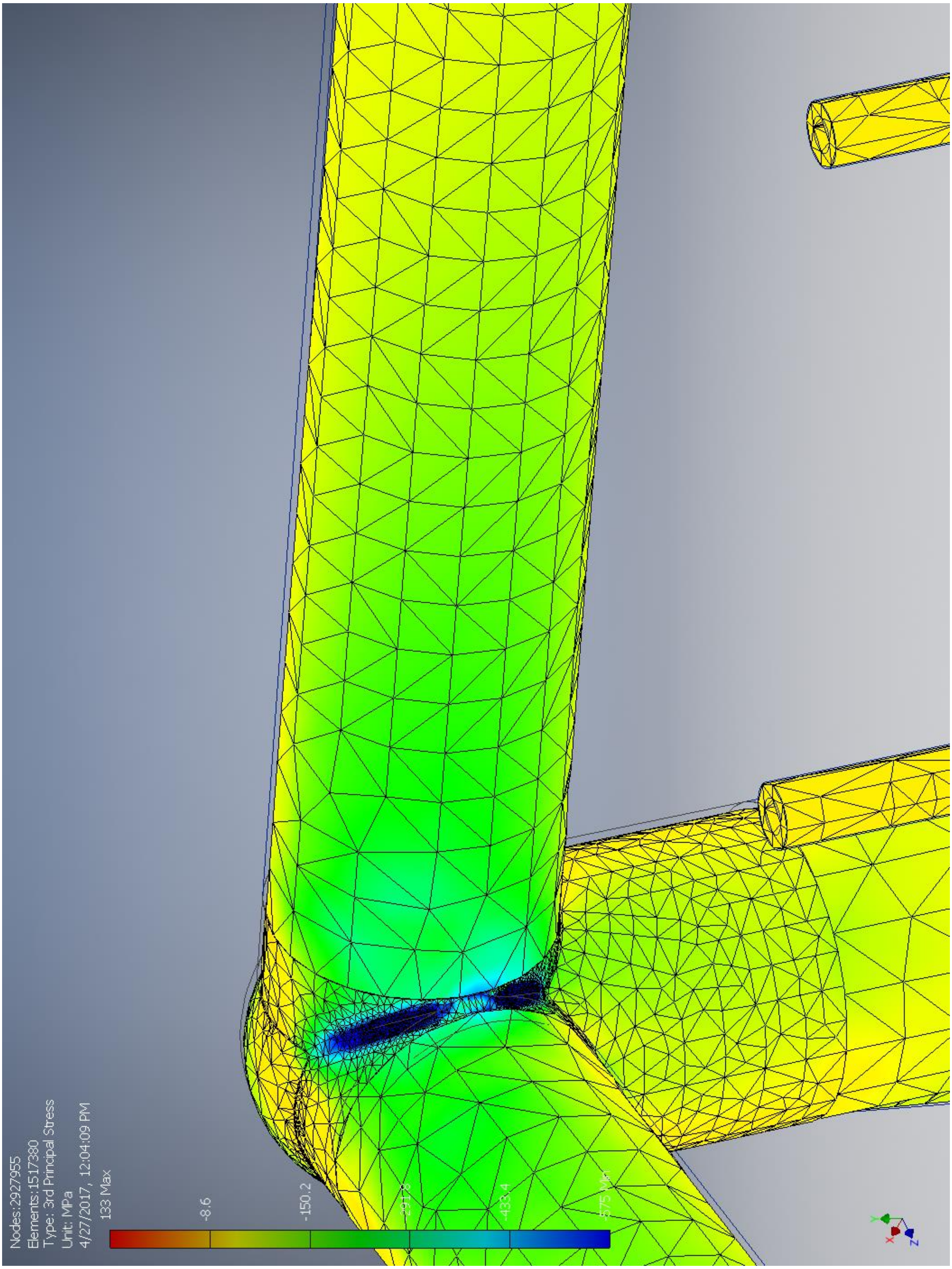

## Displacement

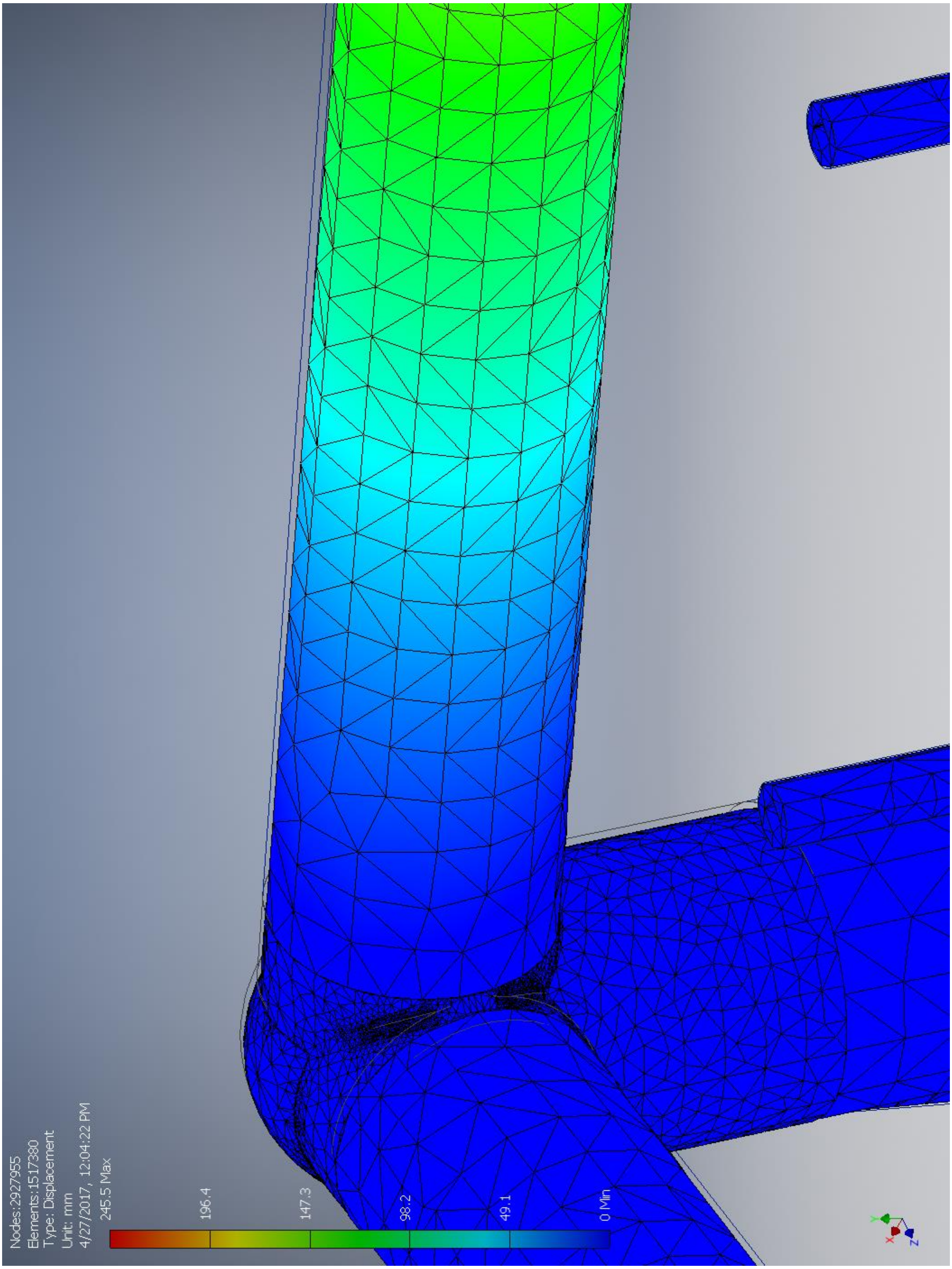

## ⊟ Safety Factor

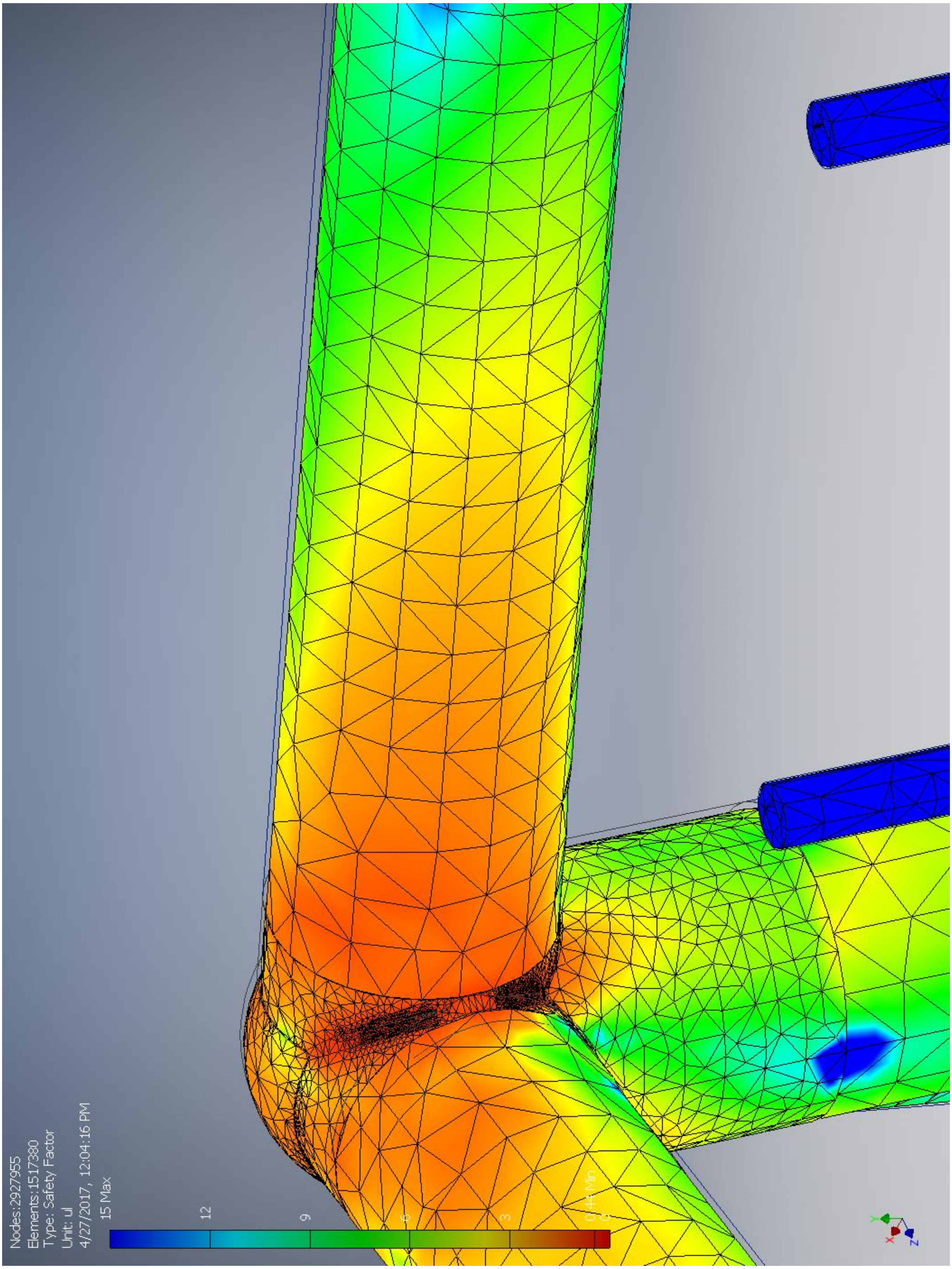

### I.3.3 With convergence on support beam

# Stress Analysis Report

| | |
|---|---|
| Analyzed File: | Assembly.iam |
| Autodesk Inventor Version: | 2017 (Build 210142000, 142) |
| Creation Date: | 4/27/2017, 11:57 AM |
| Study Author: | henrikwn |
| Summary: | |

---

## ⊟ Project Info (iProperties)

### ⊟ Summary

| | |
|---|---|
| Title | |
| Author | henrikwn |

### ⊟ Project

| | |
|---|---|
| Designer | henrikwn |

### ⊟ Physical

| | |
|---|---|
| Mass | 182983 kg |
| Area | 3.56846E+09 mm^2 |
| Volume | 6.09185E+10 mm^3 |
| Center of Gravity | x=-41359.7 mm<br>y=-19499.7 mm<br>z=32758.2 mm |

Note: Physical values could be different from Physical values used by FEA reported below.

---

## ⊟ Case-C

**General objective and settings:**

| | |
|---|---|
| Design Objective | Single Point |
| Study Type | Static Analysis |
| Last Modification Date | 4/27/2017, 11:50 AM |
| Detect and Eliminate Rigid Body Modes | No |
| Separate Stresses Across Contact Surfaces | No |
| Motion Loads Analysis | No |

### ⊟ Operating conditions

## ⊟ Force:1

| | |
|---|---|
| Load Type | Force |
| Magnitude | 1000000.000 N |
| Vector X | 936001.935 N |
| Vector Y | -341194.991 N |
| Vector Z | -86523.732 N |

### ⊟ Selected Face(s)

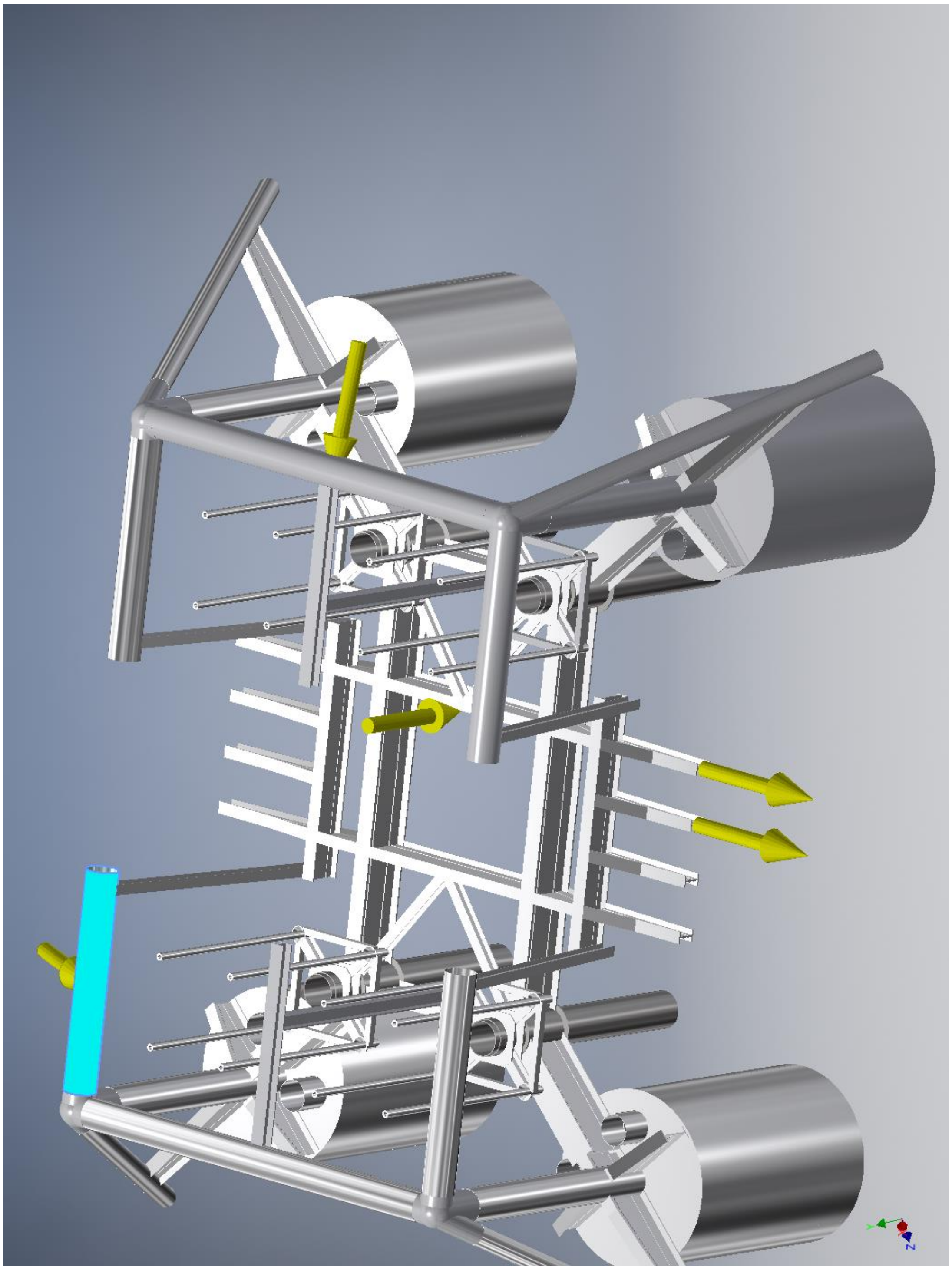

## ⊟ Force:2

| | |
|---|---|
| Load Type | Force |
| Magnitude | 1000000.000 N |
| Vector X | 319421.899 N |
| Vector Y | 439526.628 N |
| Vector Z | 839515.333 N |

### ⊟ Selected Face(s)

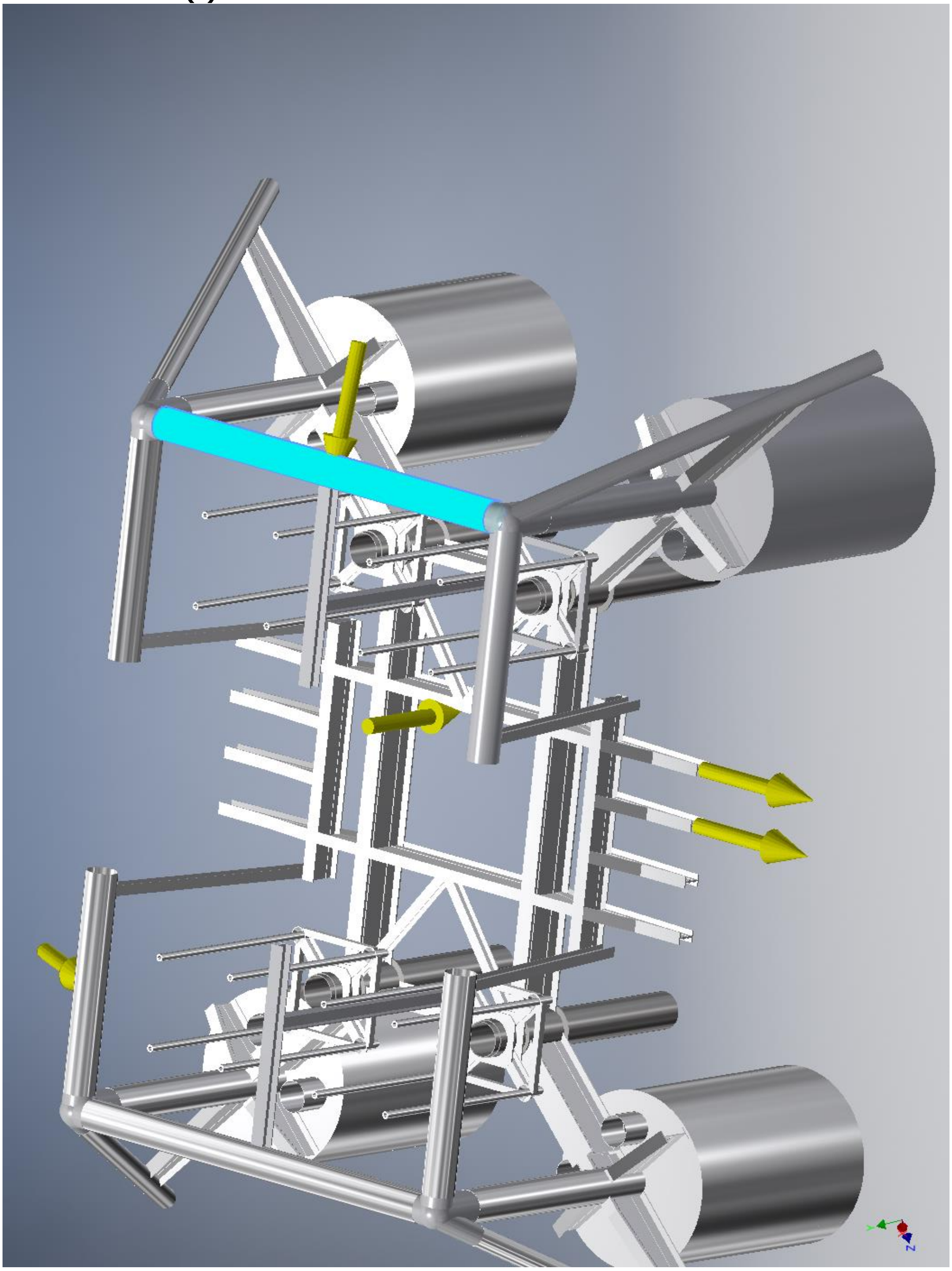

## Force:3

| Load Type | Force |
|---|---|
| Magnitude | 80000.000 N |
| Vector X | -57568.709 N |
| Vector Y | -45668.912 N |
| Vector Z | 31625.847 N |

### Selected Face(s)

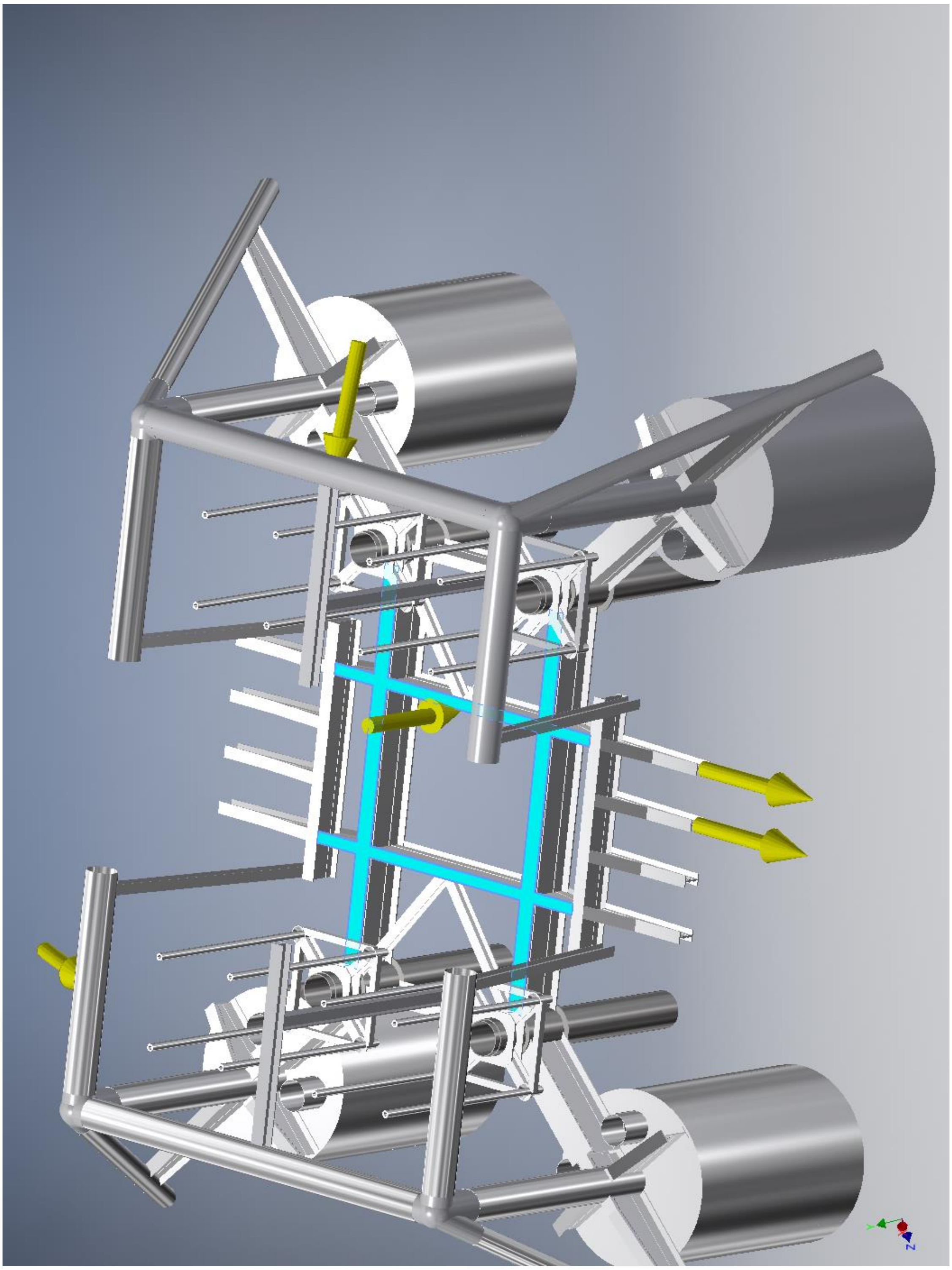

## ⊟ Force:4

| Load Type | Force |
|---|---|
| Magnitude | 300000.000 N |
| Vector X | 198108.677 N |
| Vector Y | -221589.070 N |
| Vector Z | 40635.406 N |

### ⊟ Selected Face(s)

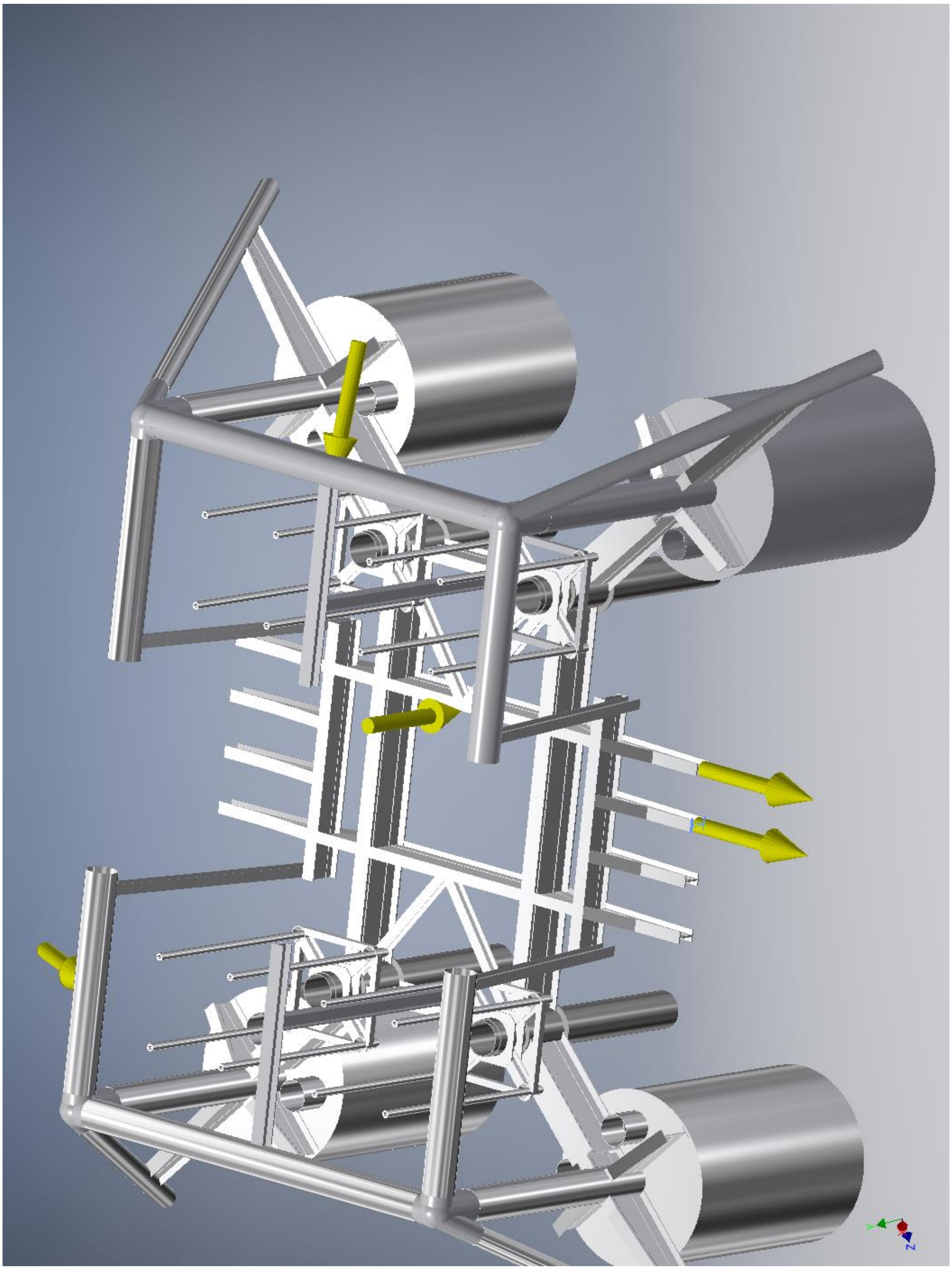

## ⊟ Force:5

| | |
|---|---|
| Load Type | Force |
| Magnitude | 300000.000 N |
| Vector X | 198108.677 N |
| Vector Y | -221589.070 N |
| Vector Z | 40635.406 N |

### ⊟ Selected Face(s)

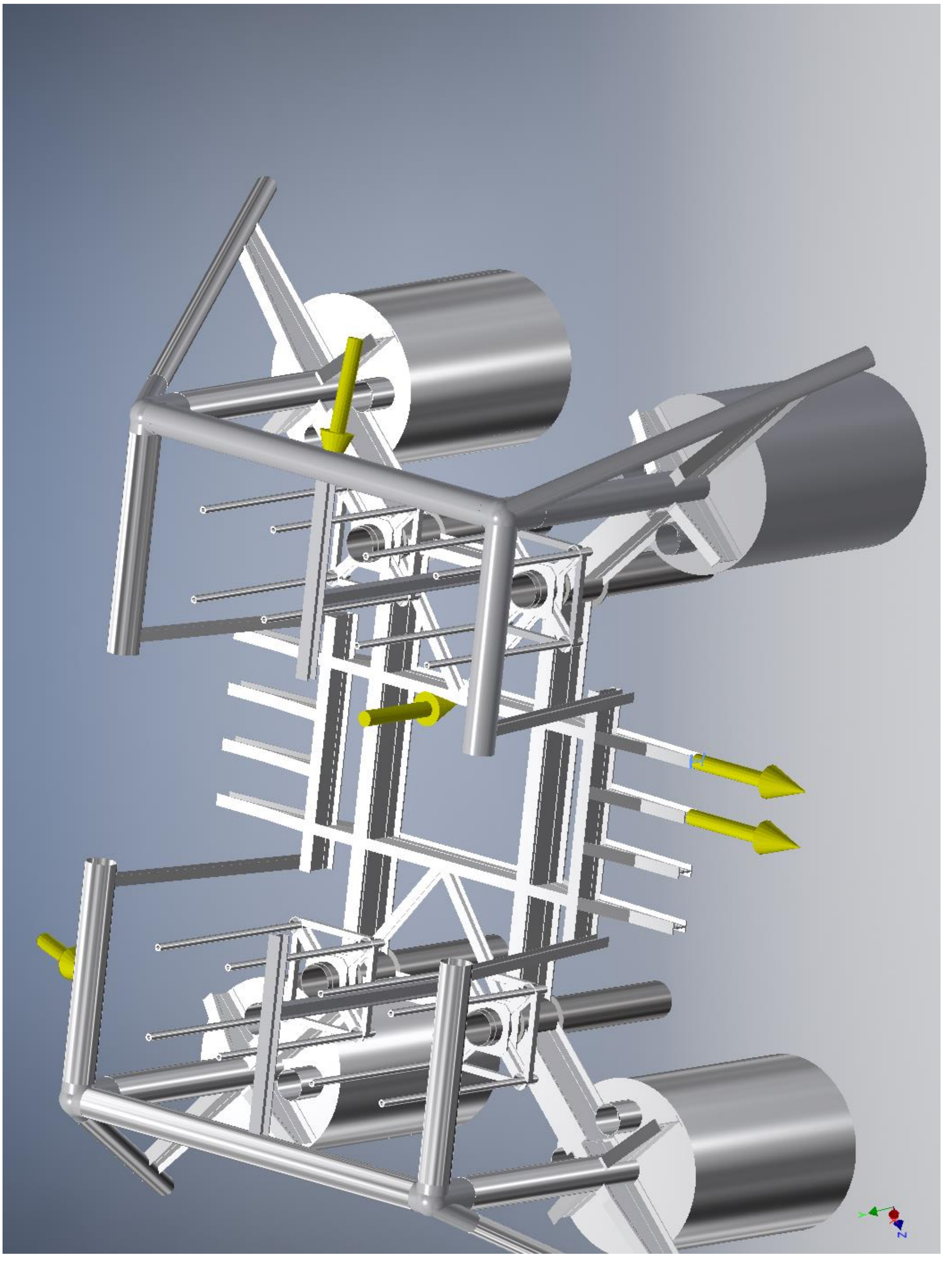

## ⊟ Fixed Constraint:1

| | |
|---|---|
| Constraint Type | Fixed Constraint |

### ⊟ Selected Face(s)

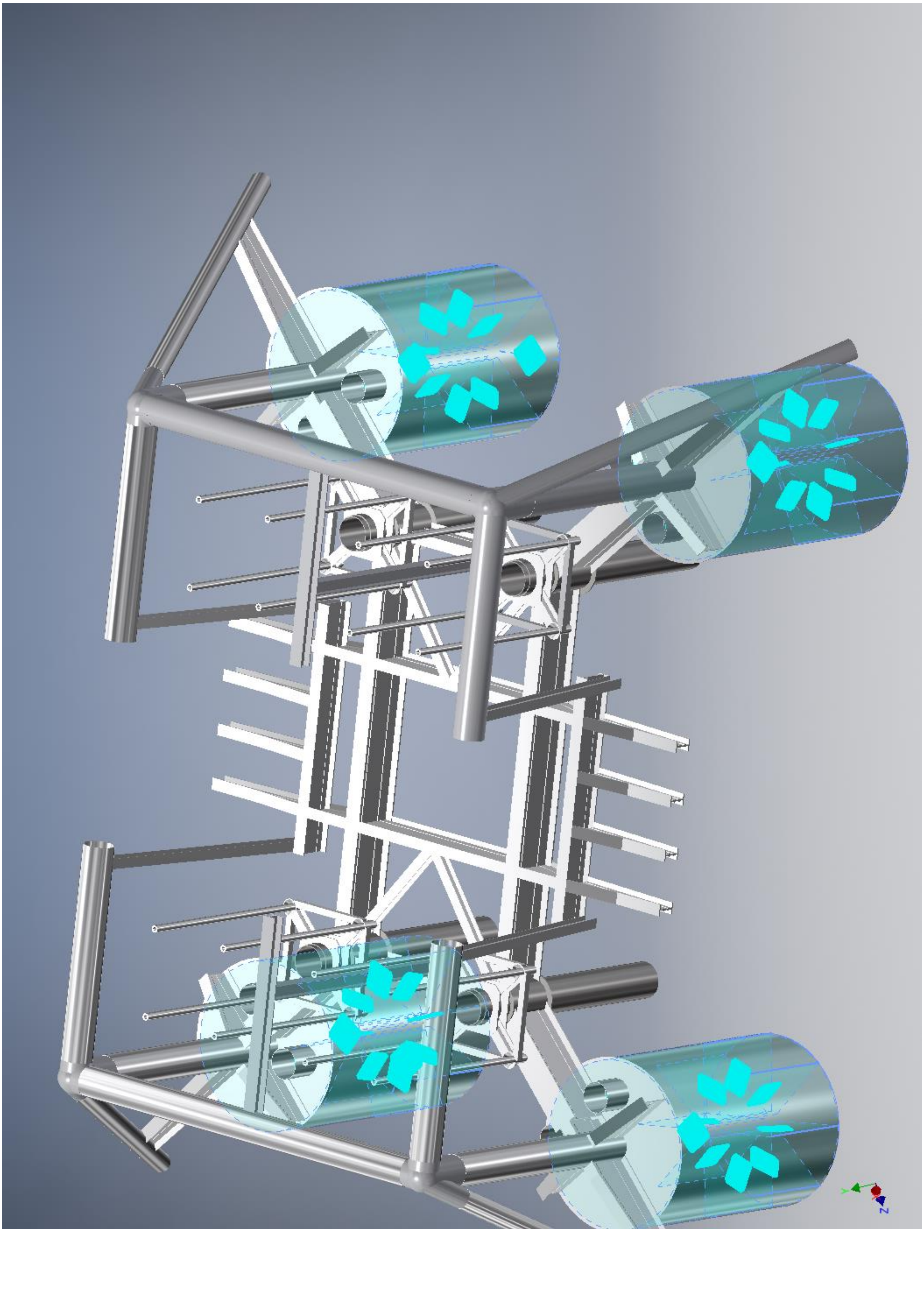

# ⊟ Results

## ⊟ Reaction Force and Moment on Constraints

| Constraint Name | Reaction Force | | Reaction Moment | |
|---|---|---|---|---|
| | Magnitude | Component (X,Y,Z) | Magnitude | Component (X,Y,Z) |
| Fixed Constraint:1 | 1855620 N | -1594070 N | 20792300 N m | -6465650 N m |
| | | 390515 N | | 11709100 N m |
| | | -865888 N | | 15918900 N m |

## ⊟ Result Summary

| Name | Minimum | Maximum |
|---|---|---|
| Volume | 6.09185E+10 mm^3 | |
| Mass | 182983 kg | |
| Von Mises Stress | 0 MPa | 483.624 MPa |
| 1st Principal Stress | -97.5239 MPa | 589.698 MPa |
| 3rd Principal Stress | -575.036 MPa | 133.04 MPa |
| Displacement | 0 mm | 245.483 mm |
| Safety Factor | 0.444559 ul | 15 ul |

## ⊟ Figures

## ⊟ Von Mises Stress

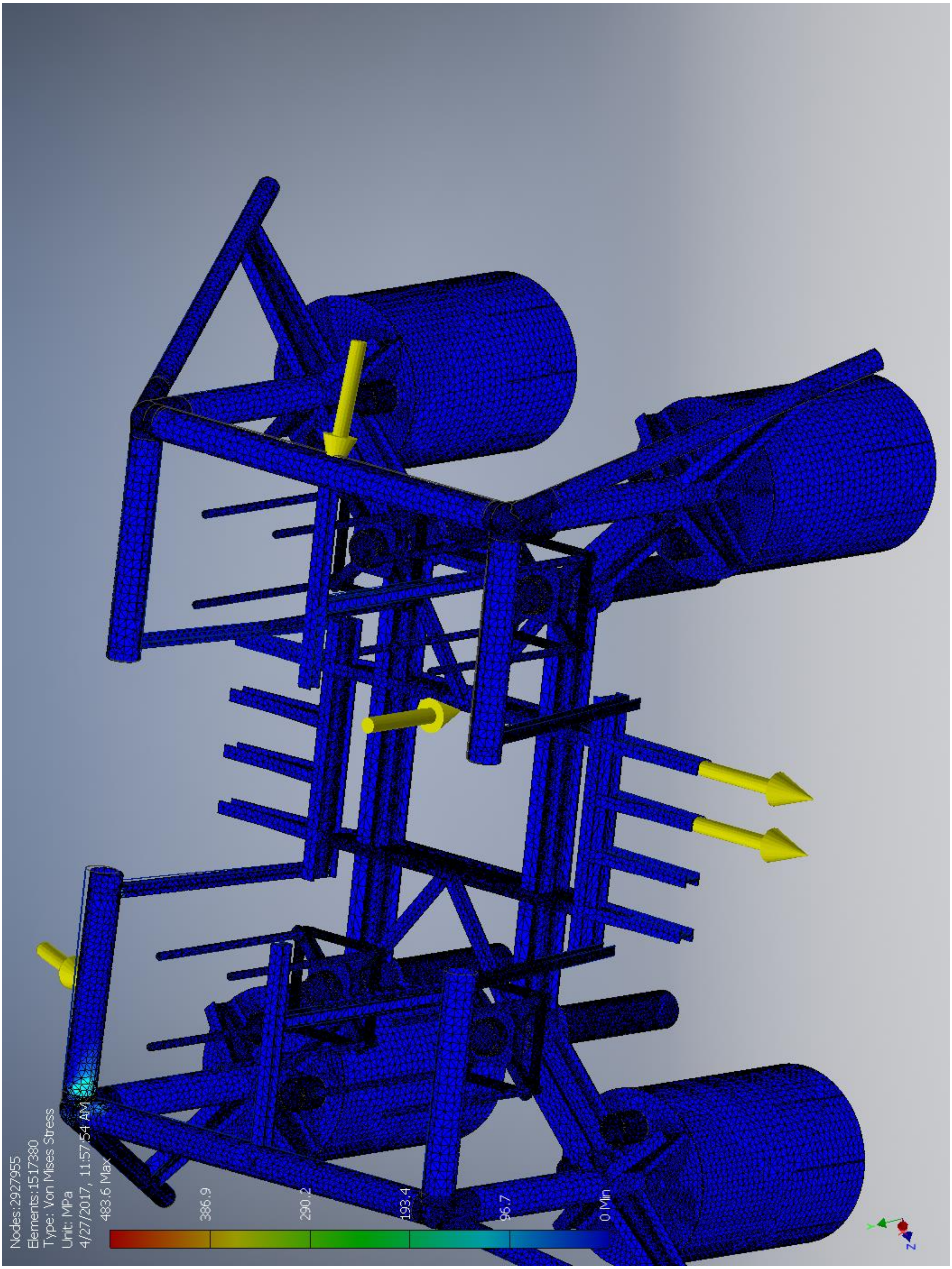

## 1st Principal Stress

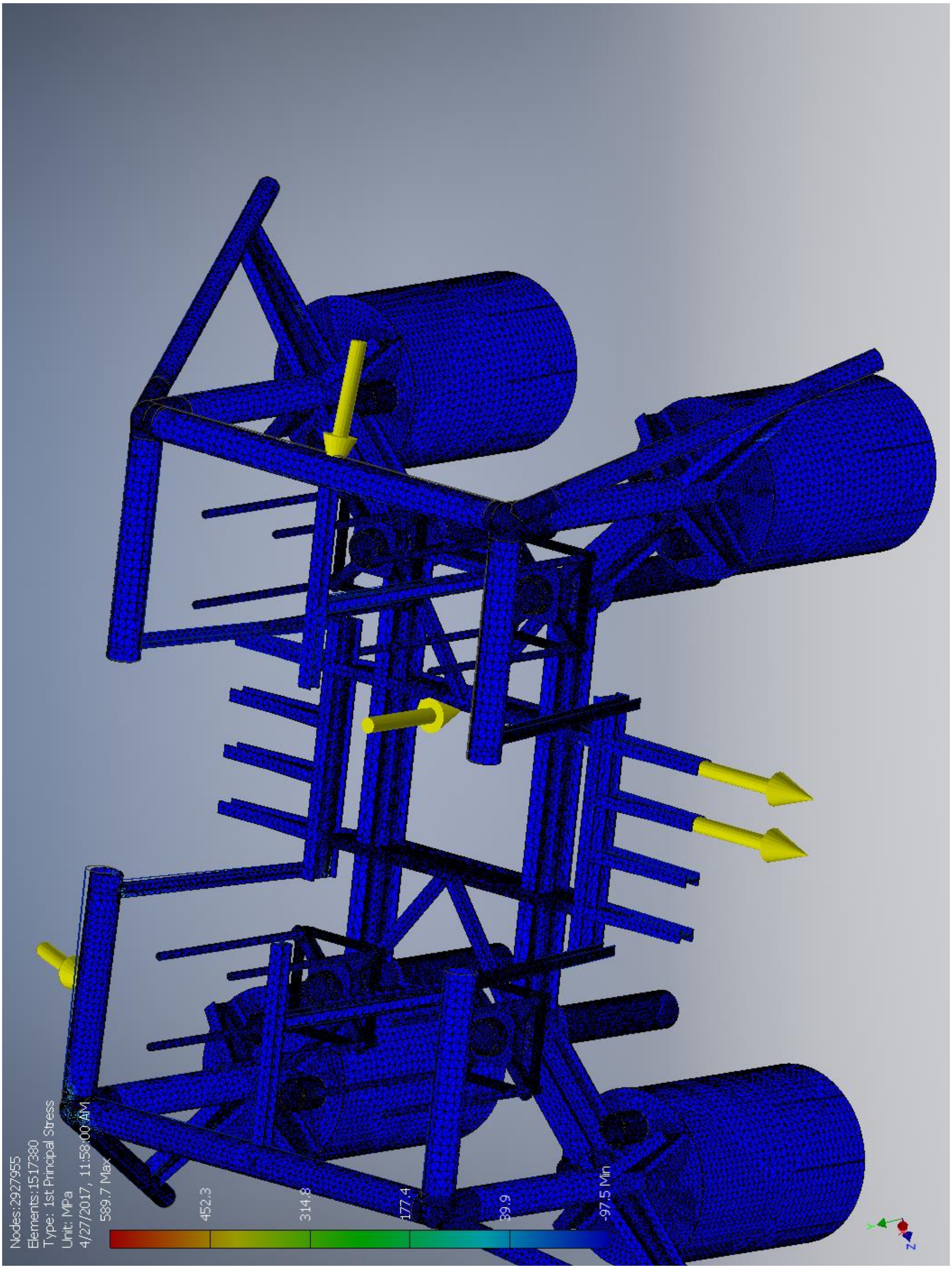

## ⊟ 3rd Principal Stress

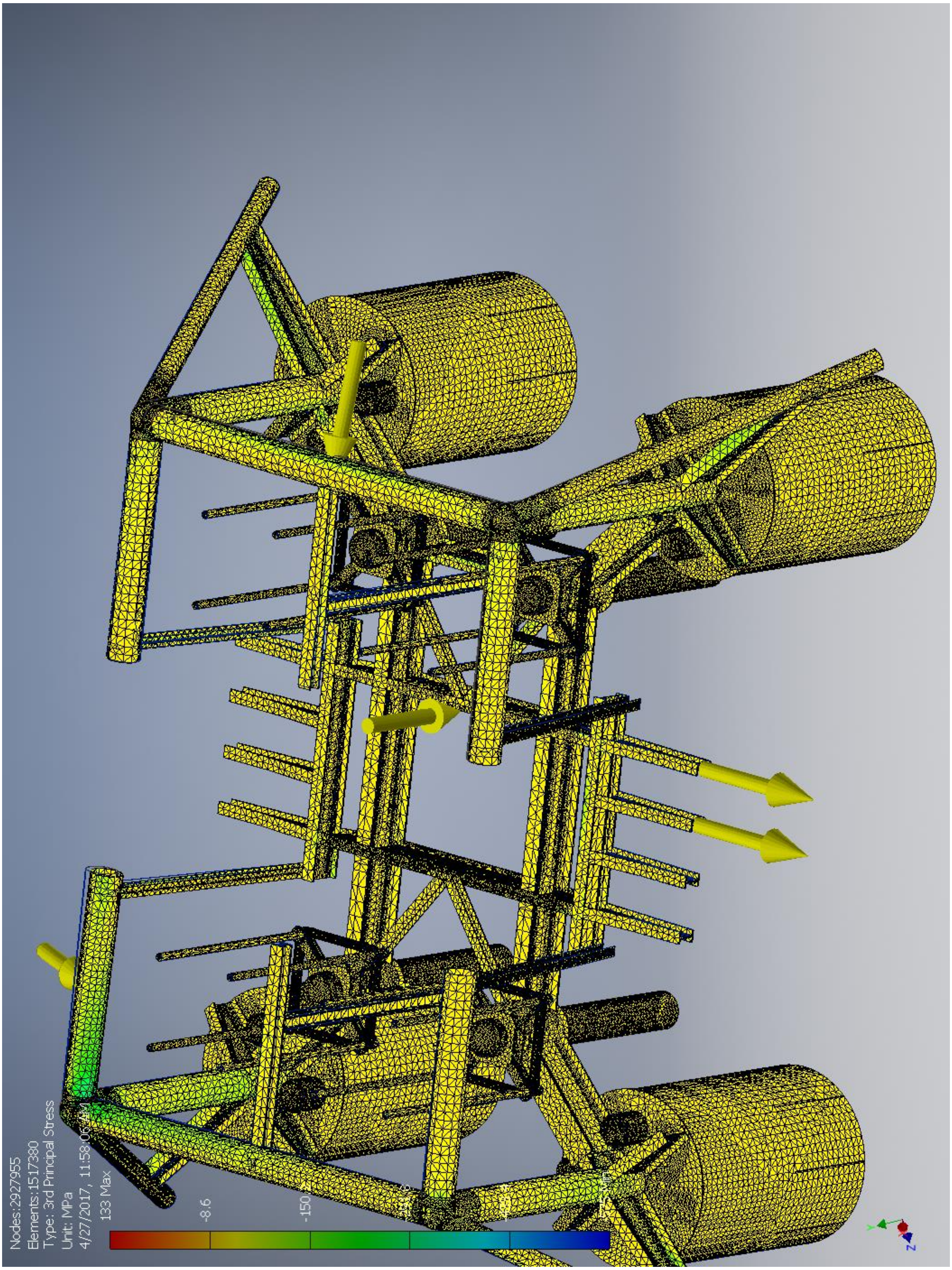

⊟ **Displacement**

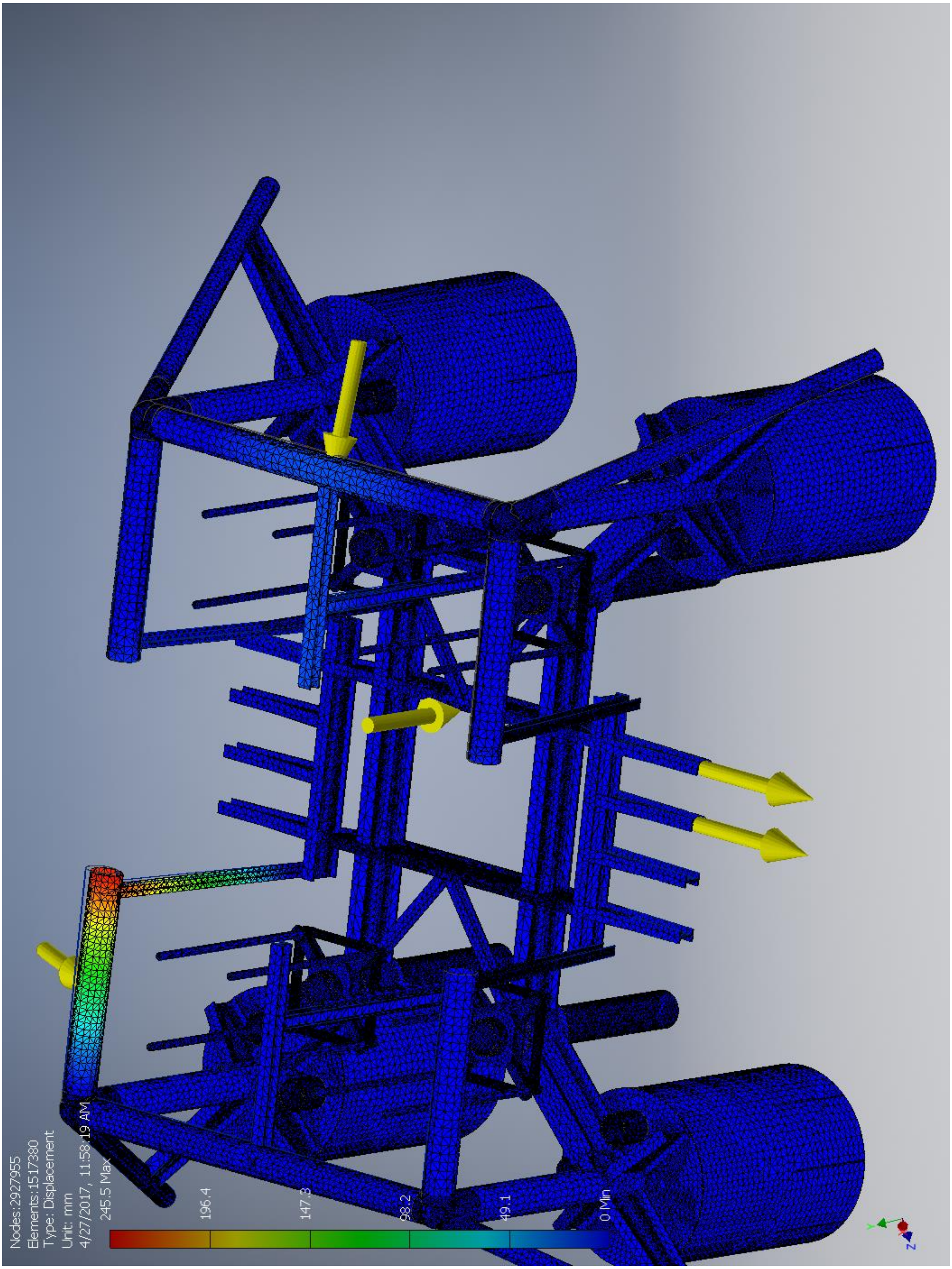

## ⊟ Safety Factor

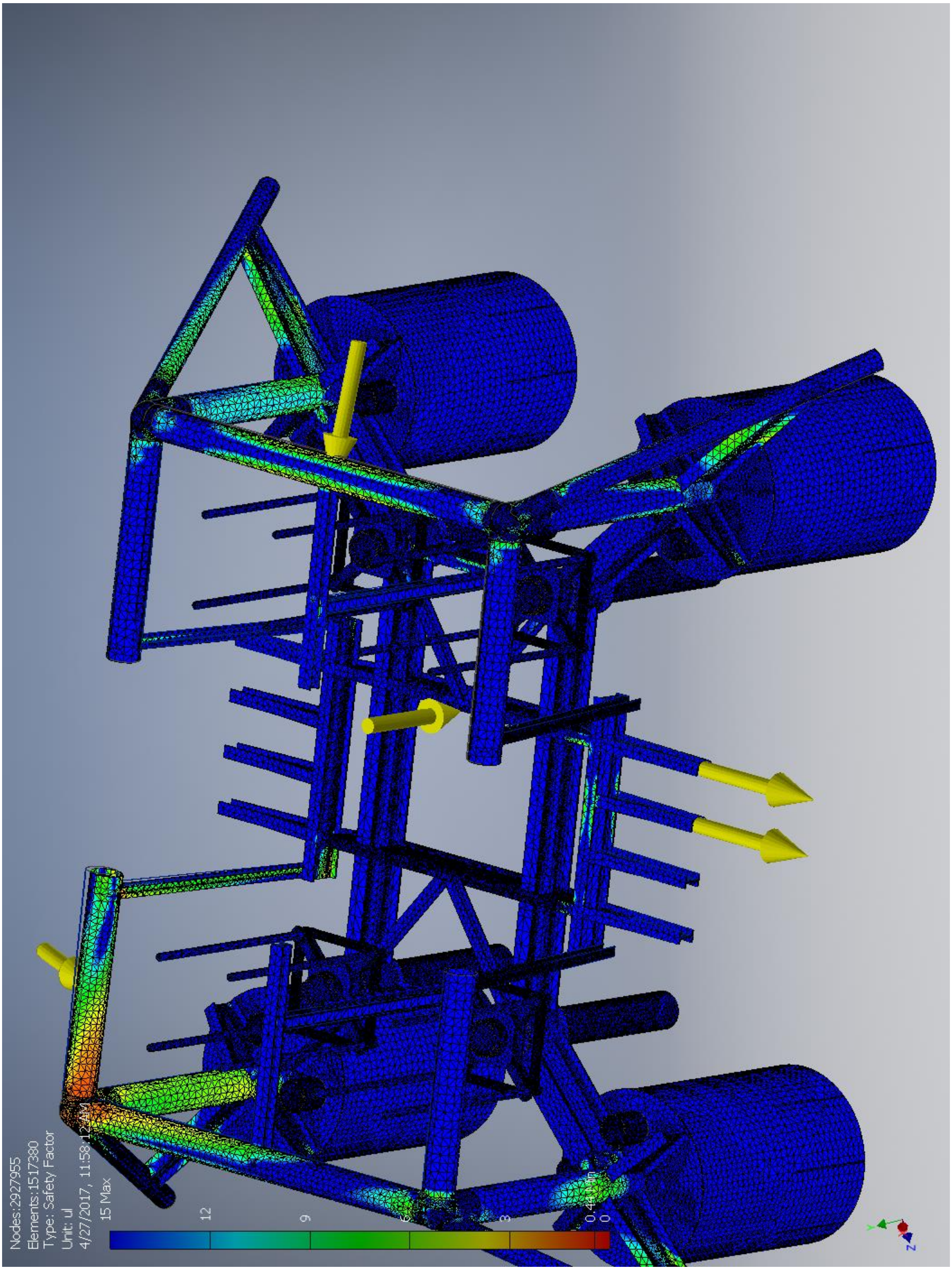

### I.3.4 Overtrawlable/snagfree design load, 400kN instead of 1000kN.

# Stress Analysis Report

AUTODESK

| | |
|---|---|
| Analyzed File: | Assembly.iam |
| Autodesk Inventor Version: | 2017 (Build 210142000, 142) |
| Creation Date: | 5/1/2017, 10:16 AM |
| Study Author: | henrikwn |
| Summary: | |

---

## ⊟ Project Info (iProperties)

### ⊟ Summary

| | |
|---|---|
| Title | |
| Author | henrikwn |

### ⊟ Project

| | |
|---|---|
| Designer | henrikwn |

### ⊟ Physical

| | |
|---|---|
| Mass | 181171 kg |
| Area | 3.52908E+09 mm^2 |
| Volume | 6.02475E+10 mm^3 |
| Center of Gravity | x=-8288.42 mm<br>y=6548.24 mm<br>z=9857.84 mm |

Note: Physical values could be different from Physical values used by FEA reported below.

---

## ⊟ Case-C

**General objective and settings:**

| | |
|---|---|
| Design Objective | Single Point |
| Study Type | Static Analysis |
| Last Modification Date | 5/1/2017, 10:11 AM |
| Detect and Eliminate Rigid Body Modes | No |
| Separate Stresses Across Contact Surfaces | No |
| Motion Loads Analysis | No |

## ⊟ Operating conditions

### ⊟ Force:1

| | |
|---|---|
| Load Type | Force |
| Magnitude | 400000.000 N |
| Vector X | 130246.406 N |
| Vector Y | -378200.838 N |
| Vector Z | 0.000 N |

### ⊟ Selected Face(s)

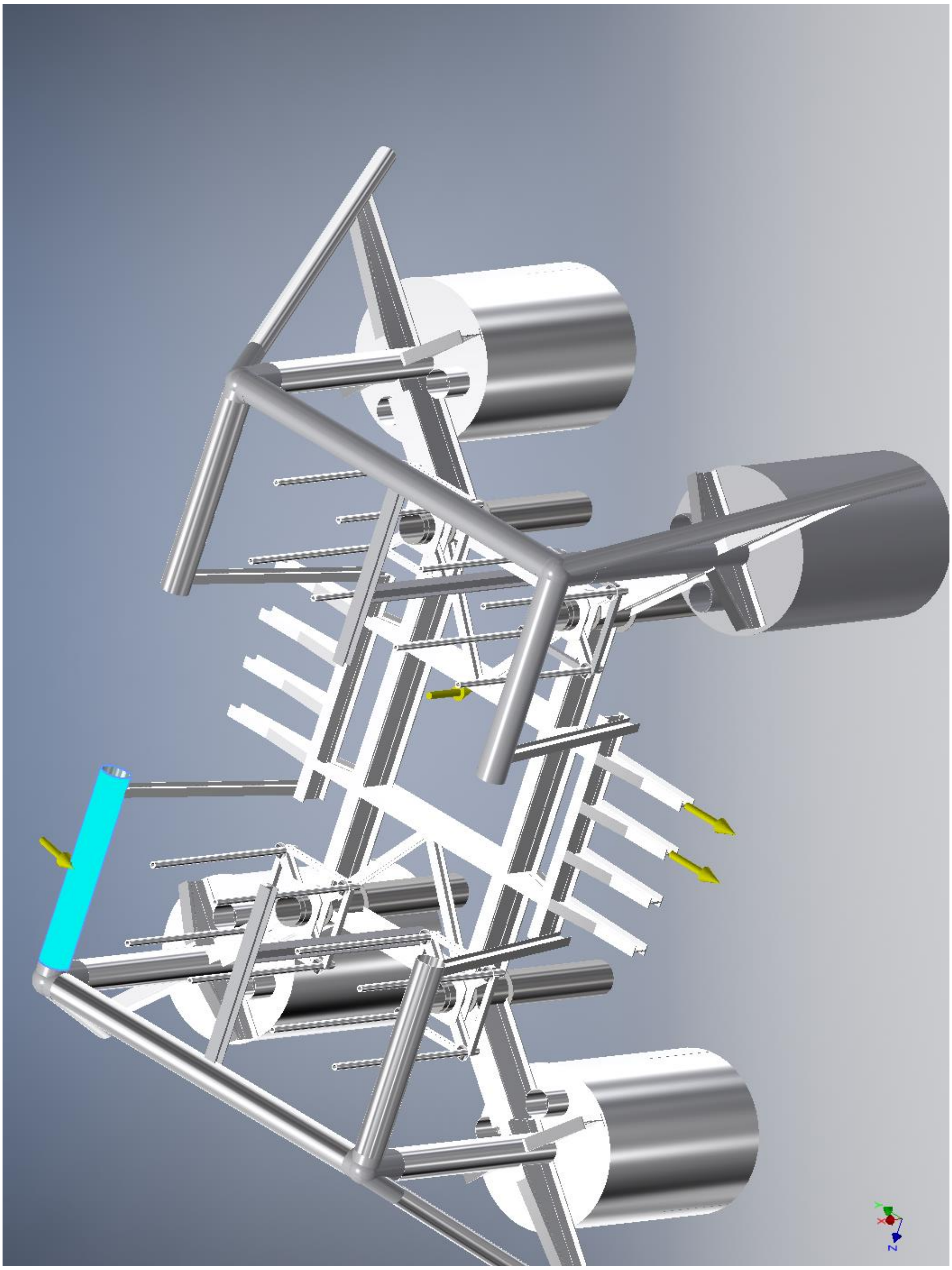

## ⊟ Force:3

| | |
|---|---|
| Load Type | Force |
| Magnitude | 800000.000 N |
| Vector X | -800000.000 N |
| Vector Y | -0.000 N |
| Vector Z | -0.000 N |

### ⊟ Selected Face(s)

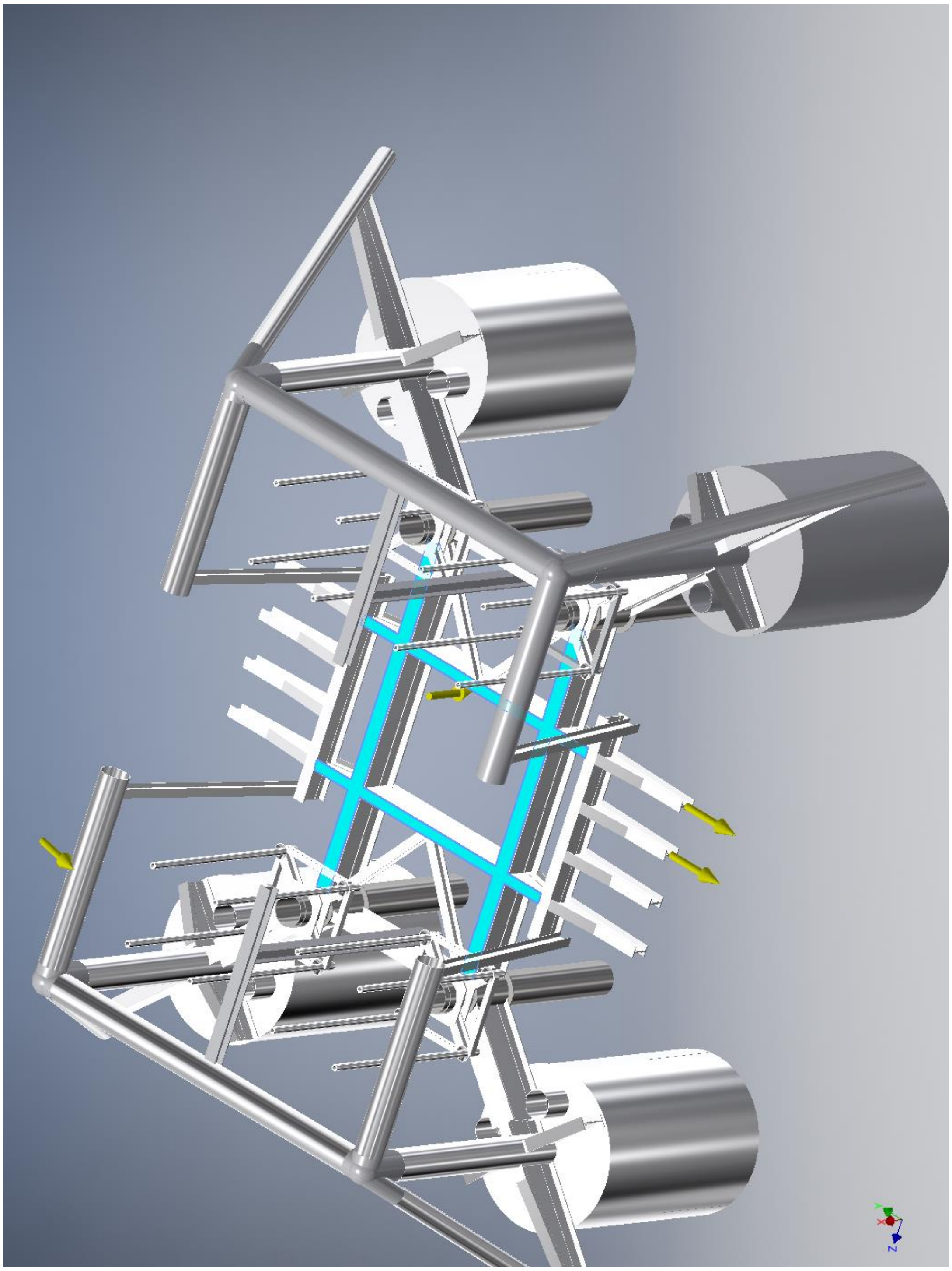

## Force:4

| | |
|---|---|
| Load Type | Force |
| Magnitude | 300000.000 N |
| Vector X | 0.000 N |
| Vector Y | -300000.000 N |
| Vector Z | 0.000 N |

### Selected Face(s)

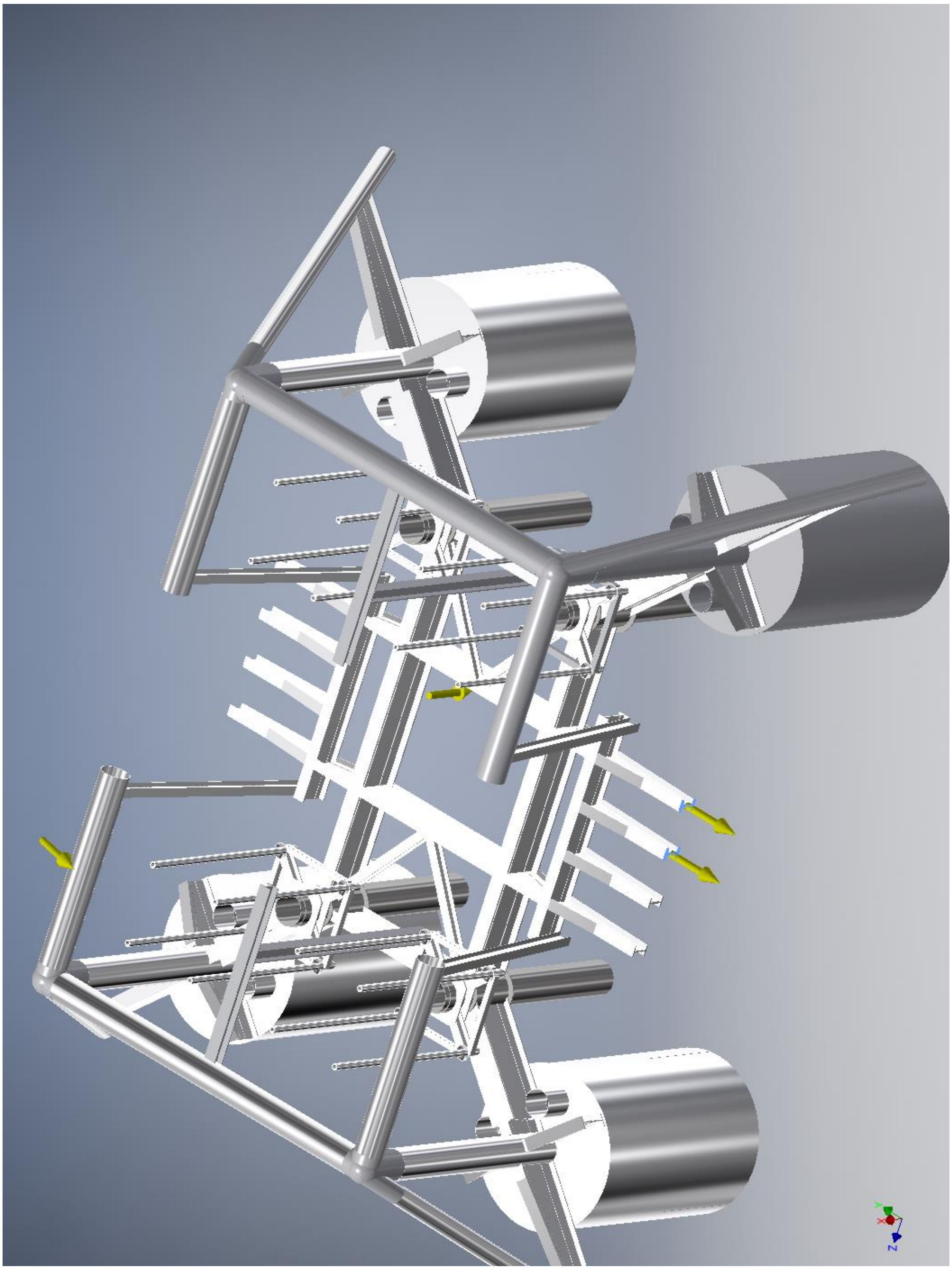

## ⊟ Fixed Constraint:1

| | |
|---|---|
| Constraint Type | Fixed Constraint |

### ⊟ Selected Face(s)

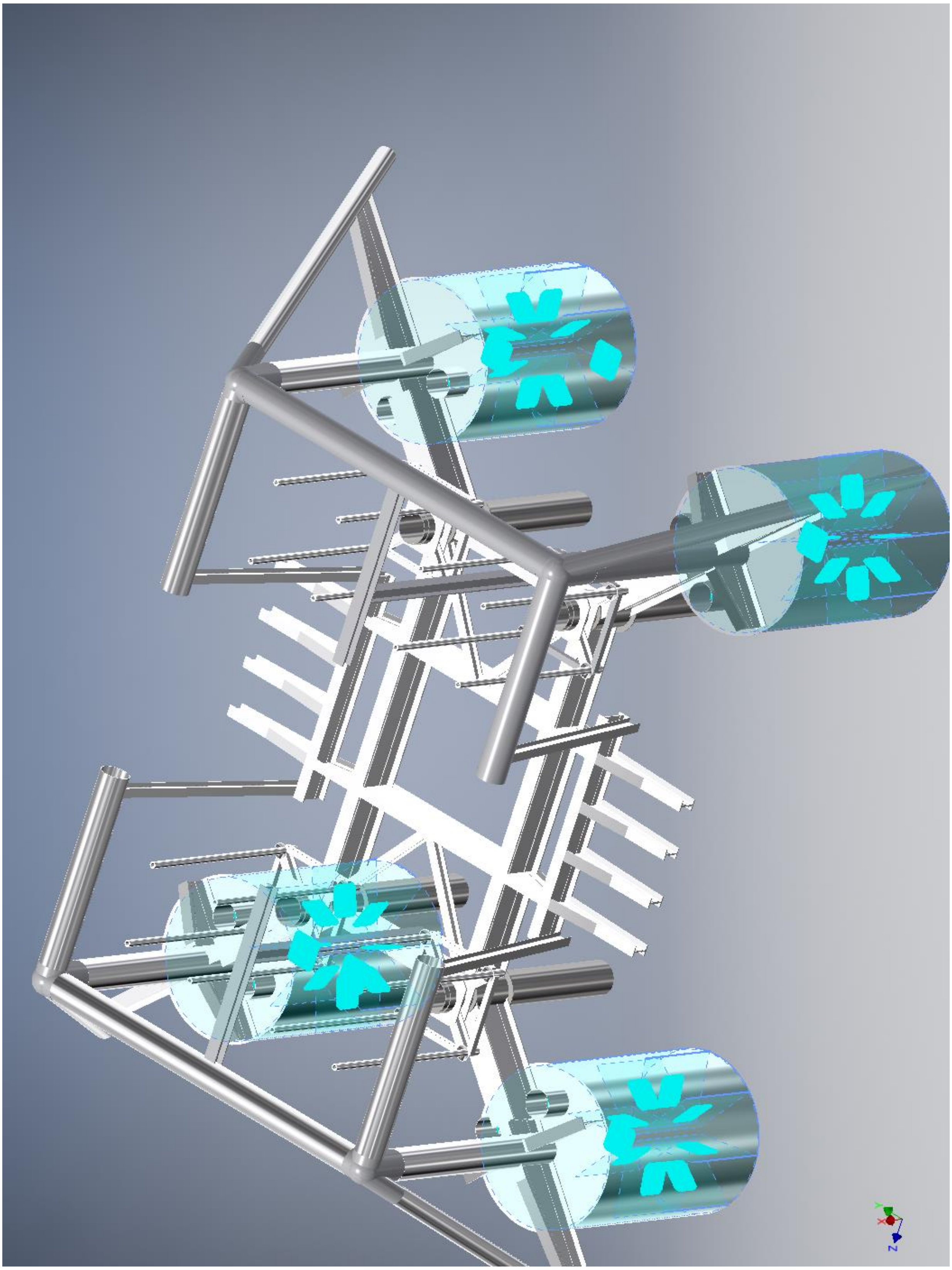

## ⊟ Results

### ⊟ Reaction Force and Moment on Constraints

| Constraint Name | Reaction Force | | Reaction Moment | |
|---|---|---|---|---|
| | Magnitude | Component (X,Y,Z) | Magnitude | Component (X,Y,Z) |
| Fixed Constraint:1 | 953166 N | 669754 N | 7388730 N m | -1858890 N m |
| | | 678201 N | | -890576 N m |
| | | 0 N | | 7095400 N m |

### ⊟ Result Summary

| Name | Minimum | Maximum |
|---|---|---|
| Volume | 6.02475E+10 mm^3 | |
| Mass | 181171 kg | |
| Von Mises Stress | 0 MPa | 230.383 MPa |
| 1st Principal Stress | -56.8608 MPa | 229.68 MPa |
| 3rd Principal Stress | -222.992 MPa | 70.3542 MPa |
| Displacement | 0 mm | 101.754 mm |
| Safety Factor | 0.95315 ul | 15 ul |

### ⊟ Figures

## ⊟ Von Mises Stress

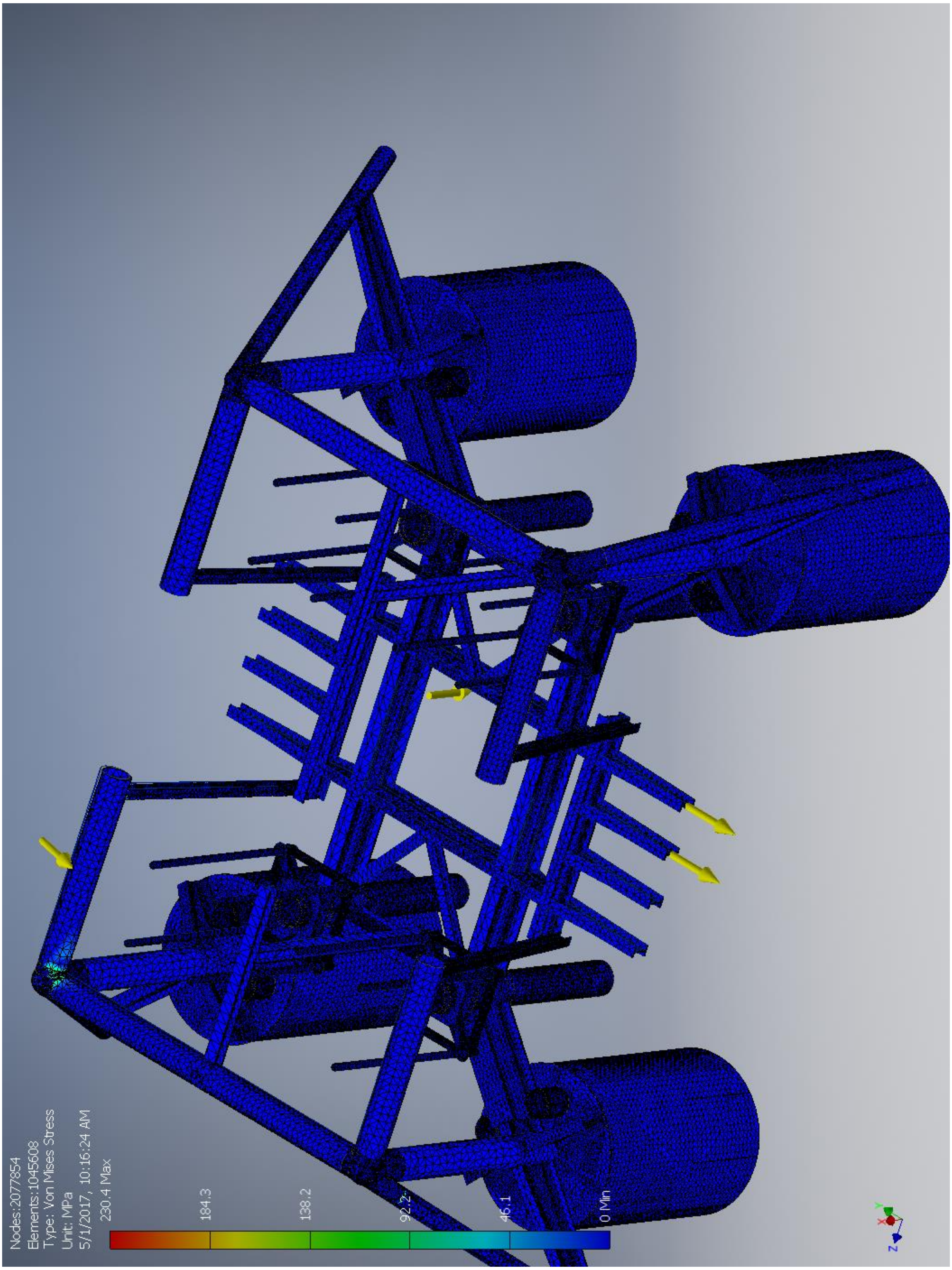

## ⊟ 1st Principal Stress

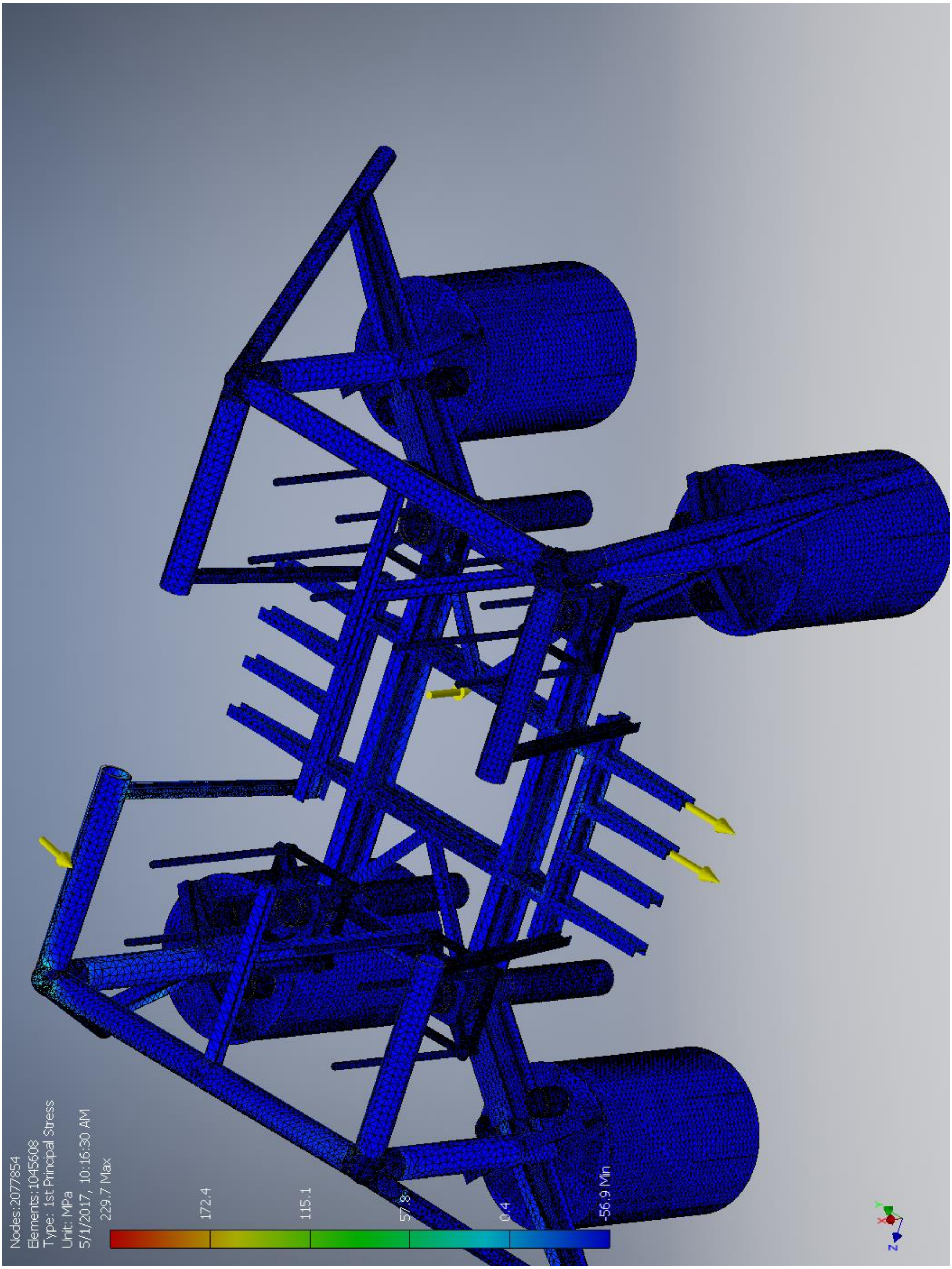

## ⊟ 3rd Principal Stress

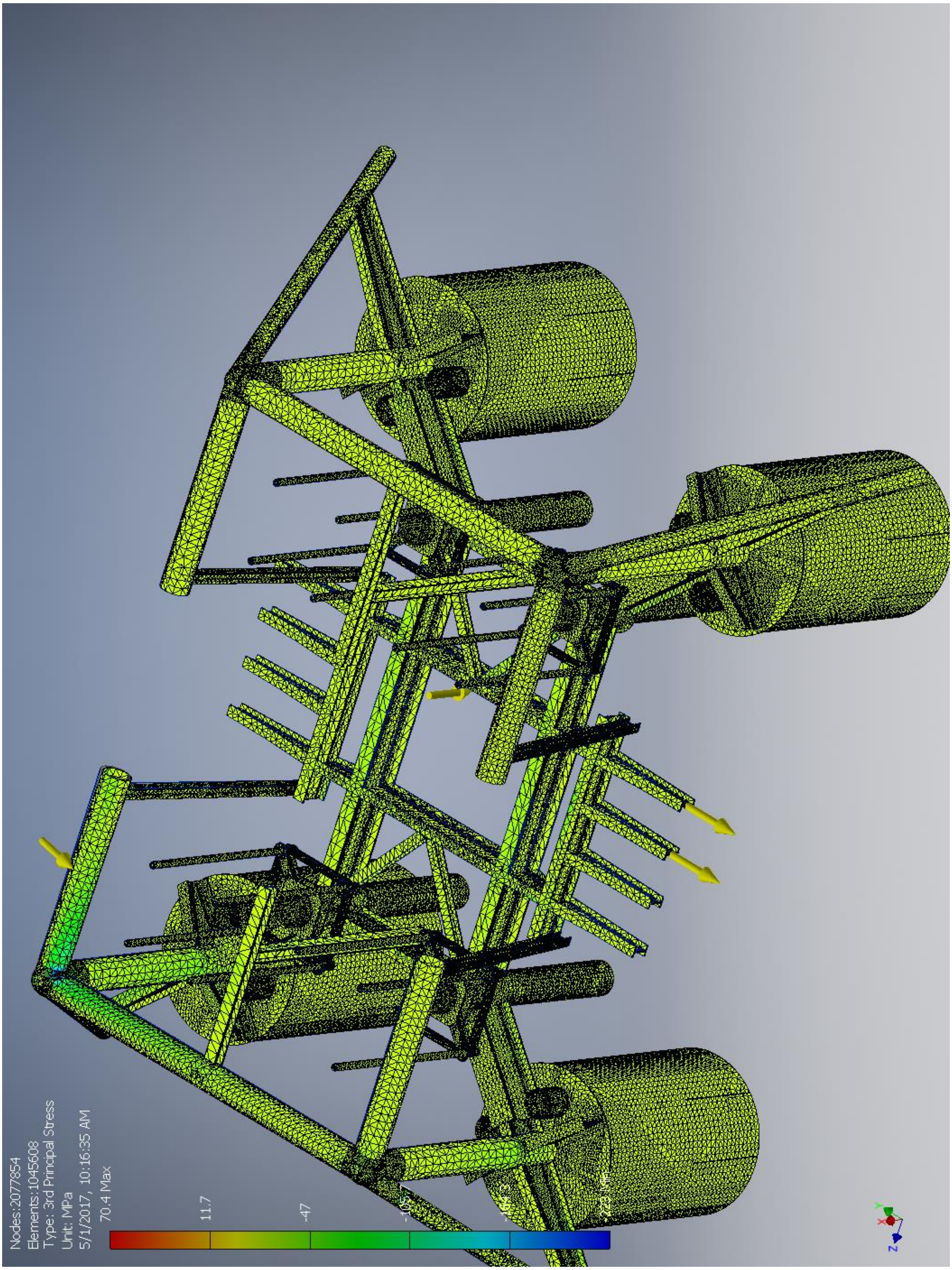

## ⊟ Displacement

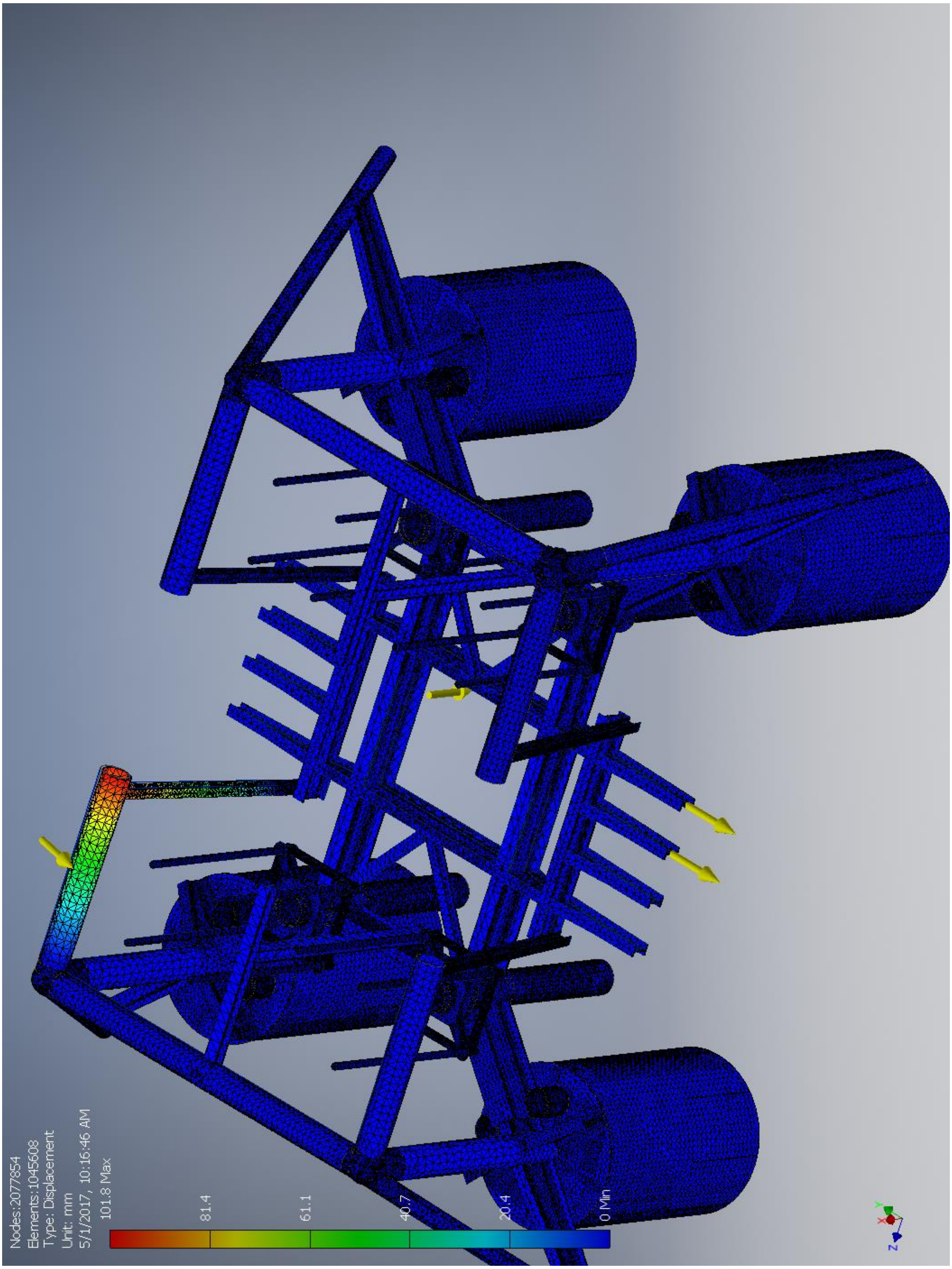

## ⊟ Safety Factor

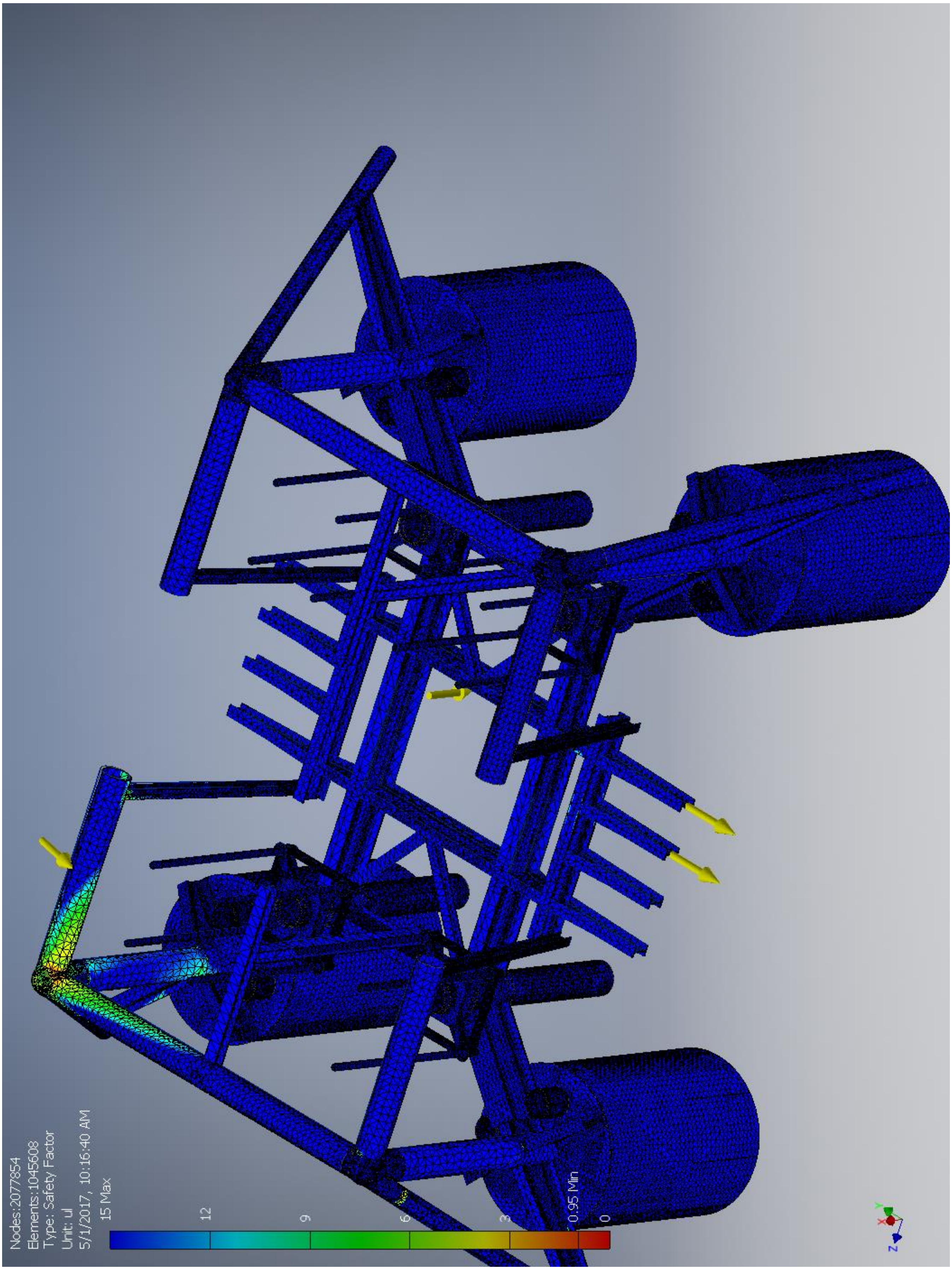

## I.4 Case-D

# Stress Analysis Report

AUTODESK.

| | |
|---|---|
| Analyzed File: | Assembly.iam |
| Autodesk Inventor Version: | 2017 (Build 210142000, 142) |
| Creation Date: | 4/28/2017, 5:10 PM |
| Study Author: | henrikwn |
| Summary: | |

---

## ⊟ Project Info (iProperties)

### ⊟ Summary

| | |
|---|---|
| Title | |
| Author | henrikwn |

### ⊟ Project

| | |
|---|---|
| Designer | henrikwn |

### ⊟ Physical

| | |
|---|---|
| Mass | 181171 kg |
| Area | 3.52908E+09 mm^2 |
| Volume | 6.02475E+10 mm^3 |
| Center of Gravity | x=-8288.42 mm<br>y=6548.24 mm<br>z=9857.84 mm |

Note: Physical values could be different from Physical values used by FEA reported below.

---

## ⊟ Case-D

**General objective and settings:**

| | |
|---|---|
| Design Objective | Single Point |
| Study Type | Static Analysis |
| Last Modification Date | 4/28/2017, 5:09 PM |
| Detect and Eliminate Rigid Body Modes | No |
| Separate Stresses Across Contact Surfaces | No |
| Motion Loads Analysis | No |

## ⊟ Operating conditions

## ⊟ Force:1

| | |
|---|---|
| Load Type | Force |
| Magnitude | 600000.000 N |
| Vector X | -600000.000 N |
| Vector Y | -0.000 N |
| Vector Z | -0.000 N |

### ⊟ Selected Face(s)

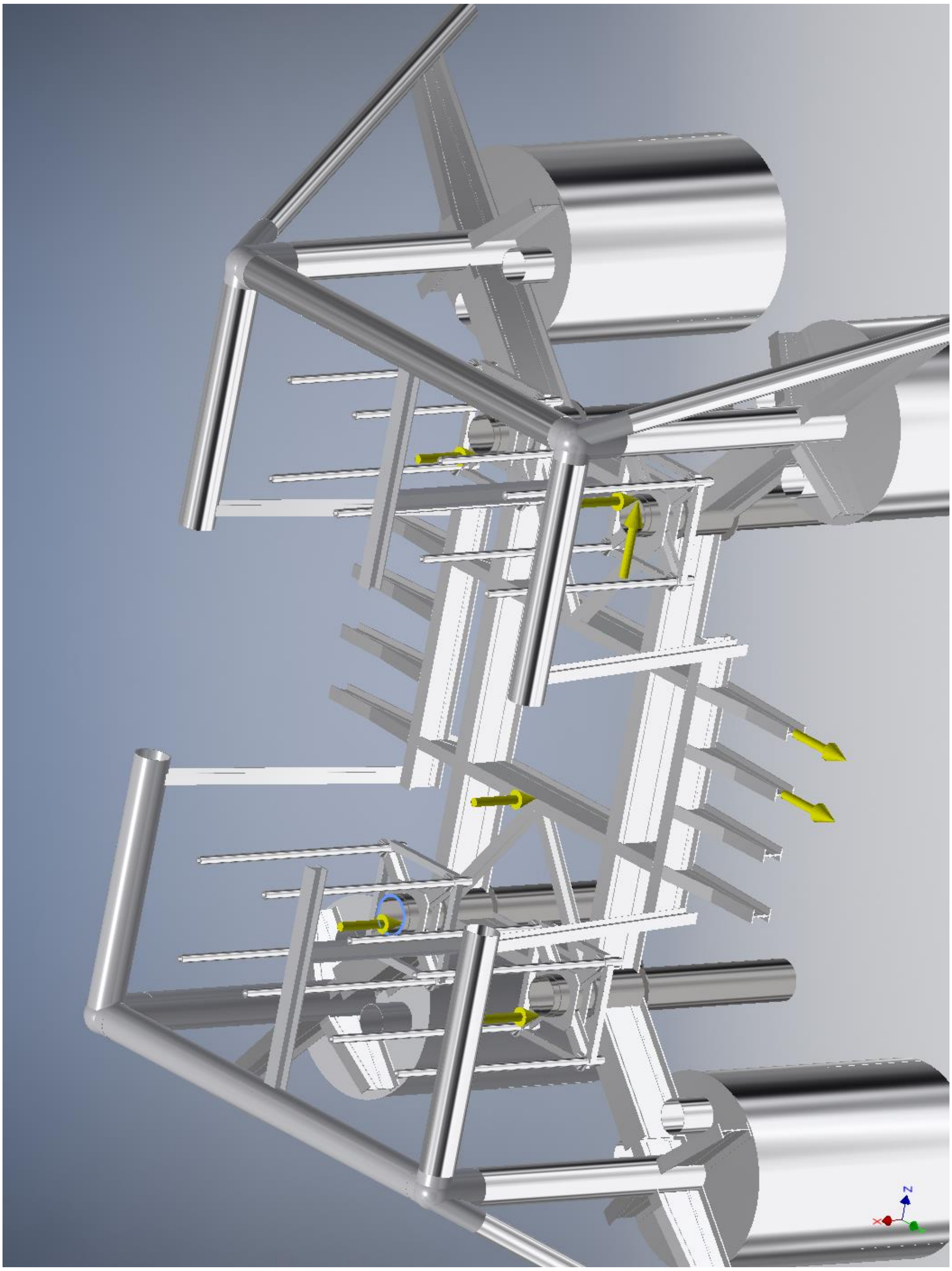

## ⊟ Force:2

| | |
|---|---|
| Load Type | Force |
| Magnitude | 600000.000 N |
| Vector X | -600000.000 N |
| Vector Y | -0.000 N |
| Vector Z | -0.000 N |

### ⊟ Selected Face(s)

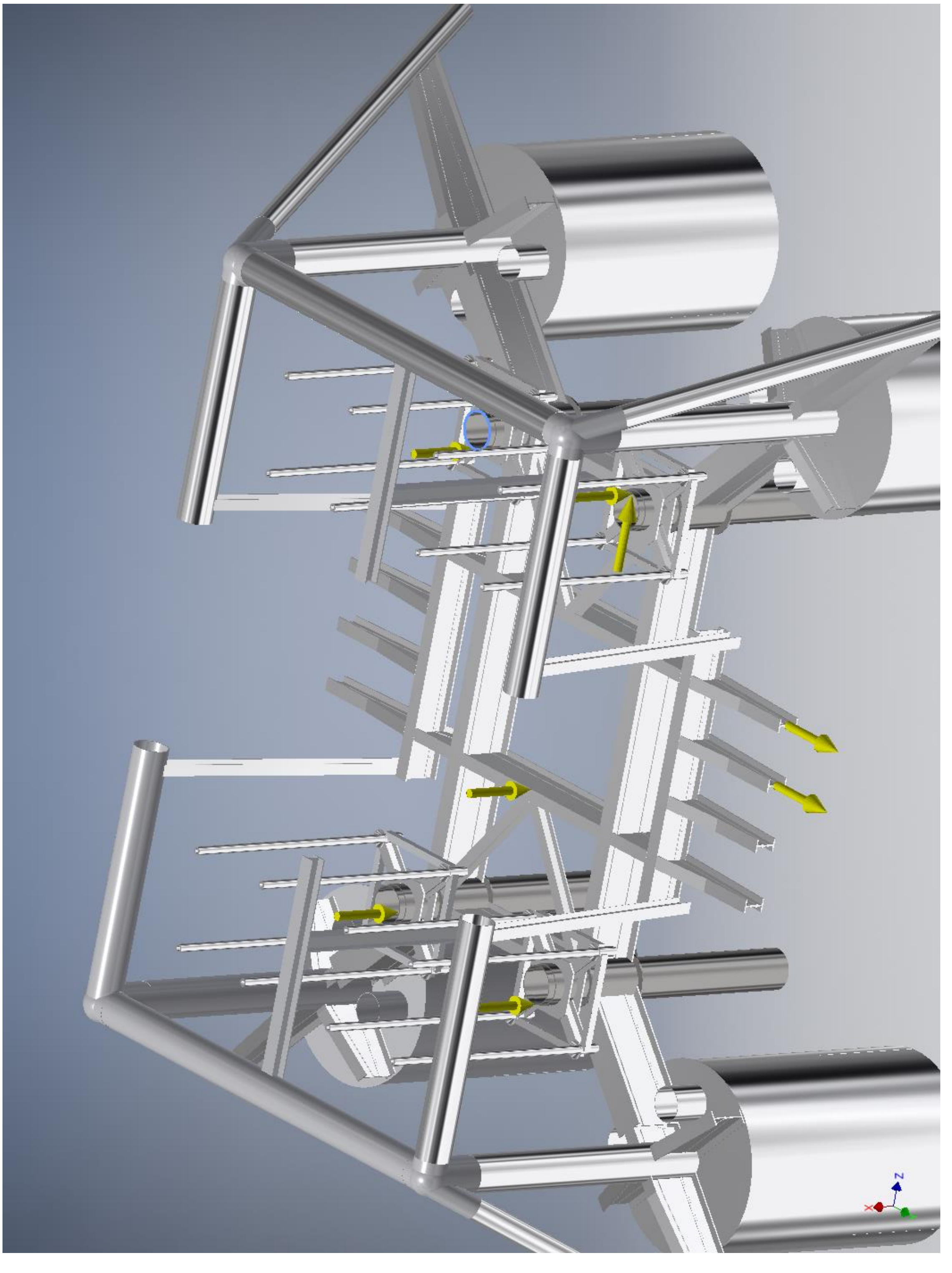

## Force:3

| | |
|---|---|
| Load Type | Force |
| Magnitude | 600000.000 N |
| Vector X | -600000.000 N |
| Vector Y | -0.000 N |
| Vector Z | -0.000 N |

### Selected Face(s)

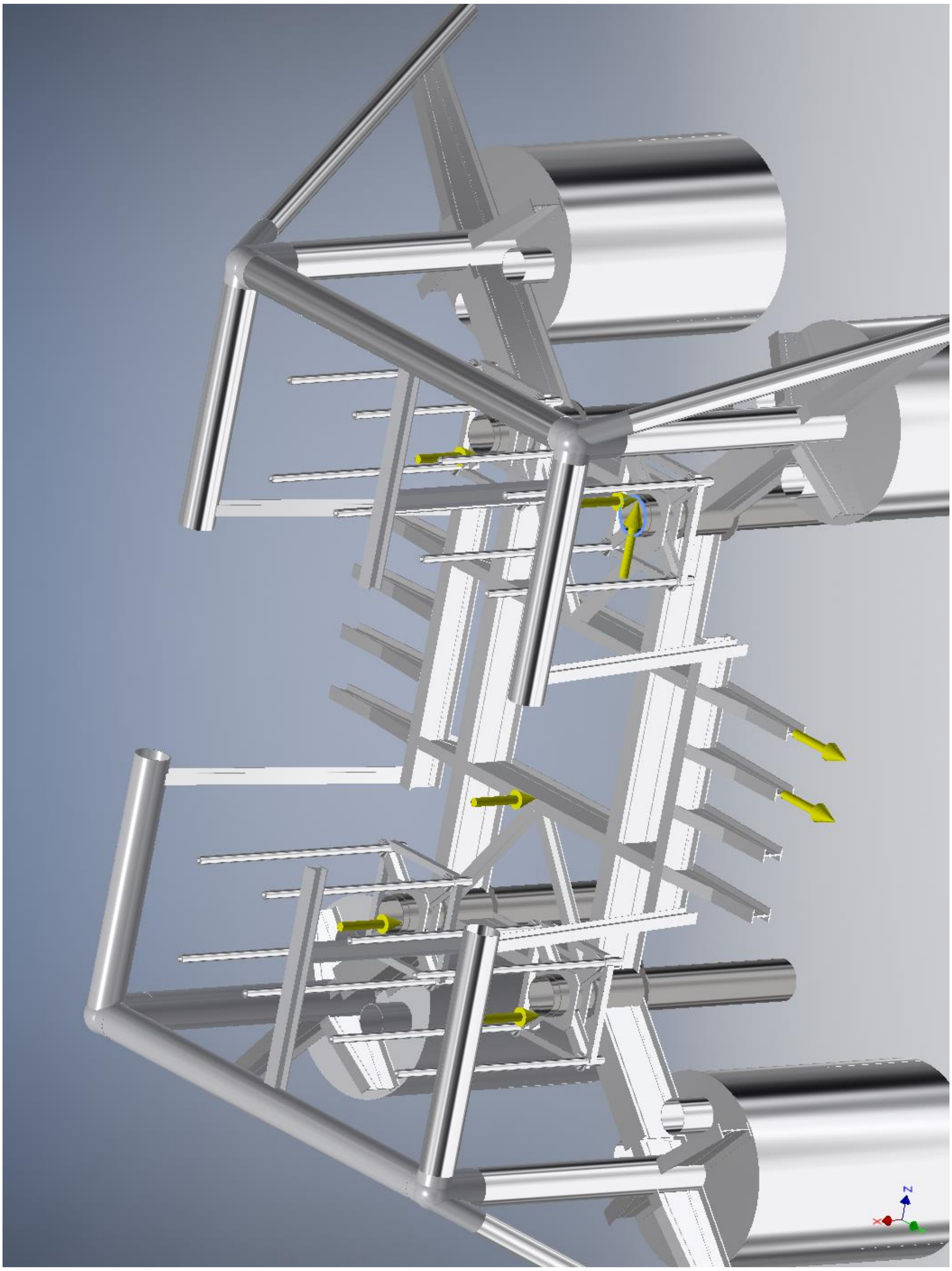

## ⊟ Force:4

| | |
|---|---|
| Load Type | Force |
| Magnitude | 600000.000 N |
| Vector X | -600000.000 N |
| Vector Y | -0.000 N |
| Vector Z | -0.000 N |

### ⊟ Selected Face(s)

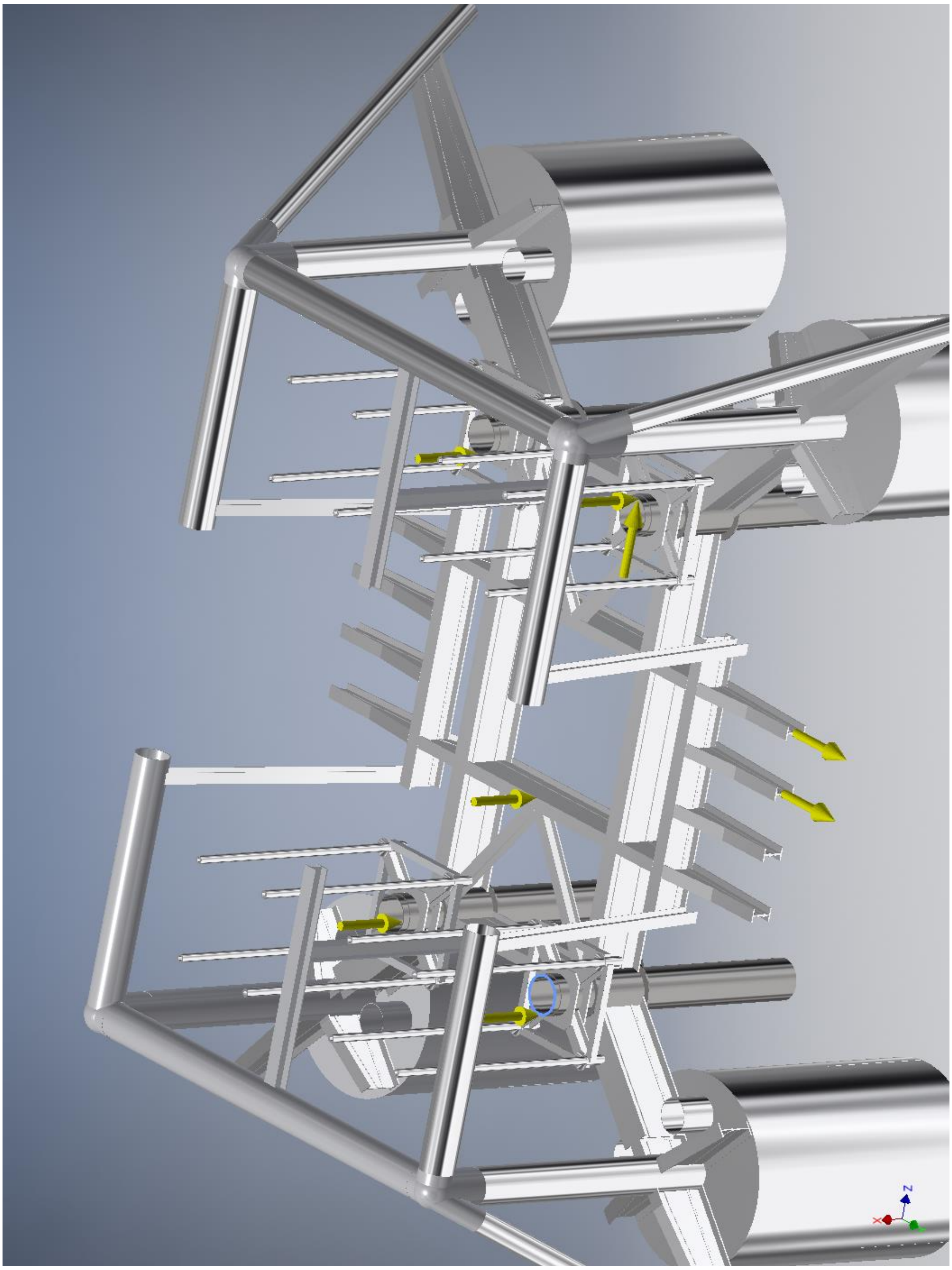

## ⊟ Force:5

| | |
|---|---|
| Load Type | Force |
| Magnitude | 450000.000 N |
| Vector X | -450000.000 N |
| Vector Y | -0.000 N |
| Vector Z | -0.000 N |

### ⊟ Selected Face(s)

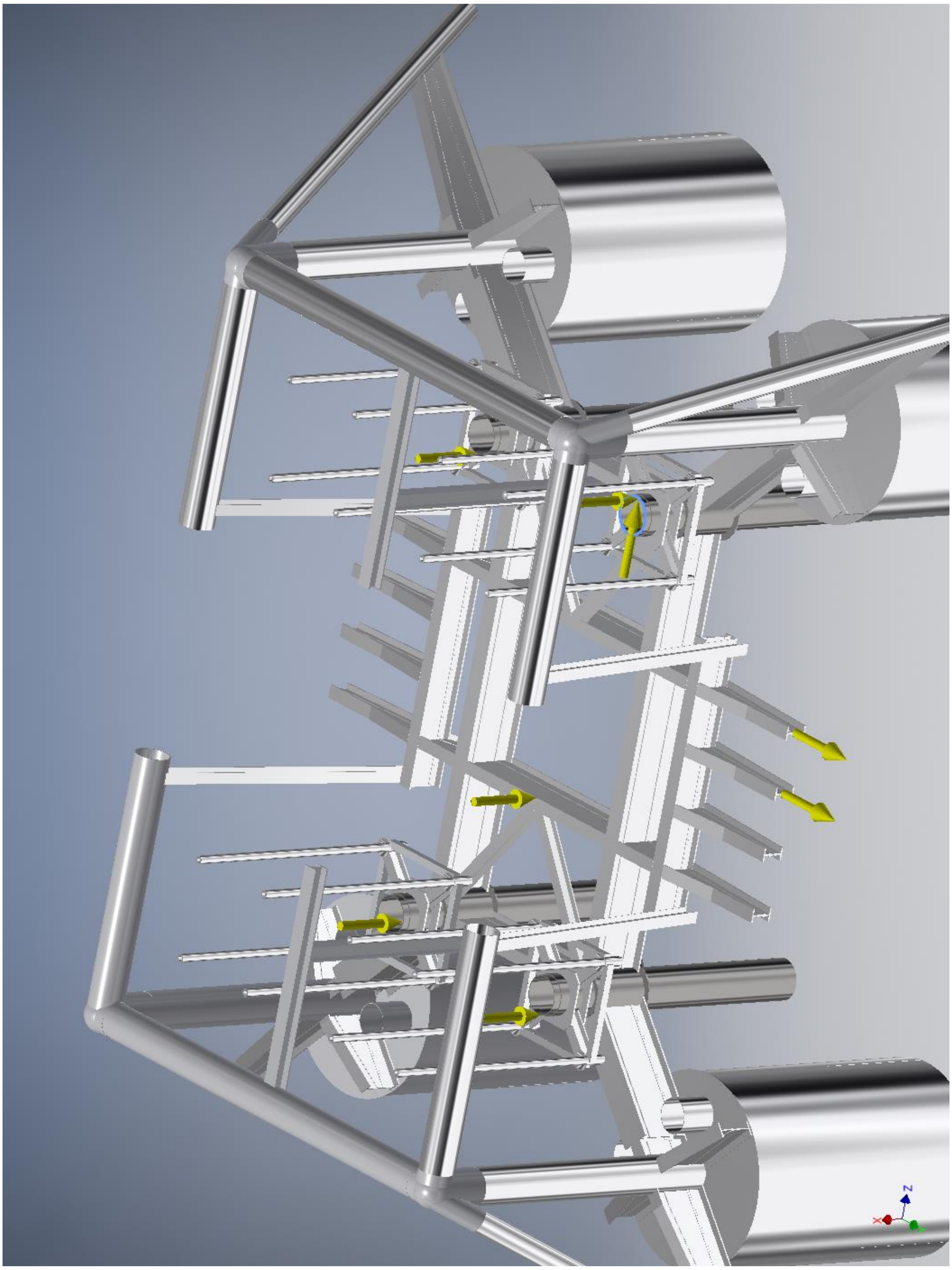

## ⊟ Force:6

| | |
|---|---|
| Load Type | Force |
| Magnitude | 200000.000 N |
| Vector X | 0.000 N |
| Vector Y | -0.000 N |
| Vector Z | 200000.000 N |

### ⊟ Selected Face(s)

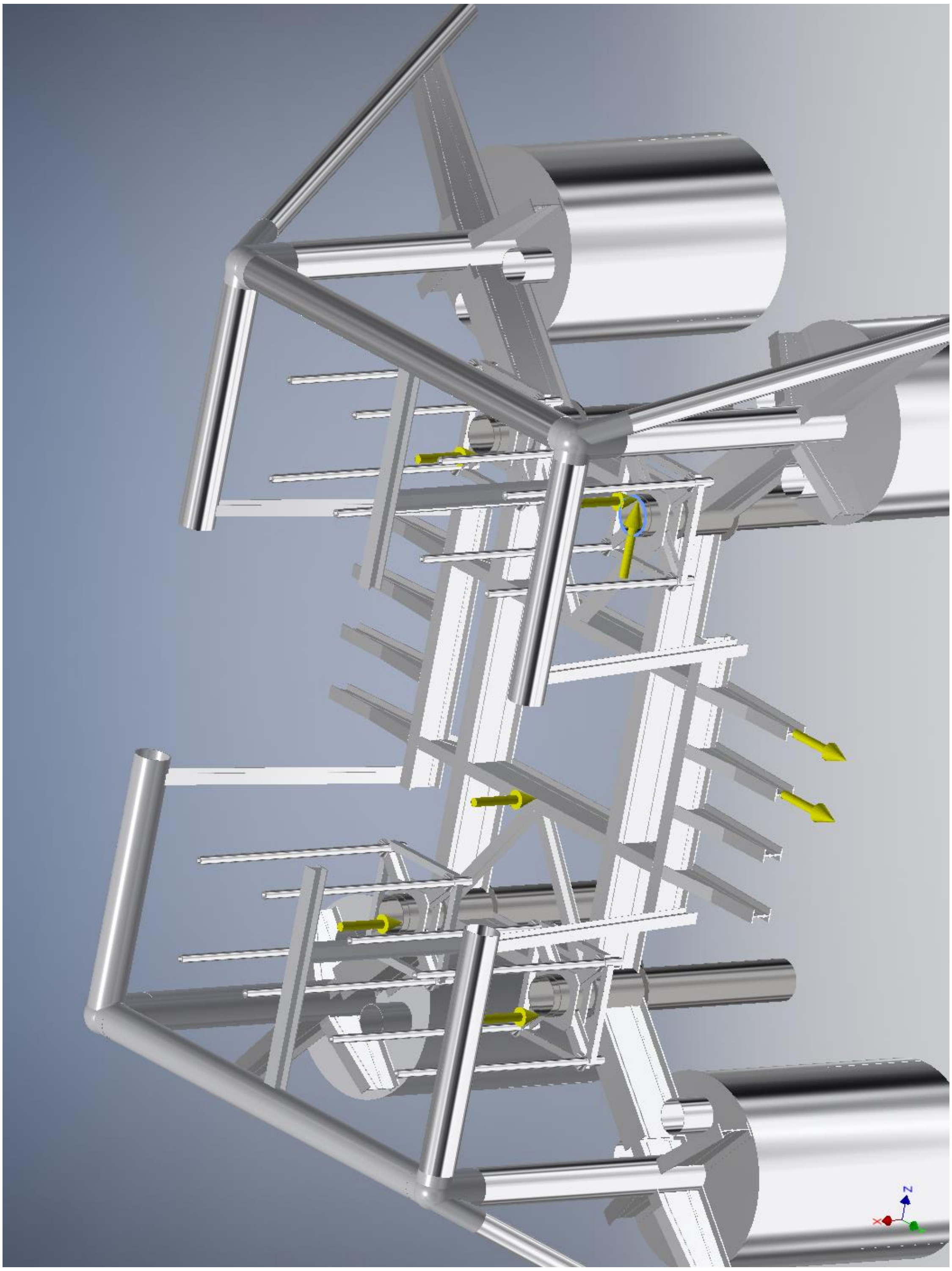

## ⊟ Force:7

| | |
|---|---|
| Load Type | Force |
| Magnitude | 800000.000 N |
| Vector X | -800000.000 N |
| Vector Y | -0.000 N |
| Vector Z | -0.000 N |

### ⊟ Selected Face(s)

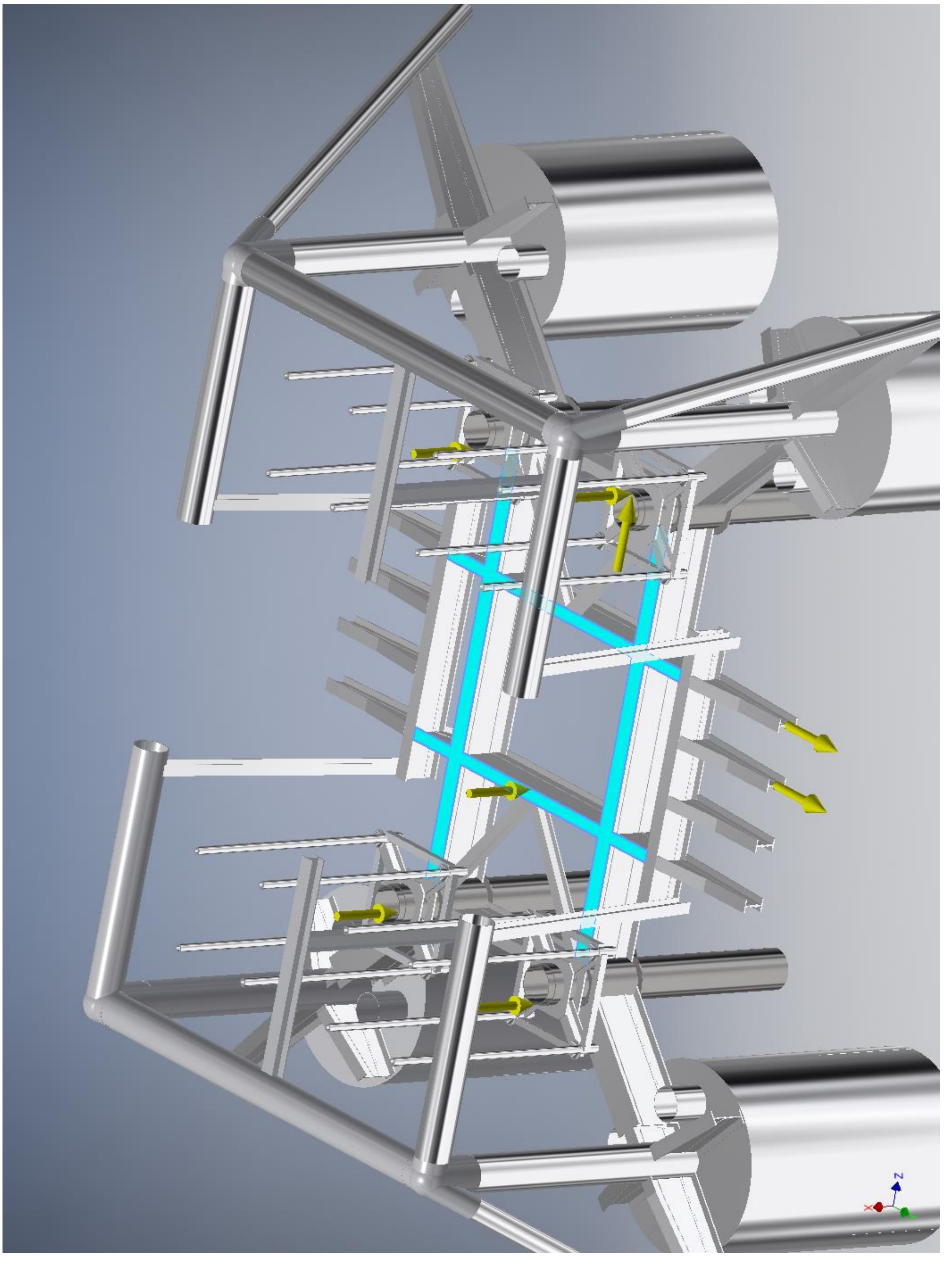

## ⊟ Force:8

| | |
|---|---|
| Load Type | Force |
| Magnitude | 300000.000 N |
| Vector X | 0.000 N |
| Vector Y | 300000.000 N |
| Vector Z | -0.000 N |

### ⊟ Selected Face(s)

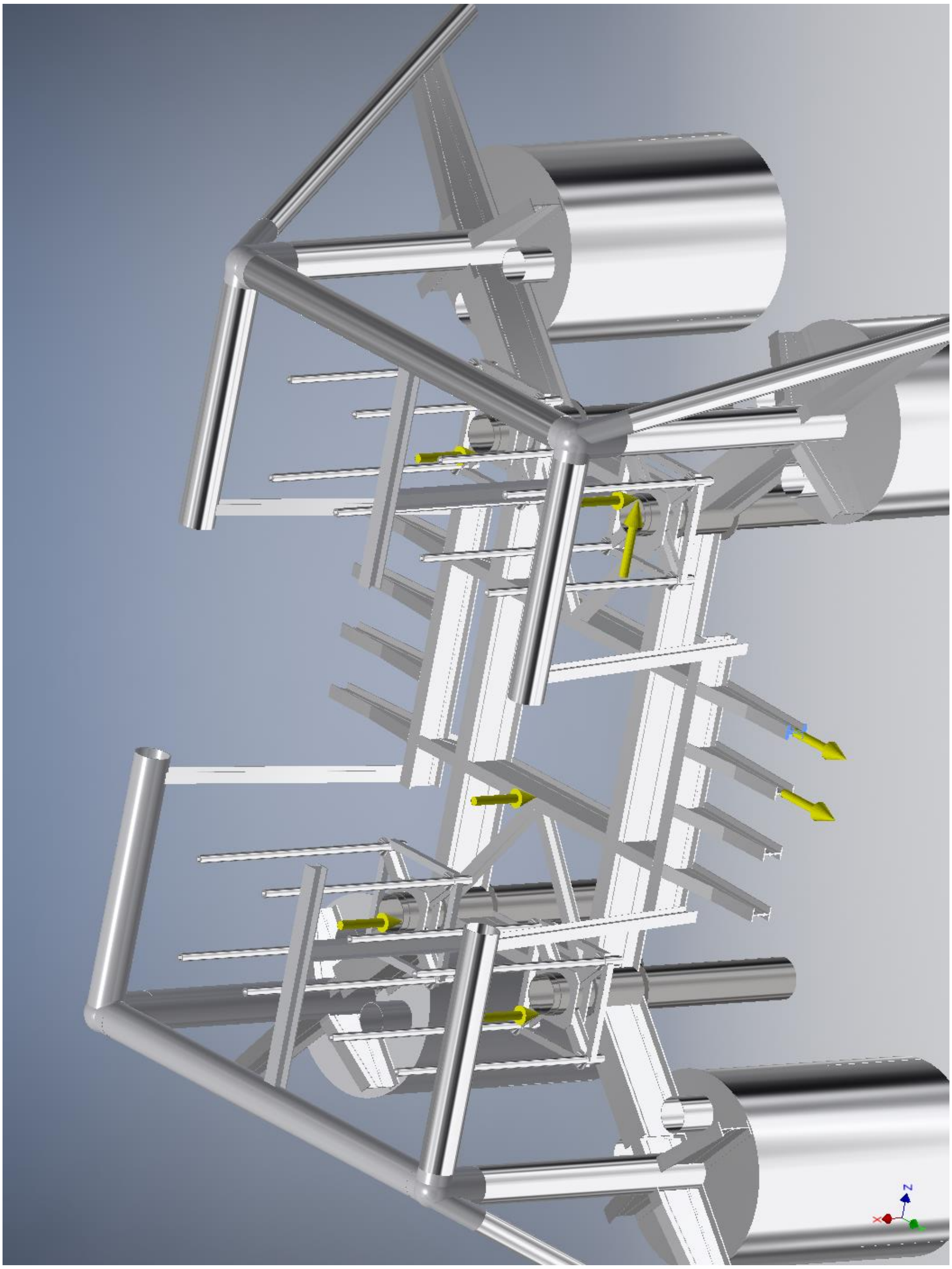

## ⊟ Force:9

| | |
|---|---|
| Load Type | Force |
| Magnitude | 300000.000 N |
| Vector X | 0.000 N |
| Vector Y | 300000.000 N |
| Vector Z | -0.000 N |

### ⊟ Selected Face(s)

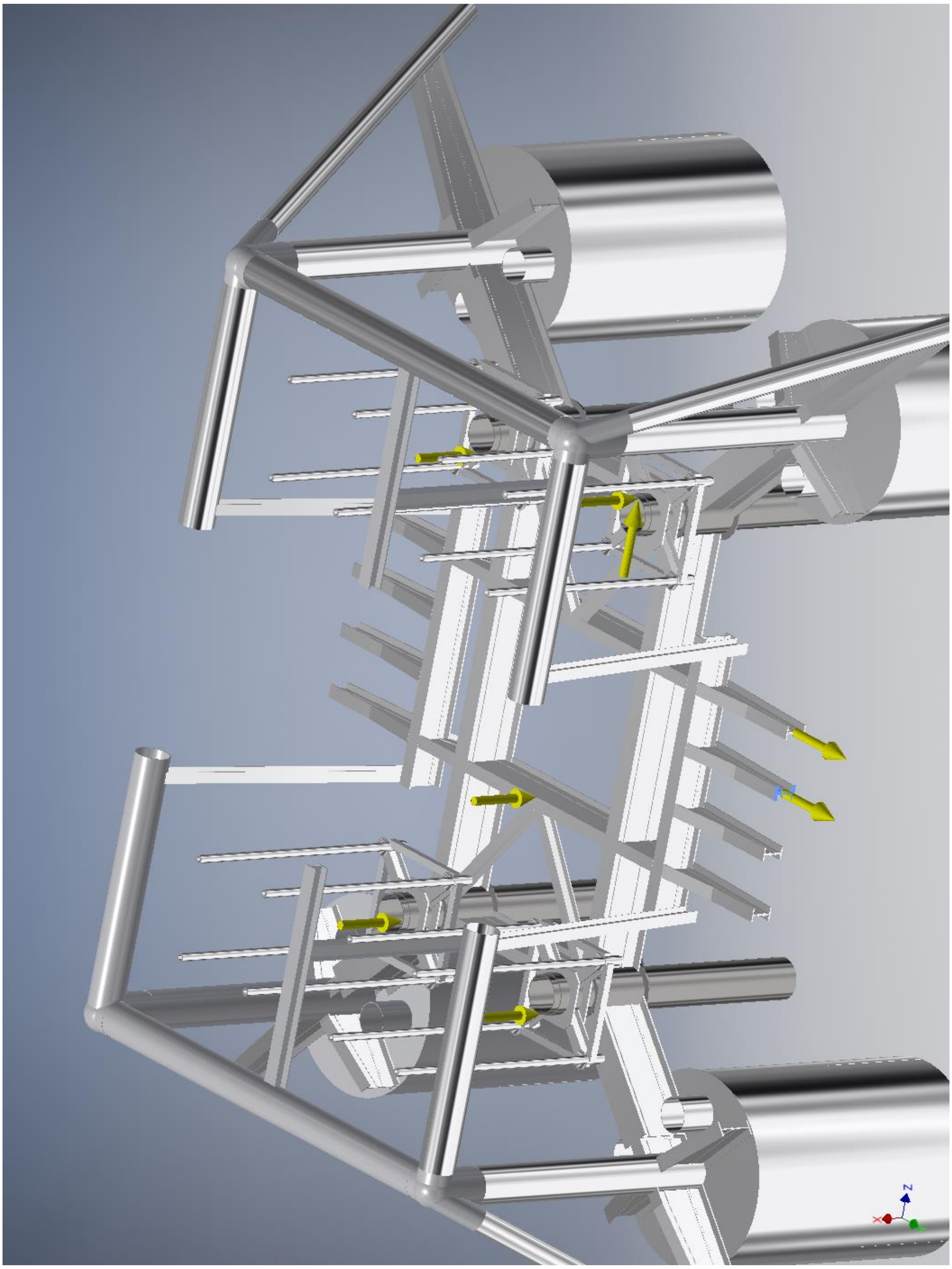

## ⊟ Fixed Constraint:1

| Constraint Type | Fixed Constraint |
|---|---|

### ⊟ Selected Face(s)

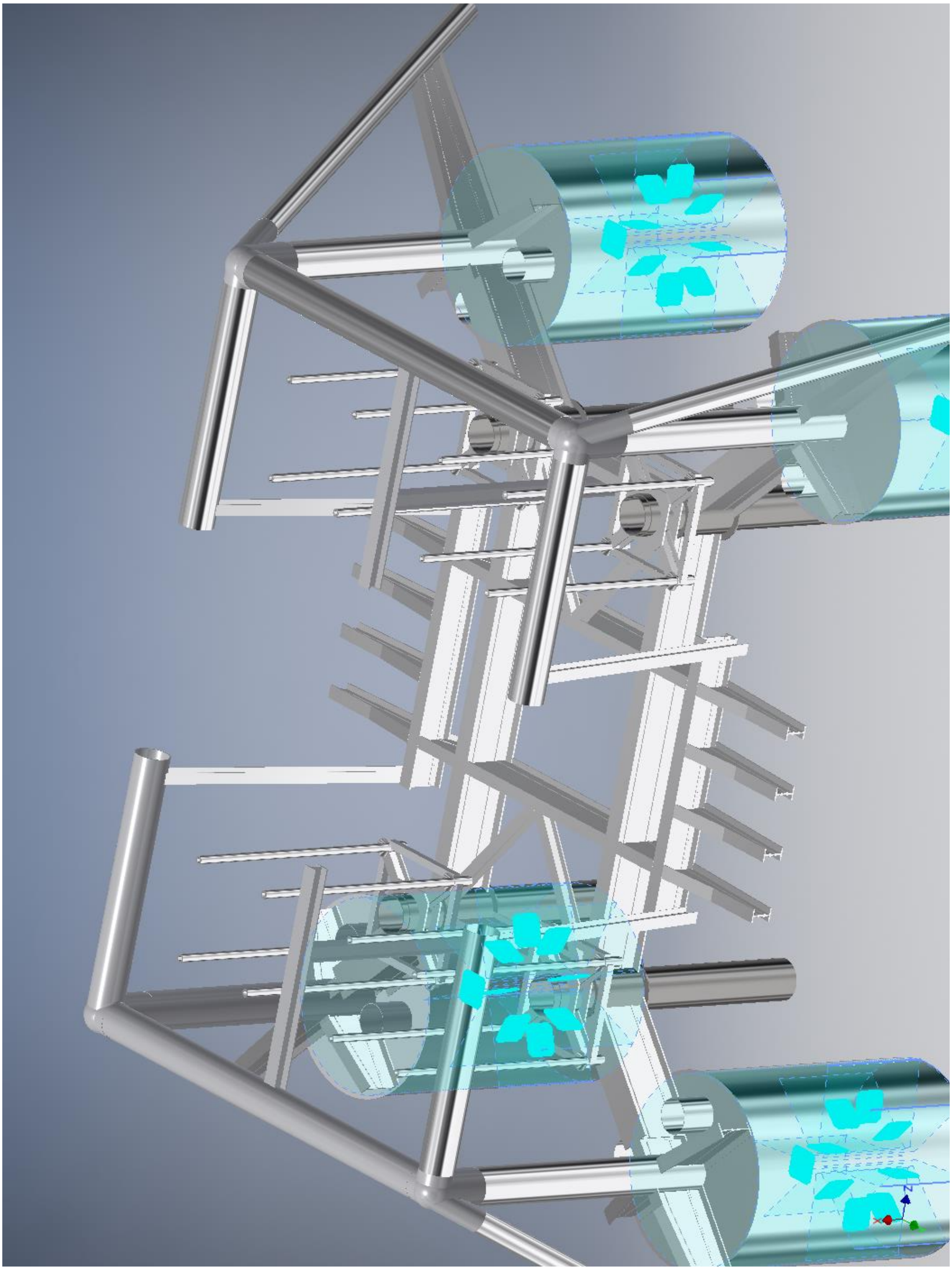

# ⊟ Results

## ⊟ Reaction Force and Moment on Constraints

<table>
<tr><th rowspan="2">Constraint Name</th><th colspan="2">Reaction Force</th><th colspan="2">Reaction Moment</th></tr>
<tr><th>Magnitude</th><th>Component (X,Y,Z)</th><th>Magnitude</th><th>Component (X,Y,Z)</th></tr>
<tr><td rowspan="3">Fixed Constraint:1</td><td rowspan="3">3704390 N</td><td>3650000 N</td><td rowspan="3">6204470 N m</td><td>365904 N m</td></tr>
<tr><td>-600000 N</td><td>4253910 N m</td></tr>
<tr><td>-200000 N</td><td>-4501760 N m</td></tr>
</table>

## ⊟ Result Summary

| Name | Minimum | Maximum |
|---|---|---|
| Volume | 6.02475E+10 mm^3 | |
| Mass | 181171 kg | |
| Von Mises Stress | 0 MPa | 127.049 MPa |
| 1st Principal Stress | -41.9479 MPa | 101.938 MPa |
| 3rd Principal Stress | -146.946 MPa | 39.752 MPa |
| Displacement | 0 mm | 17.6941 mm |
| Safety Factor | 2.71356 ul | 15 ul |

## ⊟ Figures

### Von Mises Stress

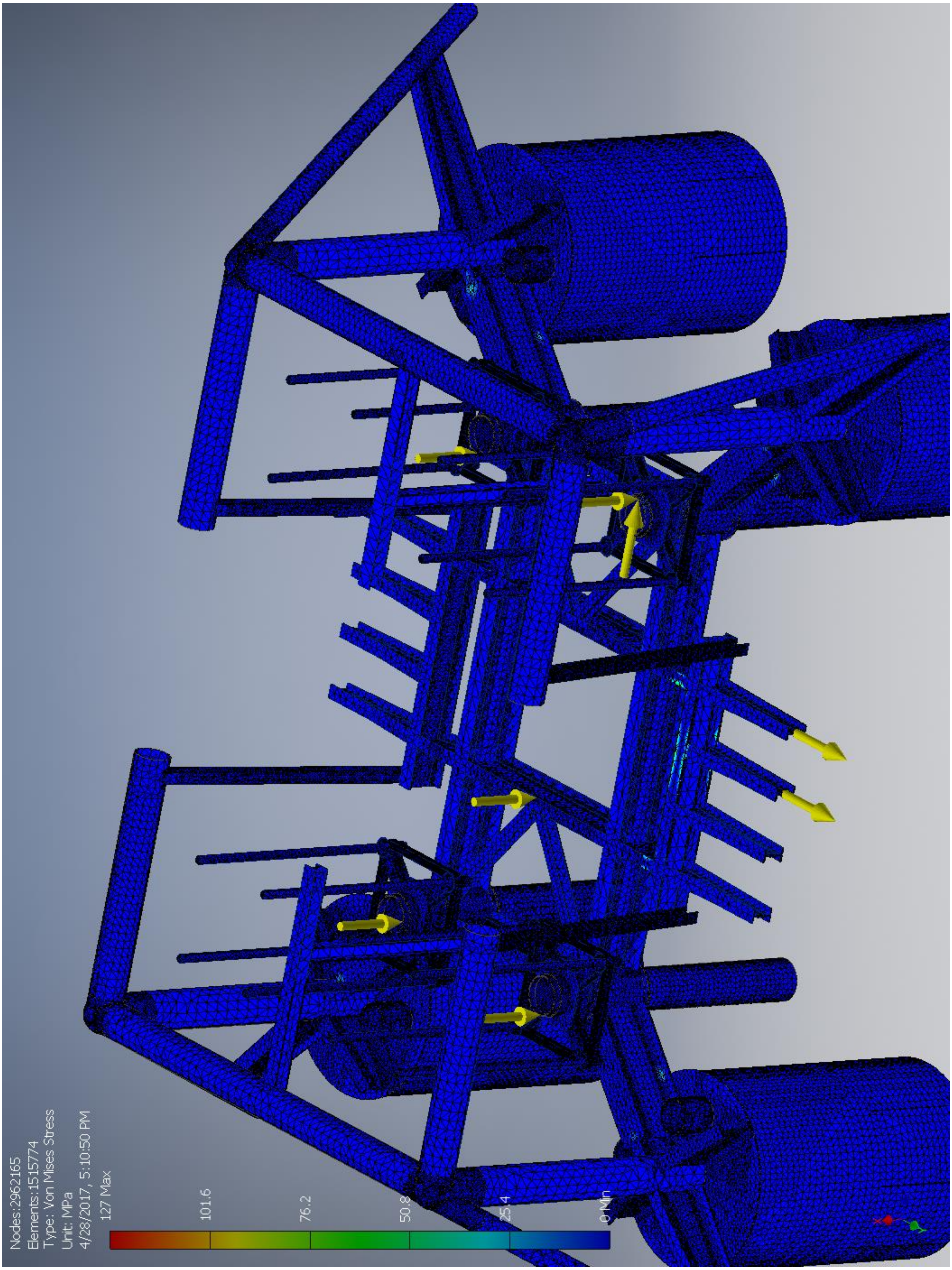

## 1st Principal Stress

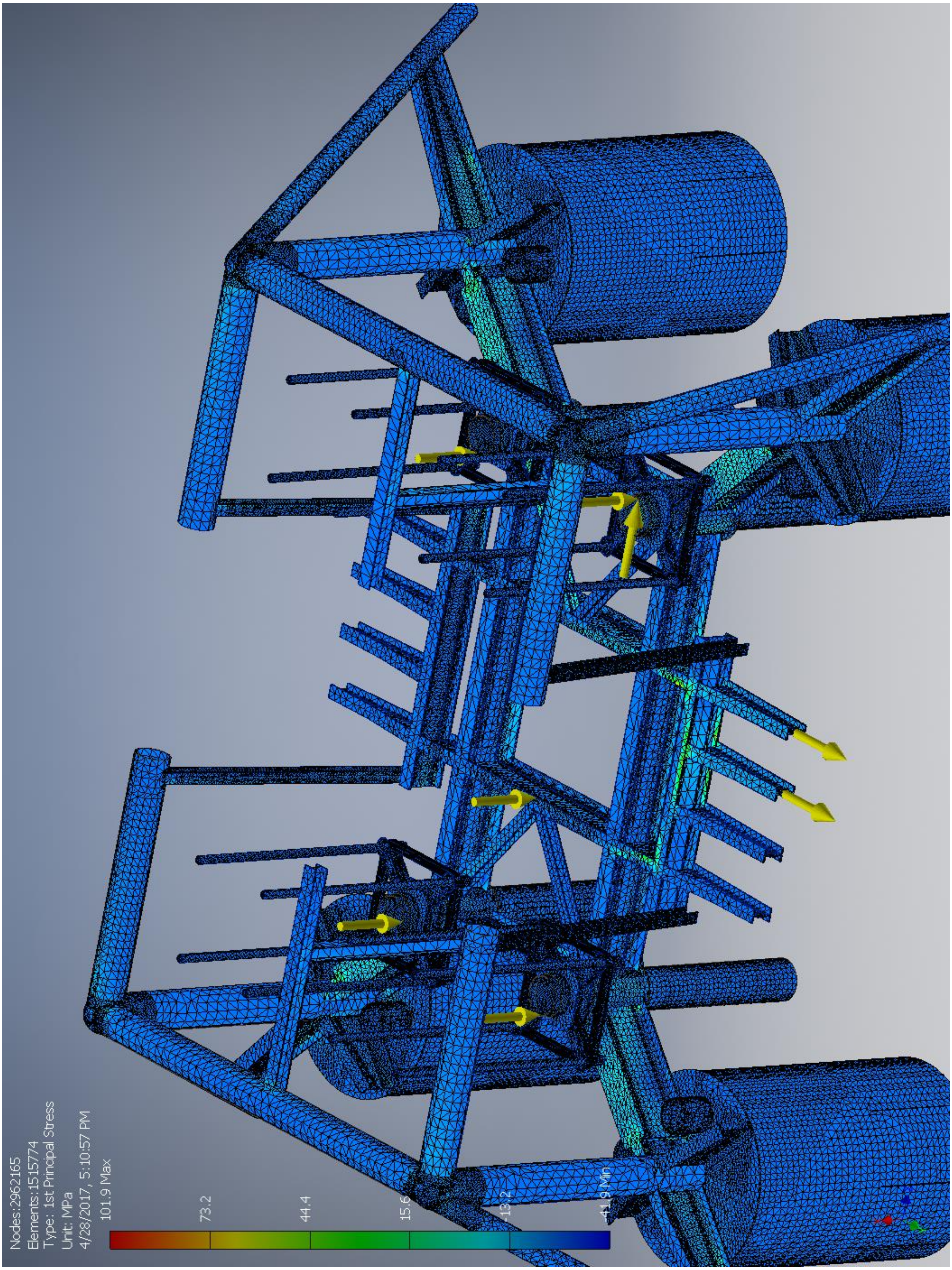

## ⊟ 3rd Principal Stress

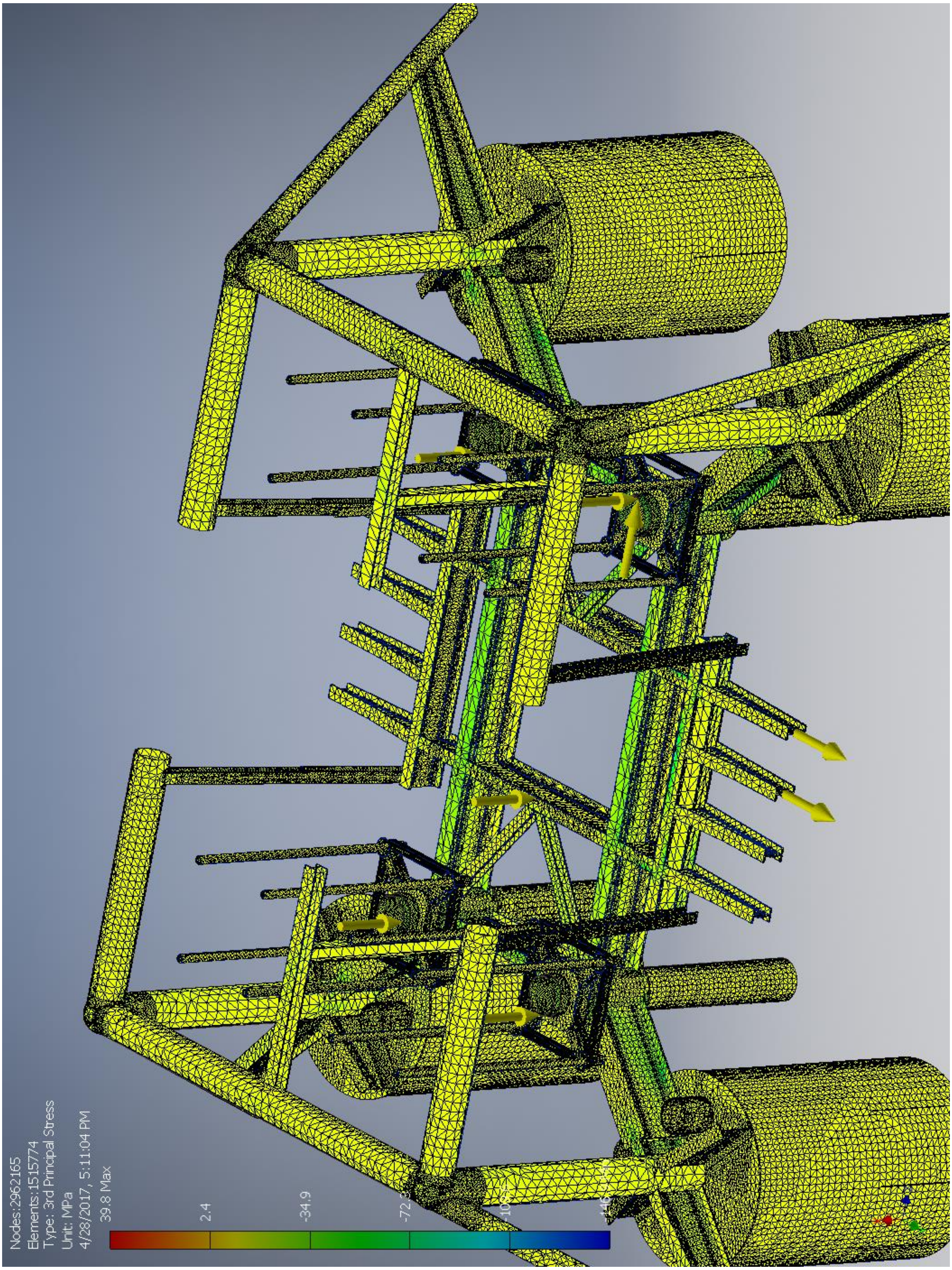

## ⊟ Displacement

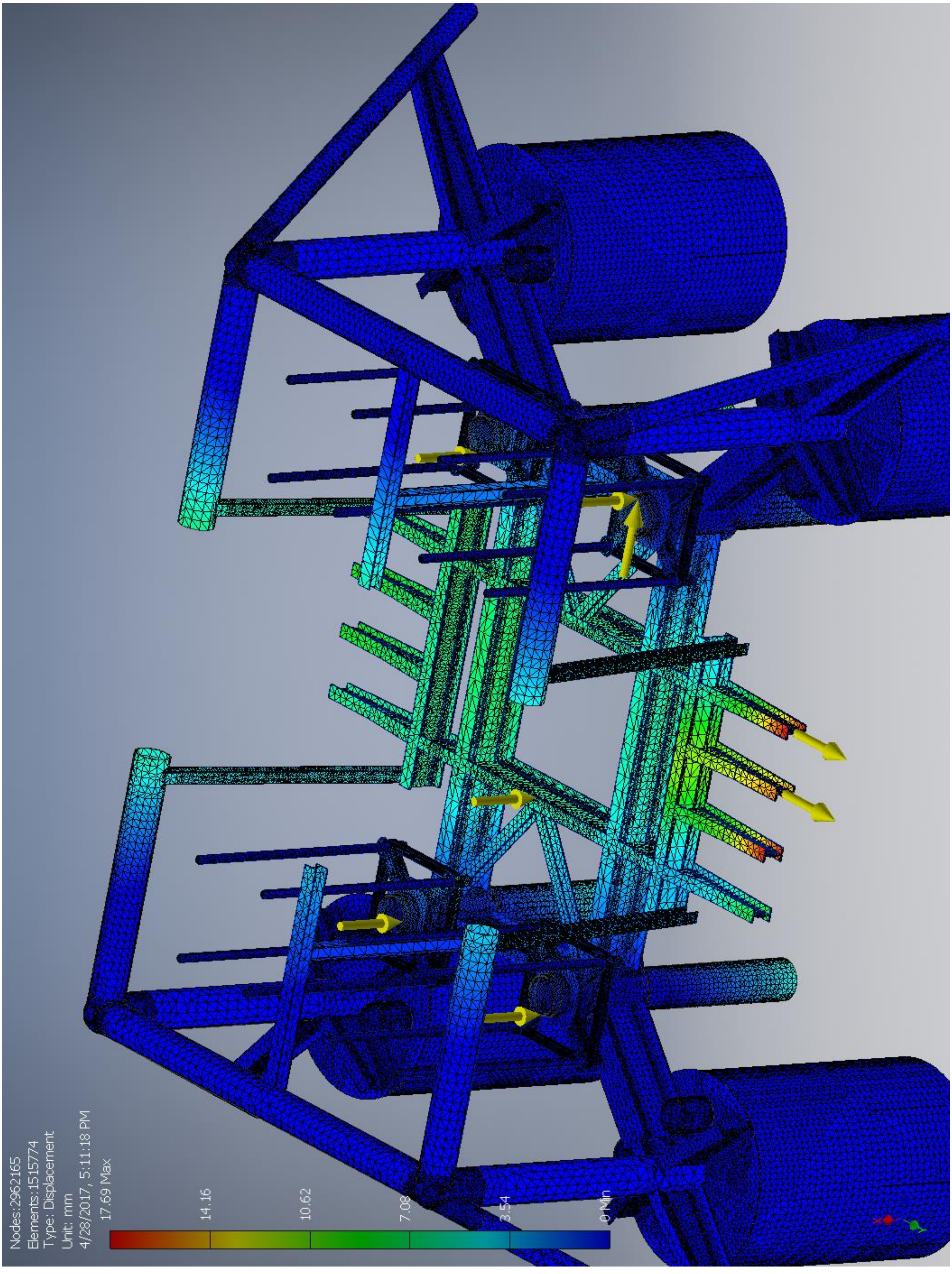

## ⊟ Safety Factor

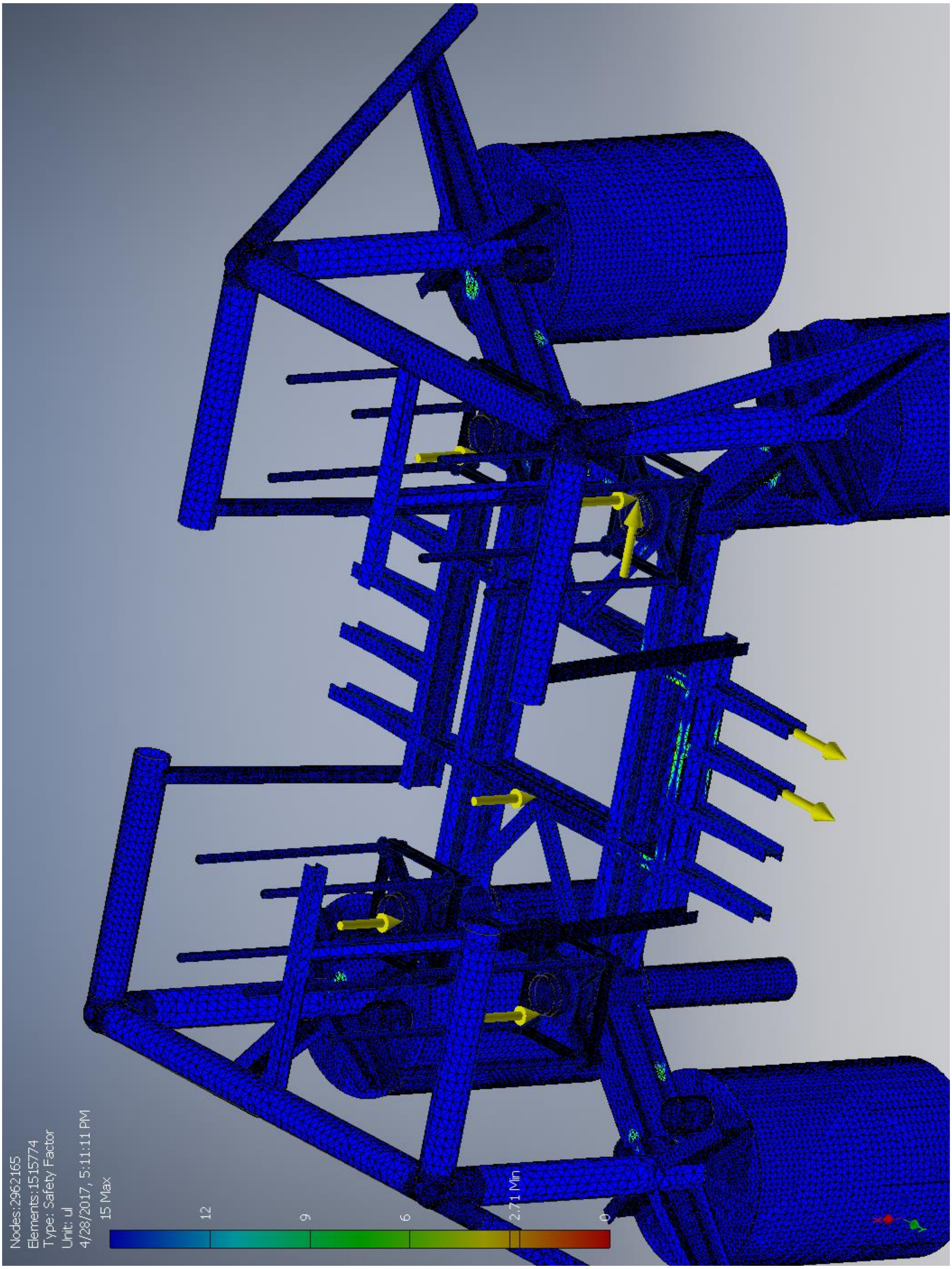

## I.5 Case-E

### I.5.1 Without convergence

# Stress Analysis Report

AUTODESK

| | |
|---|---|
| Analyzed File: | Assembly.iam |
| Autodesk Inventor Version: | 2017 (Build 210142000, 142) |
| Creation Date: | 4/27/2017, 5:19 PM |
| Study Author: | henrikwn |
| Summary: | |

---

## ⊟ Project Info (iProperties)

### ⊟ Summary

| | |
|---|---|
| Title | |
| Author | henrikwn |

### ⊟ Project

| | |
|---|---|
| Designer | henrikwn |

### ⊟ Physical

| | |
|---|---|
| Mass | 181171 kg |
| Area | 3.52908E+09 mm^2 |
| Volume | 6.02475E+10 mm^3 |
| Center of Gravity | x=-8288.42 mm<br>y=6548.24 mm<br>z=9857.84 mm |

Note: Physical values could be different from Physical values used by FEA reported below.

---

## ⊟ Case_E

**General objective and settings:**

| | |
|---|---|
| Design Objective | Single Point |
| Study Type | Static Analysis |
| Last Modification Date | 4/27/2017, 5:10 PM |
| Detect and Eliminate Rigid Body Modes | No |
| Separate Stresses Across Contact Surfaces | No |
| Motion Loads Analysis | No |

### ⊟ Operating conditions

## ⊟ Force:1

| | |
|---|---|
| Load Type | Force |
| Magnitude | 600000.000 N |
| Vector X | -600000.000 N |
| Vector Y | -0.000 N |
| Vector Z | -0.000 N |

### ⊟ Selected Face(s)

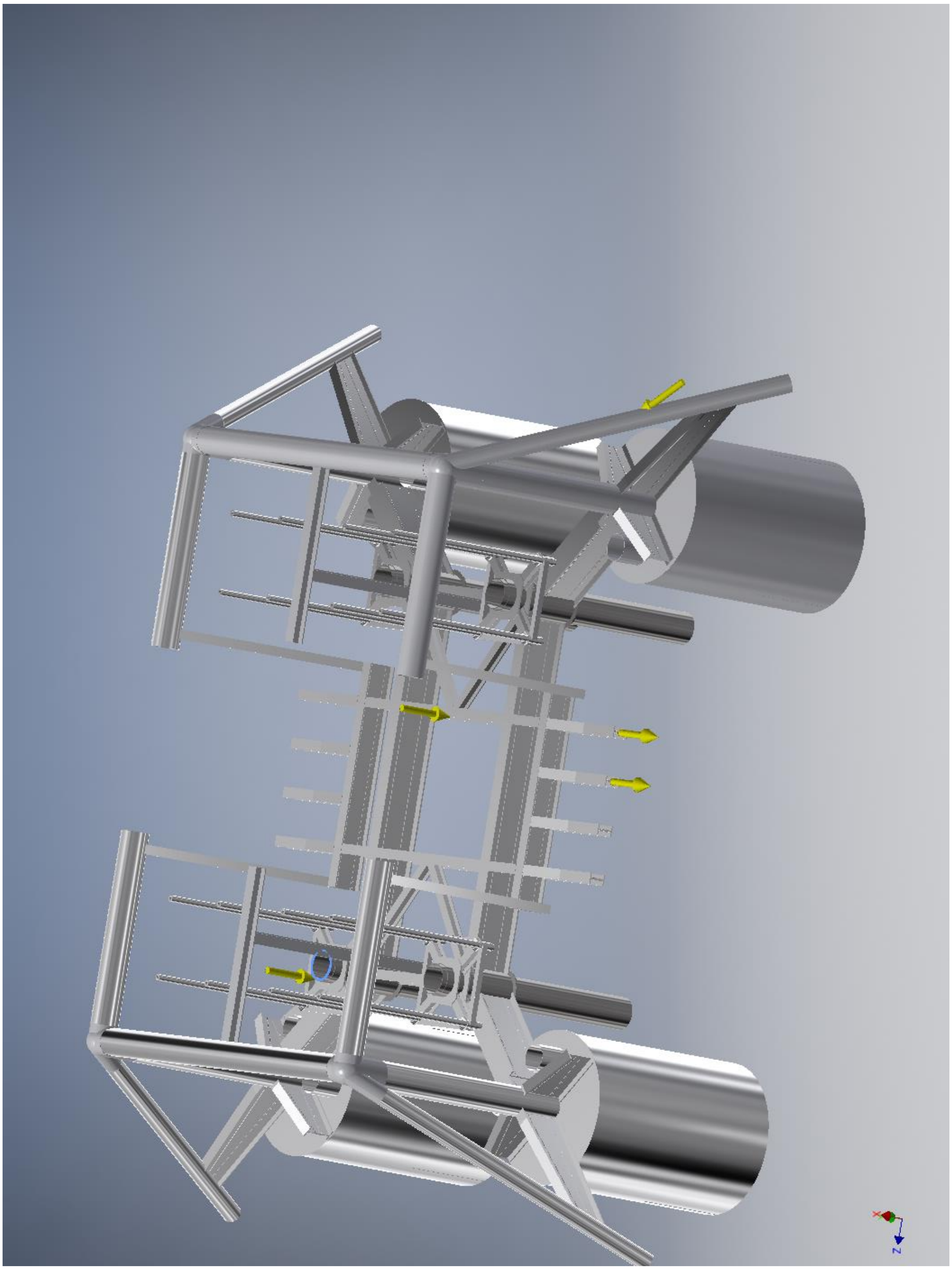

## ⊟ Force:2

| | |
|---|---|
| Load Type | Force |
| Magnitude | 800000.000 N |
| Vector X | -800000.000 N |
| Vector Y | -0.000 N |
| Vector Z | -0.000 N |

### ⊟ Selected Face(s)

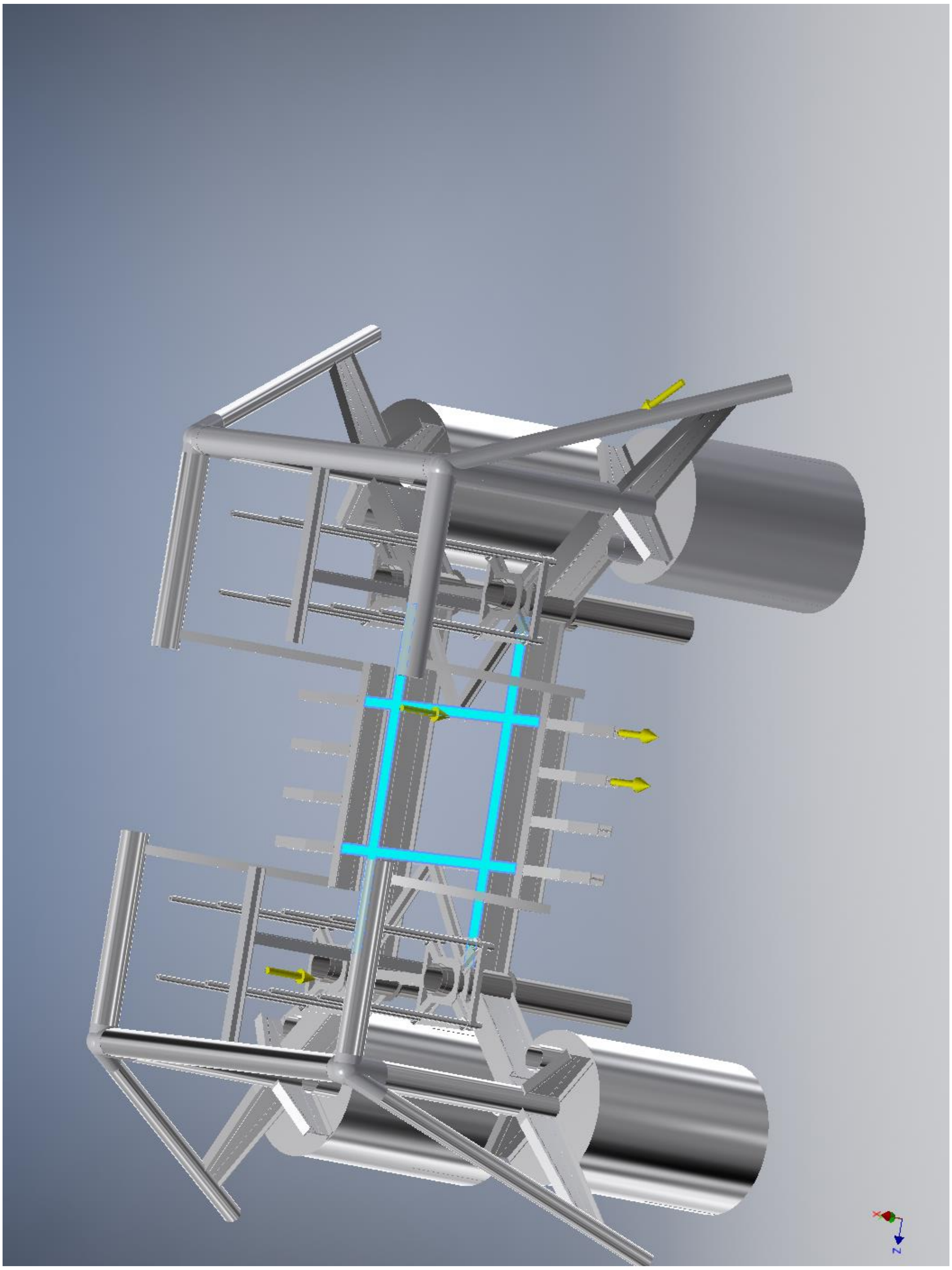

## ⊟ Force:3

| | |
|---|---|
| Load Type | Force |
| Magnitude | 300000.000 N |
| Vector X | 0.000 N |
| Vector Y | -300000.000 N |
| Vector Z | 0.000 N |

### ⊟ Selected Face(s)

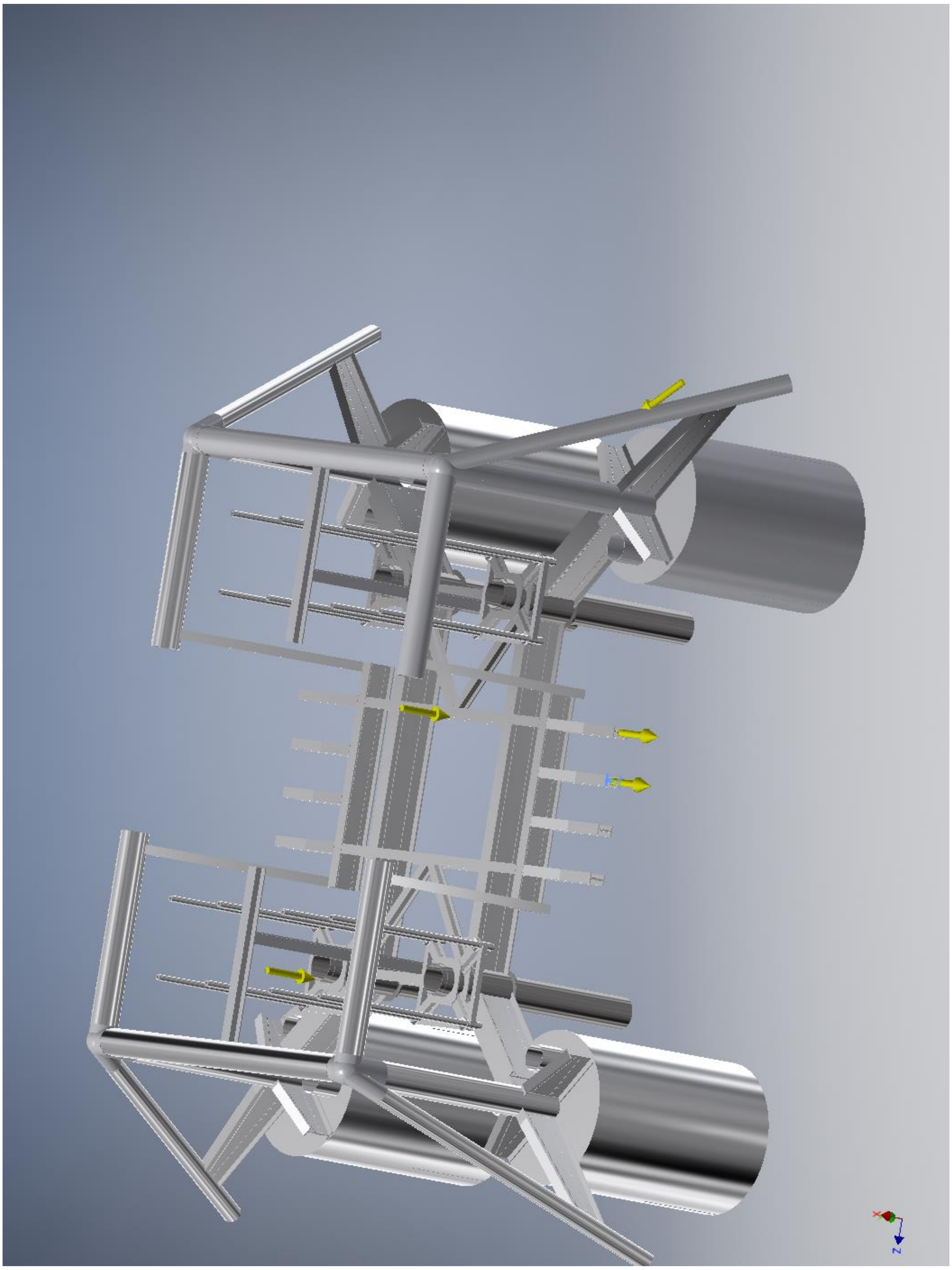

## ⊟ Force:4

| | |
|---|---|
| Load Type | Force |
| Magnitude | 300000.000 N |
| Vector X | -0.000 N |
| Vector Y | -300000.000 N |
| Vector Z | 0.000 N |

### ⊟ Selected Face(s)

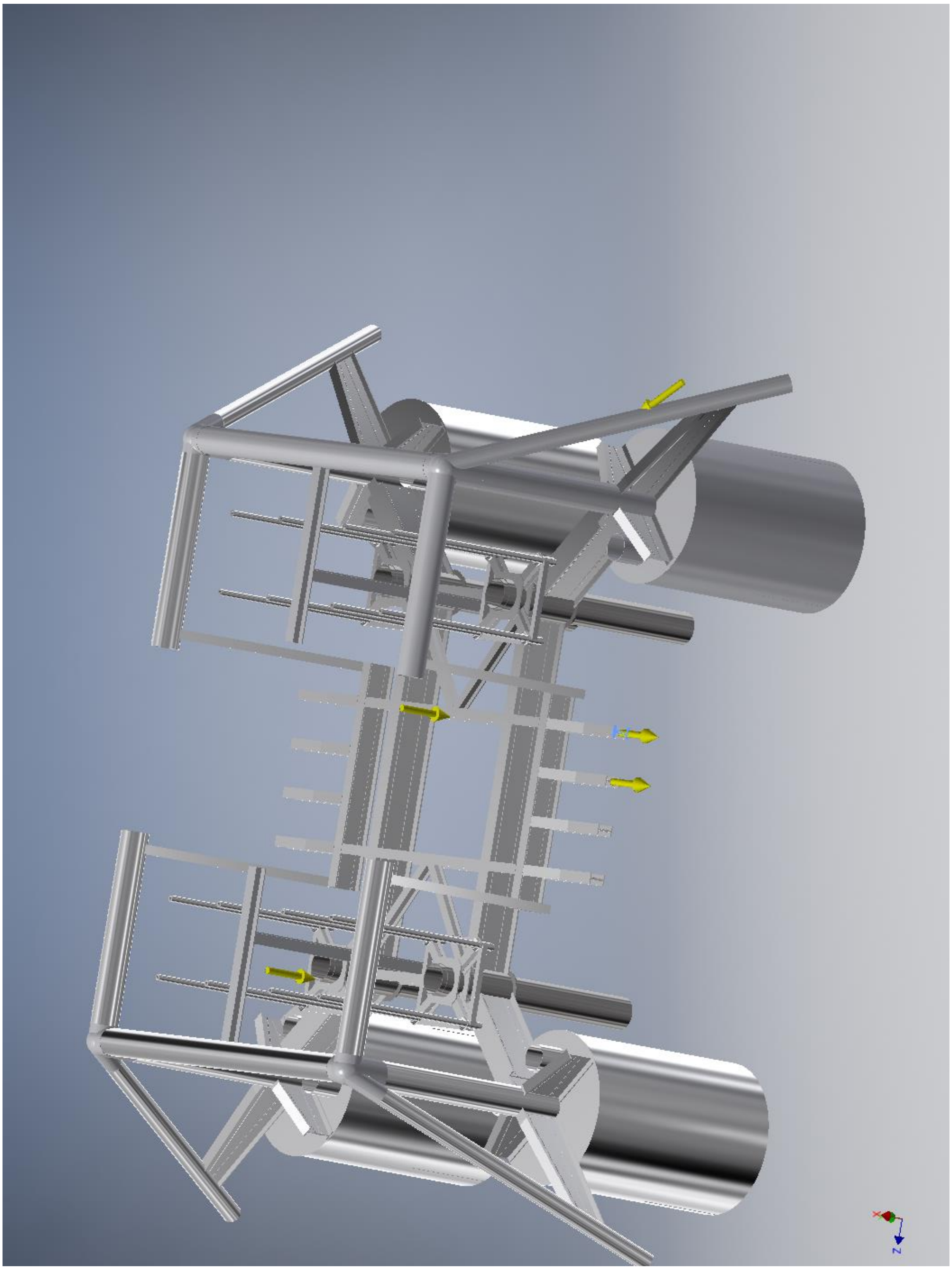

## ⊟ Force:5

| | |
|---|---|
| Load Type | Force |
| Magnitude | 1047367.023 N |
| Vector X | 342020.000 N |
| Vector Y | 700000.000 N |
| Vector Z | 700000.000 N |

### ⊟ Selected Face(s)

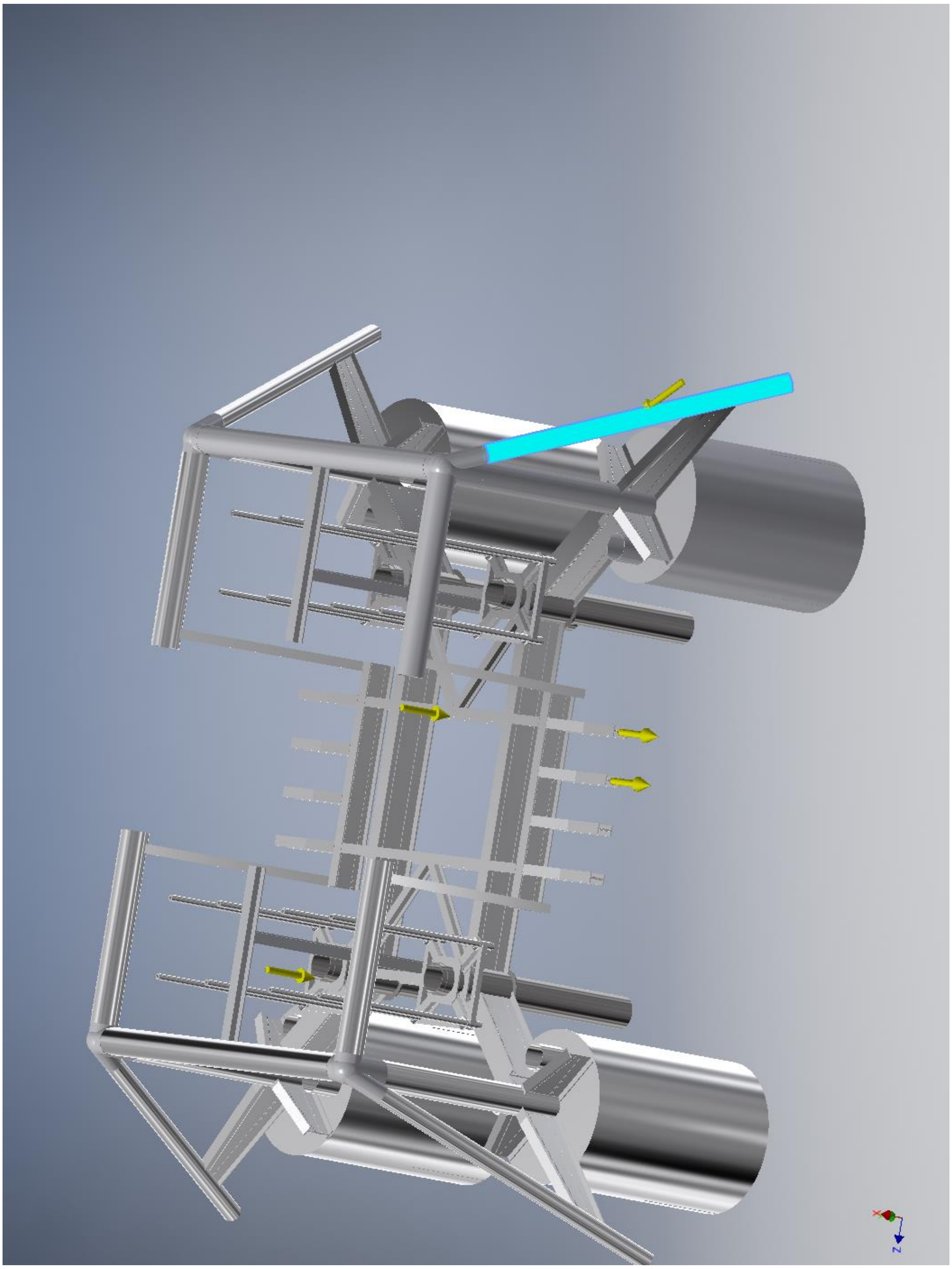

## ⊟ Fixed Constraint:1

| | |
|---|---|
| Constraint Type | Fixed Constraint |

### ⊟ Selected Face(s)

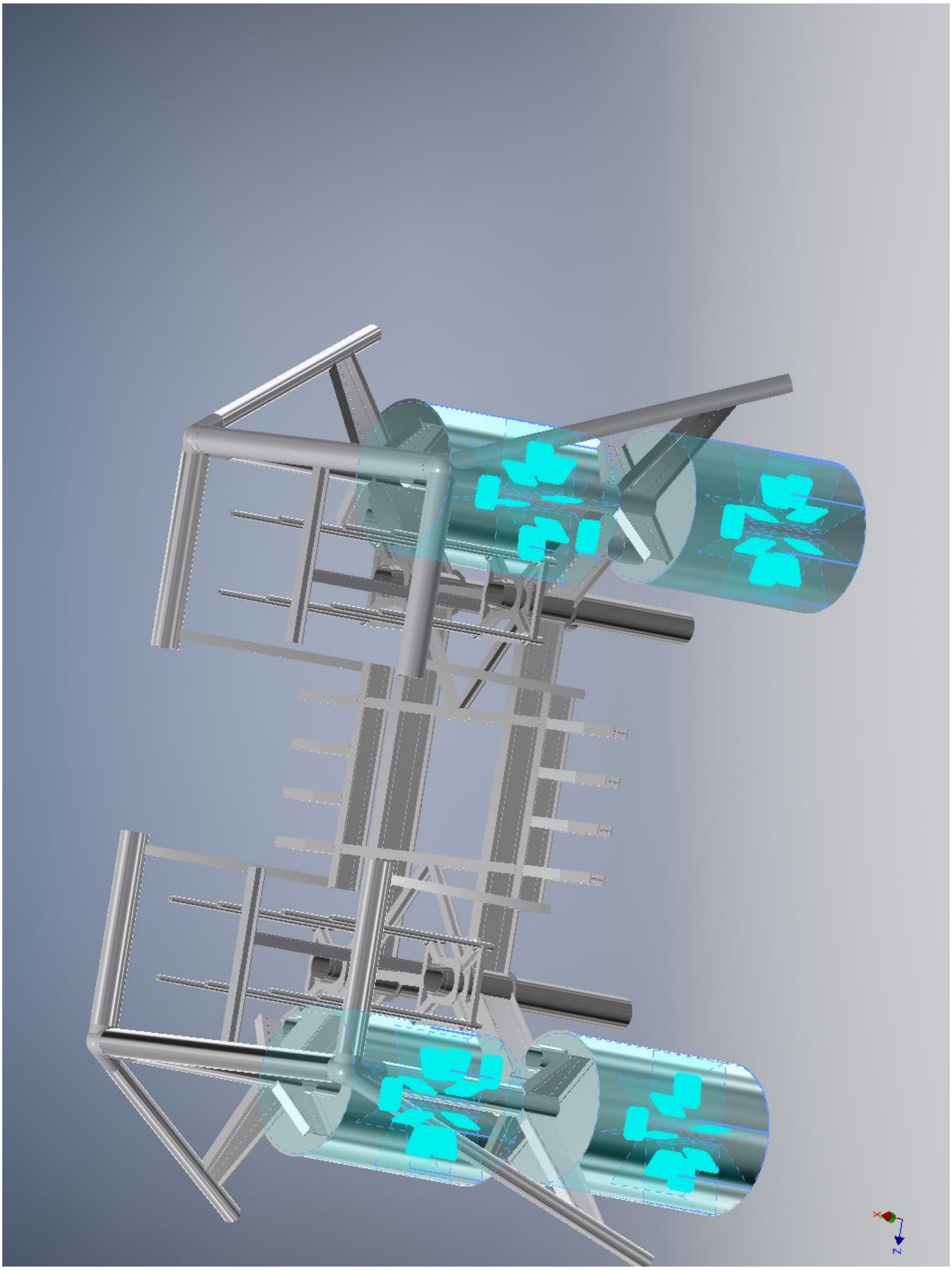

## ⊟ Results

### ⊟ Reaction Force and Moment on Constraints

| Constraint Name | Reaction Force | | Reaction Moment | |
|---|---|---|---|---|
| | Magnitude | Component (X,Y,Z) | Magnitude | Component (X,Y,Z) |
| Fixed Constraint:1 | 1272530 N | 1057980 N | 14744600 N m | -1340550 N m |
| | | -100000 N | | 13024400 N m |
| | | -700000 N | | -6780180 N m |

### ⊟ Result Summary

| Name | Minimum | Maximum |
|---|---|---|
| Volume | 6.02475E+10 mm^3 | |
| Mass | 181171 kg | |
| Von Mises Stress | 0 MPa | 283.315 MPa |
| 1st Principal Stress | -61.317 MPa | 137.09 MPa |
| 3rd Principal Stress | -227.754 MPa | 39.9197 MPa |
| Displacement | 0 mm | 19.5821 mm |
| Safety Factor | 0.97065 ul | 15 ul |

### ⊟ Figures

## ⊟ Von Mises Stress

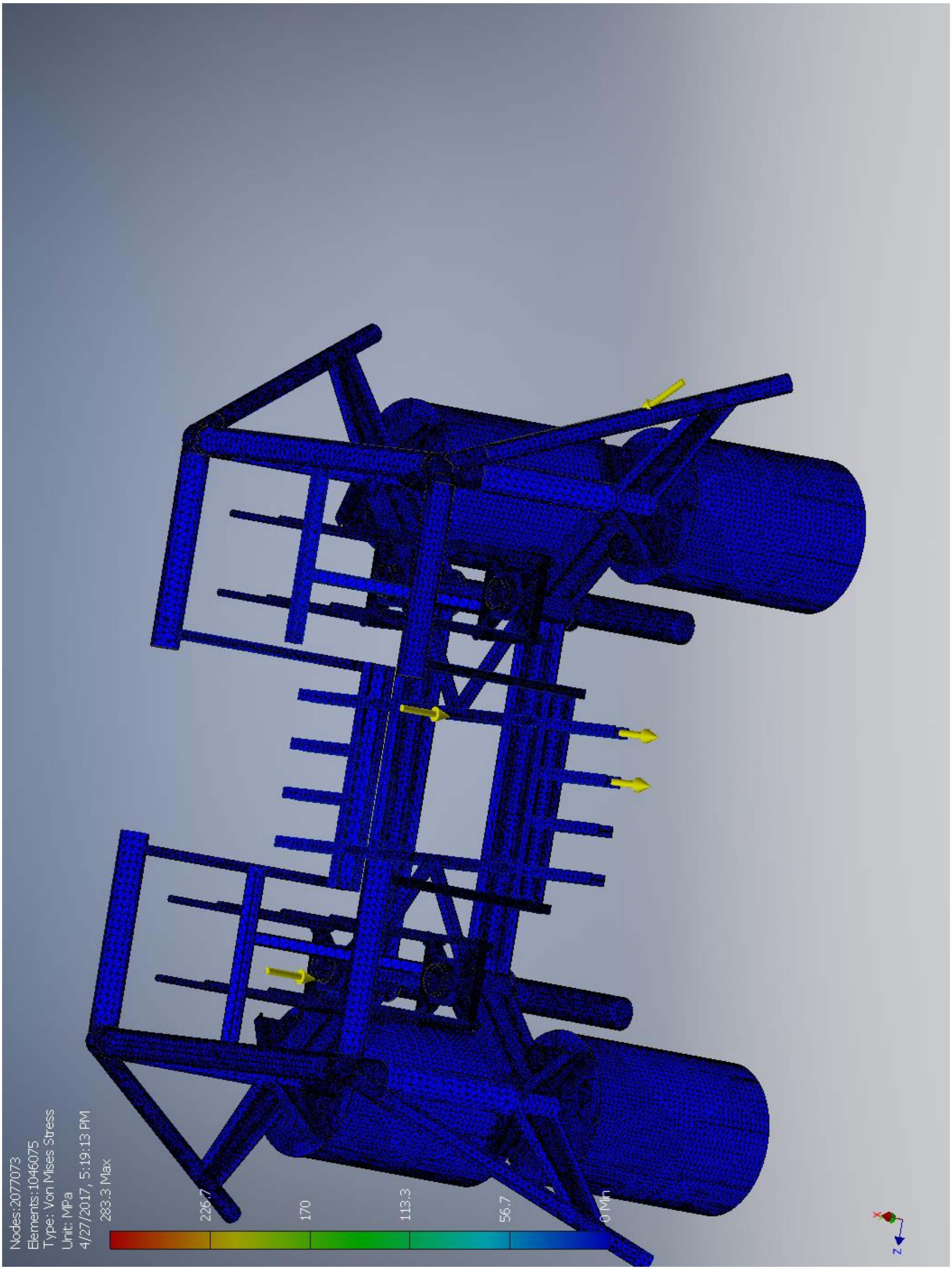

## ⊟ 1st Principal Stress

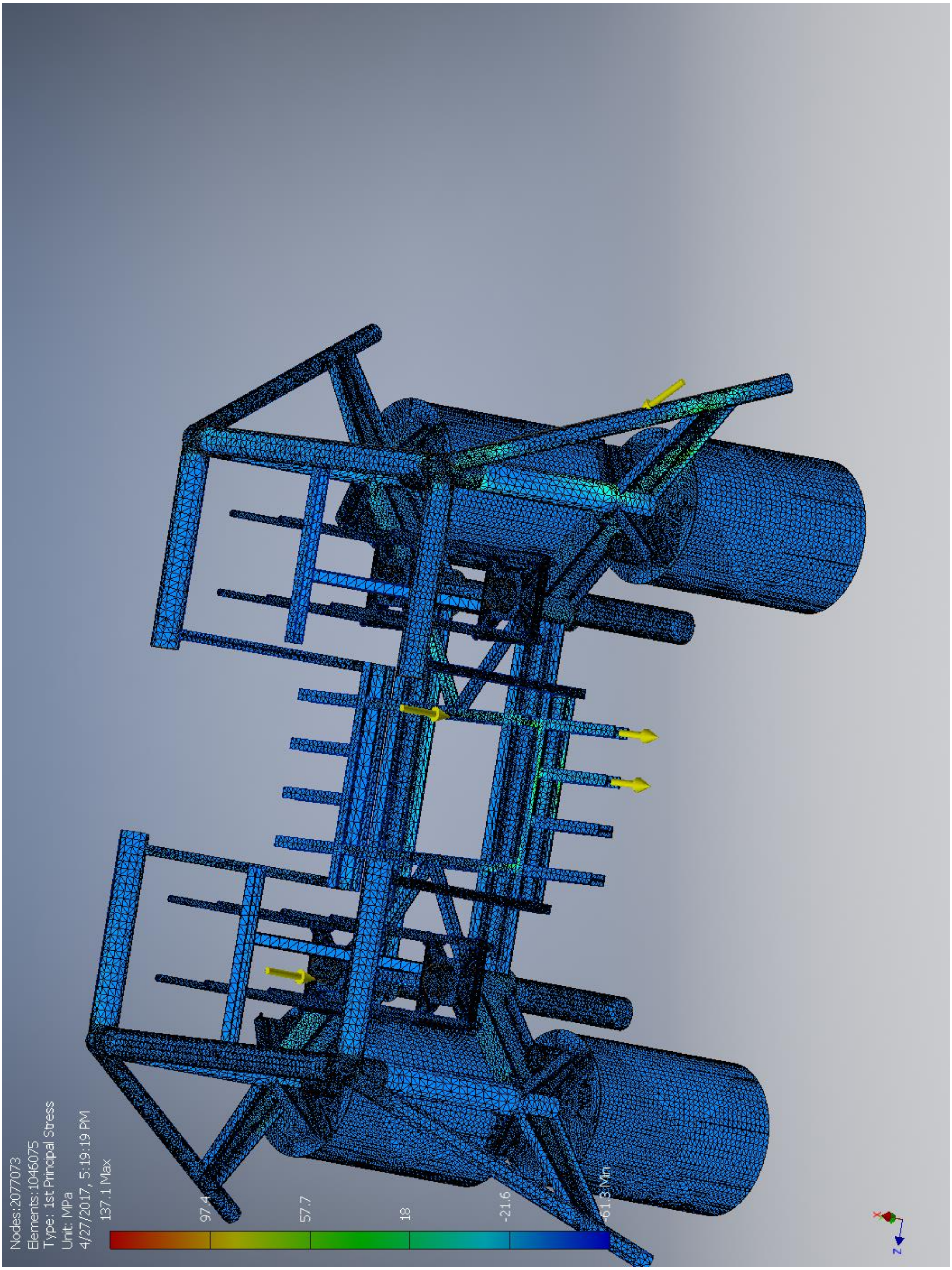

## ⊟ 3rd Principal Stress

## ⊟ Displacement

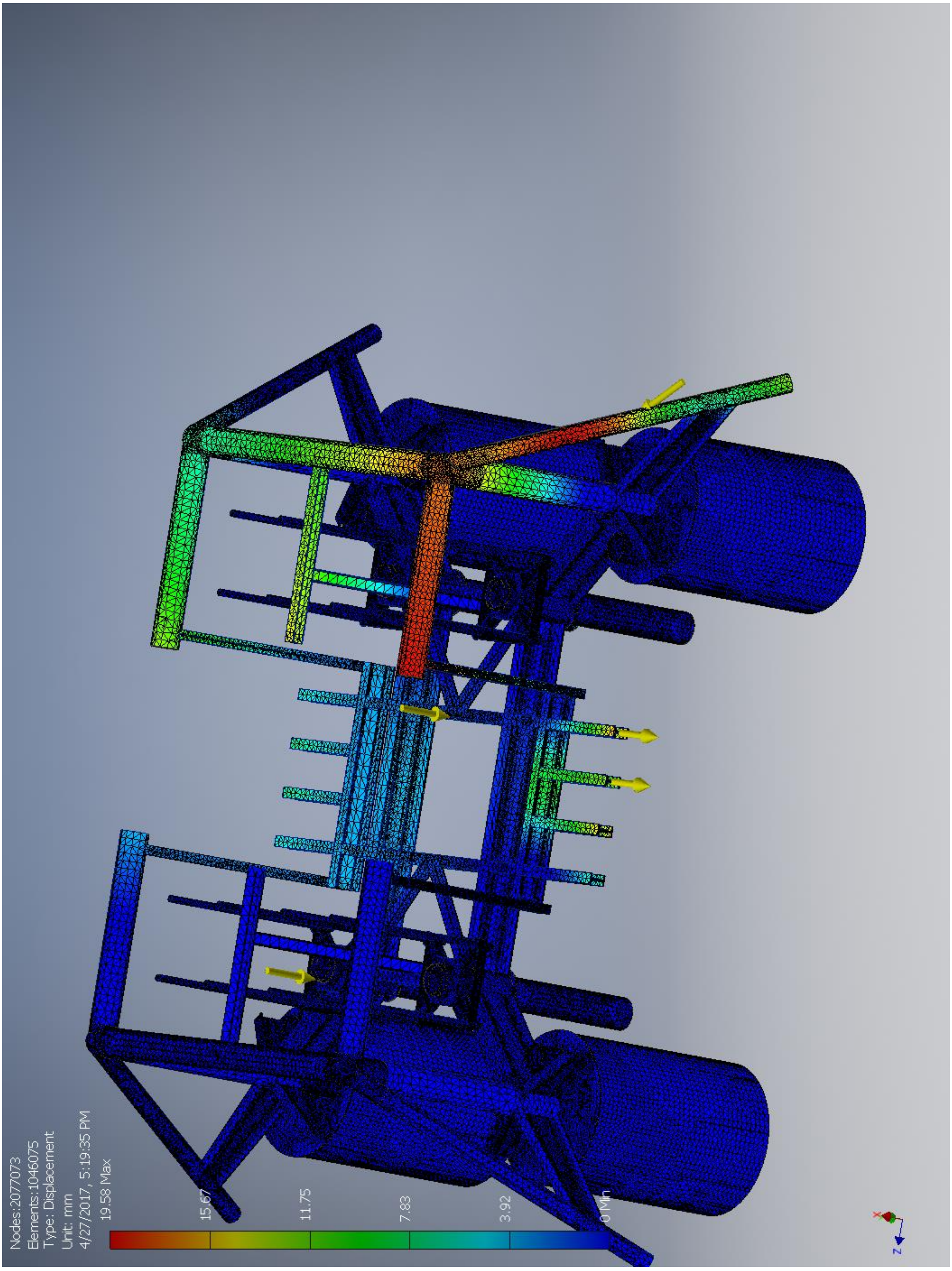

## ⊟ Safety Factor

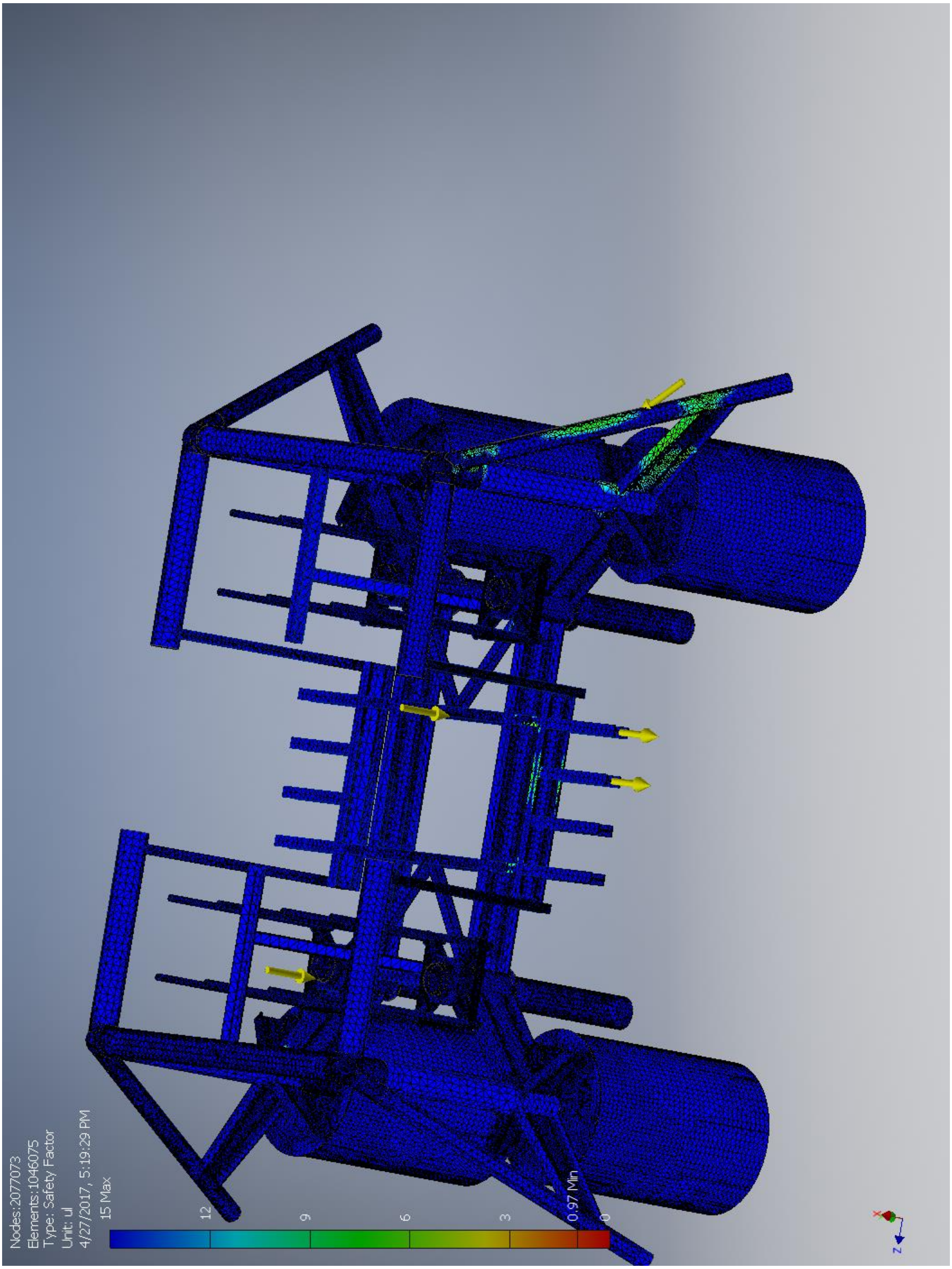

### I.5.2 With convergence

# Stress Analysis Report

| | |
|---|---|
| Analyzed File: | Assembly.iam |
| Autodesk Inventor Version: | 2017 (Build 210142000, 142) |
| Creation Date: | 4/28/2017, 9:16 AM |
| Study Author: | henrikwn |
| Summary: | |

---

## ⊟ Project Info (iProperties)

### ⊟ Summary

| | |
|---|---|
| Title | |
| Author | henrikwn |

### ⊟ Project

| | |
|---|---|
| Designer | henrikwn |

### ⊟ Physical

| | |
|---|---|
| Mass | 181171 kg |
| Area | 3.52908E+09 mm^2 |
| Volume | 6.02475E+10 mm^3 |
| Center of Gravity | x=-8288.42 mm<br>y=6548.24 mm<br>z=9857.84 mm |

Note: Physical values could be different from Physical values used by FEA reported below.

---

## ⊟ Case_E

**General objective and settings:**

| | |
|---|---|
| Design Objective | Single Point |
| Study Type | Static Analysis |
| Last Modification Date | 4/27/2017, 6:26 PM |
| Detect and Eliminate Rigid Body Modes | No |
| Separate Stresses Across Contact Surfaces | No |
| Motion Loads Analysis | No |

## ⊟ Operating conditions

## ⊟ Force:1

| | |
|---|---|
| Load Type | Force |
| Magnitude | 600000.000 N |
| Vector X | -600000.000 N |
| Vector Y | -0.000 N |
| Vector Z | -0.000 N |

### ⊟ Selected Face(s)

## ⊟ Force:2

| | |
|---|---|
| Load Type | Force |
| Magnitude | 800000.000 N |
| Vector X | -800000.000 N |
| Vector Y | -0.000 N |
| Vector Z | -0.000 N |

### ⊟ Selected Face(s)

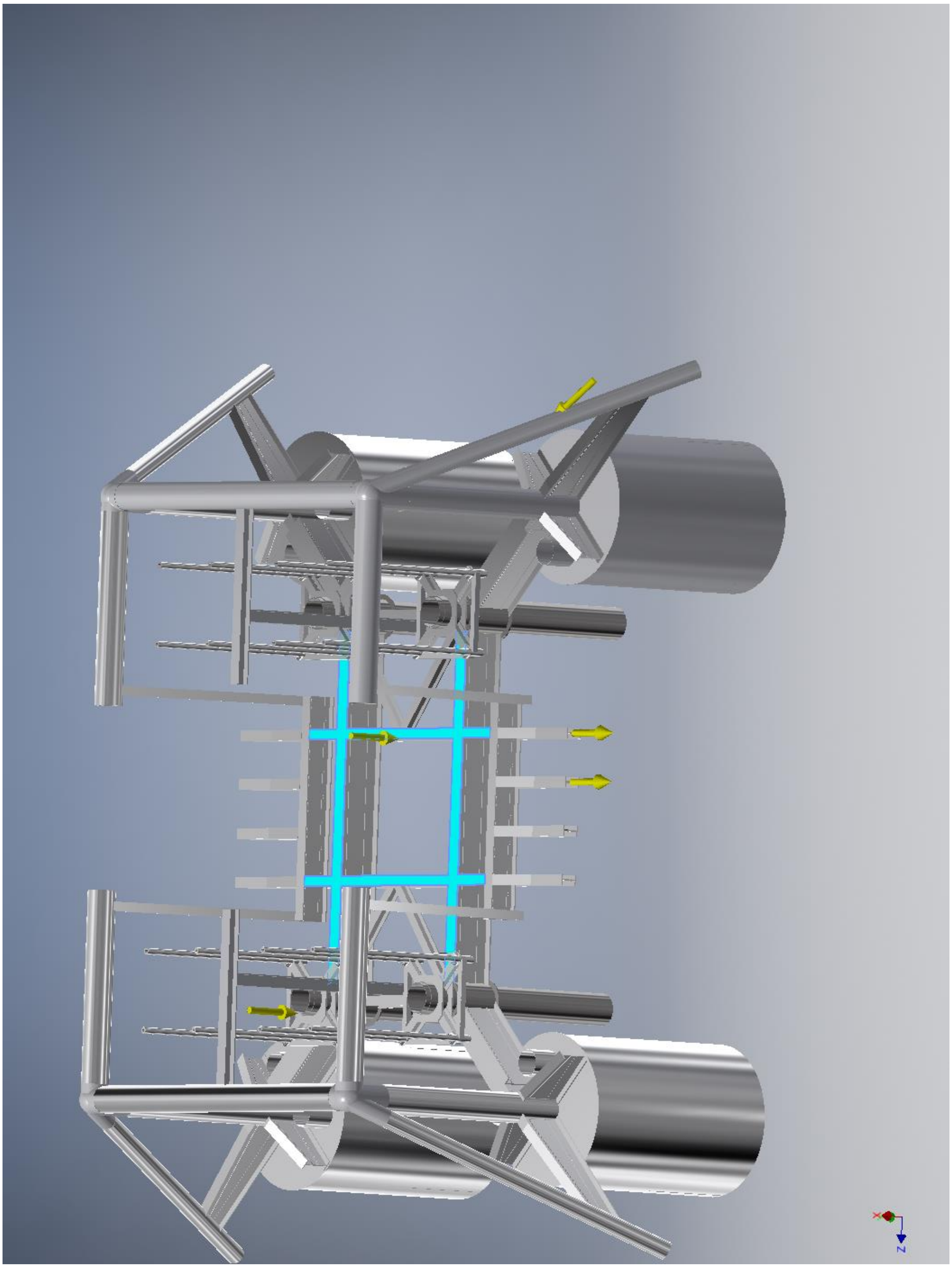

## ⊟ Force:3

| | |
|---|---|
| Load Type | Force |
| Magnitude | 300000.000 N |
| Vector X | 0.000 N |
| Vector Y | -300000.000 N |
| Vector Z | 0.000 N |

### ⊟ Selected Face(s)

### ⊟ Force:4

| | |
|---|---|
| Load Type | Force |
| Magnitude | 300000.000 N |
| Vector X | -0.000 N |
| Vector Y | -300000.000 N |
| Vector Z | 0.000 N |

#### ⊟ Selected Face(s)

## ⊟ Force:5

| | |
|---|---|
| Load Type | Force |
| Magnitude | 1047367.023 N |
| Vector X | 342020.000 N |
| Vector Y | 700000.000 N |
| Vector Z | 700000.000 N |

### ⊟ Selected Face(s)

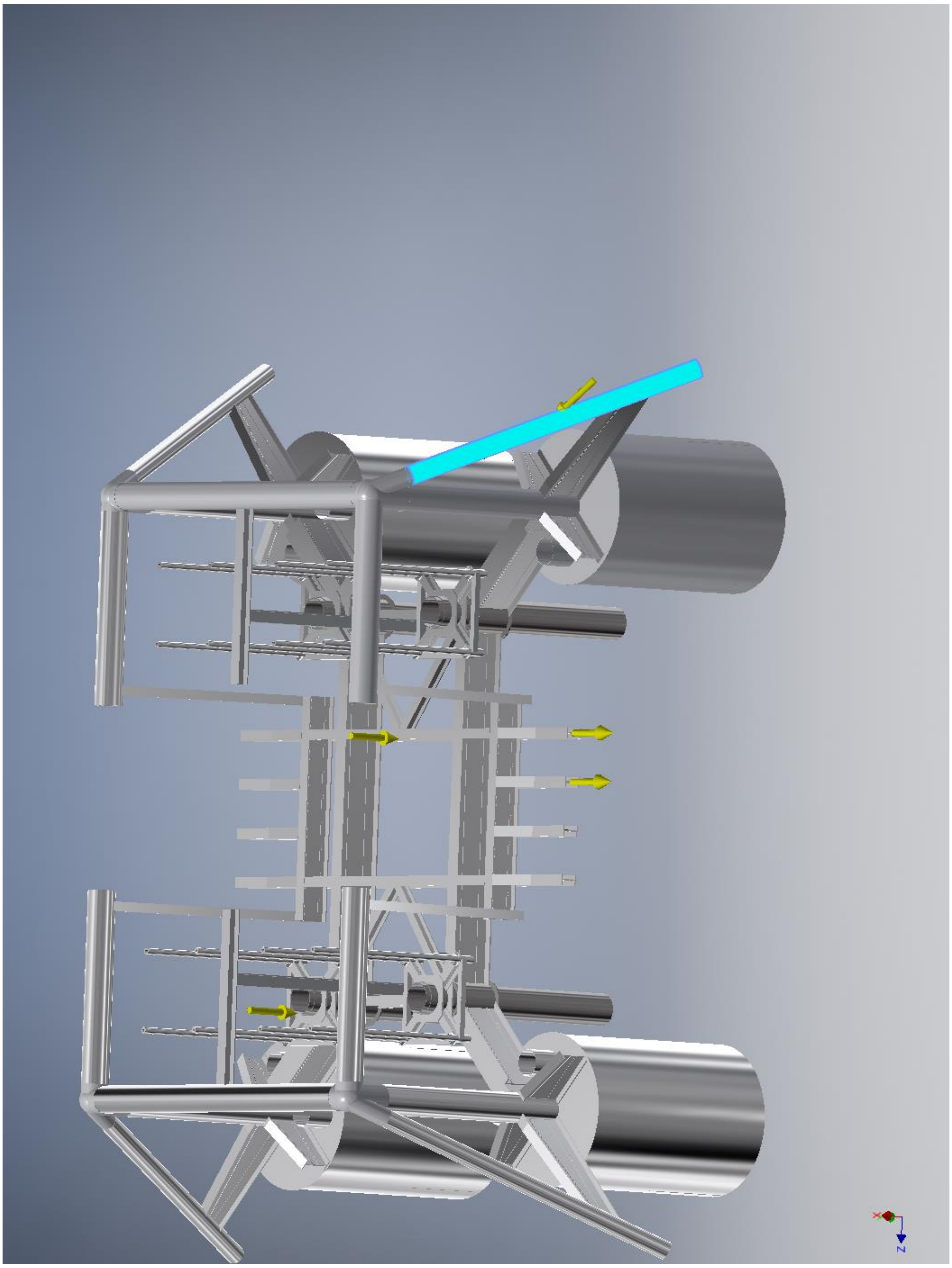

## ⊟ Fixed Constraint:1

| Constraint Type | Fixed Constraint |
|---|---|

### ⊟ Selected Face(s)

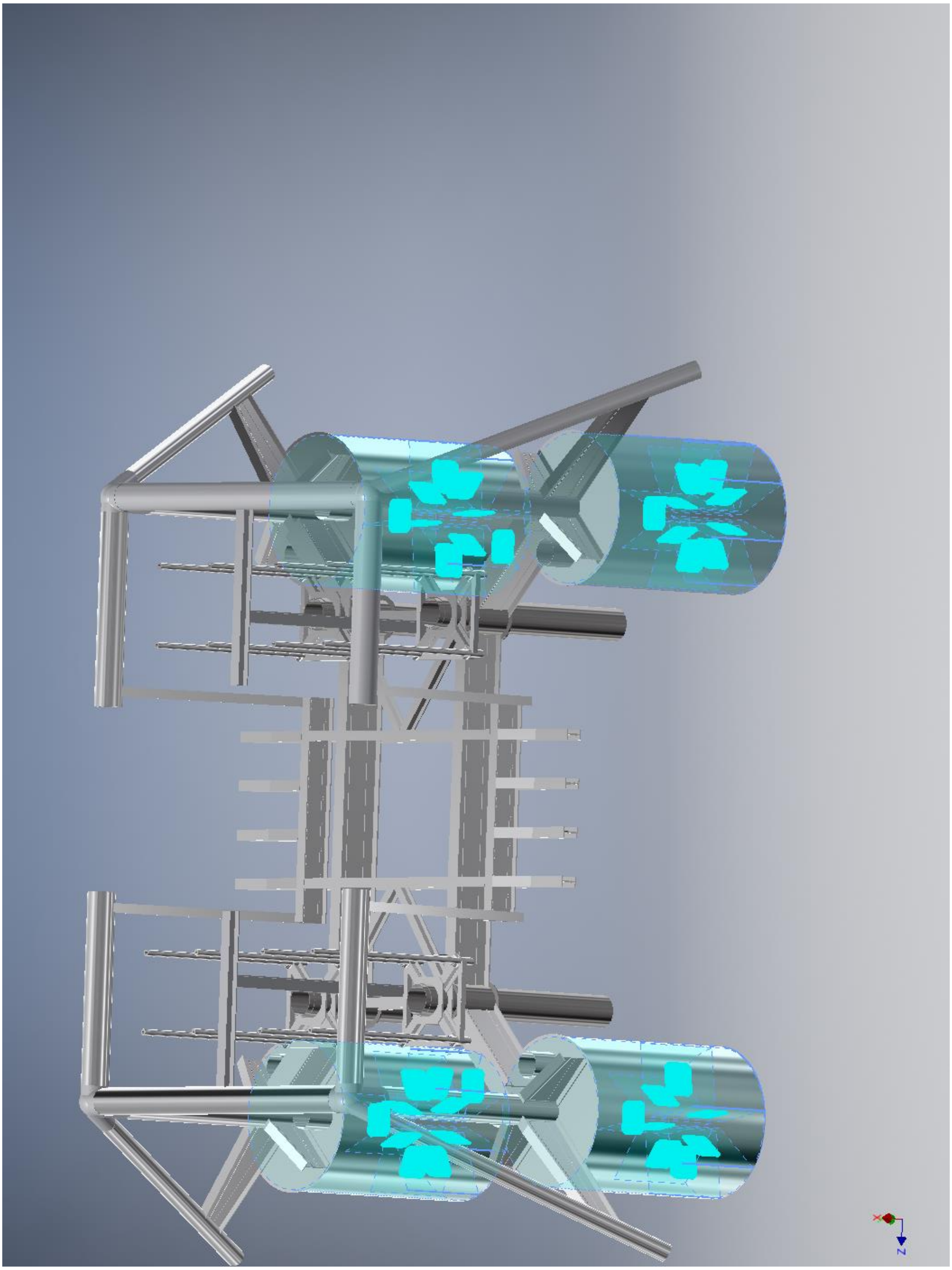

## ⊟ Results

### ⊟ Reaction Force and Moment on Constraints

| Constraint Name | Reaction Force | | Reaction Moment | |
|---|---|---|---|---|
| | **Magnitude** | **Component (X,Y,Z)** | **Magnitude** | **Component (X,Y,Z)** |
| Fixed Constraint:1 | 1272530 N | 1057980 N | 14740800 N m | -1341780 N m |
| | | -100000 N | | 13020700 N m |
| | | -700000 N | | -6778770 N m |

### ⊟ Result Summary

| Name | Minimum | Maximum |
|---|---|---|
| Volume | 6.02475E+10 mm^3 | |
| Mass | 181171 kg | |
| Von Mises Stress | 0 MPa | 7059.03 MPa |
| 1st Principal Stress | -1334.08 MPa | 4306.8 MPa |
| 3rd Principal Stress | -8525.02 MPa | 64.9763 MPa |
| Displacement | 0 mm | 20.6414 mm |
| Safety Factor | 0.0389572 ul | 15 ul |

### ⊟ Figures

## ⊟ Von Mises Stress

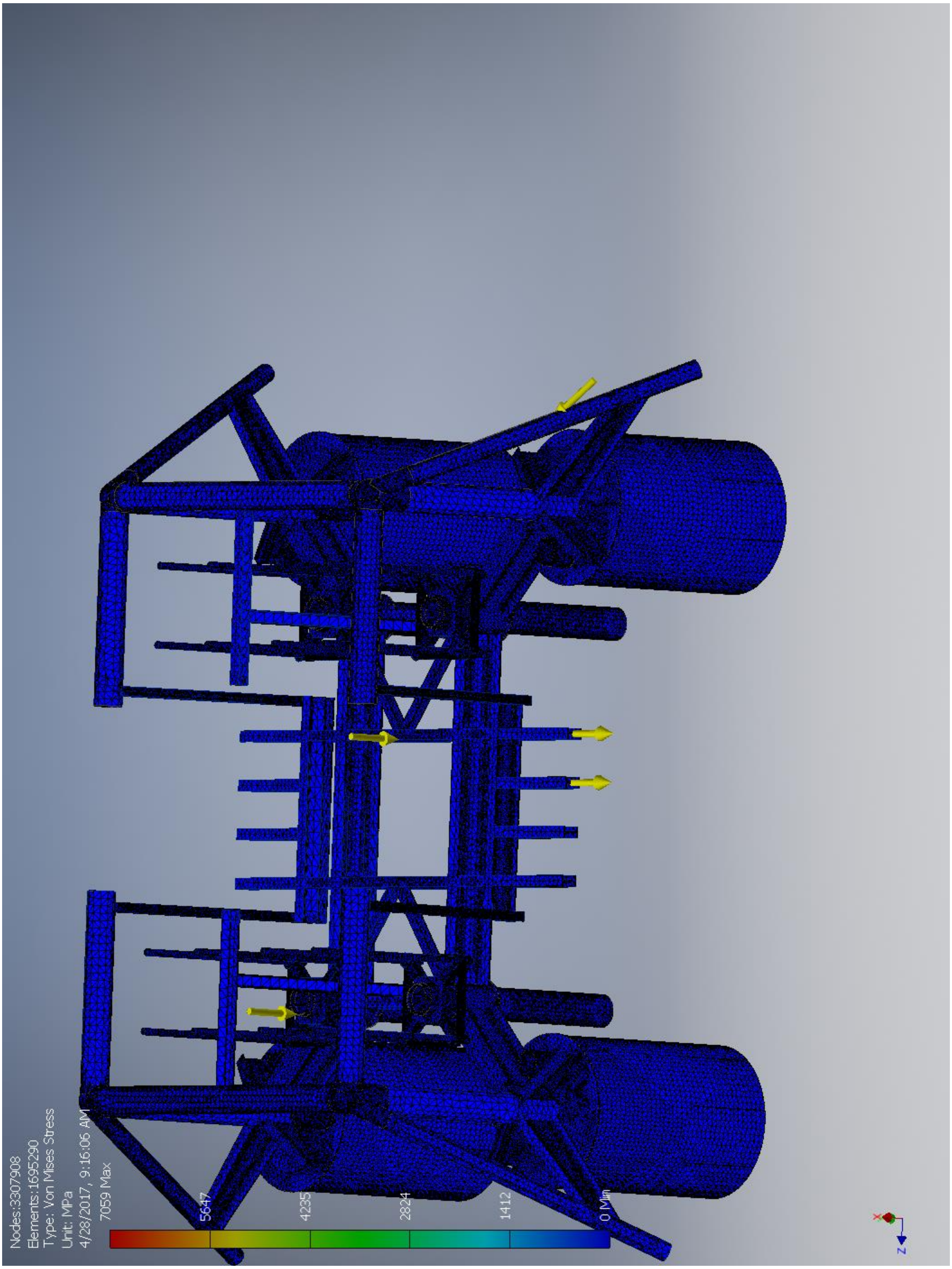

## ⊟ 1st Principal Stress

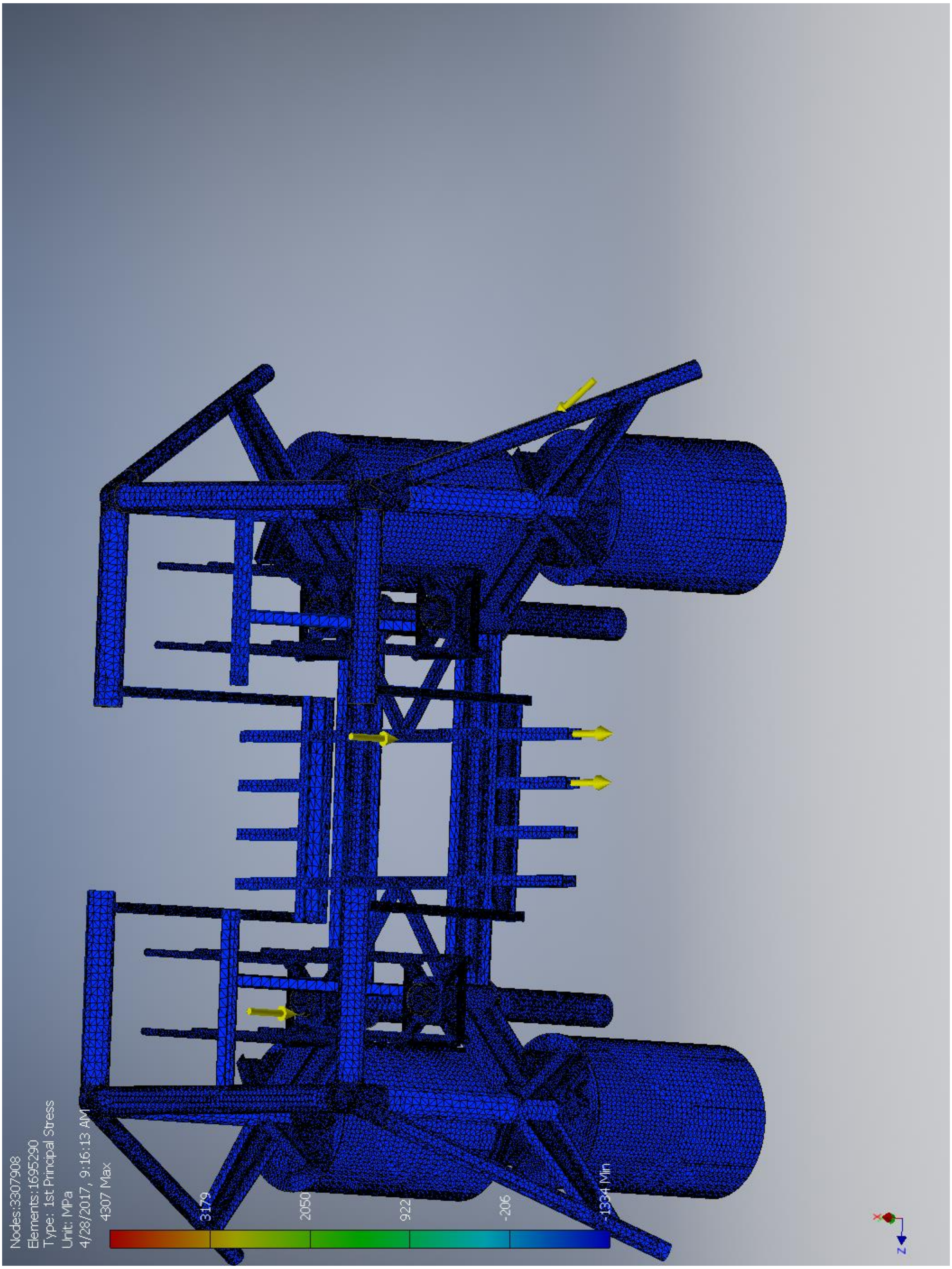

## ⊟ 3rd Principal Stress

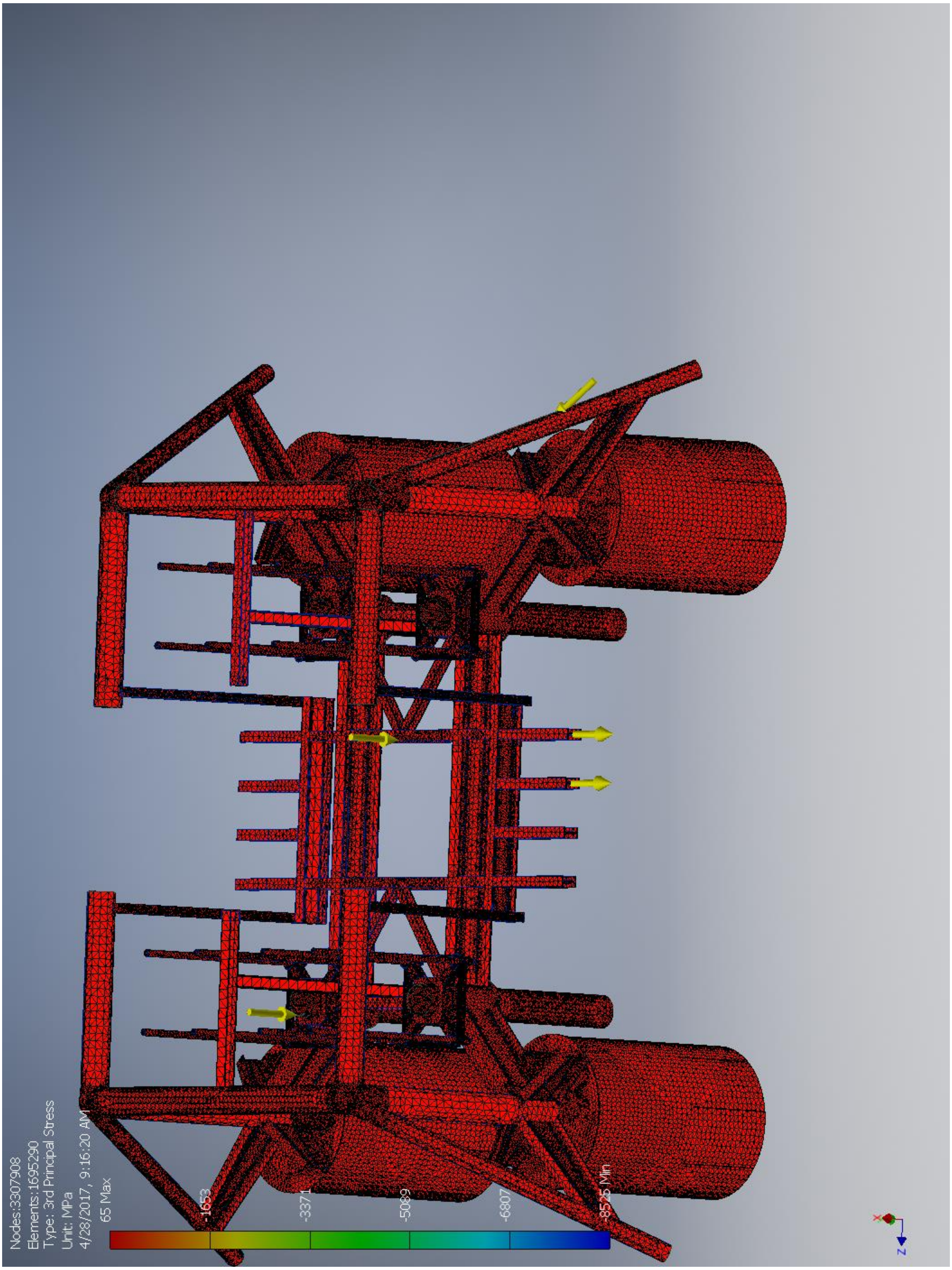

## ⊟ Displacement

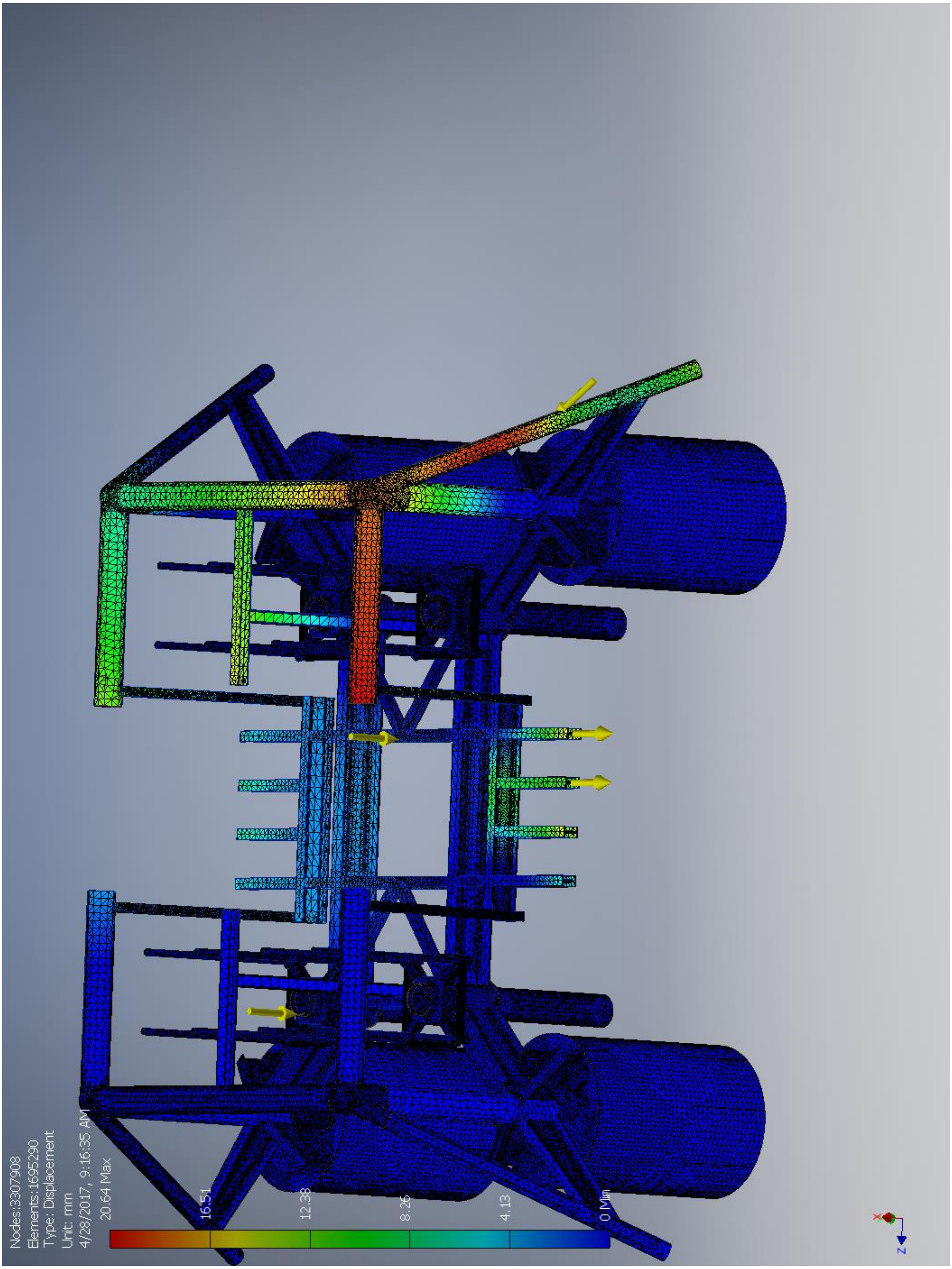

## ⊟ Safety Factor

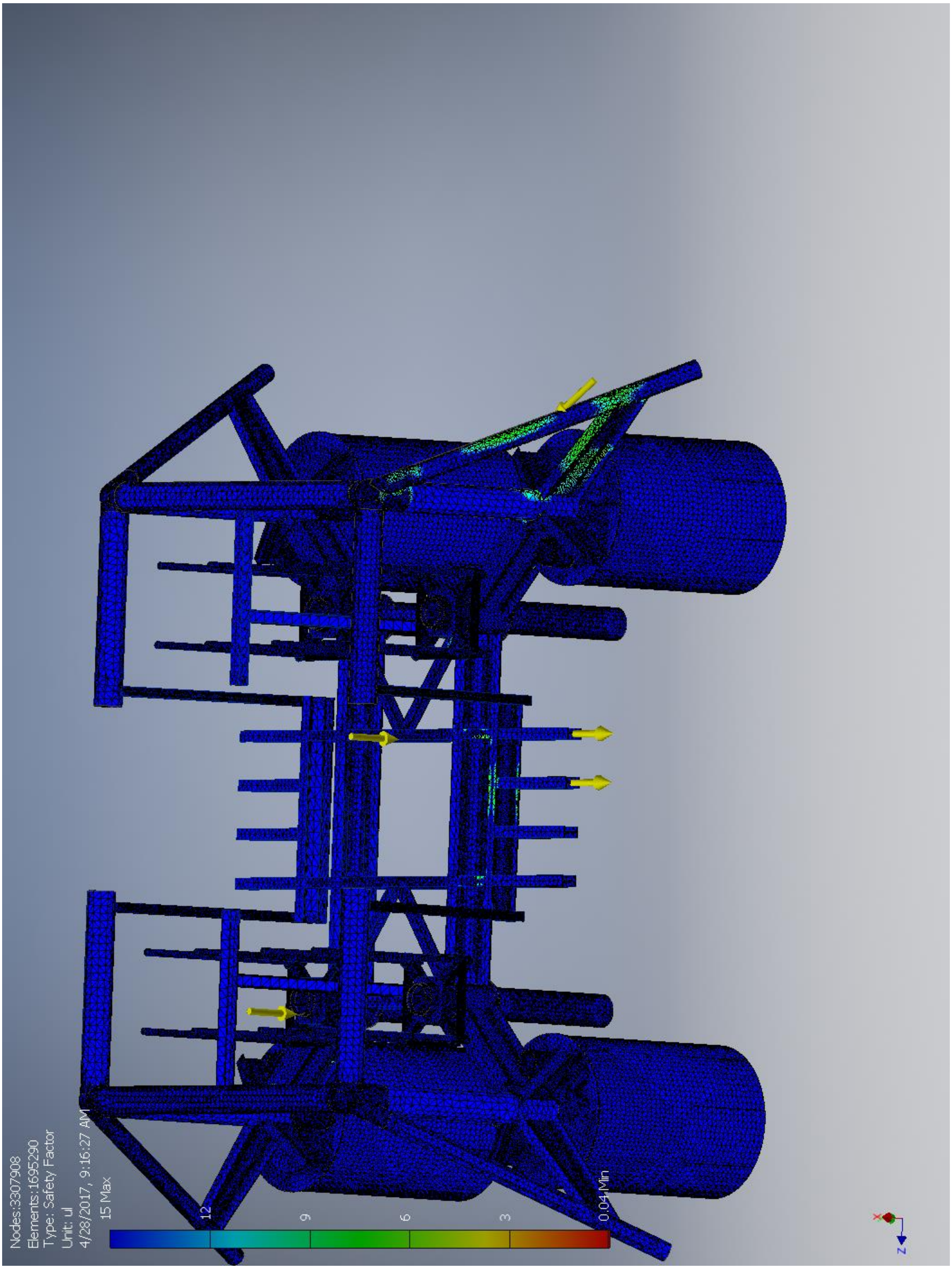

## I.6 Case-F

### I.6.1 Without convergence

# Stress Analysis Report

AUTODESK

| | |
|---|---|
| Analyzed File: | Assembly.iam |
| Autodesk Inventor Version: | 2017 (Build 210142000, 142) |
| Creation Date: | 4/28/2017, 12:02 PM |
| Study Author: | henrikwn |
| Summary: | |

---

## ⊟ Project Info (iProperties)

### ⊟ Summary

| | |
|---|---|
| Title | |
| Author | henrikwn |

### ⊟ Project

| | |
|---|---|
| Designer | henrikwn |

### ⊟ Physical

| | |
|---|---|
| Mass | 181171 kg |
| Area | 3.52908E+09 mm^2 |
| Volume | 6.02475E+10 mm^3 |
| Center of Gravity | x=-8288.42 mm<br>y=6548.24 mm<br>z=9857.84 mm |

Note: Physical values could be different from Physical values used by FEA reported below.

---

## ⊟ Case-F

**General objective and settings:**

| | |
|---|---|
| Design Objective | Single Point |
| Study Type | Static Analysis |
| Last Modification Date | 4/28/2017, 11:46 AM |
| Detect and Eliminate Rigid Body Modes | No |
| Separate Stresses Across Contact Surfaces | No |
| Motion Loads Analysis | No |

## ⊟ Operating conditions

## ⊟ Force:1

| | |
|---|---|
| Load Type | Force |
| Magnitude | 1000000.293 N |
| Vector X | 342021.000 N |
| Vector Y | 0.000 N |
| Vector Z | -939692.621 N |

### ⊟ Selected Face(s)

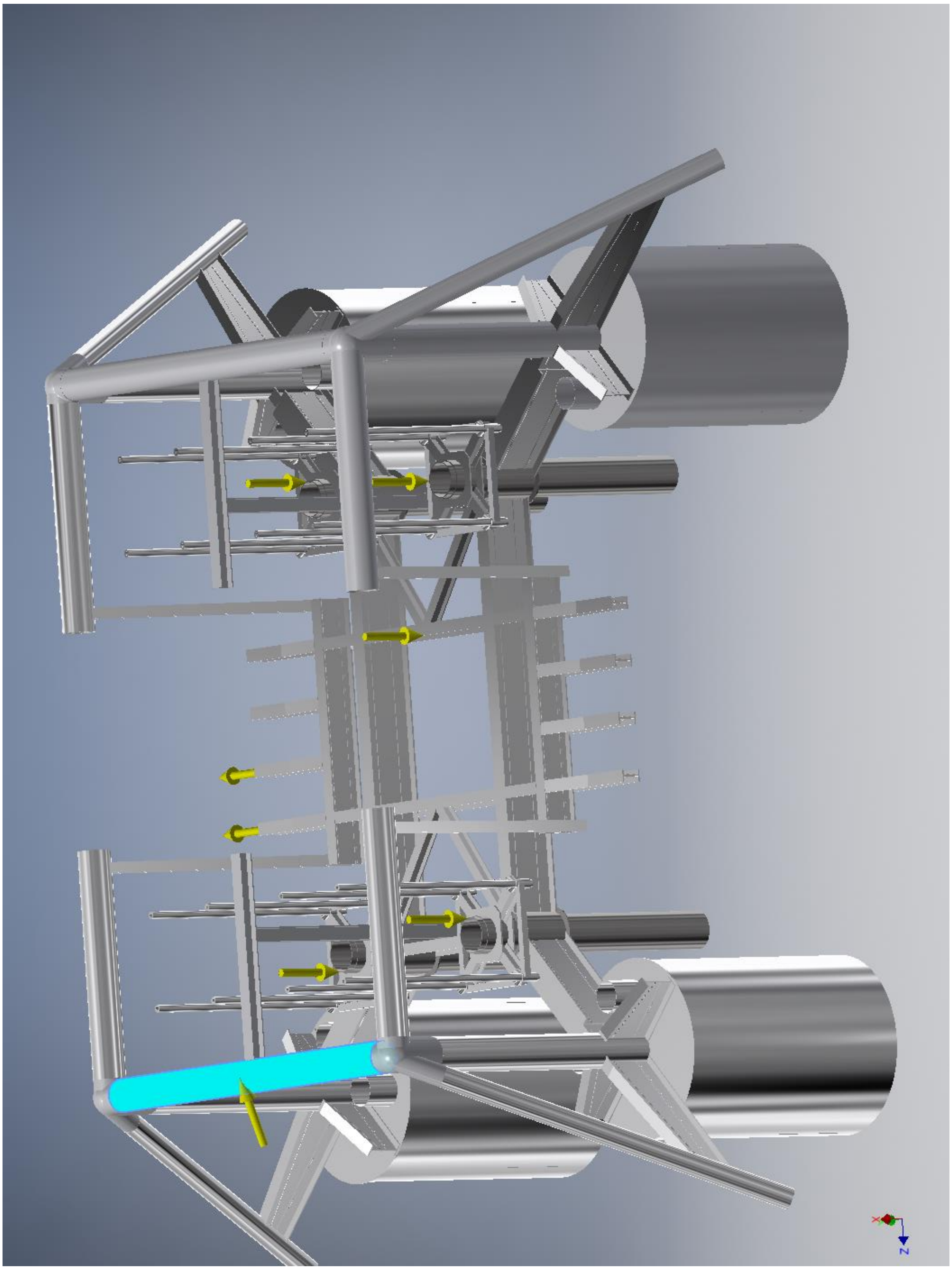

## ⊟ Force:2

| | |
|---|---|
| Load Type | Force |
| Magnitude | 600000.000 N |
| Vector X | -600000.000 N |
| Vector Y | -0.000 N |
| Vector Z | -0.000 N |

## ⊟ Selected Face(s)

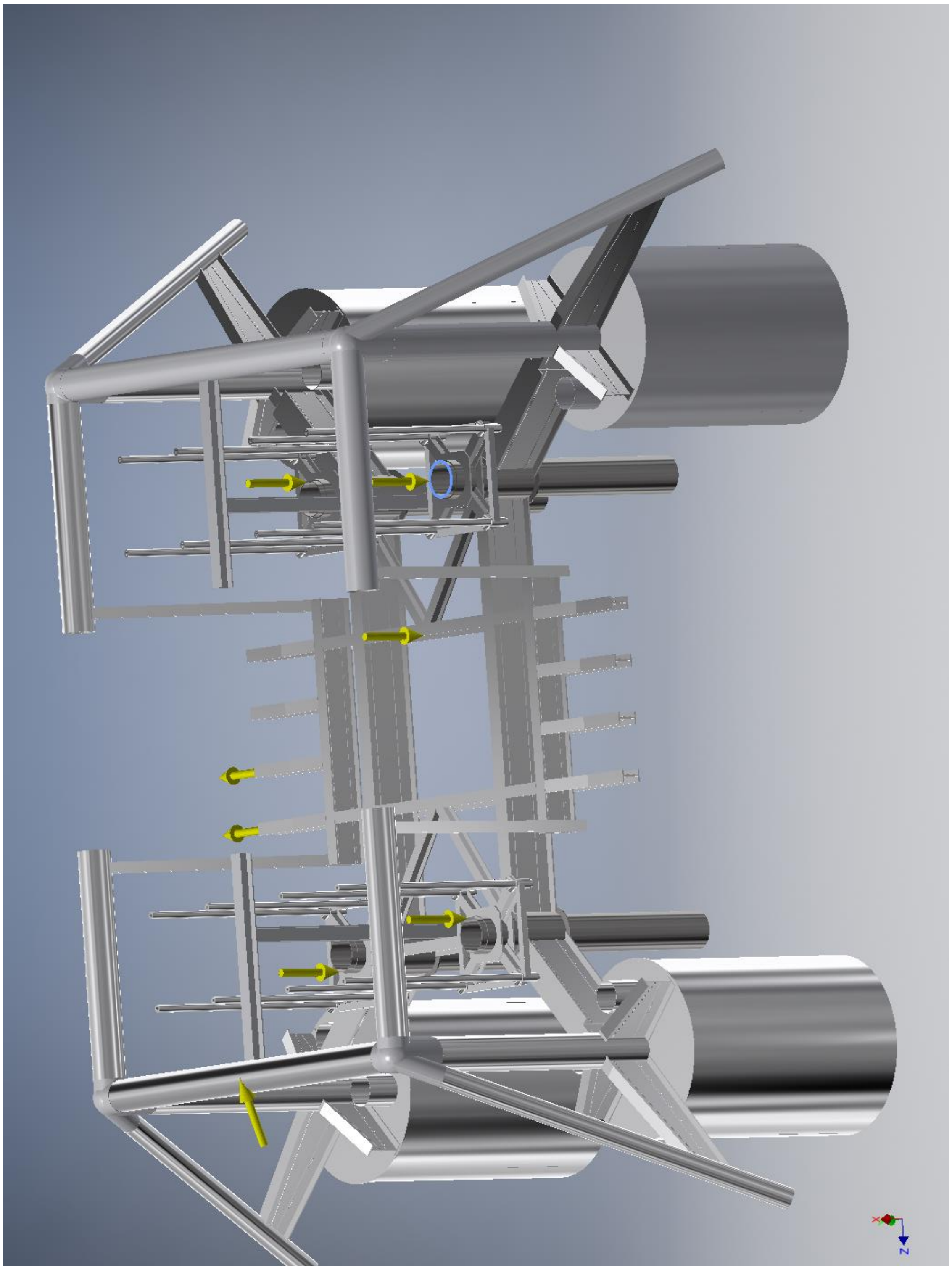

## ⊟ Force:3

| | |
|---|---|
| Load Type | Force |
| Magnitude | 600000.000 N |
| Vector X | -600000.000 N |
| Vector Y | -0.000 N |
| Vector Z | -0.000 N |

### ⊟ Selected Face(s)

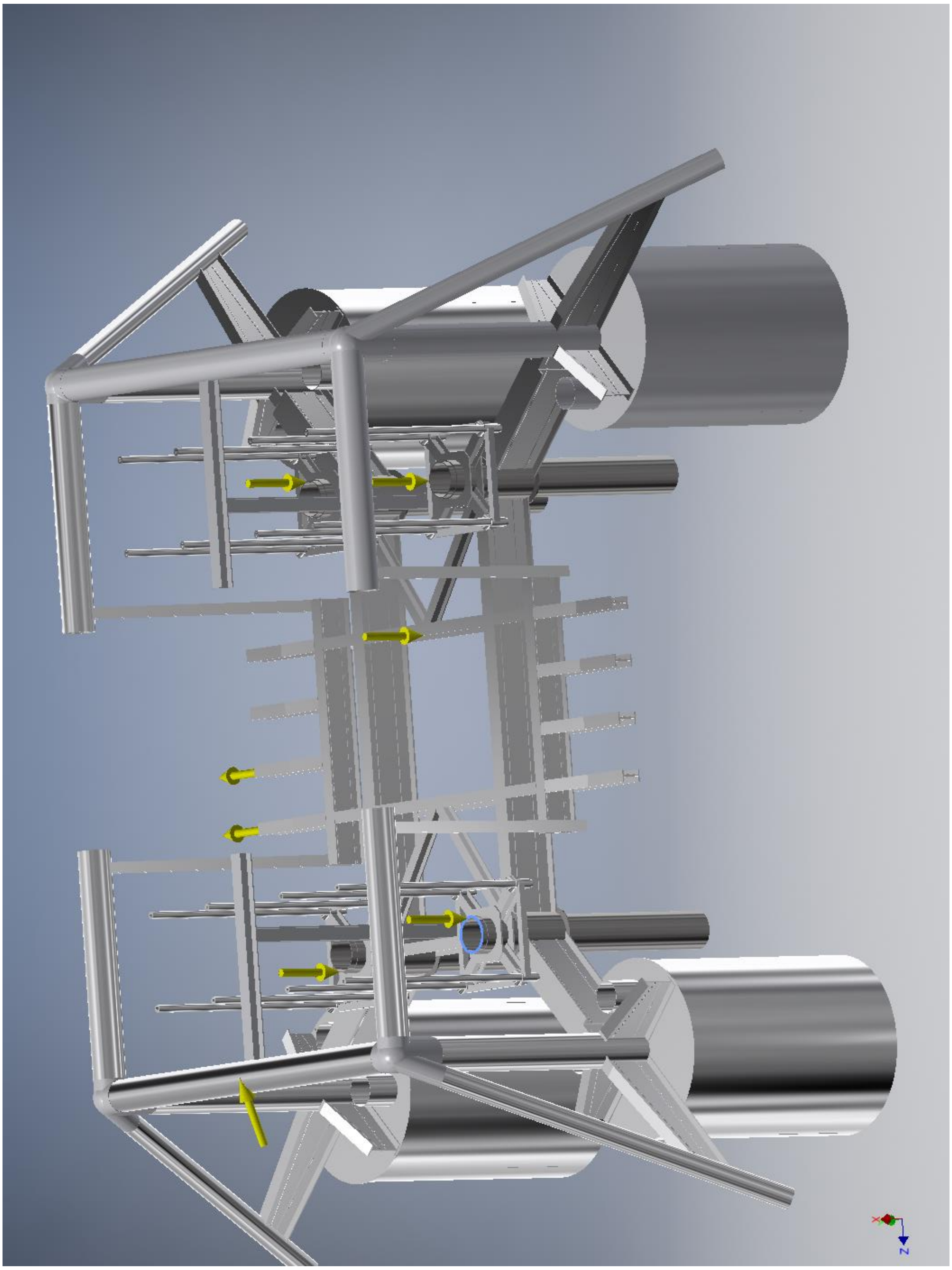

## ⊟ Force:4

| | |
|---|---|
| Load Type | Force |
| Magnitude | 600000.000 N |
| Vector X | -600000.000 N |
| Vector Y | -0.000 N |
| Vector Z | -0.000 N |

### ⊟ Selected Face(s)

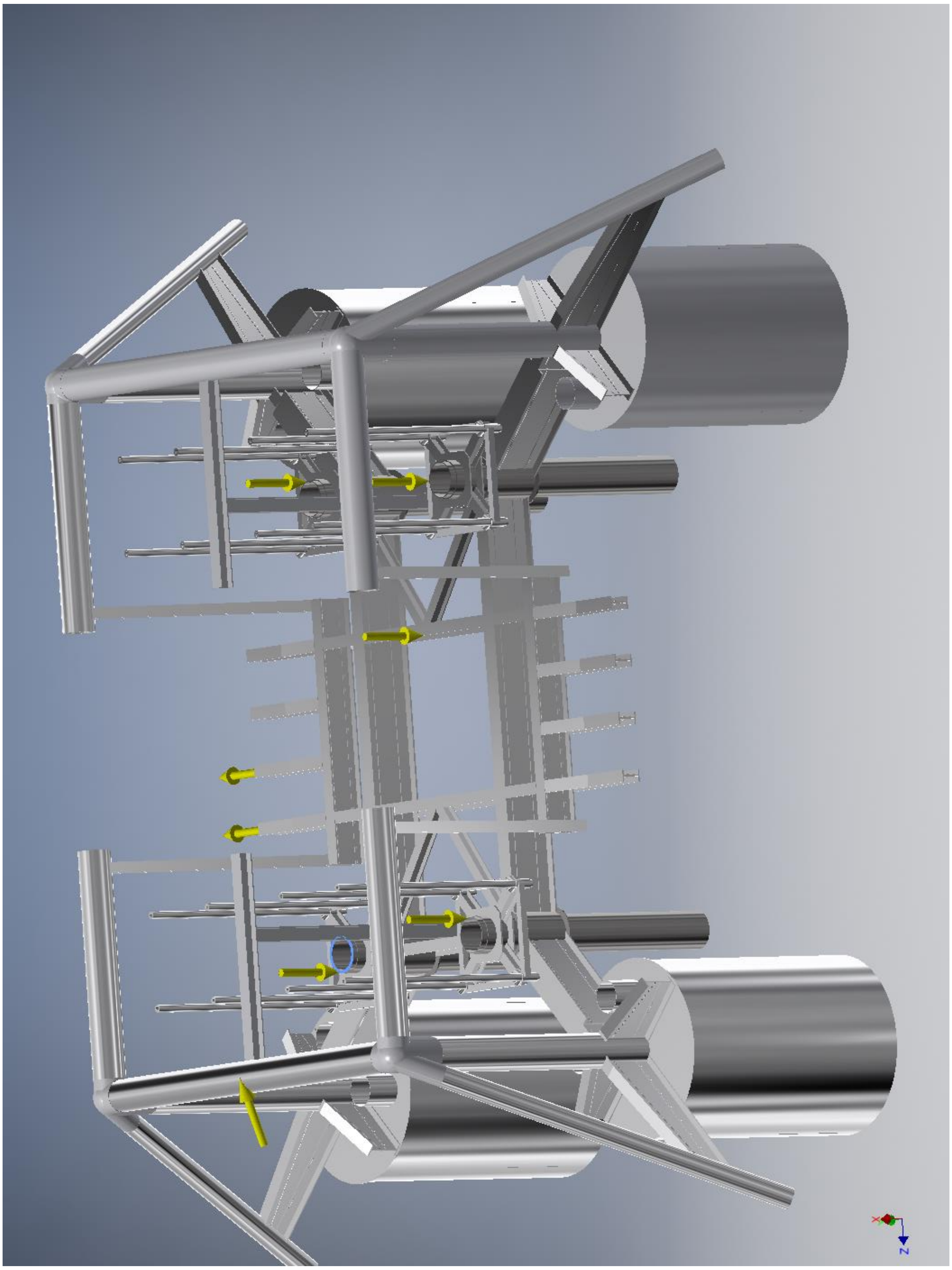

## ⊟ Force:5

| | |
|---|---|
| Load Type | Force |
| Magnitude | 600000.000 N |
| Vector X | -600000.000 N |
| Vector Y | -0.000 N |
| Vector Z | -0.000 N |

### ⊟ Selected Face(s)

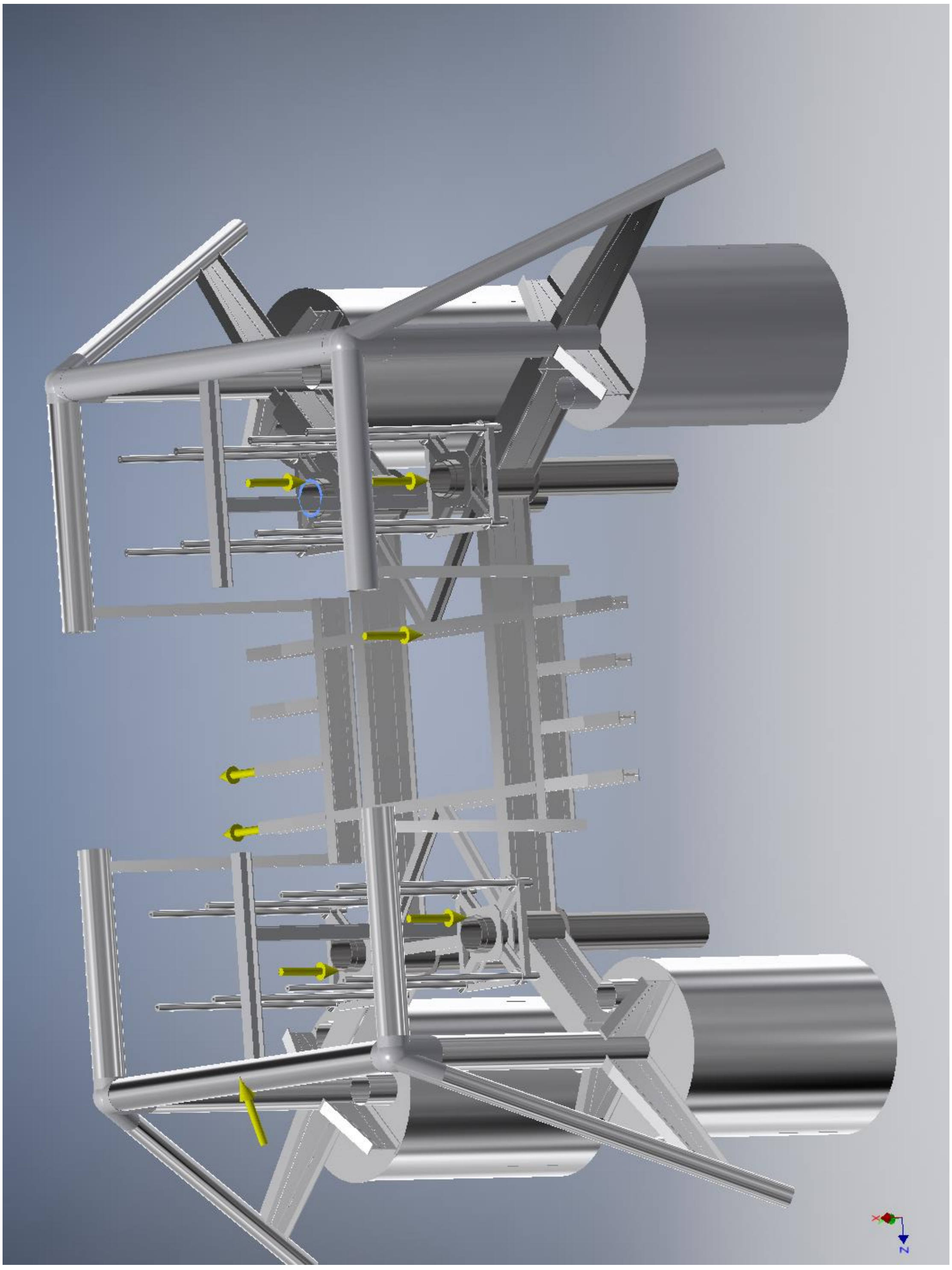

## ⊟ Force:6

| | |
|---|---|
| Load Type | Force |
| Magnitude | 800000.000 N |
| Vector X | -800000.000 N |
| Vector Y | -0.000 N |
| Vector Z | -0.000 N |

### ⊟ Selected Face(s)

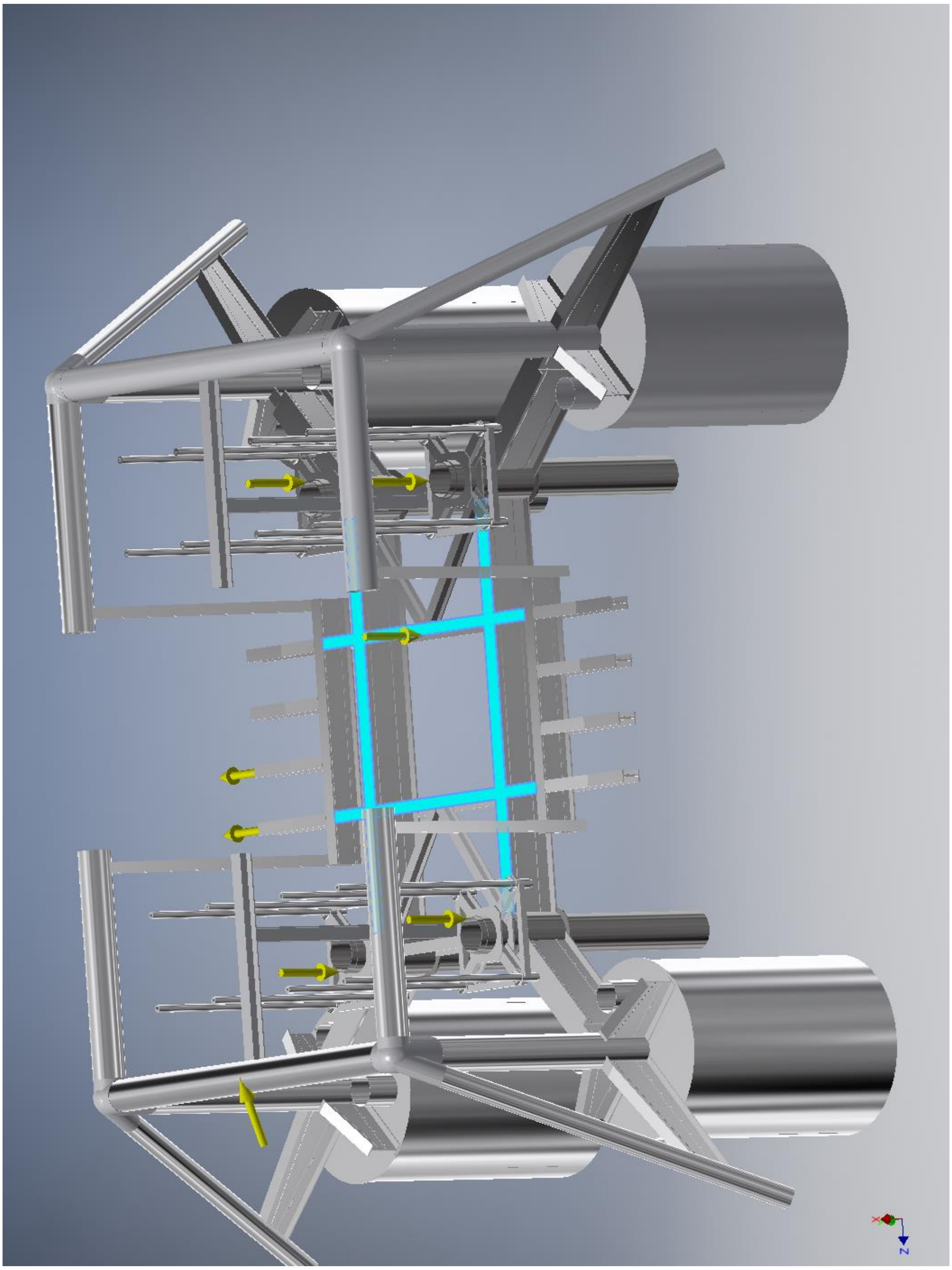

## ⊟ Force:7

| | |
|---|---|
| Load Type | Force |
| Magnitude | 300000.000 N |
| Vector X | -0.000 N |
| Vector Y | 300000.000 N |
| Vector Z | -0.000 N |

### ⊟ Selected Face(s)

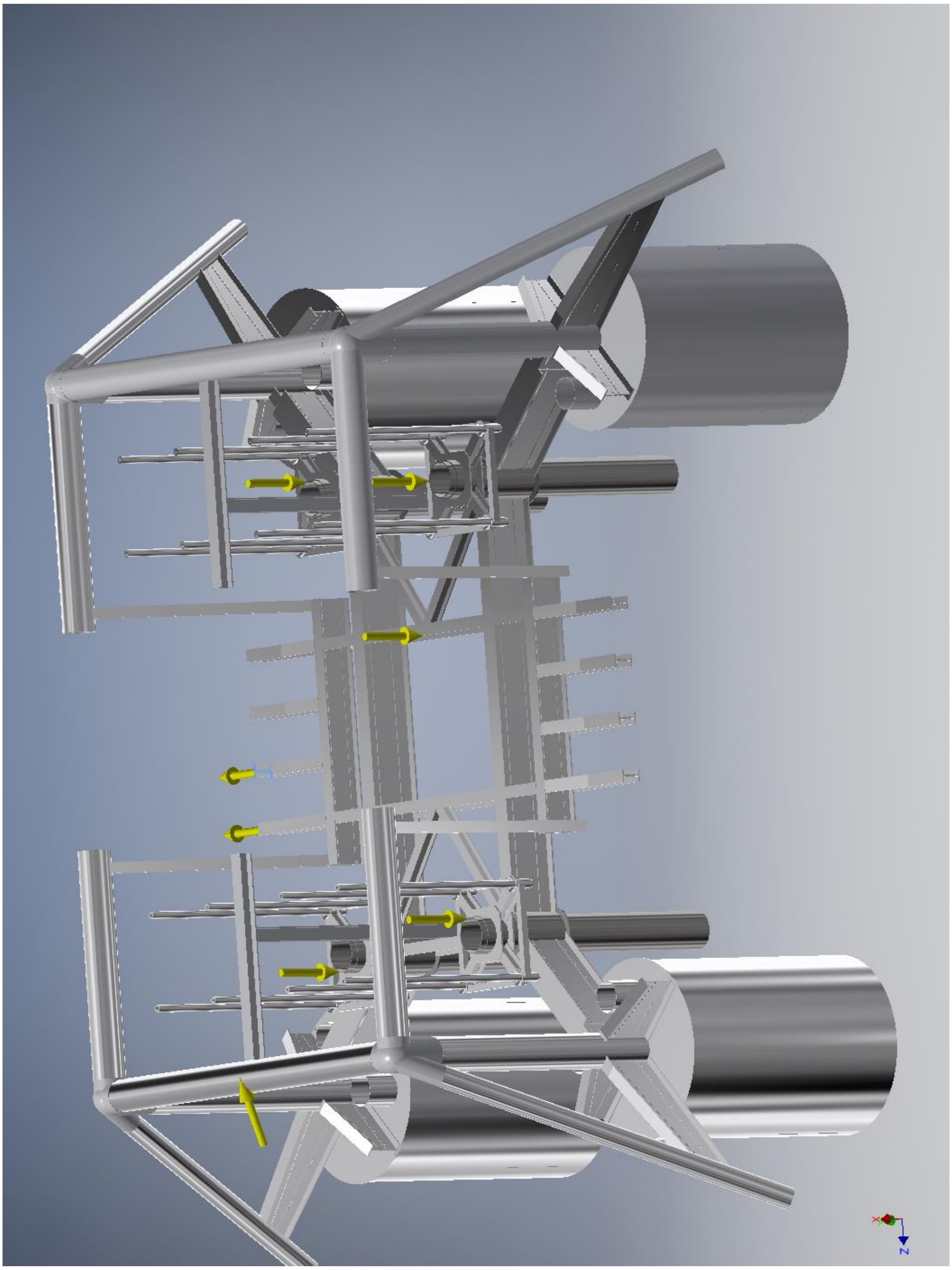

## ⊟ Force:8

| | |
|---|---|
| Load Type | Force |
| Magnitude | 300000.000 N |
| Vector X | 0.000 N |
| Vector Y | 300000.000 N |
| Vector Z | -0.000 N |

### ⊟ Selected Face(s)

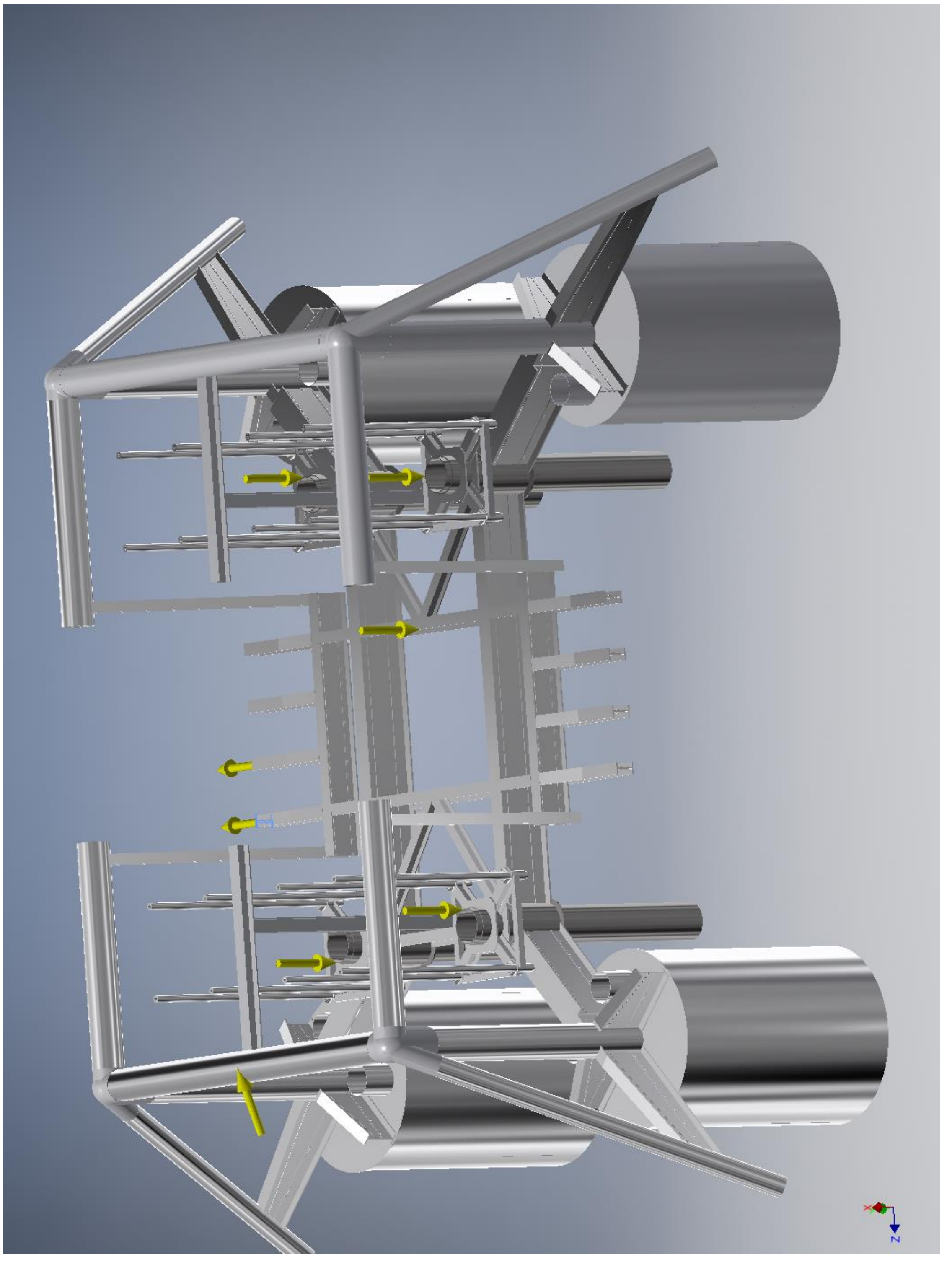

## ⊟ Fixed Constraint:1

| Constraint Type | Fixed Constraint |
| --- | --- |

### ⊟ Selected Face(s)

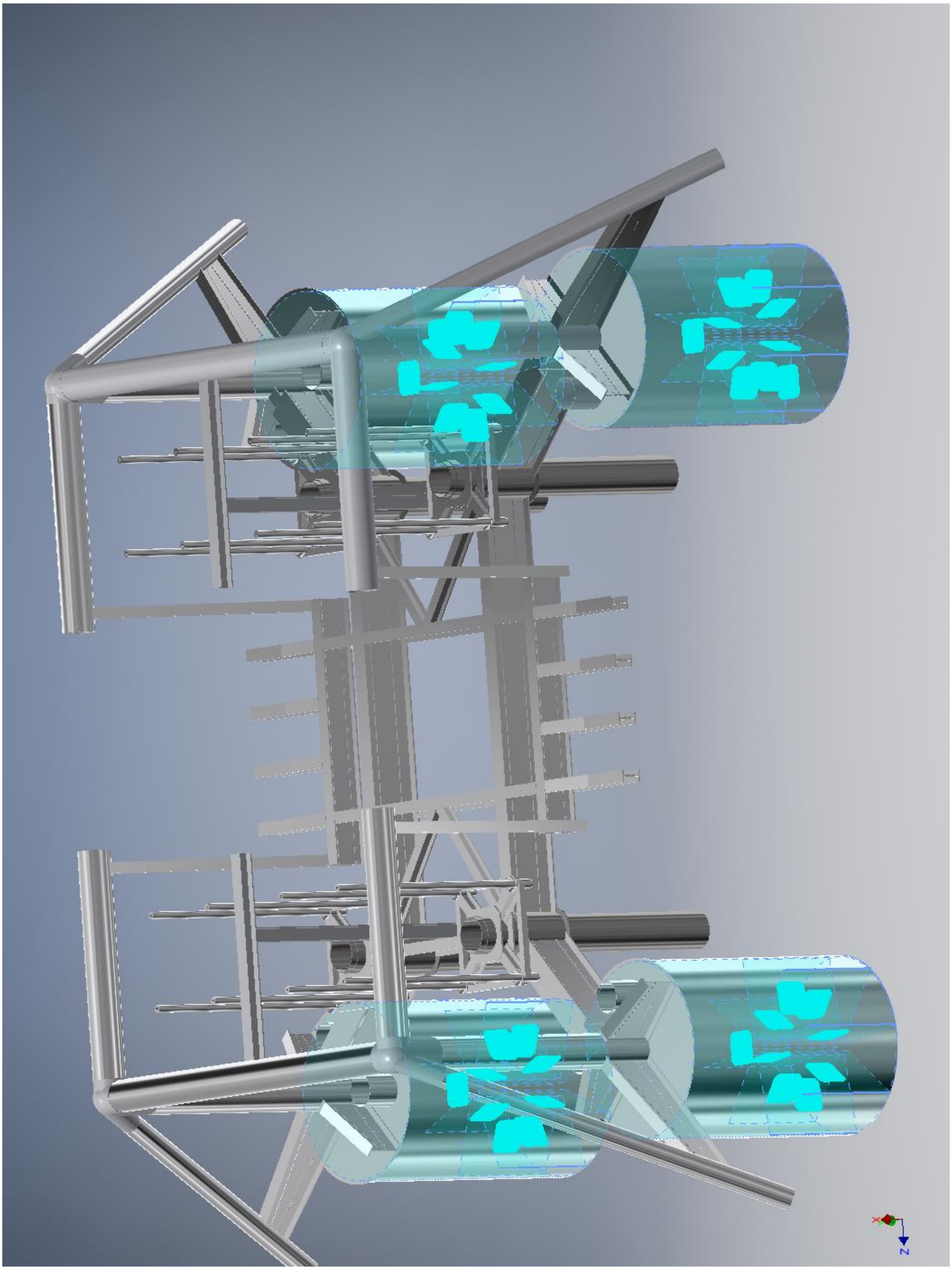

## ⊟ Results

### ⊟ Reaction Force and Moment on Constraints

| Constraint Name | Reaction Force | | Reaction Moment | |
|---|---|---|---|---|
| | Magnitude | Component (X,Y,Z) | Magnitude | Component (X,Y,Z) |
| Fixed Constraint:1 | 3067750 N | 2857980 N | 15469400 N m | 1016440 N m |
| | | -600000 N | | -15111800 N m |
| | | 939693 N | | -3146730 N m |

### ⊟ Result Summary

| Name | Minimum | Maximum |
|---|---|---|
| Volume | 6.02475E+10 mm^3 | |
| Mass | 181171 kg | |
| Von Mises Stress | 0 MPa | 343.71 MPa |
| 1st Principal Stress | -44.5052 MPa | 286.756 MPa |
| 3rd Principal Stress | -268.213 MPa | 44.1763 MPa |
| Displacement | 0 mm | 65.0658 mm |
| Safety Factor | 0.687916 ul | 15 ul |

### ⊟ Figures

## ⊟ Von Mises Stress

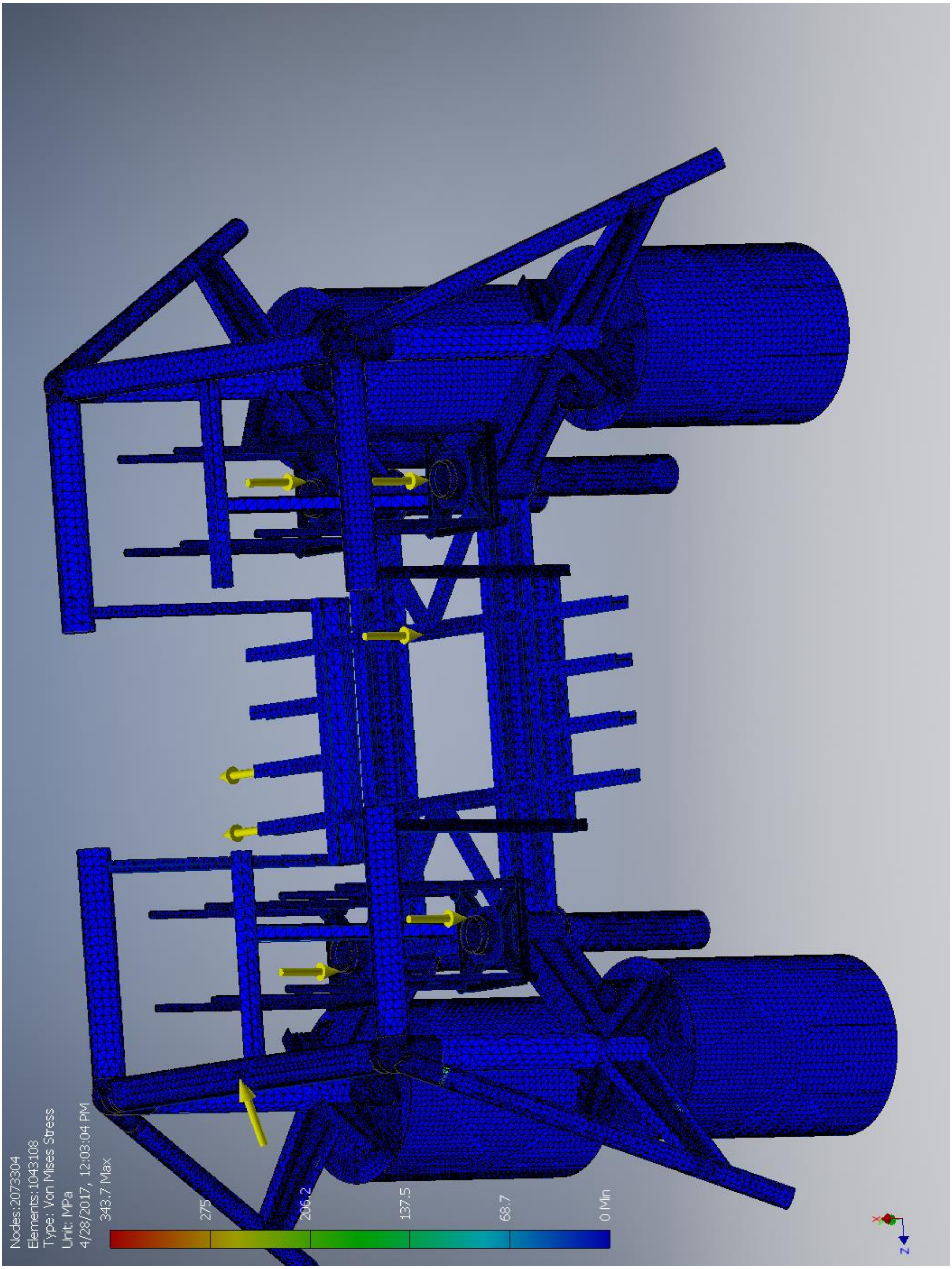

## ⊟ 1st Principal Stress

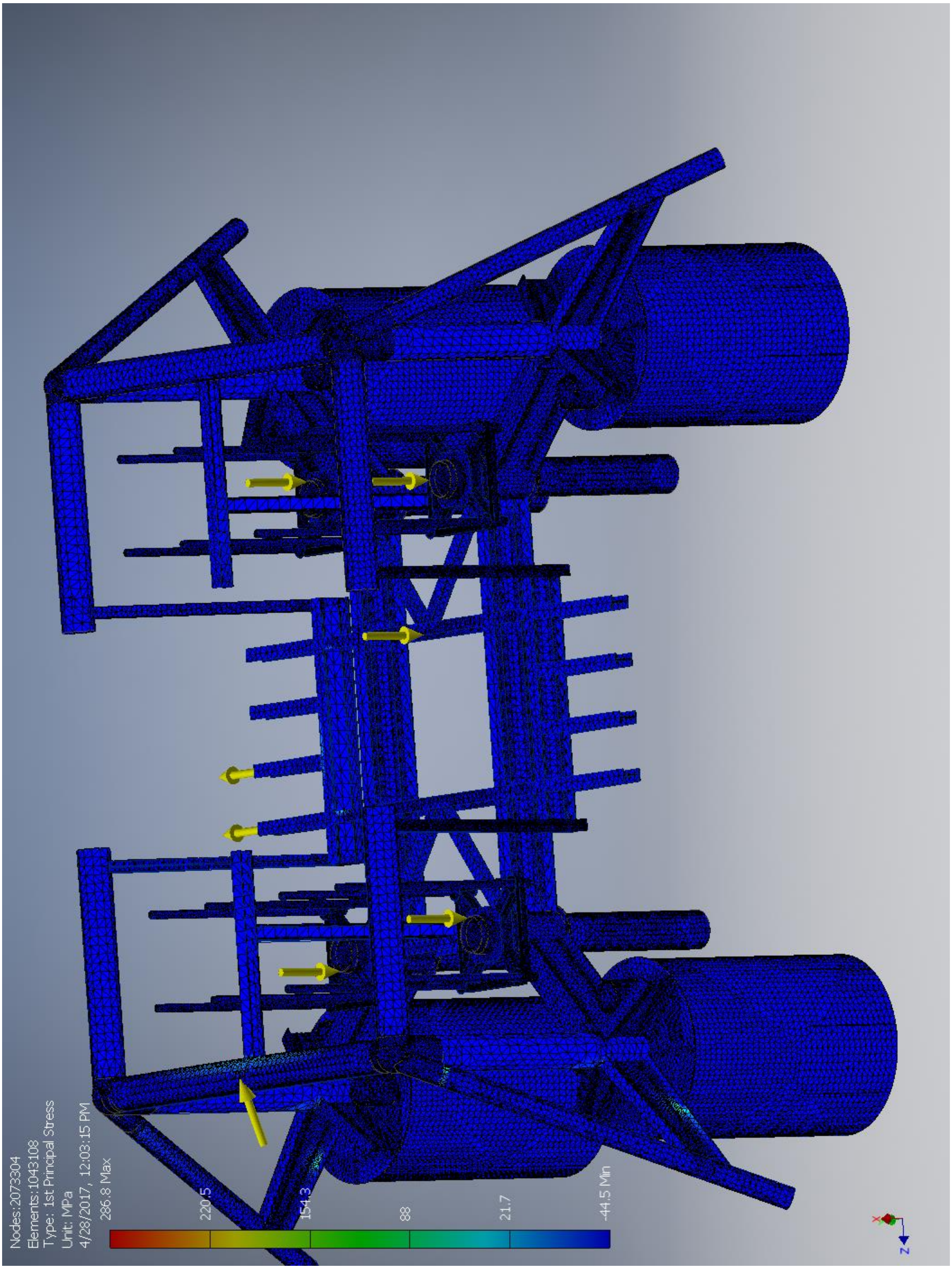

## ⊟ 3rd Principal Stress

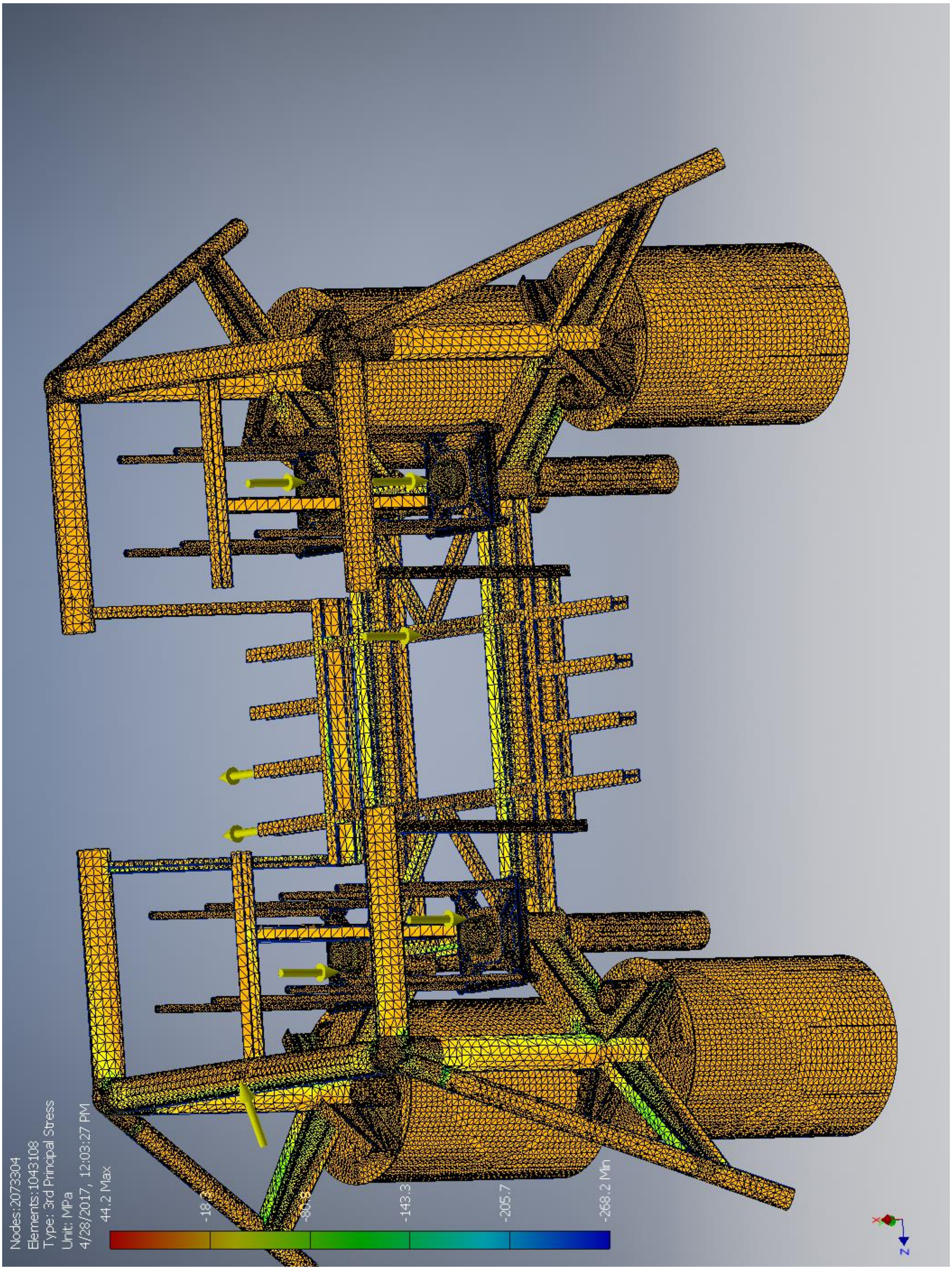

## ⊟ Displacement

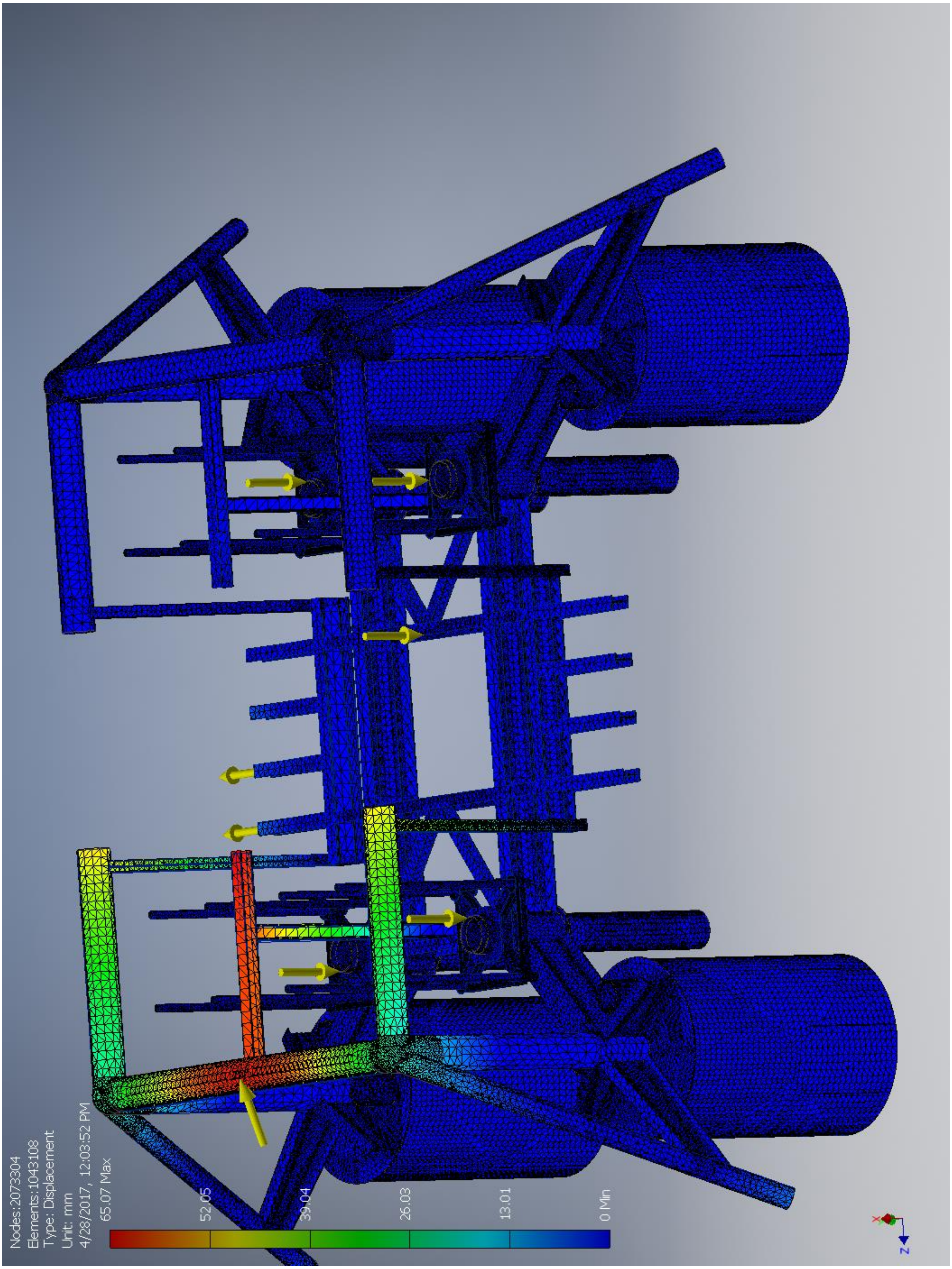

### ⊟ Safety Factor

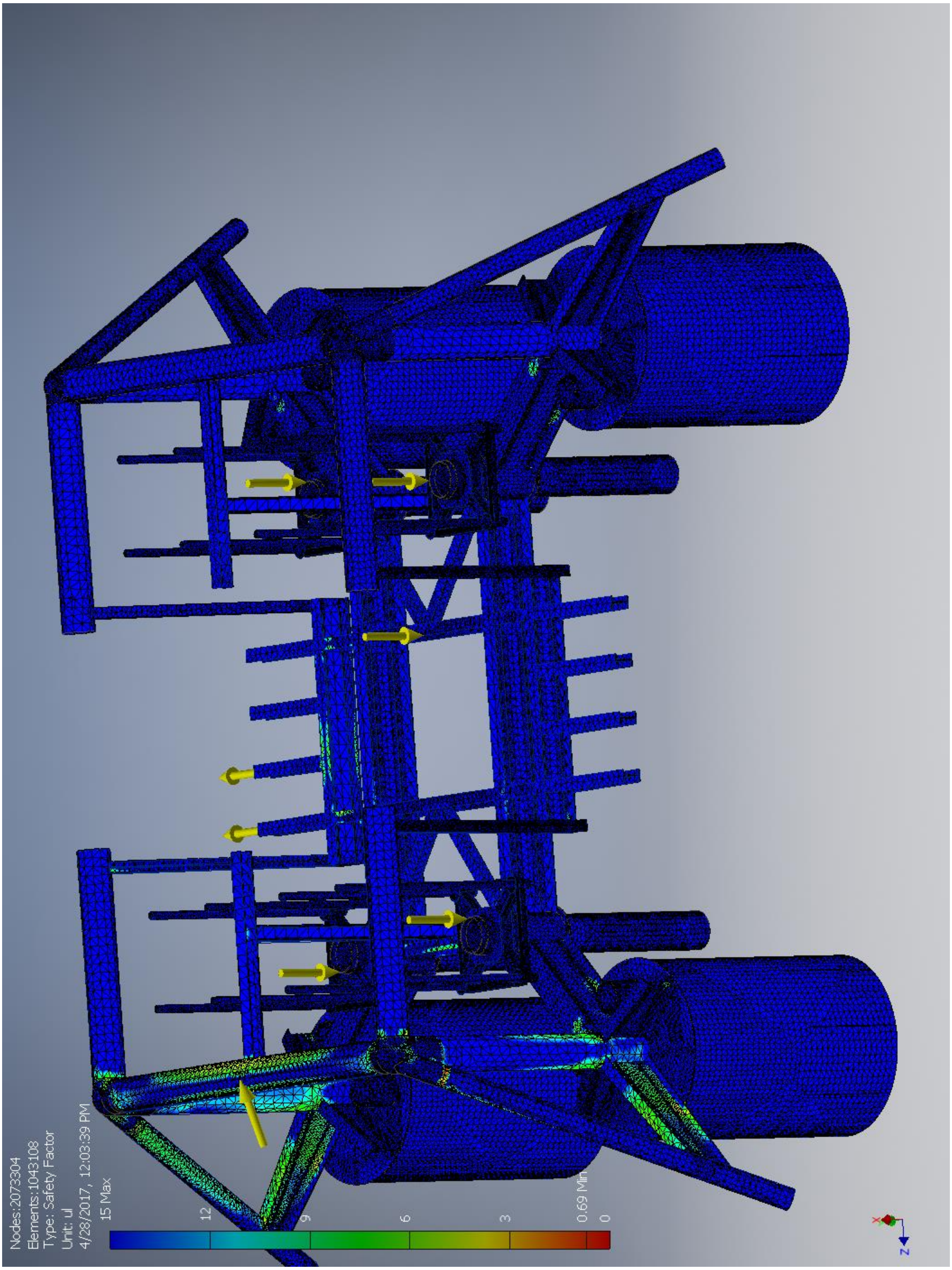

### I.6.2 With convergence

# Stress Analysis Report

| | |
|---|---|
| Analyzed File: | Assembly.iam |
| Autodesk Inventor Version: | 2017 (Build 210142000, 142) |
| Creation Date: | 4/28/2017, 11:30 AM |
| Study Author: | henrikwn |
| Summary: | |

## ⊟ Project Info (iProperties)

### ⊟ Summary

| | |
|---|---|
| Title | |
| Author | henrikwn |

### ⊟ Project

| | |
|---|---|
| Designer | henrikwn |

### ⊟ Physical

| | |
|---|---|
| Mass | 181171 kg |
| Area | 3.52908E+09 mm^2 |
| Volume | 6.02475E+10 mm^3 |
| Center of Gravity | x=-8288.42 mm<br>y=6548.24 mm<br>z=9857.84 mm |

Note: Physical values could be different from Physical values used by FEA reported below.

## ⊟ Case-F

**General objective and settings:**

| | |
|---|---|
| Design Objective | Single Point |
| Study Type | Static Analysis |
| Last Modification Date | 4/28/2017, 10:56 AM |
| Detect and Eliminate Rigid Body Modes | No |
| Separate Stresses Across Contact Surfaces | No |
| Motion Loads Analysis | No |

## ⊟ Operating conditions

## ⊟ Force:1

| | |
|---|---|
| Load Type | Force |
| Magnitude | 1000000.293 N |
| Vector X | 342021.000 N |
| Vector Y | 0.000 N |
| Vector Z | -939692.621 N |

### ⊟ Selected Face(s)

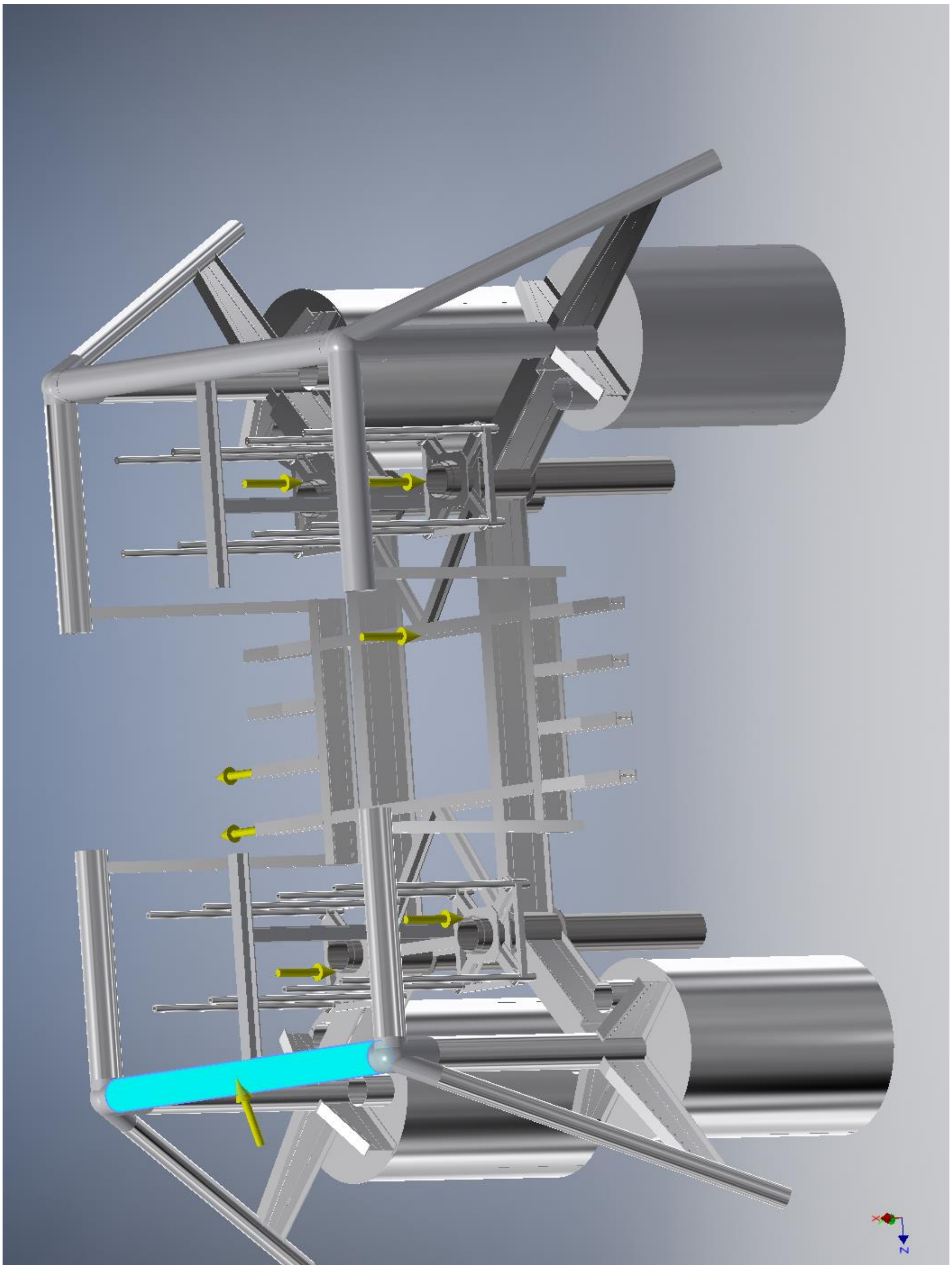

## ⊟ Force:2

| | |
|---|---|
| Load Type | Force |
| Magnitude | 600000.000 N |
| Vector X | -600000.000 N |
| Vector Y | -0.000 N |
| Vector Z | -0.000 N |

### ⊟ Selected Face(s)

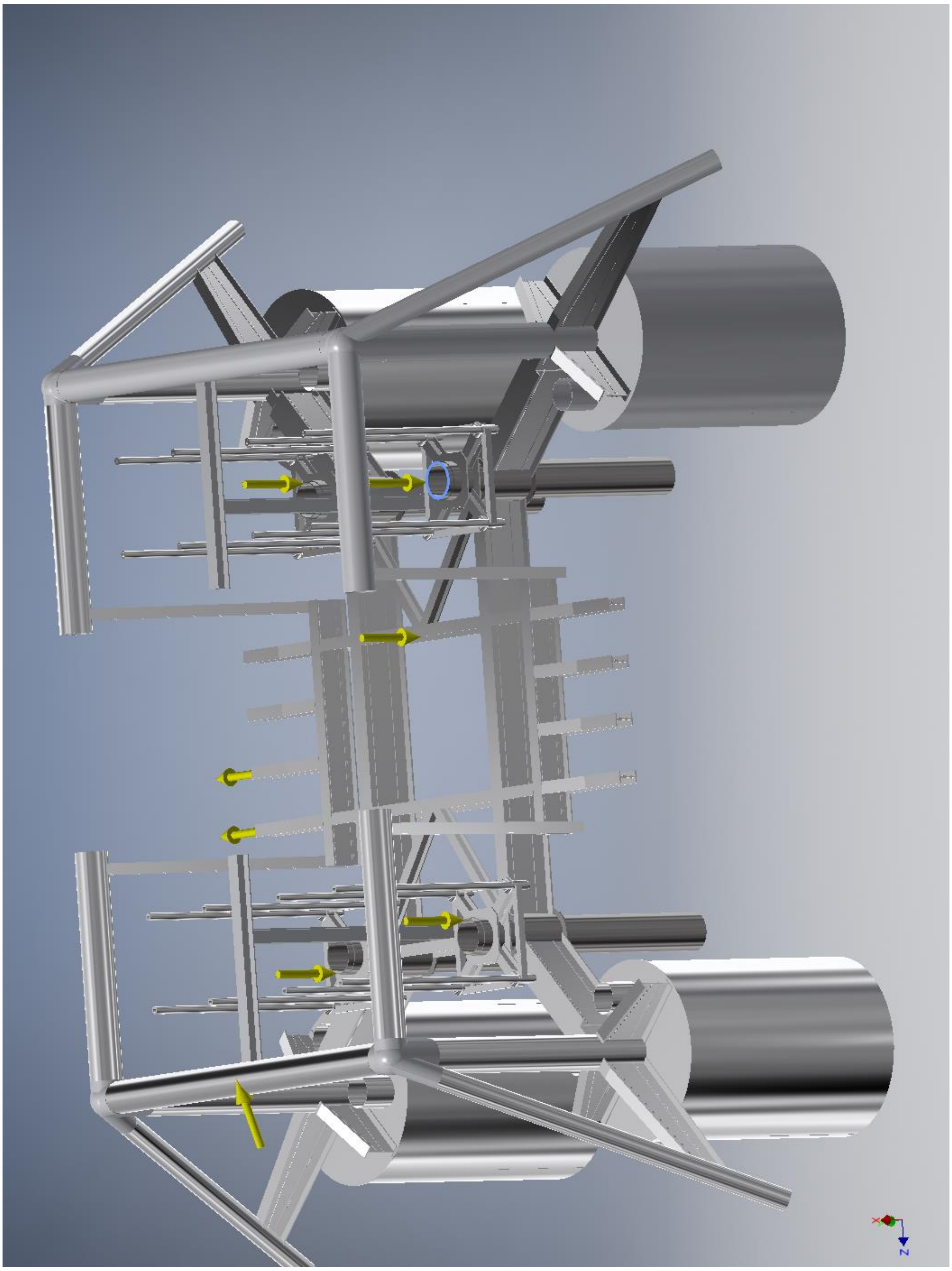

## ⊟ Force:3

| | |
|---|---|
| Load Type | Force |
| Magnitude | 600000.000 N |
| Vector X | -600000.000 N |
| Vector Y | -0.000 N |
| Vector Z | -0.000 N |

### ⊟ Selected Face(s)

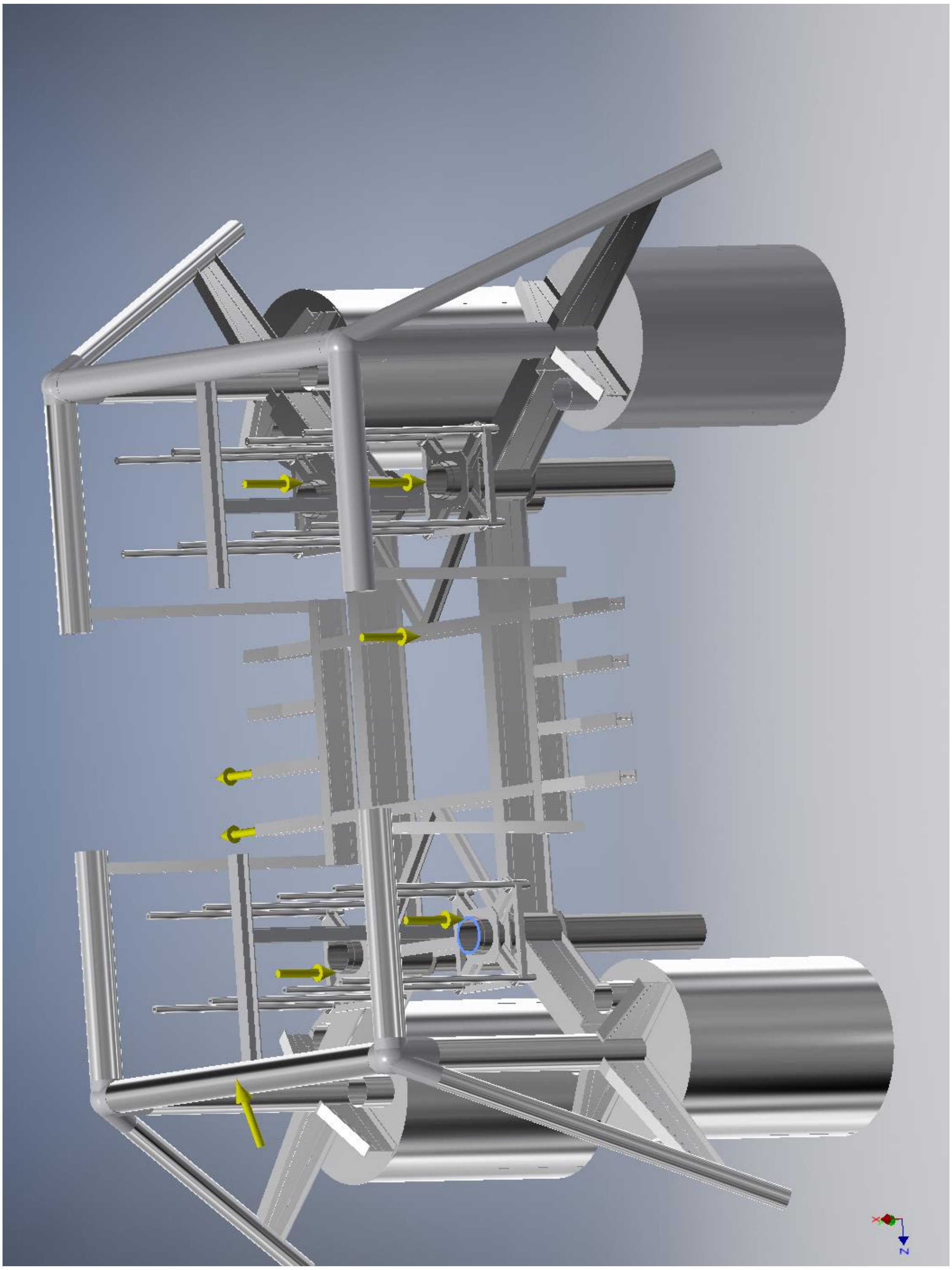

## ⊟ Force:4

| | |
|---|---|
| Load Type | Force |
| Magnitude | 600000.000 N |
| Vector X | -600000.000 N |
| Vector Y | -0.000 N |
| Vector Z | -0.000 N |

### ⊟ Selected Face(s)

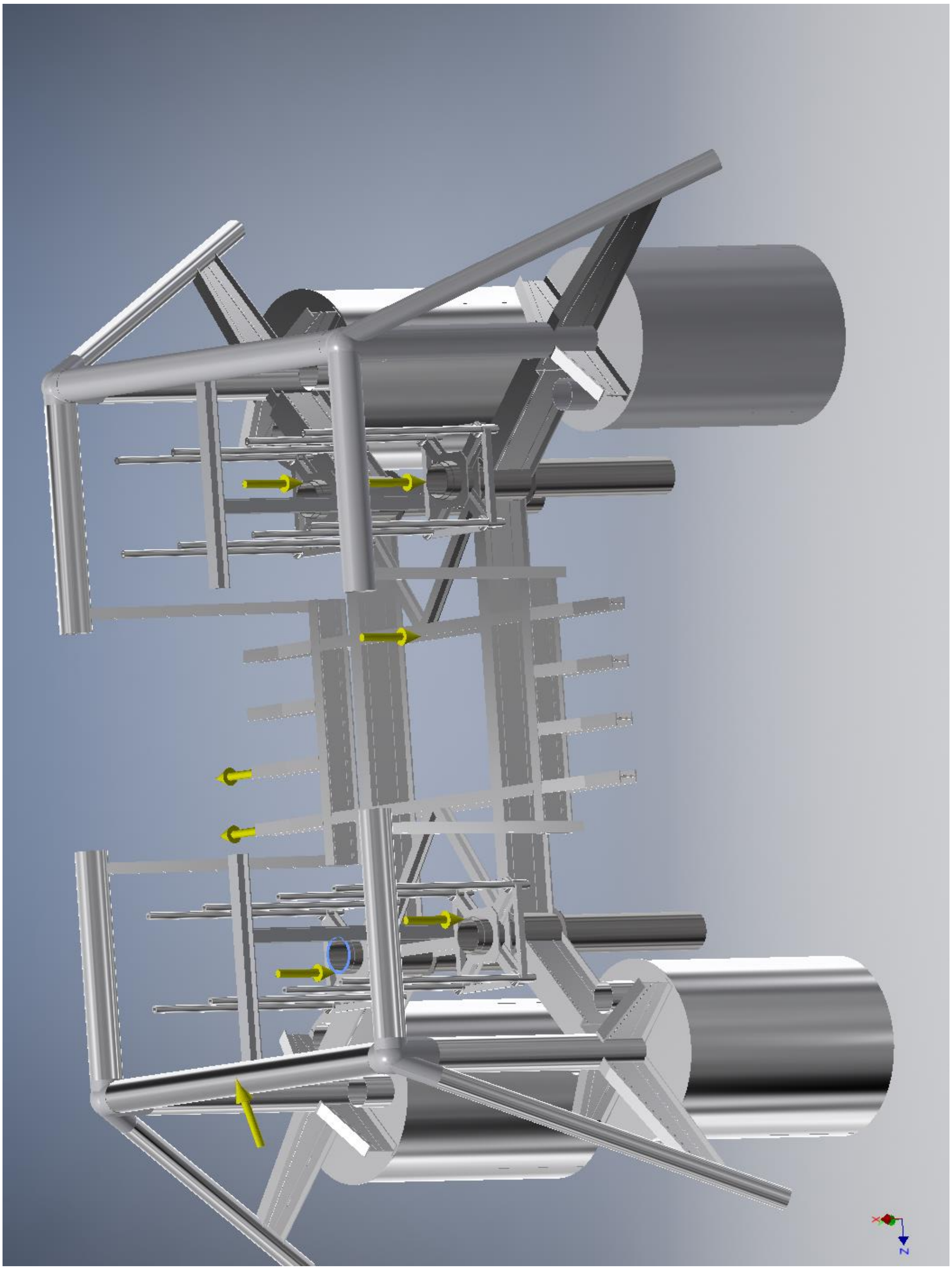

## ⊟ Force:5

| | |
|---|---|
| Load Type | Force |
| Magnitude | 600000.000 N |
| Vector X | -600000.000 N |
| Vector Y | -0.000 N |
| Vector Z | -0.000 N |

### ⊟ Selected Face(s)

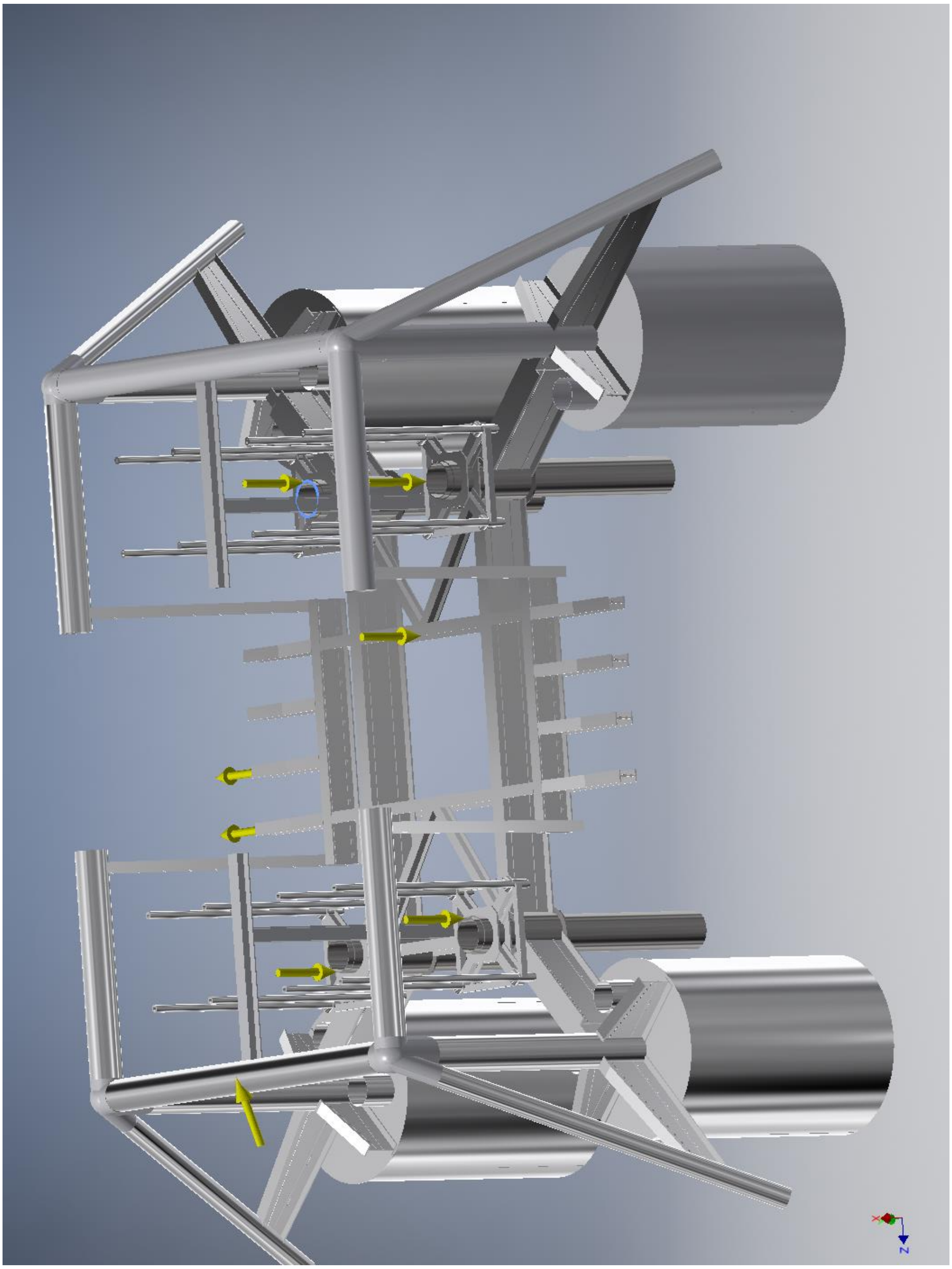

## ⊟ Force:6

| | |
|---|---|
| Load Type | Force |
| Magnitude | 800000.000 N |
| Vector X | -800000.000 N |
| Vector Y | -0.000 N |
| Vector Z | -0.000 N |

### ⊟ Selected Face(s)

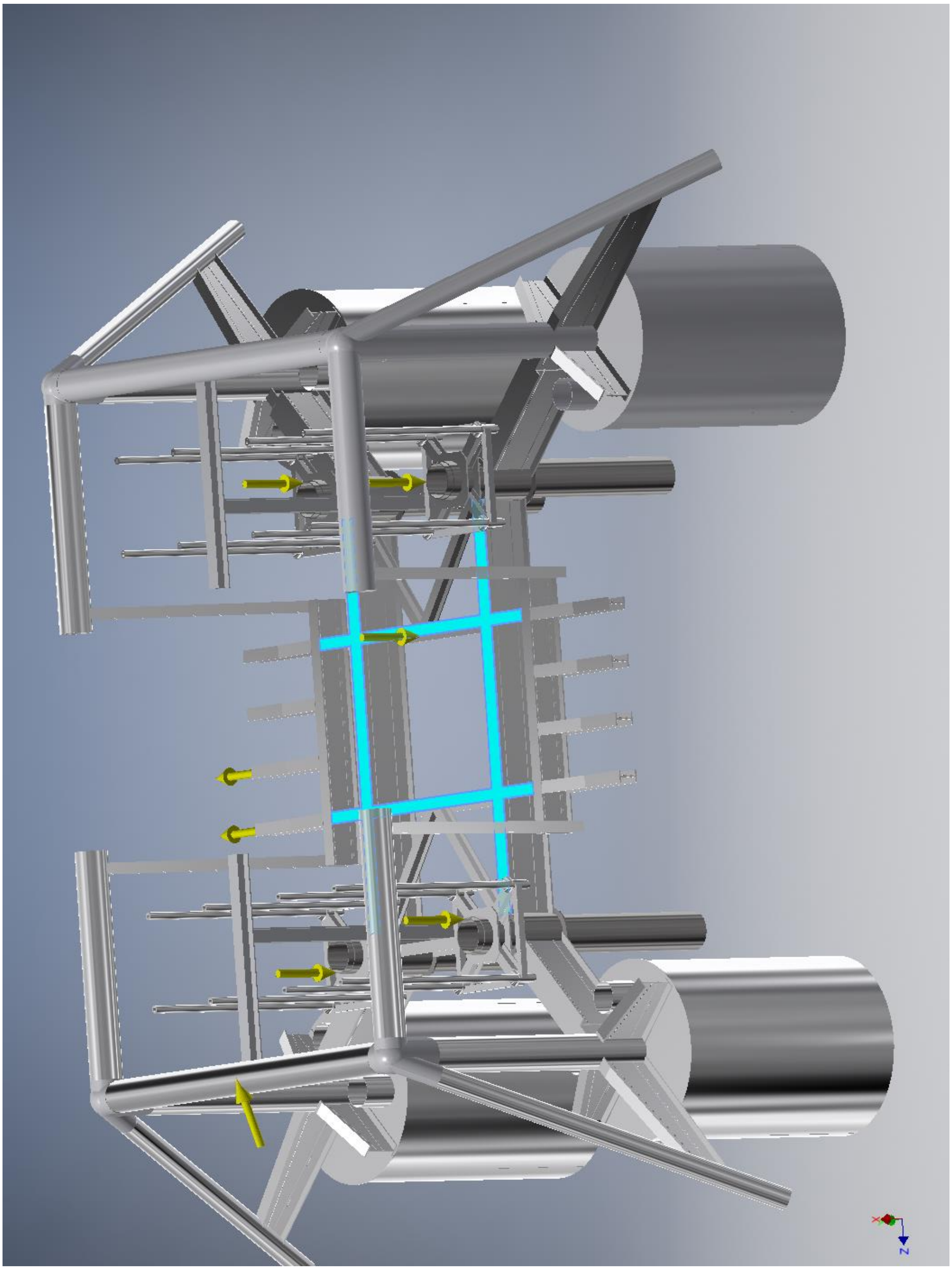

## ⊟ Force:7

| | |
|---|---|
| Load Type | Force |
| Magnitude | 300000.000 N |
| Vector X | -0.000 N |
| Vector Y | 300000.000 N |
| Vector Z | -0.000 N |

### ⊟ Selected Face(s)

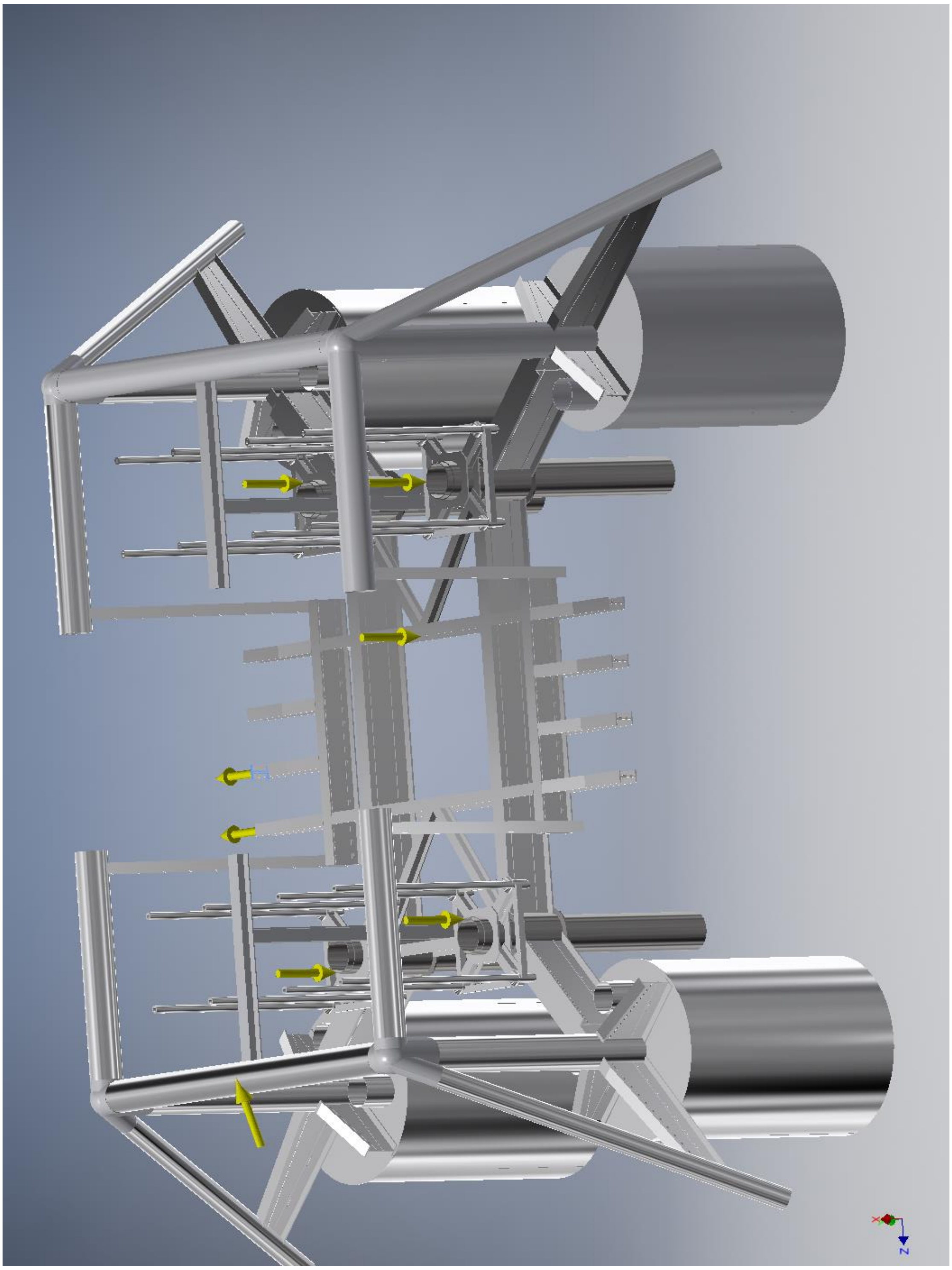

### ⊟ Force:8

| | |
|---|---|
| Load Type | Force |
| Magnitude | 300000.000 N |
| Vector X | 0.000 N |
| Vector Y | 300000.000 N |
| Vector Z | -0.000 N |

### ⊟ Selected Face(s)

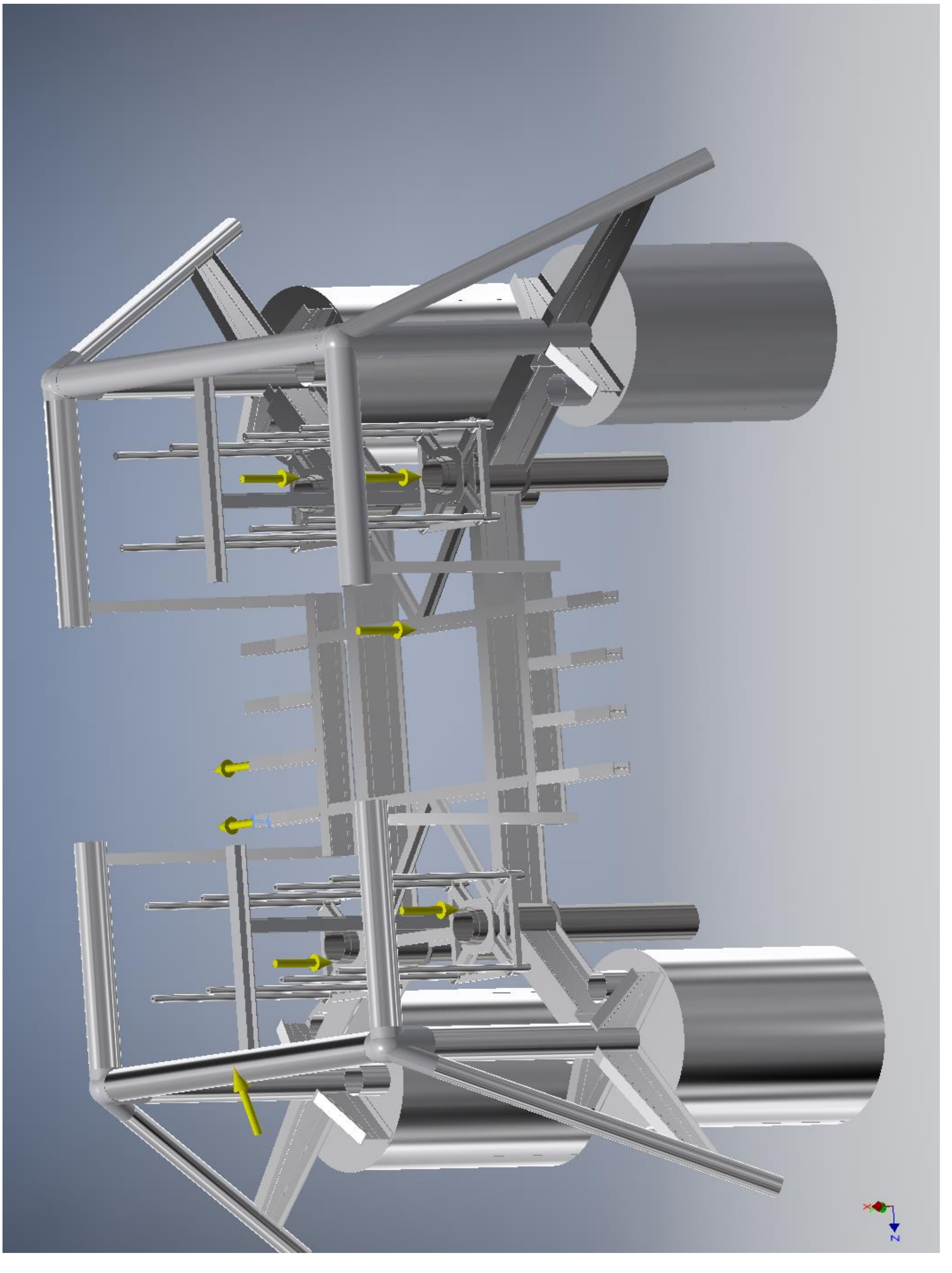

## ⊟ Fixed Constraint:1

| Constraint Type | Fixed Constraint |
|---|---|

### ⊟ Selected Face(s)

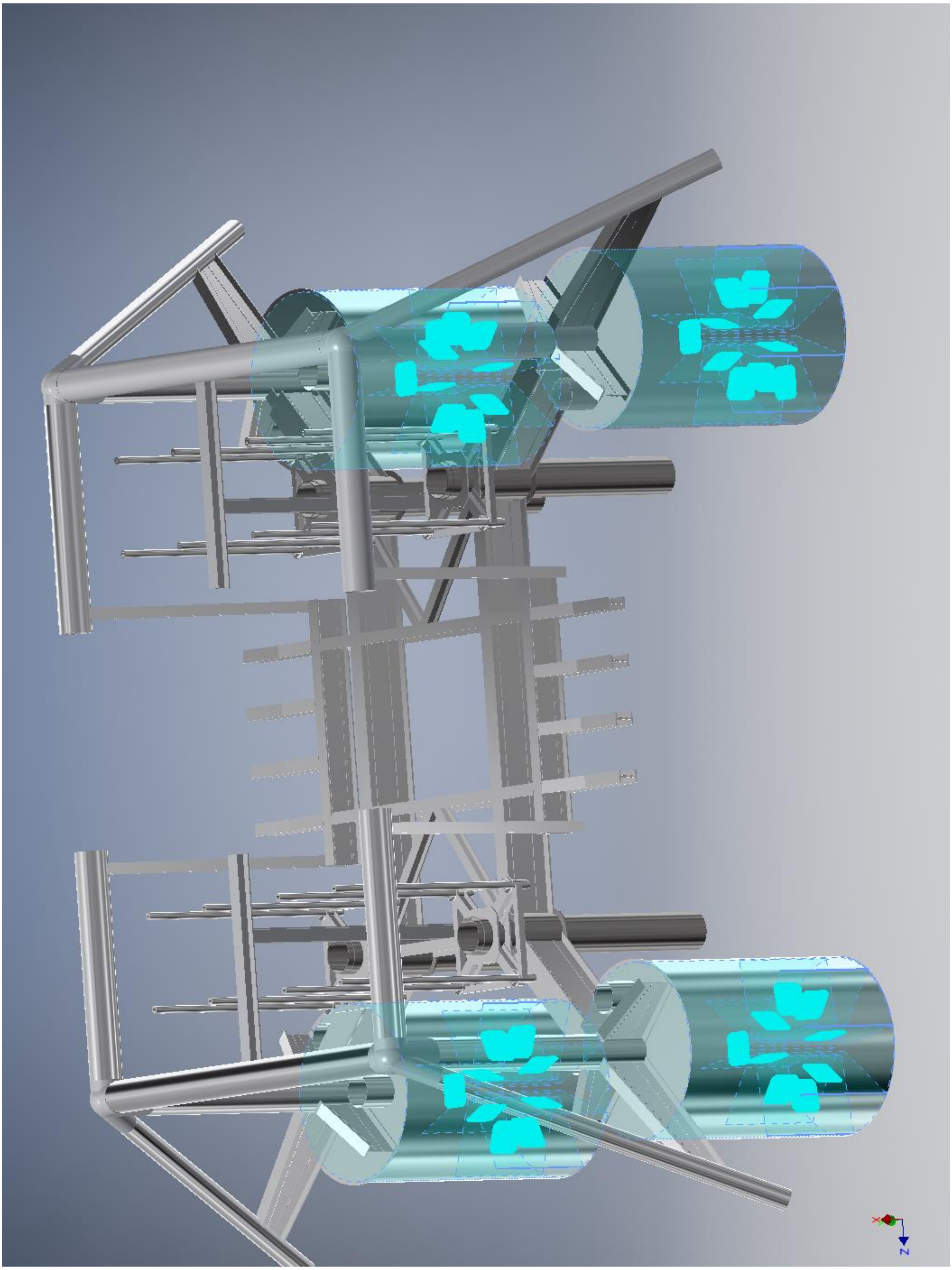

# ⊟ Results

## ⊟ Reaction Force and Moment on Constraints

| Constraint Name | Reaction Force | | Reaction Moment | |
|---|---|---|---|---|
| | Magnitude | Component (X,Y,Z) | Magnitude | Component (X,Y,Z) |
| Fixed Constraint:1 | 3067750 N | 2857980 N | 15457700 N m | 1025160 N m |
| | | -600000 N | | -15100700 N m |
| | | 939693 N | | -3140050 N m |

## ⊟ Result Summary

| Name | Minimum | Maximum |
|---|---|---|
| Volume | 6.02475E+10 mm^3 | |
| Mass | 181171 kg | |
| Von Mises Stress | 0 MPa | 6214.6 MPa |
| 1st Principal Stress | -1286.42 MPa | 1009.56 MPa |
| 3rd Principal Stress | -7647.63 MPa | 145.504 MPa |
| Displacement | 0 mm | 65.9224 mm |
| Safety Factor | 0.0442506 ul | 15 ul |

## ⊟ Figures

### ⊟ Von Mises Stress

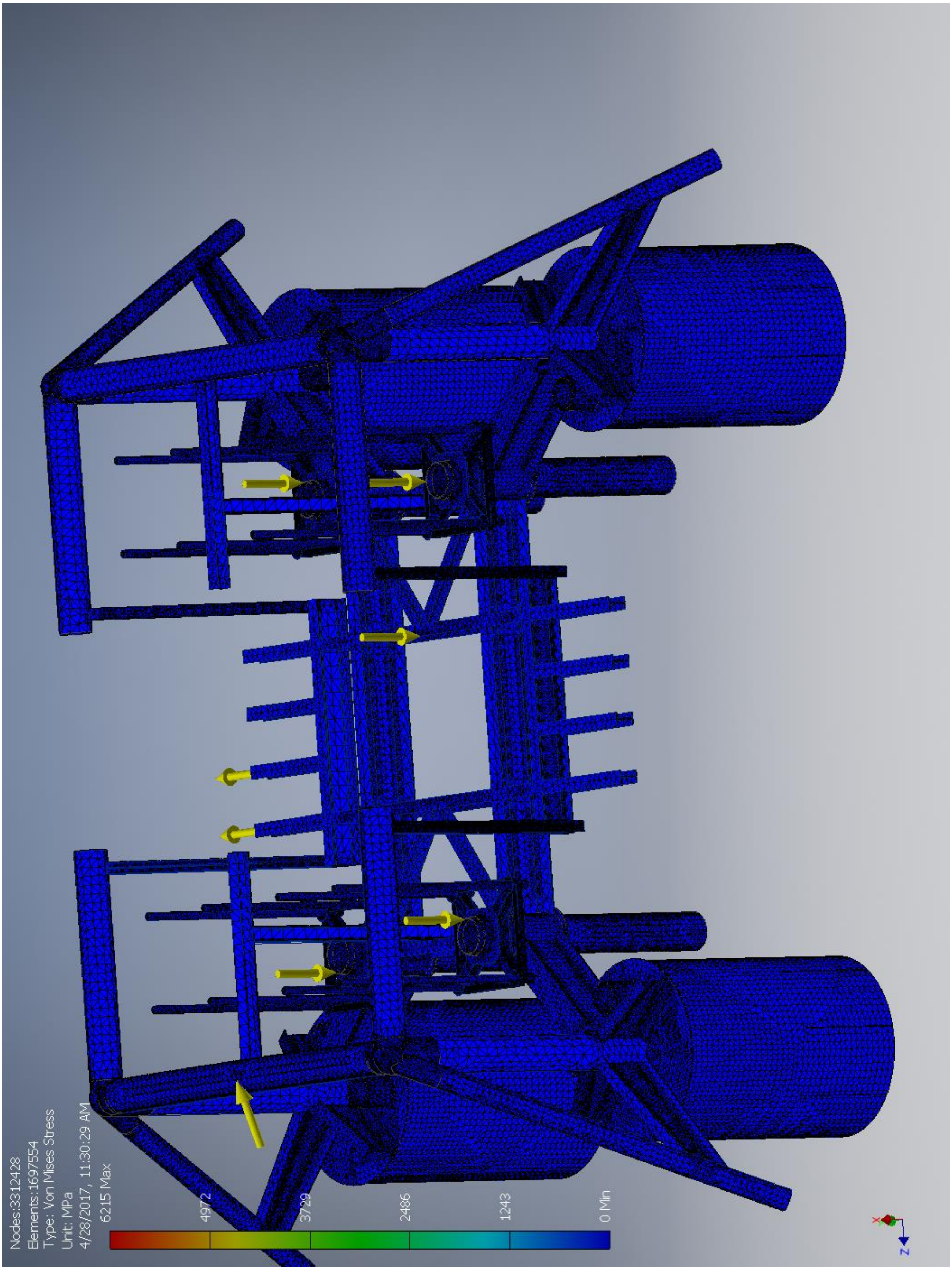

## ⊟ 1st Principal Stress

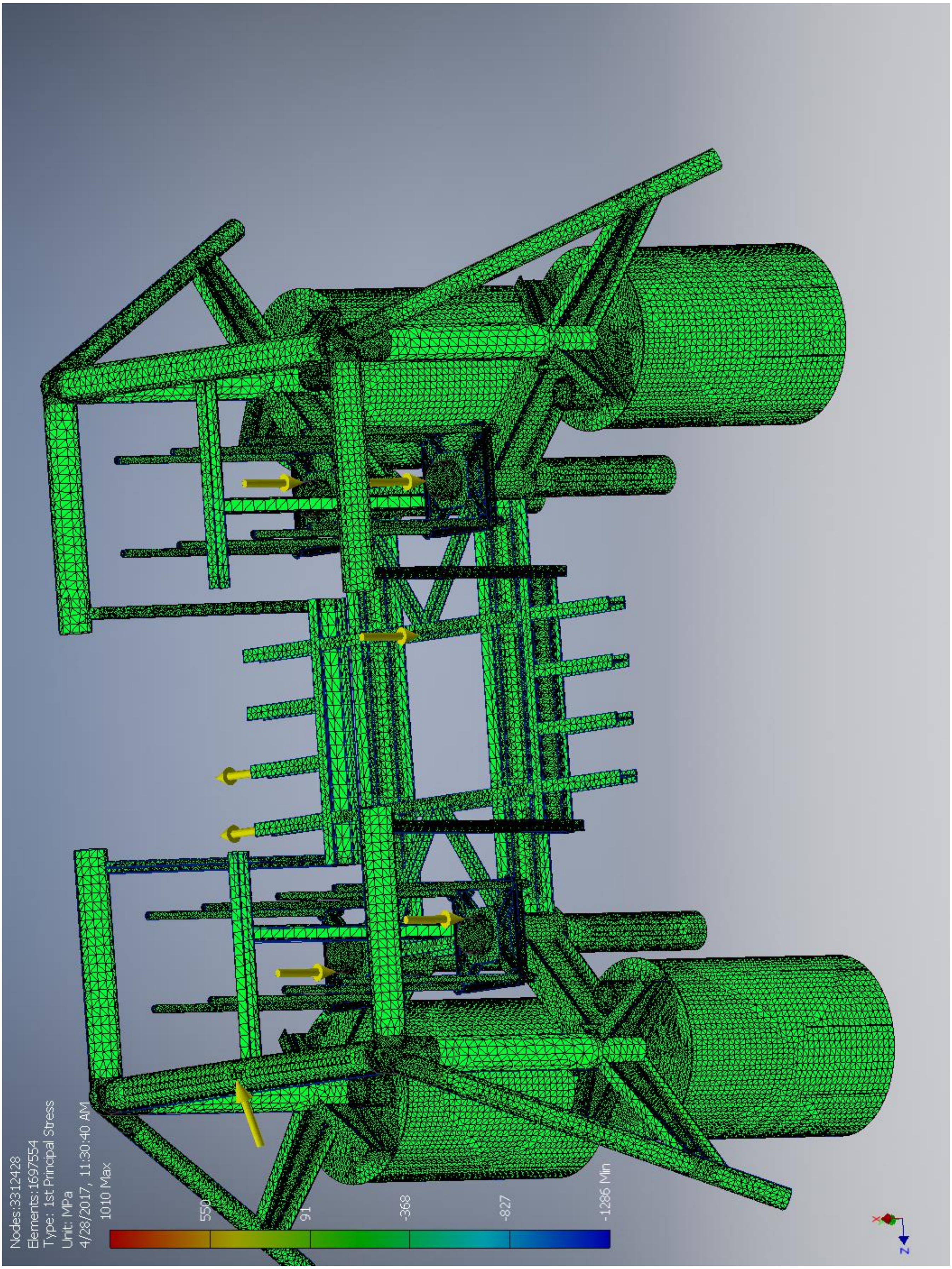

## ⊟ 3rd Principal Stress

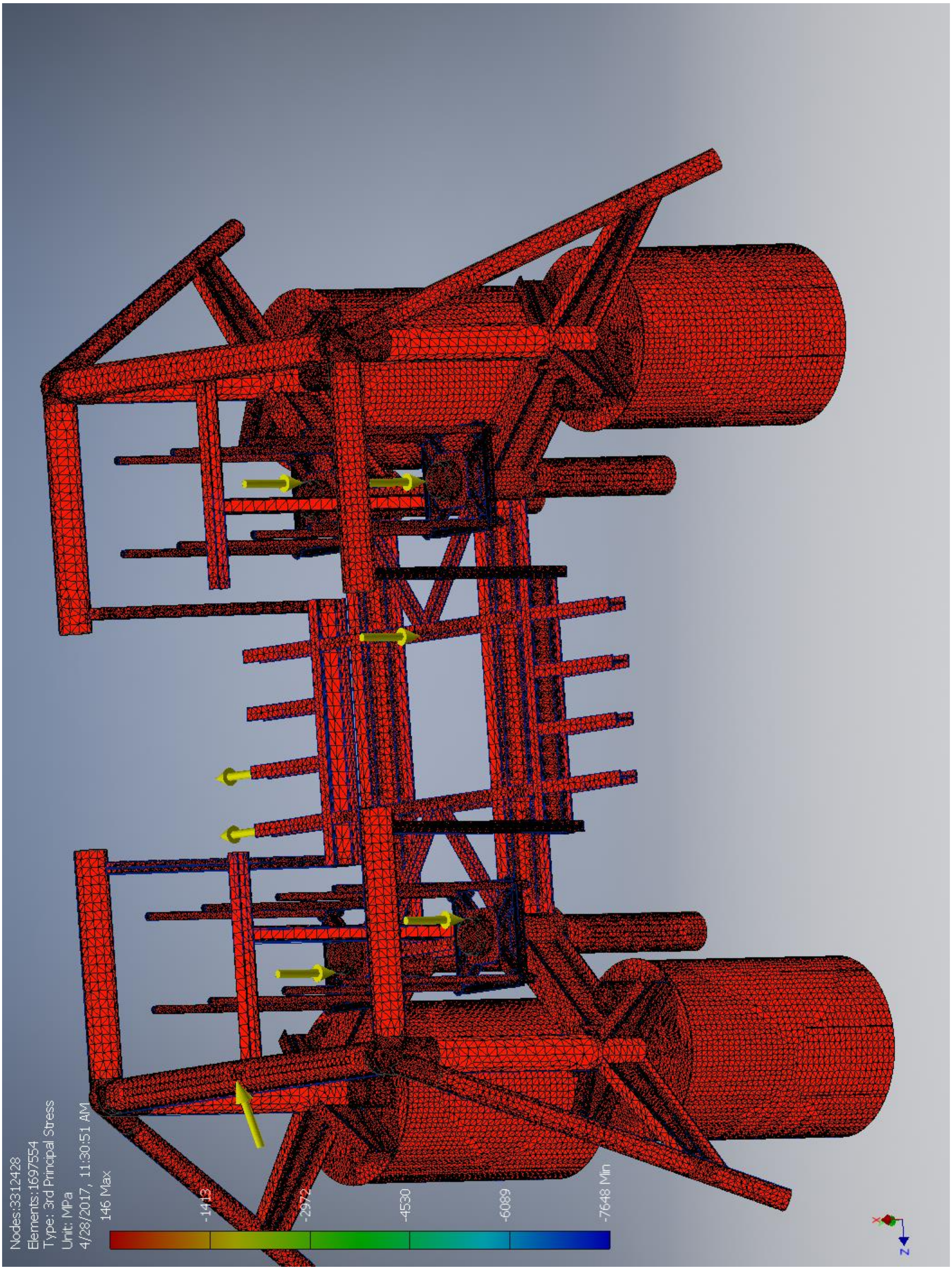

## ⊟ Displacement

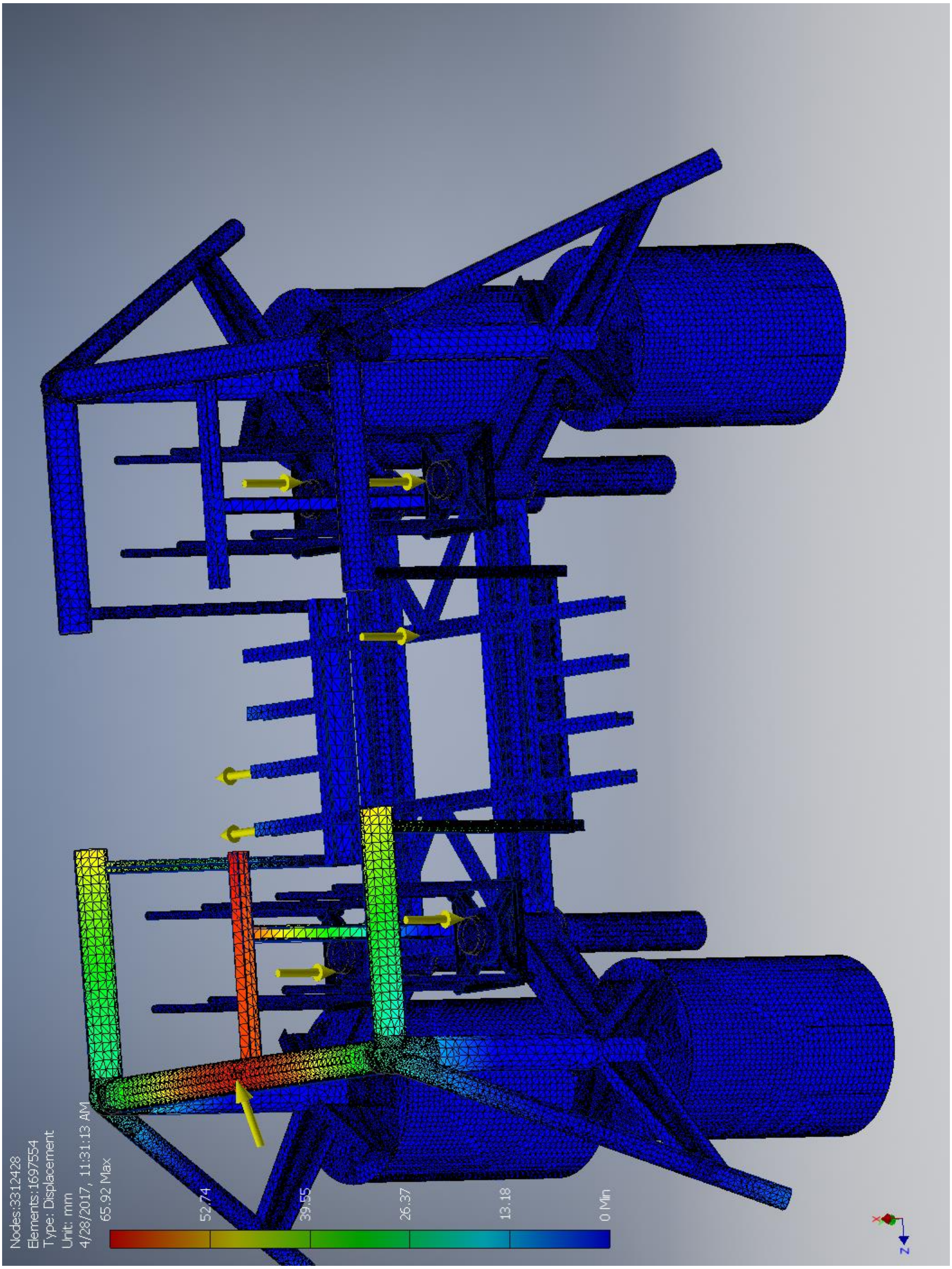

## ⊟ Safety Factor

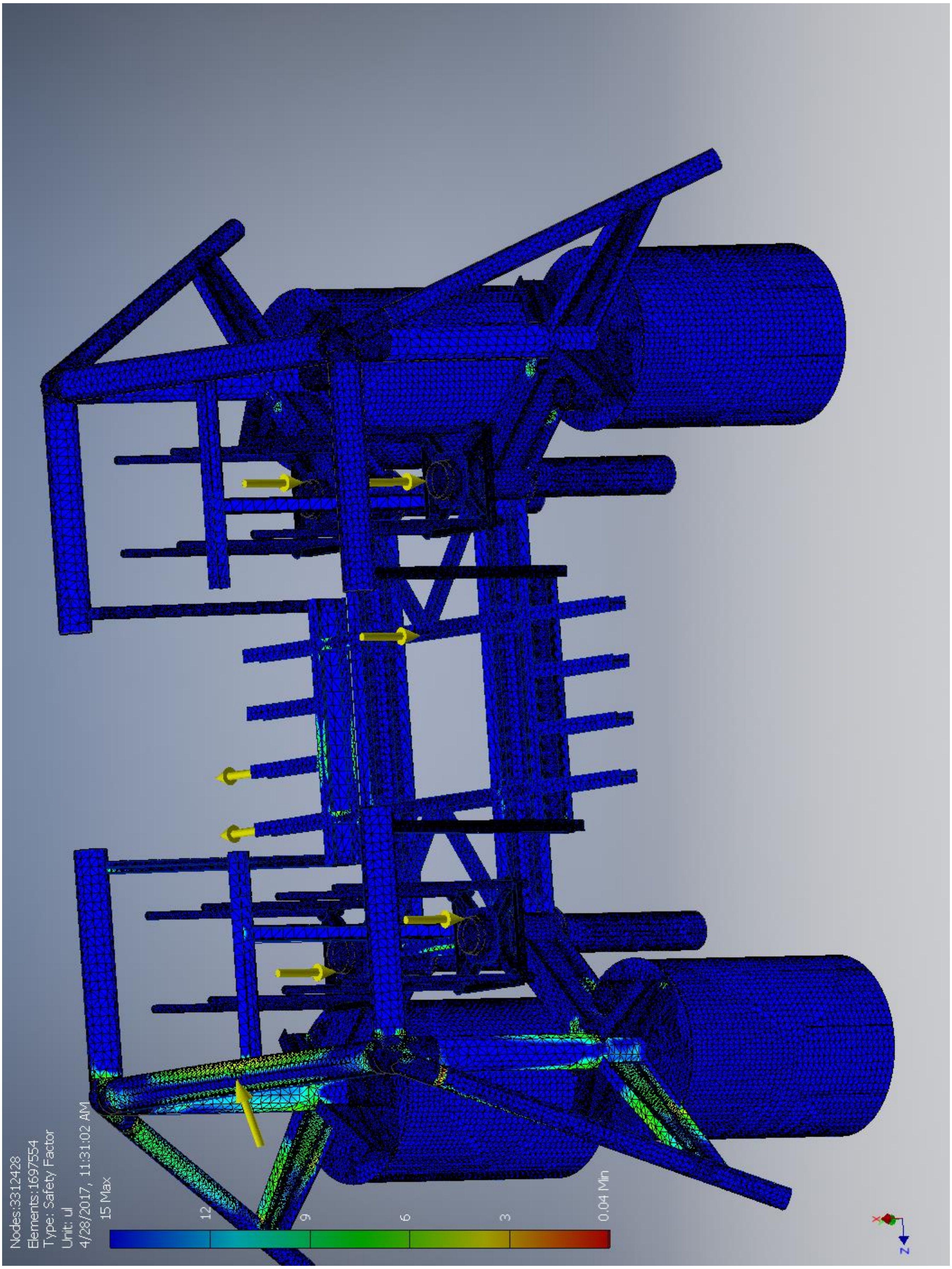

## I.7 Case-G

# Stress Analysis Report

AUTODESK

| | |
|---|---|
| Analyzed File: | Assembly.iam |
| Autodesk Inventor Version: | 2017 (Build 210142000, 142) |
| Creation Date: | 4/28/2017, 4:19 PM |
| Study Author: | henrikwn |
| Summary: | |

---

## ⊟ Project Info (iProperties)

### ⊟ Summary

| | |
|---|---|
| Title | |
| Author | henrikwn |

### ⊟ Project

| | |
|---|---|
| Designer | henrikwn |

### ⊟ Physical

| | |
|---|---|
| Mass | 182182 kg |
| Area | 3.5408E+09 mm^2 |
| Volume | 6.06219E+10 mm^3 |
| Center of Gravity | x=-8278.87 mm<br>y=6548.2 mm<br>z=9857.83 mm |

Note: Physical values could be different from Physical values used by FEA reported below.

---

## ⊟ Case-G

**General objective and settings:**

| | |
|---|---|
| Design Objective | Single Point |
| Study Type | Static Analysis |
| Last Modification Date | 4/28/2017, 3:30 PM |
| Detect and Eliminate Rigid Body Modes | No |
| Separate Stresses Across Contact Surfaces | No |
| Motion Loads Analysis | No |

⊟ Operating conditions

## ⊟ Bearing Load:1

| | |
|---|---|
| Load Type | Bearing Load |
| Magnitude | 371080.984 N |
| Vector X | 331905.000 N |
| Vector Y | -117346.000 N |
| Vector Z | 117346.000 N |

### ⊟ Selected Face(s)

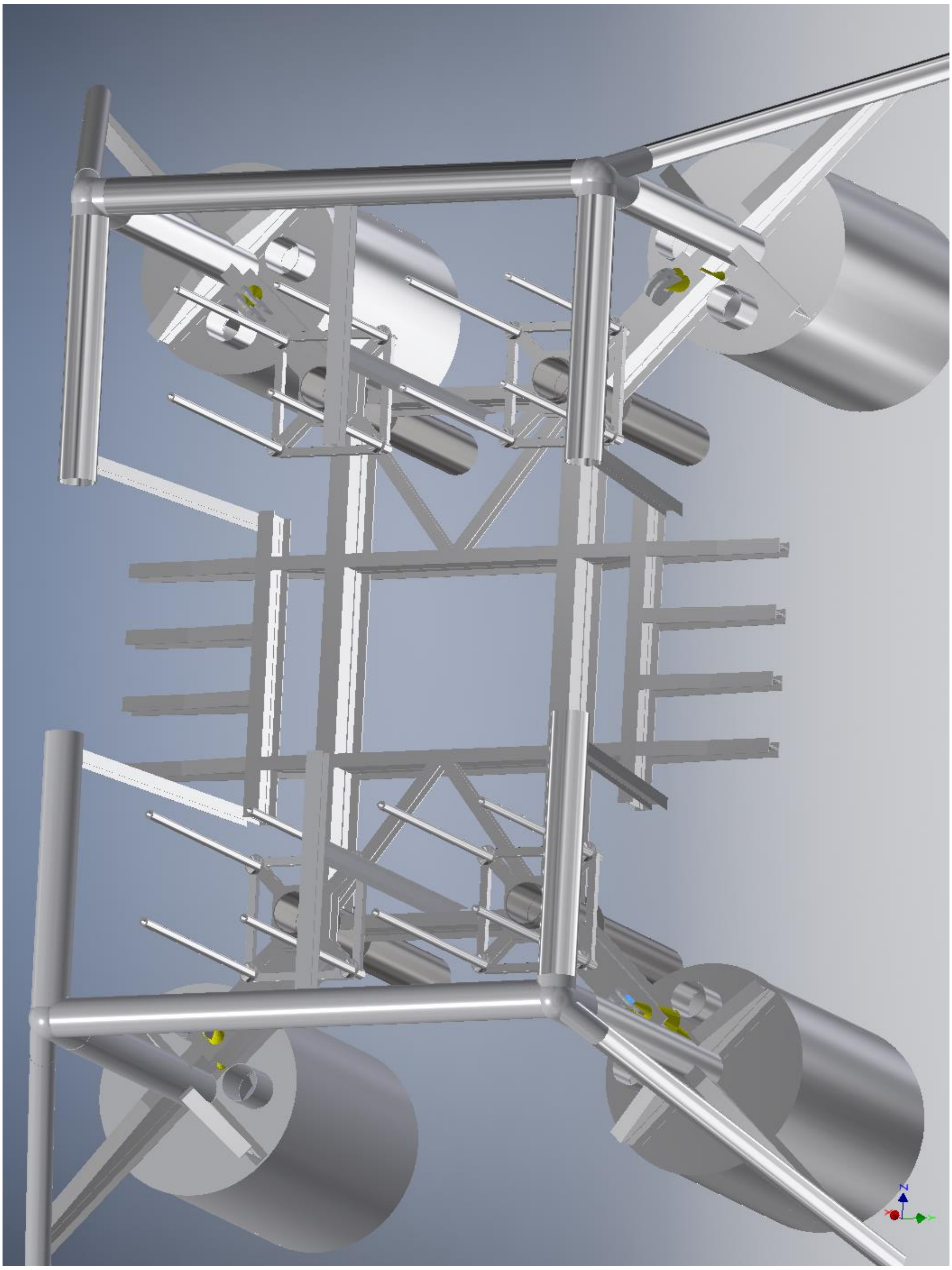

## ⊟ Bearing Load:2

| | |
|---|---|
| Load Type | Bearing Load |
| Magnitude | 371080.984 N |
| Vector X | 331905.000 N |
| Vector Y | -117346.000 N |
| Vector Z | 117346.000 N |

### ⊟ Selected Face(s)

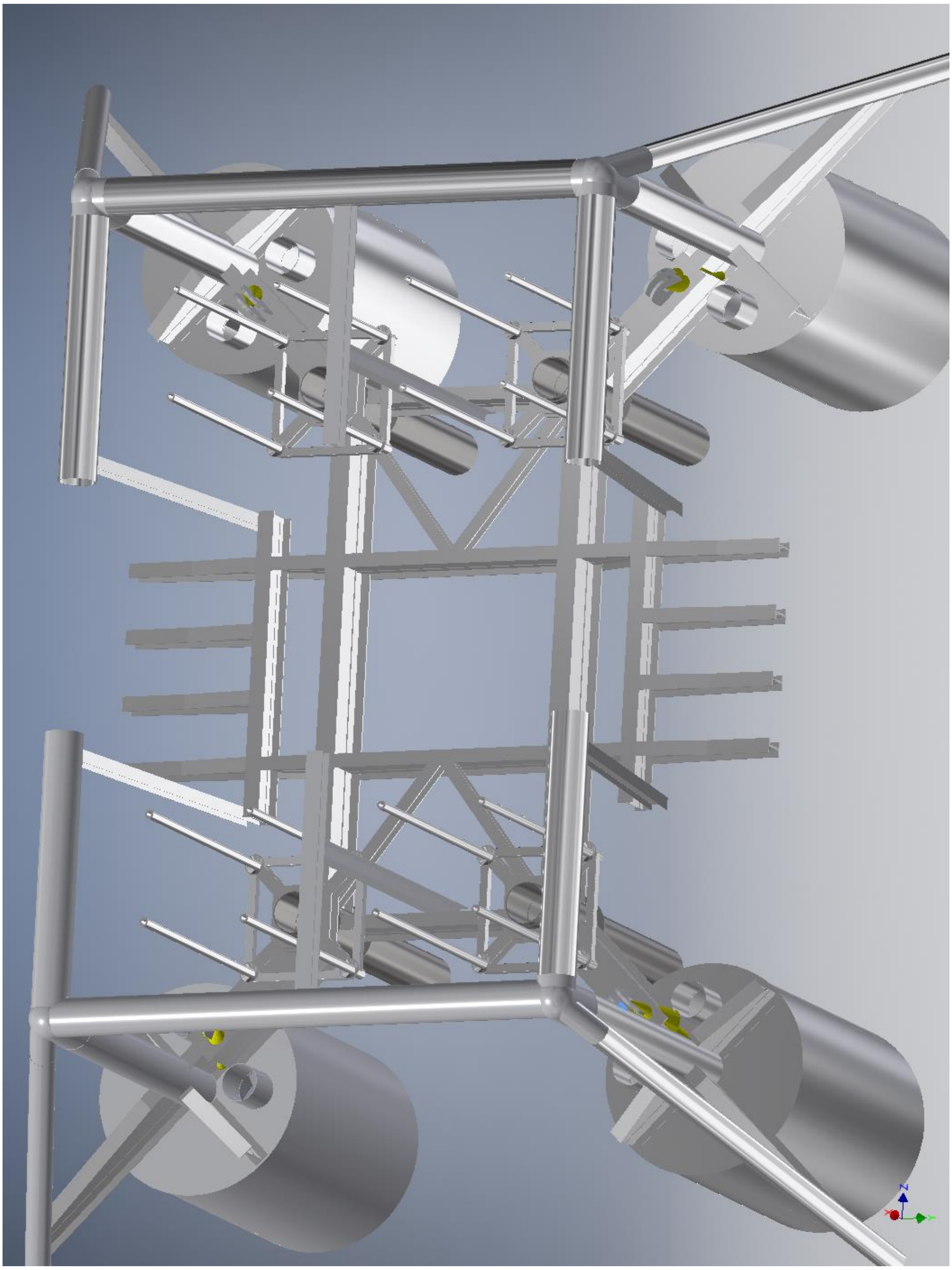

## ⊟ Bearing Load:3

| | |
|---|---|
| Load Type | Bearing Load |
| Magnitude | 371080.984 N |
| Vector X | 331905.000 N |
| Vector Y | 117346.000 N |
| Vector Z | 117346.000 N |

### ⊟ Selected Face(s)

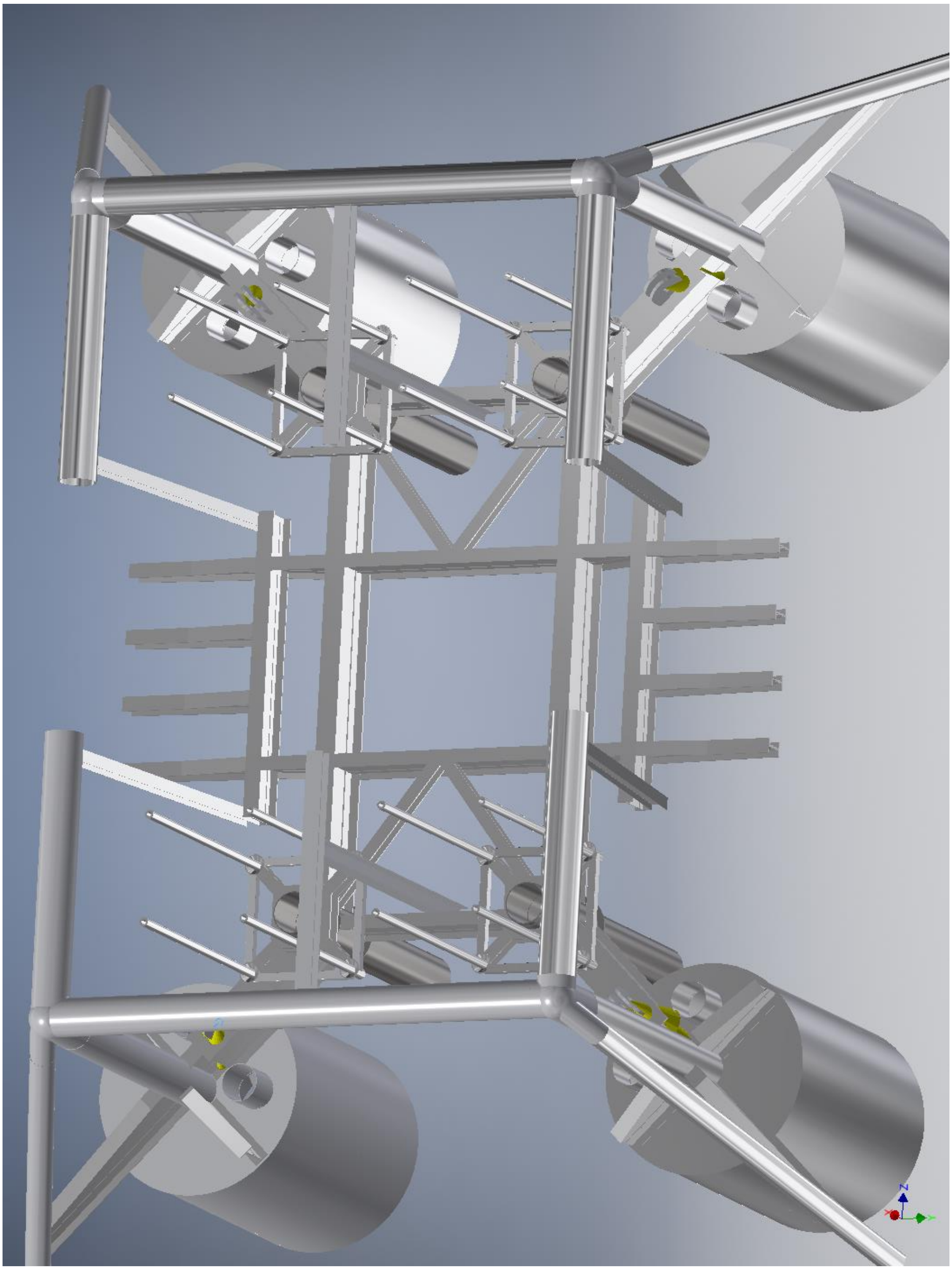

## ⊟ Bearing Load:4

| | |
|---|---|
| Load Type | Bearing Load |
| Magnitude | 371080.984 N |
| Vector X | 331905.000 N |
| Vector Y | 117346.000 N |
| Vector Z | 117346.000 N |

### ⊟ Selected Face(s)

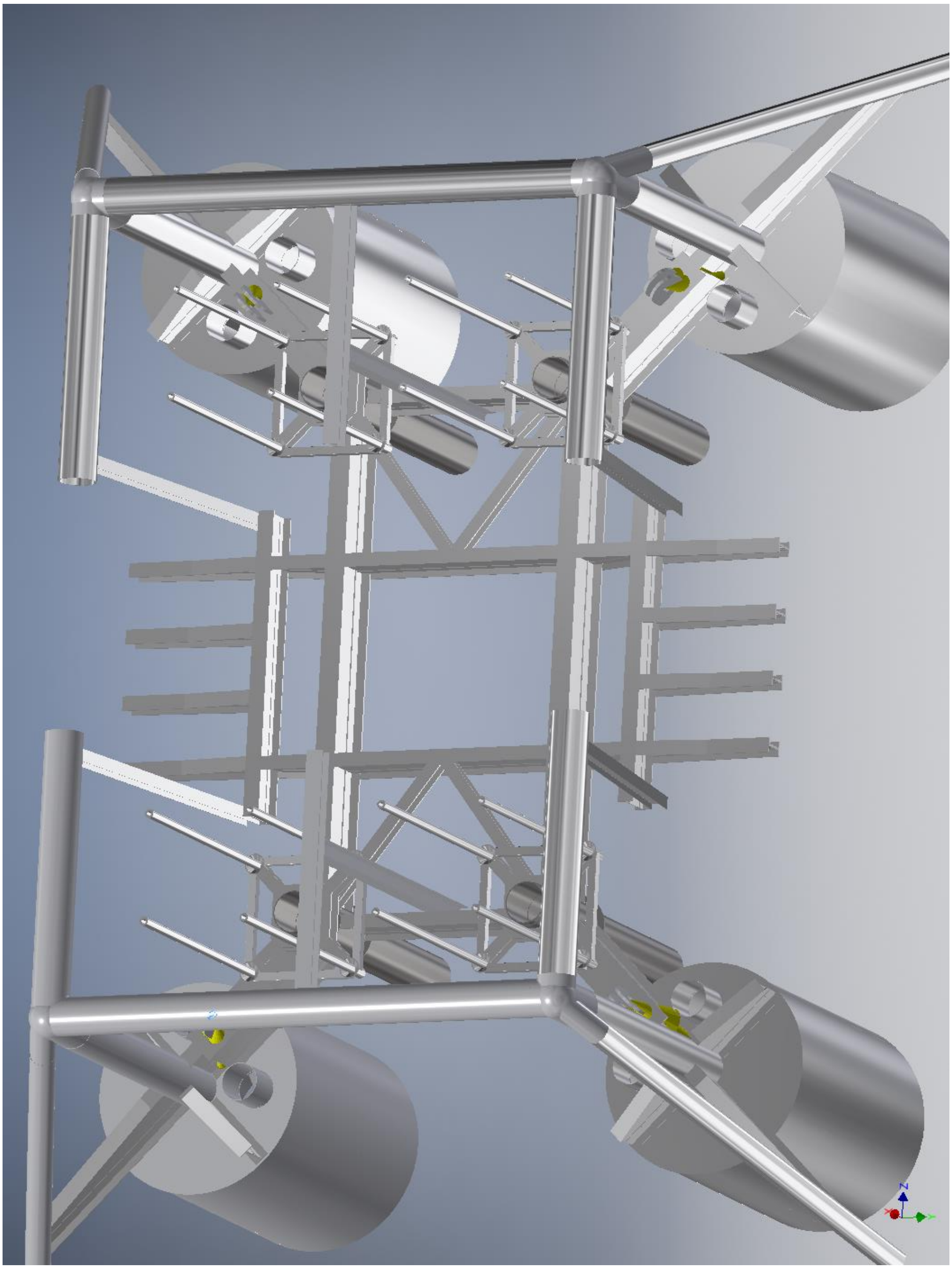

## ⊟ Bearing Load:5

| | |
|---|---|
| Load Type | Bearing Load |
| Magnitude | 371080.984 N |
| Vector X | 331905.000 N |
| Vector Y | 117346.000 N |
| Vector Z | -117346.000 N |

### ⊟ Selected Face(s)

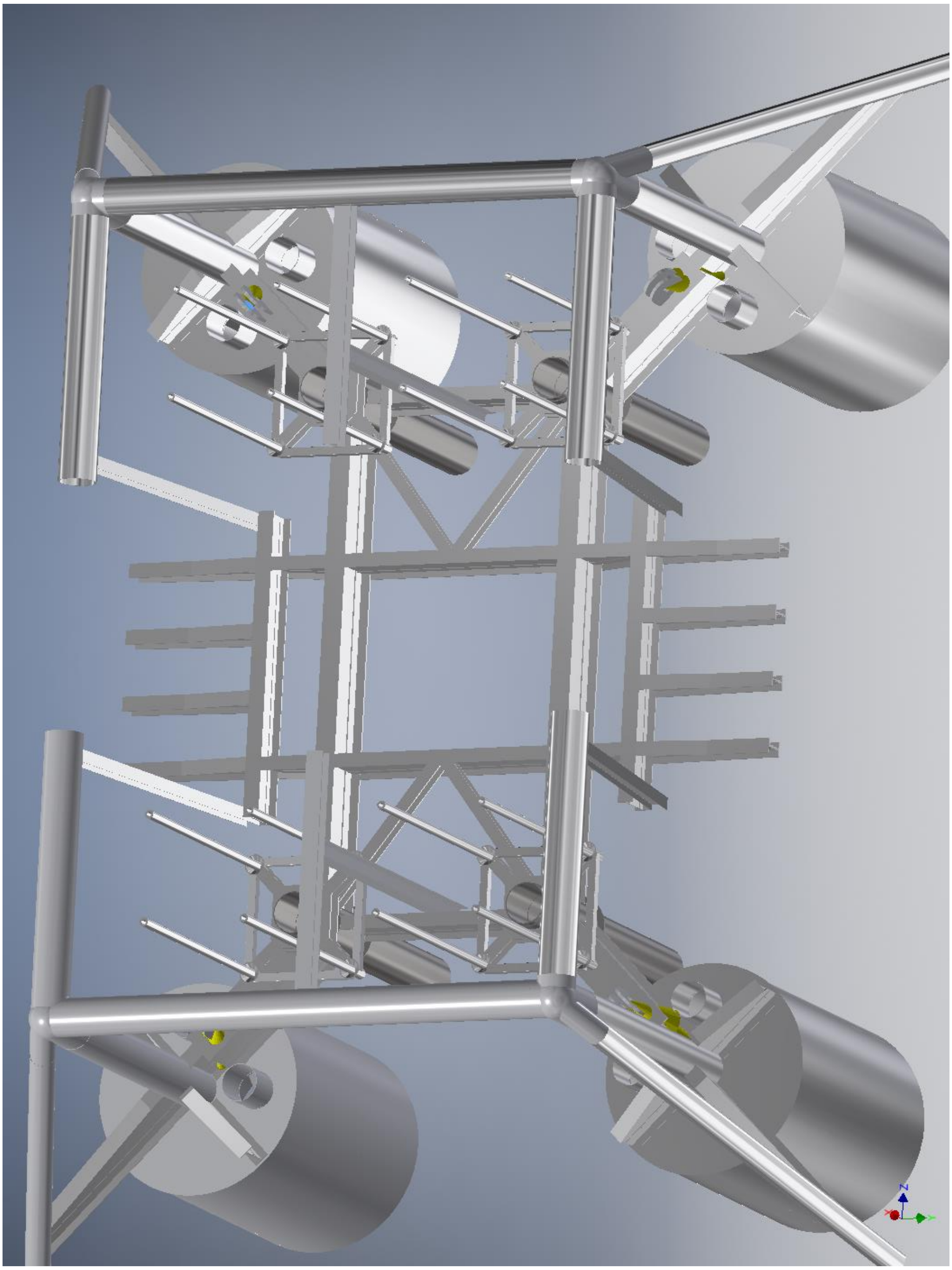

## ⊟ Bearing Load:6

| | |
|---|---|
| Load Type | Bearing Load |
| Magnitude | 371080.984 N |
| Vector X | 331905.000 N |
| Vector Y | 117346.000 N |
| Vector Z | -117346.000 N |

### ⊟ Selected Face(s)

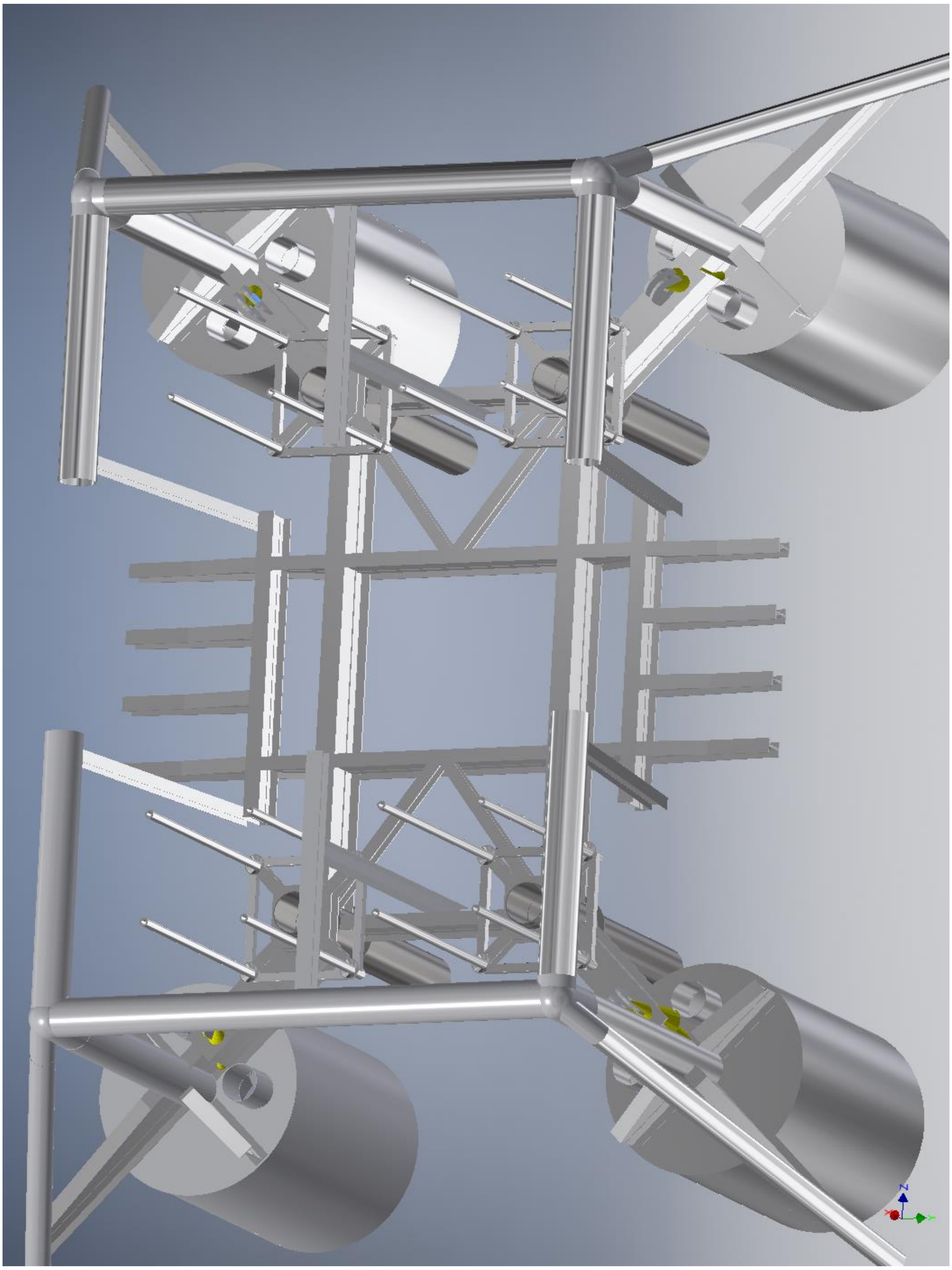

## ⊟ Bearing Load:7

| | |
|---|---|
| Load Type | Bearing Load |
| Magnitude | 371080.984 N |
| Vector X | 331905.000 N |
| Vector Y | -117346.000 N |
| Vector Z | -117346.000 N |

### ⊟ Selected Face(s)

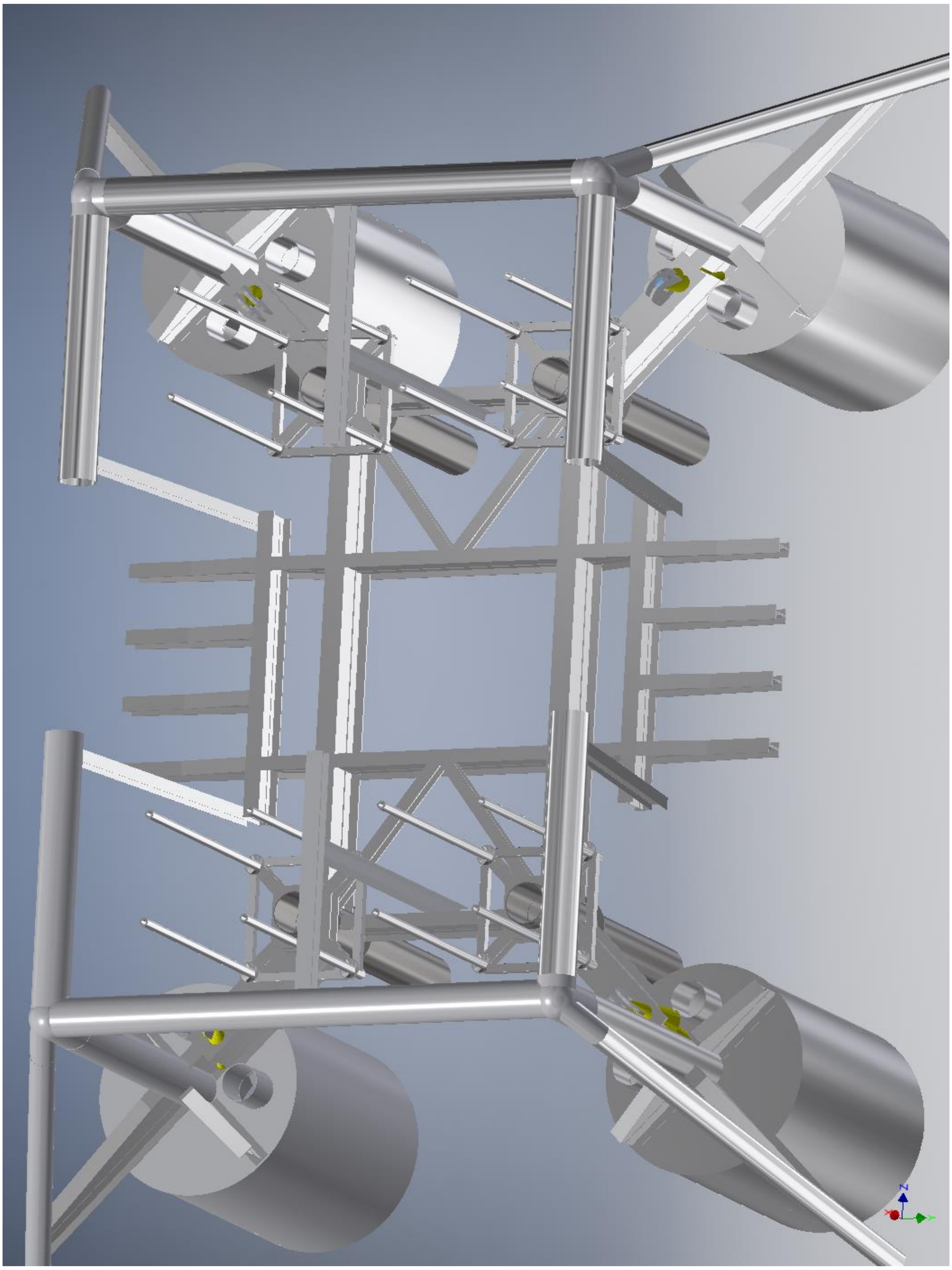

## ⊟ Bearing Load:8

| | |
|---|---|
| Load Type | Bearing Load |
| Magnitude | 371080.984 N |
| Vector X | 331905.000 N |
| Vector Y | -117346.000 N |
| Vector Z | -117346.000 N |

### ⊟ Selected Face(s)

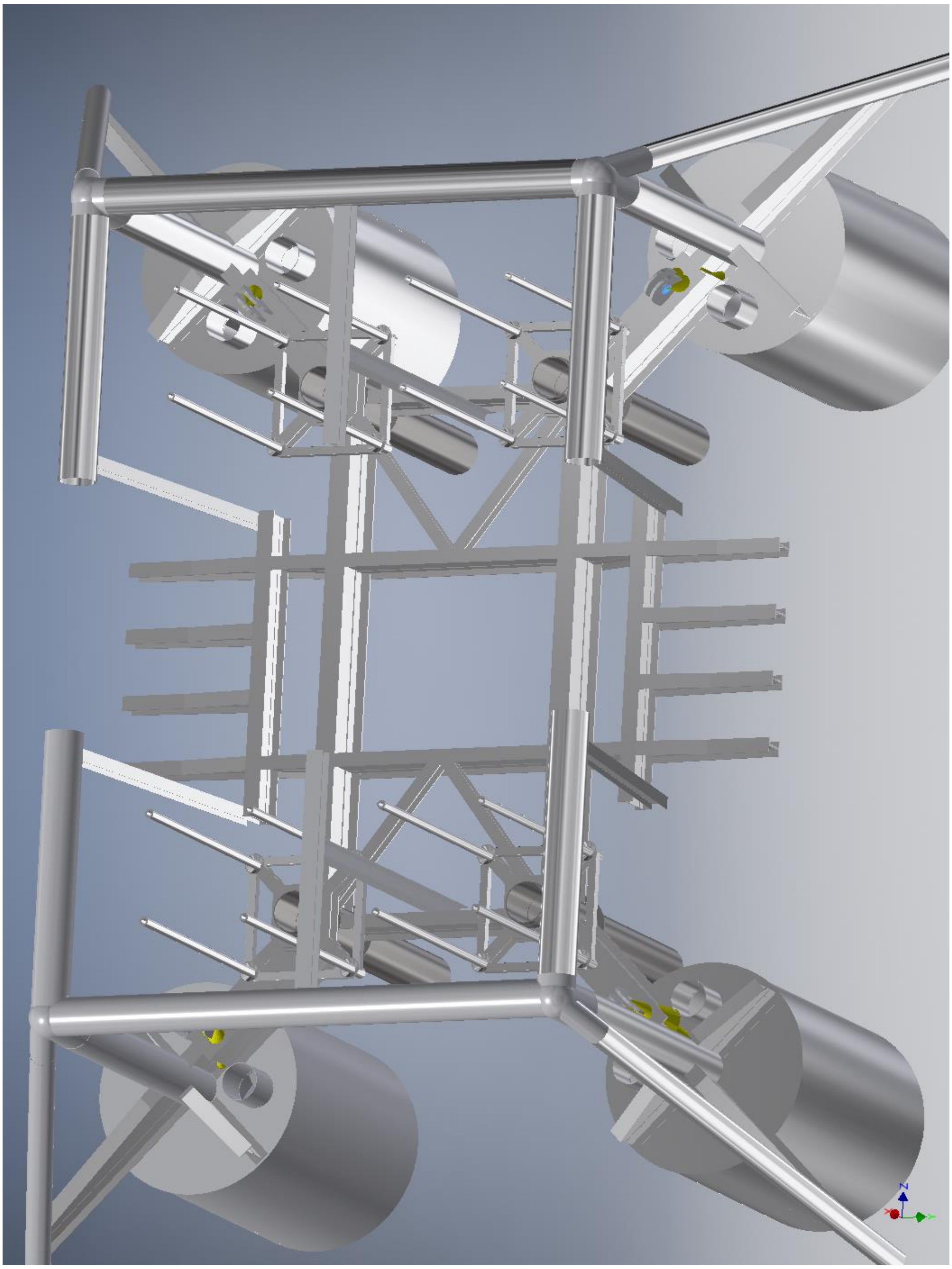

## ⊟ Fixed Constraint:1

| Constraint Type | Fixed Constraint |
| --- | --- |

### ⊟ Selected Face(s)

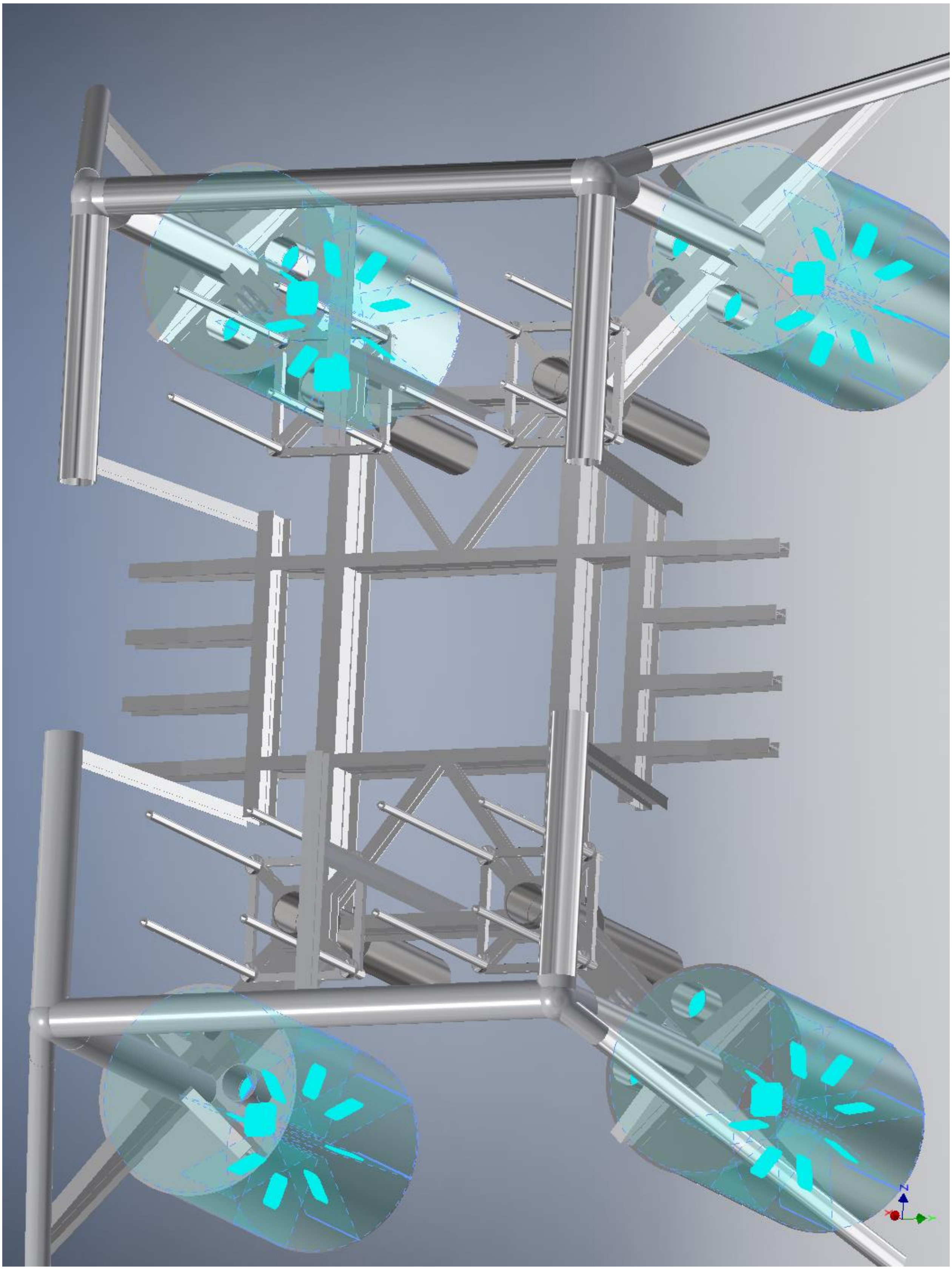

# Results

## Reaction Force and Moment on Constraints

| Constraint Name | Reaction Force | | Reaction Moment | |
|---|---|---|---|---|
| | Magnitude | Component (X,Y,Z) | Magnitude | Component (X,Y,Z) |
| Fixed Constraint:1 | 2655240 N | -2655240 N | 0 N m | 0 N m |
| | | 0 N | | 0 N m |
| | | 0 N | | 0 N m |

## Result Summary

| Name | Minimum | Maximum |
|---|---|---|
| Volume | 6.06219E+10 mm^3 | |
| Mass | 182182 kg | |
| Von Mises Stress | 0 MPa | 65.5253 MPa |
| 1st Principal Stress | -8.15124 MPa | 76.2729 MPa |
| 3rd Principal Stress | -57.1178 MPa | 22.3187 MPa |
| Displacement | 0 mm | 2.51266 mm |
| Safety Factor | 4.19686 ul | 15 ul |

## Figures

## Von Mises Stress

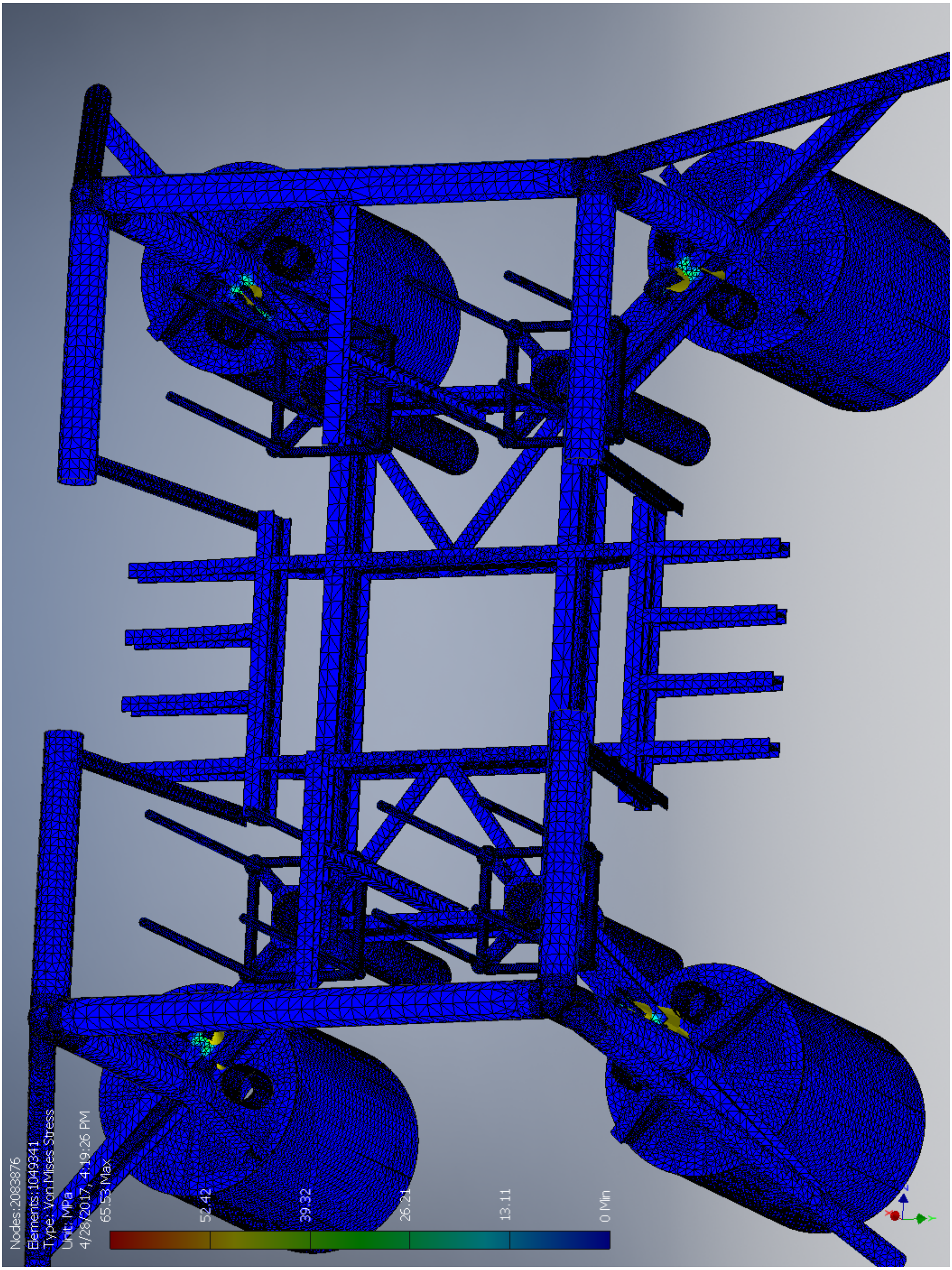

## ⊟ 1st Principal Stress

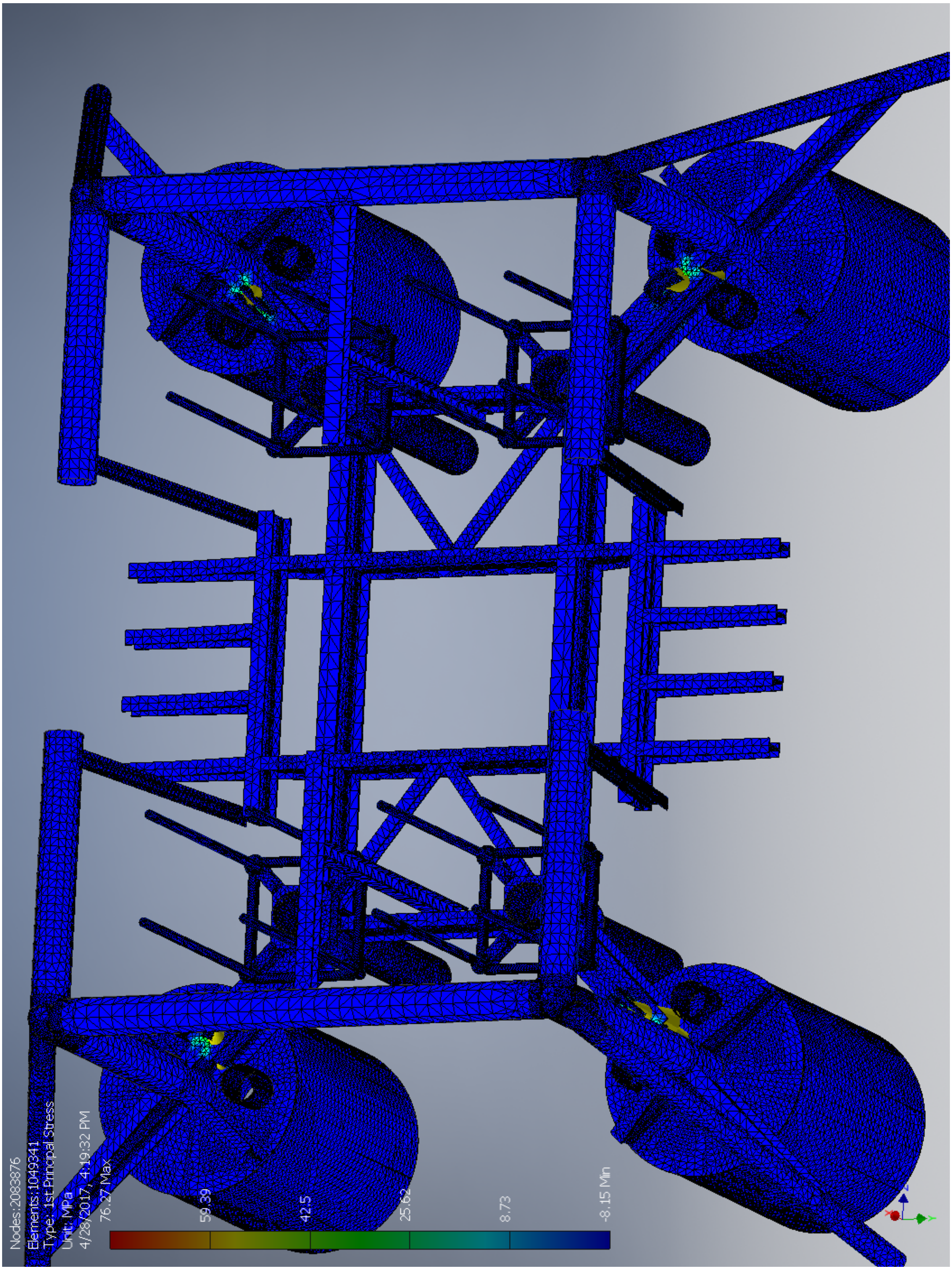

### ⊟ 3rd Principal Stress

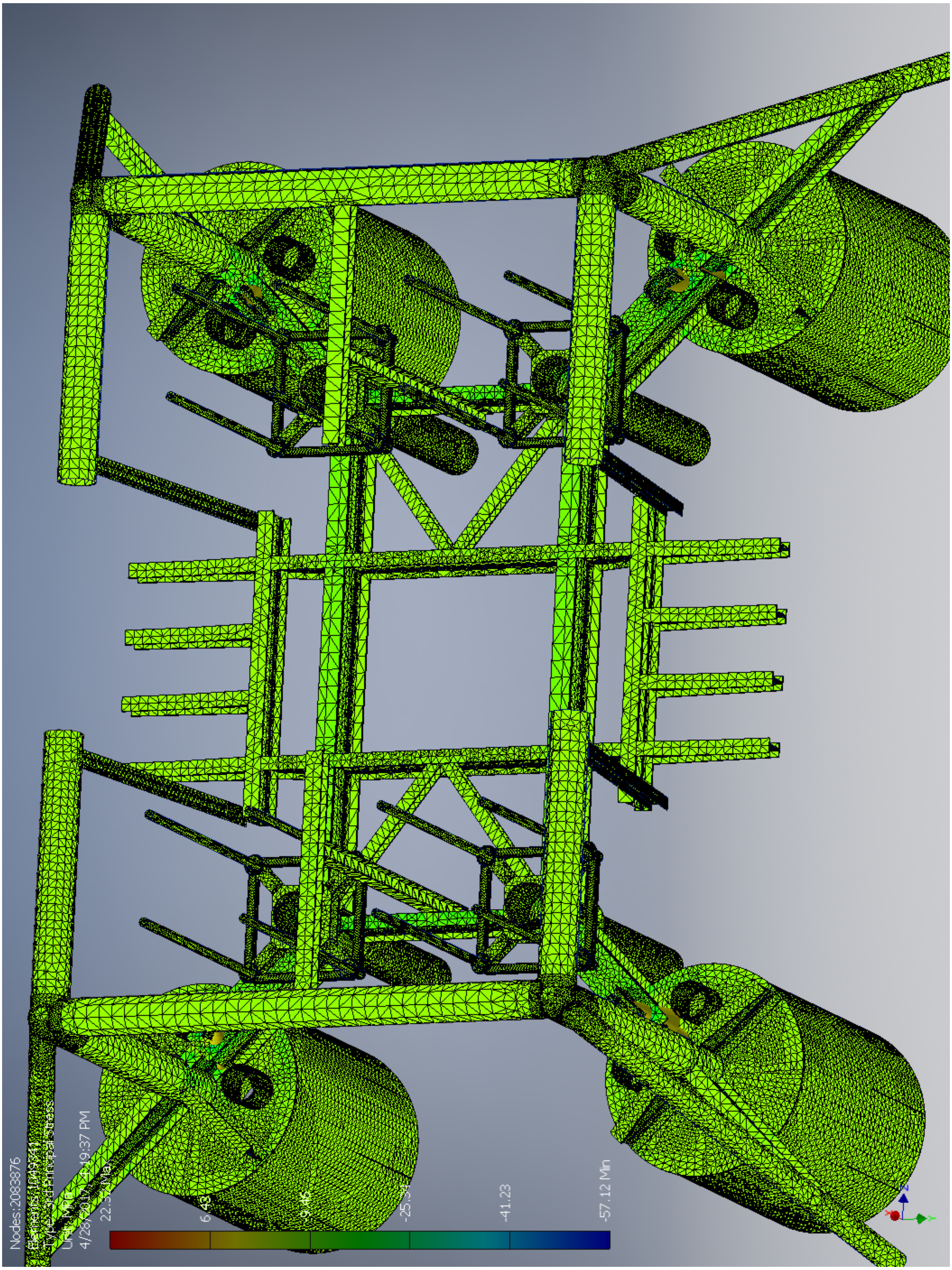

### ⊟ Displacement

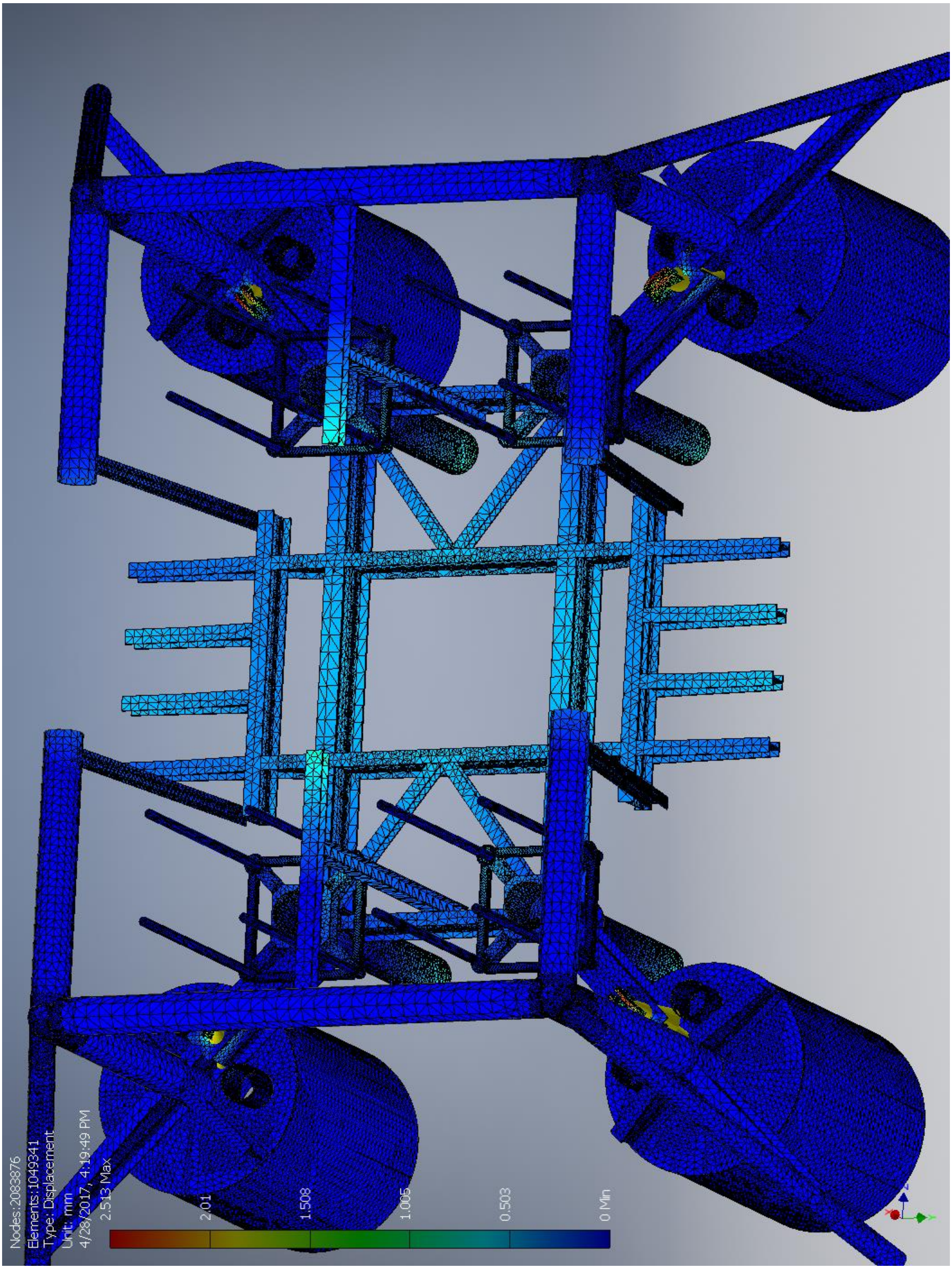

## ⊟ Safety Factor